

Michael J. Sofia *Editor*

HCV: The Journey from Discovery to a Cure

Volume I

31

Topics in Medicinal Chemistry

Series Editors

P.R. Bernstein, Philadelphia, USA

A.L. Garner, Ann Arbor, USA

G.I. Georg, Minneapolis, USA

T. Kobayashi, Tokyo, Japan

J.A. Lowe, Stonington, USA

N.A. Meanwell, Princeton, USA

A.K. Saxena, Lucknow, India

U. Stilz, Boston, USA

C.T. Supuran, Sesto Fiorentino, Italy

A. Zhang, Pudong, China

Aims and Scope

Topics in Medicinal Chemistry (TMC) covers all relevant aspects of medicinal chemistry research, e.g. pathobiochemistry of diseases, identification and validation of (emerging) drug targets, structural biology, drugability of targets, drug design approaches, chemogenomics, synthetic chemistry including combinatorial methods, bioorganic chemistry, natural compounds, high-throughput screening, pharmacological in vitro and in vivo investigations, drug-receptor interactions on the molecular level, structure-activity relationships, drug absorption, distribution, metabolism, elimination, toxicology and pharmacogenomics. Drug research requires interdisciplinary team-work at the interface between chemistry, biology and medicine. To fulfil this need, TMC is intended for researchers and experts working in academia and in the pharmaceutical industry, and also for graduates that look for a carefully selected collection of high quality review articles on their respective field of expertise.

Medicinal chemistry is both science and art. The science of medicinal chemistry offers mankind one of its best hopes for improving the quality of life. The art of medicinal chemistry continues to challenge its practitioners with the need for both intuition and experience to discover new drugs. Hence sharing the experience of drug research is uniquely beneficial to the field of medicinal chemistry.

All chapters from Topics in Medicinal Chemistry are published OnlineFirst with an individual DOI. In references, Topics in Medicinal Chemistry is abbreviated as Top Med Chem and cited as a journal.

More information about this series at <http://www.springer.com/series/7355>

Michael J. Sofia
Editor

HCV: The Journey from Discovery to a Cure

Volume I

With contributions by

S. A. Alqahtani · H. J. Alter · R. Bartenschlager ·
E. Billerbeck · H.-J. Chen · A. Cho · P. A. Furman · Y. Gai ·
R. G. Gentles · C. S. Graham · M. Houghton · L.-J. Jiang ·
D. Kempf · Y.-Y. Ku · A. D. Kwong · N. J. Liverton ·
V. Lohmann · J. Long · J. Ma · J. A. McCauley ·
K. F. McDaniel · N. A. Meanwell · T. Middleton · Y. S. Or ·
R. B. Perni · R. Rajamani · C. M. Rice · M. T. Rudd ·
M. Saeed · P. M. Scola · J. Shanley · M. J. Sofia ·
L.-Q. Sun · Y. Sun · M. S. Sulkowski · J. G. Taylor ·
S. Venkatraman · B. Wang · G. Wang · W. J. Watkins



Springer

Editor

Michael J. Sofia
Arbutus Biopharma, Inc.
Warminster, PA, USA

ISSN 1862-2461

ISSN 1862-247X (electronic)

Topics in Medicinal Chemistry

ISBN 978-3-030-28206-6

ISBN 978-3-030-28207-3 (eBook)

<https://doi.org/10.1007/978-3-030-28207-3>

© Springer Nature Switzerland AG 2019

This work is subject to copyright. All rights are reserved by the Publisher, whether the whole or part of the material is concerned, specifically the rights of translation, reprinting, reuse of illustrations, recitation, broadcasting, reproduction on microfilms or in any other physical way, and transmission or information storage and retrieval, electronic adaptation, computer software, or by similar or dissimilar methodology now known or hereafter developed.

The use of general descriptive names, registered names, trademarks, service marks, etc. in this publication does not imply, even in the absence of a specific statement, that such names are exempt from the relevant protective laws and regulations and therefore free for general use.

The publisher, the authors, and the editors are safe to assume that the advice and information in this book are believed to be true and accurate at the date of publication. Neither the publisher nor the authors or the editors give a warranty, expressed or implied, with respect to the material contained herein or for any errors or omissions that may have been made. The publisher remains neutral with regard to jurisdictional claims in published maps and institutional affiliations.

This Springer imprint is published by the registered company Springer Nature Switzerland AG.
The registered company address is: Gewerbestrasse 11, 6330 Cham, Switzerland

Preface

The story of how the battle against hepatitis C was won began in 1975 with the realization that a previously unknown virus, non-A non-B hepatitis (NANBH), was responsible for a liver disease that plagued millions of individuals worldwide and took the lives of hundreds of thousands. It wasn't until the efforts of Harvey Alter, Michael Houghton, and their collaborators that in 1989 the hepatitis C virus (HCV) was identified as the new virus. Through their efforts, the development of a way to screen the blood supply was achieved and the risk of contracting this disease was dramatically reduced. However, there were still tens of millions of individuals who remained infected and transmitting the disease either sexually, via IV drug use or by coming in contact with contaminated blood by other means. The need for a cure was critical. This two-volume book attempts to chronicle the scientific story of the discovery of the virus, the development of tools important to the search for a cure, and the many drug discovery and development efforts that eventually delivered curative therapies to the millions of chronically infected HCV patients. It also attempts to put context around the impact of this work for the patient and society.

In conceiving this book, *HCV: The Journey from Discovery to a Cure*, I wanted to not simply have a series of isolated accounts of drug discovery efforts that led to marketed products. I wanted to take the reader along the entire historical scientific journey from the beginning to the end. It is rare in the annals of science that within a lifetime the full story of the identification of the key causative agent for a disease is found, and a cure is identified and made available to patients. In fact, cures of diseases are extremely rare, and the cure for HCV is the only example of a cure for a chronic viral disease. Therefore, I felt that the entire story needed to be told in one place.

In this two-volume account of how an HCV cure was achieved, the journey is communicated by those scientists and clinicians, including five Lasker Award Laureates, who were making those critical contributions integral in making this achievement happen. It begins with accounts of the discovery of the virus, elucidation of the virus life cycle and the role of each viral protein, development of the replicon system, and the use of interferon as early therapy. It continues with sections

focused on each of the key viral drug discovery targets. Each of these drug discovery sections first provides a general overview of the evolution of medicinal chemistry efforts against the target followed by detailed accounts of the discovery of each drug that is now a marketed HCV therapy. Yet the account of how HCV was cured would not be complete without addressing the evolution of innovative clinical trials and how combination therapies evolved to deliver therapies that are now pan-genotypic, provide exceptionally high cure rates in 8–12 weeks, and exhibit high barriers to resistance. Finally, the true indicator of medical achievement is not the commercial launch of a drug but the benefits that medicines bring to the patient and society; therefore, Volume 2 of the book ends with several perspectives speaking to the benefits achieved by an HCV cure and the possibilities for eliminating HCV as a global health threat.

What this two-volume book does not attempt to do is capture the vast body of work that was published over the 24 years that spanned the time from identification of the virus in 1989 to the approval of the first interferon-free HCV cure, sofosbuvir, in 2013. It also doesn't attempt to capture in detail the stories of the many failed avenues of investigation or accounts of the many investigational drugs that never made it to regulatory approval. However, this book does capture what I feel are the seminal contributions to the field and the important drug discovery success stories that matter to patients.

Finally, I have to thank all the chapter authors who committed a great deal of time outside of their busy schedules to tell the stories contained in this book. Each of them made their contribution because they too saw the need to tell the full story and wanted to be part of it. I also must thank all those researchers and clinicians who have contributed to the HCV cure story over 24 years but whose names are not explicitly mentioned in this work. Your contributions are not lost on those who have authored these chapters.

Warminster, PA, USA

Michael J. Sofia

Contents

Part I The Virus & Early Therapy

From B to Non-B to C: The Hepatitis C Virus in Historical Perspective	3
Harvey J. Alter	
The Discovery of the Hepatitis C Virus	19
Michael Houghton	
HCV Molecular Virology and Animal Models	29
Mohsan Saeed, Eva Billerbeck, and Charles M. Rice	
The Hepatitis C Virus Replicon System and Its Role in Drug Development	69
Ralf Bartenschlager and Volker Lohmann	
The Role of Interferon for the Treatment of Chronic Hepatitis C Virus Infection	97
Saleh A. Alqahtani and Mark S. Sulkowski	

Part II HCV NS5B Polymerase Inhibitors

Evolution of HCV NS5B Nucleoside and Nucleotide Inhibitors	117
Aesop Cho	
The Discovery of Sofosbuvir: A Liver-Targeted Nucleotide Prodrug for the Treatment and Cure of HCV	141
Michael J. Sofia and Phillip A. Furman	
Evolution of HCV NS5B Non-nucleoside Inhibitors	171
William J. Watkins	
Discovery of Beclabuvir: A Potent Allosteric Inhibitor of the Hepatitis C Virus Polymerase	193
Robert G. Gentles	

Part III HCV NS3/4a Protease Inhibitors

Evolution of HCV NS3/4a Protease Inhibitors	231
Nigel J. Liverton	
Development and Marketing of INCIVEK (Telaprevir; VX-950): A First-Generation HCV Protease Inhibitor, in Combination with PEGylated Interferon and Ribavirin	261
Ann D. Kwong, Robert B. Perni, and Camilla S. Graham	
Discovery of Boceprevir, a Ketoamide-Derived HCV NS3 Protease Inhibitor, for Treatment of Genotype 1 Infections	293
Srikanth Venkatraman	
The Discovery and Early Clinical Evaluation of the HCV NS3/4A Protease Inhibitor Asunaprevir (BMS-650032)	317
Nicholas A. Meanwell, Ramkumar Rajamani, Paul M. Scola, and Li-Qiang Sun	
The Invention of Grazoprevir: An HCV NS3/4a Protease Inhibitor	355
John A. McCauley and Michael T. Rudd	
The Discovery and Development of HCV NS3 Protease Inhibitor Paritaprevir	389
Keith F. McDaniel, Yi-Yin Ku, Ying Sun, Hui-Ju Chen, Jason Shanley, Timothy Middleton, Yat Sun Or, and Dale Kempf	
Discovery and Development of the Next-Generation HCV NS3 Protease Inhibitor Glecaprevir	415
Guoqiang Wang, Jun Ma, Li-Juan Jiang, Yonghua Gai, Jiang Long, Bin Wang, Keith F. McDaniel, and Yat Sun Or	
Discovery of Voxilaprevir (GS-9857): The Pan-Genotypic Hepatitis C Virus NS3/4A Protease Inhibitor Utilized as a Component of Vosevi[®]	441
James G. Taylor	
Index	459

Part I
The Virus & Early Therapy

From B to Non-B to C: The Hepatitis C Virus in Historical Perspective



Harvey J. Alter

Contents

1	The Era of Observation Prior to Testing	4
2	The Australia Antigen Transformation	5
3	The Advent and Ascent of Non-A, Non-B Hepatitis: The Blood Transfusion Story	8
4	The Cloning of HCV	11
5	The Virtual Eradication of Transfusion-Associated Hepatitis	12
6	The End of the Beginning and the Beginning of the End	13
	References	15

Abstract The discovery of HCV was an evolutionary process beginning with the serendipitous identification of the Australia antigen that later proved to be the surface protein of the hepatitis B virus (HBV) and the first marker for any human hepatitis virus. Studies of transfusion-associated hepatitis made it evident that most cases were unrelated to HBV. The later discovery of the hepatitis A virus (HAV) made it apparent that non-B cases were also non-A leading to the awkward terminology non-A, non-B hepatitis (NANBH). While NANBH was identified only by exclusion and had no specific serologic or molecular marker, using chimpanzee transmission studies, it was possible to show that the NANBH agent was small and enveloped and most consistent with being a flavivirus as it later proved to be. Clinical studies showed that NANBH could lead to cirrhosis, hepatocellular carcinoma, and liver-related fatality. The major breakthrough occurred in the late 1980s when the Chiron Corporation cloned the NANBH agent and renamed it the hepatitis C virus (HCV). Adding HCV serologic testing, and later molecular testing, to routine donor screening virtually eradicated TAH with current risk estimated to be one case in two million transfusions. More recently, direct-acting antiviral agents have been shown to result in sustained virologic responses, tantamount to cure, in 98% of treated subjects. The existing challenges are to identify currently unrecognized HCV carriers and to make treatment accessible to all.

H. J. Alter (✉)

National Institutes of Health, Bethesda, MD, USA

e-mail: halter@cc.nih.gov

Keywords Australia antigen, HBV, HCV, Hepatitis B virus, Hepatitis C virus, NANBH, NANBV, Non-A, Non-B hepatitis, Posttransfusion hepatitis, Transfusion-associated hepatitis

Preface

This chapter is not intended to be a comprehensive review of the evolution of HCV but rather a personal vignette of how I saw the story from my vantage point at the NIH where much of the early story played out. The HCV story is historically and integrally related to the HBV story in that only by the ability to serologically or molecularly exclude HBV, and later HAV, was non-A, non-B hepatitis (NANBH) identified, setting the stage for the subsequent cloning of the NANBH agent and its renaming as HCV. I apologize for many omissions in this narrative, but the essential early history of HBV and HCV is chronicled herein, and perhaps the story is best told by one old enough to have been there. Sadly, many of the key early players are now deceased including Baruch Blumberg, Thomas London, Irving Millman, JS Dane, Palmer Beasley, Wolf Szmunes, Saul Krugman, and Hans Popper. I dedicate this chapter to their memory.

1 The Era of Observation Prior to Testing

Clinical observation, recurrent war, and serendipity have forged the approximate 2,000-year history of viral hepatitis. The original descriptions of hepatitis have been attributed to Hippocrates circa 425 BCE. He observed yellowing of the skin that he termed “ikterus” and hardening of the liver that he termed “kirros.” These observations antedated the germ theory of disease and could have had diverse etiologies but most likely were cases of hepatitis A and B related to contaminated water supplies and medical practices that involved percutaneous exposure with shared devices. The ancient nature of hepatitis viruses is also confirmed by the finding of HBV sequences in a sixteenth-century Korean mummy [1]. In the seventeenth and eighteenth centuries, many outbreaks of parenterally transmitted hepatitis were traced to contaminated vaccines for syphilis, smallpox, and other infectious agents of the time. Generally the vaccines were fortified with human plasma that was later proved to be contaminated, as in a well-documented outbreak among vaccinated shipyard workers in Bremen Germany in 1885 [2]. In essence, medical history from Hippocrates forward was marked by wartime outbreaks of hepatitis that became known as campaign jaundice and by injection-transmitted hepatitis traced to therapeutic or preventive measures that utilized pooled human plasma. A very well-characterized vaccine-induced outbreak was traced to contaminated lots of yellow fever vaccine during World War II [3]; 50,000 soldiers developed clinical hepatitis, and undoubtedly many fold that number were asymptotically infected. Retrospective seroepidemiology showed these cases to be caused by HBV [4]. The frequent and debilitating role of hepatitis during wartime fostered many studies primarily supported by the army. These studies clearly distinguished a short incubation, highly

infectious, and generally self-limited form of hepatitis that was designated hepatitis A and a more protracted form that was parenterally transmitted and designated hepatitis B [5]. These were superb epidemiologic studies but failed to identify either a causative agent or develop a specific assay for their detection. Early human volunteer studies added important pieces to the transmission of these two forms of hepatitis and to clinical outcomes but have come under ethical criticism because they employed prisoners or institutionalize children [6, 7]. These studies could not be performed under current patient protection mandates, but they did have institutional approval and participant or parent consent at the time they were performed. Studies performed at the Division of Biologic Standards, the forerunner of the FDA, utilized dilutions of hepatitis B infectious sera and defined the minimum infectious dose and the incubation period as related to dose showing that more diluted inocula had a longer incubation period [6]. Studies at the Willowbrook State School in NJ confirmed two epidemiologic forms of hepatitis and importantly identified a single patient (MS) who sequentially developed a short incubation form of hepatitis, designated MS-1, and a long incubation form, designated MS-2 [7]; these temporal characteristics were maintained when passaged to other study subjects. Years later when the Australia antigen was identified, it was shown that MS-1 was Australia antigen negative and MS-2 was Australia antigen positive and hence HBV related. It was also shown that MS-2 could be inactivated by boiling and induce protective antibody when fed to naïve subjects [8]. This was the first proof of principal for a hepatitis B vaccine.

Despite these many studies, the viruses that caused hepatitis A and B were never observed, and no test for their presence was developed. Diagnosis depended solely on epidemiology, clinical observation, and elevations of serum transaminase in temporal relationship to clinical presentation. This all changed by the serendipitous finding of the Australia antigen in the early 1960s [9] and the linking of Australia antigen to cases of hepatitis in 1967 [10].

2 The Australia Antigen Transformation

In the late 1950s and early 1960s, Baruch Blumberg, a geneticist working at NIH, performed studies that focused on protein polymorphisms in human subjects. He discovered polymorphic variations in beta-lipoproteins that were detected by Ouchterlony agar gel diffusion. In these studies, serum from a multiply transfused patient was arrayed against normal sera in a 7-well agar diffusion pattern. The underlying presumption was that multiply transfused subjects might develop antibodies against normal serum components antigenically different than their own. When these antibodies diffused into the agar, they would react with distinct and specific antigens diffusing in the opposite direction. The antigen-antibody reaction was characterized by a curved precipitin line that was then overlaid with a lipid stain (Sudan Black). A blue precipitin band was indicative of a lipoprotein polymorphism. Against this background, Harvey Alter was at NIH at the same time and using similar

Ouchterlony technology to search for protein differences that might be the cause of febrile or other transfusion-associated reactions. Dick Aster, also working in the NIH Blood Bank at that time, heard a lecture by Blumberg and reported back on the similarity between these research approaches. Within days, a collaboration was formed between the Blumberg and the Alter labs. The first element of serendipity in this story struck when Alter, while looking for additional beta-lipoprotein polymorphisms, detected a precipitin line that did not take up the lipid stain but rather turned red when a protein counterstain, azocarmine, was applied to the agar plate. This unique precipitin was found to represent an immune reaction between the serum of a multiply transfused hemophiliac and an Australian aborigine. The aborigines were one of many global populations whose sera were stored in Blumberg's serum bank for genetic studies. The significance of this finding, if indeed there was any, was unknown at the time. For a brief period, the unique antigen was called the "red antigen" for its staining characteristics, but then debate ensued as to whether to call it the Bethesda antigen for the place where it was discovered or the Australia antigen for the person in whom it was discovered. Blumberg decided on the latter terminology because it was consistent with the nomenclature for newly discovered hemoglobin polymorphisms; hence, the birth of the Australia antigen (Au).

In the next phase of investigations, we studied the prevalence of Au in healthy subjects and various NIH patient populations. Strikingly, it was found in only 0.1% of healthy donors, and in under 1% of most diseases tested, but in 10% of patients with leukemia. The first publication of this finding [9] stressed the association with leukemia and even speculated that this might be an antigen on a then postulated leukemia virus or represent the product of a gene that induced susceptibility to leukemia. There was no hint at that time (1965) that there was any relationship to hepatitis, but in retrospect the high prevalence in patients with leukemia reflected their high exposure to blood transfusion and their immune deficiency state that prevented clearance of the virus once infected. At this point in the story, Blumberg left NIH to head a research division at the Institute for Cancer Research in Fox Chase, Philadelphia. The rest of this early hepatitis virus history played out in Philadelphia. Blumberg, who was a geneticist and had a penchant for hypothesizing, believed that Au was genetically determined and predisposed individuals to leukemia. He thus initiated studies to test patients who had a known genetic predisposition to develop leukemia, namely, patients with Down's syndrome. In collaboration with Alton Sutnick and the late Tom London, institutionalized patients with Down's syndrome were tested, and strikingly, near 30% were found Au positive [11]. Although this supported the genetic hypothesis, much to the investigators' credit, they performed additional studies of Down's patients in different environmental settings. While the prevalence in large institutions for the mentally retarded approximated 30%, it was only 10% in smaller institutions, zero among Down's patients living at home and zero in newborns with Down's. This was inconsistent with the genetic hypothesis and the first clue that Au might be associated with an infectious disease. Thus, a failed hypothesis serendipitously led to a major insight in the Au story, namely, its link to an infectious disease. The third serendipitous event was that a technologist in the Blumberg lab, Barbara Werner, who had always served

as the Au-negative control came to work with classic symptoms of hepatitis and tested her own blood to find that she had seroconverted to Au positivity. This was a eureka moment that tied the Au story together and strongly suggested that Au was integrally linked to a hepatitis virus [10]. This was easily confirmed in subsequent studies of patients in various settings with and without hepatitis [11]. Subsequently, the late Fred Prince at the New York Blood Center confirmed the relationship to hepatitis and showed that Au was specifically linked to serum hepatitis (hepatitis B) and not to epidemic hepatitis A [12]. This led to a series of nomenclature revisions whereupon Au was sequentially called the SH antigen for serum hepatitis, the hepatitis-associated antigen (HAA), and finally the hepatitis B surface antigen (HBsAg) after it was shown to be a component of the viral envelop and not of other components of the virion. Studies by Bayer et al. in the Blumberg lab [13], Gerin and Purcell at NIH [14], and Dane at the Royal Free Hospital in London [15] showed that HBsAg was distributed on small circular and tubular particles that were in great abundance as compared to the whole virion which came to be known as the Dane particle. It was the great excess of non-virion antigen that made this agent detectable by a technique as insensitive as agar gel diffusion.

With the sudden availability of a serum marker for HBV, studies by Okochi in Japan [16] and Gocke in the USA [17, 18] unequivocally linked the Australia antigen to posttransfusion hepatitis B. Other studies used this new assay to measure prevalence and incidence among healthy and diseased populations throughout the world, to test disease associations, and to assess interventions to control or eradicate HBV transmission. Three studies are of particular note. In 1980, Szmuness et al. [19] tested the clinical efficacy of a plasma-derived HBV subunit vaccine developed by Maurice Hilleman at Merck. This vaccine was evaluated in 1,083 gay men in New York City where half received vaccine and half served as controls. Greater than 95% of susceptible vaccinees developed protective antibody to HBsAg, and the hepatitis attack rate in vaccine recipients was 3.2% compared to 25.6% in controls ($p < 0.0001$). Vaccine failures were presumed due to high-risk enrollees who were already incubating HBV infection at the time of vaccination. Indeed, in those who received the full course of the three-dose vaccine, efficacy was 100%. Although this vaccine had low uptake in the population because of fear of the then emerging AIDS epidemic, it served as proof that an HBV vaccine could be highly efficacious and stimulated the development of a recombinant vaccine that has become a universal vaccine in the USA and much of the developed and developing world. A second study of particular note was conducted by the late Palmer Beasley and coworkers in Taiwan [20] wherein they tested the value of hepatitis B immune globulin (HBIG) and the serum-derived HBV vaccine to prevent neonatal HBV transmission from highly infectious HBV e-antigen-positive mothers. In the absence of HBIG or vaccine, 90% of offspring were HBV infected and became HBsAg chronic carriers. In those who received three doses of HBIG alone or vaccine alone, the carrier rate was reduced to 23%, and in those who received the combination of HBIG and vaccine, only 5% became carriers; the 5% failure rate was presumed due to intra-uterine infection. The third critical study was also conducted by Beasley and coworkers [21] wherein they enrolled 22,707 Taiwanese government workers and

investigated the cause of death in those who were HBsAg positive or negative at the onset of the study. There were 105 deaths in the HBsAg-positive cohort of which 40 (38%) were attributed to hepatocellular carcinoma (HCC) and 17 (16%) to cirrhosis. In contrast, there were 202 deaths in the much larger cohort of HBsAg-negative subjects among whom only 1 died of HCC and 2 of cirrhosis. The relative risk of these fatal hepatitis B events was greater than 200-fold higher in those who were HBsAg positive. Michael Kew performed meticulous and comprehensive studies in Africa that confirmed the strong association between HBV infection and HCC [22].

One cannot overestimate the importance of the Australia antigen discovery as it led to the first diagnostic test for any hepatitis agent, the first specific viral marker for screening blood donors that dramatically reduced HBV transmission by blood transfusion, the first means to screen pregnant women and interdict perinatal HBV infection, and the basis for a first-generation hepatitis B vaccine that was 95% protective in clinical trials [16]. HBsAg also served as a link and predictive marker of hepatocellular carcinoma, the most prevalent form of liver cancer in Africa and Asia. The ability to prevent HBV infection with a virus-specific vaccine made this, in essence, the first cancer vaccine.

3 The Advent and Ascent of Non-A, Non-B Hepatitis: The Blood Transfusion Story

In 1965, Paul Holland, Paul Schmidt, and Bob Purcell initiated a prospective study of transfusion-associated hepatitis (TAH) among open heart surgery patients at the NIH Clinical Center. I became chief investigator in that study in 1970, and it has continued with some modifications to the present time. The basic study design was to obtain and store samples pre-transfusion and then every 1–2 weeks posttransfusion for 3 months followed by monthly samples for an additional 3 months. The retention of linked donor samples was added later. Since no specific viral markers were available at that time, hepatitis was diagnosed solely on the basis of ALT elevations that exceed 2.5 times the upper limit of normal (ULN) from 2 to 26 weeks posttransfusion followed by a second weekly sample that exceeded 2.0 times ULN. Patients with such elevations had additional sampling and were generally followed long-term.

The first major finding from these studies was that prior to 1970, open heart surgery patients at NIH had an astounding 30% incidence of TAH. This inordinate number was predicated on three factors, namely, the high volume of blood received (average 17 units per procedure), the prospective nature of the study which detected anicteric cases that would not have otherwise been reported, and the use of paid-donor blood. In an early and definitive analysis of this population, Walsh et al. [23] showed that patients who received at least one unit of paid-donor blood had a 51% incidence of TAH compared to only 7% in those who received only volunteer donor

blood. In 1970, based on the Walsh study and earlier published studies by John Allen [24], we adopted an all-volunteer donor system. Simultaneously, we initiated screening of blood donors for HBsAg using an unlicensed agar gel diffusion technology identical to that used in the discovery of the Australia antigen. This combined approach resulted in a dramatic 70% reduction in TAH incidence [25]. Indeed, no subsequent intervention has had as much impact on TAH, since the incidence was so high at the time. Although two variables were introduced at the same time, we could deduce that the primary factor in the massive reduction in hepatitis incidence was the introduction of an all-volunteer donor system. The source of blood proved to be the dominant factor in blood safety.

Assays for HBsAg became increasingly sensitive, and by 1973, a licensed enzyme immunoassay (EIA) was used to test stored samples from the periods before and after HBsAg screening. This revealed that even before HBsAg donor screening, no more than 30% of TAH was due to the hepatitis B virus [25], leaving open the causation of the observed non-B cases. In 1973, Feinstone, Kapikian, and Purcell at NIH [26] discovered the hepatitis A virus (HAV) using immune electron microscopy to test acute and chronic phase samples from an outbreak of hepatitis A. This method, while tedious, was accurate and sensitive, and we immediately sent samples from our non-B hepatitis cases to the Feinstone lab. Not a single non-B case was found to be HAV infected coincident with transfusion, suggesting that the main cause of TAH was a previously unknown virus or group of viruses. This resulted in the first publication to describe this previously unrecognized agent of transfusion-transmitted hepatitis [27]. We gave this new entity the nondescript name, non-A, non-B hepatitis (NANBH) rather than hepatitis C virus because we had not yet proven its viral nature nor the number of agents that might be involved.

Two important elements helped elucidate the nature of NANBH. First were transmission studies in chimpanzees. Inoculating samples from patients with acute and chronic NANBH and from implicated donors, the Alter and Purcell labs were able to routinely transmit infection to chimpanzees and then serially passage the infection in this model [28]. Tabor and coworkers at FDA [29], in parallel studies, also transmitted NANBH to chimpanzees. Infected chimpanzees were asymptomatic but developed ALT elevations in a pattern that closely mimicked human infection, and liver biopsies confirmed histologic evidence of hepatitis. Having this model, we were then fortunate to obtain an apheresis collection early in NANBH infection from a patient (WH) who was developing a severe case of icteric TAH. The Purcell lab then made dilutions of the WH plasma unit and used these to perform titration studies in chimpanzees. It was determined that WH plasma had an infectivity titer of $10^{6.5}$ chimpanzee infectious doses per milliliter. Interestingly, a decade later when PCR became available, we showed that the HCV titer of the WH sample was 10^7 and hence almost identical to the infectious titer in chimps. Having the titered NANB inoculum and the chimpanzee model allowed for further studies to characterize the agent. Steve Feinstone performed chloroform extraction of the WH inoculum, and in a carefully controlled study [30] that included a mock extraction, he was able to show that chloroform abrogated infectivity in the chimp indicating that the agent was enveloped and contained essential lipid in its membrane. Subsequently, Li-Fang He

in the Purcell lab [31] performed filtration studies wherein WH plasma was placed on filters of varying sizes and the filtrates tested for infectivity in the chimpanzee. This showed that the agent passed through a 50 nm filter, but not through a 30 nm filter. Thus, even before the agent was observed and before there was either an antigen or antibody test for specific identification, it could be deduced that the NANBH agent was small and lipid encapsulated. This narrowed the field of potential viral classes and, having ruled out any relation to HBV, was most consistent with NANBH being a small RNA virus in the alpha or flavivirus family or representing an entirely new class of viral agents. It is my recollection that Daniel Bradley at CDC was the first to suggest that the data were most consistent with the agent being a flavivirus, as it proved to be.

Not only was the precise nature of the virus obscure, but so too was its clinical significance. Because most cases were asymptomatic and identified only through prospective studies and since enzyme elevations in those cases were generally modest, there were some who considered NANBH a simple transaminitis of minor significance. The benignity of the disease was dispelled by a study conducted by the Clinical Center Liver Service. In this study, Berman et al. [32] performed liver biopsy on 39 patients with NANBH, most derived from our prospective study of TAH. While the majority of these patients had only mild to moderate hepatitis without significant fibrosis, 10% already had cirrhosis when first biopsied, and an additional 13% had what was then called chronic active hepatitis (CAH). When 20 patients were re-biopsied several years later, 5 more cases of cirrhosis had evolved such that the total with cirrhosis was 8 of 39 or 20%. Moreover, three of those with cirrhosis died of their liver disease and three others died of their underlying heart disease but also had severe liver disease as a cofounding event. This study and many others to follow [33–35] established NANBH as a generally mild disease but one that could progress to cirrhosis and ultimate fatality. Interestingly, the 20% rate of progression to cirrhosis has held up over the years, although current estimates with longer duration of follow-up are closer to 30–40%. Because of the vast number of persons with chronic HCV infection, estimated to be 350 million globally and 3 to 5 million in the USA, the disease burden is enormous, even if only 30–40% progress to dire outcomes. In the USA, HCV is the most common hepatitis infection, the most prevalent cause of end-stage liver disease, and the leading indication for liver transplantation. Despite the urgent need for a diagnostic and therapeutic breakthrough, up through the late 1980s, we remained without a specific diagnostic assay, without a visualized agent, and without therapy for chronic NANBH except for interferon, an arduous and toxic therapy that was only 10–20% effective at that time. All this changed with the unexpected cloning of the NANBH/HCV agent in 1989 [36] and the subsequent development of sensitive serologic and molecular assays and the evolution of drugs that sequentially have seen sustained virologic response rates, tantamount to cure, that exceed 95%.

4 The Cloning of HCV

From 1975, when NANBH was first identified as a clinical entity, through 1989 when the agent was cloned by Houghton and coworkers at Chiron [36], multiple efforts in the USA, Europe, and Japan to identify a specific antigen or antibody and hence to develop a serologic assay were unsuccessful, demonstrating how difficult it is to identify one component of a serologic reaction in the absence of the other. Further, molecular detection was not possible until the advent of PCR and advances in molecular technology and, as we later learned, was further limited by the generally low titer of the NANBH agent. In the 1980s, molecular biology was in its infancy, and techniques that are simple and routine today were state of the art at that time. The quest for the NANBH agent was a black box, a seemingly insoluble equation because none of the variables were known. From 1975 to 1985, multiple laboratories in the USA, Europe, and Japan attacked this conundrum, but none were able to solve the riddle as evidenced by failure to break the code on a well-characterized NANBH panel. Into this void entered the Chiron Corporation that unbeknownst to the general hepatitis community worked for 6 years to blindly clone the NANBH agent. The Chiron team led by Michael Houghton, Qui-Lim Choo, George Kuo, and Amy Weiner in collaboration with Daniel Bradley at CDC embarked on this arduous path to discovery that hinged on three critical elements. First, Bradley, in meticulously designed studies, extensively characterized infectious NANBH inocula in the chimpanzee model [37, 38]. These samples were titered, serially passaged, collected in relatively large volumes, and made available to Chiron for their cloning studies. The starting point was to pellet the source material, extract RNA, and then reverse transcribe to cDNA. The second key element of the study was to use a phage gt-11 expression vector such that genetic information in cDNA fragments would be expressed as protein when the phage infected *E. coli*. The third critical element of study design was to assume that patients with resolved or chronic NANBH would have circulating antibody to the virus even though no such antibody had been detected in the preceding decade. The fourth key element of this endeavor was perseverance, because success was slow in coming, and corporate leadership began to question the soundness of their investment. The Houghton team persisted despite sometimes demoralizing setbacks, and it has been said by the late Lacy Overby, another collaborator, that six million clones were screened with presumed antibody before there was a single positive reaction. This single reactive clone was then subcloned and the contained nucleic acid sequenced. A short genomic segment was characterized, and subsequent cloning allowed the investigators to “walk” the genome and express an antigen that could serve as a target for antibody screening [39]. A prototype antibody assay was developed, principally by Kuo [40], and was ready to be challenged by the NANBH panel held at the Alter lab. This small panel consisted of NANBH samples from patients and donors that had proven infectious in the chimpanzee and control samples from healthy donors whose blood had been transfused to at least ten recipients without being implicated in hepatitis transmission. Importantly, all samples in the panel were present in duplicate, and duplicates

were placed in random positions. Although 19 other purported NANB virus assays had failed this panel, the Chiron assay detected antibody in all known chronic NANBH carriers and, importantly, failed to detect antibody in 14 samples from 7 pedigreed donor controls. Samples from two patients with acute NANBH were missed, but that was because antibody had not yet developed; subsequent samples from these patients demonstrated antibody seroconversion. Thus, in this small but difficult panel, the Chiron assay had perfect sensitivity and specificity. The specificity of the assay for the agent of NANBH was further validated by testing cases and controls in the NIH prospective cohort wherein it became clear that this assay had it been applied to routine donor screening could have prevented 80% of TAH [41]. Analysis of a second-generation antibody assay introduced in 1992 predicted the prevention of 88% of TAH cases in the NIH cohort. Hence, 1990 introduced the first specific assay for the NANBH agent and a suitable test for blood donor screening, as well as a diagnostic assay to evaluate hepatitis cases and to screen populations. The non-A, non-B virus was renamed the hepatitis C virus (HCV) and 1990 ushered in the age of HCV.

Following this breakthrough, Chiron investigators sequenced the entire genome and showed that it coded for a polypeptide that was then posttranslationally cleaved into structural and nonstructural units. Using other flaviviruses as a model, they and other investigators identified genomic regions with enzymatic functions critical to viral replication [39]. These regions, including NS3, NS4, NS5A, and NS5B, have become targets of highly efficacious inhibitors that completely block viral replication as will be described in subsequent chapters of this book.

5 The Virtual Eradication of Transfusion-Associated Hepatitis

As described above, the most important measure in the prevention of TAH was the prohibition of paid-donor blood [23]. Those who sold their blood, particularly prior to 1970, often came from derelict populations where abusive alcohol and drug use and other high-risk behaviors were prevalent. Further, such individuals donated as frequently as possible, which could be weekly if they were selling plasma rather than whole blood. Hence, a single hepatitis-carrier donor could inflict major damage to multiple recipients with no viral screening assays in place to interdict this practice. As indicated above, the prohibition of paid donors at the NIH Clinical Center in 1970 was primarily responsible for the dramatic decline in TAH incidence from 30 to 10% [25]. By 1971, all US blood establishments adopted an all-volunteer donor system under mandate from the FDA. In 1973, improved enzyme immunoassays for HBsAg entered the market and caused a further decline in HBV transmission to very low levels. However, the absence of a test for non-A, non-B hepatitis kept total TAH incidence at around 6% in the NIH prospective study [42]. A retrospective analyses of the NIH cohort predicted that ALT testing of blood donors might affect a 30%

decline in hepatitis transmission [43]. Similar predictions came from a multicenter prospective study (Transfusion-Transmitted Virus Study, TTVS) that was supported by the National Heart Lung and Blood Institute (NHLBI) [44]. Hence, in 1981, we and a few other hospitals introduced routine donor ALT testing, but disappointingly ongoing studies did not show a benefit of such testing. We next anticipated that testing for HIV, which was introduced in 1985, would indirectly reduce TAH incidence because HIV-infected patients were frequently coinfecting with hepatitis viruses. We did not observe the anticipated collateral benefit of HIV testing because HBV blood transmission was already well controlled and because the primary victims of the early HIV epidemic were men who had sex with men and NANBH was not prevalent in that population until sexual promiscuity was later compounded by intravenous drug use. It was the use of shared needles that gave rise to the HCV epidemic, not promiscuous sexual activity. Thus by 1986, TAH incidence continued to hover around 6%. At that time another retrospective analysis by the TTVS and NIH groups [45, 46] indicated that using antibody to hepatitis B core antigen (anti-HBc) as a surrogate for NANBH might affect a 30–40% reduction in TAH. Indeed that was the case when we introduced this test as a donor screen in 1986 and when it was FDA mandated in 1987. After anti-HBc screening, TAH incidence in the NIH prospective study fell to 4%. On that background, HCV was cloned in 1989 and a first-generation commercial anti-HCV assay introduced into blood screening in 1990; an improved second-generation assay was introduced in 1992. It was routine HCV testing that broke through the resistant wall of TAH, and by 1997, the NIH prospective study demonstrated the virtual eradication of TAH [42]. We saw no further cases of HCV transmission and no cases of the then postulated non-A, non-B, non-C hepatitis. While the NIH prospective study is too small to claim eradication, the extent of transfusion transmission is now so low that it has to be estimated mathematically. It has been estimated that the current risk of transfusion-transmitted HCV is approximately 1:2,000,000 [47]. HBV transmission has also been dramatically reduced. It is my current contention that there is no specific non-A, non-B, non-C hepatitis agent and that those reported cases represented surgery-related inflammation, drug toxicity, or nonalcoholic fatty liver disease (NAFLD)/steatohepatitis (NASH). Hence, in three decades, TAH incidence declined from approximately 30% to virtual zero, a triumph of a series of donor interventions and the introduction of increasingly specific and sensitive assays for HBV and HCV. This triumph is another important piece of the HCV story.

6 The End of the Beginning and the Beginning of the End

We are clearly at the “end of the beginning” of the HCV saga. Transfusion-associated hepatitis has been virtually eradicated; excellent population screening assays are in place as are sensitive methods to detect HCV RNA and to separate chronic carriers from those who spontaneously or therapeutically cleared the infection. As described in this book, amazing therapies have been developed that could

not have been imagined only a decade ago. It is now possible to cure 98% of HCV carriers, even if they have already progressed to cirrhosis [48]. Viral clearance has been shown to halt fibrosis progression and, in some cases, to induce fibrosis regression [49]. In those who achieve a sustained virologic response that is tantamount to cure, progression to hepatocellular carcinoma is markedly diminished [50], though not totally prevented because cancerous transformation had already been initiated at the time of virologic cure. In only four decades since the first recognition of non-A, non-B hepatitis, it is possible to envision the near eradication of HCV infection even in the absence of an HCV vaccine. In theory, from this day forward, no one identified with HCV infection should succumb to its long-term sequelae of cirrhosis, HCC, and end-stage liver disease. However, this optimistic projection is marred by several impediments to eradication. First, the CDC estimates that only half of HCV-infected individuals are aware of their infection, and hence there is a vast pool of infected individuals who might never be treated or who might not be identified until they present with severe liver disease. Eradication of HCV will depend on large-scale antibody screening of all populations at high risk and possibly even those without identified risk. The CDC has identified the birth cohort of 1945–1965, the Baby Boomers, as a fertile source to detect silent carriers, but this is not sufficient to detect the majority of infected individuals. I would suggest that every person seeking medical care in emergency rooms, outpatient clinics, hospital admissions or through their personal physicians of any specialty should have their HCV status identified and any true positives referred for treatment or close evaluation. The same would be true for those incarcerated or otherwise institutionalized. Testing could also be routine upon entry to college or vocational schools and is, I believe, already mandatory in the military service. While these measures would still not capture those who do not seek medical care, higher education, or military service, it would capture a large number of currently unidentified carriers and would be well worth the cost of testing.

Nonetheless, testing is only fully meaningful if it is the first measure on the path to curative therapy. Thus, the second major impediment to HCV eradication in the USA is access to care. Currently, many persons already identified as HCV carriers have not been treated because the cost of treatment is so high that is beyond the bounds of most individual health budgets and is not covered by many insurance companies. Many patients have thus far been treated in clinical trials and compassionate use protocols, but this is the minority, and some balance must be reached between industry, insurance companies, and the government to find a middle ground that assures reasonable, but not usurious, profits and wide access to treatment even among the most indigent and those whose habits have put them at risk. The treatment of intravenous drug users, for example, is a strong public health measure because every carrier taken out of a needle-sharing population diminishes spread within that population, a community which is now the primary incubator of new HCV infections. Since new treatments are simple and with few side effects or drug interactions, they can be administered not only by hepatologists, gastroenterologists, and infectious disease specialists but also by general practitioners, nurses, and nonphysician support staff [51]. Hence, if drugs were available at affordable and reimbursable

cost, there would be no lack of medical personnel to administer and oversee treatment.

Thus, in the USA and most developed nations, the primary impediments to the potential for HCV eradication are the need to identify the large mass of silent carriers and then to triage them into treatment programs that are not limited by cost. This is a tall order, but not impossible if there is a collective will to do so. A universal HCV vaccine would be the long-term solution, but as with HIV, vaccine development has been hindered by the quasispecies nature of the virus and the failure of vaccines developed to date to induce broadly protective neutralizing antibodies or adequate T-cell responses. If such a vaccine were to be developed and proven safe and efficacious in clinical trials, it would be at least a decade before it was available for mass vaccination. Hence, the current strategy is to “test and treat,” and both parts of that equation must be expanded dramatically.

The dilemma of HCV treatment is greatly compounded in developing nations where the routes of HCV spread are multifactorial, where access to care of any kind is limited, and where financial constraints to treatment are maximized. Thus, global eradication of HCV in the absence of vaccine will require strategies to change medical practice to eliminate the reuse of needles and multidose vials and syringes, cultural changes in practices of scarification, tattooing and ritual surgery, and the infusion of HCV therapeutics and financial resources from world health communities, resource-rich governments, private philanthropy, and industry. The PEPFAR program for HIV surveillance and treatment could serve as proven model.

So the end is in sight, though still far down the pike, but clearly we are at the beginning of the end, and it is the remarkable recent advances in HCV therapeutics that have made this vision possible.

Compliance with Ethical Standards

Ethical Statement: All patient studies described herein were performed under NIH IRB approved protocols with appropriate informed consent.

Chimpanzee studies were approved by the animal use committees of the Southwest Foundation for Biomedical Research, San Antonio Texas or the NIH, Intramural program.

References

1. Bar-Gal GK, Kim MJ, Klein A et al (2012) Tracing hepatitis B to the 16th century in a Korean mummy. *Hepatology* 56:1671–1680
2. Lurman A (1885) Eine Icterus-epidemie. *Berl Klin Wochenschr* 22:2023
3. Editorial (1942) Jaundice following yellow fever immunization. *JAMA* 119:1110
4. Seeff LB, Beebe GW, Hoofnagle JH (1987) A serological follow-up of the 1942 epidemic of post-vaccination hepatitis in the United States Army. *N Engl J Med* 316:965–970
5. Paul JR, Havens WP, Sabin AB et al (1945) Transmission experiments in serum jaundice and infectious hepatitis. *JAMA* 128:911–915
6. Barker LF, Shulman NR, Murray R et al (1970) Transmission of serum hepatitis. *JAMA* 211:1509–1512
7. Krugman S, Giles JP, Hammonds J (1967) Infectious hepatitis: evidence for two distinctive clinical, epidemiological and immunological types of infection. *JAMA* 200:365

8. Krugman S, Giles JP, Hammond J (1971) Viral hepatitis, type B (MS-2 strain): studies on active immunization. *JAMA* 217:41–45
9. Blumberg BS, Alter HJ, Visnich S (1965) A “new” antigen in leukemia sera. *JAMA* 191:541–546
10. Blumberg BS, Gerstley BJS, Hungerford DA et al (1967) A serum antigen (Australia antigen) in Down’s syndrome, leukemia and hepatitis. *Ann Intern Med* 66:924–931
11. Sutnick AI, London WT, Bayer M et al (1968) Anicteric hepatitis associated with Australia antigen; occurrence in patients with Down’s syndrome. *JAMA* 205:670–674
12. Prince AM (1968) An antigen detected in the blood during the incubation period of serum hepatitis. *Proc Natl Acad Sci* 60:814–821
13. Bayer ME, Blumberg BS, Werner B (1968) Particles associated with Australia antigen in the sera of patients with leukemia, Down’s syndrome and hepatitis. *Nature* 218:1057–1059
14. Gerin JL, Purcell RH, Hoggan MD et al (1969) Biophysical properties of Australia antigen. *J Virol* 4:763–768
15. Dane OS, Cameron CH, Briggs M (1970) Virus-like particles in serum of patients with Australia antigen-associated hepatitis. *Lancet* 1:695–698
16. Okochi K, Murakami S (1968) Observations on Australia antigen in Japanese. *Vox Sang* 15:374–385
17. Gocke DJ, Greenberg HB, Kavey NB (1970) Correlation of Australia antigen with posttransfusion hepatitis. *JAMA* 212:877–879
18. Gocke DJ, Kavey NB (1969) Hepatitis antigen: correlation with disease and infectivity of blood donors. *Lancet* 2:1055–1059
19. Szmunes W, Stevens CE, Harley EJ et al (1980) Hepatitis B vaccine: demonstration of efficacy in a controlled clinical trial in a high risk population in the United States. *N Engl J Med* 303:833–841
20. Beasley RP, Hwang L-Y, Lee GC-Y et al (1983) Prevention of perinatally transmitted hepatitis B virus infections with hepatitis B immune globulin and hepatitis B vaccine. *Lancet* 2:1099–1102
21. Beasley RP, Hwang L-Y, Lin C-C et al (1981) Hepatocellular carcinoma and hepatitis B virus: a prospective study of 22,707 men in Taiwan. *Lancet* 2i:1006–1008
22. Kew MC, Rossouw E, Hodgkinson J et al (1983) Hepatitis B virus status of southern African Blacks with hepatocellular carcinoma: comparison between rural and urban patients. *Hepatology* 3:65–68
23. Walsh JH, Purcell RH, Morrow AG et al (1970) Posttransfusion hepatitis after open-heart operations: incidence after the administration of blood from commercial and volunteer donor populations. *JAMA* 211:261–265
24. Allen JG (1970) Commercially obtained blood and serum hepatitis. *Surg Gynecol Obstet* 131:277–281
25. Alter HJ, Holland PV, Purcell RH et al (1972) Posttransfusion hepatitis after exclusion of the commercial and hepatitis B antigen positive donor. *Ann Intern Med* 77:691–699
26. Feinstone SM, Kapikian AZ, Purcell RH (1973) Hepatitis A: detection by immune electron microscopy of a virus-like antigen associated with acute illness. *Science* 182:1026–1028
27. Feinstone SM, Kapikian AZ, Purcell RH et al (1975) Transfusion-associated hepatitis not due to viral hepatitis type A or B. *N Engl J Med* 292:767–770
28. Alter HJ, Purcell RH, Holland PV et al (1978) Transmissible agent in “non-A, non-B” hepatitis. *Lancet* 1:459–463
29. Tabor E, Gerety RJ, Drucker JA et al (1978) Transmission on non-A, non-B hepatitis from man to chimpanzee. *Lancet* 1:463–466
30. Feinstone JM, Mihalik KB, Kamimura J et al (1983) Inactivation of hepatitis B virus and non-A, non-B virus by chloroform. *Infect Immun* 4:816–821
31. He L-F, Alling DW, Popkin TJ et al (1987) Determining the size of non-A, non-B hepatitis virus by filtration. *J Infect Dis* 156:636–640

32. Berman MD, Alter HJ, Ishak KG et al (1979) The chronic sequelae of non-A, non-B hepatitis. *Ann Intern Med* 91:1–6
33. Rakela J, Redeker AG (1979) Chronic liver disease after acute non-A, non-B viral hepatitis. *Gastroenterology* 77:1200–1202
34. Realdi G, Alberti A, Ruggi M et al (1982) Long-term follow-up of acute and chronic non-A, non-B post-transfusion hepatitis: evidence of progression to liver cirrhosis. *Gut* 23:270–275
35. Ghany MG, Kleiner DE, Alter HJ et al (2003) Progression of fibrosis in chronic hepatitis C. *Gastroenterology* 124:97–104
36. Choo Q-L, Kuo G, Weiner AJ et al (1989) Isolation of a cDNA clone derived from a blood-borne non-A, non-B viral hepatitis genome. *Science* 244:359–362
37. Bradley DW, Cook EH, Maynard JE et al (1979) Experimental infection of chimpanzees with antihemophilic (factor VIII) materials: recovery of virus like particles associated with non-A, non-B hepatitis. *J Med Virol* 3:253–269
38. Bradley DW, McCaustland KA, Cook EH et al (1985) Post-transfusion non-A, non-B hepatitis in chimpanzees: physicochemical evidence that the tubular forming agent is a small enveloped virus. *Gastroenterology* 88:773–779
39. Kuo G, Choo Q, Alter HJ et al (1989) An assay for circulating antibodies to a major etiologic virus of human non-A, non-B hepatitis. *Science* 244:362–364
40. Alter HJ, Purcell RH, Shih JW et al (1989) Detection of antibody to hepatitis C virus in prospectively followed transfusion recipients with acute and chronic non-A, non-B hepatitis. *New Engl J Med* 321:1494–1500
41. Alter HJ, Houghton M (2000) Hepatitis C virus and eliminating post-transfusion hepatitis. *Nat Med* 6:1082–1086
42. Alter HJ, Purcell RH, Holland PV et al (1981) The relationship of donor transaminase (ALT) to recipient hepatitis: impact on blood transfusion services. *JAMA* 246:630–634
43. Aach RD, Szmunn W, Mosley JW (1981) Serum alanine amino transferase of donors in relation to the risk of non-A, non-B hepatitis in recipients: the transfusion-transmitted viruses study. *N Engl J Med* 304:989–994
44. Stevens CE, Aach RD, Hollinger FB (1984) Hepatitis B virus antibody in blood donors and the occurrence of non-A, non-B hepatitis in transfusion recipients; an analysis of the transfusion-transmitted virus study. *Ann Intern Med* 101:733–738
45. Koziol DE, Holland PV, Alling DW et al (1986) Antibody to hepatitis B Core antigen as a paradoxical marker for non-A, non-B hepatitis agents in donated blood. *Ann Intern Med* 104:488–495
46. Dodd RY, Notari EP, Stramer SL (2002) Current prevalence and incidence of infectious disease markers and estimated window period risk in the American Rd cross blood donor population. *Transfusion* 42:975–979
47. Feld JJ, Jacobson IM, Hezode C et al (2015) Sofosbuvir and velpatasvir for HCV genotype 1,2,4, 5 and 6 infection. *N Engl J Med* 373:2599–2607
48. Casado JL, Esteban MA, Banon S (2015) Fibrosis regression explains differences in outcome in HIV-HCV coinfecting patients with cirrhosis after sustained virologic response. *Dig Dis Sci* 60:3473–3481
49. Morgan RL, Baack B, Smith BD et al (2013) Eradication of hepatitis C virus infection and the development of hepatocellular carcinoma: a meta-analysis of observational studies. *Ann Intern Med* 158:329–337
50. Kattakuzhy S, Gross C, Emmanuel B et al (2017) Expansion of treatment for hepatitis C virus infection by task shifting to community-based nonspecialist providers: a nonrandomized clinical trial. *Ann Intern Med* 167:311–318

The Discovery of the Hepatitis C Virus



Michael Houghton

Contents

1	Introduction	20
2	NANBH	20
3	1982–1986: Dead Ends	21
4	1985–1986: Getting Warmer	22
5	Very Hot!	23
6	What’s Next?	25
	References	26

Abstract After a 6-year intensive search for the causative agent of parenteral non-A, non-B hepatitis using a large variety of pre-PCR molecular biological, immunological, and virological methods, HCV was discovered using a cDNA immunoscreening method in which infectious chimpanzee plasma was used as the source of cloning material and NANBH patient sera as a presumptive source of NANBH-specific antibodies. Clone 5-1-1 and overlapping clones were shown to be extrachromosomal in origin, to be derived from a large single-stranded RNA found only in NANBH materials and which directly encoded an antigen shown to specifically bind antibodies in most parenteral NANBH-infected chimpanzees and patients. The nucleotide sequence of the RNA genome exhibited low homology with flaviviruses which in combination proved that HCV was the major cause of blood-borne NANBH and that it was a distant relative of the *Flaviviridae* family. Since 1990, a series of HCV-specific antibody- and RNA-detecting blood screening tests have effectively eliminated posttransfusion HCV infections. Subsequent decades of research by the field into the viral life cycle and the development of direct-acting antivirals have now led to HCV becoming the first curable, chronically infecting virus of man. It is now important to focus on a prophylactic vaccine to curtail this global epidemic.

M. Houghton (✉)

Li Ka Shing Institute of Virology, Department of Medical Microbiology and Immunology,
University of Alberta, Edmonton, AB, Canada
e-mail: michael.houghton@ualberta.ca

Keywords Blood-borne NANBH, Flaviviridae, HCV, HCV blood tests, HCV discovery, HCV identification, Hepatitis C virus, Non-A, non-B hepatitis

1 Introduction

It is now exactly 30 years ago when I first announced that a group of us from the Chiron Corporation in California in collaboration with the CDC had identified hepatitis C virus (HCV) for the first time and that it was distantly related to the flaviviruses. The history leading up to this discovery now follows (see [1–4] for earlier accounts) as part of this volume detailing the successful development of HCV direct-acting antivirals (DAAs) that can now cure most patients within 1–3 months of oral therapy.

My own work on HCV or non-A, non-B hepatitis (NANBH) as it was then known began in 1982 when I joined the Chiron Corporation shortly after its start-up as a biotechnology company by the University of California Professors, Bill Rutter and Ed Penhoet. Emigrating from the UK where I worked on characterizing the human fibroblast interferon gene using the newly evolved recombinant DNA technologies, I intended originally to study artificial chimeric interferons and to explore the existence of possible epithelial interferons (now known as the lambda interferons which are important in the mucosal antiviral response). However, Dino Dina (Virology Head) and Bill Rutter suggested that I may be interested to focus my laboratory on trying to identify the etiological cause of NANBH which would match my prior experience in studying rare interferon mRNAs. I readily accepted this formidable challenge little realizing that it would take 6 years before achieving success, a very long time in the rapidly evolving California biotechnology industry.

2 NANBH

The existence of NANBH first came to light in 1974 when Fred Prince and colleagues showed that unexpectedly, most transfusion-associated cases of hepatitis were not due to HBV [5]. This was then followed by a paper from Steve Feinstone and colleagues at the NIH showing that most transfusion-associated NANBH was not due to either HAV or HBV [6]. Thus began a 15 year search by the field for the elusive infectious agent causing parenteral, blood-borne NANBH. Unfortunately, methods used successfully to identify HBV and then HAV were not successful at identifying HCV, which we now know was due to the much lower viral titers of HCV and to the absence of the identification of any NANBH-specific viral morphology, antigen, or antibody and the absence of cell culture propagation methods. Such methods had led to the successive discoveries of HBV and HAV and later, HIV [7–9]. When I started searching for HCV in 1982, it had been shown by Harvey Alter of the NIH and separately by the transfusion-transmitted viruses study (TTVS) group

that NANBH persisted as chronic hepatitis with alternating flares of liver damage [10, 11]. Later, Miriam Alter of the CDC showed evidence for sporadic NANBH occurring in the absence of obvious parenteral transmission (now known to be due to prior intravenous drug use [12]). Dan Bradley of the CDC had been leading one of the several groups showing that human NANBH could be transmitted and serially passaged in the common chimpanzee, *Pan troglodytes* [13]. Using this animal model (which remains to this day as the only reliable immunocompetent animal model for HCV infection), he then went on to show good evidence for the existence of two distinct NANBH agents [14], one sensitive to organic solvents (and therefore presumably lipid-enveloped) causing extensive proliferation of the endoplasmic reticulum in chimpanzee hepatocytes (earlier termed the “tubule-forming agent (TFA)” by Yoko Shimizu and colleagues [15]) and the other a solvent-resistant agent. Dan Bradley also showed in 1985 that the TFA could be filtered through a 80 nm pore-sized filter which together with the observed proliferation of the endoplasmic reticulum typical of RNA viruses in cell cultures, prompted him to suggest that the TFA may be a small enveloped RNA virus such as a member of the *Togaviridae* or *Flaviviridae* [16]. Later, Bob Purcell’s lab showed that the TFA could not pass through a 50 nm filter consistent with it being either toga- or flavi-like or a new viral agent [17].

3 1982–1986: Dead Ends

Work in my own laboratory at Chiron started off working with samples from Tatsuo Miyamura of the Japanese NIH who spent a year in my lab and brought autopsied liver samples from Japanese NANBH patients. Other colleagues in my laboratory then and over the next many years were Qui-Lim Choo and Amy Weiner along with Kansheng Wang, as well as valuable mentorship from Dr. Lacy Overby who had previously pioneered Abbott laboratories’ HAV and HBV diagnostics unit. Unfortunately, we soon realized that the quality of liver mRNA derived from autopsies was poor and far from ideal. Seeking to collaborate with a laboratory expert in the chimpanzee model so as to access fresh and intact biological samples, Bill Rutter and I then made a visit to the CDC in Phoenix to propose a collaboration with Dan Bradley to identify the elusive etiology of blood-borne NANBH using recombinant DNA and allied methodologies. The CDC readily agreed, and over the next 6 years, I received a constant supply of liver biopsy and blood samples from Dan Bradley’s NANBH-infected chimpanzees.

Initially, we went on a long fishing expedition isolating bacterially cloned cDNAs derived from liver poly-A⁺-mRNAs specific to NANBH-infected chimpanzee livers and absent in control, NANBH-uninfected livers. This work preceded the discovery of the powerful PCR amplification methodologies that did not become routine for interrogating mRNA/cDNA until the late 1980s. While successful at identifying many upregulated mRNAs (and downregulated ones also), we showed that all of them were derived from the host chimpanzee DNA genome and not from any

potential NANBH viral DNA or RNA genome. Attempts to use hybridization probes derived from the genomes of hepadnaviruses, picornaviruses, flaviviruses, pestiviruses, and togaviruses all failed. Prolonged attempts to grow the virus in tissue culture also proved fruitless (we now know because only one strain of HCV, the JFH-1 strain of Dr. Takaji Wakita, can grow efficiently in human hepatoma cell lines [18]). Brave efforts by Amy Weiner in trying to visualize a putative large NANBH RNA or DNA genome on agarose gels from highly concentrated plasma extracts also proved fruitless. Spurred on by data from Bob Purcell's NIH laboratory that the delta hepatitis agent may be related to HCV, I collaborated with John Gerin's laboratory at the NIH, and we succeeded in showing that this agent comprised a most interesting plant viroid-like RNA genome [19]. Unfortunately, attempts to use what we now called the hepatitis D virus (HDV) genome as a hybridization probe for HCV did not work [20]. We now know HCV is a very different agent from HDV. Many other attempts using other experimental approaches also failed.

4 1985–1986: Getting Warmer

Now back in Japan, Yohko Shimizu identified a monoclonal antibody that bound specifically to an antigen in NANBH-infected chimpanzee livers and not in control tissues [21]. Following her pioneering work, another Chiron colleague attempted to identify our own Mabs, but this proved highly difficult. We also received Yohko Shimizu's antibody and tried to identify its target antigen by immunoscreening bacterial cDNA expression libraries derived from NANBH-infected chimpanzee livers. However, as was often the case with this immunoscreening approach, neither we nor Dr. Shimizu's laboratory could isolate the target antigen using this method (later found by her to be a host protein following affinity purification and protein sequencing). Back in 1983 and 1984, I had discussed with Dino Dina and experts in cDNA immunoscreening the possibility of performing this method using NANBH patient sera as a presumptive source of HCV-specific antibodies. However, knowing that NANBH was highly persistent, possibly implying a poor immune response as was known to be the case in chronic persistent HBV infections, and knowing that even with well-characterized antisera or monoclonal antibodies this method often failed, I considered the approach too risky. Meanwhile, after several years of failing to identify HCV, we requested that Dan Bradley try to provide us with chimpanzee materials of at least equal infectivity titer to those identified earlier by other groups in the USA and Japan who had identified human and chimpanzee blood of 10^5 – $10^{6.5}$ chimp infectious doses per mL (CID/mL) several years before [22, 23]. There followed a CDC/Chiron co-funded program performed in Dan Bradley's CDC facility which resulted in the identification of large volumes of chimpanzee plasma of 10^5 (chimp Don) and 10^6 (chimp Rodney) CID/mL being available to us in 1985 along with liver samples of similar CID/g tissue.

Meanwhile in 1985, in discussing the Shimizu-type monoclonal antibody approaches with George Kuo, my next door neighbor at Chiron who worked on

human Factor VIII and TNF-alpha, he enthusiastically suggested immunoscreening cDNA expression libraries with NANBH patient sera as a presumptive source of viral antibodies. He argued that NANBH-specific antigen in such bacterial clones would likely be of a very high concentration and capable of binding and detecting any NANBH-specific antibody that was present in patient sera, thus facilitating identification of its target NANBH viral cDNA (indeed, knowing the approximate NANBH viral titers in the CDC's chimpanzee liver samples enabled us to conclude that NANBH antigen levels in hepatocytes would likely be below the level required for conventional detection of specific antibodies using thin liver sections as the target antigens, thus possibly explaining why the existence of NANBH antibodies had not been demonstrated to date). Shortly afterward, Dan Bradley also suggested using this cDNA immunoscreening approach and was embarking on it with a competing company (only for it to be eventually discontinued there as having a low probability of success as indeed many of our own internal and external experts opined).

Largely as a result of the discussion with George, I decided to include this approach in our ongoing search for the NANBH agent. Initially, I extracted poly-A⁺ from liver biopsy samples from four of Dan Bradley's chimpanzees all harvested deliberately at different points in the acute phase of NANBH infection so as to maximize the chance of having some actual HCV mRNA present. After conversion into cDNA, I cloned the mixture into the bacteriophage cDNA expression vector, lambda gt11. George tested various published detection methods for identifying cDNA clones by expression screening and concluded that the use of an I¹²⁵-radiolabelled anti-human/chimpanzee Ig would offer optimal detection sensitivity. Qui-Lim Choo then successfully validated the resulting cDNA library using antibodies specific to the rare liver proteins superoxide dismutase and alpha1 antitrypsin. However, when he screened this library with sera from NANBH humans and chimps, no HCV clones could be identified. I next made a cDNA library from the CDC's chimpanzee Rodney (#910) plasma of 10⁶ CID/mL, but again, Qui-Lim Choo could not identify any HCV clones using NANBH patient sera as a screening tool. We next applied this method to a model viral system, that of HDV, a genome that was far more abundant than HCV and one that we had recently shown possessed a plant viroid-like RNA genome [19]. I prepared a random-primed cDNA library derived from HDV chimpanzee plasma from which Kangsheng Wang and Qui-Lim Choo readily identified numerous HDV viral clones using serum from a HDV-infected individual as a source of antibodies. Adjusting for the large difference in chimp infectivity titer between HDV (>10¹¹) and HCV (10⁶) plasma, I was able to calculate that we were just within the limits of sensitivity for detecting HCV clones using this technique.

5 Very Hot!

This led to another try in which I cloned both RNA and DNA from chimp Rodney plasma into the lambda gt11 cDNA expression vector, and then Qui-Lim Choo and I decided that we should screen it using serum from a patient with chronic NANBH

that had unusually high liver damage (reflected in very high serum aminotransferase levels). Previously we had tended to use NANBH sera obtained after the acute phase of infection when serum aminotransferase levels had normalized possibly indicating convalescence as a result of strong protective immune responses (we now know that the titer of HCV antibodies tend to be higher in chronic NANBH infections as compared with acute, resolved infections). Qui-Lim identified about six positive clones from this screening, some of which he showed were derived from the chimpanzee genome and some from the small amounts of carrier MS2 bacteriophage RNA that I had needed to add to the plasma extraction. One small clone remained named 5-1-1 by Qui-Lim. Whatever it was, it encoded an antigen that was clearly detectable using sera from NANBH patients (8/12 were positive) and not from control humans (0/10 positive). *So far so good!* To test whether it was derived from the chimpanzee genome, we pulled out a larger overlapping clone (81) with which we could perform a sensitive Southern blot analysis of the chimp and human genome (it's important to note that powerful PCR amplification methods were not in routine use by this time). While we could easily detect hybridization of the single-copy human fibroblast interferon gene to host DNA, clone 81 showed no hybridization whatsoever. Pinching ourselves to believe that finally this clone could really be derived from HCV, we next investigated if we could detect *seroconversion* to the 5-1-1 antigen in cases of human posttransfusion NANBH and in chimps infected by Dan Bradley with HAV, HBV, or NANBH. Unbelievably, we only saw seroconversion to anti-5-1-1 following NANBH infection not in preinfection samples! Critical concurrent experiments showed that clone 81 hybridized to a large RNA molecule of ~10,000 nucleotides on Northern blots and that this RNA was single- and positive-stranded with the RNA encoding the 5-1-1 and 81 antigens. *On fire!* The cream on the cake was then provided by sequencing more overlapping clones and observing very limited but significant sequence homologies with dengue flavivirus. *HCV was a flavi-like virus!* At this point, Qui-Lim, George, and I felt that we had indeed identified HCV for the first time and filed a patent application to that effect in late 1987 later published in *Science* ([24]; Fig. 1).

Later on in 1988, we screened blinded panels of NANBH and control blood samples from Harvey Alter at the NIH and successfully identified 6/7 NANBH samples of proven infectivity along with at least one positive blood donor implicated in 9/10 posttransfusion NANBH cases. We also showed that the majority of NANBH patients from Italy and Japan (provided by Ferruccio Bonino and Tatsuo Miyamura) were positive for antibodies to our antigens [25]. Not only did this confirm the association of 5-1-1 and related clones with parenteral NANBH but this also meant that we had the basis for the first specific HCV/NANBH screening test for infectious blood donors.

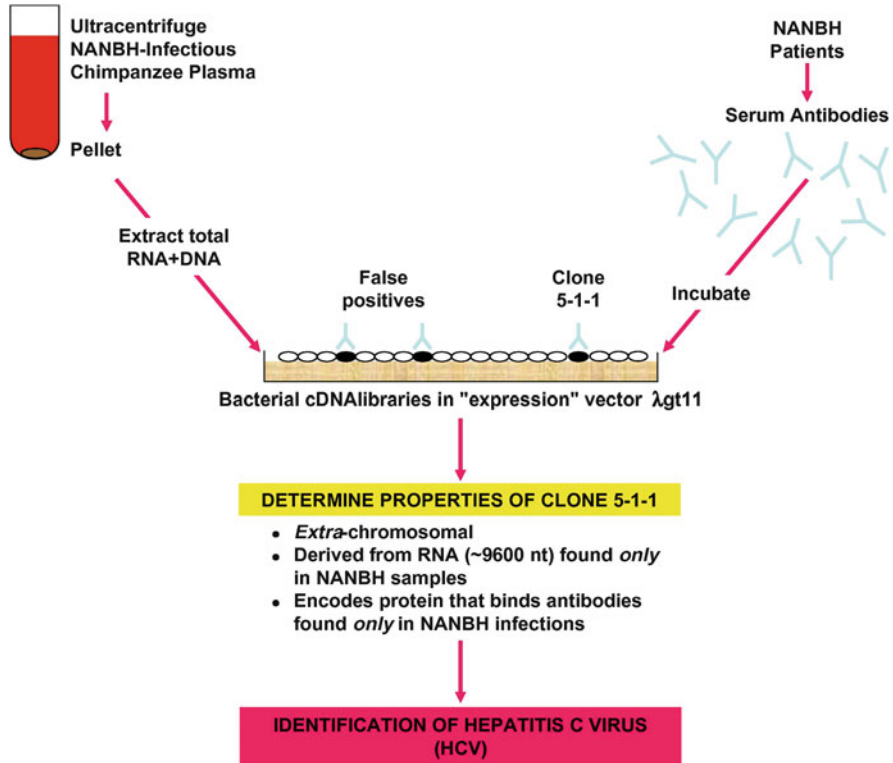


Fig. 1 Experimental scheme for the identification of the hepatitis C virus

6 What's Next?

Our first diagnostic (licensed to Ortho Diagnostics) using the clone 81 antigen was approved for blood screening ~1990 and detected around two-thirds of infectious blood donors around the world thus preventing millions of HCV infections. Subsequently, we were able to add other HCV antigens to 5-1-1 and 81 improving the sensitivity to >95%. PCR and TMA RNA amplification methods then became available to be able to detect acutely infected, infectious blood donors that had not yet seroconverted to HCV antibody after which the threat of posttransfusion HCV was effectively eliminated. The field of HCV was now borne with the 1st International Meeting on HCV and Related Viruses being convened by myself and Ferruccio Bonino in 1992 at the Cini Foundation in Venice, Italy. Later this year, we will be celebrating the 25th of these annual meetings from which great knowledge from numerous excellent laboratories in the field regarding the replication cycle and biology of HCV has been elucidated including outstanding contributions from the laboratories of Ralf Bartenschlager and Charles Rice.

This book deals with the great advances that have occurred in HCV therapy since the virus discovery and details the development of very potent direct-acting

antivirals (DAAs) targeting the HCV polymerase, NS5a protein, and serine protease that can now cure nearly all patients within 1–3 months of oral administration. However, the long history of infectious disease has taught us that epidemic infections cannot be eliminated or effectively controlled without a potent vaccine. While promising work on a HCV vaccine is in progress from numerous laboratories including mine at the University of Alberta, another future edition of this book will be required before concluding that this key objective has been attained.

Compliance with Ethical Standards

Funding This study was funded by the Canada Excellence in Research Chairs program, Alberta Innovates and the Li Ka Shing Institute of Virology.

Conflict of Interest Author is a director and stock holder of Aurora Vaccines Inc.

Ethical Approval All applicable international, national, and/or institutional guidelines for the care and use of animals were followed. All procedures performed in the studies involving human participants were in accordance with the ethical standards of the institutional and/or national research committee and with the 1964 Helsinki declaration and its later amendments or comparable ethical standards.

Informed Consent Informed consent was obtained from all individual participants included in the study.

References

1. Houghton M (2000) Identification of the hepatitis C virus. *Nat Med* 6(10):1084–1086
2. Houghton M (2009) Discovery of the hepatitis C virus. *Liver Int* 29(Suppl 1):82–88
3. Houghton M (2009) The long and winding road leading to the identification of the hepatitis C virus. *J Hepatol* 51(5):939–948
4. Houghton M (2016) Towards the control of hepatitis C. In: Miyamura T, Lemon S, Walker C, Wakita T (eds) *Hepatitis C virus I*. Springer, Tokyo
5. Prince AM, Brotman B, Grady GF, Kuhns WJ, Hazzi C, Levine RW, Millian SJ (1974) Long-incubation post-transfusion hepatitis without serological evidence of exposure to hepatitis-B virus. *Lancet* 2(7875):241–246
6. Feinstone SM, Kapikian AZ, Purcell RH, Alter HJ, Holland PV (1975) Transfusion-associated hepatitis not due to viral hepatitis type A or B. *N Engl J Med* 292(15):767–770
7. Bayer ME, Blumberg BS, Werner B (1968) Particles associated with Australia antigen in the sera of patients with leukaemia, Down's Syndrome and hepatitis. *Nature* 218:1057–1059
8. Feinstone SM, Kapikian AZ, Purcell RH (1973) Hepatitis A: detection by immune electron microscopy of a viruslike antigen associated with acute illness. *Science* 182:1026–1028
9. Barré-Sinoussi F, Chermann JC, Rey F, Nugeyre MT, Chamaret S, Gruest J, Dauguet C, Axler-Blin C, Vézinet-Brun F, Rouzioux C, Rozenbaum W, Montagnier L (1983) Isolation of a T-lymphotropic retrovirus from a patient at risk for acquired immune deficiency syndrome (AIDS). *Science* 220(4599):868–871
10. Hollinger FB, Mosley JW, Szmuness W, Aach RD, Peters RL, Stevens C (1980) Transfusion-transmitted viruses study: experimental evidence for two non-A, non-B, hepatitis agents. *J Infect Dis* 142(3):400–407

11. Alter HJ (1980) The dominant role of non-A, non-B in the pathogenesis of post-transfusion hepatitis: a clinical assessment. *Clin Gastroenterol* 9(1):155–170 Review
12. Alter MJ, Gerety RJ, Smallwood LA, Sampliner RE, Tabor E, Deinhardt F, Frösner G, Matanoski GM (1982) Sporadic non-A, non-B hepatitis: frequency and epidemiology in an urban U.S. population. *J Infect Dis* 145(6):886–893
13. Bradley DW, Cook EH, Maynard JE, McCaustland KA, Ebert JW, Dolana GH, Petzel RA, Kantor RJ, Heilbrunn A, Fields HA, Murphy BL (1979) Experimental infection of chimpanzees with antihemophilic (factor VIII) materials: recovery of virus-like particles associated with non-A, non-B hepatitis. *J Med Virol* 3(4):253–269
14. Bradley DW, Maynard JE, Popper H, Cook EH, Ebert JW, McCaustland KA, Schable CA, Fields HA (1983) Posttransfusion non-A, non-B hepatitis: physicochemical properties of two distinct agents. *J Infect Dis* 148(2):254–265
15. Shimizu YK, Feinstone SM, Purcell RH, Alter HJ, London WT (1979) Non-A, non-B hepatitis: ultrastructural evidence for two agents in experimentally infected chimpanzees. *Science* 205:197–200
16. Bradley DW, McCaustland KA, Cook EH, Schable CA, Ebert JW, Maynard JE (1985) Posttransfusion non-A, non-B hepatitis in chimpanzees. Physicochemical evidence that the tubule-forming agent is a small, enveloped virus. *Gastroenterology* 88(3):773–779
17. He LF, Alling D, Popkin T, Shapiro M, Alter HJ, Purcell RH (1987) Determining the size of non-A, non-B hepatitis virus by filtration. *J Infect Dis* 156(4):636–640
18. Wakita T, Pietschmann T, Kato T, Date T, Miyamoto M, Zhao Z, Murthy K, Habermann A, Kräusslich HG, Mizokami M, Bartenschlager R, Liang TJ (2005) Production of infectious hepatitis C virus in tissue culture from a cloned viral genome. *Nat Med* 11(7):791–796. Epub 2005 Jun 12. Erratum in: *Nat Med.* 2005 Aug;11(8):905
19. Wang KS, Choo QL, Weiner AJ, Ou JH, Najarian RC, Thayer RM, Mullenbach GT, Denniston KJ, Gerin JL, Houghton M (1986) Structure, sequence and expression of the hepatitis delta (delta) viral genome. *Nature* 323(6088):508–514 Erratum in: *Nature* 1987 Jul 30–Aug 5;328(6129):456
20. Weiner AJ, Wang KS, Choo QL, Gerin JL, Bradley DW, Houghton M (1987) Hepatitis delta (delta) cDNA clones: undetectable hybridization to nucleic acids from infectious non-A, non-B hepatitis materials and hepatitis B DNA. *J Med Virol* 21(3):239–247
21. Shimizu YK, Oomura M, Abe K, Uno M, Yamada E, Ono Y, Shikata T (1985) Production of antibody associated with non-A, non-B hepatitis in a chimpanzee lymphoblastoid cell line established by in vitro transformation with Epstein-Barr virus. *Proc Natl Acad Sci U S A* 82(7):2138–2142
22. Feinstone SM, Alter HJ, Dienes HP, Shimizu Y, Popper H, Blackmore D, Sly D, London WT, Purcell RH (1981) Non-A, non-B hepatitis in chimpanzees and marmosets. *J Infect Dis* 144(6):588–598
23. Prince AM (1985) Reliability of chimpanzee model for non-A, non-B hepatitis. *Lancet* 2(8464):1134
24. Choo QL, Kuo G, Weiner AJ, Overby LR, Bradley DW, Houghton M (1989) Isolation of a cDNA clone derived from a blood-borne non-A, non-B viral hepatitis genome. *Science* 244(4902):359–362
25. Kuo G, Choo QL, Alter HJ, Gitnick GL, Redeker AG, Purcell RH, Miyamura T, Dienstag JL, Alter MJ, Stevens CE et al (1989) An assay for circulating antibodies to a major etiologic virus of human non-A, non-B hepatitis. *Science* 244(4902):362–364

HCV Molecular Virology and Animal Models



Mohsan Saeed, Eva Billerbeck, and Charles M. Rice

Contents

1	Introduction	30
2	HCV Genome Organization	31
3	Summary of the HCV Life Cycle	32
4	Functional HCV RNA Elements	34
4.1	The HCV 5' UTR	34
4.2	The HCV 3' UTR	35
5	HCV Proteins	36
5.1	Core	36
5.2	HCV Glycoproteins	38
5.3	P7	39
5.4	NS2	40
5.5	NS3-4A Complex	41
5.6	NS4B	43
5.7	NS5A	43
5.8	NS5B	45
6	Summary	47
7	HCV Animal Studies	47
7.1	Animal Models	47
7.2	Chimpanzees	48
7.3	HCV Mouse Models	50
8	HCV-Related Hepaciviruses	53
8.1	GB Virus B	53
8.2	Non-primate Hepaciviruses	54
8.3	Rodent Hepaciviruses	54
9	Concluding Remarks	55
	References	56

M. Saeed, E. Billerbeck, and C. M. Rice (✉)

Laboratory of Virology and Infectious Disease, The Rockefeller University, New York, NY, USA

e-mail: msaeed@rockefeller.edu; ebillerbec@rockefeller.edu; ricec@rockefeller.edu

Abstract Hepatitis C virus (HCV) infection was once considered a threat to life but is now curable. This miraculous achievement is the result of years of effort to understand basic HCV biology, which led to the development of HCV cell culture systems eventually enabling drug discovery. Initial studies focused on biochemical characterization of viral proteins and dissected their roles in the virus life cycle. Two of the viral proteins, NS3-4A protease and NS5B polymerase, were selected early on as potential drug targets, and subsequent collaborative efforts of academia and industry led to the development of highly effective inhibitors against these enzymes. Another HCV protein, NS5A that has no known enzymatic activity, was more recently identified as an unexpected target of a highly potent class of anti-HCV inhibitors. Various combinations of these protease, polymerase, and NS5A inhibitors now constitute the current anti-HCV regimens with cure rates of above 95%. This chapter is divided into two parts. The first part begins with a short introduction to HCV and its life cycle and reviews insights into biochemical and functional characteristics of HCV RNA elements and proteins. The second part discusses the HCV animal models and how their use yielded important insights into the viral life cycle, immunity, and disease pathogenesis.

Keywords HCV proteins, HCV replication, HCV RNA, Human liver chimeric mice, Non-primate hepaciviruses, Rodent hepaciviruses

1 Introduction

Identification of HCV in 1989 as the major cause of non-A, non-B chronic hepatitis elicited intense research. Initially, lack of suitable cell culture systems and small animal models slowed progress, but still great strides were made toward biochemical and functional characterization of various HCV RNA elements and proteins. These studies mainly relied on *in vitro* biochemical assays and/or expression of individual proteins in cell culture, and the results were at times validated in chimpanzees, the only HCV animal model available. Remarkable knowledge gained over these years set the stage for development of the first HCV *in vitro* replication system in 1999 [1]. This system uses truncated HCV genomes, called HCV subgenomic replicons that encode a subset of the viral nonstructural proteins and can autonomously replicate in cell culture. Although a great tool for studying various aspects of the HCV RNA replication, this system did not allow virus particle production. Eventually, success came in 2005 when the first efficient HCV cell culture (HCVcc) infection systems were reported [2, 3], finally allowing dissection of all the steps of the HCV life cycle. The HCVcc system has since been extensively used to expand our knowledge of HCV molecular biology.

2 HCV Genome Organization

HCV is a positive-sense, single-stranded RNA virus. Its genome is approximately 9.6 kb and comprises a long open reading frame (ORF) flanked at its 5' and 3' ends by untranslated regions (UTRs) [4–7] (Fig. 1). These UTRs contain important signals for replication and translation of the viral RNA. For example, the 5' UTR has an internal ribosomal entry site (IRES) required for HCV RNA translation [9], and interaction between the 5' and 3' UTRs has been shown to be essential for genome replication [10–12]. Moreover, nucleotide sequences and RNA secondary structures in the ORF have also been implicated in translation and replication [13, 14].

The ORF encodes a polyprotein of just over 3,000 amino acids. This polyprotein then undergoes a series of cleavage events to generate three structural and seven nonstructural proteins. The structural proteins are produced at the N-terminus of the polyprotein and include the core protein and two viral glycoproteins, E1 and E2. The nonstructural proteins include the p7 viroporin, the NS2 protease, the NS3-4A protease/NTPase/RNA helicase, the NS4B membrane-remodeling protein, the NS5A phosphoprotein, and the NS5B RNA-dependent RNA polymerase (RdRp). The structural proteins and p7 are processed by two host proteases, signal peptidase

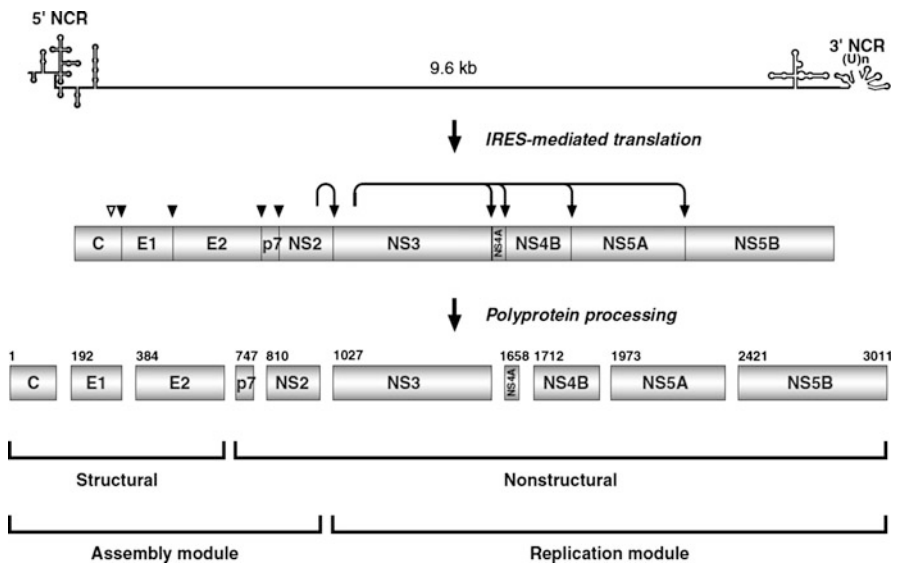


Fig. 1 HCV polyprotein processing. The HCV genome, shown on the top, is translated in an IRES-dependent manner to yield a polyprotein precursor that is processed by the host and viral proteases. Solid arrowheads indicate signal peptidase-mediated cleavages, while the open arrowhead indicates further C-terminal processing of the core protein by signal peptide peptidase. Arrows indicate cleavages by the HCV NS2 and NS3-4A proteases. Amino acid numbering above each protein refers to the HCV H strain (genotype 1a; GenBank accession number AF009606). Reproduced from “Hepatitis C Virus Proteins: From Structure to Function” [8], with permission from Springer

and signal peptide peptidase (SPP) [15], while maturation of the other proteins requires two viral proteases, NS2 and NS3-4A [16]. NS2 is an autoprotease that cleaves the polyprotein at the NS2/3 site, while all other cleavages are performed by NS3-4A.

3 Summary of the HCV Life Cycle

To enter a hepatocyte, HCV first interacts with glycans on the cell surface thereby docking onto the surface of the cell [17, 18]. The virus envelope proteins and virion-associated lipoproteins then interact with HCV receptors to facilitate virus internalization. Four key HCV receptors include scavenger receptor B1 (SR-B1), CD81, claudin-1 (CLDN1), and occludin (OCLN), which complete the viral entry process with the help of a number of host proteins, such as epidermal growth factor receptor (EGFR), ephrin receptor A2 (EphA2), and Niemann-Pick C1-like1 (NPC1L1) (reviewed in [19]). HCV is a hepatotropic virus that only infects humans, and this specificity for human hepatocytes is at least partially defined by the entry step. For example, SR-B1, CLDN1, and NPC1L1 are highly expressed in hepatocytes and thought to be responsible for HCV hepatotropism, while CD81 and OCLN are critical for HCV human tropism – mouse cells refractory to HCV infection become susceptible when human CD81 and OCLN are expressed (reviewed in [20]).

Receptor-bound HCV is endocytosed in a clathrin-dependent process [21] and trafficked to early endosomes, where low pH-induced fusion between the viral and endosomal membranes releases the viral RNA into the cytoplasm [22, 23]. This RNA is then translated in an IRES-dependent manner to generate the ten major HCV proteins, which can be functionally classified into two modules: an assembly module (C-NS2, required for virion assembly) and a replication module (NS3-NS5B, components of the replicase complex) (Fig. 2). These modules do not operate in isolation though, as almost all replicase proteins have been shown to assist assembly (reviewed in [25]). The assembly module, however, is dispensable for HCV RNA replication.

HCV replicates its genome in a membrane-associated replication complex, which is composed of viral and host proteins [26]. Analogous to other positive-strand RNA viruses, HCV replication occurs in two steps, both of which are catalyzed by the viral NS5B polymerase. In the first step, HCV genomic RNA is used as a template to generate a complementary negative strand, which in turn serves as a template in the second step to produce molar excess of positive-strand progeny RNA. This progeny RNA has three possible fates: (1) it is translated to produce viral proteins, (2) it is used as a template to generate more negative-strand intermediates, or (3) it is trafficked to the assembly site where it is packaged into new virions.

Our understanding of how virions are assembled is incomplete. For assembly to occur, the HCV glycoproteins E1 and E2, the core protein, the newly generated viral RNA, and several viral and host proteins must come together. The current model posits that HCV core protein at the surface of lipid droplets (LD) recruits HCV

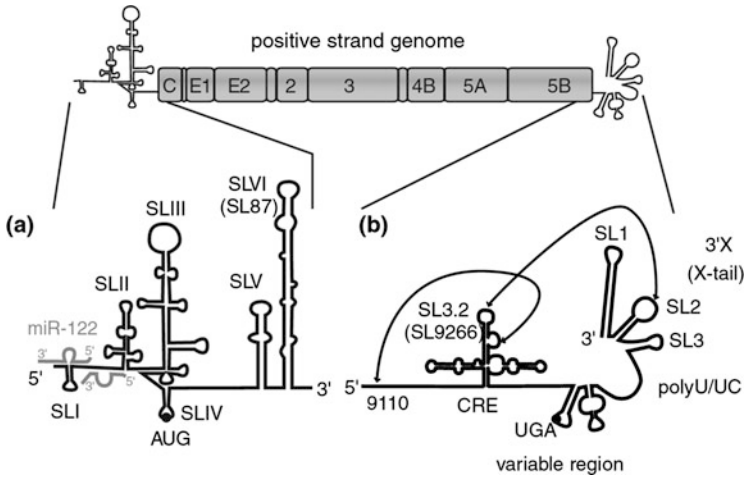


Fig. 2 Schematic representation of HCV genome. **(a)** 5' UTR of the viral genome. Two copies of miR-122 bound to the genome are shown in gray. **(b)** 3' UTR of the viral genome. Arrows indicate the long-range interactions of SL3.2 with sequences around 9,110 and with SL2 of the 3' UTR. Reproduced from “Hepatitis C Virus RNA Replication” [24], with permission from Springer

replication complexes, primarily through its interaction with the NS5A protein [27]. This brings newly synthesized viral RNA in close juxtaposition to the assembly site and facilitates formation of nucleocapsids, which then acquire an HCV glycoprotein-studded envelope through budding into the ER lumen (reviewed in [28]). Once inside the ER lumen, the HCV particles appear to follow the canonical secretory pathway. Consistent with this, treating HCV infected cells with Brefeldin A, a potent inhibitor of ER-Golgi transport, blocks HCVcc egress and causes accumulation of infectious particles inside cells [29].

HCV particles further mature throughout the secretory pathway. This is reflected by differential biochemical properties of extracellular and intracellular particles. For example, the glycoproteins on the surface of extracellular virions contain complex glycans, whereas intracellular particles largely harbor simple, high-mannose glycans [30]. Since glycan maturation occurs in the Golgi, this suggests that HCV particles pass through Golgi en route to release at the cell membrane. Also, in contrast to the extracellular virions, intracellular HCV particles are highly sensitive to a low pH. It is believed that the ion channel activity of the HCV p7 protein blocks acidification of the secretory vesicles and protects the transiting virions from low pH [31]. Another difference is the comparatively lower buoyant density of the extracellular virions, implying that HCV undergoes post-synthesis lipidation, most likely in the post-ER compartment [29, 32].

Outside the cell, HCV exists as a lipoprotein-virus hybrid, sometimes called a lipo-viro-particle (LVP) that has an extremely low buoyant density (1.03–1.10 g/mL) [33, 34]. Sucrose gradient fractionation of HCVcc yields two virus populations: one with higher density but low specific infectivity and another of

low density and high infectivity [3, 35]. Interestingly, treatment with cholesterol, an essential component of the lipoproteins, improves the infectivity of the higher-density virus population [36]. Moreover, the lipid composition of highly purified infectious HCV particles closely resembles that of the lipoproteins [37]. However, despite compelling evidence that HCV is secreted from cells as LVP, it is unclear how and when during its assembly the virus associates with the lipoproteins or lipoprotein components. Future studies should shed light on this and several other aspects of the rather poorly understood steps of HCV assembly and egress.

4 Functional HCV RNA Elements

The HCV genomic RNA serves as a template for both translation and replication. Each of these processes requires *cis*-acting viral RNA elements and transacting cellular RNAs, such as micro-RNA-122 (miR-122). Since most of the functionally important *cis*-acting RNA elements are located in the HCV 5' and 3' UTRs, in this section, we will limit our discussion to these genomic regions.

4.1 The HCV 5' UTR

The 5' UTR is a highly structured 341 nucleotide region comprising four stem-loops (I–IV) (Fig. 2). The first two stem-loops (nucleotides 5–125) are essential for replication, as their deletion blocks RNA synthesis [38]. Although other regions of the 5' UTR are not required for replication, their presence markedly enhances replication efficiency, suggesting that the signals for RNA replication are distributed throughout the UTR [38].

Stem-loops II–IV (nucleotides 40–341) plus a few nucleotides of the core-coding region form the HCV IRES, a class III IRES that requires only a subset of host translation initiation factors (eIFs) [39]. Indeed, the purified ribosomal 40S subunit can bind the HCV IRES in the absence of any eIFs or other proteins [40]. Inside infected cells, the 40S subunit directly binds to a pseudoknot structure in stem-loop III and positions itself such that the initiator AUG codon sits in the 40S P site [41]. Next, the eIF3 and the ternary complex (eIF2/GTP/Met-tRNA_i^{Met}) are recruited to form a 48S intermediate [40, 42]. GTP hydrolysis and subsequent release of initiation factors then allow 60S subunit joining and formation of a functional 80S ribosome complex [43, 44].

HCV requires a liver-specific and abundant micro-RNA, miR-122, for its replication [45, 46]. Two copies of miR-122 bind to two highly conserved target sites located between the first two stem-loops of the 5' UTR (Fig. 2). Ablating these target sites or sequestering miR-122 by antisense locked nucleic acid (LNA) inhibitors blocks HCV replication. Multiple mechanisms for miR-122 function have been proposed, including (1) it protects the HCV 5' end from exonuclease

Xrn-mediated decay [47–49]; (2) it promotes IRES-mediated translation of the HCV genome [50, 51]; (3) it increases the fraction of HCV RNA available for replication, possibly by displacing the translation-associated proteins from the RNA template [52]; and (4) HCV RNA-mediated sequestration of miR-122 derepresses the normal, presumably proviral, host miR-122 targets and thereby promotes virus replication [53].

The absolute conservation of the miR-122 binding sites across HCV isolates and the indispensability of miR-122 for HCV replication made it an attractive target for antiviral therapy. Indeed, weekly administration of a miR-122 antagonist, SPC3649, decreased HCV titers in chronically infected chimpanzees by more than two orders of magnitude following 12 weeks of therapy. This first-in-class inhibitor (miravirsen/SPC3649) has shown promise in clinical trials [54], but was not developed as a first-line HCV therapy. It may however be considered as a salvage therapy in rare instances of treatment failure or as a component of one-shot injectable cure cocktail for difficult-to-treat PWID (people who inject drugs) populations.

4.2 *The HCV 3' UTR*

The 3' UTR has a tripartite structure comprising an about 40-nucleotide variable region immediately following the stop codon, a poly (U/UC) tract of varying length, and a highly conserved 98-nucleotide region, designated as the X-tail or 3'X [6, 55]. While the variable region and the X-tail are highly structured, with two and three stem-loops, respectively, the poly (U/UC) tract is unstructured (Fig. 2). The poorly conserved 40-nucleotide variable region is dispensable for RNA replication, although its presence enhances replication efficiency [56, 57]. Of interest, despite high-sequence diversity, the variable region contains an invariable sequence motif – a binding site for miR-122 [45]. Although no functional role for this miR-122 binding site has been demonstrated in cell culture, such high conservation suggests that it might have an as yet undefined function(s) in vivo.

The poly (U/UC) tract highly varies in length. It comprises a homouridine core (U core) flanked by 5' and 3' arms that contain stretches of uridines with interspersed cytidines. The poly (U/UC) tract is essential for replication [56, 58]. Also, its base composition appears to be under strong selection pressure, as replacement of the U core with any other nucleotide homopolymers is not tolerated [56, 58]. Additionally, shortening the U core beyond a certain length inhibits HCV; however, such mutants can extend their U core in cell culture and revert to the parental replication levels [58]. The fact that these revertants always acquire uridines, and not other nucleotides, further suggests that this region may have sequence-specific roles, such as recruitment of important viral or cellular proteins. This is in line with the observation that the HCV NS3 helicase, NS5A, and NS5B preferentially bind to uridine homopolymers [59–61].

The X-tail spans the last 98 nucleotides of the HCV genome and is the most highly conserved region in the 3' UTR [6]. This region has three stem-loops

(SL1–3), and all of them are essential for replication [56, 57, 62, 63]. Importantly, both the structures and sequences of these stem-loops are critical, as even mutations that maintain the structures are barely tolerated [57, 63]. This could be due to the multiple interactions each nucleotide in this region is engaged in. For example, nucleotides in the SL2 base pair with a stem-loop in the NS5B-coding region to form a kissing-loop interaction (Fig. 2), which is essential for virus replication [13]. Alternatively, these sequences could be important for recruiting essential viral and/or host proteins.

The 3' UTR also appears to communicate with the 5' UTR and enhance RNA translation [10–12]. This communication is possibly a way to ensure that only complete, non-degraded HCV RNAs are translated and replicated. Exactly how HCV UTRs communicate with each other is unknown, but it seems to involve multiple regions in the 3' UTR. A few host proteins, such as the NFAR complex and IMP-1, have also been implicated in this process [64, 65]. Our understanding of how 3' UTR enhances HCV RNA translation is incomplete, but evidence suggests that it involves translation termination and ribosome recycling.

5 HCV Proteins

The HCV genome encodes ten proteins. The first three proteins (core, E1, and E2) are the structural components of the virus particles, while the remaining seven proteins (p7, NS2, NS3, NS4A, NS4B, NS5A, and NS5B) function in genome replication and virion biogenesis without being incorporated into mature virions. In this section, we provide a brief overview of the contemporary knowledge of these proteins. For detailed insights, the readers are referred to reviews of individual proteins.

5.1 Core

The core protein constitutes the virion capsid and is synthesized at the most N-terminal portion of the HCV polyprotein (Fig. 1). During polyprotein biogenesis, an internal signal sequence between core and the E1 glycoprotein docks the nascent polypeptide on the ER membrane and induces translocation of E1 into the ER lumen [66]. The mature form of core is then released by two catalytic events: first, an ER-resident signal peptidase cleaves between E1 and the signal peptide, leaving behind an immature membrane-bound core of 191-aa. The signal peptide is further processed by an intramembrane SPP, releasing mature 177-aa core (core¹⁷⁷) from the membrane [67–69] (Fig. 3). This protein is then free for trafficking to LD, where it drives virion assembly [70]. A recent mass spec analysis of highly purified HCV particles identified core¹⁷⁷ as the protein form that is incorporated into mature virions [71].

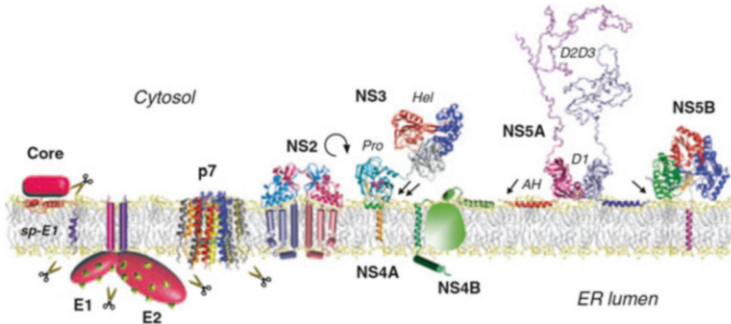


Fig. 3 Structure and membrane association of HCV proteins. Scissors on the ER luminal side indicate cleavages by the signal peptidases, while the one on the cytosolic side indicates the additional cleavage of core by signal peptide peptidase. The cyclic arrow shows NS2-mediated cleavage, while the black arrows denote NS3-4A-mediated cleavages. Reproduced from “Hepatitis C Virus Proteins: From Structure to Function” [8], with permission from Springer

The three-dimensional structure of the core protein is yet to be solved. The hydropathy profile suggests that the mature core comprises two domains: an N-terminal hydrophilic domain of ~122-aa (domain 1) and a C-terminal hydrophobic domain (domain 2) [72]. Domain 1 is highly enriched in basic residues, has RNA binding and homo-oligomerization activities, and is a key player in virion assembly. Domain 2 contains two amphipathic α -helices and a central hydrophobic loop and anchors the core protein to the membrane [73]. An important step during nucleocapsid formation is the packaging and compaction of the viral RNA, a process that requires substantial structural remodeling of the RNA. This is typically achieved by the RNA chaperone activity of the viral capsid proteins, and in the case of HCV, this function appears to reside in the domain 1 of the core protein [74].

How core and the viral RNA come together to assemble nucleocapsids, and exactly where in the cell this assembly occurs, is unknown. However, it is widely accepted that assembly occurs on the surface of LDs where the functional core protein resides. Interaction between core and NS5A appears to be important for the delivery of the viral RNA to the assembly site. It is unclear, however, if NS5A alone carries the viral RNA from an HCV replication complex to the assembly site or if the whole replication complex is moved to the LD. Once bound to the viral RNA, core is assumed to oligomerize and drive nucleocapsid formation (reviewed in [28]).

Additional core species, most likely produced by internal translation initiation, have also been reported [75]. Originally identified in cell culture systems, these 6–14-kDa minicores have recently been detected in patient sera as well [76]; however, their biological relevance is unclear. Evidence of an alternate reading frame (ARF) overlapping the core-coding region also exists. Although ARF proteins appear to elicit antibodies in patients, their function in viral persistence and pathogenesis is also unknown (reviewed in [77]).

5.2 HCV Glycoproteins

The HCV genome encodes two envelope glycoproteins, E1 and E2, that are released from the polyprotein by signal peptidase cleavage. As a general feature of the viral envelope proteins, HCV glycoproteins exhibit marked conformational plasticity, allowing them to play distinct roles at different stages of the virus life cycle, such as virion production and maturation, receptor binding, and fusion between the viral and cellular membranes.

HCV glycoproteins are type I transmembrane proteins with a large N-terminal ER-luminal ectodomain and a C-terminal hydrophobic transmembrane domain (TMD) (Fig. 3). A unique feature of the E1 and E2 TMDs is their dynamic topology provided by their special architecture – each TMD comprises a short stretch of hydrophilic residues connecting two hydrophobic segments, with the second segment serving as a signal sequence for the downstream protein. Before signal peptide cleavage, the TMDs have a hairpin structure with both ends of the hairpin oriented toward the ER lumen, but following cleavage, the second hydrophobic segment is reoriented toward the cytosol, resulting in a single membrane-spanning domain [78].

The TMDs contribute to several of the HCV glycoprotein properties, such as membrane association, ER retention, and E1E2 non-covalent heterodimer formation (reviewed in [79]). Like many ER-resident membrane proteins, the hydrophilic residues in the middle of the TMD appear to mediate the ER retention of E1 and E2. Replacing these residues with alanine abolishes ER retention. Similarly, deleting the E2 TMD or replacing it by the anchor signal from another protein disrupts E1 and E2 heterodimer formation, indicating that TMDs play critical roles in protein heterodimerization. Interestingly, although E1 and E2 makes non-covalent heterodimers at the ER membrane, they appear to be covalently bound on secreted virus particles [30].

It is unclear how and when E1E2 dimers acquire intermolecular disulfide linkages during HCV assembly. Although E1 and E2 ectodomains have numerous highly conserved cysteine residues, as first predicted and later confirmed by structural data, these cysteines are engaged in intramolecular disulfide associations and are therefore unavailable for intermolecular linkages [80–82]. However, as several regions of the HCV glycoproteins appear to possess remarkable conformational flexibility, it is possible that structural rearrangements at some point during virion assembly expose the cysteines and allow formation of intermolecular disulfide bonds.

In contrast to the flavivirus envelope (E) protein, HCV glycoproteins are heavily glycosylated, a feature required for proper protein folding, transport through the secretory pathway, and escape from the host immune surveillance. E1 and E2 have 4–6 and 9–11 N-linked glycosylation sites, respectively, which are decorated by high-mannose-type glycans as the proteins translocate into the ER lumen. These glycans then interact with an ER chaperone, calnexin, and assist in protein folding [83, 84]. As the assembled HCV particles pass through the Golgi, several of the high-mannose glycans are converted into complex glycans [30] and presumably protect the secreted virions from the humoral immune response [85].

HCV E1E2 heterodimers interact with cell surface receptors to initiate virus entry, which is a highly coordinated multistep process leading to virus uptake into endosomes. Low pH in the early endosomes then induces fusion between the viral and endosomal membrane, facilitating escape of the viral genome into the cytoplasm. Our knowledge of how fusion occurs is incomplete. In the case of flaviviruses, the E protein has a fusion peptide that is buried at the dimer interface at neutral pH. Upon exposure to low endosomal pH, the E protein undergoes structural rearrangement exposing the fusion peptide, which then inserts into the endosomal membrane and brings it closer to the viral membrane for fusion (reviewed in [86]). However, for HCV, which of the two glycoproteins mediates fusion is unclear.

For years, E2 was proposed to be a fusion protein; however, recent structures of the E2 ectodomain appear to disprove this notion. For example, type II fusion proteins, such as that of flaviviruses, have an elongated, three-dimensional architecture of over 140 Å in length, whereas HCV E2 ectodomain is a compact, globular protein of only 32 Å. Also, the predicted fusion peptide is buried inside the hydrophobic core of the E2 ectodomain where it is part of the secondary structural elements, seemingly ruling out a role in fusion [87]. Moreover, in contrast to typical fusion proteins, HCV E2 does not undergo major structural and oligomeric changes upon exposure to lower pH [80]. Is then E1 the fusion protein?

The crystal structure of the E1 N-terminal portion (aa 1–79) was recently solved. This so-called nE1 is 59 Å in length, and although it exists as a dimer in solution, its structure has no resemblance to other viral fusion proteins [88]. This raises the possibility that HCV fusion occurs by a completely different mechanism. Alternatively, the fusion peptide could be located in the regions of the HCV glycoproteins that were not part of the crystal structures, or fusion could be mediated by the E1E2 heterodimer. Also, the possibility of virion-associated lipoproteins or cellular receptors and cofactors mediating HCV fusion cannot be ruled out.

In addition to mediating cell entry, the HCV glycoproteins elicit neutralizing antibodies in patients. Consequently, the genes encoding glycoproteins are highly variable, and E2 further contains two hypervariable regions (HVR), differing by up to 80% among HCV isolates. HVR1 spans the first 27 amino acids of E2 and is the immunodominant region containing several epitopes that elicit type-specific antibodies [89]. HVR2 comprises amino acid 76–101 and shows massive sequence diversity. However, the significance of such a high diversity is unknown, as this region appears to play no roles in humoral immune responses [90].

5.3 P7

P7 is a small 63-aa protein located at the junction of the structural and nonstructural region in the HCV polyprotein and is processed by the signal peptidase cleavage. It is an integral membrane protein comprising two antiparallel transmembrane segments separated by a hydrophilic cytosolic loop [91] (Fig. 3). When reconstituted in

artificial membranes, p7 assembles into hexamers or heptamers and exhibits cation channel activity that is abolished by classical ion channel inhibitors, suggesting that p7 is a viroporin [92, 93].

To date, no high-resolution 3D structure of p7 has been solved. NMR studies of p7 monomers embedded in artificial membranes have revealed the following structural features [94]: (1) an N-terminal transmembrane segment comprising two α -helices connected by a turn, (2) a cytosolic loop containing a highly conserved dibasic motif, (3) a C-terminal transmembrane segment comprising an α -helix, and (4) an unstructured 7-aa C-terminal segment. P7 monomers oligomerize to make ion channels, but what these channels look like and how monomers are packed within these channels are unclear. Two studies, one based on a single-particle EM analysis and the other on structure simulation, have provided contrasting pictures: while the former revealed a conical-shaped channel, the latter showed a cylindrical, upright architecture [93, 95]. This discrepancy is likely due to the difference in the thickness of the artificial membranes the two groups used to reconstitute p7. In fact, the ability to adapt to the membrane thickness is a general feature of viroporins.

Several lines of evidence indicate that p7 is dispensable for HCV RNA replication *in vitro*. It is however essential for HCV infectivity in chimpanzees and for production of infectious particles in cell culture, suggesting that p7 is required at later stages of the virus life cycle (reviewed in [96]). To support this, an HCV mutant lacking the p7 viroporin activity failed to produce infectious particles, and this defect could be partially rescued by the influenza virus M2 viroporin. However, M2 failed to rescue infectivity of an HCV mutant lacking the whole p7 protein, suggesting p7 has additional viroporin-independent roles [31]. The p7 viroporin activity is believed to protect intracellular viruses from acidification, whereas its non-channel activity involves its interactions with other viral, and possibly host, proteins (reviewed in [96]).

5.4 NS2

NS2 is the first nonstructural protein encoded by the HCV genome and is processed by the signal peptidase at its N-terminus and by an intrinsic *cis*-protease activity at its C-terminus [97]. For efficient enzymatic activity, NS2 requires the protease domain, but not the protease activity, of the downstream NS3 protein [98] and is therefore described as NS2-3 protease. The protease-mediated NS2-NS3 cleavage is essential for HCV RNA replication [99]; however, following cleavage, NS2 loses its enzymatic activity and is no longer required for replication in cell culture. Consistent with this, HCV subgenomic replicons devoid of NS2 can efficiently replicate in cell culture. NS2 however is important for the production of infectious virions [1].

NS2-3 protease has no sequence or structural similarity with any known eukaryotic proteases. However, the finding that classical cysteine protease inhibitors such as iodoacetamide inhibit NS2-3 led to the suggestion that it is a cysteine protease [100]. Later, crystallization of the NS2 protease domain confirmed this assumption

and revealed a catalytic triad of His, Cys, and Glu, which is conserved across all HCV genotypes [101]. Replacing catalytic His and Cys with alanine abolishes NS2-3 enzymatic activity, whereas substitution of Glu is largely tolerated [97, 102]. NS2 forms a homodimer with two composite active sites (Fig. 3), each of which contains catalytic His and Glu residues contributed by one monomer together with a nucleophilic Cys contributed by the other [101].

The NS2-3 autoprotease activity leads to its inactivation, presumably because after cleavage, NS2 C-terminal residues occupy the active site [101]. The liberated NS2 is a 23-kDa protein localized at the ER membranes through its three N-terminal transmembrane segments (TMS), while the protease domain is cytoplasmically oriented [100, 103]. A number of mutations in the TMS and protease domain have been found to influence infectious particle production, suggesting an important role for NS2 [104–109]. Exactly how NS2 contributes to virus production is poorly understood but may involve a complex network of interactions with structural and other nonstructural viral proteins [104, 107, 110, 111].

5.5 NS3-4A Complex

NS3 is a multifunctional protein that makes a complex with and uses NS4A as a cofactor. The N-terminal one-third of NS3 is a chymotrypsin-like serine protease, while the C-terminal two-thirds has NTPase/RNA helicase activity. Both of these activities are essential for HCV replication (reviewed in [112]).

NS3-4A protease NS3-4A is responsible for all downstream cleavages that occur in the HCV polyprotein [113]. The cleavage at the NS3/4A site occurs in *cis*, while the rest require *trans*-cleavage activity of NS3-4A. There seems to be a preferential order in which NS3-4A processes the polyprotein: first NS5A/5B site is cleaved to produce the NS4A-5A intermediate, followed by cleavage at the NS4A/4B site to produce a relatively stable NS4B-5A precursor, which is the final intermediate to be processed [114]. The significance of this cleavage order is unknown, but the intermediates generated may have regulatory roles in the viral life cycle [115].

NS3-4A is an integral membrane protein complex, anchored on the ER membrane by an NS3 N-terminal amphipathic α -helix and an NS4A N-terminal transmembrane segment [116] (Fig. 3). The protease region of NS3 has a typical chymotrypsin-like fold and is composed of two β -barrel domains flanked by two short α -helices. At the interface of these domains lies the active site, with a catalytic triad of His, Asp, and Ser; His and Asp are contributed by one domain, while the nucleophilic Ser by the other. Three Cys residues and a water molecule coordinate a Zn^{2+} ion required for enzyme stabilization (reviewed in [117]). The NS3 protease requires an obligate cofactor, NS4A, which is a 54-aa polypeptide comprising three regions: the N-terminal hydrophobic region that forms a transmembrane α -helix, the

central β -strand that is incorporated into the N-terminal β -barrel of NS3, and the C-terminal acidic region that forms a negatively charged α -helix. The C-terminal helix appears to play multiple roles in HCV RNA replication and virus particle production, most likely through binding with NS3 helicase and other replicase components [118, 119].

Aside from HCV polyprotein processing, NS3-4A cleaves several host proteins (reviewed in [120]). Its most well-defined target is MAVS, an adapter protein in the RIG-I branch of the interferon (IFN) production pathway. By cleaving MAVS, NS3-4A blocks RIG-I signaling and thereby antagonizes the major cellular antiviral immune pathway. Another immune component that NS3-4A has been shown to cleave is TRIF, an adaptor protein in the TLR branch of the IFN production pathway. Several other proteins, such as T cell protein tyrosine phosphatase (TC-PTP), UV-damaged DNA binding protein 1 (DDB1), and a membrane-associated peroxidase GPx8, are also targeted by NS3-4A, but the functional significance of these cleavages is poorly understood. This however shows that NS3-4A protease is a multifunctional protein, required on one hand for the maturation of viral proteins and, on the other hand, to disrupt cellular antiviral defenses.

Inspired by the clinical success of human immunodeficiency virus (HIV) protease inhibitors, and given the fact that NS3-4A protease has multiple essential roles in the HCV life cycle, intense efforts were started early to develop NS3-4A protease inhibitors. These efforts culminated in the development of highly effective HCV protease inhibitors that are now in clinical use. The details of these inhibitors are provided in the later sections of this book.

NS3 helicase The C-terminus of NS3 is a superfamily 2, 3'-5' RNA helicase, which is thought to separate viral RNA strands, disrupt RNA secondary structures, and/or remove nucleic acid-associated proteins during HCV RNA replication (reviewed in [117]). An inherent NTPase activity of NS3 hydrolyzes ATP and thereby provides fuel for the translocation and RNA unwinding functions of the protein ([121] and references therein). Although NS3 NTPase/helicase is an independent enzyme, the presence of the NS3 protease domain and NS4A appears to modulate at least some of its activities. Ablating NS3 helicase function blocks HCV replication in vivo and in vitro, indicative of an essential enzymatic role (reviewed in [25]). However, exactly how NS3 helicase unwinds HCV RNA and its precise role in the virus life cycle remains elusive. Interestingly, in vitro assays have shown that NS3 also has a DNA helicase activity [122, 123], raising the formal possibility that it could interact with cellular DNA.

Crystal structures of the NS3 helicase domain as well as of the full-length NS3 protein in complex with its NS4A cofactor have been solved (reviewed in [117]). These structures revealed a Y-shaped helicase, where the N-terminal domain (D1) and the middle domain (D2) make arms, while the C-terminal domain (D3) makes stem of the "Y" (Fig. 3). D1 and D2 have similar topologies and contain all of the conserved helicase sequence motifs, including the signature DExH/D-box motif required for the binding and hydrolysis of NTP and coordination of a metal ion cofactor (Mg^{2+} or Mn^{2+}). Crystallization of NS3 helicase with bound nucleic acids

revealed that the substrate binding pocket of the enzyme resides in the cleft separating domain 3 from the other two domains [124].

Although HCV NTPase/helicase is not as extensively developed as a drug target as HCV protease and polymerase, it undoubtedly represents a potential target for antiviral therapy. Progress, however, has been slowed by a number of factors, including poor grasp of the NS3 helicase mechanism, a paucity of high-throughput assays for compound screening, and striking similarities between NS3 and cellular RNA helicases impeding identification of HCV-specific, nontoxic inhibitors. Improved understanding of the NS3 helicase could help overcome some of these barriers.

5.6 *NS4B*

Like all positive-sense RNA viruses, HCV replication occurs on highly remodeled cellular membranes, and although several viral and cellular proteins play roles in the biogenesis of these membranes, the NS4B protein is believed to be a major player [125, 126]. This 27-kDa, highly hydrophobic protein strongly associates with ER membranes and induces specific membranous structures designated the membranous web, which is the site of HCV RNA replication [127, 128]. In addition, NS4B has been reported to have RNA binding [129], NTP hydrolysis [130], and adenylate kinase [131] activities.

NS4B is an integral membrane protein comprising two amphipathic α -helices at its N-terminus, four transmembrane segments in the middle of the protein, and two α -helices at the C-terminus (reviewed in [132]). In addition, two palmitoylation sites in the NS4B C-terminus also appear to contribute to the membrane association [133]. How NS4B induces the formation of the membranous web is unknown; however, one way that membrane proteins induce membrane curvature and vesicle formation is by making oligomeric complexes. Multiple lines of evidence suggest that NS4B forms oligomers, involving a number of homo- and heterotypic interactions [125, 133, 134]. Mutations disrupting the NS4B membrane association and/or oligomerization severely impair the size and morphology of membrane vesicles with concomitant effects on virus replication [125, 134].

Different NS4B functions, including RNA binding, oligomerization, and enzymatic activities (NTP hydrolase and adenylate kinase), represent potential drug targets. It is therefore no surprise that NS4B has been pursued as a target for antiviral therapy, although as yet with little clinical success (reviewed in [135]).

5.7 *NS5A*

NS5A, the only HCV nonstructural protein without any apparent enzymatic activity, is perhaps the most enigmatic HCV protein and also the target of the most potent

clinically available drugs. This multifunctional, RNA-binding phosphoprotein plays essential roles in HCV RNA replication, virion assembly, and disease pathogenesis through its interactions with viral and cellular proteins (reviewed in [136]).

NS5A is a ~450-aa protein that is anchored on the ER membrane through an N-terminal amphipathic α -helix (Fig. 3). It comprises three domains (DI, II, and III) separated by two trypsin-sensitive low complexity sequences (LCS I and II) [137]. DI contains zinc-binding and RNA-binding motifs, is well conserved across HCV genotypes, plays essential roles in HCV RNA replication, and is the only domain crystallized so far [138]. The intrinsically unfolded DII and DIII are relatively less conserved than DI [139, 140]. Approximately, two-third of DII can be deleted without significant effects on HCV replication and virus particle production in culture [141]. DIII on the other hand is not needed for replication, as it can be deleted [141] or engineered to accommodate heterologous proteins such as GFP [142, 143], with no significant effects on viral RNA synthesis. However, this domain is essential for virion assembly, presumably through its interaction with the HCV core protein at the assembly site [141].

NS5A exists in the HCV infected cells in two major phospho-isoforms: p56 or basal phosphorylation form and p58 or hyperphosphorylation form. The p58 is converted from p56 and requires polyprotein processing [144]. Interestingly, the p56:p58 ratio appears to function as a molecular switch between virus replication and assembly, with p56 favoring RNA replication and p58 mediating a transition to virion assembly. This model stems from the observations that a high p56:p58 ratio achieved through genetic or chemical inhibition of NS5A hyperphosphorylation enhances HCV RNA replication in cell culture [145–147], while it inhibits HCV propagation in chimpanzees [148] and impairs virion assembly in the HCVcc-based experiments [149]. It should however be noted that some HCV isolates have yielded results which do not agree with the above model. One example is of the HCV JFH1 isolate for which high p56:p58 ratio has been shown to inhibit rather than enhance RNA replication [150].

NS5A is an integral part of the HCV replication complexes (RC), and several NS5A inhibitors have been shown to disrupt RC formation [151]. However, it is unclear if NS5A is directly recruited to RC through its N-terminal membrane anchor or if other viral or host proteins are involved. At least some evidence suggests that the NS4B protein may contribute to NS5A membrane localization [152]. Similarly, at least two host membrane-anchor proteins, VAPA [153] and FBL2 [154], bind with NS5A and are presumed to play a role in NS5A membrane localization. Inside the RC, NS5A binds with other components of the viral replicase machinery and seems to recruit host proteins essential for HCV replication. For example, NS5A-mediated recruitment of two host enzymes, PI4KIII α [155] and cyclophilin A (CYPA) [156], is essential for the formation of functional RC. Several other proteins have been shown to bind NS5A, but the significance of these interactions is poorly understood.

NS5A plays important roles in virus particle production by channeling the progeny viral RNA to LDs, the assembly site. This function requires NS5A interaction with the core protein located on the surface of LDs and appears to be mediated

through NS5A DIII, as deletion of this domain blocks core-mediated NS5A trafficking to LDs and inhibits virion production. In contrast, this deletion has no effect on NS5A localization to the RC or HCV RNA replication (reviewed in [28]).

Due to the lack of a known enzymatic activity, NS5A was once considered a non-druggable protein. However, some of its important and extensively validated catalytic binding partners such as CYPA and PI4KIII α , both of which are essential for HCV replication, have been long pursued as antiviral drug targets. An unexpected discovery came in 2010, when a small molecule, BMS-790052 (Daclatasvir), was found to directly target NS5A [157]. This compound inhibits HCV with half-maximal inhibitory concentration (IC₅₀) in the low picomolar range, and compounds in this class are now part of the HCV standard-of-care treatment. How daclatasvir hinders NS5A activity is an active area of investigation, but it seems to interfere with multiple functions, including NS5A hyperphosphorylation, dimerization, and NS5A protein-protein interactions, partly explaining the unusually high potency of this compound (reviewed in [158]).

5.8 NS5B

HCV NS5B polymerase is the catalytic subunit of the viral replicase complex responsible for two RNA polymerization steps. In the first step, it uses HCV genomic RNA as a template to generate the complementary negative-strand RNA intermediate, which, in the second step, serves as a template for the synthesis of the positive-strand progeny RNA. NS5B has been extensively characterized and contains all the sequence and structural motifs conserved among known viral RNA-dependent RNA polymerases (RdRp) [61, 159, 160]. The N-terminal 530 amino acids of this 591-aa protein constitute the catalytic domain that is connected to the C-terminal 21-aa membrane-anchor domain through a 40-aa linker (Fig. 3). The membrane association of NS5B is essential, as deletion of the C-terminal domain abrogates HCV RNA replication in cell culture [161]; however, this domain contributes minimally to nucleotide polymerization [162].

As a general feature of RdRp, the NS5B catalytic domain has discernable finger, thumb, and palm subdomains in reference to the catalytic domain's likeness to a cupped right hand. The purified catalytic domain is capable of performing de novo and primer-dependent RNA synthesis, requiring only divalent metals such as Mg²⁺ or Mn²⁺ as cofactors [163]; however, HCV RNA synthesis in vivo likely occurs by de novo initiation. The catalytic nucleotidyl transferase pocket is located in the palm subdomain and contains the signature sequences of D²²⁰_{xxxx}D²²⁵ and G³¹⁷D³¹⁸D³¹⁹ ("x" represent any residue). The D²²⁰ and D³¹⁸ chelate two catalytic metal ions that are crucial for the polymerase function. The template RNA enters the active site through a hydrophobic groove between the fingers and thumb subdomains, while NTPs access the active site via a specific tunnel beginning at the backside periphery of the palm subdomain.

Structural studies have revealed two unusual features of the NS5B polymerase [164–167]. First, the fingers and thumb subdomains heavily interact with each other resulting in a completely encircled active site and low intra-domain and possibly inter-domain flexibility, which may restrict structural rearrangements generally required during nucleotide binding and polymerization. Second, a thumb subdomain β -hairpin loop of 12 amino acids protrudes into the active site, presumably contributing to the positioning of the HCV 3' terminus for correct initiation [168]. Also, the β loop imposes steric hindrance against docking the dsRNA, thus ensuring the preferential use of the HCV 3' terminus as a template for de novo initiation of RNA synthesis. Consistently, deleting the β loop promotes primer-dependent RNA synthesis, which requires binding of several base pairs of dsRNA [168].

The de novo RNA synthesis is a complex process, and a recent study that captured snapshots of the ternary assemblies (NS5B, template RNA, and NTPs) at different stages of HCV RNA replication suggests the following sequence of events [167] (Fig. 4): (1) in the NS5B apo enzyme, the active site is partially occupied by the β loop and the C-terminus linker; (2) once the 3' end of the HCV RNA and an initiating nucleotide enter the active site, the β loop and the C-terminus linker are slightly retracted (~ 5 Å) to create space for the formation of a dinucleotide primer; (3) the first nucleotidyl transferase reaction then generates a dinucleotide primer; (4) extension of this primer by one to three nucleotides completely displaces the β loop and the C-terminus linker, opening the RNA duplex exit channel; and (5) once the “path” is cleared of the β loop and the C-terminus linker, the polymerase transitions from the dinucleotide-primed state to a rapid, processive elongation state.

NS5B does not replicate the viral genome in isolation, rather as a part of the replicase complex anchored on the ER membrane. The replicase complex is thought to comprise the host and viral proteins that might affect HCV replication activity. For example, protein kinase C-related kinase, PRK2, has been proposed to phosphorylate NS5B and thereby regulate HCV replication [169]. Similarly, NS5B binds to NS3, and the NS3 interacts with NS4A and possibly NS4B and NS5B [170]. NS5B has also been shown to directly interact with NS5A, which can possibly modulate NS5B functions [171]. How this complex array of interactions affects and/or regulates NS5B-catalyzed RNA synthesis is unclear.

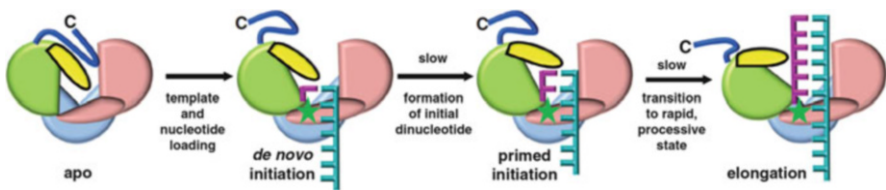


Fig. 4 Model of HCV replication by NS5B. NS5B C-terminus and the β loop that occlude the RNA binding groove of the apo form of the polymerase are shown in blue and yellow color, respectively. See text for details of each step. Reproduced from Appleby et al. [167] with permission from the American Association for the Advancement of Science (AAAS)

Along with the NS3 protease, NS5B has long been extensively pursued as the most druggable HCV protein (reviewed in [172]). Although both nucleoside and non-nucleoside inhibitors of NS5B have been reported, only nucleoside inhibitors have demonstrated broad genotype coverage and high resistance barrier both in the laboratory and in human clinical studies. For these reasons, the nucleotide inhibitor sofosbuvir is now a backbone for several of the current interferon-free anti-HCV regimens containing HCV protease and NS5A inhibitors, with cure rates approaching almost 100%. The details of these inhibitors and their mechanisms of action are provided in subsequent chapters.

6 Summary

Thanks to the years of elegant research, we now have extensive knowledge of HCV proteins and how they contribute to the virus life cycle and pathogenesis. However, still much remains to be learnt. For example, high-resolution structures of most of the viral full-length membrane proteins are yet to be solved. Although X-ray crystallography of membrane proteins remains challenging, continuously improving methodologies and increasingly popular alternative systems such as cryo-EM should facilitate progress on this front. The ultimate success would be to solve the structure of the entire HCV replicase complex that will yield insights into the stoichiometric ratios and functions of individual replicase components. These structural and the associated functional studies will deepen our understanding of the replication mechanisms of HCV and potentially other positive-strand RNA viruses.

7 HCV Animal Studies

While the study of HCV molecular biology and the development of antivirals have greatly benefited from the availability of cell culture models, the key contributions of animal studies toward discovery of HCV and establishment of *in vitro* culture systems cannot be overstated. As the efforts to develop prophylactic HCV vaccines intensify, the use of animal models to test vaccine candidates and concepts will become even more important. In the next section, we provide an overview of HCV animal models, past and present, and their importance for studying HCV virology, immunology, and pathogenesis.

7.1 *Animal Models*

It took a decade from the discovery of HCV as the etiologic agent of non-A, non-B hepatitis (NANBH) in 1989 [173] to the development of HCV replicon system and

another 5 years to establish an HCV infectious cell culture system that would allow the study of the entire viral life cycle *in vitro* [1, 2, 174]. These experimental systems were milestones in HCV research that paved the way for the development of HCV DAAs that achieve a cure from chronic HCV infection [175]. On the organismal level, analyses of samples from HCV-infected patients have provided valuable insights into the natural history of infection, host immune responses, and pathogenesis [176]. Clinical research on HCV, however, is limited by the heterogeneity of human study cohorts and restricted access to human liver tissue.

HCV has a narrow host tropism limited only to humans and chimpanzees [177]. Studies in chimpanzees led to the discovery of HCV and were essential for many other breakthroughs in HCV research [178]. However, studies in these nonhuman primates were hampered by limited availability, high costs, and ethical concerns. The latter eventually led to a moratorium on government-funded chimpanzee research in 2015. Given these limitations, significant effort has been put into the development of alternative animal models for HCV.

Various species, such as woodchucks and numerous Old and New World monkeys, have been challenged with HCV and shown to be resistant [179–181]. Interestingly, the tree shrew (*Tupaia belangeri*) is susceptible to HCV infection [182]. However, the utility of this outbred species as a small animal model of HCV infection has been limited.

Numerous approaches have been taken to develop laboratory mouse models of HCV infection, including transgenic expression of viral proteins, xenotransplantation, genetic humanization, and viral adaptation [183]. Finally, HCV-related animal hepaciviruses provide the possibility to develop surrogate models of HCV infection [184].

In this section of the chapter, we discuss the chimpanzee model and selected HCV mouse models as well as models based on novel animal hepaciviruses in the context of HCV drug and vaccine development (see Table 1).

7.2 Chimpanzees

Chimpanzees are the only species besides humans that is readily susceptible to HCV infection. This first became apparent in the 1970s when NANBH virus was discovered as a new hepatitis-causing agent in human blood products and the only animal susceptible to the mysterious virus was a chimpanzee [185–187]. Ever since the chimpanzee model has played an essential role in HCV research.

In 1989, HCV was discovered as the etiological agent of NANBH by using the serum of an experimentally infected chimpanzee [173]. In the following decade, experiments in which *in vitro* transcribed viral RNA was directly injected into the liver of chimpanzees were essential to define the sequence of a full-length infectious clone [148, 188]. This was a prerequisite for the development of HCV replicon system, the first cell culture model of HCV [1, 174]. However, until the first HCV infectious cell culture system was developed in 2005, the chimpanzee remained the

Table 1 Summary of animal models for HCV and related hepaciviruses

Model	Infection	Immune response	Drug and antibody testing	Vaccine testing
<i>Hepatitis C virus</i>				
Chimpanzees	Acute and chronic	Yes, fully immune-competent	Yes	Yes
Liver chimeric mice	Chronic	No, highly immune-deficient	Yes	No
HCV entry factor transgenic mice	Prolonged low level viremia	No, immune-deficient	Yes	No
<i>HCV-related hepaciviruses</i>				
Monkeys (GBV-B)	Acute and chronic	Yes, fully immune-competent	n.d.	n.d.
Horses (NPHV)	Acute and chronic	Yes, fully immune-competent	n.d.	n.d.
Rats (RHV/NrHV)	Chronic	Yes, fully immune-competent	Yes	n.d.
Mice (RHV/NrHV)	Acute, chronic after transient immunosuppression	Yes, fully immune-competent	n.d.	n.d.

n.d. not determined

only experimental model recapitulating the entire HCV life cycle. Chimpanzees are susceptible to all six HCV genotypes, and infection can be initiated by intravenous injection of clinical isolates or HCVcc or by intrahepatic injection of in vitro transcribed RNA of infectious HCV cDNA clones [2, 185, 187–189].

The course of HCV infection in chimpanzees has been well characterized and differs from that in humans [177]. In humans, around 70% of infected individuals develop chronic infection, which frequently progresses to liver fibrosis and hepatocellular carcinoma (HCC). In contrast, chimpanzees mostly clear HCV in the acute phase of infection, and the animals that progress to chronicity do not develop fibrosis and HCC [178].

Nevertheless, the chimpanzee model has been of critical importance for defining antiviral immune responses and the nature of protective immunity following reinfection. Importantly, results from these immunological studies are in line with observations from HCV infection in humans. HCV infection in chimpanzees induces significant innate and adaptive immune responses in peripheral blood and liver and is associated with elevated ALT levels and hepatitis [190–193]. Acute clearance is associated with a strong hepatic innate immune response involving upregulation of hundreds of interferon-stimulated genes (ISGs) in hepatocytes and the expansion of HCV-specific CD4+ and CD8+ T cells [192–194]. The chronic phase of disease is

characterized by persistent viremia, sustained expression of intrahepatic ISGs, emergence of viral escape mutations in T cell epitopes, and mild hepatitis [192, 195, 196].

Experiments in chimpanzees further showed that clearance of a primary infection does not provide complete protective immunity against challenges with homologous or heterologous viruses [197, 198]. However, HCV viremia was often significantly shorter following reinfection and the likelihood of chronic infection reduced. Rapid HCV clearance post reinfection was associated with the induction of an HCV-specific memory T cell response. Antibody-mediated depletion of CD4+ or CD8+ T cells prolonged HCV viremia after re-challenge, thus directly demonstrating the critical role of both lymphocyte subsets in the clearance of HCV infection [199, 200]. Chimpanzees were also used to show that neutralizing antibodies may confer partial protection in primary HCV infection and upon reinfection [201, 202].

Chimpanzees have also been used to test numerous HCV therapeutic strategies, such as proof-of-concept that an interferon-free cure of HCV infection is possible with combinations of DAAs [203]. Further, it was shown that blockade of the liver-specific HCV host factor miR-122 by an antisense oligonucleotide prevents viral replication in vivo and leads to a slow but consistent decline of HCV viremia [204].

Chimpanzee studies have provided important insights into HCV vaccine design, and the animals have been used to assess the preclinical efficacy of vaccine candidates [205]. Immunization with an antibody vaccine comprising recombinant envelope E1/E2 glycoproteins or with a T cell vaccine consisting of adenovirus or plasmid DNA expressing HCV nonstructural genes has not led to induction of sterilizing immunity, but has prevented chronicity following experimental infection in chimpanzees [206, 207].

Finally the chimpanzee studies provided first insights into the functionality of the antiviral immune response post DAA cure. One animal cured of chronic infection with DAAs showed expansion of HCV-specific T cells post re-challenge but eventually progressed to a second chronic infection indicating that a DAA cure might not result in protective immunity [208]. These preliminary results may have further implications for vaccine design.

Overall chimpanzees have been of great importance for HCV research, and now historical studies in this model remain the gold standard for all other animal models.

7.3 HCV Mouse Models

Laboratory mice are the favorite model organism of biomedical research with numerous genetic variants and tools available to perform in-depth mechanistic studies. Consequently, significant effort has been put into the development of mouse models of HCV infection [209]. Since mice are resistant to natural HCV infection, sophisticated approaches were necessary to render them susceptible to

infection. Here we outline three strategies: (1) xenotransplantation, (2) genetic humanization, and (3) viral adaptation.

7.3.1 Xenotransplantation

Humanization of the mouse liver by transplantation of HCV-permissive human cells, such as hepatoma cell lines or primary hepatocytes, has been evolved as the most widely used strategy to study HCV infection in rodents. Xenotransplantation models have contributed to our understanding of many aspects of HCV biology, such as viral entry and mechanisms of neutralizing antibodies. However, a prerequisite of xenotransplantation is immunodeficiency of the host to prevent xenograft rejection. Thus, these models are not suitable to study antiviral immune responses. Here we describe distinct approaches of liver xenotransplantation and highlight strategies to overcome the lack of immune responses in these models.

Hepatoma Cell Transplantation Models

The human Huh7 hepatoma cell line containing an HCV replicon can be transplanted into severe combined immunodeficient (SCID) mice. In this model, HCV RNA replication was detectable *in vivo*, and responses to antiviral treatment such as interferon- α (IFN- α) could be analyzed [210]. A recent study from 2017 further developed the replicon cell transplantation mouse model to overcome its immune deficiency [211]. In this model, instead of human hepatoma cells, an H-2b positive mouse hepatoma cell line previously shown to support the HCV replicon [212] was transplanted into syngeneic immune-competent H-2b-restricted mice (C57BL/6). This approach led to HCV replication *in vivo* and the induction of HCV NS3- and NS4-specific T cell responses [211]. This model may become useful for HCV vaccine development. However, one has to keep in mind that immune responses induced against a replicon-containing hepatoma cell line are likely to be different from immune responses elicited during a natural infection.

Human Liver Chimeric Mice

In human liver chimeric mouse models, the liver of mice is xeno-engrafted with primary human hepatocytes. This can be achieved by intrasplenic injections of human cells into immunodeficient mice carrying a genetically engineered liver injury. The liver has a remarkable regenerative capacity upon injury, and the induction of murine liver injury before xenotransplantation gives human hepatocytes a growth and engraftment advantage. Two different liver injury mouse models are commonly used to generate liver chimeric mice: (1) urokinase plasminogen activator (alb-uPA) transgenic mice in which transgenic overexpression of uPA under the albumin promoter leads to liver injury [213, 214] and (2) fumaryl acetoacetate

hydrolase (FAH^{-/-})-deficient mice in which defects in the tyrosine breakdown pathway lead to accumulation of hepatotoxic metabolites [215, 216]. When uPA mice are backcrossed on the immunodeficient strain SCID and FAH^{-/-} mice on the RAG2^{-/-} IL-2R^{null} strain, respectively, the resulting uPA-SCID and FRG mouse models can achieve high levels of human liver cell chimerism and susceptibility to HCV infection with high titer viremia [214, 217–219].

Both the uPA-SCID and the FRG model have been widely used in HCV research [220]. Studies in these mice have contributed to our current understanding of basic aspects of HCV virology, the viral life cycle, and HCV particle composition [221]. Further, it has been shown that broadly neutralizing antibodies targeting viral envelope proteins as well as antibodies specific for HCV entry factors can protect against infection or abrogate a chronic infection in vivo in human liver chimeric mice [222–226]. Finally, these models have been proven useful for the preclinical evaluation of HCV DAAs [227, 228].

Significant effort has also been put into overcoming the immune deficiency in liver chimeric mice to broaden their application to immunological studies. A strategy to achieve this is to combine the xenotransplantation of human hepatocytes with that of human hematopoietic stem cells (HSC) into one immunodeficient host [183, 229]. In fact, approaches to engraft mice with human immune cells by transplantation of human fetal liver or cord blood-derived HSC have been developed for decades and applied in many research fields [230]. Only recently, however, the successful double engraftment of human hepatocytes and immune cells into mice was reported [231–233].

Despite significant progress, these complicated models still suffer from a variety of shortcomings in the functionality of the transplanted human immune system, e.g., caused by mismatches in mouse and human hematopoietic cytokines or MHC molecules [230]. These problems currently limit their utility to study HCV-specific immune responses or vaccine strategies. Efforts to improve these models will hopefully solve these caveats in the coming years.

7.3.2 Genetic Humanization of Mice

Genetic manipulation of the host, such as expression of human host factors or inactivation of inhibitory murine molecules, has been explored as another strategy to develop an HCV mouse model. For this approach, a detailed knowledge of factors that define HCV host tropism is necessary. Most progress in this regard has been made at the level of viral entry into hepatocytes. It has been shown that CD81, SR-B1, CLDN1, and OCLN represent the minimal set of entry factors required for HCV uptake into mouse hepatocytes and that CD81 and OCLN need to be of human origin [234]. Based on this knowledge, a genetically humanized C57BL/6 mouse model expressing all four human entry factors was constructed and shown to support HCV entry into the mouse liver in vivo [235, 236]. This model was then used to evaluate the efficacy of HCV envelope-specific neutralizing antibodies [237]. In addition, when innate immune signaling pathways (e.g., STAT-1 signaling) were blunted in

these mice, low levels of viral replication were detected suggesting that the entire HCV life cycle can be completed in mouse hepatocytes [235]. Using a similar approach, another study showed low-level HCV infection without immunosuppression in outbred ICR mice transgenic for CD81 and OCLN [238].

7.3.3 Viral Adaptation

A complementary approach to mouse humanization is the attempt to adapt HCV to entry and replication in mouse hepatocytes without the need of human factors. In fact, one adaptation strategy resulted in the selection of adaptive mutations in HCV E1 and E2 that enabled a so-called murine-tropic HCV (mtHCV) to enter mouse hepatocytes in vitro [239]. A recent follow-up study from 2016 further showed that mtHCV could infect the mouse liver in vivo. Viral replication, however, was not detected even when the mice were highly immune-compromised [240]. In conclusion, additional studies are needed to evaluate whether mice humanization and HCV mouse adaptation approaches can eventually lead to robust HCV replication in mice.

8 HCV-Related Hepaciviruses

For decades, the hepacivirus genus of the family *Flaviviridae* consisted of only two known members: HCV and GB virus B. In recent years, however, the phylogenetic diversity of hepaciviruses has expanded significantly [184, 241]. In 2011, a non-primate hepacivirus (NPHV) was discovered first in dogs and later in horses. Shortly thereafter more animal hepaciviruses were found in rodents, bats, cows, colobus monkeys, and even sharks. The discovery of these viruses reveals a so far unappreciated genetic diversity and host tropism of hepaciviruses and might help to provide new insight into HCV evolution and origin [242]. HCV-related hepaciviruses could also serve as a basis for the development of immune-competent surrogate HCV animal models. Here we discuss the potential of GB virus B, NPHV, and rodent hepaciviruses to serve as such models.

8.1 GB Virus B

GB virus B (GBV-B) was first described in 1967 following the experimental inoculation of marmosets with serum from a surgeon (GB: George Baker) suffering from acute hepatitis. In 1995 two viral genomes, GBV-A and GBV-B, were isolated from serum and liver of experimentally infected marmosets; however, only GBV-B caused hepatitis [243]. It has since been shown that a variety of other New World monkeys, such as tamarins and owl monkeys, are susceptible to GBV-B infection [244]. While GBV-B infection in monkeys is mostly acute and self-limiting, some

cases of chronic infection following intrahepatic inoculation of viral RNA have been reported [245]. Although GBV-B was supposedly isolated from a human sample, GBV-B infections in human populations have not been observed, and a potential viral reservoir in monkeys has also not been identified. As such the natural host of GBV-B remains unknown [184].

While HCV and GBV-B are related viruses with similar genome organization, there is significant divergence on the nucleotide and amino acid level. This limits the utility of GBV-B for HCV drug and vaccine testing.

8.2 *Non-primate Hepaciviruses*

In 2011, using high-throughput sequencing, a novel hepacivirus was identified in the respiratory tract of dogs during a respiratory illness outbreak in these animals [246]. The isolated virus was initially name canine hepacivirus (CHV). However, a follow-up screen performed in multiple species to further define the distribution and host tropism of this new virus revealed that CHV is actually most prevalent in horses and not in dogs [247, 248]. Following this discovery, the virus was renamed to non-primate hepacivirus (NPHV) [247]. NPHV is the closest known viral homolog to HCV with a nucleotide sequence convergence of approximately 50%. Multiple recent studies have characterized the natural course of infection and tissue tropism of NPHV in horses [249–251]. Collectively, these data show that NPHV causes a hepatotropic infection that can either be acute and self-limiting or progress to chronicity. Infection can be initiated by inoculation of horses with NPHV-positive horse plasma or intrahepatic injection of in vitro transcribed RNA derived from a NPHV cDNA clone [250].

Acute infection of NPHV is associated with mild hepatitis and liver damage. Interestingly, infection of immunodeficient foals led to significantly less pronounced liver disease as compared to immune-competent foals suggesting immune-mediated viral hepatitis [251]. Further, NPHV-infected horses showed activation of immune cells and delayed seroconversion. After clearance of primary infection, the horses were protected against reinfection [252].

In conclusion, NPHV infection in horses shows important similarities to HCV infection in humans. Thus this infection system might become a useful surrogate model to evaluate HCV vaccine strategies in the future. However, horses are large animals that are not genetically amenable or tractable, and there are limited equine-specific research tools available.

8.3 *Rodent Hepaciviruses*

In 2013, two studies independently reported the discovery of multiple rodent hepaciviruses (RHV) after screening over 5,000 individual rodents from 45 different

species [253, 254]. RHVs were isolated from species such as deer mice, desert wood rats, or bank voles. Further, in 2014 another report described the isolation of an RHV in rats from New York City, named Norway rat hepatitis virus (NrHV) [255]. Phylogenetic comparison of RHVs with other hepaciviruses revealed that RHVs are more divergent from HCV than NPHV, but closer to HCV than the primate virus GBV-B [184].

The identification of hepaciviruses in wild rodents opened the possibility for the development of small laboratory animal models of hepacivirus infection. In fact, a recent study provided a detailed characterization of NrHV infection in laboratory rats, thus establishing an immune-competent rat surrogate model for HCV [256]. Rats developed a hepatotropic and miR-122-dependent chronic infection upon challenge with NrHV-positive serum or intrahepatic inoculation with *in vitro* transcribed RNA from an infectious clone. While spontaneous clearance was not observed, rats could be cured by treatment with the HCV DAA sofosbuvir. Similar to HCV infection in humans, chronic NrHV infection in rats was characterized by sustained intrahepatic immune activation, including persistent upregulation of type 1 interferon pathways [256].

Rodent hepaciviruses were not discovered in wild house mice [257]. However, it was recently shown that NrHV infection is not restricted to rats and that the virus can efficiently replicate in laboratory mouse strains [258]. Immunodeficient mouse strains developed a chronic infection while fully immune-competent C57BL/6 and Balb/c mice cleared NrHV within 3–5 weeks. Similar to rats, NrHV infection in mice was hepatotropic and miR-122-dependent. Acute clearance in mice was associated with the induction of a strong intrahepatic immune response and acute hepatitis. Transient depletion of CD4+ T cells resulted in viral chronicity in immune-competent mice indicating a major role of T cells in clearance of NrHV infection [258]. This is consistent with the T cell depletion studies performed in HCV-infected chimpanzees. Similar to HCV reinfection in chimpanzees and humans, mice were also not completely protected against secondary NrHV infection.

Both, the NrHV/RHV rat and mouse models provide fully immune-competent rodent HCV surrogate models that share important similarities with HCV infection in chimpanzees and humans. Both models provide for the first time a platform to mechanistically study basic aspects of hepacivirus infection and immunity in the liver. The utility of these models for HCV vaccine development still needs to be determined. Given the significant genetic divergence between HCV and RHVs, it remains to be determined if RHV models will be useful for the preclinical testing of HCV vaccine strategies.

9 Concluding Remarks

From the discovery of HCV until today, the chimpanzees have remained the only immune-competent animal model of HCV infection. As such studies in these large apes have been instrumental for achieving the medical milestone of HCV cure.

Nevertheless numerous other animal models of HCV infection have also provided valuable insight into HCV biology and served as platforms to test drug and vaccine candidates. A remaining challenge for HCV research is the development of a protective vaccine. Novel immune-competent HCV models that allow the mechanistic studies of immune responses and potentially the prioritization of vaccine candidates might help to achieve this goal.

Acknowledgments We thank William Schneider for critical reading of the manuscript. We apologize to colleagues whose work was not cited due to space constraints.

Compliance with Ethical Standards

Funding We thank NIAID, NIDDK, NCI, the Greenberg Medical Research Institute, and the Starr Foundation for their financial support over the years.

Conflict of Interest The authors have no conflict of interest.

Ethical Approval This article does not contain any studies with human participants or animals performed by any of the authors.

References

1. Lohmann V et al (1999) Replication of subgenomic hepatitis C virus RNAs in a hepatoma cell line. *Science* 285:110–113
2. Wakita T et al (2005) Production of infectious hepatitis C virus in tissue culture from a cloned viral genome. *Nat Med* 11:791–796. <https://doi.org/10.1038/nm1268>
3. Lindenbach BD et al (2005) Complete replication of hepatitis C virus in cell culture. *Science* 309:623–626. <https://doi.org/10.1126/science.1114016>
4. Choo QL et al (1991) Genetic organization and diversity of the hepatitis C virus. *Proc Natl Acad Sci U S A* 88:2451–2455
5. Han JH et al (1991) Characterization of the terminal regions of hepatitis C viral RNA: identification of conserved sequences in the 5' untranslated region and poly(A) tails at the 3' end. *Proc Natl Acad Sci U S A* 88:1711–1715
6. Kolykhalov AA, Feinstone SM, Rice CM (1996) Identification of a highly conserved sequence element at the 3' terminus of hepatitis C virus genome RNA. *J Virol* 70:3363–3371
7. Tanaka T, Kato N, Cho MJ, Sugiyama K, Shimotohno K (1996) Structure of the 3' terminus of the hepatitis C virus genome. *J Virol* 70:3307–3312
8. Moradpour D, Penin F (2013) Hepatitis C virus proteins: from structure to function. *Curr Top Microbiol Immunol* 369:113–142. https://doi.org/10.1007/978-3-642-27340-7_5
9. Wang C, Sarnow P, Siddiqui A (1993) Translation of human hepatitis C virus RNA in cultured cells is mediated by an internal ribosome-binding mechanism. *J Virol* 67:3338–3344
10. Bradrick SS, Walters RW, Gromeier M (2006) The hepatitis C virus 3'-untranslated region or a poly(A) tract promote efficient translation subsequent to the initiation phase. *Nucleic Acids Res* 34:1293–1303. <https://doi.org/10.1093/nar/gkl019>
11. Bung C et al (2010) Influence of the hepatitis C virus 3'-untranslated region on IRES-dependent and cap-dependent translation initiation. *FEBS Lett* 584:837–842. <https://doi.org/10.1016/j.febslet.2010.01.015>

12. Song Y et al (2006) The hepatitis C virus RNA 3'-untranslated region strongly enhances translation directed by the internal ribosome entry site. *J Virol* 80:11579–11588. <https://doi.org/10.1128/JVI.00675-06>
13. Friebe P, Boudet J, Simorre JP, Bartenschlager R (2005) Kissing-loop interaction in the 3' end of the hepatitis C virus genome essential for RNA replication. *J Virol* 79:380–392. <https://doi.org/10.1128/JVI.79.1.380-392.2005>
14. Pirakitikulr N, Kohlway A, Lindenbach BD, Pyle AM (2016) The coding region of the HCV genome contains a network of regulatory RNA structures. *Mol Cell* 62:111–120. <https://doi.org/10.1016/j.molcel.2016.01.024>
15. Hijikata M, Kato N, Ootsuyama Y, Nakagawa M, Shimotohno K (1991) Gene mapping of the putative structural region of the hepatitis C virus genome by in vitro processing analysis. *Proc Natl Acad Sci U S A* 88:5547–5551
16. Grakoui A, Wychowski C, Lin C, Feinstone SM, Rice CM (1993) Expression and identification of hepatitis C virus polyprotein cleavage products. *J Virol* 67:1385–1395
17. Barth H et al (2006) Viral and cellular determinants of the hepatitis C virus envelope-heparan sulfate interaction. *J Virol* 80:10579–10590. <https://doi.org/10.1128/JVI.00941-06>
18. Jiang J et al (2012) Hepatitis C virus attachment mediated by apolipoprotein E binding to cell surface heparan sulfate. *J Virol* 86:7256–7267. <https://doi.org/10.1128/JVI.07222-11>
19. Lindenbach BD, Rice CM (2013) The ins and outs of hepatitis C virus entry and assembly. *Nat Rev Microbiol* 11:688–700. <https://doi.org/10.1038/nrmicro3098>
20. Ding Q, von Schaewen M, Ploss A (2014) The impact of hepatitis C virus entry on viral tropism. *Cell Host Microbe* 16:562–568. <https://doi.org/10.1016/j.chom.2014.10.009>
21. Blanchard E et al (2006) Hepatitis C virus entry depends on clathrin-mediated endocytosis. *J Virol* 80:6964–6972. <https://doi.org/10.1128/JVI.00024-06>
22. Hsu M et al (2003) Hepatitis C virus glycoproteins mediate pH-dependent cell entry of pseudotyped retroviral particles. *Proc Natl Acad Sci U S A* 100:7271–7276. <https://doi.org/10.1073/pnas.0832180100>
23. Meertens L, Bertaux C, Dragic T (2006) Hepatitis C virus entry requires a critical postinternalization step and delivery to early endosomes via clathrin-coated vesicles. *J Virol* 80:11571–11578. <https://doi.org/10.1128/JVI.01717-06>
24. Lohmann V (2013) Hepatitis C virus RNA replication. *Curr Top Microbiol Immunol* 369:167–198. https://doi.org/10.1007/978-3-642-27340-7_7
25. Murray CL, Jones CT, Rice CM (2008) Architects of assembly: roles of Flaviviridae non-structural proteins in virion morphogenesis. *Nat Rev Microbiol* 6:699–708. <https://doi.org/10.1038/nrmicro1928>
26. Paul D, Madan V, Bartenschlager R (2014) Hepatitis C virus RNA replication and assembly: living on the fat of the land. *Cell Host Microbe* 16:569–579. <https://doi.org/10.1016/j.chom.2014.10.008>
27. Miyanari Y et al (2007) The lipid droplet is an important organelle for hepatitis C virus production. *Nat Cell Biol* 9:1089–1097. <https://doi.org/10.1038/ncb1631>
28. Bartenschlager R, Penin F, Lohmann V, Andre P (2011) Assembly of infectious hepatitis C virus particles. *Trends Microbiol* 19:95–103. <https://doi.org/10.1016/j.tim.2010.11.005>
29. Gastaminza P et al (2008) Cellular determinants of hepatitis C virus assembly, maturation, degradation, and secretion. *J Virol* 82:2120–2129. <https://doi.org/10.1128/JVI.02053-07>
30. Vieyres G et al (2010) Characterization of the envelope glycoproteins associated with infectious hepatitis C virus. *J Virol* 84:10159–10168. <https://doi.org/10.1128/JVI.01180-10>
31. Wozniak AL et al (2010) Intracellular proton conductance of the hepatitis C virus p7 protein and its contribution to infectious virus production. *PLoS Pathog* 6:e1001087. <https://doi.org/10.1371/journal.ppat.1001087>
32. Gastaminza P, Kapadia SB, Chisari FV (2006) Differential biophysical properties of infectious intracellular and secreted hepatitis C virus particles. *J Virol* 80:11074–11081. <https://doi.org/10.1128/JVI.01150-06>
33. Bradley D et al (1991) Hepatitis C virus: buoyant density of the factor VIII-derived isolate in sucrose. *J Med Virol* 34:206–208
34. Hijikata M et al (1993) Equilibrium centrifugation studies of hepatitis C virus: evidence for circulating immune complexes. *J Virol* 67:1953–1958

35. Cai Z et al (2005) Robust production of infectious hepatitis C virus (HCV) from stably HCV cDNA-transfected human hepatoma cells. *J Virol* 79:13963–13973. <https://doi.org/10.1128/JVI.79.22.13963-13973.2005>
36. Aizaki H et al (2008) Critical role of virion-associated cholesterol and sphingolipid in hepatitis C virus infection. *J Virol* 82:5715–5724. <https://doi.org/10.1128/JVI.02530-07>
37. Merz A et al (2011) Biochemical and morphological properties of hepatitis C virus particles and determination of their lipidome. *J Biol Chem* 286:3018–3032. <https://doi.org/10.1074/jbc.M110.175018>
38. Friebe P, Lohmann V, Krieger N, Bartenschlager R (2001) Sequences in the 5' nontranslated region of hepatitis C virus required for RNA replication. *J Virol* 75:12047–12057. <https://doi.org/10.1128/JVI.75.24.12047-12057.2001>
39. Wang C, Le SY, Ali N, Siddiqui A (1995) An RNA pseudoknot is an essential structural element of the internal ribosome entry site located within the hepatitis C virus 5' noncoding region. *RNA* 1:526–537
40. Pestova TV, Shatsky IN, Fletcher SP, Jackson RJ, Hellen CU (1998) A prokaryotic-like mode of cytoplasmic eukaryotic ribosome binding to the initiation codon during internal translation initiation of hepatitis C and classical swine fever virus RNAs. *Genes Dev* 12:67–83
41. Berry KE, Waghray S, Mortimer SA, Bai Y, Doudna JA (2011) Crystal structure of the HCV IRES central domain reveals strategy for start-codon positioning. *Structure* 19:1456–1466. <https://doi.org/10.1016/j.str.2011.08.002>
42. Ji H, Fraser CS, Yu Y, Leary J, Doudna JA (2004) Coordinated assembly of human translation initiation complexes by the hepatitis C virus internal ribosome entry site RNA. *Proc Natl Acad Sci U S A* 101:16990–16995. <https://doi.org/10.1073/pnas.0407402101>
43. Locker N, Easton LE, Lukavsky PJ (2007) HCV and CSFV IRES domain II mediate eIF2 release during 80S ribosome assembly. *EMBO J* 26:795–805. <https://doi.org/10.1038/sj.emboj.7601549>
44. Pestova TV, de Breyne S, Pisarev AV, Abaeva IS, Hellen CU (2008) eIF2-dependent and eIF2-independent modes of initiation on the CSFV IRES: a common role of domain II. *EMBO J* 27:1060–1072. <https://doi.org/10.1038/emboj.2008.49>
45. Jopling CL, Yi M, Lancaster AM, Lemon SM, Sarnow P (2005) Modulation of hepatitis C virus RNA abundance by a liver-specific MicroRNA. *Science* 309:1577–1581. <https://doi.org/10.1126/science.1113329>
46. Jopling CL, Schutz S, Sarnow P (2008) Position-dependent function for a tandem microRNA miR-122-binding site located in the hepatitis C virus RNA genome. *Cell Host Microbe* 4:77–85. <https://doi.org/10.1016/j.chom.2008.05.013>
47. Li Y, Masaki T, Yamane D, McGivern DR, Lemon SM (2013) Competing and noncompeting activities of miR-122 and the 5' exonuclease Xrn1 in regulation of hepatitis C virus replication. *Proc Natl Acad Sci U S A* 110:1881–1886. <https://doi.org/10.1073/pnas.1213515110>
48. Li Y, Yamane D, Lemon SM (2015) Dissecting the roles of the 5' exoribonucleases Xrn1 and Xrn2 in restricting hepatitis C virus replication. *J Virol* 89:4857–4865. <https://doi.org/10.1128/JVI.03692-14>
49. Sedano CD, Sarnow P (2014) Hepatitis C virus subverts liver-specific miR-122 to protect the viral genome from exoribonuclease Xrn2. *Cell Host Microbe* 16:257–264. <https://doi.org/10.1016/j.chom.2014.07.006>
50. Henke JI et al (2008) microRNA-122 stimulates translation of hepatitis C virus RNA. *EMBO J* 27:3300–3310. <https://doi.org/10.1038/emboj.2008.244>
51. Jangra RK, Yi M, Lemon SM (2010) Regulation of hepatitis C virus translation and infectious virus production by the microRNA miR-122. *J Virol* 84:6615–6625. <https://doi.org/10.1128/JVI.00417-10>
52. Masaki T et al (2015) miR-122 stimulates hepatitis C virus RNA synthesis by altering the balance of viral RNAs engaged in replication versus translation. *Cell Host Microbe* 17:217–228. <https://doi.org/10.1016/j.chom.2014.12.014>

53. Luna JM et al (2015) Hepatitis C virus RNA functionally sequesters miR-122. *Cell* 160:1099–1110. <https://doi.org/10.1016/j.cell.2015.02.025>
54. Janssen HL et al (2013) Treatment of HCV infection by targeting microRNA. *N Engl J Med* 368:1685–1694. <https://doi.org/10.1056/NEJMoa1209026>
55. Tanaka T, Kato N, Cho MJ, Shimotohno K (1995) A novel sequence found at the 3' terminus of hepatitis C virus genome. *Biochem Biophys Res Commun* 215:744–749. <https://doi.org/10.1006/bbrc.1995.2526>
56. Friebe P, Bartenschlager R (2002) Genetic analysis of sequences in the 3' nontranslated region of hepatitis C virus that are important for RNA replication. *J Virol* 76:5326–5338
57. Yi M, Lemon SM (2003) 3' nontranslated RNA signals required for replication of hepatitis C virus RNA. *J Virol* 77:3557–3568
58. You S, Rice CM (2008) 3' RNA elements in hepatitis C virus replication: kissing partners and long poly(U). *J Virol* 82:184–195. <https://doi.org/10.1128/JVI.01796-07>
59. Gwack Y, Kim DW, Han JH, Choe J (1996) Characterization of RNA binding activity and RNA helicase activity of the hepatitis C virus NS3 protein. *Biochem Biophys Res Commun* 225:654–659. <https://doi.org/10.1006/bbrc.1996.1225>
60. Huang L et al (2005) Hepatitis C virus nonstructural protein 5A (NS5A) is an RNA-binding protein. *J Biol Chem* 280:36417–36428. <https://doi.org/10.1074/jbc.M508175200>
61. Lohmann V, Korner F, Herian U, Bartenschlager R (1997) Biochemical properties of hepatitis C virus NS5B RNA-dependent RNA polymerase and identification of amino acid sequence motifs essential for enzymatic activity. *J Virol* 71:8416–8428
62. Blight KJ, Rice CM (1997) Secondary structure determination of the conserved 98-base sequence at the 3' terminus of hepatitis C virus genome RNA. *J Virol* 71:7345–7352
63. Yi M, Lemon SM (2003) Structure-function analysis of the 3' stem-loop of hepatitis C virus genomic RNA and its role in viral RNA replication. *RNA* 9:331–345
64. Isken O et al (2003) Members of the NF90/NFAR protein group are involved in the life cycle of a positive-strand RNA virus. *EMBO J* 22:5655–5665. <https://doi.org/10.1093/emboj/cdg562>
65. Weinlich S et al (2009) IGF2BP1 enhances HCV IRES-mediated translation initiation via the 3'UTR. *RNA* 15:1528–1542. <https://doi.org/10.1261/rna.1578409>
66. Santolini E, Migliaccio G, La Monica N (1994) Biosynthesis and biochemical properties of the hepatitis C virus core protein. *J Virol* 68:3631–3641
67. McLauchlan J, Lemberg MK, Hope G, Martoglio B (2002) Intramembrane proteolysis promotes trafficking of hepatitis C virus core protein to lipid droplets. *EMBO J* 21:3980–3988. <https://doi.org/10.1093/emboj/cdf414>
68. Oehler V et al (2012) Structural analysis of hepatitis C virus core-E1 signal peptide and requirements for cleavage of the genotype 3a signal sequence by signal peptide peptidase. *J Virol* 86:7818–7828. <https://doi.org/10.1128/JVI.00457-12>
69. Okamoto K et al (2008) Intramembrane processing by signal peptide peptidase regulates the membrane localization of hepatitis C virus core protein and viral propagation. *J Virol* 82:8349–8361. <https://doi.org/10.1128/JVI.00306-08>
70. Kopp M, Murray CL, Jones CT, Rice CM (2010) Genetic analysis of the carboxy-terminal region of the hepatitis C virus core protein. *J Virol* 84:1666–1673. <https://doi.org/10.1128/JVI.02043-09>
71. Lussignol M et al (2016) Proteomics of HCV virions reveals an essential role for the nucleoporin Nup98 in virus morphogenesis. *Proc Natl Acad Sci U S A* 113:2484–2489. <https://doi.org/10.1073/pnas.1518934113>
72. Boulant S, Vanbelle C, Ebel C, Penin F, Lavergne JP (2005) Hepatitis C virus core protein is a dimeric alpha-helical protein exhibiting membrane protein features. *J Virol* 79:11353–11365. <https://doi.org/10.1128/JVI.79.17.11353-11365.2005>
73. Boulant S et al (2006) Structural determinants that target the hepatitis C virus core protein to lipid droplets. *J Biol Chem* 281:22236–22247. <https://doi.org/10.1074/jbc.M601031200>
74. Cristofari G et al (2004) The hepatitis C virus Core protein is a potent nucleic acid chaperone that directs dimerization of the viral (+) strand RNA in vitro. *Nucleic Acids Res* 32:2623–2631. <https://doi.org/10.1093/nar/gkh579>

75. Eng FJ et al (2009) Internal initiation stimulates production of p8 minicore, a member of a newly discovered family of hepatitis C virus core protein isoforms. *J Virol* 83:3104–3114. <https://doi.org/10.1128/JVI.01679-08>
76. Eng FJ et al (2018) Newly discovered hepatitis C virus minicores circulate in human blood. *Hepatol Commun* 2:21–28. <https://doi.org/10.1002/hep4.1125>
77. Branch AD, Stump DD, Gutierrez JA, Eng F, Walewski JL (2005) The hepatitis C virus alternate reading frame (ARF) and its family of novel products: the alternate reading frame protein/F-protein, the double-frameshift protein, and others. *Semin Liver Dis* 25:105–117. <https://doi.org/10.1055/s-2005-864786>
78. Cocquerel L et al (2002) Topological changes in the transmembrane domains of hepatitis C virus envelope glycoproteins. *EMBO J* 21:2893–2902. <https://doi.org/10.1093/emboj/cdf295>
79. Voisset C, Dubuisson J (2004) Functional hepatitis C virus envelope glycoproteins. *Biol Cell* 96:413–420. <https://doi.org/10.1016/j.biolcel.2004.03.008>
80. Khan AG et al (2014) Structure of the core ectodomain of the hepatitis C virus envelope glycoprotein 2. *Nature* 509:381–384. <https://doi.org/10.1038/nature13117>
81. Kong L et al (2013) Hepatitis C virus E2 envelope glycoprotein core structure. *Science* 342:1090–1094. <https://doi.org/10.1126/science.1243876>
82. Krey T et al (2010) The disulfide bonds in glycoprotein E2 of hepatitis C virus reveal the tertiary organization of the molecule. *PLoS Pathog* 6:e1000762. <https://doi.org/10.1371/journal.ppat.1000762>
83. Choukhi A, Ung S, Wychowski C, Dubuisson J (1998) Involvement of endoplasmic reticulum chaperones in the folding of hepatitis C virus glycoproteins. *J Virol* 72:3851–3858
84. Goffard A et al (2005) Role of N-linked glycans in the functions of hepatitis C virus envelope glycoproteins. *J Virol* 79:8400–8409. <https://doi.org/10.1128/JVI.79.13.8400-8409.2005>
85. Helle F, Duverlie G, Dubuisson J (2011) The hepatitis C virus glycan shield and evasion of the humoral immune response. *Viruses* 3:1909–1932. <https://doi.org/10.3390/v3101909>
86. Smit JM, Moesker B, Rodenhuis-Zybert I, Wilschut J (2011) Flavivirus cell entry and membrane fusion. *Viruses* 3:160–171. <https://doi.org/10.3390/v3020160>
87. Khan AG, Miller MT, Marcotrigiano J (2015) HCV glycoprotein structures: what to expect from the unexpected. *Curr Opin Virol* 12:53–58. <https://doi.org/10.1016/j.coviro.2015.02.004>
88. El Omari K et al (2014) Unexpected structure for the N-terminal domain of hepatitis C virus envelope glycoprotein E1. *Nat Commun* 5:4874. <https://doi.org/10.1038/ncomms5874>
89. Weiner AJ et al (1992) Evidence for immune selection of hepatitis C virus (HCV) putative envelope glycoprotein variants: potential role in chronic HCV infections. *Proc Natl Acad Sci U S A* 89:3468–3472
90. Farci P et al (1996) Prevention of hepatitis C virus infection in chimpanzees by hyperimmune serum against the hypervariable region 1 of the envelope 2 protein. *Proc Natl Acad Sci U S A* 93:15394–15399
91. Carrere-Kremer S et al (2002) Subcellular localization and topology of the p7 polypeptide of hepatitis C virus. *J Virol* 76:3720–3730
92. Griffin SD et al (2003) The p7 protein of hepatitis C virus forms an ion channel that is blocked by the antiviral drug, amantadine. *FEBS Lett* 535:34–38
93. Luik P et al (2009) The 3-dimensional structure of a hepatitis C virus p7 ion channel by electron microscopy. *Proc Natl Acad Sci U S A* 106:12712–12716. <https://doi.org/10.1073/pnas.0905966106>
94. Montserret R et al (2010) NMR structure and ion channel activity of the p7 protein from hepatitis C virus. *J Biol Chem* 285:31446–31461. <https://doi.org/10.1074/jbc.M110.122895>
95. Chandler DE, Penin F, Schulten K, Chipot C (2012) The p7 protein of hepatitis C virus forms structurally plastic, minimalist ion channels. *PLoS Comput Biol* 8:e1002702. <https://doi.org/10.1371/journal.pcbi.1002702>
96. Steinmann E, Pietschmann T (2010) Hepatitis C virus p7-a viroporin crucial for virus assembly and an emerging target for antiviral therapy. *Viruses* 2:2078–2095. <https://doi.org/10.3390/v2092078>

97. Grakoui A, McCourt DW, Wychowski C, Feinstone SM, Rice CM (1993) A second hepatitis C virus-encoded proteinase. *Proc Natl Acad Sci U S A* 90:10583–10587
98. Schregel V, Jacobi S, Penin F, Tautz N (2009) Hepatitis C virus NS2 is a protease stimulated by cofactor domains in NS3. *Proc Natl Acad Sci U S A* 106:5342–5347. <https://doi.org/10.1073/pnas.0810950106>
99. Kolykhalov AA, Mihalik K, Feinstone SM, Rice CM (2000) Hepatitis C virus-encoded enzymatic activities and conserved RNA elements in the 3' nontranslated region are essential for virus replication in vivo. *J Virol* 74:2046–2051
100. Pallaoro M et al (2001) Characterization of the hepatitis C virus NS2/3 processing reaction by using a purified precursor protein. *J Virol* 75:9939–9946. <https://doi.org/10.1128/JVI.75.20.9939-9946.2001>
101. Lorenz IC, Marcotrigiano J, Dentzer TG, Rice CM (2006) Structure of the catalytic domain of the hepatitis C virus NS2-3 protease. *Nature* 442:831–835. <https://doi.org/10.1038/nature04975>
102. Hijikata M et al (1993) Two distinct proteinase activities required for the processing of a putative nonstructural precursor protein of hepatitis C virus. *J Virol* 67:4665–4675
103. Santolini E, Pacini L, Fipaldini C, Migliaccio G, Monica N (1995) The NS2 protein of hepatitis C virus is a transmembrane polypeptide. *J Virol* 69:7461–7471
104. Jirasko V et al (2008) Structural and functional characterization of nonstructural protein 2 for its role in hepatitis C virus assembly. *J Biol Chem* 283:28546–28562. <https://doi.org/10.1074/jbc.M803981200>
105. Jirasko V et al (2010) Structural and functional studies of nonstructural protein 2 of the hepatitis C virus reveal its key role as organizer of virion assembly. *PLoS Pathog* 6: e1001233. <https://doi.org/10.1371/journal.ppat.1001233>
106. Phan T, Beran RK, Peters C, Lorenz IC, Lindenbach BD (2009) Hepatitis C virus NS2 protein contributes to virus particle assembly via opposing epistatic interactions with the E1-E2 glycoprotein and NS3-NS4A enzyme complexes. *J Virol* 83:8379–8395. <https://doi.org/10.1128/JVI.00891-09>
107. Stapleford KA, Lindenbach BD (2011) Hepatitis C virus NS2 coordinates virus particle assembly through physical interactions with the E1-E2 glycoprotein and NS3-NS4A enzyme complexes. *J Virol* 85:1706–1717. <https://doi.org/10.1128/JVI.02268-10>
108. Yi M, Ma Y, Yates J, Lemon SM (2009) Trans-complementation of an NS2 defect in a late step in hepatitis C virus (HCV) particle assembly and maturation. *PLoS Pathog* 5:e1000403. <https://doi.org/10.1371/journal.ppat.1000403>
109. de la Fuente C, Goodman Z, Rice CM (2013) Genetic and functional characterization of the N-terminal region of the hepatitis C virus NS2 protein. *J Virol* 87:4130–4145. <https://doi.org/10.1128/JVI.03174-12>
110. Bosen B, Granio O, Bartenschlager R, Cosset FL (2011) A concerted action of hepatitis C virus p7 and nonstructural protein 2 regulates core localization at the endoplasmic reticulum and virus assembly. *PLoS Pathog* 7:e1002144. <https://doi.org/10.1371/journal.ppat.1002144>
111. Popescu CI et al (2011) NS2 protein of hepatitis C virus interacts with structural and non-structural proteins towards virus assembly. *PLoS Pathog* 7:e1001278. <https://doi.org/10.1371/journal.ppat.1001278>
112. De Francesco R, Steinkuhler C (2000) Structure and function of the hepatitis C virus NS3-NS4A serine proteinase. *Curr Top Microbiol Immunol* 242:149–169
113. Grakoui A, McCourt DW, Wychowski C, Feinstone SM, Rice CM (1993) Characterization of the hepatitis C virus-encoded serine proteinase: determination of proteinase-dependent polyprotein cleavage sites. *J Virol* 67:2832–2843
114. Pietschmann T, Lohmann V, Rutter G, Kurpanek K, Bartenschlager R (2001) Characterization of cell lines carrying self-replicating hepatitis C virus RNAs. *J Virol* 75:1252–1264. <https://doi.org/10.1128/JVI.75.3.1252-1264.2001>
115. Herod MR, Jones DM, McLauchlan J, McCormick CJ (2012) Increasing rate of cleavage at boundary between non-structural proteins 4B and 5A inhibits replication of hepatitis C virus. *J Biol Chem* 287:568–580. <https://doi.org/10.1074/jbc.M111.311407>

116. Brass V et al (2008) Structural determinants for membrane association and dynamic organization of the hepatitis C virus NS3-4A complex. *Proc Natl Acad Sci U S A* 105:14545–14550. <https://doi.org/10.1073/pnas.0807298105>
117. Raney KD, Sharma SD, Moustafa IM, Cameron CE (2010) Hepatitis C virus non-structural protein 3 (HCV NS3): a multifunctional antiviral target. *J Biol Chem* 285:22725–22731. <https://doi.org/10.1074/jbc.R110.125294>
118. Lindenbach BD et al (2007) The C terminus of hepatitis C virus NS4A encodes an electrostatic switch that regulates NS5A hyperphosphorylation and viral replication. *J Virol* 81:8905–8918. <https://doi.org/10.1128/JVI.00937-07>
119. Phan T, Kohlway A, Dimberu P, Pyle AM, Lindenbach BD (2011) The acidic domain of hepatitis C virus NS4A contributes to RNA replication and virus particle assembly. *J Virol* 85:1193–1204. <https://doi.org/10.1128/JVI.01889-10>
120. Morikawa K et al (2011) Nonstructural protein 3-4A: the Swiss army knife of hepatitis C virus. *J Viral Hepat* 18:305–315. <https://doi.org/10.1111/j.1365-2893.2011.01451.x>
121. Gu M, Rice CM (2010) Three conformational snapshots of the hepatitis C virus NS3 helicase reveal a ratchet translocation mechanism. *Proc Natl Acad Sci U S A* 107:521–528. <https://doi.org/10.1073/pnas.0913380107>
122. Levin MK, Patel SS (2002) Helicase from hepatitis C virus, energetics of DNA binding. *J Biol Chem* 277:29377–29385. <https://doi.org/10.1074/jbc.M112315200>
123. Porter DJ et al (1998) Product release is the major contributor to kcat for the hepatitis C virus helicase-catalyzed strand separation of short duplex DNA. *J Biol Chem* 273:18906–18914
124. Kim JL et al (1998) Hepatitis C virus NS3 RNA helicase domain with a bound oligonucleotide: the crystal structure provides insights into the mode of unwinding. *Structure* 6:89–100
125. Gouttenoire J, Roingard P, Penin F, Moradpour D (2010) Amphipathic alpha-helix AH2 is a major determinant for the oligomerization of hepatitis C virus nonstructural protein 4B. *J Virol* 84:12529–12537. <https://doi.org/10.1128/JVI.01798-10>
126. Paul D et al (2011) NS4B self-interaction through conserved C-terminal elements is required for the establishment of functional hepatitis C virus replication complexes. *J Virol* 85:6963–6976. <https://doi.org/10.1128/JVI.00502-11>
127. Egger D et al (2002) Expression of hepatitis C virus proteins induces distinct membrane alterations including a candidate viral replication complex. *J Virol* 76:5974–5984
128. Gosert R et al (2003) Identification of the hepatitis C virus RNA replication complex in Huh-7 cells harboring subgenomic replicons. *J Virol* 77:5487–5492
129. Einav S et al (2008) Discovery of a hepatitis C target and its pharmacological inhibitors by microfluidic affinity analysis. *Nat Biotechnol* 26:1019–1027. <https://doi.org/10.1038/nbt.1490>
130. Einav S, Elazar M, Danieli T, Glenn JS (2004) A nucleotide binding motif in hepatitis C virus (HCV) NS4B mediates HCV RNA replication. *J Virol* 78:11288–11295. <https://doi.org/10.1128/JVI.78.20.11288-11295.2004>
131. Thompson AA et al (2009) Biochemical characterization of recombinant hepatitis C virus nonstructural protein 4B: evidence for ATP/GTP hydrolysis and adenylate kinase activity. *Biochemistry* 48:906–916. <https://doi.org/10.1021/bi801747p>
132. Gouttenoire J, Penin F, Moradpour D (2010) Hepatitis C virus nonstructural protein 4B: a journey into unexplored territory. *Rev Med Virol* 20:117–129. <https://doi.org/10.1002/rmv.640>
133. Yu GY, Lee KJ, Gao L, Lai MM (2006) Palmitoylation and polymerization of hepatitis C virus NS4B protein. *J Virol* 80:6013–6023. <https://doi.org/10.1128/JVI.00053-06>
134. Paul D et al (2018) Glycine zipper motifs in hepatitis C virus nonstructural protein 4B are required for the establishment of viral replication organelles. *J Virol* 92. <https://doi.org/10.1128/JVI.01890-17>
135. Wang Z, Chen X, Wu C, Xu H, Liu H (2016) Current drug discovery for anti-hepatitis C virus targeting NS4B. *Curr Top Med Chem* 16:1362–1371
136. Ross-Thriepland D, Harris M (2015) Hepatitis C virus NS5A: enigmatic but still promiscuous 10 years on! *J Gen Virol* 96:727–738. <https://doi.org/10.1099/jgv.0.000009>

137. Tellinghuisen TL, Marcotrigiano J, Gorbalenya AE, Rice CM (2004) The NS5A protein of hepatitis C virus is a zinc metalloprotein. *J Biol Chem* 279:48576–48587. <https://doi.org/10.1074/jbc.M407787200>
138. Tellinghuisen TL, Marcotrigiano J, Rice CM (2005) Structure of the zinc-binding domain of an essential component of the hepatitis C virus replicase. *Nature* 435:374–379. <https://doi.org/10.1038/nature03580>
139. Liang Y, Ye H, Kang CB, Yoon HS (2007) Domain 2 of nonstructural protein 5A (NS5A) of hepatitis C virus is natively unfolded. *Biochemistry* 46:11550–11558. <https://doi.org/10.1021/bi700776e>
140. Verdegem D et al (2011) Domain 3 of NS5A protein from the hepatitis C virus has intrinsic alpha-helical propensity and is a substrate of cyclophilin A. *J Biol Chem* 286:20441–20454. <https://doi.org/10.1074/jbc.M110.182436>
141. Appel N et al (2008) Essential role of domain III of nonstructural protein 5A for hepatitis C virus infectious particle assembly. *PLoS Pathog* 4:e1000035. <https://doi.org/10.1371/journal.ppat.1000035>
142. Moradpour D et al (2004) Insertion of green fluorescent protein into nonstructural protein 5A allows direct visualization of functional hepatitis C virus replication complexes. *J Virol* 78:7400–7409. <https://doi.org/10.1128/JVI.78.14.7400-7409.2004>
143. Schaller T et al (2007) Analysis of hepatitis C virus superinfection exclusion by using novel fluorochrome gene-tagged viral genomes. *J Virol* 81:4591–4603. <https://doi.org/10.1128/JVI.02144-06>
144. Neddermann P, Clementi A, De Francesco R (1999) Hyperphosphorylation of the hepatitis C virus NS5A protein requires an active NS3 protease, NS4A, NS4B, and NS5A encoded on the same polyprotein. *J Virol* 73:9984–9991
145. Appel N, Pietschmann T, Bartenschlager R (2005) Mutational analysis of hepatitis C virus nonstructural protein 5A: potential role of differential phosphorylation in RNA replication and identification of a genetically flexible domain. *J Virol* 79:3187–3194. <https://doi.org/10.1128/JVI.79.5.3187-3194.2005>
146. Evans MJ, Rice CM, Goff SP (2004) Phosphorylation of hepatitis C virus nonstructural protein 5A modulates its protein interactions and viral RNA replication. *Proc Natl Acad Sci U S A* 101:13038–13043. <https://doi.org/10.1073/pnas.0405152101>
147. Neddermann P et al (2004) Reduction of hepatitis C virus NS5A hyperphosphorylation by selective inhibition of cellular kinases activates viral RNA replication in cell culture. *J Virol* 78:13306–13314. <https://doi.org/10.1128/JVI.78.23.13306-13314.2004>
148. Bukh J et al (2002) Mutations that permit efficient replication of hepatitis C virus RNA in Huh-7 cells prevent productive replication in chimpanzees. *Proc Natl Acad Sci U S A* 99:14416–14421. <https://doi.org/10.1073/pnas.212532699>
149. Masaki T et al (2014) Involvement of hepatitis C virus NS5A hyperphosphorylation mediated by casein kinase I-alpha in infectious virus production. *J Virol* 88:7541–7555. <https://doi.org/10.1128/JVI.03170-13>
150. Fridell RA et al (2013) Intragenic complementation of hepatitis C virus NS5A RNA replication-defective alleles. *J Virol* 87:2320–2329. <https://doi.org/10.1128/JVI.02861-12>
151. McGivern DR et al (2014) Kinetic analyses reveal potent and early blockade of hepatitis C virus assembly by NS5A inhibitors. *Gastroenterology* 147:453–462.e457. <https://doi.org/10.1053/j.gastro.2014.04.021>
152. Biswas A, Treadaway J, Tellinghuisen TL (2016) Interaction between nonstructural proteins NS4B and NS5A is essential for proper NS5A localization and hepatitis C virus RNA replication. *J Virol* 90:7205–7218. <https://doi.org/10.1128/JVI.00037-16>
153. Gao L, Aizaki H, He JW, Lai MM (2004) Interactions between viral nonstructural proteins and host protein hVAP-33 mediate the formation of hepatitis C virus RNA replication complex on lipid raft. *J Virol* 78:3480–3488
154. Wang C et al (2005) Identification of FBL2 as a geranylgeranylated cellular protein required for hepatitis C virus RNA replication. *Mol Cell* 18:425–434. <https://doi.org/10.1016/j.molcel.2005.04.004>

155. Reiss S et al (2011) Recruitment and activation of a lipid kinase by hepatitis C virus NS5A is essential for integrity of the membranous replication compartment. *Cell Host Microbe* 9:32–45. <https://doi.org/10.1016/j.chom.2010.12.002>
156. Liu Z, Yang F, Robotham JM, Tang H (2009) Critical role of cyclophilin A and its prolyl-peptidyl isomerase activity in the structure and function of the hepatitis C virus replication complex. *J Virol* 83:6554–6565. <https://doi.org/10.1128/JVI.02550-08>
157. Gao M et al (2010) Chemical genetics strategy identifies an HCV NS5A inhibitor with a potent clinical effect. *Nature* 465:96–100. <https://doi.org/10.1038/nature08960>
158. Nakamoto S, Kanda T, Wu S, Shirasawa H, Yokosuka O (2014) Hepatitis C virus NS5A inhibitors and drug resistance mutations. *World J Gastroenterol* 20:2902–2912. <https://doi.org/10.3748/wjg.v20.i11.2902>
159. Behrens SE, Tomei L, De Francesco R (1996) Identification and properties of the RNA-dependent RNA polymerase of hepatitis C virus. *EMBO J* 15:12–22
160. Simister P et al (2009) Structural and functional analysis of hepatitis C virus strain JFH1 polymerase. *J Virol* 83:11926–11939. <https://doi.org/10.1128/JVI.01008-09>
161. Moradpour D et al (2004) Membrane association of the RNA-dependent RNA polymerase is essential for hepatitis C virus RNA replication. *J Virol* 78:13278–13284. <https://doi.org/10.1128/JVI.78.23.13278-13284.2004>
162. Yamashita T et al (1998) RNA-dependent RNA polymerase activity of the soluble recombinant hepatitis C virus NS5B protein truncated at the C-terminal region. *J Biol Chem* 273:15479–15486
163. Ranjith-Kumar CT et al (2002) Mechanism of de novo initiation by the hepatitis C virus RNA-dependent RNA polymerase: role of divalent metals. *J Virol* 76:12513–12525
164. Ago H et al (1999) Crystal structure of the RNA-dependent RNA polymerase of hepatitis C virus. *Structure* 7:1417–1426
165. Bressanelli S et al (1999) Crystal structure of the RNA-dependent RNA polymerase of hepatitis C virus. *Proc Natl Acad Sci U S A* 96:13034–13039
166. Lesburg CA et al (1999) Crystal structure of the RNA-dependent RNA polymerase from hepatitis C virus reveals a fully encircled active site. *Nat Struct Biol* 6:937–943. <https://doi.org/10.1038/13305>
167. Appleby TC et al (2015) Viral replication. Structural basis for RNA replication by the hepatitis C virus polymerase. *Science* 347:771–775. <https://doi.org/10.1126/science.1259210>
168. Hong Z et al (2001) A novel mechanism to ensure terminal initiation by hepatitis C virus NS5B polymerase. *Virology* 285:6–11. <https://doi.org/10.1006/viro.2001.0948>
169. Kim SJ, Kim JH, Kim YG, Lim HS, Oh JW (2004) Protein kinase C-related kinase 2 regulates hepatitis C virus RNA polymerase function by phosphorylation. *J Biol Chem* 279:50031–50041. <https://doi.org/10.1074/jbc.M408617200>
170. Piccininni S et al (2002) Modulation of the hepatitis C virus RNA-dependent RNA polymerase activity by the non-structural (NS) 3 helicase and the NS4B membrane protein. *J Biol Chem* 277:45670–45679. <https://doi.org/10.1074/jbc.M204124200>
171. Shirota Y et al (2002) Hepatitis C virus (HCV) NS5A binds RNA-dependent RNA polymerase (RdRP) NS5B and modulates RNA-dependent RNA polymerase activity. *J Biol Chem* 277:11149–11155. <https://doi.org/10.1074/jbc.M111392200>
172. Patil VM, Gupta SP, Samanta S, Masand N (2011) Current perspective of HCV NS5B inhibitors: a review. *Curr Med Chem* 18:5564–5597
173. Choo QL et al (1989) Isolation of a cDNA clone derived from a blood-borne non-A, non-B viral hepatitis genome. *Science* 244:359–362
174. Blight KJ, Kolykhalov AA, Rice CM (2000) Efficient initiation of HCV RNA replication in cell culture. *Science* 290:1972–1974
175. Vilarinho S, Lifton RP (2016) Pioneering a global cure for chronic hepatitis C virus infection. *Cell* 167:12–15. <https://doi.org/10.1016/j.cell.2016.08.038>
176. Shin EC, Sung PS, Park SH (2016) Immune responses and immunopathology in acute and chronic viral hepatitis. *Nat Rev Immunol* 16:509–523. <https://doi.org/10.1038/nri.2016.69>

177. Bukh J (2004) A critical role for the chimpanzee model in the study of hepatitis C. *Hepatology* 39:1469–1475. <https://doi.org/10.1002/hep.20268>
178. Lanford RE, Walker CM, Lemon SM (2017) The Chimpanzee model of viral hepatitis: advances in understanding the immune response and treatment of viral hepatitis. *ILAR J* 58:172–189. <https://doi.org/10.1093/ilar/ilx028>
179. Abe K, Kurata T, Teramoto Y, Shiga J, Shikata T (1993) Lack of susceptibility of various primates and woodchucks to hepatitis C virus. *J Med Primatol* 22:433–434
180. Sithebe NP et al (2002) Lack of susceptibility of Chacma baboons (*Papio ursinus orientalis*) to hepatitis C virus infection. *J Med Virol* 66:468–471. <https://doi.org/10.1002/jmv.2167>
181. Garson JA, Whitty K, Watkins P, Morgan AJ (1997) Lack of susceptibility of the cottontop tamarin to hepatitis C infection. *J Med Virol* 52:286–288. [https://doi.org/10.1002/\(SICI\)1096-9071\(199707\)52:3<286::AID-JMV9>3.0.CO;2-Z](https://doi.org/10.1002/(SICI)1096-9071(199707)52:3<286::AID-JMV9>3.0.CO;2-Z)
182. Xie ZC et al (1998) Transmission of hepatitis C virus infection to tree shrews. *Virology* 244:513–520. <https://doi.org/10.1006/viro.1998.9127>
183. Billerbeck E, de Jong Y, Dorner M, de la Fuente C, Ploss A (2013) Animal models for hepatitis C. *Curr Top Microbiol Immunol* 369:49–86. https://doi.org/10.1007/978-3-642-27340-7_3
184. Hartlage AS, Cullen JM, Kapoor A (2016) The strange, expanding world of animal hepaciviruses. *Ann Rev Virol* 3:53–75. <https://doi.org/10.1146/annurev-virology-100114-055104>
185. Alter HJ, Purcell RH, Holland PV, Popper H (1978) Transmissible agent in non-A, non-B hepatitis. *Lancet* 1:459–463
186. Hollinger FB et al (1978) Non-A, non-B hepatitis transmission in chimpanzees: a project of the transfusion-transmitted viruses study group. *Intervirology* 10:60–68
187. Tabor E et al (1978) Transmission of non-A, non-B hepatitis from man to chimpanzee. *Lancet* 1:463–466
188. Kolykhalov AA et al (1997) Transmission of hepatitis C by intrahepatic inoculation with transcribed RNA. *Science* 277:570–574
189. Lindenbach BD et al (2006) Cell culture-grown hepatitis C virus is infectious in vivo and can be recultured in vitro. *Proc Natl Acad Sci U S A* 103:3805–3809. <https://doi.org/10.1073/pnas.0511218103>
190. Cooper S et al (1999) Analysis of a successful immune response against hepatitis C virus. *Immunity* 10:439–449
191. Major ME et al (2004) Hepatitis C virus kinetics and host responses associated with disease and outcome of infection in chimpanzees. *Hepatology* 39:1709–1720. <https://doi.org/10.1002/hep.20239>
192. Bigger CB, Brasky KM, Lanford RE (2001) DNA microarray analysis of chimpanzee liver during acute resolving hepatitis C virus infection. *J Virol* 75:7059–7066. <https://doi.org/10.1128/JVI.75.15.7059-7066.2001>
193. Thimme R et al (2002) Viral and immunological determinants of hepatitis C virus clearance, persistence, and disease. *Proc Natl Acad Sci U S A* 99:15661–15668. <https://doi.org/10.1073/pnas.202608299>
194. Abe K, Inchauspe G, Shikata T, Prince AM (1992) Three different patterns of hepatitis C virus infection in chimpanzees. *Hepatology* 15:690–695
195. Thomson M et al (2001) Emergence of a distinct pattern of viral mutations in chimpanzees infected with a homogeneous inoculum of hepatitis C virus. *Gastroenterology* 121:1226–1233
196. Erickson AL et al (2001) The outcome of hepatitis C virus infection is predicted by escape mutations in epitopes targeted by cytotoxic T lymphocytes. *Immunity* 15:883–895
197. Farci P et al (1992) Lack of protective immunity against reinfection with hepatitis C virus. *Science* 258:135–140
198. Prince AM et al (1992) Immunity in hepatitis C infection. *J Infect Dis* 165:438–443
199. Grakoui A et al (2003) HCV persistence and immune evasion in the absence of memory T cell help. *Science* 302:659–662. <https://doi.org/10.1126/science.1088774302/5645/659>

200. Shoukry NH et al (2003) Memory CD8+ T cells are required for protection from persistent hepatitis C virus infection. *J Exp Med* 197:1645–1655. <https://doi.org/10.1084/jem.20030239>
201. Bukh J et al (2015) Immunoglobulin with high-titer in vitro cross-neutralizing hepatitis C virus antibodies passively protects chimpanzees from homologous, but not heterologous, challenge. *J Virol* 89:9128–9132. <https://doi.org/10.1128/JVI.01194-15>
202. Morin TJ et al (2012) Human monoclonal antibody HCV1 effectively prevents and treats HCV infection in chimpanzees. *PLoS Pathog* 8:e1002895. <https://doi.org/10.1371/journal.ppat.1002895>
203. Olsen DB et al (2011) Sustained viral response in a hepatitis C virus-infected chimpanzee via a combination of direct-acting antiviral agents. *Antimicrob Agents Chemother* 55:937–939. <https://doi.org/10.1128/AAC.00990-10>
204. Lanford RE et al (2010) Therapeutic silencing of microRNA-122 in primates with chronic hepatitis C virus infection. *Science* 327:198–201. <https://doi.org/10.1126/science.1178178>
205. Houghton M (2011) Prospects for prophylactic and therapeutic vaccines against the hepatitis C viruses. *Immunol Rev* 239:99–108. <https://doi.org/10.1111/j.1600-065X.2010.00977.x>
206. Choo QL et al (1994) Vaccination of chimpanzees against infection by the hepatitis C virus. *Proc Natl Acad Sci U S A* 91:1294–1298
207. Folgori A et al (2006) A T-cell HCV vaccine eliciting effective immunity against heterologous virus challenge in chimpanzees. *Nat Med* 12:190–197. <https://doi.org/10.1038/nm1353>
208. Callendret B et al (2016) Persistent hepatitis C viral replication despite priming of functional CD8+ T cells by combined therapy with a vaccine and a direct-acting antiviral. *Hepatology* 63:1442–1454. <https://doi.org/10.1002/hep.28309>
209. Ploss A, Rice CM (2009) Towards a small animal model for hepatitis C. *EMBO Rep* 10:1220–1227. <https://doi.org/10.1038/embor.2009.223>
210. Zhu Q et al (2006) Novel robust hepatitis C virus mouse efficacy model. *Antimicrob Agents Chemother* 50:3260–3268. <https://doi.org/10.1128/AAC.00413-06>
211. Levander S et al (2018) Immune-mediated effects targeting hepatitis C virus in a syngeneic replicon cell transplantation mouse model. *Gut* 67:1525–1535. <https://doi.org/10.1136/gutjnl-2016-313579>
212. Long G et al (2011) Mouse hepatic cells support assembly of infectious hepatitis C virus particles. *Gastroenterology* 141:1057–1066. <https://doi.org/10.1053/j.gastro.2011.06.010>
213. Sandgren EP et al (1991) Complete hepatic regeneration after somatic deletion of an albumin-plasminogen activator transgene. *Cell* 66:245–256
214. Mercer DF et al (2001) Hepatitis C virus replication in mice with chimeric human livers. *Nat Med* 7:927–933. <https://doi.org/10.1038/90968>
215. Grompe M et al (1993) Loss of fumarylacetoacetate hydrolase is responsible for the neonatal hepatic dysfunction phenotype of lethal albino mice. *Genes Dev* 7:2298–2307
216. Grompe M et al (1995) Pharmacological correction of neonatal lethal hepatic dysfunction in a murine model of hereditary tyrosinaemia type I. *Nat Genet* 10:453–460. <https://doi.org/10.1038/ng0895-453>
217. Bissig KD, Le TT, Woods NB, Verma IM (2007) Repopulation of adult and neonatal mice with human hepatocytes: a chimeric animal model. *Proc Natl Acad Sci U S A* 104:20507–20511. <https://doi.org/10.1073/pnas.0710528105>
218. Bissig KD et al (2010) Human liver chimeric mice provide a model for hepatitis B and C virus infection and treatment. *J Clin Invest* 120:924–930. <https://doi.org/10.1172/JCI40094>
219. Azuma H et al (2007) Robust expansion of human hepatocytes in Fah^{-/-}/Rag2^{-/-}/Il2rg^{-/-} mice. *Nat Biotechnol* 25:903–910. <https://doi.org/10.1038/nbt1326>
220. Grompe M, Strom S (2013) Mice with human livers. *Gastroenterology* 145:1209–1214. <https://doi.org/10.1053/j.gastro.2013.09.009>
221. Vercauteren K, de Jong YP, Meuleman P (2015) Animal models for the study of HCV. *Curr Opin Virol* 13:67–74. <https://doi.org/10.1016/j.coviro.2015.04.009>

222. de Jong YP et al (2014) Broadly neutralizing antibodies abrogate established hepatitis C virus infection. *Sci Transl Med* 6:254ra129. <https://doi.org/10.1126/scitranslmed.3009512>
223. Desombere I et al (2016) Monoclonal anti-envelope antibody AP33 protects humanized mice against a patient-derived hepatitis C virus challenge. *Hepatology* 63:1120–1134. <https://doi.org/10.1002/hep.28428>
224. Mailly L et al (2015) Clearance of persistent hepatitis C virus infection in humanized mice using a claudin-1-targeting monoclonal antibody. *Nat Biotechnol* 33:549–554. <https://doi.org/10.1038/nbt.3179>
225. Akazawa D et al (2013) Neutralizing antibodies induced by cell culture-derived hepatitis C virus protect against infection in mice. *Gastroenterology* 145:447–455.e441–444. <https://doi.org/10.1053/j.gastro.2013.05.007>
226. Meuleman P et al (2012) A human monoclonal antibody targeting scavenger receptor class B type I precludes hepatitis C virus infection and viral spread in vitro and in vivo. *Hepatology* 55:364–372. <https://doi.org/10.1002/hep.24692>
227. Kneteman NM et al (2009) HCV796: a selective nonstructural protein 5B polymerase inhibitor with potent anti-hepatitis C virus activity in vitro, in mice with chimeric human livers, and in humans infected with hepatitis C virus. *Hepatology* 49:745–752. <https://doi.org/10.1002/hep.22717>
228. Ohara E et al (2011) Elimination of hepatitis C virus by short term NS3-4A and NS5B inhibitor combination therapy in human hepatocyte chimeric mice. *J Hepatol* 54:872–878. <https://doi.org/10.1016/j.jhep.2010.08.033>
229. Kremsdorf D, Strick-Marchand H (2017) Modeling hepatitis virus infections and treatment strategies in humanized mice. *Curr Opin Virol* 25:119–125. <https://doi.org/10.1016/j.coviro.2017.07.029>
230. Shultz LD, Brehm MA, Garcia-Martinez JV, Greiner DL (2012) Humanized mice for immune system investigation: progress, promise and challenges. *Nat Rev Immunol* 12:786–798. <https://doi.org/10.1038/nri3311>
231. Washburn ML et al (2011) A humanized mouse model to study hepatitis C virus infection, immune response, and liver disease. *Gastroenterology*. <https://doi.org/10.1053/j.gastro.2011.01.001>
232. Strick-Marchand H et al (2015) A novel mouse model for stable engraftment of a human immune system and human hepatocytes. *PLoS One* 10:e0119820. <https://doi.org/10.1371/journal.pone.0119820>
233. Billerbeck E et al (2016) Humanized mice efficiently engrafted with fetal hepatoblasts and syngeneic immune cells develop human monocytes and NK cells. *J Hepatol* 65:334–343. <https://doi.org/10.1016/j.jhep.2016.04.022>
234. Ploss A et al (2009) Human occludin is a hepatitis C virus entry factor required for infection of mouse cells. *Nature* 457:882–886. <https://doi.org/10.1038/nature07684>
235. Dorner M et al (2013) Completion of the entire hepatitis C virus life cycle in genetically humanized mice. *Nature* 501:237–241. <https://doi.org/10.1038/nature12427>
236. Dorner M et al (2011) A genetically humanized mouse model for hepatitis C virus infection. *Nature* 474:208–211. <https://doi.org/10.1038/nature10168>
237. Giang E et al (2012) Human broadly neutralizing antibodies to the envelope glycoprotein complex of hepatitis C virus. *Proc Natl Acad Sci U S A* 109:6205–6210. <https://doi.org/10.1073/pnas.1114927109>
238. Chen J et al (2014) Persistent hepatitis C virus infections and hepatopathological manifestations in immune-competent humanized mice. *Cell Res* 24:1050–1066. <https://doi.org/10.1038/cr.2014.116>
239. Bitzegeio J et al (2010) Adaptation of hepatitis C virus to mouse CD81 permits infection of mouse cells in the absence of human entry factors. *PLoS Pathog* 6:e1000978. <https://doi.org/10.1371/journal.ppat.1000978>
240. von Schaeuwen M et al (2016) Expanding the host range of hepatitis C virus through viral adaptation. *MBio* 7:e01915–e01916. <https://doi.org/10.1128/mBio.01915-16>

241. Scheel TK, Simmonds P, Kapoor A (2015) Surveying the global virome: identification and characterization of HCV-related animal hepaciviruses. *Antivir Res* 115:83–93. <https://doi.org/10.1016/j.antiviral.2014.12.014>
242. Simmonds P (2013) The origin of hepatitis C virus. *Curr Top Microbiol Immunol* 369:1–15. https://doi.org/10.1007/978-3-642-27340-7_1
243. Simons JN et al (1995) Identification of two flavivirus-like genomes in the GB hepatitis agent. *Proc Natl Acad Sci U S A* 92:3401–3405
244. Bukh J, Appgar CL, Govindarajan S, Purcell RH (2001) Host range studies of GB virus-B hepatitis agent, the closest relative of hepatitis C virus, in New World monkeys and chimpanzees. *J Med Virol* 65:694–697. <https://doi.org/10.1002/jmv.2092>
245. Martin A et al (2003) Chronic hepatitis associated with GB virus B persistence in a tamarin after intrahepatic inoculation of synthetic viral RNA. *Proc Natl Acad Sci U S A* 100:9962–9967. <https://doi.org/10.1073/pnas.1731505100>
246. Kapoor A et al (2011) Characterization of a canine homolog of hepatitis C virus. *Proc Natl Acad Sci U S A* 108:11608–11613. <https://doi.org/10.1073/pnas.1101794108>
247. Burbelo PD et al (2012) Serology enabled discovery of genetically diverse hepaciviruses in a new host. *J Virol* 86:6171–6178. <https://doi.org/10.1128/JVI.00250-12>
248. Lyons S et al (2014) Viraemic frequencies and seroprevalence of non-primate hepacivirus and equine pegiviruses in horses and other mammalian species. *J Gen Virol* 95:1701–1711. <https://doi.org/10.1099/vir.0.065094-0>
249. Pfaender S et al (2015) Clinical course of infection and viral tissue tropism of hepatitis C virus-like nonprimate hepaciviruses in horses. *Hepatology* 61:447–459. <https://doi.org/10.1002/hep.27440>
250. Scheel TK et al (2015) Characterization of nonprimate hepacivirus and construction of a functional molecular clone. *Proc Natl Acad Sci U S A* 112:2192–2197. <https://doi.org/10.1073/pnas.1500265112>
251. Ramsay JD et al (2015) Experimental transmission of equine hepacivirus in horses as a model for hepatitis C virus. *Hepatology* 61:1533–1546. <https://doi.org/10.1002/hep.27689>
252. Pfaender S et al (2017) Immune protection against reinfection with nonprimate hepacivirus. *Proc Natl Acad Sci U S A* 114:E2430–E2439. <https://doi.org/10.1073/pnas.1619380114>
253. Kapoor A et al (2013) Identification of rodent homologs of hepatitis C virus and pegiviruses. *MBio* 4:e00216–e00213. <https://doi.org/10.1128/mBio.00216-13>
254. Drexler JF et al (2013) Evidence for novel hepaciviruses in rodents. *PLoS Pathog* 9:e1003438. <https://doi.org/10.1371/journal.ppat.1003438>
255. Firth C et al (2014) Detection of zoonotic pathogens and characterization of novel viruses carried by commensal *Rattus norvegicus* in New York City. *MBio* 5:e01933–e01914. <https://doi.org/10.1128/mBio.01933-14>
256. Trivedi S et al (2017) Viral persistence, liver disease and host response in hepatitis C-like virus rat model. *Hepatology*. <https://doi.org/10.1002/hep.29494>
257. Williams SH et al (2018) Viral diversity of house mice in New York City. *MBio* 9:e01354–e01317. <https://doi.org/10.1128/mBio.01354-17>
258. Billerbeck E et al (2017) Mouse models of acute and chronic hepacivirus infection. *Science* 357:204–208. <https://doi.org/10.1126/science.aal1962>

The Hepatitis C Virus Replicon System and Its Role in Drug Development



Ralf Bartenschlager and Volker Lohmann

Contents

1	Introduction	71
2	HCV Molecular Virology: A 3-Minute Course	71
3	Early Attempts to Establish Infection-Based HCV Replication Systems	72
4	Early Attempts to Establish Transfection-Based HCV Replication Systems Using Complete Genomes	73
5	Subgenomic HCV Replicons: The Work-Around	74
6	Improvements of the HCV Replicon System	76
6.1	Identification of Replication-Enhancing Mutations	76
6.2	Establishment of Highly Permissive Cell Clones	79
6.3	Genomic HCV Replicons	79
6.4	Development of Replicons for All Major HCV Genotypes	80
6.5	HCV Permissive Cell Lines Beyond Huh7	81
6.6	Alternative HCV Replicon Formats	81
7	The HCVcc System	82
7.1	The JFH-1 Paradigm	82
7.2	Improvements of the JFH-1 Based HCVcc System	82
7.3	The HCVcc System Beyond the JFH-1 Isolate and Huh7 Cells	84
8	Role of the HCV Replicon System for Drug Development	85
9	Concluding Remarks	88
	References	89

R. Bartenschlager (✉)
Department of Infectious Diseases, Molecular Virology, Heidelberg University, Heidelberg, Germany

Division of Virus-Associated Carcinogenesis, German Cancer Research Center (DKFZ), Heidelberg, Germany
e-mail: ralf.bartenschlager@med.uni-heidelberg.de

V. Lohmann
Department of Infectious Diseases, Molecular Virology, Heidelberg University, Heidelberg, Germany

Abstract Infections with the hepatitis C virus (HCV) are an important medical problem as they can lead to chronic liver disease, including liver cirrhosis and hepatocellular carcinoma. The HCV genome was cloned molecularly in 1989, and around 25 years later, antiviral therapy has been established that eliminates the virus in more than 95% of infected individuals. To reach this goal, several hurdles had to be overcome, a major one having been the development of robust cell culture systems that were suitable for drug development, but also to study the individual steps of the HCV replication cycle. Here we summarize the step-by-step establishment of HCV cell culture systems with a focus on the replicon system that played a major role in the development of HCV-specific direct-acting antiviral drugs.

Keywords Antiviral therapy, Direct acting antiviral drugs, Drug development, HCV cell culture system, NS5A inhibitor, Replicon

Abbreviations

cDNA	Complementary DNA
DAA	Direct-acting antiviral
EMCV	Encephalomyocarditis virus
HBV	Hepatitis B virus
HCV	Hepatitis C virus
HCVcc	Cell culture grown HCV
HDV	Hepatitis D virus
hVAP-A	Human vesicle-associated membrane protein-associated protein A
IFN	Interferon
IRES	Internal ribosomal entry site
MDA5	Melanoma differentiation antigen 5
MEF	Mouse embryonic fibroblasts
miR-122	microRNA-122
Npt	Neomycin phosphotransferase
NS	Nonstructural protein
NTR	Nontranslated region
PHHs	Primary human hepatocytes
PI4KA	Phosphatidylinositol-4-phosphate kinase III α
PI4P	Phosphatidylinositol-4-phosphate
RdRp	RNA-dependent RNA polymerase
REM	Replication-enhancing mutation
RIG-I	Retinoic acid inducible gene I
RT-PCR	Reverse transcription-polymerase chain reaction
TEM	Virus titer-enhancing mutation

1 Introduction

Viruses are obligate intracellular parasites and therefore can only replicate in a living cell. For this reason, cell culture systems are an inevitable precondition to study how a virus replicates and how this process can be blocked. Hepatitis C virus (HCV) is not an exception to this rule, but it turned out that cultured cells inoculated with virus contained in primary patient materials such as serum do not support HCV replication. The molecular cloning of the HCV genome in 1989 [1] raised hope that the direct transfer of a synthetic version of the HCV genome would overcome this cell culture block, but also this hope did not materialize. Several major roadblocks had to be overcome until engineered HCV minigenomes, called subgenomic replicons, capable of replicating with high efficiency in an easy to culture cell line became available in 1999 [2]. This HCV replicon system was the long-awaited breakthrough that rapidly became the gold standard in drug development. At the same time, the replicon system opened the door to study HCV-host cell interaction, and it laid the groundwork for improved culture models ultimately supporting the complete viral life cycle. Here we summarize the current status of HCV cell culture systems, focusing on the HCV replicon system and its use for the development of direct-acting antivirals (DAAs) that are in clinical use and described in great detail in this book. We will exclude all surrogate HCV cell culture and animal models. The reader interested in a more global overview is referred to excellent recent reviews [3, 4].

2 HCV Molecular Virology: A 3-Minute Course

Since the molecular virology of HCV is described in more detail in Saeed et al. [5], here we will only briefly summarize those aspects of the viral replication cycle that are required to understand the basic principle of the replicon system. Upon entry into the host cell, the HCV genome is released into the cytoplasm. Owing to the positive polarity of this RNA and the internal ribosome entry site (IRES) in the 5' nontranslated region, the viral genome is recognized by ribosomes and used for protein synthesis (Fig. 1). The resulting polyprotein is co- and posttranslationally cleaved into the following ten products: the structural proteins that build up the virus particle (core protein, envelope proteins 1 and 2), two proteins required for the assembly of infectious virions (ρ 7 and nonstructural protein (NS) 2), and five proteins required and sufficient for viral RNA replication (NS3 containing a serine-type protease and a helicase activity in the N- and C-terminal domain, respectively; the NS3 protease cofactor NS4A; NS4B; NS5A which is required for HCV RNA replication and virion assembly; and the NS5B RNA-dependent RNA polymerase (RdRp)) (Fig. 1). The viral proteins, together with several host cell factors, induce the formation of a cytoplasmic membranous replication organelle, designated the membranous web, which is the site where the viral RNA genome is amplified via a negative-strand RNA copy ([6], reviewed in [7]). This serves as template for the

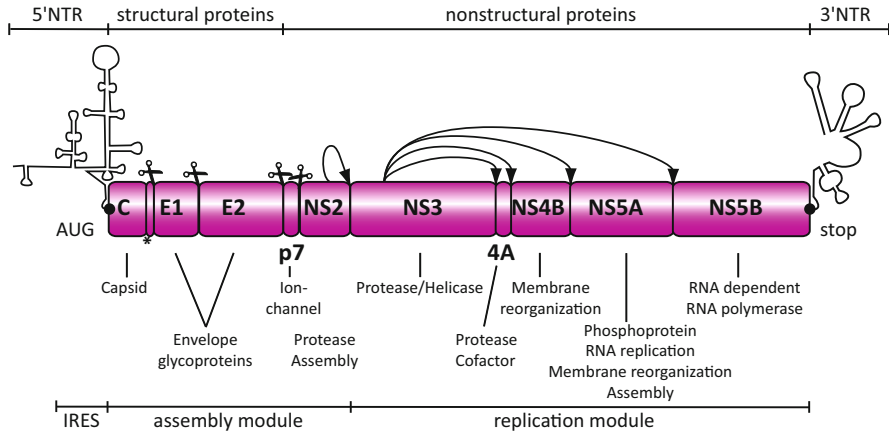


Fig. 1 HCV genome organization. The 5' and 3' NTRs are indicated by their proposed secondary structures; coding regions are given as boxes. Scissors and arrows point to polyprotein cleavages mediated by cellular signal peptidase and viral proteases, respectively. The asterisk in the capsid region points to a signal peptide peptidase cleavage site

production of excessive amounts of positive-strand RNAs that can be used for polyprotein synthesis and the formation of new negative-strand RNAs or become incorporated into HCV particles. These are released out of the cell via a non-cytolytic mechanism.

3 Early Attempts to Establish Infection-Based HCV Replication Systems

Soon after the first molecular cloning of the cDNA of an HCV genome [1], diagnostic tests to screen blood supplies [8] as well as detection methods for viral antigen and RNA for research purposes were established. This enabled attempts to propagate HCV contained in the serum of infected patients in cell culture, but these attempts were of limited success (e.g., [9–13]). Replication, if any, was extremely low, poorly reproducible, and not reliable. The detection of viral antigens by widely used methods such as immunofluorescence or Western blot was not possible, probably because of limited sensitivity, and the production of infectious progeny could not be demonstrated. Therefore, almost all read-out methods in these early days relied on RT-PCR-based approaches, which have limited reliability when trying to measure negative-strand RNA in the presence of excessive amounts of positive-strand RNA. Some of these limitations could be overcome by using primary hepatocytes that are permissive for HCV, but replication was still very low and transient, and the outcome of infection very much depended on the particular hepatocyte donor [3].

4 Early Attempts to Establish Transfection-Based HCV Replication Systems Using Complete Genomes

HCV is a positive-strand RNA virus, i.e., the RNA genome itself is infectious and can initiate a complete replication cycle when introduced into the cytoplasm, e.g., via transfection of RNA generated by *in vitro* transcription. For this purpose a full-length cDNA copy of the genome is inserted downstream of a bacteriophage promoter, usually derived from the bacteriophage T7, and a restriction site or the hepatitis D virus (HDV) ribozyme is placed right at the 3' end of the viral sequence (Fig. 2). This vector is linearized with the restriction enzyme and the DNA template

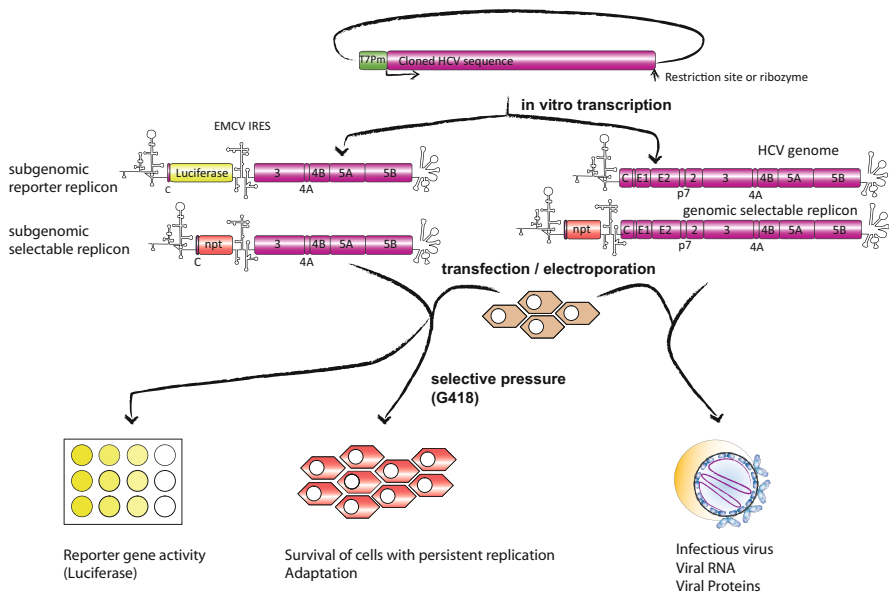


Fig. 2 Experimental strategies to establish cell culture models for HCV replication based on cloned viral isolates. Viral genome sequences are flanked at the 5' end by the T7-RNA polymerase promoter and at the 3' end either by a ribozyme of the hepatitis D virus or a unique recognition sequence for a restriction enzyme. The plasmid is amplified in *E. coli*, and purified DNA is linearized by restriction enzyme digest. T7-RNA polymerase is used to generate *in vitro* transcripts that are transfected into permissive cells. Left half: Subgenomic replicons containing the encephalomyocarditis virus (EMCV) IRES to allow translation of the HCV nonstructural proteins and the encoded reporter gene (e.g., firefly luciferase) or selection marker (e.g., neomycin phosphotransferase, npt). These replicons allow detection of viral replication by reporter assays or selection for drug-resistant cell clones (e.g., by using G418 in case of npt-containing replicons), respectively. In the latter case, the number of cell clones reflects replication capacity with cell clones containing persistently replicating HCV replicon RNAs. Right half: In case of the HCVcc system, used full-length genomes give rise to infectious virus particles. In this case, HCV replication can be judged by quantification of viral RNA and proteins and determination of virus titer. Selectable genomic replicons were designed to generate cell clones with persistent HCV replication allowing virus production. For further details see text

used for *in vitro* transcription using the T7 RNA polymerase. In the case of the HDV ribozyme, the DNA does not need to be linearized as the ribozyme will fold after *in vitro* transcription and cut itself off the HCV RNA. In either way, RNAs with precisely defined 5' and 3' ends can be produced in unlimited quantities *in vitro* and transfected into a cell line or primary cells, thus bypassing virus entry. Within the cell these RNAs are used for the synthesis of viral proteins that should initiate the amplification of the RNA and finally the production of infectious virus particles. Although this approach has been used with great success for many positive-strand RNA viruses [14], they were not successful for HCV. Retrospectively, we know that at least two reasons were responsible for the failures. First, the HCV genomes cloned in the early days lacked an important element at the 3' end of the RNA. This element, designated the "X-tail," contains extensive secondary structures [15, 16]; therefore it was difficult to clone and missed in the first molecular HCV cDNA clones. The second reason was the presence of replication-inactivating mutations in the original molecular HCV clones. These mutations were either introduced during the molecular cloning procedure or present in the virus isolate cloned from a given sample. As HCV is an RNA virus with high genomic plasticity, a high proportion of progeny viruses contain mutations, many of them impairing or destroying replication fitness. Such mutations can be eliminated by using so-called consensus genomes that are derived from nucleotide and amino acid sequence alignments of multiple independent genomes cloned from the very same source. Any sequence difference present in a minority of cDNA clones is considered as undesired mutation that might have been introduced either during the cloning procedure or present already in the particular viral genome. In this way a "consensus sequence" was established that was used to create the matching molecular clone. This concept that was used with great success, e.g., for pestiviruses [17], was also successful in the case of HCV. In fact, two HCV consensus genomes, both based on the genotype 1a isolate H77, were shown to be fully functional upon intrahepatic inoculation of chimpanzees [18, 19]. This result raised great hope to establish a cell culture system for HCV, but disappointingly, the molecular clones that replicated so well *in vivo* did not in cultured cells [20].

5 Subgenomic HCV Replicons: The Work-Around

At around this time, we also attempted to establish a cell culture system for HCV. While our initial focus was HCV polyprotein cleavage [21] and the characterization of the viral enzymes, i.e., the NS3-4A protease [22] and the NS5B RdRp [23], it was obvious that our research would soon come to an end without a robust cell culture system. Therefore, we established a molecular genotype 1b HCV cDNA clone that we designated Con1, an acronym referring to the fact that it also corresponded to a consensus sequence, and conducted numerous transfection-based experiments. However, all these attempts failed and several reasons could account for that. First, HCV replication might have been too low to be detected with available methodology. In fact, we had focused on the detection of replicating RNA by

sensitive strand-specific RT-PCR methodology (in these early days, quantitative PCR was not yet available), but this read-out turned out to be flawed because input RNA used for transfection contained residual plasmid DNA. Therefore, we developed methods to remove traces of contaminating plasmid DNA from *in vitro* transcripts and to specifically detect negative-strand HCV RNA. However, even this improved method was not reliable because the sheer amount of input RNA (10^{13} – 10^{14} copies) was too high to allow the unambiguous detection of negative-strand RNA, a marker for *de novo* replication. Second, we did not know which cell line was permissive for HCV and therefore tested all liver-derived cell lines we had in hand, including the human hepatoma cell line Huh7, that one of the authors had used extensively for studying hepatitis B virus [24]. However, also these attempts were not successful, and we concluded that either the selected HCV genome or the cell lines might not be the right one or that HCV might replicate in transfected cells, but with efficiency too low to be detected with our methods.

Hoping that the second explanation would be right, we searched for alternative read-out methods of viral replication and resorted to an approach in which the survival of a cell is coupled to the efficient replication of a HCV RNA (Fig. 2). This strategy took advantage of observations made with other positive-strand RNA viruses: the region encoding for the structural proteins is dispensable for RNA replication [25–29]. Therefore, we deleted the region encoding core to NS2 or core to p7 (we did not know whether NS2 might be required for RNA replication) and inserted two heterologous sequence elements: first, the IRES of the encephalomyocarditis virus (EMCV) directing the expression of the HCV replicase proteins NS3 to NS5B and, second, the gene encoding for neomycin phosphotransferase (npt) which confers resistance against the cytotoxic drug geneticin (G418). Npt was translated under the control of the HCV IRES residing in the 5' NTR of the viral genome (Fig. 2). As reference, we generated analogous constructs encoding an inactive NS5B RdRp. We transfected various cell lines, including Huh7 cells, with *in vitro* transcripts of these constructs and cultured the cells in the presence of different concentrations of G418 to select for those cells that supported efficient replication of these engineered HCV “minigenomes” (most often called replicons). Only in the case of Huh7 cells we obtained a low number of G418-resistant cell clones, around twofold higher as compared to cells transfected with the NS5B-inactive mutant [2]. In fact, out of a total of around 4×10^{-7} cells, we could isolate around 40 cell clones, indicating that HCV replicated robustly in only one out of ten million transfected cells. However, to our great delight, when we examined G418-resistant cells from which we established stable cell clones, we found that they contained 1,000–5,000 HCV positive-strand RNAs per cell and around tenfold less negative-strand RNA, consistent with the positive-/negative-strand RNA ratio reported for other viruses. Of note, RNA amount in selected cell clones was substantially higher as compared to HCV cell culture systems reported prior to this replicon system, thus allowing for the first time the direct detection of HCV RNA without amplification. In addition, viral proteins could be monitored by Western blot and immunofluorescence microscopy. Most importantly, viral RNA could be radiolabeled metabolically with [^3H] uridine in the presence of dactinomycin, a

strong inhibitor of DNA-dependent RNA polymerase, thus demonstrating autonomous replication of HCV RNAs in these cells [2]. Although initially confronted with skepticism by some scientists, our results were reproduced later on by others using either the identical Con1 HCV isolate [20] or another genotype 1b isolate (HCV-N) that had been cloned from the serum of a chronically HCV-infected patient [30].

6 Improvements of the HCV Replicon System

6.1 Identification of Replication-Enhancing Mutations

The fact that on the one hand we obtained only a low number of G418-resistant cell clones but on the other hand a high HCV replication in selected cells argued that we had selected either for mutated (adapted) HCV RNA or for individual cells being highly permissive of viral replication. Both assumptions turned out to be right. With respect to *replication-enhancing mutations* (REMs), more generically called cell culture adaptive mutations, we and others found that HCV replicons stably replicating in selected cell clones contained one or several mutations that were not present in the original replicon cDNA construct (Fig. 3a). These mutations clustered in three particular regions of the NS3 to NS5B coding region. The most prominent site was the center of NS5A. In addition, these mutations accumulated in NS3 either close to the C-terminal region of the protease or the N-terminal region of the helicase domain and at a very distinct site in NS4B [20, 30–38]. An additional site was found in NS5B [39]. These REMs enhanced HCV replication by up to several orders of magnitude and could be categorized into two “complementation groups”: one group corresponding to mutations in NS3 and the other group corresponding to mutations residing in the other replicase proteins [32, 39]. Of note, a mutation in one group could be combined with a mutation in another group, and this combination often enhanced RNA replication synergistically (Fig. 3b, c), whereas the combination of mutations of the same group suppressed or even destroyed replication competence of the replicon RNA. Moreover, the degree of replication enhancement differs between individual mutations. A profound enhancement is mediated by the S2204I and S2204R mutation in NS5A or the K1846T mutation in NS4B (numbers refer to the amino acid sequence of the Con1 isolate; Fig. 3a). In contrast, mutations residing in NS3 enhance RNA replication only very moderately suggesting that these mutations act by different modes of action (Fig. 3b, c) [32, 34, 38, 40].

The molecular mechanism by which these mutations enhance HCV RNA replication is only partially understood. The fact that these mutations are rarely, if ever, found in natural isolates argues for specific adaptation to hepatoma cells. Consistent with that we recently found that some REMs are loss-of-function mutations that reduce the interaction between NS5A and the host cell lipid kinase phosphatidylinositol-4-phosphate kinase III α (PI4KA) [41]. This kinase is expressed at low levels in hepatocytes *in vivo*, but at very high levels in many hepatoma cells, including Huh7-derived cells. Interaction between the viral replicase, most notably

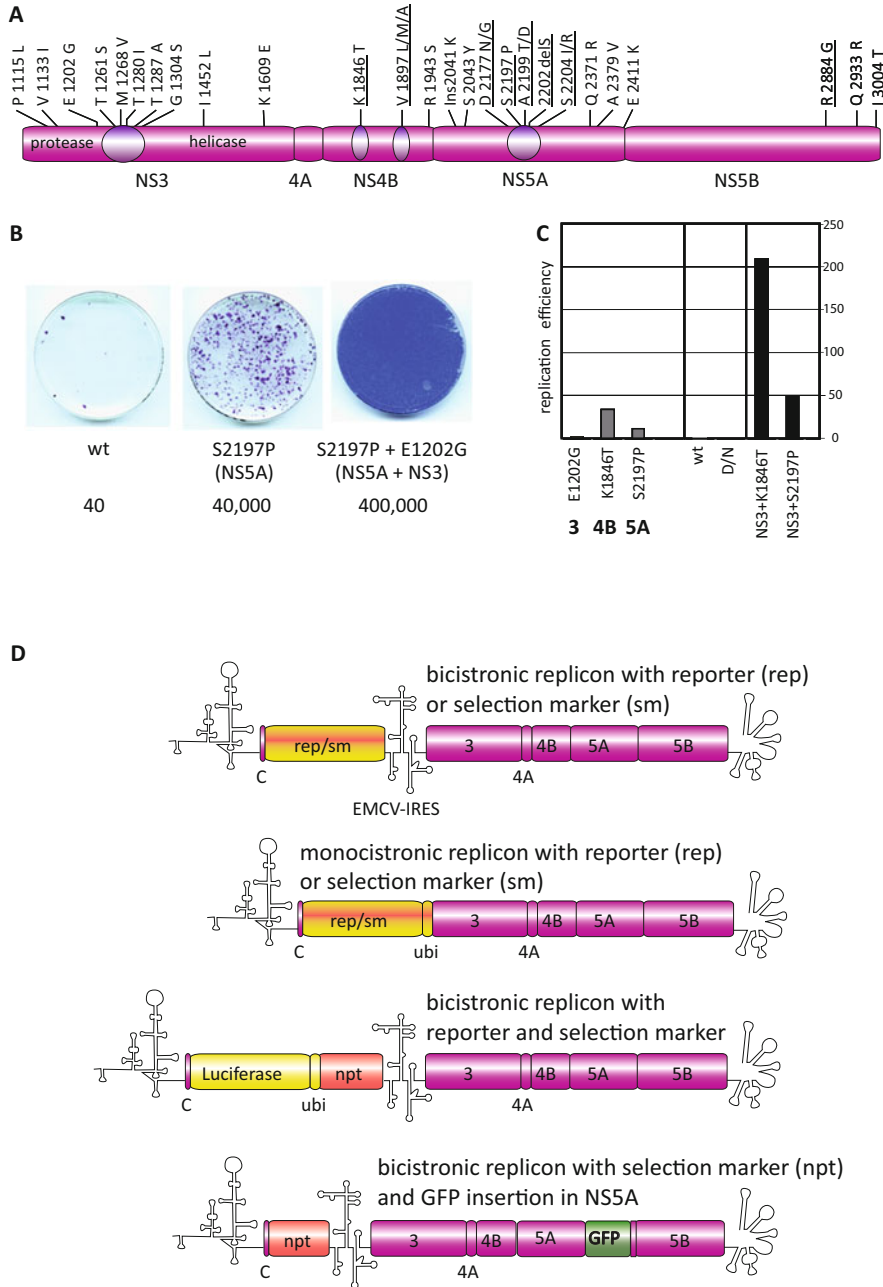


Fig. 3 Subgenomic HCV replicons. (a) Schematic of the NS3-5B coding region with hotspots for replication-enhancing mutations (REMs) indicated. Underlined mutations enhanced replication substantially and were found as sole mutations in replicon cell clones. (b) Enhancement of colony formation efficiency by REMs. Huh7 cells transfected with selectable replicons were cultured in the

NS5A, and this kinase leads to massive accumulation of phosphatidylinositol-4-phosphate (PI4P), the product generated by PI4KA, in the membranes containing the viral replicase (the membranous web) [42, 43]. There, elevated PI4P amounts appear to be required for the non-vesicular transport of cholesterol [44, 45], and perhaps also other lipids [46], to the membranous web with these lipids possibly enhancing replicase activity, e.g., in the form of lipid microdomains (reviewed in [7]). In the case of non-adapted replicons, PI4KA appears to be over-activated, and at least some REMs reduce kinase activation arguing that too much cholesterol and possibly other lipids might be deleterious for HCV replication.

Although plausible, this model does not explain why REMs block the assembly of infectious HCV particles [47, 48]. Interestingly, most REMs reduce the abundance of hyperphosphorylated NS5A suggesting that the phosphorylation status of NS5A is important for regulating a transition from RNA replication to assembly. Indeed, a reduction of NS5A hyperphosphorylation by using kinase inhibitors was found to enhance the replication of Con1 replicons that do not contain REMs [49]. In contrast, when REM-containing Con1 replicons were treated with these inhibitors, RNA replication was impaired suggesting that a minimal amount of hyperphosphorylated NS5A might be required for replication.

How the phosphorylation status of NS5A might regulate HCV RNA replication versus assembly is not clear. Since NS5A interacts with several host cell factors, it is plausible to assume that host cell factor-NS5A interaction might be affected by the phosphorylation status of the latter. One possible cellular interactant is the human vesicle-associated membrane protein-associated protein A (hVAP-A) [50]. This protein plays an important role for efficient HCV RNA replication with interaction between hVAP-A and NS5A depending on the NS5A phosphorylation status [50]. Another candidate is PI4KA that modulates NS5A phosphorylation by shifting the balance toward the replication-favoring basal phosphorylation status of NS5A. Moreover, the predominant interaction site in NS5A required for the association with PI4KA resides in a region adjacent to a hotspot of REMs [43]. However, the molecular mechanism remains to be determined.

Fig. 3 (continued) presence of G418. Resistant cell clones were stained with Coomassie brilliant blue. Colony formation efficiency per microgram of transfected replicon RNA is indicated below each plate. A single REM in NS5A can increase colony formation by about 1,000-fold; addition of NS3 mutations has an additive effect. **(c)** Replication enhancement of reporter replicons by REMs. Bicistronic replicons containing the indicated mutations and encoding firefly luciferase were transfected into Huh7 cells. Replication efficiency is expressed as luciferase activity obtained 48 h after transfection compared to the wild type (wt). D/N, replication deficient control. **(d)** Subgenomic mono- and bicistronic replicons with reporter gene (rep; e.g., firefly luciferase) and/or selection marker (sm; e.g., neomycin phosphotransferase (npt)). The HCV 5' and 3' NTRs as well as the EMCV IRES are indicated by their proposed secondary structure

6.2 *Establishment of Highly Permissive Cell Clones*

Apart from the identification of REMs, the use of selectable replicons allowed the isolation of highly permissive Huh7-derived cell clones. This has been achieved by treating cell clones containing a stably replicating subgenomic replicon RNA with interferon (IFN) [32, 34, 51, 52], which profoundly suppresses HCV replication [29, 52], and by keeping these cells under confluency for extended time spans. Both conditions are deleterious for viral replication [54], thus giving rise to so-called “cured” cell lines. By using this method, several highly permissive cell clones such as Huh7-Lunet [55] or Huh7.5 cells [51] have been established that provide a much more favorable environment for HCV replication as compared to naïve Huh7 cells. This might be due to low expression of HCV-targeting restriction factors or to high level expression of HCV dependency factors. In the case of Huh7.5 cells, high permissiveness has been linked to a mutation in RIG-I, a pattern recognition receptor originally thought to be responsible for sensing HCV RNA and activation of the IFN response [56]. However, more recent studies identified MDA5 as primary sensor of HCV [57, 58]. Moreover, ectopic expression of functional RIG-I in Huh7.5 cells has no effect on HCV RNA replication, arguing that other factors contribute to the high permissiveness of Huh7.5 cells [59]. Finally, other human liver cell lines such as HepG2 also support HCV RNA replication only poorly, yet have a defective IFN response [60]. Therefore, the reason for the high permissiveness of Huh7.5 cells remains to be determined.

Although these novel cell systems are of great value to study HCV replication, they do not support robust replication of primary HCV isolates. In fact, save for JFH-1, only HCV variants containing REMs replicate in these cell systems. Assuming that the underlying reason might be the insufficient expression of a host cell factor that is necessary for the replication of non-adapted HCV strains, Saeed and colleagues conducted an unbiased expression-based screen and identified SEC14L2 that was sufficient to enable RNA replication of non-adapted HCV derived from various genotypes and even primary isolates contained in patient samples [61]. Although the underlying mechanism is not yet clarified, the earlier observation that save for JFH-1, HCV replication is sensitive to lipid peroxidation [62] and the fact that SEC14L2 is a vitamin E-binding protein argue that SEC14L2 might stimulate HCV replication by enhancing vitamin E-mediated protection against lipid peroxidation [61]. Interestingly, a comparable replication stimulation of primary HCV isolates and non-adapted strains could be achieved by treatment of Huh7 cells with PI4KA-specific inhibitors also pointing toward a lipid-dependent regulation of HCV replication and its modulation by REMs [41].

6.3 *Genomic HCV Replicons*

Taking advantage of REMs and highly permissive cell clones, the next step was obvious: to construct genomic replicons corresponding to complete HCV genomes

with the aim to achieve the production of infectious HCV particles (Fig. 2). While it was straightforward to establish Huh7-derived cell lines containing stably replicating genomic replicons, these cells did not support HCV particle production [31, 34, 51, 63]. Although viral RNA that was resistant to nuclease treatment because of shielding in membranous structures was released from these cells, analogous structures were released from cells containing a subgenomic HCV replicon [63]. These structures most likely correspond to exosomes, containing HCV RNA and being released from cells via the multivesicular body pathway [64]. However, authentic virus particles could not be detected in culture supernatants of these cells [63]. Deletion of the heterologous IRES or the selection marker did not render REM-containing genomes assembly competent, and even in transient replication assays, no virus production was found. It was therefore assumed that REMs block HCV particle production. Consistent with this assumption, in collaboration with Jens Bukh at the NIH, we found that intrahepatic inoculation of chimpanzees with *in vitro* transcripts derived from the authentic Con1 genome caused persistent infection, whereas a Con1 genome containing three REMs was unable to establish infection *in vivo* [47]. Importantly, a Con1 genome containing only one REM rapidly reverted to wild type that caused viremia in the animal. This result argued for a strong selection against REMs *in vivo*, most likely due to blocking virus particle production, an assumption that we could confirm several years later: Huh7 cells transfected with a highly adapted HCV genome did not support virus production, whereas cells transfected with the wild-type Con1 genome released HCV particles with proven *in vivo* infectivity [48]. However, owing to the low replication of the wild-type genome, virus release was very transient and mainly driven from input RNA transfected into the cells.

6.4 Development of Replicons for All Major HCV Genotypes

First-generation replicons covered only a few HCV isolates and only the genotype 1. These included the isolates Con1 [2], HCV-N [31], and HCV-BK [35], all belonging to genotype 1b, and the H77 isolate belonging to genotype 1a. Replication of these isolates also depended on REMs, albeit to various extents. This dependency was most pronounced for the H77 isolate that did not replicate at all in cell culture and first required the insertion of REMs to allow further adaptation to cell culture [34]. Since then, several additional functional replicons derived from various genotype 1 isolates have been established. This was achieved either by the insertion of defined REMs or by starting with *de novo* adaptation (reviewed in [3]). Of note, all replicons selected for similar sets of REMs, arguing that comparable or even identical mechanisms account for the adaptation.

Important extensions of the repertoire of HCV replicons to cover all genotypes have been made by using analogous experimental approaches. For instance, in the case of the genotype 3a isolate S310, a consensus sequence was used to construct a selectable subgenomic replicon very much alike the original Con1 replicon [65]; the

same was applied for another genotype 3a isolate (S52) [66] and the genotype 4a isolate ED43 [66, 67]. REMs were identified in all of these replicons, often at positions very similar or even identical to those reported for other replicons. For instance, a mutation affecting a putative NS5A phosphorylation site and abrogating PI4KA activation [41] was found to increase RNA replication of replicons derived from genotype 1a, 1b, 3a, and 4a isolates. This high conservation of REMs was also the key to establish replicons of genotypes 5 and 6 [68, 69], thus closing the gap in our replicon tool box.

6.5 *HCV Permissive Cell Lines Beyond Huh7*

Original HCV replicon systems were mostly based on Huh7 cells, but since the original discovery in 1999, the spectrum could be expanded profoundly. Replicons in non-Huh7 cells such as HeLa or the mouse hepatoma cell line Hepa 1–6 have been reported already in 2003 [70]. While having been an important add-on to available culture systems, this study also demonstrated that HCV RNA replication as such is not restricted to hepatocytes. Nevertheless, it should be noted that the establishment of stable replicons in these cell lines was very inefficient arguing that host cell factors present in liver cells might enhance HCV replication.

With the advent of the highly replication-competent JFH-1 isolate (see below), replicons derived from this isolate could be established in many other cell lines. These include the human liver cell lines HepG2 and IMY-9, the non-liver cell lines 293 and HeLa, and even mouse embryonic fibroblasts (MEFs) [71–73]. However, also with the JFH-1 isolate, the establishment of stable replicons was much less efficient as compared to Huh7 cells. Of note for some cell lines like HepG2 [74] and Hep3B [75], the lack of permissiveness could be linked to low levels of microRNA-122 (miR-122), an essential host cell dependency factor for HCV [76].

6.6 *Alternative HCV Replicon Formats*

The identification of REMs and the availability of highly permissive cell clones as well as the JFH-1 isolate allowed the rapid development of alternative HCV replicon formats (reviewed in [3]). These include (Fig. 3d):

1. Efficient reporter replicons containing, e.g., the luciferase gene and applicable for transient (short-term) HCV replication assays (e.g., [3, 38, 52, 77]). Such replicon systems allow, e.g., the rapid testing of drug resistance mutations, and they reflect replication capacity of a given HCV RNA much more accurately than selection for stable cell clones.
2. Cell lines containing selectable reporter replicons and being well applicable for high-throughput screening purposes (e.g., [78]).

3. Monocistronic replicons containing only the HCV IRES, thus excluding possible confounding effects exerted by the heterologous EMCV IRES (e.g., [34]).
4. Reporter replicons suitable for live cell imaging, e.g., by the insertion of the gene encoding the green fluorescent protein (GFP) into domain 3 of NS5A [79, 80].

7 The HCVcc System

7.1 *The JFH-1 Paradigm*

Subgenomic replicons have been a major tool for drug development, but owing to REMs they did not support virus production. For this reason, they were suitable to target every step of the intracellular replication cycle, most notably the viral enzymes, but not useful to study virus entry as well as virus particle assembly and release. This was a dilemma because on the one hand, REMs were required for robust viral RNA replication, but hindered assembly, and, on the other hand, in the absence of REMs, replication was insufficient. The solution of this problem was the identification of an HCV isolate capable of replicating to high levels independent from REMs. This “holy grail” was found by our colleague Takaji Wakita, in those days at the university in Tokyo, who had cloned a cDNA of an HCV isolate in a Japanese patient with fulminant hepatitis C, hence the name JFH-1 for this isolate [37]. A subgenomic replicon designed like our original Con-1 replicon produced an uncountable number of G418-resistant cell clones upon transfection of Huh7 cells. Notably, most replicon RNAs isolated from stable JFH-1 replicon cell clones did not contain REMs, consistent with the high G418 transduction efficiency [37]. Very much in line with our assumption, a full-length molecular clone of this JFH-1 isolate supported virus production, and virus particles released from transfected cells were infectious for Huh7 cells and in a chimpanzee [81]. In addition, in collaboration with the Wakita group, we constructed a chimeric HCV genome composed of the JFH-1 replicase (NS3 to NS5B) fused N-terminally with the Con1 sequence encoding the missing structural proteins as well as p7 and NS2 (Fig. 4a). Also this chimeric genome supported the production of infectious HCV particles [81]. Together with a similar result that was published around the same time [82], these observations laid the foundation for a fully permissive HCV cell culture system allowing study of the complete viral life cycle in an easy-to-culture liver cell line. In order to distinguish HCV present in patient sera from HCV produced in cell culture, the term “HCVcc” (cell culture-grown) was coined [82].

7.2 *Improvements of the JFH-1 Based HCVcc System*

Since the first reports of the JFH-1-based HCVcc system, numerous improvements have been made. One important discovery was the identification of virus

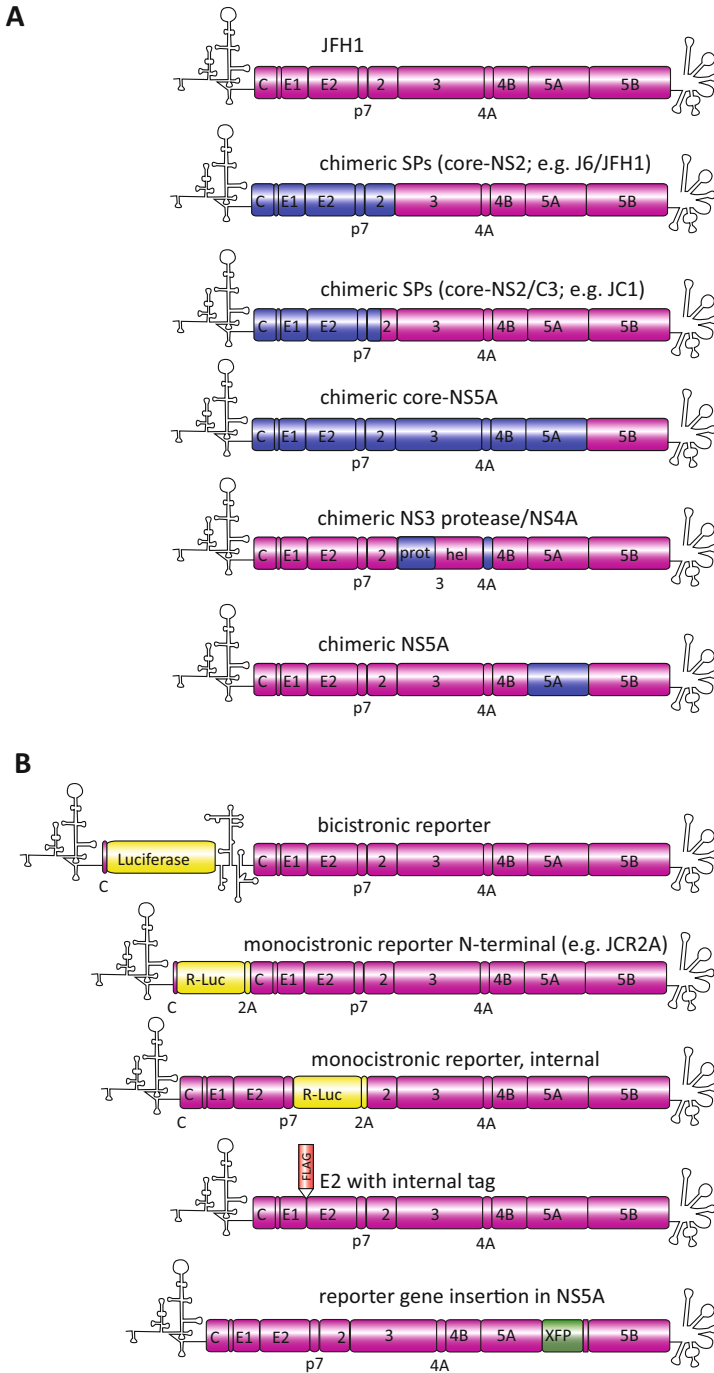


Fig. 4 HCV genomes replicating in vitro. (a) Wild-type JFH-1, different chimeras and (b) a selected set of reporter virus genomes (bi- and monocistronic). JFH-1 sequences are shown in

titer-enhancing mutations (TEMs). The first report in this direction was based on the observation that Huh7.5.1 cells (a subclone of the Huh7.5 cell clone) transfected with full-length RNA of the JFH-1 strain released only low amounts of infectious HCV, but upon serial passage of transfected cells, virus titer increased around 200-fold [83]. This observation argued for the emergence of a cell culture-adapted JFH-1 variant, a conclusion that was not considered in this initial study [84], but confirmed in a subsequent report from the same group [85].

Numerous TEMs were reported in several follow-up studies by various groups and found to reside both in the structural proteins and in several nonstructural proteins, arguing for the involvement also of replicase components, notably the NS3 helicase, in the assembly process [85–91]. Moreover, we found that assembly efficiency of intra- and inter-genotypic chimeric HCV genomes could be improved by fusing the genome segments at a distinct position within NS2 (i.e., right after the first transmembrane segment of NS2; [92]) (Fig. 4a). This fusion site was most efficient for a J6-JFH-1 chimera that we designated Jc1 yielding virus titers that were around 1,000-fold higher as compared to the original JFH-1 genome [92]. By using an analogous approach, chimeric JFH-1-derived HCV genomes allowing the production of virus particles corresponding to all seven HCV genotypes have been achieved [89–94].

Similar to the subgenomic replicon system, numerous reporter-based HCVcc systems derived from the JFH-1 isolate have been developed (Fig. 4b). These include bi- and monocistronic genomes containing the luciferase gene that are well suitable, e.g., for high-content screens [42, 81, 95–98], virus genomes encoding fluorescence proteins to allow for image-based analysis [42, 80, 99–101], or JFH-1 genomes with insertions of tags to allow high-affinity capture, e.g., of infectious HCV particles or replicase components [102–104].

7.3 *The HCVcc System Beyond the JFH-1 Isolate and Huh7 Cells*

As alluded to above, the JFH-1 isolate is unique in its ability to replicate in cell culture with very high efficiency without the requirement for REMs while being fully functional *in vivo*. This is not the case for all the other HCV molecular clones with proven *in vivo* infectivity that to the best of our knowledge unanimously require cell culture adaptation. One example is the H77-S strain (genotype 1a), a highly adapted H77-derived genome that contains a total of five mutations increasing RNA

Fig. 4 (continued) pink. In case of chimeric genomes, viral sequences of the second genotype are indicated by blue color. Heterologous coding sequences are shown yellow (luciferase), green (autofluorescent proteins), and red (FLAG-tag). Note that the reporter virus genomes are often chimeric as depicted in panel (a) which is not indicated in panel (b). Further details are given in the text

replication and virus production [105, 106]. Other examples are the HCV TNcc strain (genotype 1a) [107], the highly cell culture-adapted J6cc genome (genotype 2a) containing a total of six adaptive mutations [108], the JFH-2 strain (genotype 2a) that was isolated from another patient with fulminant hepatitis C [109], three highly adapted genotype 2b isolates [108, 110], and the cell culture-adapted genotype 3a strain S310 [111]. Very recently, a highly adapted genotype 3a virus model has been established with similar efficiency as JFH-1 but based on isolate DBN3a and containing 17 adaptive mutations [112]. In addition, a large panel of chimeric HCV genomes containing replacements of, e.g., NS5A or the NS3 protease/4A cofactor sequences or even the entire core-NS5A sequence have been developed allowing the measurement of the genotype specificity of drugs against all major HCV genotypes (Fig. 4a) [113–115].

Apart from increasing the spectrum of HCV strains replicating in cell culture, progress has also been made with respect to HCV permissive cell lines supporting the complete HCV life cycle. Initially focused on Huh7 cells, notably Huh7.5 cells that express high level of the entry molecule CD81 [116], it turned out that important aspects of HCV-host cell interaction cannot be recapitulated properly in this cell system. One example is the poor lipidation of HCVcc produced in Huh7 cells as compared to virions produced *in vivo* [117–119]. Another example is the lack of a proper IFN response in these cells [56, 59]. Therefore, attempts have been undertaken to improve HCV cell culture models. Examples are human hepatocytic cell lines like HuH-6 [120], IMY-N9 [71, 74], and LH86 [121], non-hepatocytic human cell lines such as HEK293 [72, 122], Hela [70, 72], neuroepithelioma cells [123], and even nonhuman cells [70, 73, 124–127].

Since replication in virtually all of these cell lines is lower than in Huh7 cells, important host dependency factors have been introduced into these cells with the aim to increase HCV permissiveness. A focus has been put on miR-122 and apolipoprotein E that are expressed only to low level in most of these cells but very critical for efficient HCV RNA replication and virus production, respectively (see [5]). Indeed, ectopic overexpression of these factors renders Hep3B cells [75], HepG2 cells [74], and even mouse hepatic cells [124, 125, 127] more permissive for HCV. Finally, with respect to HCV-induced IFN response, primary human hepatocytes (PHHs) or hepatocyte-like cells derived from induced pluripotent stem cells (reviewed in [128]) are probably closest to the *in vivo* situation. Although HCV replication is only transient and often rather low, a major advantage, beyond the authentic IFN response, is the permissiveness of these cell systems for primary human isolates.

8 Role of the HCV Replicon System for Drug Development

The development of DAAs was tightly linked to the establishment of the HCV replicon system, and to the best of our knowledge, all DAAs that are in clinical use have been developed by using this cell culture model. One reason is timing because the subgenomic replicon system was the first robust cell culture model established

for HCV. This happened at a time when two obvious drug targets, the NS3-4A protease [21, 129–131] and the NS5B RdRp [23, 132], had been identified. However, studies of these drug targets were limited to *in vitro* assays or the use of surrogate cell-based systems with little predictive value for antiviral efficacy in an HCV-based replication system. For that reason, surrogate systems also did not allow reliable high-content cell-based screens or were limited to just one defined HCV target (e.g., the NS3-4A protease). In contrast, subgenomic HCV replicons overcame these hurdles while being robust and easy to handle. For instance, subgenomic replicons do not support virus production and thus can be used in a standard cell culture laboratory without particular biosafety precautions. Moreover, the first HCV replicons were based on genotype 1 isolates, which are most widespread and among the most difficult to treat with IFN-based therapy, which was the standard of care for many years [133]. Importantly, replicons not only allowed the validation of compounds against a predefined target but also enabled the discovery of new drug targets. The most striking example are inhibitors of NS5A, a protein that lacks enzymatic activity and promotes different steps of the HCV replication cycle by regulated interaction with several viral and host cell factors. Owing to these properties, NS5A had not been considered as druggable target; however, pioneering work by the group of Min Gao and Nicolas Meanwell at Bristol-Myers Squibb led to the discovery of daclatasvir, the first in-class NS5A inhibitor [134] (see Min Gao, “NS5A as a Target for HCV Drug Discovery” and Nicholas Meanwell, “Discovery and Development of Daclatasvir” of this book). A hallmark of this inhibitor class is its unprecedented antiviral potency explaining, while virtually all DAA combinations used in the clinic contain one NS5A inhibitor. Without the replicon system, this drug class might not have been discovered.

The identification of a drug target and the selection for drug resistance are other examples where subgenomic replicons played an important role for drug discovery. For instance, the target of NS5A inhibitors was initially identified by the selection for drug resistance that mapped to distinct sites in NS5A (Fig. 5). Moreover, the double selection of cells containing a stably replicating HCV replicon, e.g., with G418 and a given DAA, allows the rapid identification of resistant variants because it selects for clonal cell populations in which resistance-conferring mutations are conserved in most, if not all, replicon RNAs of that given cell clone (Fig. 5). By using this approach, drug resistance mutations and the genetic resistance barrier (inferred from the time required until a resistant variant emerges) could be identified. Of note, most of these mutations were confirmed later on in patients, thus validating the predictive value of the replicon system for DAA-treated patients (reviewed in [135, 136]). Moreover, the replication fitness of drug-resistant variants could be predicted which laid the ground for phenotypic resistance assays and *in silico*-based prediction algorithms ([137] and references cited therein).

Subgenomic replicons also paved the way for the discovery of host targets, notably cyclophilin A [138–140] and miR-122 [76, 141, 142] and compounds directed against them. Although these compounds have strong antiviral activity against HCV *in vitro* and in clinical trials, it is uncertain whether they will be developed further to clinical approval. Nevertheless, these studies provided

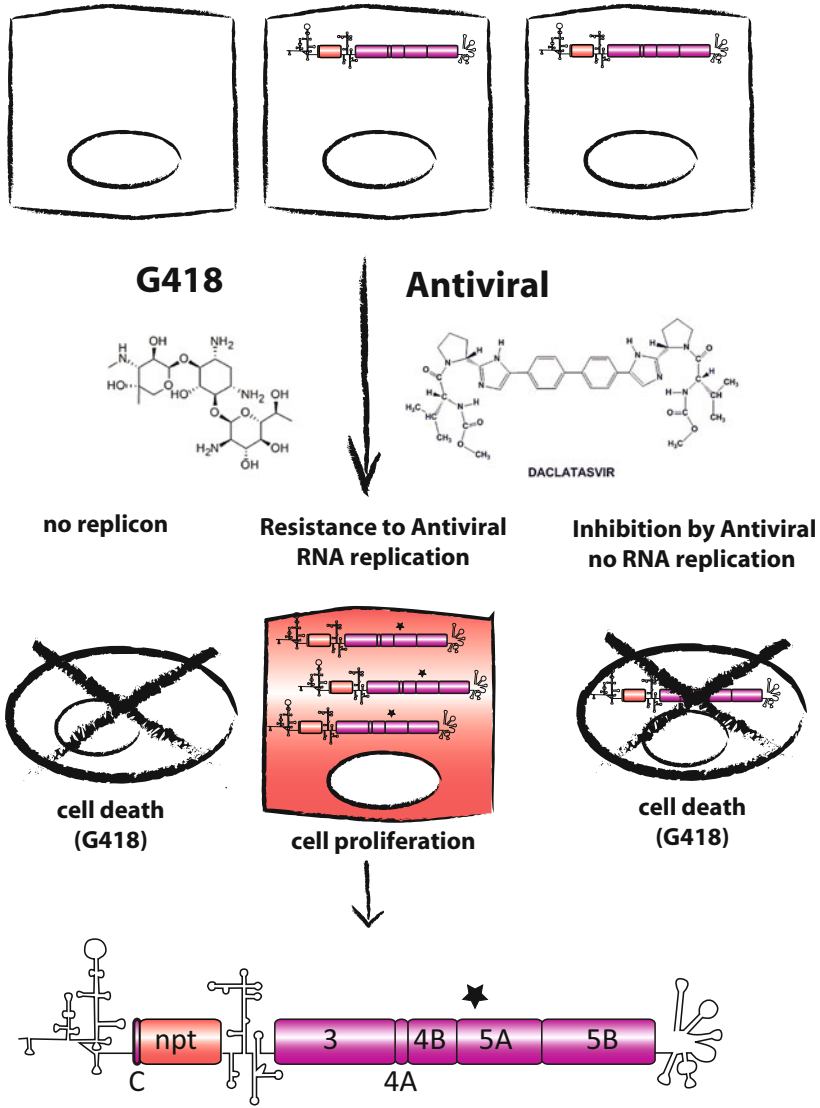


Fig. 5 Selection of drug-resistant variants using replicon cell lines. Cell lines containing persistent selectable replicons are treated with G418 and a DAA (here, daclatasvir). Inhibition of HCV replication by the DAA will result in loss of G418 resistance and cell death. Only replicons acquiring mutations conferring drug resistance will replicate and give rise to surviving cell clones. These mutations are conserved in the surviving cell clones and point to the mode of action of the drug

important lessons on host-directed therapy and its possible application for broad-spectrum antiviral therapy (reviewed in [143]).

While subgenomic replicons played a key role for HCV drug development, this was not the case with the HCVcc system. Several reasons might account for that. First, at the time the HCVcc system was robust enough to allow high-throughput screenings, many companies had already closed their HCV drug discovery programs. Second, while the HCVcc system requires a high-containment laboratory (corresponding to BSL3* in Europe), subgenomic replicons require only BSL1 conditions because there is no risk of infection. Thus, high-content screens or other approaches requiring a technically demanding infrastructure do not need to be installed in a high-containment laboratory. Third, DAA sensitivity and resistance assays have given comparable results with both systems. Fourth, owing to the high SVR rates achievable with IFN-based therapy of genotype 2 infections, the genotype 2a-based HCVcc system was probably less attractive than the replicon system based on the difficult-to-treat genotype 1. The fact that initial replicon systems were based exclusively on genotype 1 strains probably explains why many (first-generation) DAAs had a strong bias toward genotype 1. This limitation of the tool box was overcome later on by the development of inter-genotypic chimeras and with the advent of non-genotype 1 replicons.

9 Concluding Remarks

Twenty-eight years have elapsed since the first report about the successful molecular cloning of a near full-length HCV genome. During these years, basic scientists in academia and industry, experts in medicinal chemistry, and clinicians have worked hard, and today patients can be offered an antiviral therapy that can eliminate HCV in more than 95% of treated individuals. This cure rate is unprecedented for any chronic infection and the result of a step-by-step process in which overcoming one hurdle almost instantly confronted the scientific community with the next one. For sure, the seminal publication by Mike Houghton and his team in 1989 was the starting point as it provided the blue print of the HCV genome organization and opened the field that had the ultimate goal to develop a most effective, ideally curative therapy. To reach this goal, replicons have been most instrumental, but their development occurred in a stepwise process requiring 10 years from the original discovery of HCV until success. It required the discovery of the correct 3' end of the HCV genome, the construction of functional consensus genomes, and the identification of proper cell lines. In the course of these studies, many research groups made important contributions and discoveries, and these joint efforts paved the way to highly effective all-oral IFN-free antiviral therapy.

Owing to this success, HCV is now mistakenly considered as a vanquished virus that can be controlled or even eradicated on a global scale by sole antiviral treatment. However, this view is short-sighted and does not take into account important challenges that prevail at several levels. At the level of public health, DAAs are expensive and therefore will likely remain out of the reach of a majority of infected

persons worldwide for many years. Moreover, most persistent HCV infections are clinically silent, are often undiagnosed, and will not be recognized by patients or practitioners until liver damage is advanced. Thus, more efforts are required to identify those that are unaware of their infection. Considering the clinical level, it is well possible that clinically relevant DAA resistance, which thus far is rather uncommon, might increase with broader use of the drugs. Considering translational research, the jury is still out whether or not a vaccine will be required for global control of HCV. It should be kept in mind that HCV infection does not induce protective immunity, neither after acute self-limiting infection nor after DAA-based virus elimination. In fact, reinfection is rather common, and during the last few years, we have seen a striking increase in the number of new infections, e.g., in the USA, where it is linked to extensive opioid addiction. Clearly, the high cure rate achievable with DAA-based therapy is a major medical success, but whether this is sufficient for global eradication of HCV in the absence of a vaccine remains questionable. If we do not want to take the risk, the answer is obvious: join forces to develop a vaccine.

Acknowledgments We are deeply indebted to all past and present members of our research groups, who made valuable contributions to all of our work. Studies in the authors' laboratories were supported by the Deutsche Forschungsgemeinschaft, the German Ministry for Research and Education (BMBF), and the European Union.

Compliance with Ethical Standards

Funding Work in the authors' laboratory has been supported by the Deutsche Forschungsgemeinschaft, the Bundesministerium für Bildung und Forschung and the European Union.

Conflict of Interest V.L. and R.B. are co-founders of ReBLikon GmbH, which holds commercial rights to hepatitis C virus replicon technology.

Ethical Approval Work conducted in the authors' laboratory did not involve studies with human participants or animals.

References

1. Choo QL, Kuo G, Weiner AJ, Overby LR, Bradley DW, Houghton M (1989) Isolation of a cDNA clone derived from a blood-borne non-A, non-B viral hepatitis genome. *Science* 244(4902):359–362
2. Lohmann V, Korner F, Koch J, Herian U, Theilmann L, Bartenschlager R (1999) Replication of subgenomic hepatitis C virus RNAs in a hepatoma cell line. *Science* 285(5424):110–113
3. Steinmann E, Pietschmann T (2013) Cell culture systems for hepatitis C virus. *Curr Top Microbiol Immunol* 369:17–48
4. Billerbeck E, de Jong Y, Dorner M, de la FC, Ploss A (2013) Animal models for hepatitis C. *Curr Top Microbiol Immunol* 369:49–86

5. Saeed M, Billerbeck E, Rice CM (2019) Molecular virology and animal models. *Top Med Chem.* https://doi.org/10.1007/7355_2018_51
6. Egger D, Wolk B, Gosert R, Bianchi L, Blum HE, Moradpour D et al (2002) Expression of hepatitis C virus proteins induces distinct membrane alterations including a candidate viral replication complex. *J Virol* 76(12):5974–5984
7. Paul D, Madan V, Bartenschlager R (2014) Hepatitis C virus RNA replication and assembly: living on the fat of the land. *Cell Host Microbe* 16(5):569–579
8. Kuo G, Choo QL, Alter HJ, Gitnick GL, Redeker AG, Purcell RH et al (1989) An assay for circulating antibodies to a major etiologic virus of human non-A, non-B hepatitis. *Science* 244(4902):362–364
9. Seipp S, Mueller HM, Pfaff E, Stremmel W, Theilmann L, Goeser T (1997) Establishment of persistent hepatitis C virus infection and replication in vitro. *J Gen Virol* 78.(Pt 10):2467–2476
10. Tagawa M, Kato N, Yokosuka O, Ishikawa T, Ohto M, Omata M (1995) Infection of human hepatocyte cell lines with hepatitis C virus in vitro. *J Gastroenterol Hepatol* 10(5): 523–527
11. Kato N, Nakazawa T, Mizutani T, Shimotohno K (1995) Susceptibility of human T-lymphotropic virus type I infected cell line MT-2 to hepatitis C virus infection. *Biochem Biophys Res Commun* 206(3):863–869
12. Shimizu YK, Iwamoto A, Hijikata M, Purcell RH, Yoshikura H (1992) Evidence for in vitro replication of hepatitis C virus genome in a human T-cell line. *Proc Natl Acad Sci U S A* 89(12):5477–5481
13. Nakajima N, Hijikata M, Yoshikura H, Shimizu YK (1996) Characterization of long-term cultures of hepatitis C virus. *J Virol* 70(5):3325–3329
14. Boyer JC, Haenni AL (1994) Infectious transcripts and cDNA clones of RNA viruses. *Virology* 198(2):415–426
15. Tanaka T, Kato N, Cho MJ, Shimotohno K (1995) A novel sequence found at the 3' terminus of hepatitis C virus genome. *Biochem Biophys Res Commun* 215(2):744–749
16. Kolykhalov AA, Feinstone SM, Rice CM (1996) Identification of a highly conserved sequence element at the 3' terminus of hepatitis C virus genome RNA. *J Virol* 70(6):3363–3371
17. Moormann RJ, van Gennip HG, Miedema GK, Hulst MM, van Rijn PA (1996) Infectious RNA transcribed from an engineered full-length cDNA template of the genome of a pestivirus. *J Virol* 70(2):763–770
18. Kolykhalov AA, Agapov EV, Blight KJ, Mihalik K, Feinstone SM, Rice CM (1997) Transmission of hepatitis C by intrahepatic inoculation with transcribed RNA. *Science* 277(5325): 570–574
19. Yanagi M, Purcell RH, Emerson SU, Bukh J (1997) Transcripts from a single full-length cDNA clone of hepatitis C virus are infectious when directly transfected into the liver of a chimpanzee. *Proc Natl Acad Sci U S A* 94(16):8738–8743
20. Blight KJ, Kolykhalov AA, Rice CM (2000) Efficient initiation of HCV RNA replication in cell culture. *Science* 290:1972–1974
21. Bartenschlager R, Ahlborn LL, Mous J, Jacobsen H (1993) Nonstructural protein 3 of the hepatitis C virus encodes a serine-type proteinase required for cleavage at the NS3/4 and NS4/5 junctions. *J Virol* 67(7):3835–3844
22. Bartenschlager R (1999) The NS3/4A proteinase of the hepatitis C virus: unravelling structure and function of an unusual enzyme and a prime target for antiviral therapy. *J Viral Hepat* 10(11):1–2
23. Lohmann V, Korner F, Herian U, Bartenschlager R (1997) Biochemical properties of hepatitis C virus NS5B RNA-dependent RNA polymerase and identification of amino acid sequence motifs essential for enzymatic activity. *J Virol* 71(11):8416–8428
24. Bartenschlager R, Schaller H (1992) Hepadnaviral assembly is initiated by polymerase binding to the encapsidation signal in the viral RNA genome. *EMBO J* 11(9):3413–3420
25. Kaplan G, Racaniello VR (1988) Construction and characterization of poliovirus subgenomic replicons. *J Virol* 62(5):1687–1696

26. Mittelholzer C, Moser C, Tratschin JD, Hofmann MA (1997) Generation of cytopathogenic subgenomic RNA of classical swine fever virus in persistently infected porcine cell lines. *Virus Res* 51(2):125–137
27. Castillo L, Diaz P, Inostroza J, Espinoza R, Millaqueo L, Calderara M et al (1993) Prevalence of hepatitis C virus antibodies in chronic hemodialysis and kidney transplantation patients. *Rev Med Chil* 121(9):1024–1028
28. Behrens SE, Grassmann CW, Thiel HJ, Meyers G, Tautz N (1998) Characterization of an autonomous subgenomic pestivirus RNA replicon. *J Virol* 72(3):2364–2372
29. Khromykh AA, Westaway EG (1997) Subgenomic replicons of the flavivirus Kunjin: construction and applications. *J Virol* 71(2):1497–1505
30. Guo JT, Bichko VV, Seeger C (2001) Effect of alpha interferon on the hepatitis C virus replicon. *J Virol* 75(18):8516–8523
31. Ikeda M, Yi M, Li K, Lemon SM (2002) Selectable subgenomic and genome-length dicistronic RNAs derived from an infectious molecular clone of the HCV-N strain of hepatitis C virus replicate efficiently in cultured Huh7 cells. *J Virol* 76(6):2997–3006
32. Lohmann V, Hoffmann S, Herian U, Penin F, Bartenschlager R (2003) Viral and cellular determinants of hepatitis C virus RNA replication in cell culture. *J Virol* 77(5):3007–3019
33. Kishine H, Sugiyama K, Hijikata M, Kato N, Takahashi H, Noshi T et al (2002) Subgenomic replicon derived from a cell line infected with the hepatitis C virus. *Biochem Biophys Res Commun* 293(3):993–999
34. Blight KJ, McKeating JA, Marcotrigiano J, Rice CM (2003) Efficient replication of hepatitis C virus genotype 1a RNAs in cell culture. *J Virol* 77(5):3181–3190
35. Grobler JA, Markel EJ, Fay JF, Graham DJ, Simcoe AL, Ludmerer SW et al (2003) Identification of a key determinant of hepatitis C virus cell culture adaptation in domain II of NS3 helicase. *J Biol Chem* 278(19):16741–16746
36. Gu B, Gates AT, Isken O, Behrens SE, Sarisky RT (2003) Replication studies using genotype 1a subgenomic hepatitis C virus replicons. *J Virol* 77(9):5352–5359
37. Kato T, Date T, Miyamoto M, Furusaka A, Tokushige K, Mizokami M et al (2003) Efficient replication of the genotype 2a hepatitis C virus subgenomic replicon. *Gastroenterology* 125(6):1808–1817
38. Krieger N, Lohmann V, Bartenschlager R (2001) Enhancement of hepatitis C virus RNA replication by cell culture-adaptive mutations. *J Virol* 75(10):4614–4624
39. Lohmann V, Körner F, Dobierzewska A, Bartenschlager R (2001) Mutations in hepatitis C virus RNAs conferring cell culture adaptation. *J Virol* 75:1437–1449
40. Yi M, Lemon SM (2002) Replication of subgenomic hepatitis A virus RNAs expressing firefly luciferase is enhanced by mutations associated with adaptation of virus to growth in cultured cells. *J Virol* 76(3):1171–1180
41. Harak C, Meyrath M, Romero-Brey I, Schenk C, Gondeau C, Schult P et al (2016) Tuning a cellular lipid kinase activity adapts hepatitis C virus to replication in cell culture. *Nat Microbiol* 2:16247
42. Reiss S, Rebhan I, Backes P, Romero-Brey I, Erfle H, Matula P et al (2011) Recruitment and activation of a lipid kinase by hepatitis C virus NS5A is essential for integrity of the membranous replication compartment. *Cell Host Microbe* 9(1):32–45
43. Reiss S, Harak C, Romero-Brey I, Radujkovic D, Klein R, Ruggieri A et al (2013) The lipid kinase phosphatidylinositol-4 kinase III alpha regulates the phosphorylation status of hepatitis C virus NS5A. *PLoS Pathog* 9(5):e1003359
44. Wang H, Perry JW, Lauring AS, Neddermann P, De FR, Tai AW (2014) Oxysterol-binding protein is a phosphatidylinositol 4-kinase effector required for HCV replication membrane integrity and cholesterol trafficking. *Gastroenterology* 146(5):1373–1385
45. Stoeck IK, Lee JY, Tabata K, Romero-Brey I, Paul D, Schult P et al (2018) Hepatitis C virus replication depends on Endosomal cholesterol homeostasis. *J Virol* 92(1):e01196–e01117

46. Khan I, Katikaneni DS, Han Q, Sanchez-Felipe L, Hanada K, Ambrose RL et al (2014) Modulation of hepatitis C virus genome replication by glycosphingolipids and four-phosphate adaptor protein 2. *J Virol* 88(21):12276–12295
47. Bukh J, Pietschmann T, Lohmann V, Krieger N, Faulk K, Engle RE et al (2002) Mutations that permit efficient replication of hepatitis C virus RNA in Huh-7 cells prevent productive replication in chimpanzees. *Proc Natl Acad Sci U S A* 99(22):14416–14421
48. Pietschmann T, Zayas M, Meuleman P, Long G, Appel N, Koutsoudakis G et al (2009) Production of infectious genotype 1b virus particles in cell culture and impairment by replication enhancing mutations. *PLoS Pathog* 5(6):e1000475
49. Neddermann P, Quintavalle M, Di Pietro C, Clementi A, Cerretani M, Altamura S et al (2004) Reduction of hepatitis C virus NS5A hyperphosphorylation by selective inhibition of cellular kinases activates viral RNA replication in cell culture. *J Virol* 78(23):13306–13314
50. Evans MJ, Rice CM, Goff SP (2004) Phosphorylation of hepatitis C virus nonstructural protein 5A modulates its protein interactions and viral RNA replication. *Proc Natl Acad Sci U S A* 101(35):13038–13043
51. Blight KJ, McKeating JA, Rice CM (2002) Highly permissive cell lines for subgenomic and genomic hepatitis C virus RNA replication. *J Virol* 76(24):13001–13014
52. Murray EM, Grobler JA, Markel EJ, Pagnoni MF, Paonessa G, Simon AJ et al (2003) Persistent replication of hepatitis C virus replicons expressing the beta-lactamase reporter in subpopulations of highly permissive Huh7 cells. *J Virol* 77(5):2928–2935
53. Frese M, Pietschmann T, Moradpour D, Haller O, Bartenschlager R (2001) Interferon-alpha inhibits hepatitis C virus subgenomic RNA replication by an MxA-independent pathway. *J Gen Virol* 82.(Pt 4):723–733
54. Pietschmann T, Lohmann V, Rutter G, Kurpanek K, Bartenschlager R (2001) Characterization of cell lines carrying self-replicating hepatitis C virus RNAs. *J Virol* 75(3):1252–1264
55. Friebe P, Boudet J, Simorre JP, Bartenschlager R (2005) Kissing-loop interaction in the 3' end of the hepatitis C virus genome essential for RNA replication. *J Virol* 79(1):380–392
56. Sumpter Jr R, Loo YM, Foy E, Li K, Yoneyama M, Fujita T et al (2005) Regulating intracellular antiviral defense and permissiveness to hepatitis C virus RNA replication through a cellular RNA helicase, RIG-I. *J Virol* 79(5):2689–2699
57. Hiet MS, Bauhofer O, Zayas M, Roth H, Tanaka Y, Schirmacher P et al (2015) Control of temporal activation of hepatitis C virus-induced interferon response by domain 2 of nonstructural protein 5A. *J Hepatol* 63(4):829–837
58. Cao X, Ding Q, Lu J, Tao W, Huang B, Zhao Y et al (2015) MDA5 plays a critical role in interferon response during hepatitis C virus infection. *J Hepatol* 62(4):771–778
59. Binder M, Kochs G, Bartenschlager R, Lohmann V (2007) Hepatitis C virus escape from the interferon regulatory factor 3 pathway by a passive and active evasion strategy. *Hepatology* 46(5):1365–1374
60. Keskinen P, Nyqvist M, Sareneva T, Pirhonen J, Melén K, Julkunen I (1999) Impaired antiviral response in human hepatoma cells. *Virology* 263:364–375
61. Saeed M, Andreo U, Chung HY, Espiritu C, Branch AD, Silva JM et al (2015) SEC14L2 enables pan-genotype HCV replication in cell culture. *Nature* 524(7566):471–475
62. Yamane D, McGivern DR, Wauthier E, Yi M, Madden VJ, Welsch C et al (2014) Regulation of the hepatitis C virus RNA replicase by endogenous lipid peroxidation. *Nat Med* 20(8): 927–935
63. Pietschmann T, Lohmann V, Kaul A, Krieger N, Rinck G, Rutter G et al (2002) Persistent and transient replication of full-length hepatitis C virus genomes in cell culture. *J Virol* 76(8):4008–4021
64. Dreux M, Garaigorta U, Boyd B, Decembre E, Chung J, Whitten-Bauer C et al (2012) Short-range exosomal transfer of viral RNA from infected cells to plasmacytoid dendritic cells triggers innate immunity. *Cell Host Microbe* 12(4):558–570
65. Saeed M, Gondeau C, Hmwe S, Yokokawa H, Date T, Suzuki T et al (2013) Replication of hepatitis C virus genotype 3a in cultured cells. *Gastroenterology* 144(1):56–58

66. Saeed M, Scheel TK, Gottwein JM, Marukian S, Dustin LB, Bukh J et al (2012) Efficient replication of genotype 3a and 4a hepatitis C virus replicons in human hepatoma cells. *Antimicrob Agents Chemother* 56(10):5365–5373
67. Peng B, Yu M, Xu S, Lee YJ, Tian Y, Yang H et al (2013) Development of robust hepatitis C virus genotype 4 subgenomic replicons. *Gastroenterology* 144(1):59–61
68. Wose Kinge CN, Espiritu C, Prabdi-Sing N, Sithebe NP, Saeed M, Rice CM (2014) Hepatitis C virus genotype 5a subgenomic replicons for evaluation of direct-acting antiviral agents. *Antimicrob Agents Chemother* 58(9):5386–5394
69. Yu M, Peng B, Chan K, Gong R, Yang H, Delaney W et al (2014) Robust and persistent replication of the genotype 6a hepatitis C virus replicon in cell culture. *Antimicrob Agents Chemother* 58(5):2638–2646
70. Zhu Q, Guo JT, Seeger C (2003) Replication of hepatitis C virus subgenomes in nonhepatic epithelial and mouse hepatoma cells. *J Virol* 77(17):9204–9210
71. Date T, Kato T, Miyamoto M, Zhao Z, Yasui K, Mizokami M et al (2004) Genotype 2a hepatitis C virus subgenomic replicon can replicate in HepG2 and IMY-N9 cells. *J Biol Chem* 279(21):22371–22376
72. Kato T, Date T, Miyamoto M, Zhao Z, Mizokami M, Wakita T (2005) Nonhepatic cell lines HeLa and 293 support efficient replication of the hepatitis C virus genotype 2a subgenomic replicon. *J Virol* 79(1):592–596
73. Chang KS, Cai Z, Zhang C, Sen GC, Williams BR, Luo G (2006) Replication of hepatitis C virus (HCV) RNA in mouse embryonic fibroblasts: protein kinase R (PKR)-dependent and PKR-independent mechanisms for controlling HCV RNA replication and mediating interferon activities. *J Virol* 80(15):7364–7374
74. Narbus CM, Israelow B, Sourisseau M, Michta ML, Hopcraft SE, Zeiner GM et al (2011) HepG2 cells expressing microRNA miR-122 support the entire hepatitis C virus life cycle. *J Virol* 85(22):12087–12092
75. Thibault PA, Huys A, Dhillon P, Wilson JA (2013) MicroRNA-122-dependent and -independent replication of hepatitis C virus in Hep3B human hepatoma cells. *Virology* 436(1):179–190
76. Jopling CL, Yi M, Lancaster AM, Lemon SM, Sarnow P (2005) Modulation of hepatitis C virus RNA abundance by a liver-specific MicroRNA. *Science* 309(5740):1577–1581
77. Yi M, Bodola F, Lemon SM (2002) Subgenomic hepatitis C virus replicons inducing expression of a secreted enzymatic reporter protein. *Virology* 304(2):197–210
78. Vrolijk JM, Kaul A, Hansen BE, Lohmann V, Haagmans BL, Schalm SW et al (2003) A replicon-based bioassay for the measurement of interferons in patients with chronic hepatitis C. *J Virol Methods* 110(2):201–209
79. Moradpour D, Evans MJ, Gosert R, Yuan Z, Blum HE, Goff SP et al (2004) Insertion of green fluorescent protein into nonstructural protein 5A allows direct visualization of functional hepatitis C virus replication complexes. *J Virol* 78(14):7400–7409
80. Wolk B, Buchele B, Moradpour D, Rice CM (2008) A dynamic view of hepatitis C virus replication complexes. *J Virol* 82(21):10519–10531
81. Wakita T, Pietschmann T, Kato T, Date T, Miyamoto M, Zhao Z et al (2005) Production of infectious hepatitis C virus in tissue culture from a cloned viral genome. *Nat Med* 11(7):791–796
82. Lindenbach BD, Evans MJ, Syder AJ, Wolk B, Tellinghuisen TL, Liu CC et al (2005) Complete replication of hepatitis C virus in cell culture. *Science* 309(5734):623–626
83. Zhong J, Gastaminza P, Cheng G, Kapadia S, Kato T, Burton DR et al (2005) Robust hepatitis C virus infection in vitro. *Proc Natl Acad Sci U S A* 102(26):9294–9299
84. Bartenschlager R, Pietschmann T (2005) Efficient hepatitis C virus cell culture system: what a difference the host cell makes. *Proc Natl Acad Sci U S A* 102(28):9739–9740
85. Zhong J, Gastaminza P, Chung J, Stamataki Z, Isogawa M, Cheng G et al (2006) Persistent hepatitis C virus infection in vitro: coevolution of virus and host. *J Virol* 80(22):11082–11093

86. Russell RS, Meunier JC, Takikawa S, Faulk K, Engle RE, Bukh J et al (2008) Advantages of a single-cycle production assay to study cell culture-adaptive mutations of hepatitis C virus. *Proc Natl Acad Sci U S A* 105(11):4370–4375
87. Kaul A, Woerz I, Meuleman P, Leroux-Roels G, Bartenschlager R (2007) Cell culture adaptation of hepatitis C virus and in vivo viability of an adapted variant. *J Virol* 81(23):13168–13179
88. Delgrange D, Pillez A, Castelain S, Cocquerel L, Rouille Y, Dubuisson J et al (2007) Robust production of infectious viral particles in Huh-7 cells by introducing mutations in hepatitis C virus structural proteins. *J Gen Virol* 88.(Pt 9):2495–2503
89. Yi M, Ma Y, Yates J, Lemon SM (2007) Compensatory mutations in E1, p7, NS2, and NS3 enhance yields of cell culture-infectious intergenotypic chimeric hepatitis C virus. *J Virol* 81(2):629–638
90. Scheel TK, Gottwein JM, Carlsen TH, Li YP, Jensen TB, Spengler U et al (2011) Efficient culture adaptation of hepatitis C virus recombinants with genotype-specific core-NS2 by using previously identified mutations. *J Virol* 85(6):2891–2906
91. Gottwein JM, Scheel TK, Jensen TB, Lademann JB, Prentoe JC, Knudsen ML et al (2009) Development and characterization of hepatitis C virus genotype 1-7 cell culture systems: role of CD81 and scavenger receptor class B type I and effect of antiviral drugs. *Hepatology* 49(2):364–377
92. Pietschmann T, Kaul A, Koutsoudakis G, Shavinskaya A, Kallis S, Steinmann E et al (2006) Construction and characterization of infectious intra- and intergenotypic hepatitis c virus chimeras. *Proc Natl Acad Sci U S A* 103(19):7408–7413
93. Gottwein JM, Scheel TK, Hoegh AM, Lademann JB, Eugen-Olsen J, Lisby G et al (2007) Robust hepatitis C genotype 3a cell culture releasing adapted intergenotypic 3a/2a (S52/JFH1) viruses. *Gastroenterology* 133(5):1614–1626
94. Jensen TB, Gottwein JM, Scheel TK, Hoegh AM, Eugen-Olsen J, Bukh J (2008) Highly efficient JFH1-based cell-culture system for hepatitis C virus genotype 5a: failure of homologous neutralizing-antibody treatment to control infection. *J Infect Dis* 198(12):1756–1765
95. Koutsoudakis G, Kaul A, Steinmann E, Kallis S, Lohmann V, Pietschmann T et al (2006) Characterization of the early steps of hepatitis C virus infection by using luciferase reporter viruses. *J Virol* 80(11):5308–5320
96. Tschernie DM, Jones CT, Evans MJ, Lindenbach BD, McKeating JA, Rice CM (2006) Time- and temperature-dependent activation of hepatitis C virus for low-pH-triggered entry. *J Virol* 80(4):1734–1741
97. Jones CT, Murray CL, Eastman DK, Tassello J, Rice CM (2007) Hepatitis C virus p7 and NS2 proteins are essential for production of infectious virus. *J Virol* 81(16):8374–8383
98. Gottwein JM, Jensen TB, Mathiesen CK, Meuleman P, Serre SB, Lademann JB et al (2011) Development and application of hepatitis C reporter viruses with genotype 1 to 7 core- nonstructural protein 2 (NS2) expressing fluorescent proteins or luciferase in modified JFH1 NS5A. *J Virol* 85(17):8913–8928
99. Schaller T, Appel N, Koutsoudakis G, Kallis S, Lohmann V, Pietschmann T et al (2007) Analysis of hepatitis C virus superinfection exclusion by using novel fluorochrome gene-tagged viral genomes. *J Virol* 81(9):4591–4603
100. Schoggins JW, Wilson SJ, Panis M, Murphy MY, Jones CT, Bieniasz P et al (2011) A diverse range of gene products are effectors of the type I interferon antiviral response. *Nature* 472(7344):481–485
101. Yi M, Ma Y, Yates J, Lemon SM (2009) Trans-complementation of an NS2 defect in a late step in hepatitis C virus (HCV) particle assembly and maturation. *PLoS Pathog* 5(5):e1000403
102. Merz A, Long G, Hiet MS, Brugger B, Chlanda P, Andre P et al (2011) Biochemical and morphological properties of hepatitis C virus particles and determination of their lipidome. *J Biol Chem* 286(4):3018–3032
103. Catanese MT, Uryu K, Kopp M, Edwards TJ, Andrus L, Rice WJ et al (2013) Ultrastructural analysis of hepatitis C virus particles. *Proc Natl Acad Sci U S A* 110(23):9505–9510

104. Paul D, Hoppe S, Saher G, Krijnse-Locker J, Bartenschlager R (2013) Morphological and biochemical characterization of the membranous hepatitis C virus replication compartment. *J Virol* 87(19):10612–10627
105. Yi M, Villanueva RA, Thomas DL, Wakita T, Lemon SM (2006) Production of infectious genotype 1a hepatitis C virus (Hutchinson strain) in cultured human hepatoma cells. *Proc Natl Acad Sci U S A* 103(7):2310–2315
106. Yi M, Lemon SM (2004) Adaptive mutations producing efficient replication of genotype 1a hepatitis C virus RNA in normal Huh7 cells. *J Virol* 78(15):7904–7915
107. Li YP, Ramirez S, Jensen SB, Purcell RH, Gottwein JM, Bukh J (2012) Highly efficient full-length hepatitis C virus genotype 1 (strain TN) infectious culture system. *Proc Natl Acad Sci U S A* 109(48):19757–19762
108. Li YP, Ramirez S, Gottwein JM, Scheel TK, Mikkelsen L, Purcell RH et al (2012) Robust full-length hepatitis C virus genotype 2a and 2b infectious cultures using mutations identified by a systematic approach applicable to patient strains. *Proc Natl Acad Sci U S A* 109(18):E1101–E1110
109. Date T, Kato T, Kato J, Takahashi H, Morikawa K, Akazawa D et al (2012) Novel cell culture-adapted genotype 2a hepatitis C virus infectious clone. *J Virol* 86(19):10805–10820
110. Ramirez S, Li YP, Jensen SB, Pedersen J, Gottwein JM, Bukh J (2014) Highly efficient infectious cell culture of three HCV genotype 2b strains and sensitivity to lead protease, NS5A, and polymerase inhibitors. *Hepatology* 59(2):395–407
111. Kim S, Date T, Yokokawa H, Kono T, Aizaki H, Maurel P et al (2014) Development of hepatitis C virus genotype 3a cell culture system. *Hepatology* 60(6):1838–1850
112. Ramirez S, Mikkelsen LS, Gottwein JM, Bukh J (2016) Robust HCV genotype 3a infectious cell culture system permits identification of escape variants with resistance to sofosbuvir. *Gastroenterology* 151(5):973–985
113. Scheel TK, Gottwein JM, Mikkelsen LS, Jensen TB, Bukh J (2011) Recombinant HCV variants with NS5A from genotypes 1–7 have different sensitivities to an NS5A inhibitor but not interferon-alpha. *Gastroenterology* 140(3):1032–1042
114. Gottwein JM, Scheel TK, Jensen TB, Ghanem L, Bukh J (2011) Differential efficacy of protease inhibitors against HCV genotypes 2a, 3a, 5a, and 6a NS3/4A protease recombinant viruses. *Gastroenterology* 141(3):1067–1079
115. Li YP, Ramirez S, Humes D, Jensen SB, Gottwein JM, Bukh J (2014) Differential sensitivity of 5'UTR-NS5A recombinants of hepatitis C virus genotypes 1–6 to protease and NS5A inhibitors. *Gastroenterology* 146(3):812–821
116. Koutsoudakis G, Herrmann E, Kallis S, Bartenschlager R, Pietschmann T (2007) The level of CD81 cell surface expression is a key determinant for productive entry of hepatitis C virus into host cells. *J Virol* 81(2):588–598
117. Scholtes C, Ramiere C, Rainteau D, Perrin-Cocon L, Wolf C, Humbert L et al (2012) High plasma level of nucleocapsid-free envelope glycoprotein-positive lipoproteins in hepatitis C patients. *Hepatology* 56(1):39–48
118. Andre P, Komurian-Pradel F, Deforges S, Perret M, Berland JL, Sodoyer M et al (2002) Characterization of low- and very-low-density hepatitis C virus RNA-containing particles. *J Virol* 76(14):6919–6928
119. Bartenschlager R, Penin F, Lohmann V, Andre P (2011) Assembly of infectious hepatitis C virus particles. *Trends Microbiol* 19(2):95–103
120. Windisch MP, Frese M, Kaul A, Trippler M, Lohmann V, Bartenschlager R (2005) Dissecting the interferon-induced inhibition of hepatitis C virus replication by using a novel host cell line. *J Virol* 79(21):13778–13793
121. Zhu H, Dong H, Eksioglu E, Hemming A, Cao M, Crawford JM et al (2007) Hepatitis C virus triggers apoptosis of a newly developed hepatoma cell line through antiviral defense system. *Gastroenterology* 133(5):1649–1659
122. Ali S, Pellerin C, Lamarre D, Kukulj G (2004) Hepatitis C virus subgenomic replicons in the human embryonic kidney 293 cell line. *J Virol* 78(1):491–501

123. Fletcher NF, Yang JP, Farquhar MJ, Hu K, Davis C, He Q et al (2010) Hepatitis C virus infection of neuroepithelioma cell lines. *Gastroenterology* 139(4):1365–1374
124. Long G, Hiet MS, Windisch MP, Lee JY, Lohmann V, Bartenschlager R (2011) Mouse hepatic cells support assembly of infectious hepatitis C virus particles. *Gastroenterology* 141(3):1057–1066
125. Frentzen A, Kusuma A, Guerlevik E, Hueging K, Knocke S, Ginkel C et al (2014) Cell entry, efficient RNA replication, and production of infectious hepatitis C virus progeny in mouse liver-derived cells. *Hepatology* 59(1):78–88
126. Uprichard SL, Chung J, Chisari FV, Wakita T (2006) Replication of a hepatitis C virus replicon clone in mouse cells. *Virology* 343:89
127. Vogt A, Scull MA, Friling T, Horwitz JA, Donovan BM, Dorner M et al (2013) Recapitulation of the hepatitis C virus life-cycle in engineered murine cell lines. *Virology* 444(1–2):1–11
128. Bengrine A, Brochot E, Louchet M, Herpe YE, Duverlie G (2016) Modeling of HBV and HCV hepatitis with hepatocyte-like cells. *Front Biosci (Schol Ed)* 8:97–105
129. Grakoui A, McCourt DW, Wychowski C, Feinstone SM, Rice CM (1993) Characterization of the hepatitis C virus-encoded serine proteinase: determination of proteinase-dependent polyprotein cleavage sites. *J Virol* 67(5):2832–2843
130. Tomei L, Failla C, Santolini E, De FR, La MN (1993) NS3 is a serine protease required for processing of hepatitis C virus polyprotein. *J Virol* 67(7):4017–4026
131. Hijikata M, Mizushima H, Tanji Y, Komoda Y, Hirowatari Y, Akagi T et al (1993) Proteolytic processing and membrane association of putative nonstructural proteins of hepatitis C virus. *Proc Natl Acad Sci U S A* 90(22):10773–10777
132. Behrens SE, Tomei L, De FR (1996) Identification and properties of the RNA-dependent RNA polymerase of hepatitis C virus. *EMBO J* 15(1):12–22
133. Pawlotsky JM (2003) The nature of interferon-alpha resistance in hepatitis C virus infection. *Curr Opin Infect Dis* 16(6):587–592
134. Gao M, Nettles RE, Belema M, Snyder LB, Nguyen VN, Fridell RA et al (2010) Chemical genetics strategy identifies an HCV NS5A inhibitor with a potent clinical effect. *Nature* 465(7294):96–100
135. Delang L, Neyts J, Vliegen I, Abrignani S, Neddermann P, De FR (2013) Hepatitis C virus-specific directly acting antiviral drugs. *Curr Top Microbiol Immunol* 369:289–320
136. Sarrazin C, Hezode C, Zeuzem S, Pawlotsky JM (2012) Antiviral strategies in hepatitis C virus infection. *J Hepatol* 56(Suppl 1):S88–S100
137. Kalaghatgi P, Sikorski AM, Knops E, Rupp D, Sierra S, Heger E et al (2016) Geno2pheno [HCV] – a web-based interpretation system to support hepatitis C treatment decisions in the era of direct-acting antiviral agents. *PLoS One* 11(5):e0155869
138. Watashi K, Hijikata M, Hosaka M, Yamaji M, Shimotohno K (2003) Cyclosporin A suppresses replication of hepatitis C virus genome in cultured hepatocytes. *Hepatology* 38(5):1282–1288
139. Yang F, Robotham JM, Nelson HB, Irsigler A, Kenworthy R, Tang H (2008) Cyclophilin A is an essential cofactor for hepatitis C virus infection and the principal mediator of cyclosporine resistance in vitro. *J Virol* 82(11):5269–5278
140. Kaul A, Stauffer S, Berger C, Pertel T, Schmitt J, Kallis S et al (2009) Essential role of cyclophilin A for hepatitis C virus replication and virus production and possible link to polyprotein cleavage kinetics. *PLoS Pathog* 5(8):e1000546
141. Lanford RE, Hildebrandt-Eriksen ES, Petri A, Persson R, Lindow M, Munk ME et al (2010) Therapeutic silencing of microRNA-122 in primates with chronic hepatitis C virus infection. *Science* 327(5962):198–201
142. van der Ree MH, van der Meer AJ, de BJ, Maan R, van VA, Welzel TM et al (2014) Long-term safety and efficacy of microRNA-targeted therapy in chronic hepatitis C patients. *Antivir Res* 111:53–59
143. Kaufmann SHE, Dorhoi A, Hotchkiss RS, Bartenschlager R (2018) Host-directed therapies for bacterial and viral infections. *Nat Rev Drug Discov* 17(1):35–56

The Role of Interferon for the Treatment of Chronic Hepatitis C Virus Infection



Saleh A. Alqahtani and Mark S. Sulkowski

Contents

1	Introduction	98
2	Interferons	99
3	Standard Interferon Alfa Monotherapy	100
4	Standard Interferon Alfa and Ribavirin Combination Therapy	101
5	Pegylated Interferon Alfa Monotherapy	102
6	Pegylated Interferon Alfa and Ribavirin Combination Therapy	103
7	Other Types of Interferons	106
8	The Addition of HCV Direct-Acting Antivirals to Peginterferons Plus Ribavirin	107
9	Conclusions	108
	References	108

Abstract For many years the only available therapy for chronic hepatitis C virus (HCV) infection was interferon-based therapy. Interferons are a family of cytokines that are an essential part of the body's natural response to viral pathogens. In 1991, interferon- α (IFN- α) injections were first approved by the Food and Drug Administration for the treatment of HCV infection and remained the backbone of therapy until late 2014. As monotherapy, IFN- α injected thrice weekly yielded low sustained virologic response (SVR) rates. In 1998, the addition of ribavirin, a broad-spectrum, non-specific antiviral agent, decreased liver inflammation alone and, in combination with IFN- α , increased the SVR rate; however, the addition of ribavirin also increased side effects. In the early 2000s, IFN- α plus ribavirin combination treatment was further improved by the development of longer-acting pegylated IFN- α (PegIFN- α). While this reduced the need for subcutaneous injections from three times a week to

S. A. Alqahtani

Johns Hopkins University School of Medicine, Baltimore, MD, USA

M. S. Sulkowski (✉)

Johns Hopkins University School of Medicine, Baltimore, MD, USA

Department of Medicine, Viral Hepatitis Center, The Johns Hopkins Hospital, Baltimore, MD, USA

e-mail: msulkowski@jhmi.edu

once a week which improved patients' adherence, the increase in SVR with PegIFN- α over standard IFN- α was relatively modest. Further, drug-related side effects remained problematic, limiting HCV treatment uptake and effectiveness. In the early direct-acting antiviral (DAA) era, PegIFN- α and ribavirin were used in combination with DAAs to prevent drug resistance and increase the SVR rate. With the advent of combination DAA regimens, the role of IFN- α decreased dramatically and, in late 2017, IFN- α was no longer recommended by professional societies as a first-line treatment for any HCV genotype or patient population, marking the end of the IFN- α era.

Keywords Chronic infection, Hepatitis C virus, Inflammation, Interferon, Therapy

1 Introduction

Scientific discoveries related to the structure and replication of the hepatitis C virus (HCV) set the stage for the development of direct-acting antivirals (DAAs) for the treatment of HCV infection [1]. Prior to these breakthroughs, the foundation of HCV treatment was recombinant interferon alfa (IFN- α) which induce non-specific antiviral and immunologic activity against HCV in infected persons (Table 1).

Table 1 The timeline of interferon therapy for hepatitis C viral infection

Year	Therapeutic development
1986	IFN- α first used to treat "non-A, non-B hepatitis"
	Normalized ALT levels for 25–40% patients after 2–3 months
1989	HCV identified as the cause of most cases on non-A, non-B hepatitis
1991	FDA approval of IFN- α 3MU by subcutaneous injection thrice weekly for 24 or 48 weeks
	SVR of 12–16% for persons with HCV genotype infection
1999	The addition of ribavirin to IFN- α significantly improved rates of SVR to 35–45%
2001	PegIFN- α subcutaneous injection weekly plus ribavirin emerges as the standard of care for the treatment of chronic HCV infection
	SVR of 70–90% in genotypes 2 and 3 HCV infection
	SVR of 40–50% in other genotypes (including genotype 1)
2011	Boceprevir and telaprevir (NS3/4A protease inhibitor) approved by the FDA in combination with PegIFN- α and ribavirin
	Triple therapy introduced with PegIFN- α , ribavirin, and DAA
	SVR of 75% in genotype 1 HCV infection
2013	FDA approval of sofosbuvir (NS5B polymerase inhibitor) plus PegIFN- α and ribavirin as well as the first interferon-free regimen of sofosbuvir plus ribavirin
2017	AASLD/IDSA guidelines no longer recommend the use of interferon for any patient population or HCV genotype infection

IFN interferon, *HCV* hepatitis C virus, *ALT* alanine aminotransferase, *FDA* Food and Drug Administration, *SVR* sustained virologic response, *DAA* direct-acting antivirals, *AASLD* American Association for the Study of Liver Diseases, *IDSA* Infectious Diseases Society of America

While in the era of combination HCV DAA therapy the role of interferon has dramatically diminished, IFN- α was the cornerstone of HCV treatment from 1991 until late 2014 [2].

Interferons are soluble glycoproteins and cytokines, small proteins involved in cell signaling, that are an essential part of the body's natural response to viral infection [3]. There are many different interferons, and they are classified as types I, II, and III according to their receptor binding [3]. For HCV treatment, type I interferons are the most commonly used, mainly interferon- α (IFN- α) but also IFN- β [3], while the type III IFN- λ showed some promise [4].

Before HCV was identified as the agent mainly responsible for non-A, non-B hepatitis, IFN- α showed promise as an effective treatment [5]. However, early treatment regimens had some shortcomings; in many patients, the responses were disappointing, and as IFN- α has a short half-life, this meant patients needed subcutaneous injections three times a week. The addition of daily ribavirin, a broad-spectrum antiviral agent, improved the number of patients with a favorable response, however, at the expense of increasing side effects [6]. Moreover, the attachment of inert polyethylene glycol to create pegylated IFN- α (PegIFN- α) reduced the rapid degradation and clearance of IFN- α . Improved pharmacokinetics meant high levels of IFN- α could be sustained for extended periods of time, reducing the frequency of injection to once weekly [7]. However, even with these improvements, cure from HCV remained suboptimal with PegIFN- α and ribavirin, which lead to further research to discover more effective therapy with a better safety profile [3].

IFN- β has achieved excellent results for patients with genotype 1 infection who are mainly poor responders to standard treatment [8]. Receptors for type I interferons are expressed on all cells, whereas the expression of IFN- λ receptors is more localized. This observation suggests that IFN- λ is a useful alternative treatment for patients who experience severe side effects from interferon treatment [4]. Other recombinant interferon proteins have also been investigated including IFN- α 2b fused with human serum albumin, known as albinterferon [9], and the consensus interferon (CIFN), an artificial interferon with the most common human IFN- α subtype amino acid at each position in the protein sequence [10].

As DAAs have become more widely available and less expensive, interferon alfa is no longer used to treat HCV infection in most regions, and very few persons with chronic HCV infection patients are expected to use this agent in the future [2]. This review aims to present the history of interferon therapy for patients infected with HCV.

2 Interferons

Interferons are a heterogeneous class of soluble glycoproteins that are expressed in response to viral or bacterial infection [3]. Interferons are released as the first line of defense by infected cells, and this then protects the neighboring uninfected cells against viral infection [11]. There are three types of interferon, types I, II, and III,

classified according to the structure of their membrane cell surface receptors. The antiviral properties of these proteins have led to the therapeutic use of recombinant interferons for viral infections including hepatitis C and B virus [11]. Also, interferon has broad application in treating various diseases including multiple sclerosis, leukemia, melanoma, human papillomavirus infection, chronic granulomatous disease, and malignant osteoporosis [12–14]. In many of these situations, they have been found to complement various antiviral drugs [11].

Type I interferons are cytokines that bind to the IFN- α/β -receptor (IFNAR). Type I interferons include multiple IFN- α subtypes and IFN- β , IFN- ϵ , IFN- κ , and IFN- ω [15]. For HCV infection, interferon therapy has mainly involved IFN- α , a type I interferon. When IFN- α binds IFNAR, this activates the Janus kinase/signal transducers and activators of transcription (JAK/STAT) signaling pathway. Several hundred interferon-stimulated genes are then stimulated by JAK/STAT to provide antiviral, antiproliferative, antitumor, or immunomodulatory actions [16]. Two subtypes of IFN- α were used to treat HCV infection, IFN- α -2a and IFN- α -2b; these are similar in structure but bind with different affinities to the IFNAR receptor subunits 1 and 2 [17]. In clinical trials, the efficacy and adverse profiles of IFN- α -2a and IFN- α -2b were similar and mostly indistinguishable from a clinical perspective [18].

3 Standard Interferon Alfa Monotherapy

HCV cure is measured by the demonstration of a sustained virologic response (SVR) defined as undetectable HCV RNA by polymerase chain reaction (PCR) after cessation of antiviral therapy [19]. SVR was initially assessed at 24 weeks after stopping therapy but, more recently, undetectable HCV RNA 12 weeks (SVR12) after therapy has been accepted as evidence of HCV cure [19]. In 1986, IFN- α was first used as a monotherapy for HCV [5], before the discovery of HCV as the cause of disease in most persons with non-A, non-B hepatitis in 1989 [20]. In these early investigations, treatment efficacy was measured biochemically by testing alanine aminotransferase (ALT) level as a measure of ongoing liver injury from HCV [21, 22].

Initially, IFN- α monotherapy regimen was administered as IFN- α -2b three million units (MU) subcutaneous injections three times a week for 24 weeks; approximately, 25 to 40% of persons treated with this regimen achieved normalization of serum ALT level by the end of the treatment which was a significant advance for a disease with no prior therapeutic options [23, 24]. Unfortunately, the ALT response was only sustained in 8–9% of patients after stopping IFN- α monotherapy, and the most effective IFN- α regimens were prolonged courses of treatment over 12 to 18 months [25]. However, in those with sustained ALT normalization, later studies confirmed these outcomes were strongly associated with the absence of detectable HCV RNA and long-term follow-up of patients indicated improved clinical outcomes [26]. In addition to low and heterogeneous response rates, IFN- α monotherapy was also associated with adverse side effects including flu-like

symptoms, hematological toxicity, elevated liver enzymes, nausea, fatigue, and autoimmune, thyroid, and psychiatric sequelae [27]. In light of long treatment durations with a low likelihood of sustained response and nearly universal side effects, many patients did not initiate or failed to complete IFN- α monotherapy.

4 Standard Interferon Alfa and Ribavirin Combination Therapy

From 1991 until 1998, IFN- α monotherapy was the only treatment available for chronic HCV infection. Due to limited effectiveness, rates of treatment uptake and, among those treated, SVR were low during this period. The next breakthrough in HCV therapy was the addition of the non-specific antiviral ribavirin to IFN- α monotherapy. Discovered in 1970, ribavirin (1- β -D-ribofuranosyl-1,2,4-triazole-3-carboxamide) is a guanosine nucleoside analogue with broad-spectrum antiviral activity [28]. Even now, its full mechanism of action in the treatment of HCV is not fully understood [31–33]. Interestingly, ribavirin monotherapy did not demonstrate antiviral activity in persons chronically infected with HCV [29]; however, serum ALT levels and liver inflammation decreased in some patients while taking ribavirin [30, 31]. The observed biochemical response led to clinical trials of IFN- α alone and in combination with ribavirin. When used in combination with IFN- α , ribavirin achieved higher SVR than IFN- α alone resulting in a sustained virologic response in approximately 40% of persons receiving combination therapy [6, 32, 33]. On the basis of large randomized controlled trials, the combination of IFN- α -2b plus ribavirin was approved for the treatment of chronic HCV infection. In the first study, McHutchison and colleagues randomized 912 HCV treatment-naïve patients with HCV infection to receive the standard IFN- α -2b alone or in combination with ribavirin for 24 or 48 weeks. The SVR rate was markedly higher in persons who received combination therapy for either 24 weeks or 48 weeks (31–38%) compared to patients who received IFN- α -2b alone for either 24 weeks or 48 weeks (6–13%) [34]. In the second study, Poynard and coworkers randomized 832 treatment-naïve patients with HCV into three groups: IFN- α -2b plus ribavirin for 24 weeks, IFN- α -2b plus ribavirin for 48 weeks, or IFN- α -2b plus placebo for 48 weeks. SVR was achieved in 43% and 35% of patients treated with combination therapy for 48 weeks and 24 weeks, respectively, and only 19% of those treated with IFN- α -2b monotherapy [35]. In these studies, response to interferon plus ribavirin was associated with HCV genotype 2 or 3 infection, lower baseline HCV RNA level (<2 million copies/mL), younger age, female sex, and less liver fibrosis. While the mechanism of action of ribavirin was and is incompletely understood, the addition of ribavirin to IFN- α led to a substantial increase in SVR, largely by reducing the number of persons who experienced HCV relapse after stopping treatment. In one study, the magnitude of the biochemical response to ribavirin monotherapy appeared to predict the response to combination therapy [36]. Regardless of the mechanism,

the combination therapy was a major advance in HCV therapy limited only by the adverse effects of the two-drug regimen [37]. Compared to placebo, the addition of ribavirin led to more side effects which were treatment-limiting for some patients, including hemolytic anemia, cough and dyspnea, rash and pruritus, and nausea. Also, ribavirin is teratogenic, bringing additional concern regarding pregnancy before and immediately after treatment with this agent [38].

The most significant adverse event related to ribavirin is dose-dependent hemolytic anemia, leading to a 2- to 3-g decline in hemoglobin in most persons. In some studies, persons with a greater magnitude of hemoglobin decline were more likely to achieve SVR, suggesting that the degree of anemia was associated with ribavirin exposure [39]. The mechanism of hemolytic anemia is thought to be related to phosphorylation of ribavirin inside the cells to ribavirin monophosphate [40]. Red blood cells lack 5' nucleotidase and alkaline phosphatase needed to dephosphorylate and transport ribavirin monophosphate, so ribavirin monophosphate accumulates [41]. Ribavirin monophosphate is also phosphorylated further to ribavirin diphosphate and then ribavirin triphosphate. High levels of ribavirin triphosphate then interfere with the normal ATP-dependent systems within the red blood cells, which can result in hemolysis [42]. This anemia was managed with ribavirin dose reduction and, in some circumstance, epoetin alfa to stimulate the production of RBC from the bone marrow.

The approval of standard IFN- α -2b plus ribavirin by the US Food and Drug Administration (1998) marked a significant step forward in HCV treatment. The duration of combination HCV treatment was 24 weeks for persons with HCV genotype 2 or 3 infection and 48 weeks for those with HCV genotype 1 infection. In Europe, the EASL International Consensus Conference allowed for the use of IFN- α -2b plus ribavirin for 24 weeks in persons with HCV genotype 1 and low levels of HCV RNA at baseline ($<2 \times 10^6$ copies/mL) [43]. Of note, the next breakthrough in HCV treatment was nearly a decade later with the approval of the HCV NS3/4A protease inhibitors, telaprevir, and boceprevir, in 2008.

5 Pegylated Interferon Alfa Monotherapy

Before the approval of the first HCV DAAs, the field witnessed an incremental advance in HCV treatment with the development of longer-acting interferon alfa injections. In 1991, standard IFN- α -2b as thrice-weekly injections led to peaks and troughs in interferon exposure which contributed to lower efficacy and also increased side effects due to the fluctuating exposure. In 2000, the issue of short interferon half-life was addressed by the addition of inert polyethylene glycol (PEG) to IFN- α which resulted in decreased degradation and clearance, increasing the half-life of interferon and consequently permitting less frequent weekly dosing while maintaining higher and sustained interferon levels [44, 45]. Ultimately, two pegylated interferons or peginterferons (PegIFNs) were approved for use in patients with chronic HCV infection, PegIFN- α -2a (Pegasys[®], Hoffmann-La

Roche, Nutley, NJ) and PegIFN- α -2b (Peg-Intron[®], Schering-Plough Corp., Kenilworth, NJ). PegIFN- α -2a is formed by the addition of a 40-kDa branched PEG moiety covalently linked to the standard interferon alfa-2a molecule. This alteration created a molecule with a mean terminal half-life of approximately 80 h and allowed for once-weekly dosing with a fixed dose of 180 μ g. PegIFN- α -2b is formed by the addition of a 12-kDa linear PEG moiety covalently linked to standard IFN- α -2b molecule [46]. This alteration created a molecule with a mean terminal half-life of approximately 40 h and allowed for once-weekly dosing with a weight-based dose of 1.5 μ g/kg of body weight. PegIFN- α -2b and PegIFN- α -2a were approved by the US Food and Drug Administration in 2001 and 2002, respectively, and replaced standard interferon.

The basis for the shift from standard to long-acting pegylated IFN was randomized studies comparing the formulations. Several clinical trials demonstrated higher rates of SVR in persons receiving PegIFN monotherapy versus standard IFN monotherapy [7, 47, 48]. In one study, Zeuzem et al. [7] randomized 531 HCV treatment-naïve patients to receive either PegIFN- α -2a weekly or IFN- α -2a thrice weekly for 48 weeks; the SVR rate was 39% in patients randomized to PegIFN group compared to only 19% in those who received standard IFN. In a dose-finding study, Reddy and colleagues found that PegIFN- α -2a 180 μ g weekly was the optimum dose for efficacy, safety, and tolerability in patients without advanced liver disease [47]. In another phase 3 trial, PegIFN- α -2a was evaluated in persons with compensated cirrhosis for whom safety and efficacy of interferon were generally worse than was observed in other patient population [49]. The cirrhotic patients were randomized to receive IFN- α -2a thrice weekly, PegIFN- α -2a 90 mcg weekly, or PegIFN- α -2a 180 mcg weekly with SVR rates of 8%, 15%, and 30% in each group, respectively [49]. These studies demonstrated that PegIFN was more effective than standard IFN, leading the way for the use of PegIFN plus ribavirin for most patients. However, PegIFN monotherapy was the standard of care for persons who were not able to take ribavirin including those not able to tolerate hemolysis such as persons with renal insufficiency, hemoglobinopathies, and cardiovascular disease.

6 Pegylated Interferon Alfa and Ribavirin Combination Therapy

The next step in HCV drug development was the combination of PegIFN plus ribavirin therapy which was the part of the standard of care for the treatment of chronic HCV infection for more than a decade from 2001 to October 2014. In phase 3 clinical trials of PegIFN- α -2a and PegIFN- α -2b in combination with ribavirin, persons with HCV genotype 1 infection had SVR rates of 46% and 42%, respectively [50–52]. However, the cross-study comparison of these combination treatments was difficult because the studies used different doses of ribavirin. The trials of PegIFN- α -2a were conducted with weight-based dosing of ribavirin (1,000 mg/day

for persons less than 75 kg and 1,200 mg/day for persons greater than or equal to 75 kg) which was the standard dosing schema with standard interferon. In contrast, the trials of PegIFN- α -2b were conducted with fixed-dose ribavirin (800 mg/day) for all participants. Since SVR rates were generally higher in persons with greater ribavirin exposure (ribavirin mg per kilogram), this led to uncertainty as to the efficacy of the two types PegIFN in combination with ribavirin. Also, differences were observed concerning the SVR rates achieved in patients enrolled in the United States and Europe with higher response rates in the non-US patient population. This uncertainty prompted the conduct of the largest HCV clinical trial ever conducted, the IDEAL study. The study was a large, multicenter, prospective, randomized, controlled study performed in the United States to provide a head-to-head comparison of the antiviral efficacy and adverse events of PegIFN- α -2a and PegIFN- α -2b [53]. Overall, 3,070 patients with HCV genotype 1 infection were randomized to 48 weeks of treatment with 1 of 3 PegIFN plus ribavirin regimens: PegIFN alfa-2b standard-dose (1.5 mcg/kg) plus weight-based ribavirin (800–1,400 mg/kg), PegIFN alfa-2b low-dose (1.0 mcg/kg) plus weight-based ribavirin (800–1,400 mg/kg), or PegIFN- α -2a 180 mcg plus weight-based ribavirin (1,000–1,200 mg/kg). The SVR rates achieved in all three groups were similar: 39.8% with the standard-dose PegIFN- α -2b, 38.0% with low-dose PegIFN- α -2b, and 40.9% with PegIFN- α -2a. The safety profile was also similar among the three groups; serious adverse events occurred in 8.6 to 11.7% of patients [53]. In contrast, two studies in Europe showed better efficacy for PegIFN- α -2a compared to PegIFN- α -2b in combination with ribavirin, mostly in HCV genotype 1 [54, 55].

The most important contribution of the IDEAL study was the identification of host genetic polymorphism by a genome-wide association study (GWAS) that explained much of the heterogeneity observed in viral response to interferon, namely, the lower SVR rates observed in persons with African ancestry compared to those with European or Asian ancestry. Ge and colleagues performed genotyping on 1,671 patients who were treated in the IDEAL study and consented to genetic testing; all were HCV treatment naïve and had HCV genotype 1 infection [56]. The researchers found that a polymorphism on chromosome 19 (rs12979860) located upstream of the gene for interleukin28B (IL28B) was strongly associated with SVR in all patient populations. The presence of the IL28B CC genotype was associated with an approximately twofold higher SVR rate compared to the presence of the CT or TT genotype. Interestingly, the frequency of the CC genotype was highest in persons of Asian ancestry and lowest in those of African ancestry and explained 56% of the observed lower SVR rates in persons with African ancestry. Thompson and coworkers incorporated this single-nucleotide polymorphism into models of existing baseline predictors of SVR following PegIFN plus ribavirin treatment and found that IL-28B genotype had the highest odds ratio favoring SVR (CC vs non-CC: odds ratio, 5.2; 95% CI, 4.1–6.7; $P < 0.0001$) [57]. After adjustment for IL28B status, other independent predictors of higher SVR were lower HCV RNA level ($<600,000$ IU/mL), Caucasian or Hispanic ethnicity, minimal liver fibrosis (METAVIR stages 0–2), and lower fasting blood glucose. Factors associated with SVR following PegIFN plus ribavirin are summarized in Table 2. In addition to the

Table 2 Factors related to response to treatment of HCV with PegIFN and ribavirin

Factor	Influence on treatment
HCV genotype	Genotypes 1 and 4 have decreased response compared to genotypes 2, 3, and 5
Baseline viral level	Patients with a low level (less than six million U/mL) show a better response
Race	Caucasians show a better response. This is related to interleukin-28B genotype and HCV-specific immune response
Host polymorphism near the gene for interleukin-28B	The chance of cure is more than doubled with homozygosity for the C allele at the rs12979860 SNP
Liver fibrosis/cirrhosis	Minimal fibrosis predicts a better response
Body weight	Patients weighing less than 85 kg have a better response
Age	Patients younger than 40 years have a better response
Gender	Females have a better response to treatment than males
Alanine aminotransferase level	Patients with ALT quotient of 3 or more (mean serum ALT level/upper limit of the normal range) have a better response
HCV-specific immune response	Patients with a high CDC+ T cell count have a better response
Insulin resistance and steatosis	The absence of these both predicts a better response
Statin use	Statin use before treatment predicts a better response to treatment
Response during treatment	Patients with either a rapid or early virologic response have a better overall response to treatment
Adherence to treatment	Patients who do not adhere to treatment (less than 80% total doses of IFN and ribavirin received less than 80% of the expected duration of therapy) have a poor response

IFN interferon, HCV hepatitis C virus, Peg pegylated, ALT alanine aminotransferase, SNP single-nucleotide polymorphism

factors identified in the IDEAL study (limited to genotype 1 infection), patients with HCV genotype 2 or 3 infection are more responsive to PegIFN plus ribavirin than those with HCV genotype 1 infection. For example, patients with genotype 2 or 3 infection achieved SVR rates between 70 and 80% following treatment of 24-week duration with a lower dose of ribavirin (800 mg daily); in contrast, those with HCV genotype 1 infection achieved SVR rates of 40% following treatment of 48-week duration with higher-dose ribavirin (1,000 or 1,200 mg daily) [58]. On-treatment HCV RNA kinetics was a significant predictor of SVR; for example, persons who failed to achieve decline from baseline in HCV RNA level $>$ two log₁₀ IU/mL (null response) were found to have a low likelihood of achieving SVR with continued treatment. This observation led to the widespread adoption of HCV RNA monitoring at treatment week 12 and the early discontinuation of PegIFN plus ribavirin for futility in persons with a null response. Similarly, the achievement of rapid virologic response (RVR) which is defined as undetectable HCV RNA after 4 weeks of PegIFN plus ribavirin was strongly associated with SVR. In a randomized controlled trial by Moreno et al. [59], it was suggested that HCV genotype 1 patients with low

baseline HCV RNA level (400,000 IU/ml) and undetectable HCV RNA at week 4 can achieve SVR with shorter duration of therapy of 24 weeks which was helpful for patients having a better side effects profile compared to patients who received extended therapy of 48 weeks [59]. In the study by Thompson et al., the achievement of RVR was not predictive of SVR in persons with the favorable IL28B CC genotype but was strongly associated with SVR in those with non-CC genotype [57]. In a model that included baseline predictive factors and RVR, RVR had the largest odds ratio for SVR (odds ratio, 9.1; 96% CI, 5.8–14.0 vs non-RVR non-CC genotype reference). Based on these findings, IL28B genotype and RVR were widely used in clinical practice to manage patients with HCV genotype 1 infection in whom treatment was considered (IL28B) or initiated (RVR) to limit the exposure to PegIFN plus ribavirin to the subset of persons most likely to achieve SVR.

7 Other Types of Interferons

Because of the limited response to PegIFN- α treatment in some patient populations with HCV and unpleasant side effects, alternative treatments have been investigated to different extents. In some Asian countries, IFN- β therapy, a type I interferon with similar antiviral activity to IFN- α , has been utilized, especially for patients who found adherence to standard IFN- α regimens difficult or who had encountered treatment failure [8, 60, 61]. Recombinant IFN- β monotherapy or in combination with ribavirin was suggested for patients intolerant to IFN- α [62]. Natural IFN- β monotherapy used short term has been shown to be useful for patients with acute HCV infection and patients infected with HCV genotype 2 with low HCV RNA levels. Its use in combination with ribavirin for 48 weeks or for 24 weeks was also effective for some patients with HCV genotype 1 or HCV genotype 2 infection and for patients who had been challenging to treat with standard PegIFN- α plus ribavirin therapy [63]. The efficacy of IFN- β therapy in persons who did not respond to IFN- α may have been due to the development of anti-IFN- α associated with non-SVR in some patients treated with this agent [64].

The systemic side effects of IFN- α may in part be due to their general expression in most cells in the body that is typical of type I interferons. IFN- λ is a type 3 interferon with more restricted tissue expression. PegIFN- λ was investigated in persons with chronic HCV infection and found to have similar rates of SVR to PegIFN- α with less systemic side effects and bone marrow suppression. However, this agent was also associated with emergent elevations in serum ALT levels; this hepatotoxicity led to the discontinuation of the development of this agent for chronic HCV infection [65]. The single-nucleotide polymorphisms (SNPs) in the IL28B gene and associated with treatment outcome in HCV patients treated with PegIFN- α /ribavirin have also been identified for IFN- λ [66]. Interestingly, studies are ongoing with PegIFN- λ as a potential treatment for chronic hepatitis D virus infection [67].

Other recombinant interferon fusion proteins have also been investigated. For example, IFN- α 2b fused with human serum albumin, known as albuferon, had

similar antiviral properties to IFN- α in cultured cells and in HCV-infected patients [9]. This albumin fusion also prolonged the half-life of albuferon compared to PegIFN- α [68]. Clinical studies showed that albuferon had similar antiviral effects to PegIFN- α [69, 70]. But concern over serious pulmonary adverse events resulted in the discontinuation of this agent.

Finally, consensus interferon (CIFN) is an artificial interferon designed to have the most common human IFN- α subtype amino acid at each position in the protein sequence [10]. In treatment-naïve patients with chronic HCV, CIFN plus ribavirin showed high SVR, and it also showed positive results in nonresponders [71–73]. However, a short half-life meant CIFN required daily injection, and therefore, this interferon was not widely adopted in clinical practice.

8 The Addition of HCV Direct-Acting Antivirals to Peginterferons Plus Ribavirin

As molecular biological methods have provided a better understanding of the viral protein structure and the life cycle of HCV, drugs that act against specific viral targets, HCV DAAs have been developed [74]. Early studies of the first-generation DAAs, the HCV NS3/4A protease inhibitors telaprevir and boceprevir, demonstrated the rapid emergence of HCV drug resistance. This observation led to the combination of these drugs with PegIFN and ribavirin, increasing the SVR to as high as 75% for persons infected with HCV genotype 1 [75–77]. However, these combination therapies were problematic in clinical practice due to the marked increase of side effects with the addition of the DAAs to PegIFN plus ribavirin. These added side effects included severe anemia (telaprevir and boceprevir) and severe skin rash (telaprevir) and coupled with a high daily pill burden led to poor patient compliance and limited uptake in clinical practice [78]. Not unexpectedly, SVR with these triple-combination therapies was also influenced by the patient and virus characteristic that had been identified in the PegIFN plus ribavirin studies. For example, the HCV RNA response to a 4-week lead-in phase of PegIFN- α plus ribavirin was highly predictive of SVR following the addition of boceprevir. Further, studies also confirmed the impact of the patients' IL28B genotype on the likelihood of SVR; in some studies persons with the favorable IL28B CC genotype could be treated for shorter durations of therapy with boceprevir triple therapy [79]. These first-generation HCV NS3/4A protease inhibitors were replaced by the safer, more effective HCV NS5B inhibitor sofosbuvir; however, the initial approval of this DAA for genotype 1 patients included the combination of sofosbuvir plus PegIFN and ribavirin [80]. Subsequently many DAAs have been approved for treatment of HCV as part of interferon-sparing regimens [81]. Currently, interferon-containing regimens are not recommended for use in clinical practice because of the excellent efficacy and safety of pan-genotypic DAA regimens; the use of these regimens has expanded dramatically with the reduced cost of the DAAs due to commercial competition and generic

manufacturing [82]. In the United States, the interferon era officially ended in September 2017 when the HCV treatment guidelines from the American Association for the Study of Liver Diseases and the Infectious Diseases Society of America removed interferon as a recommended therapy for any patient population or HCV genotype [83]. The last indication for its use had been for persons with advanced renal disease (estimated glomerular filtration rate <30 mL/min/1.73 m²) and HCV genotype 2 or 3 infection; this recommendation was dropped in favor of treatment with the pan-genotypic DAA combination of glecaprevir/pibrentasvir which includes DAAs that are not cleared by the kidneys [84].

9 Conclusions

Interferon was the backbone of HCV treatment for nearly 25 years (1991 until 2014), and, in the United States, interferon-based therapy remained a recommended HCV treatment for a least one patient population (HCV genotype 2 or infection plus advanced renal insufficiency) until September 2017. The removal of interferon from HCV treatment has had the combined effect of increasing antiviral efficacy since the response to interferon was heavily influenced by patient and virus characteristics and increasing effectiveness with the elimination of the severe side effects associated with interferon which increased the number of people eligible and willing to be treated for chronic HCV infection. Indeed, the removal of interferon has paved the way for efforts to eliminate HCV infection globally using safe, tolerable, and effective oral DAA regimens to cure persons living with chronic HCV infection.

Compliance with Ethical Standards

Conflict of Interest Author declares that he has no conflict of interest.

Ethical Approval Not applicable.

References

1. Nayak A, Pattabiraman N, Fadra N, Goldman R, Kosakovsky Pond SL, Mazumder R (2015) Structure-function analysis of hepatitis C virus envelope glycoproteins E1 and E2. *J Biomol Struct Dyn* 33(8):1682–1694
2. Parekh PJ, Shiffman ML (2014) The role of interferon in the new era of hepatitis C treatments. *Expert Rev Gastroenterol Hepatol* 8(6):649–656
3. Lin FC, Young HA (2014) Interferons: Success in anti-viral immunotherapy. *Cytokine Growth Factor Rev* 25(4):369–376
4. Muir AJ, Shiffman ML, Zaman A, Yoffe B, de la Torre A, Flamm S et al (2010) Phase 1b study of pegylated interferon lambda 1 with or without ribavirin in patients with chronic genotype 1 hepatitis C virus infection. *Hepatology* 52(3):822–832

5. Hoofnagle JH, Mullen KD, Jones DB, Rustgi V, Di Bisceglie A, Peters M et al (1986) Treatment of chronic non-A,non-B hepatitis with recombinant human alpha interferon. A preliminary report. *N Engl J Med* 315(25):1575–1578
6. Lai MY, Kao JH, Yang PM, Wang JT, Chen PJ, Chan KW et al (1996) Long-term efficacy of ribavirin plus interferon alfa in the treatment of chronic hepatitis C. *Gastroenterology* 111(5):1307–1312
7. Zeuzem S, Feinman SV, Rasenack J, Heathcote EJ, Lai MY, Gane E et al (2000) Peginterferon alfa-2a in patients with chronic hepatitis C. *N Engl J Med* 343(23):1666–1672
8. Ishikawa T, Kubota T, Abe H, Nagashima A, Hirose K, Togashi T et al (2012) Efficacy of the regimen using twice-daily beta-interferon followed by the standard of care for chronic hepatitis C genotype 1b with high viral load. *Hepatology* 42(9):864–869
9. Liu C, Zhu H, Subramanian GM, Moore PA, Xu Y, Nelson DR (2007) Anti-hepatitis C virus activity of albinterferon alfa-2b in cell culture. *Hepatology* 37(11):941–947
10. Blatt LM, Davis JM, Klein SB, Taylor MW (1996) The biologic activity and molecular characterization of a novel synthetic interferon-alpha species, consensus interferon. *J Interf Cytokine Res* 16(7):489–499
11. Ghosh D, Ghosh D, Parida P (2016) Physiological proteins in therapeutics: a current review on interferons. *Mini Rev Med Chem* 16(12):947–952
12. Carlson RJ, Doucette JR, Knox K, Nazarali AJ (2015) Pharmacogenomics of interferon-beta in multiple sclerosis: what has been accomplished and how can we ensure future progress? *Cytokine Growth Factor Rev* 26(2):249–261
13. Yoshida J, Mizuno M, Wakabayashi T (2004) Interferon-beta gene therapy for cancer: basic research to clinical application. *Cancer Sci* 95(11):858–865
14. Razaghi A, Owens L, Heimann K (2016) Review of the recombinant human interferon gamma as an immunotherapeutic: impacts of production platforms and glycosylation. *J Biotechnol* 240:48–60
15. van Pesch V, Lanaya H, Renaud JC, Michiels T (2004) Characterization of the murine alpha interferon gene family. *J Virol* 78(15):8219–8228
16. Gibbert K, Schlaak JF, Yang D, Dittmer U (2013) IFN-alpha subtypes: distinct biological activities in anti-viral therapy. *Br J Pharmacol* 168(5):1048–1058
17. Jaks E, Gavutis M, Uze G, Martal J, Piehler J (2007) Differential receptor subunit affinities of type I interferons govern differential signal activation. *J Mol Biol* 366(2):525–539
18. Sato I, Shimbo T, Kawasaki Y, Masaki N (2015) Comparison of peginterferon alfa-2a and alfa-2b for treatment of patients with chronic hepatitis C: a retrospective study using the Japanese Interferon Database. *Drug Des Devel Ther* 9:283–290
19. Chen J, Florian J, Carter W, Fleischer RD, Hammerstrom TS, Jadhav PR et al (2013) Earlier sustained virologic response end points for regulatory approval and dose selection of hepatitis C therapies. *Gastroenterology* 144(7):1450–1455.e2
20. Choo QL, Kuo G, Weiner AJ, Overby LR, Bradley DW, Houghton M (1989) Isolation of a cDNA clone derived from a blood-borne non-A, non-B viral hepatitis genome. *Science* 244(4902):359–362
21. National Institutes of Health (2002) National Institutes of Health Consensus Development Conference Statement: Management of hepatitis C: 2002 – June 10–12, 2002. *Hepatology* 36(5 Suppl 1):S3–S20
22. Liu Z, Que S, Xu J, Peng T (2014) Alanine aminotransferase-old biomarker and new concept: a review. *Int J Med Sci* 11(9):925–935
23. Davis GL, Balart LA, Schiff ER, Lindsay K, Bodenheimer HC Jr, Perrillo RP et al (1989) Treatment of chronic hepatitis C with recombinant interferon alfa. A multicenter randomized, controlled trial. *N Engl J Med* 321(22):1501–1506
24. Di Bisceglie AM, Martin P, Kassianides C, Lisker-Melman M, Murray L, Waggoner J et al (1989) Recombinant interferon alfa therapy for chronic hepatitis C. A randomized, double-blind, placebo-controlled trial. *N Engl J Med* 321(22):1506–1510

25. Poynard T, Leroy V, Cohard M, Thevenot T, Mathurin P, Opolon P et al (1996) Meta-analysis of interferon randomized trials in the treatment of viral hepatitis C: effects of dose and duration. *Hepatology* 24(4):778–789
26. Lau DT, Kleiner DE, Ghany MG, Park Y, Schmid P, Hoofnagle JH (1998) 10-Year follow-up after interferon-alpha therapy for chronic hepatitis C. *Hepatology* 28(4):1121–1127
27. Sleijfer S, Bannink M, Van Gool AR, Kruit WH, Stoter G (2005) Side effects of interferon-alpha therapy. *Pharm World Sci* 27(6):423–431
28. Wu LS, Rower JE, Burton JR Jr, Anderson PL, Hammond KP, Baouchi-Mokrane F et al (2015) Population pharmacokinetic modeling of plasma and intracellular ribavirin concentrations in patients with chronic hepatitis C virus infection. *Antimicrob Agents Chemother* 59(4):2179–2188
29. Bodenheimer HC Jr, Lindsay KL, Davis GL, Lewis JH, Thung SN, Seeff LB (1997) Tolerance and efficacy of oral ribavirin treatment of chronic hepatitis C: a multicenter trial. *Hepatology* 26(2):473–477
30. Brok J, Gluud LL, Gluud C (2009) Ribavirin monotherapy for chronic hepatitis C. *Cochrane Database Syst Rev* 4:CD005527
31. Tong MJ, Hwang SJ, Lefkowitz M, Lee SD, Co RL, Conrad A et al (1994) Correlation of serum HCV RNA and alanine aminotransferase levels in chronic hepatitis C patients during treatment with ribavirin. *J Gastroenterol Hepatol* 9(6):587–591
32. Reichard O, Norkrans G, Fryden A, Braconier JH, Sonnerborg A, Weiland O (1998) Randomised, double-blind, placebo-controlled trial of interferon alpha-2b with and without ribavirin for chronic hepatitis C. The Swedish Study Group. *Lancet* 351(9096):83–87
33. Schalm SW, Hansen BE, Chemello L, Bellobuono A, Brouwer JT, Weiland O et al (1997) Ribavirin enhances the efficacy but not the adverse effects of interferon in chronic hepatitis C. Meta-analysis of individual patient data from European centers. *J Hepatol* 26(5):961–966
34. McHutchison JG, Gordon SC, Schiff ER, Shiffman ML, Lee WM, Rustgi VK et al (1998) Interferon alfa-2b alone or in combination with ribavirin as initial treatment for chronic hepatitis C. Hepatitis Interventional Therapy Group. *N Engl J Med* 339(21):1485–1492
35. Poynard T, Marcellin P, Lee SS, Niederau C, Minuk GS, Ideo G et al (1998) Randomised trial of interferon alpha2b plus ribavirin for 48 weeks or for 24 weeks versus interferon alpha2b plus placebo for 48 weeks for treatment of chronic infection with hepatitis C virus. International Hepatitis Interventional Therapy Group (IHIT). *Lancet* 352(9138):1426–1432
36. Rotman Y, Noureddin M, Feld JJ, Guedj J, Witthaus M, Han H et al (2014) Effect of ribavirin on viral kinetics and liver gene expression in chronic hepatitis C. *Gut* 63(1):161–169
37. McHutchison JG, Poynard T (1999) Combination therapy with interferon plus ribavirin for the initial treatment of chronic hepatitis C. *Semin Liver Dis* 19(Suppl 1):57–65
38. Sulkowski MS, Cooper C, Hunyady B, Jia J, Ogurtsov P, Peck-Radosavljevic M et al (2011) Management of adverse effects of Peg-IFN and ribavirin therapy for hepatitis C. *Nat Rev Gastroenterol Hepatol* 8(4):212–223
39. Soota K, Maliakkal B (2014) Ribavirin induced hemolysis: a novel mechanism of action against chronic hepatitis C virus infection. *World J Gastroenterol* 20(43):16184–16190
40. Wu JZ, Larson G, Walker H, Shim JH, Hong Z (2005) Phosphorylation of ribavirin and viramidine by adenosine kinase and cytosolic 5'-nucleotidase II: implications for ribavirin metabolism in erythrocytes. *Antimicrob Agents Chemother* 49(6):2164–2171
41. Page T, Connor JD (1990) The metabolism of ribavirin in erythrocytes and nucleated cells. *Int J Biochem* 22(4):379–383
42. De Franceschi L, Fattovich G, Turrini F, Ayi K, Brugnara C, Manzato F et al (2000) Hemolytic anemia induced by ribavirin therapy in patients with chronic hepatitis C virus infection: role of membrane oxidative damage. *Hepatology* 31(4):997–1004
43. (1999) EASL International Consensus Conference on hepatitis C. Paris, 26–27 February 1999. Consensus statement. *J Hepatol* 31(Suppl 1):3–8

44. Glue P, Fang JW, Rouzier-Panis R, Raffanel C, Sabo R, Gupta SK et al (2000) Pegylated interferon-alpha2b: pharmacokinetics, pharmacodynamics, safety, and preliminary efficacy data. Hepatitis C Intervention Therapy Group. *Clin Pharmacol Ther* 68(5):556–567
45. Baker DE (2001) Pegylated interferons. *Rev Gastroenterol Disord* 1(2):87–99
46. Zeuzem S, Welsch C, Herrmann E (2003) Pharmacokinetics of peginterferons. *Semin Liver Dis* 23(Suppl 1):23–28
47. Reddy KR, Wright TL, Pockros PJ, Shiffman M, Everson G, Reindollar R et al (2001) Efficacy and safety of pegylated (40-kd) interferon alpha-2a compared with interferon alpha-2a in noncirrhotic patients with chronic hepatitis C. *Hepatology* 33(2):433–438
48. Lindsay KL, Trepo C, Heintges T, Shiffman ML, Gordon SC, Hoefs JC et al (2001) A randomized, double-blind trial comparing pegylated interferon alpha-2b to interferon alpha-2b as initial treatment for chronic hepatitis C. *Hepatology* 34(2):395–403
49. Heathcote EJ, Shiffman ML, Cooksley WG, Dusheiko GM, Lee SS, Balart L et al (2000) Peginterferon alpha-2a in patients with chronic hepatitis C and cirrhosis. *N Engl J Med* 343(23):1673–1680
50. Fried MW, Shiffman ML, Reddy KR, Smith C, Marinos G, Goncales FL Jr et al (2002) Peginterferon alpha-2a plus ribavirin for chronic hepatitis C virus infection. *N Engl J Med* 347(13):975–982
51. Hadziyannis SJ, Sette H Jr, Morgan TR, Balan V, Diago M, Marcellin P et al (2004) Peginterferon-alpha2a and ribavirin combination therapy in chronic hepatitis C: a randomized study of treatment duration and ribavirin dose. *Ann Intern Med* 140(5):346–355
52. Manns MP, McHutchison JG, Gordon SC, Rustgi VK, Shiffman M, Reindollar R et al (2001) Peginterferon alpha-2b plus ribavirin compared with interferon alpha-2b plus ribavirin for initial treatment of chronic hepatitis C: a randomised trial. *Lancet* 358(9286):958–965
53. McHutchison JG, Lawitz EJ, Shiffman ML, Muir AJ, Galler GW, McCone J et al (2009) Peginterferon alpha-2b or alpha-2a with ribavirin for treatment of hepatitis C infection. *N Engl J Med* 361(6):580–593
54. Rumi MG, Aghemo A, Prati GM, D'Ambrosio R, Donato MF, Soffredini R et al (2010) Randomized study of peginterferon-alpha2a plus ribavirin vs peginterferon-alpha2b plus ribavirin in chronic hepatitis C. *Gastroenterology* 138(1):108–115
55. Ascione A, De Luca M, Tartaglione MT, Lampasi F, Di Costanzo GG, Lanza AG et al (2010) Peginterferon alpha-2a plus ribavirin is more effective than peginterferon alpha-2b plus ribavirin for treating chronic hepatitis C virus infection. *Gastroenterology* 138(1):116–122
56. Ge D, Fellay J, Thompson AJ, Simon JS, Shianna KV, Urban TJ et al (2009) Genetic variation in IL28B predicts hepatitis C treatment-induced viral clearance. *Nature* 461(7262):399–401
57. Thompson AJ, Muir AJ, Sulkowski MS, Ge D, Fellay J, Shianna KV et al (2010) Interleukin-28B polymorphism improves viral kinetics and is the strongest pretreatment predictor of sustained virologic response in genotype 1 hepatitis C virus. *Gastroenterology* 139(1):120–9. e18
58. Rosen HR (2011) Clinical practice. Chronic hepatitis C infection. *N Engl J Med* 364(25):2429–2438
59. Moreno C, Deltenre P, Pawlotsky JM, Henrion J, Adler M, Mathurin P (2010) Shortened treatment duration in treatment-naïve genotype 1 HCV patients with rapid virological response: a meta-analysis. *J Hepatol* 52(1):25–31
60. Ahn SH, Lee HW, Kim YS, Kim JK, Han KH, Chon CY et al (2009) Recombinant interferon-Beta-1alpha plus ribavirin for the treatment of chronic HCV infection: a prospective, randomized, comparative pilot study. *Gut Liver* 3(1):20–25
61. Inoue K, Watanabe T, Yamada M, Yoshikumi H, Ogawa O, Yoshida M (2009) Efficacy of interferon Beta combined with cyclosporine induction and intensified therapy for retreatment of chronic hepatitis C. *Transplant Proc* 41(1):246–249
62. Pellicano R, Craxi A, Almasio PL, Valenza M, Venezia G, Alberti A et al (2005) Interferon beta-1a alone or in combination with ribavirin: a randomized trial to compare efficacy and safety in chronic hepatitis C. *World J Gastroenterol* 11(29):4484–4489

63. Sasaki R, Kanda T, Nakamoto S, Haga Y, Nakamura M, Yasui S et al (2015) Natural interferon-beta treatment for patients with chronic hepatitis C in Japan. *World J Hepatol* 7(8):1125–1132
64. Matsuda F, Torii Y, Enomoto H, Kuga C, Aizawa N, Iwata Y et al (2012) Anti-interferon-alpha neutralizing antibody is associated with nonresponse to pegylated interferon-alpha plus ribavirin in chronic hepatitis C. *J Viral Hepat* 19(10):694–703
65. Ramos EL (2010) Preclinical and clinical development of pegylated interferon-lambda 1 in chronic hepatitis C. *J Interf Cytokine Res* 30(8):591–595
66. Donnelly RP, Dickensheets H, O'Brien TR (2011) Interferon-lambda and therapy for chronic hepatitis C virus infection. *Trends Immunol* 32(9):443–450
67. Elazar M, Glenn JS (2017) Emerging concepts for the treatment of hepatitis delta. *Curr Opin Virol* 24:55–59
68. Osborn BL, Olsen HS, Nardelli B, Murray JH, Zhou JX, Garcia A et al (2002) Pharmacokinetic and pharmacodynamic studies of a human serum albumin-interferon-alpha fusion protein in cynomolgus monkeys. *J Pharmacol Exp Ther* 303(2):540–548
69. Nelson DR, Benhamou Y, Chuang WL, Lawitz EJ, Rodriguez-Torres M, Flisiak R et al (2010) Albinterferon Alfa-2b was not inferior to pegylated interferon-alpha in a randomized trial of patients with chronic hepatitis C virus genotype 2 or 3. *Gastroenterology* 139(4):1267–1276
70. Zeuzem S, Sulkowski MS, Lawitz EJ, Rustgi VK, Rodriguez-Torres M, Bacon BR et al (2010) Albinterferon Alfa-2b was not inferior to pegylated interferon-alpha in a randomized trial of patients with chronic hepatitis C virus genotype 1. *Gastroenterology* 139(4):1257–1266
71. Fattovich G, Zagni I, Minola E, Felder M, Rovere P, Carlotto A et al (2003) A randomized trial of consensus interferon in combination with ribavirin as initial treatment for chronic hepatitis C. *J Hepatol* 39(5):843–849
72. Bacon BR, Shiffman ML, Mendes F, Ghalib R, Hassanein T, Morelli G et al (2009) Retreating chronic hepatitis C with daily interferon alfacon-1/ribavirin after nonresponse to pegylated interferon/ribavirin: DIRECT results. *Hepatology* 49(6):1838–1846
73. Nordstrom EM, Biggins SW, Gralla J, Rosen HR, Everson GT, Burton JR Jr (2015) Consensus interferon for recurrent hepatitis C infection in nonresponders to peginterferon and ribavirin after liver transplant. *Exp Clin Transplant* 13(6):543–549
74. Soriano V, Vispo E, Poveda E, Labarga P, Martin-Carbonero L, Fernandez-Montero JV et al (2011) Directly acting antivirals against hepatitis C virus. *J Antimicrob Chemother* 66(8):1673–1686
75. Jacobson IM, McHutchison JG, Dusheiko G, Di Bisceglie AM, Reddy KR, Bzowej NH et al (2011) Telaprevir for previously untreated chronic hepatitis C virus infection. *N Engl J Med* 364(25):2405–2416
76. Poordad F, McCone J Jr, Bacon BR, Bruno S, Manns MP, Sulkowski MS et al (2011) Boceprevir for untreated chronic HCV genotype 1 infection. *N Engl J Med* 364(13):1195–1206
77. Sherman KE, Flamm SL, Afdhal NH, Nelson DR, Sulkowski MS, Everson GT et al (2011) Response-guided telaprevir combination treatment for hepatitis C virus infection. *N Engl J Med* 365(11):1014–1024
78. Jacobson IM, Pawlotsky JM, Afdhal NH, Dusheiko GM, Forns X, Jensen DM et al (2012) A practical guide for the use of boceprevir and telaprevir for the treatment of hepatitis C. *J Viral Hepat* 19(Suppl 2):1–26
79. Poordad F, Bronowicki JP, Gordon SC, Zeuzem S, Jacobson IM, Sulkowski MS et al (2012) Factors that predict response of patients with hepatitis C virus infection to boceprevir. *Gastroenterology* 143(3):608–618 e5
80. Lawitz E, Lalezari JP, Hassanein T, Kowdley KV, Poordad FF, Sheikh AM et al (2013) Sofosbuvir in combination with peginterferon alfa-2a and ribavirin for non-cirrhotic, treatment-naïve patients with genotypes 1, 2, and 3 hepatitis C infection: a randomised, double-blind, phase 2 trial. *Lancet Infect Dis* 13(5):401–408
81. Gutierrez JA, Lawitz EJ, Poordad F (2015) Interferon-free, direct-acting antiviral therapy for chronic hepatitis C. *J Viral Hepat* 22(11):861–870

82. de Leuw P, Stephan C (2018) Protease inhibitor therapy for hepatitis C virus-infection. *Expert Opin Pharmacother* 19(6):577–587
83. AASLD-IDSA HCV Guidance Panel (2018) Hepatitis C guidance 2018 update: AASLD-IDSA recommendations for testing, managing, and treating hepatitis C virus infection. *Clin Infect Dis* 67(10):1477–1492
84. Gane E, Lawitz E, Pugatch D, Papatheodoridis G, Brau N, Brown A et al (2017) Glecaprevir and pibrentasvir in patients with HCV and severe renal impairment. *N Engl J Med* 377(15):1448–1455

Part II
HCV NS5B Polymerase Inhibitors

Evolution of HCV NS5B Nucleoside and Nucleotide Inhibitors



Aesop Cho

Contents

1	Background	118
2	Early Nucleoside Inhibitors	121
3	Advanced Nucleos(t)ide Inhibitors	123
3.1	Adenosine Analogs	123
3.2	Guanosine Analogs	126
3.3	Cytidine Analogs	129
3.4	Uridine Analogs	132
4	Conclusion	135
	References	136

Abstract Adenosine and cytidine analogs containing the 2'-C-methyl substituent were identified as initial hits from screening. These compounds displayed selective anti-HCV activity in a cell-based HCV replicon assay and, as their triphosphates, inhibited HCV NS5B polymerase enzyme in a cell-free assay. Since then, a number of new 2'-modified nucleoside analogs and nucleotide derivatives were synthesized and evaluated for direct inhibition of HCV replication. Potency, selectivity, and other drug-like properties were substantially optimized, and consequently more than a dozen compounds were advanced into preclinical and clinical evaluations. In the end, a prodrug of 2'-fluoro-2'-C-methyluridine monophosphate PSI-7977 (GS-7977, sofosbuvir) was approved for the treatment of chronic HCV infection.

Keywords HCV, Monophosphate prodrug, NS5B, Nucleoside, Nucleotide, Phosphoramidate prodrug

A. Cho (✉)

Department of Medicinal Chemistry, Gilead Sciences, Inc., Foster City, CA, USA
e-mail: Aesop.Cho@gilead.com

1 Background

The discovery of HCV NS5B nucleoside inhibitors began primarily with screening of existing collections of nucleosides for anti-HCV activity. Historically, nucleoside analogs and derivatives containing structurally diverse nucleobase and/or ribose moieties had been synthesized and evaluated toward a wide range of biological and therapeutic utilities. Accordingly, a library of these nucleoside analogs existed when both cell-based HCV replicon and cell-free NS5B enzyme assays were available, which enabled rapid screening and identification of initial hits.

At the time that a search for HCV inhibitors was initiated, nucleos(t)ide analogs had already demonstrated their therapeutic utility as antiviral agents for herpes viruses, hepatitis B virus, and human immunodeficiency virus. Over 20 nucleos(t)ides had been identified and developed for treatment of these viral infections worldwide. For this reason, there was a high expectation that nucleos(t)ide analogs would in turn serve as an effective agent in HCV therapy. However, those viruses encode a polymerase whose primary function is DNA synthesis, and thus the majority of nucleos(t)ide antiviral drugs to treat those infections are mimic of endogenous 2'-deoxynucleosides. Since HCV NS5B is an RNA polymerase, different structural elements in the nucleoside scaffold are likely to be required for recognition by the RNA polymerase. For example, presence of the 2'-hydroxyl group as in the ribonucleoside should offer such selective recognition over DNA polymerases (Fig. 1).

To be an effective and selective inhibitor of HCV replication, a nucleos(t)ide analog must enter the infected host cell and get metabolized by host kinases to its nucleoside triphosphate (NTP), which then must selectively bind to the active site of NS5B polymerase as a substrate and become incorporated into the elongating chain of viral RNA. Unlike naturally occurring canonical nucleosides, however, the incorporation into the nascent RNA should then block further RNA polymerization, consequently resulting in inhibition of production of functionally matured HCV RNA (i.e., HCV replication) (Fig. 2). On the other hand, this nucleos(t)ide analog and its metabolites must not adversely affect normal cellular processes such as *de novo* nucleoside synthesis, cellular signaling, and RNA synthesis (e.g., through being incorporated into the elongating host RNA by host RNA polymerases). Since these adverse effects to host cells could indirectly inhibit HCV replication, it is important to investigate whether the observed antiviral activity is derived from direct blockage of viral replication. Mechanistically, it is the NTP species that directly interacts with HCV NS5B and blocks generation of the matured HCV RNA.

A nucleoside analog itself is essentially a biologically inactive substance that requires the metabolic transformation to the bioactive NTP species by three distinctive kinases: ribonucleoside kinase (rNK) phosphorylates the nucleoside to the nucleoside monophosphate (NMP), nucleoside monophosphate kinase (NMPK) then phosphorylates NMP to the nucleoside diphosphate (NDP), and finally nucleoside diphosphate kinase (NDPK) phosphorylates NDP to NTP (Fig. 3). Depending on the structure of nucleoside analog, however, the efficiency of any of these

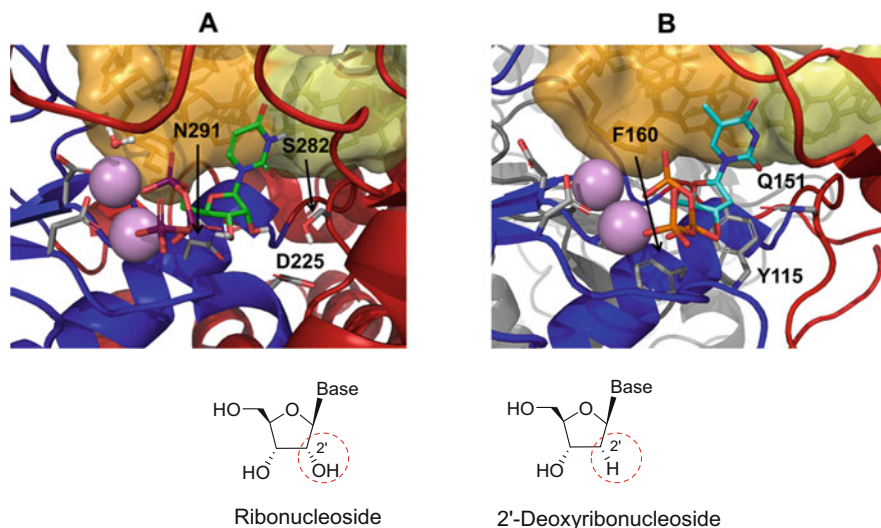


Fig. 1 RNA and DNA polymerases have different amino acid residues in the substrate-binding sites. These models show hydrophilic amino acid residues interacting with the 2'-hydroxyl group in the active site of HCV NS5B RNA polymerase (a) and hydrophobic amino acid residues interacting with the 2'-deoxy position in the active site of HIV RT DNA polymerase (b). The 2'-hydroxyl group in the ribonucleoside offers selective recognition by RNA polymerases over DNA polymerases

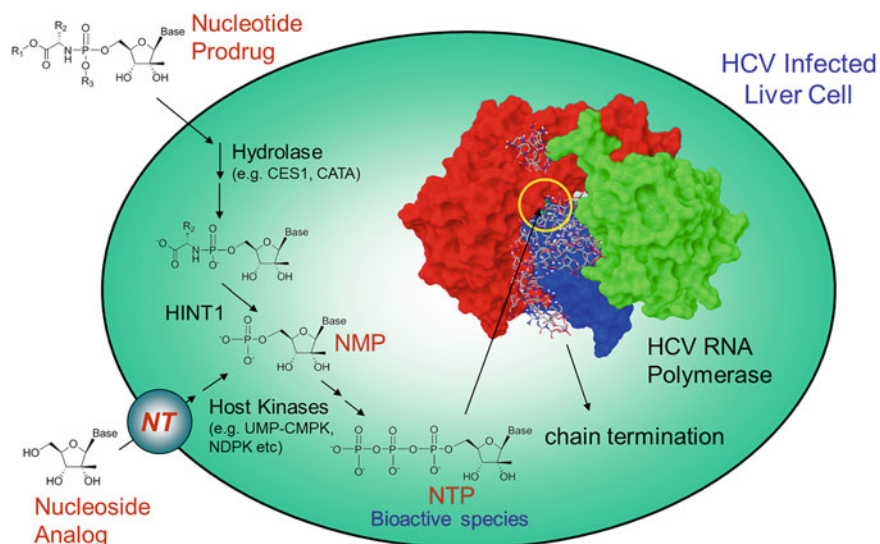


Fig. 2 Mode of action for HCV NS5B nucleos(t)ide inhibitor. Nucleoside analog or nucleotide prodrug enters the HCV-infected liver cell and is metabolized to the biologically active nucleoside triphosphate, which inhibits NS5B RNA polymerase to cause formation of degenerated HCV

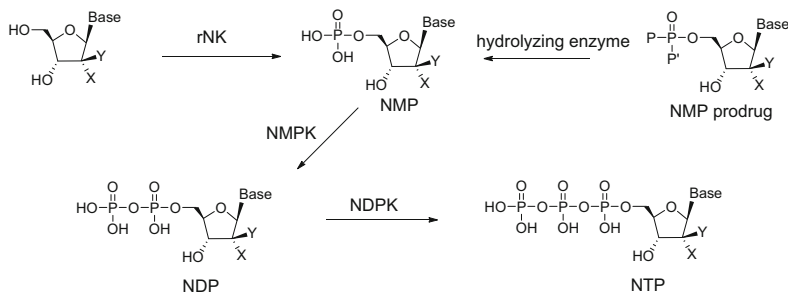


Fig. 3 A nucleoside analog is metabolized to the corresponding NTP via three distinctive kinases. NMP prodrug releases NMP, which is then transformed to NDP and NTP. *rNK* ribonucleoside kinase, *NMPK* nucleoside monophosphate kinase, *NDPK* nucleoside diphosphate kinase

enzymatic reactions may be compromised, and consequently the intracellular production of NTP may be limited. In such a case, the nucleoside analog will display a lower-than-expected antiviral activity in a cell-based assay, even if the corresponding NTP (often prepared by chemical synthesis) is found to be directly and potently active against the NS5B polymerase in a cell-free biochemical assay.

Consequently, there have been significant efforts in rescuing nucleosides that are poor substrates for the kinases yet biologically active as the triphosphates in the NS5B enzyme assay. In particular, for nucleoside analogs that are poor substrates for the first kinase in the phosphorylation cascade, monophosphate prodrug strategies have been successfully employed (Fig. 3). NMP is negatively charged at the physiological pH (i.e., pH 7.4) and thus poorly cell-permeable. However, the monophosphate prodrug that shields the charges can enter the cell and be transformed intracellularly to NMP (and subsequently to NDP and to NTP), thus bypassing the rate-limiting kinase-mediated first phosphorylation. Several prodrug tactics have been developed to efficiently deliver NMP into the target cells.

In order to achieve *in vivo* efficacy, sufficient levels of intracellular NTP must be maintained until viral replication is stopped and the remaining virus is cleared out from the infected cells. Unlike *in vitro* systems, the drug levels in the plasma of animals are dynamic and decreased over time after administration of the drug. During the transit time, a nucleos(t)ide analog present in the circulation must be taken up by the infected cells and transformed to the NTP species. The level of the intracellularly formed NTP species should then be high enough to effectively suppress the viral replication. Importantly, the intracellular half-life of the NTP should also be long enough to maintain the NTP concentration at the effective level until the nucleos(t)ide analog is re-administrated. In general, NTP is a metabolically unstable species, and its half-life varies depending on the structure of the nucleos(t)ide. Thus, designing a nucleos(t)ide analog that has a prolonged half-life as the triphosphate and meets all the requirements including potency and selectivity is challenging.

Nucleos(t)ide analogs thus meeting these requirements would have yet another hurdle to overcome – oral bioavailability. Oral administration is the most preferred

route of administration because of its simplicity and convenience. Historically, however, many nucleos(t)ide analogs suffer from poor oral bioavailability due to their high polarity and low intestinal permeability. In order to improve oral absorption of these polar drugs, a number of prodrug approaches have been explored. An ideal prodrug achieves delivery of a parent drug by attachment of a nontoxic moiety that is stable during transit but is readily cleaved to release the parent drug once reached to the target tissue. Since the hepatocytes in the liver are the major cells infected by HCV, selective loading of the parent drug into the liver over other tissues is desired. Some successful prodrug strategies employed for improved oral bioavailability and targeted liver-loading will be described in the following sections.

Finally, a major strive in direct-acting anti-HCV drug discovery and development is to achieve activity against all genotypes and high barrier of the emergence of drug-resistant variants. These are the two critically important biological properties that an antiviral agent must have to be successful in the clinic. Nucleos(t)ide analogs target the highly conserved active site of the HCV polymerase. Thus, they are expected to be equally effective across all genotypes and also have a high barrier to resistance because of poor replicative fitness of any active-site mutant variants. Accordingly, despite of a number of challenges in its drug discovery, this class has been pursued as the most attractive agent that would be a cornerstone of the treatment regimens for chronic HCV infection.

2 Early Nucleoside Inhibitors

Early on, researchers at Merck screened their own in-house collection of nucleosides for anti-HCV activity and identified two nucleoside analogs, 2'-*C*-methyladenosine (2'-*C*-MeA) and 2'-*O*-methylcytidine (2'-*O*-MeC), which inhibit HCV RNA replication (Fig. 4) [1]. In a replicon assay using a stable Huh-7 human hepatoma cell line, which supports the replication of HCV RNA and proteins, both compounds displayed antiviral activity with a 50% effective concentration (EC_{50}) of 0.25 and 21 μ M, respectively. Furthermore, they were selective in that no cytotoxicity was observed up to 100 μ M in HBI10A cells as measured by a MTS assay. MTS ([3-(4,5-dimethylthiazol-2-yl)-5-(3-carboxymethoxyphenyl)-2-(4-sulfophenyl)-2H-tetrazolium] salt) is a chemical reagent to be used to quantify metabolically active cells by a colorimetric method. When incubated with actively growing replicon cells

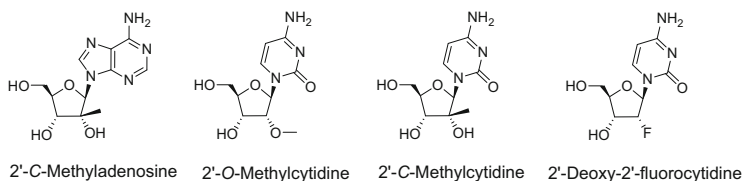


Fig. 4 Early HCV nucleoside inhibitors

in culture, these nucleoside analogs resulted in intracellular formation of the corresponding triphosphates that were potent competitive inhibitors of NS5B-catalyzed reactions *in vitro*, with a 50% inhibitory concentration (IC_{50}) of 1.9 and 3.8 μM (obtained with NS5B Δ 21), respectively. Contrarily, the triphosphates affected the function of host cell DNA polymerases α , β , and γ only minimally. Metabolism studies with the tritium-labeled nucleosides revealed that 2'-*C*-MeA was efficiently taken up into either Huh-7 cells or HBI10A cells and converted intracellularly to the corresponding triphosphate (at 75–105 pmol/million cells upon incubation of 2 μM of the nucleoside for 23 h), while incubation with 2'-*O*-MeC yielded very little triphosphate (with intracellular concentration over 500-fold less than that produced from 2'-*C*-MeA). This explains the significantly higher inhibitory activity of 2'-*C*-MeA over 2'-*O*-MeC in the cell-based assay.

2'-*C*-Methylcytidine (2'-*C*-MeC) was also evaluated, along with 2'-*C*-MeA, which was first published by a group at Pharmasset [2]. This pyrimidine nucleoside containing the 2'-*C*-methyl substituent also actively inhibited HCV viral replication, although it was approximately tenfold less potent than 2'-*C*-MeA in a replicon assay (a 90% effective concentration EC_{90} of 10.4 vs. 1.4 μM). The structural implication of this initial result was twofold: (1) the 2'-methyl substitution on the ribose ring confers anti-HCV activity and (2) the nucleobase influences antiviral potency. This discovery prompted intense efforts toward further structural refinement of the 2'-modified nucleosides.

Several other 2'-modified nucleoside analogs were also explored for their potential as HCV NS5B inhibitors, which include 2'-deoxy-2'-fluorocytidine (2'-FdC), an analog of cytidine where the 2'-hydroxy group is replaced with the fluorine (Fig. 4) [3]. In a 4-day replicon assay using Huh-7 cells, 2'-FdC had a potent inhibitory activity with a 90% effective concentration (EC_{90}) of 5.0 μM and no cytotoxicity (50% reduction in cell growth $CC_{50} > 100 \mu\text{M}$). In addition, the 2'-FdC triphosphate (2'-FdCTP) showed IC_{50} of 14.9 μM in an NS5B polymerase enzyme assay. However, prolonged incubation of the HCV replicon cells with 2'-FdC (at 8 μM over 7 days) resulted in a significant reduction in the host ribosomal RNA levels, compared to the untreated control. A closer analysis of the cell cycle distribution of the treated replicon cells revealed that 2'-FdC caused cytostasis due to an S-phase arrest. These results suggest that apart from the desired inhibition of the NS5B enzyme, 2'-FdC itself or its metabolites inhibit one or more cellular targets. For example, 2'-FdCTP was shown to be incorporated into host cell DNA and RNA, which might be a cause for the observed toxicity. However, the exact mode of action for the cytostatic effect remains unknown. Regardless, an enticing postulate from this work is that a single point isosteric replacement of canonical nucleosides (e.g., from the 2'-hydroxy to the 2'-fluoro) may be insufficient to dissociate the undesired side effects on host cells from the desired antiviral activity and provide an acceptable selectivity for HCV NS5B.

Independently, a new structural class of anti-HCV active nucleosides was identified by researchers at Roche. This discovery was based on a rational design approach. A series of 4'-substituted 2'-deoxyribonucleosides had been previously investigated as selective inhibitors of HIV reverse transcriptase. These were specifically designed to

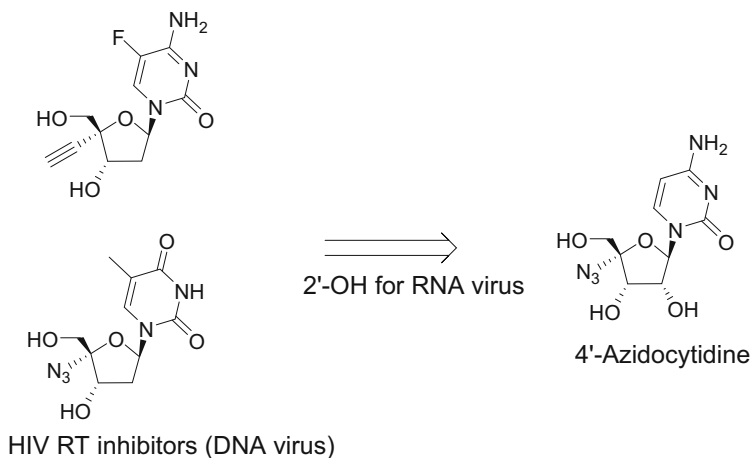


Fig. 5 Incorporation of 4'-substitutions into a ribonucleoside core for HCV activity

target DNA viruses. To build in anti-HCV activity, the 2'-hydroxy group was incorporated into these molecules. Among those synthesized and tested, 4'-azidocytidine emerged as a promising analog with an EC_{50} of 1.3 μM with no cytotoxicity up to 2,000 μM (Fig. 5) [4].

3 Advanced Nucleos(t)ide Inhibitors

3.1 Adenosine Analogs

Although 2'-C-MeA was shown to be a potent and selective HCV NS5B inhibitor in *in vitro* assays, it was far less than ideal to be developed as a therapeutic agent. Similar to naturally occurring adenosine, this compound is readily degraded by adenosine deaminase (ADA) and purine nucleoside phosphorylase (PNP) present in systemic circulation, which leads to poor pharmacokinetics (PK) (Fig. 6). PK studies with rats showed rapid decrease in the plasma nucleoside levels upon intravenous administration (i.e., the plasma clearance was in excess of hepatic blood flow; $>200 \text{ mL/min/kg}$) and no detectable drug concentration in plasma upon oral dosing (i.e., oral bioavailability of 0%). To address these issues, extensive structure-activity relationship investigation around this purine nucleoside had been conducted by a research team at Merck [5–8].

The importance of the methyl group at the 2'-C position for NS5B activity was reaffirmed by their work. Various ribose modifications including transfer of the methyl group to the 3'-C position or the 2'-O position (i.e., 2'-methoxy), incorporation of steric bulk from the methyl to the ethyl, and transposition of the stereochemistry at the 2' position (i.e., from α -hydroxy- β -methyl to β -hydroxy- α -methyl)

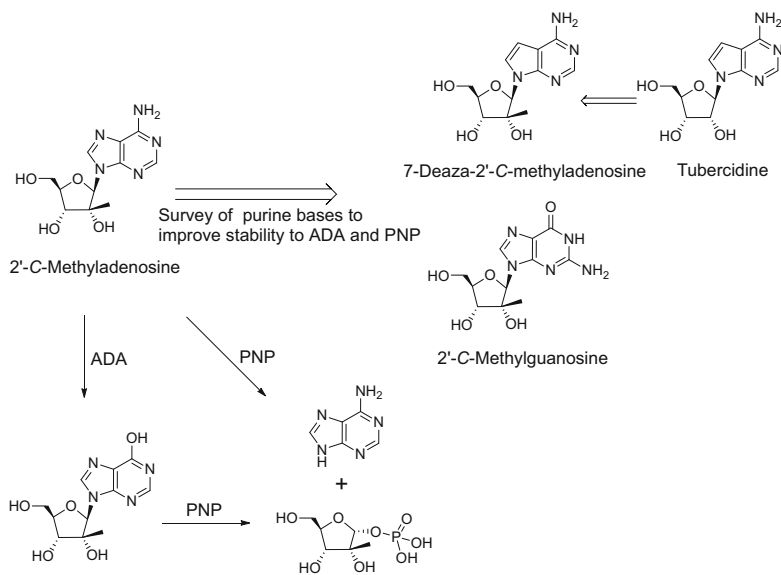


Fig. 6 7-Deaza-2'-C-methyladenosine and 2'-C-methylguanosine identified from survey of a number of purine nucleoside analogs toward achieving stability to adenosine deaminase (ADA) and purine nucleoside phosphorylase (PNP)

resulted in loss of activity. While the SAR of the ribose moiety was stringent, some flexibility was allowed for modification of the purine nucleobase moiety. Most of the nucleobases that had previously demonstrated efficient cellular uptake and conversion to the triphosphate in the context of the ribonucleoside core similarly conferred anti-HCV activity. Among those tested, two nucleosides, 7-deaza-2'-C-methyladenosine (7-deaza-2'-C-MeA) and 2'-C-methylguanosine (2'-C-MeG, discussed in detail at the following section), had emerged as new leads that exhibited antiviral activity with complete stability to ADA and PNP (Fig. 6).

In addition to providing stability to the enzymatic degradations, 7-deaza-2'-C-MeA exhibited potent antiviral activity comparable to 2'-C-MeA in the replicon assay (EC_{50} 0.3 vs. 0.25 μM). In a NS5B enzyme assay, 7-deaza-2'-C-methyladenosine triphosphate (7-deaza-2'-C-MeATP) was 17-fold more potent than 2'-C-methyladenosine triphosphate (2'-C-MeATP) (IC_{50} 0.11 vs. 1.8 μM). Furthermore, no cellular toxicity was observed with 7-deaza-2'-C-MeA in a MTS assay using the Huh-7 cells for up to 72 h at a 100 μM concentration. Given that the des-methyl analog tubercidin (7-deaza-adenosine, Fig. 6) is known to be highly cytotoxic, the lack of observed cytotoxicity by introduction of 2'-C-methyl group was remarkable. By comparison, tubercidin displayed high cytotoxicity (CC_{50} of 3 μM at 24 h, 0.15 μM at 72 h) in the same MTS assay. Additional studies were conducted to substantiate the observation. Again, no cytotoxicity was observed at up to a 1,000 μM concentration of 7-deaza-2'-C-MeA in both a MTS assay using

more sensitive Jurkat cells and a [^{14}C]thymidine uptake assay using Huh-7 cells, while tubercidin exhibited cytotoxicity at submicromolar concentrations.

One concern with noncanonical nucleobases such as 7-deaza-2'-*C*-MeA is the possibility for induction of mutagenic events. However, the 2'-*C*-methyl pharmacophore apparently prevented recognition by human polymerases, which may permit the use of nucleobases that otherwise would be unsuitable. Incubation of the tritium-labeled 7-deaza-2'-*C*-MeA with Huh-7 cells for 3 days showed undetectable to trace levels of incorporation of the radioactive nucleoside into cellular RNA, which provided further evidence that this nucleoside triphosphate was very specific for incorporation by the HCV NS5B polymerase.

Because of the promising antiviral and selectivity profile, 7-deaza-2'-*C*-MeA was advanced into preclinical *in vivo* studies. The compound exhibited a good oral bioavailability (>50%) in male beagle dogs, Sprague-Dawley rats, and rhesus macaques. The rate of compound clearance in the circulatory system was moderate in all three animal species tested (14, 1.6, 9.0 mL/min/kg, respectively). The levels of the NTP in the liver were about 100-fold higher than the plasma levels of the parent nucleoside; oral doses at 2, 20, and 200 mg/kg to male Sprague-Dawley rats resulted in the liver NTP concentrations of 12, 92, 507 $\mu\text{mol/kg}$ and the plasma nucleoside exposure of 0.1, 2.0, 4.8 μM at 8 h of post-dose, respectively. The oral 50% lethal dose (LD_{50}) to female mice was greater than 2,000 mg/kg. No deaths or other treatment-related physical signs were seen during a post-dose 14-day observation period. For comparison, the mice dosed with tubercidin at 50 mg/kg died within 6 days.

To determine an antiviral efficacy *in vivo*, 7-deaza-2'-*C*-MeA was administered to HCV-infected chimpanzees, which resulted in dose- and time-dependent decreases in plasma viral load. In one experiment, HCV-infected chimpanzees dosed for 7 days at 0.2 and 2 mg/kg/day by intravenous administration experienced average reductions in viral load of 1.0 and >5 \log_{10} IU/mL, respectively. Separately, two HCV-infected chimpanzees received daily doses of 1 mg/kg via oral administration. After 37 days of the oral dosing, one chimpanzee with a high starting viral load experienced a reduction in viral load of 4.6 \log_{10} , and the viral load in the other chimpanzee fell below the limit of quantification (LOQ). Importantly, viral load remained below the LOQ throughout the duration of dosing and for at least 12 days after dosing ended. The results demonstrated a robust *in vivo* antiviral activity of 7-deaza-2'-*C*-MeA, justifying advancement into human clinical trials (as MK-608). Despite promising results in animal studies, however, MK-608 was discontinued for undisclosed reasons after entering phase I clinical trial.

Several additional adenosine analogs were also reported to be active against HCV (Fig. 7). Further substituents on the 7 position of 7-deaza-2'-*C*-MeA (such as **7a** and **7b**), replacement of the 2'-hydroxy to the 2'-fluoro group (**7c**), and application of the *C*-nucleoside scaffold (such as **7d-7f**) afforded varied potency and selectivity. However, there have been no further developments on these adenosine analogs [9–14].

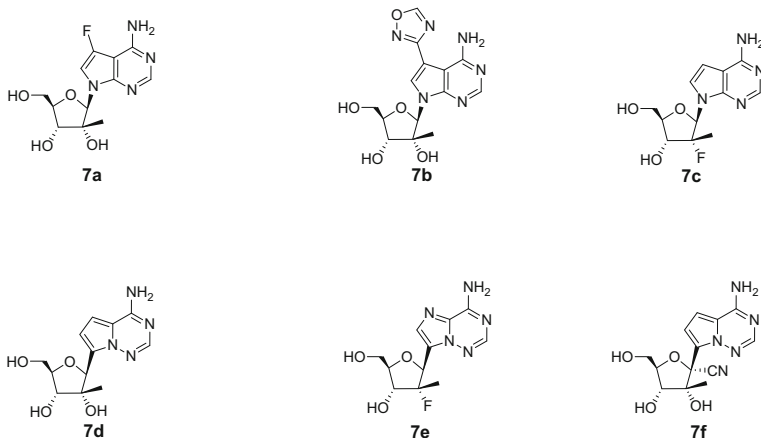


Fig. 7 Adenosine analogs with further structural variations

3.2 Guanosine Analogs

Researchers at Merck reported for the first time an analog of the guanosine series containing the signature 2'-C-methyl substituent, 2'-C-methylguanosine (2'-C-MeG) [5]. This compound exhibited a potent anti-HCV activity with EC_{50} of 3.1 μM in a cellular assay (Fig. 8). Interestingly, the corresponding NTP was exceptionally potent at inhibiting HCV NS5B enzyme activity in a cell-free assay (IC_{50} 0.13 μM). By comparison, 2'-C-MeA had EC_{50} of 0.26 μM and IC_{50} of 1.9 μM . The ratio of EC_{50} to IC_{50} for 2'-C-MeG is ~ 25 , while that for 2'-C-MeA is ~ 0.15 . This large difference was striking at a glance, but was readily explained by intracellular levels of the biologically active NTPs. The intracellular level of NTP upon incubation of 2'-C-MeG in the Huh-7 replicon cells were ~ 500 -fold lower than that from 2'-C-MeA. This result suggested that 2'-C-MeG was poorly taken up by the cells and/or inefficiently metabolized to its NTP, which limits intracellular level of 2'-C-MeGTP, resulting in the less-than-expected EC_{50} (Fig. 8).

With this information in hand, a series of monophosphate prodrug approaches were undertaken to increase cell-based activity against HCV (Fig. 8). McGuigan and his team investigated a phosphoramidate prodrug strategy and found that L-alanine 1-naphthyl phosphoramidate prodrugs (e.g., **8-1**) of 2'-C-MeG afforded a significant increase in antiviral activity (EC_{50} down to 0.28 μM) with no cytotoxicity up to 50 μM [15]. This result suggested that the first phosphorylation step of 2'-C-MeG was rate-limiting and the subsequent phosphorylation steps leading to the NTP were well proceeded. In addition, this particular phosphoramidate prodrug enabled an efficient delivery of 2'-C-MeG monophosphate (2'-C-MeGMP) into the host cells and circumvented the limitation of the first phosphorylation step. In contrast, the adenosine prodrug counterpart (**8-2**) did not show any increase in activity (EC_{50} from 0.26 to 0.24 μM). This is because the cellular uptake and intracellular

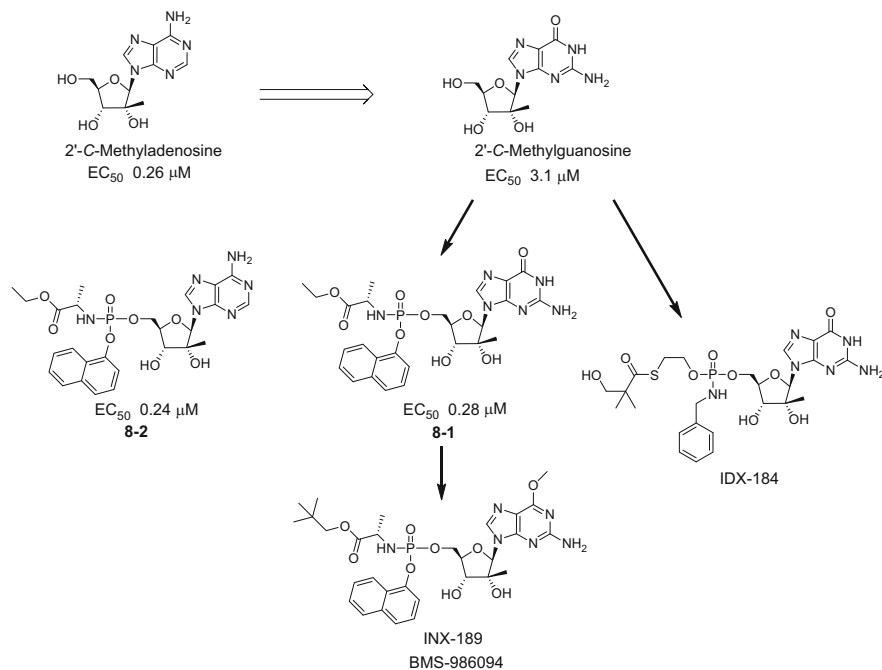


Fig. 8 Discovery of 2'-C-methyl guanosine and its monophosphate prodrugs

phosphorylation of the parent nucleoside 2'-C-MeA is already efficient so that the prodrug approach is not beneficial for NTP loading into the cells.

Continued efforts in this approach ultimately led to identification of INX-189 (Fig. 8), which is a double prodrug where a methyl group is added on the 6-*O* position of the nucleobase that is hydrolyzed upon entry to the host cells [16]. This modification was necessary to further increase the lipophilicity of the molecule for enhanced cellular permeability. A number of 6-*O*-methyl 2'-C-MeG prodrugs with various amino acid ester promoieties were prepared and evaluated, and a prodrug with L-alanine *neo*-pentyl ester was found to be optimal. INX-189 was substantially more potent than the earlier prodrug **8.1** (EC_{50} 0.013 μ M vs. 0.28 μ M) with an *in vitro* therapeutic index of >500 (CC_{50} 7.0 μ M). Intracellular 2'-C-MeGTP concentration when incubated with this prodrug at EC_{90} of 40 nM in the replicon cells was 2.4 pmol/million cells (i.e., ~240 pmol/g of liver tissue), and intracellular half-life of the triphosphate was ~24 h. Subsequently, *in vivo* pharmacokinetic studies were conducted to determine if liver 2'-C-MeGTP levels required for the 90% viral inhibition could be achieved at reasonable doses. At oral doses of ≥ 5 mg/kg in rats, the concentrations of 2'-C-MeGTP in the liver exceeded the EC_{90} soon after dosing and remained at or above the level for 72 h. Similarly, the EC_{90} level in the liver was achieved at 25 mg/kg oral dose in cynomolgus monkeys.

Mitochondrial toxicity has been observed with certain classes of nucleoside analog drugs, which was ascribed to inhibition of the mitochondrial DNA polymerase. This unwanted side effect has been well documented in the case of reverse transcriptase inhibitors used to treat HIV infection. The potential liability of INX-189 with regard to mitochondrial toxicity therefore was assessed in tissue culture studies with both a liver-derived cell line (HepG2) and a lymphocyte cell line (CEM). Treatment of the compound for 3 or 14 days produced no change in the ratio of mitochondrial genome copy number to cellular DNA, which was indicative of a lack of mitochondrion-specific toxicity [17].

INX-189 (later known as BMS-986094) was subsequently advanced to clinical development. The compound was shown to be effective and well tolerated in the early phase of trials. In a phase 1b trial, significant antiviral effects were observed in the 9, 25, 50, and 100 mg cohorts with median HCV RNA reduction at day 7 by 0.64, 1.0, 1.47, and 2.53 \log_{10} IU/mL, respectively, compared with $-0.20 \log_{10}$ IU/mL in placebo patients. In an expanded phase 1b trial with higher dosages (once-a-day 200 mg) as monotherapy or in combination (once-a-day 100 mg) with ribavirin for 7 days, BMS-986094 demonstrated potent and dose-dependent antiviral activity with a median HCV RNA reduction from baseline of 4.25 \log_{10} IU/mL.

During a phase II trial with a longer duration of the drug treatment, however, a serious safety issue was identified. A 20-year-old male treated with 200 mg dose experienced rapidly progressive heart failure and died. Additionally, 14 of 34 patients treated with BMS-986094 longer than a week had some evidence of cardiac dysfunction. BMS-986094 also had an adverse impact on the kidney, with most of the patients having increases in serum creatinine levels regardless of the degree of systolic dysfunction. The patient who died developed acute renal failure, while another required temporary hemodialysis. However, the serum creatinine levels of all other patients were improved once the drug was stopped.

To understand these findings better, a series of *in vitro* and *in vivo* investigative studies were conducted [18]. Independent researchers reported that 2'-*C*-MeGTP was rather efficiently incorporated by mitochondrial RNA polymerase and BMS-986094 induced functional reduction of mitochondrial respiration in a cultured cell line and in freshly isolated rat cardiomyocytes at clinically relevant concentrations, which contradicts the earlier assessment. Intriguingly, tissue analysis from cynomolgus monkey PK studies revealed relatively high concentrations and slow clearance of the active metabolite 2'-*C*-MeGTP in the heart and kidney, which may be associated with the observed cardiac and renal toxicity in the clinical trials. However, the link between the tissue accumulation of the metabolite and the clinically observed toxicity remains to be further investigated.

Another 2'-*C*-MeG monophosphate prodrug, IDX-184 (Fig. 8), also had an improved antiviral activity in a replicon assay (EC_{50} 0.3–0.45 μ M) and in a JFH-1 infectious system (EC_{50} 0.06–0.11 μ M), as compared to the parent 2'-*C*-MeG [19, 20]. *In vitro* metabolism experiments indicated that IDX-184 was efficient at delivering the monophosphate in the replicon cells with a boosted level of intracellular 2'-*C*-MeGTP (~100-fold), corroborated with the increased antiviral activity in the cell-based assay. In particular, IDX-184 was predominantly metabolized in the

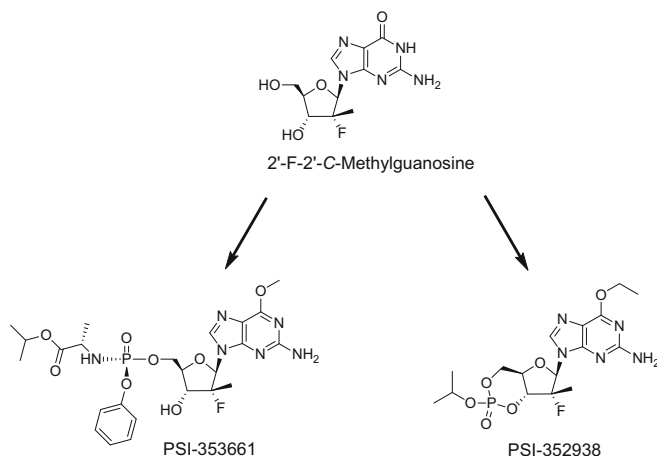


Fig. 9 Discovery of 2'-fluoro-2'-C-methylguanosine and its monophosphate prodrugs

liver via both cytochrome P (CYP)-dependent and cytochrome P (CYP)-independent processes, opening up the possibility of a liver-targeted delivery that could enhance the therapeutic margin by limiting potential off-target tissue toxicity. Consistent with the *in vitro* results, oral pharmacokinetic studies with IDX-184 in rats and monkeys showed very high extraction (approximately 95%) by the liver, with low plasma levels of the parent 2'-C-MeG, suggesting preferential loading of 2'-C-MeGTP into the liver over other tissues. IDX-184 was progressed to clinical trial, demonstrating efficacy in early trials. However, the clinical development was discontinued due to a concern of toxicity.

A guanosine analog with 2'-fluoro and 2'-C-methyl groups was only weakly active in a HCV replicon assay (EC_{90} 69 μ M), but its triphosphate was potent at inhibiting HCV NS5B polymerase enzyme (IC_{50} 5.9 μ M). Monophosphate prodrug approaches were applied, and more than 1,000-fold increased potency was achieved. PSI-353661 and PSI-352938 were chosen for clinical development, but their clinical evaluations were put on hold, presumably based on toxicity findings from nonclinical safety studies (Fig. 9) [21, 22].

3.3 Cytidine Analogs

The first pyrimidine analog discovered to be a selective inhibitor of HCV replication was 2'-C-methylcytidine (2'-C-MeC). Similar to a majority of other nucleosides, the compound was not sufficiently orally bioavailable, which hampered further development. To overcome the limitation, 3'-*O*-valinyl ester prodrug of 2'-C-MeC (NM283, valopicitabine) was devised (Fig. 10) [23, 24]. This prodrug utilized an active intestinal absorption via a peptide transport mechanism, which had been a

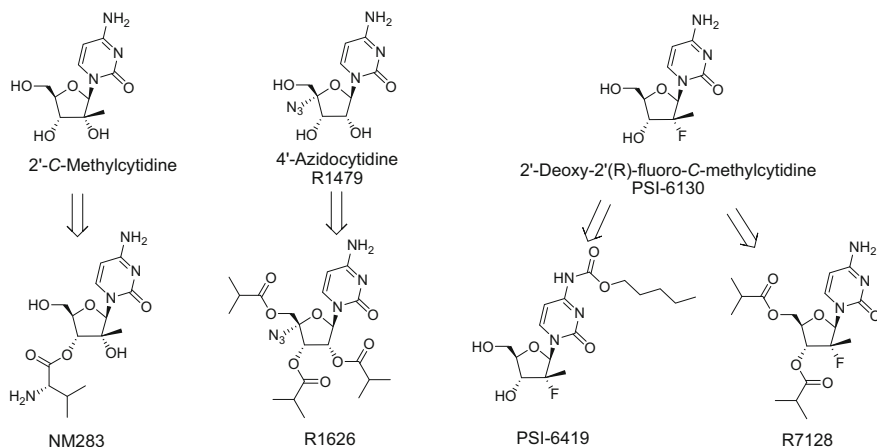


Fig. 10 Ester prodrugs of cytidine analogs for increased oral bioavailability

successful strategy employed in several nucleoside analogs. The valinyl ester prodrug was highly soluble (423 g/L in water as the dihydrochloride salt), stable in acidic media (e.g., half-life of 6 days at pH 4.5), and rapidly converted into the parent 2'-C-MeC in both human plasma and whole blood, which are all desirable attributes for an oral prodrug. As expected, the apparent bioavailability of 2'-C-MeC following oral administration of NM283 was greatly improved (34%F in rats). The prodrug also exhibited a good PK profile in monkeys and demonstrated an antiviral efficacy in the HCV-infected chimpanzee. NM283 was eventually progressed to clinical development. In a monotherapy study with HCV-infected patients, HCV viral load reductions of 0.15–1.21 log₁₀ IU/mL were observed at 2 weeks with 50–800 mg/day of NM283 in a dose-dependent manner. High doses (e.g., 800 mg/day) were necessary to achieve a clinically meaningful efficacy. However, NM283 was associated with dose-limiting gastrointestinal disturbances, nausea, and vomiting, with higher prevalence in cohorts receiving doses of 400 mg/day or above. Eventually, the development of NM283 was discontinued based on a conclusion that the benefits of NM283 did not outweigh the gastrointestinal toxicities [25].

Another pyrimidine nucleoside 4'-azidocytidine (R1479) was also advanced to clinical evaluation (Fig. 10) [26]. R1479 had a potent anti-HCV activity (EC₅₀ of 1.3 μM and IC₅₀ of 0.67 μM) with no cytotoxic or cytostatic effects. Dose-dependent viral load reduction was evident, but observed plasma exposure of R1479 was low due to poor oral absorption. Accordingly, a prodrug campaign was undertaken. Several prodrug strategies including appendages of liver-targeted promoieties (e.g., N⁶-alkyloxycarbonyl as in capecitabine), peptide transporter-targeted promoieties, and lipophilic carboxylic acid ester promoieties were investigated. Over 100 structurally diverse compounds covering a range of clogP were synthesized and evaluated for their stability, permeability, and oral bioavailability in cynomolgus monkeys. Among them, R1626 (balapiravir) (Fig. 10), a tri-isobutyl ester prodrug of R1479, was found

to have optimal properties with increased oral bioavailability and improved in vitro antiviral activity. This compound was then progressed to clinical trials. In a phase 1b study, treatment-naïve patients infected with HCV genotype 1 were treated with R1626 orally at doses of 500 mg, 1,500 mg, 3,000 mg, or 4,500 mg or placebo twice daily (BID) for 14 days with 14 days of follow-up. Doses up to and including 3,000 mg BID were well tolerated in the study. However, there was an increase in frequency of adverse events (e.g., neutropenia) at the highest dose (4,500 mg). R1626 was efficiently converted to R1479, with dose-proportional pharmacokinetics observed over the entire dose range. Dose-dependent and time-dependent reductions in HCV RNA were observed. Mean decreases in viral load after 14 days of treatment with doses of 500, 1,500, 3,000, and 4,500 mg were 0.32, 1.2, 2.6, and 3.7 log₁₀ IU/mL, respectively. However, the compound was not progressed further likely due to the insufficient efficacy.

The earlier hit 2'-deoxy-2'-fluorocytidine (2'-FdC) was followed up by a research group at Pharmasset. Further structural modification of the sugar ring, namely, addition of the key 2'-C-Me moiety, led to the identification of 2'-deoxy-2'(R)-fluoro-2'-C-methylcytidine (PSI-6130) [27–29]. This change maintained the potent anti-HCV activity and yet afforded much improved selectivity. PSI-6130 showed EC₉₀ of 4.6 μM in a HCV replicon assay, but little or no activity against bovine diarrhea virus and other flaviviruses, indicating that it was a highly selective HCV inhibitor. PSI-6130 is efficiently phosphorylated to the corresponding NTP in the cells. The steady-state inhibition constant (K_i) for PSI-6130 triphosphate with the wild-type NS5B enzyme was 4.3 μM, compared well with those of 2'-C-MeCTP (K_i 1.6 μM) and 2'-C-MeATP (K_i 1.5 μM). Furthermore, PSI-6130 showed little or no cytotoxicity/cytostasis against a variety of cell types and no mitochondrial toxicity. Incubation of the compound in monkey and human whole blood revealed deamination leading to formation of a metabolite 2'-deoxy-2'(R)-fluoro-2'-methyluracil (PSI-6206) which had no anti-HCV activity on its own. This biologically inactive metabolite was also detected in vivo. PK studies in rhesus monkeys revealed significant metabolism upon oral administration of PSI-6130. The oral bioavailability of PSI-6130 was 24%, but the total bioavailability including the parent drug PSI-6130 and the deaminated metabolite PSI-6206 was 64%. In addition, the plasma exposure of PSI-6206 following administration by the oral route was three- to fourfold higher than for the intravenous route, suggesting that deamination likely took place predominantly during first-pass metabolism in the liver or the gastrointestinal lining. PSI-6130 was advanced into clinical evaluation. In a phase I study with healthy male volunteers, single oral doses of PSI-6130 were generally well tolerated, and no serious adverse events were seen with doses up to 3,000 mg [30].

To improve oral absorption and drug exposure while suppressing formation of the uridine metabolite, a prodrug campaign was undertaken with PSI-6130. PSI-6419 (*N*⁴-pentylloxycarbonyl PSI-6130) was designed inspired by capecitabine, an orally bioavailable nucleoside analog prodrug. However, this prodrug did not yield high levels of PSI-6130 in serum, when administered orally to cynomolgus monkeys. Additional prodrug approaches were then investigated, which resulted in discovery of

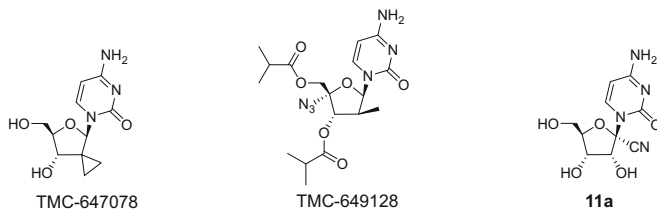


Fig. 11 Additional cytidine analogs for anti-HCV activity

R7128 (3',5'-diisobutyrate prodrug of PSI-6130) with an improved oral bioavailability. R-7128 (mericitabine) (Fig. 10) was progressed to clinical development [30]. In a phase I dose range finding PK study in healthy subjects, single oral doses of R-7128 (500–9,000 mg) revealed efficient delivery of PSI-6130. While plasma exposure to the prodrug R-7128 was negligible, plasma levels of the parent PSI-6130 and the uridine metabolite PSI-6206 were increased dose proportionally. At dose of 1,500 mg, for example, the C_{\max} for PSI-6130 was 7.5 $\mu\text{g/mL}$, median t_{\max} 2.0 h, $t_{1/2}$ 5.6 h, and $\text{AUC}_{(0-\text{inf})}$ 59 $\mu\text{g h/mL}$. In subjects administered a dose of 1,500 mg with food, the respective C_{\max} , median t_{\max} , $t_{1/2}$, and $\text{AUC}_{(0-\text{inf})}$ were 8.9 $\mu\text{g/mL}$, 3.0 h, 5.2 h, and 71 $\mu\text{g h/mL}$. In 14-day monotherapy studies in patients with genotype 1 HCV infection, a 1,500 mg BID dose afforded the mean decline in HCV RNA of 2.7 \log_{10} IU/mL with the range of the decline being 1.2–4.2 \log_{10} IU/mL after completion of the treatment. Once-a-day (QD) administrations of 750 mg and 1,500 mg were less effective, resulting in viral load reduction by 2.1 and 1.5 \log_{10} IU/mL, respectively. R7128 was moved to phase II studies with longer treatment duration as well as a combination regimen with PEG-IFN- α and ribavirin. However, those studies showed no clear clinical benefits, and no further clinical development had been reported since then.

Some additional cytidine analogs with modifications of the ribose ring such as TMC-647078, TMC-649128, and **11a** were identified as anti-HCV inhibitors (Fig. 11). These new cytidine analogs exhibited no advantages over the previous analogs with respect to potency and selectivity [31–33].

3.4 Uridine Analogs

Metabolism studies with PSI-6130 in primary human hepatocytes revealed multiple phosphorylated metabolites (Fig. 12). In addition to PSI-6130 and its 5'-phosphorylated derivatives as predicted, the deaminated derivative of PSI-6130 (PSI-6206) and its corresponding phosphorylated metabolites were present in the PSI-6130-treated hepatocytes [34]. Both triphosphate species are enzymatically active (IC_{50} of 0.13 μM for the CTP and 0.52 μM for the UTP). Interestingly, both species were formed equally well, but an intracellular half-life of the UTP was much longer than that of the CTP (38 h vs. 4.7 h). 2'-F-2'-C-MeU (PSI-6206) was

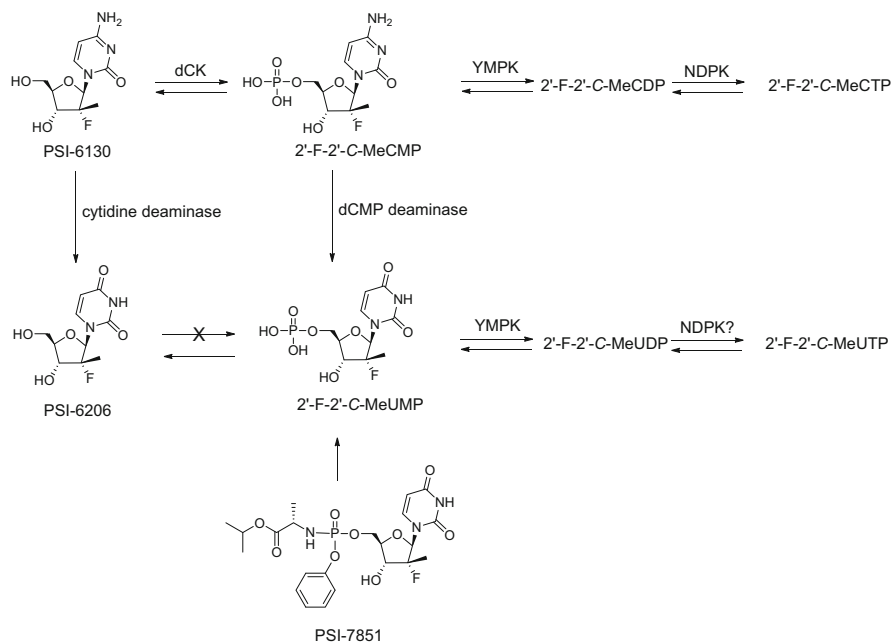


Fig. 12 Metabolic pathway of PSI-1630 and discovery of PSI-7851

intrinsically inactive in a cell-based HCV replicon assay and found to be not metabolized to its phosphorylated species. Therefore, 2'-F-2'-C-MeUMP present in the human hepatocytes was most likely formed through the deamination of 2'-F-2'-C-MeCMP by the cellular dCMP deaminase and subsequently further phosphorylated to the corresponding UDP and UTP. Accordingly, the monophosphate strategy was applied, which ultimately led to the discovery of PSI-7851 [35, 36].

PSI-7851 was highly potent in a HCV replicon assay (EC_{90} 0.52 μ M) and, when incubated in primary human hepatocytes, produced intracellularly a significant level of the biologically active 2'-F-2'-C-MeUTP (\sim 500 μ M after 48 h of incubation with 100 μ M of PSI-7851). The compound showed essentially no toxicity when tested in expanded cell lines including Huh7, HepG2, BxBC3, and CEM. In addition, no inhibition of mitochondrial DNA synthesis up to the highest concentration tested (50 μ M) was observed. Oral administration of PSI-7851 in dogs and cynomolgus monkeys showed an adequate level of the plasma exposure of the prodrug PSI-7851 and the liver exposure of 2'-F-2'-C-MeUTP. Nonclinical single-dose acute toxicity studies determined a no-observed-adverse-effect-level (NOAEL) of >1,800 mg/kg. PSI-7851 was then advanced to clinical development and demonstrated a promising efficacy in chronic HCV-infected patients. Once-a-day oral administration of 400 mg of PSI-7851 afforded the mean decline in HCV RNA of 2.0 \log_{10} IU/mL at day 3. By comparison, twice daily administration of 1,500 mg of R7128 resulted in the decline in HCV RNA of only 1.0 \log_{10} IU/mL. Since PSI-7851 was a mixture

of diastereomers at the phosphorous center of the phosphoramidate moiety, it was not ideal for drug development. Thus, a single stereoisomer from the mixture, PSI-7977 (GS-7977, sofosbuvir), was eventually selected for further development. A full account of discovery and development of sofosbuvir will be discussed in the ensuing chapter.

As a result of the discovery of PSI-7851 and PSI-7977 exhibiting impressive efficacy and tolerability in the clinical setting, prodrugs of other uridine nucleosides were investigated. Unlike 2'-C-MeC, the 2'-C-methyl-substituted uridine (2'-C-MeU) was only weakly active in a HCV replicon assay, while its triphosphate 2'-C-MeUTP was equally potent as 2'-C-MeCTP in a NS5B enzyme assay. Therefore, monophosphate prodrug approaches were again investigated to improve potency, which resulted in discovery of a series of compounds with submicromolar EC_{50} in replicon assays (Fig. 13). Researchers at Alios BioPharma has explored thio-monophosphate prodrugs of various 2'-C-methyl-substituted nucleosides for anti-HCV activity and identified a uridine thiophosphate prodrug ALS-2200 [37]. The compound had a potent activity in a replicon assay ($EC_{50} < 1 \mu M$) and its thiotriphosphate (thio-NTP) had enzymatic activity comparable to the oxo-NTP counterpart. Incubation of the prodrug in plated human hepatocytes produced the thio-NTP intracellularly, suggesting that the observed replicon activity comes from the thio-NTP. Because the sulfur atom is introduced, two diastereoisomeric thio-NTPs can be possibly formed. Interestingly, however, only one isomer was found from the metabolism study. ALS-2200 is a mixture of the two diastereoisomers at the phosphorus, and one single diastereoisomer, VX-135 (absolute stereochemistry information not available), was advanced to clinical development. Although VX-135 demonstrated efficacy at reducing viral loads in HCV-infected patients, it

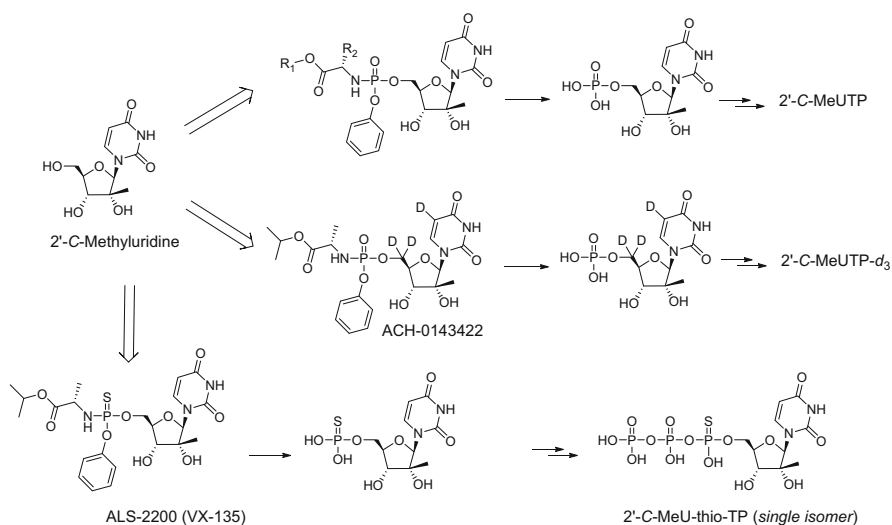


Fig. 13 Uridine monophosphate prodrugs

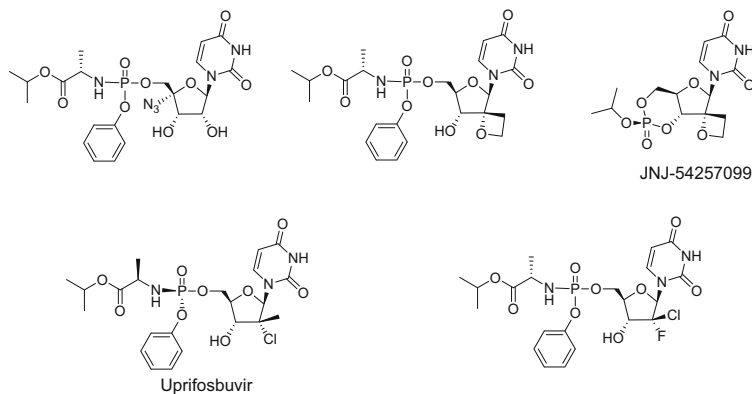


Fig. 14 Ribose-modified uridine monophosphate prodrugs for anti-HCV activity

showed liver toxicity in some patients who received a 400 mg dose. Lowering dose could avoid toxicity at the expense of reduced or compromised efficacy. For this reason, further clinical development was stopped. A research team at Achillion Pharmaceuticals investigated a prodrug of deuterated 2'-C-MeU, ACH-0143422, where the 5'-deuterium had a significant positive effect on in vitro metabolism [38]. The 5'-deuterium increased the stability toward dephosphorylation of the 5'-monophosphate, thereby increasing the bioactive triphosphate pool, which might result in increased efficacy in the clinic. ACH-0143422 entered clinical studies. However, it did not progress beyond phase II clinical studies.

Independently, a number of structurally related uridine derivatives were evaluated for anti-HCV activity (Fig. 14) [39–44]. Various modifications on the ribose ring were tolerated, and all these uridine analogs required monophosphate prodrug approaches for cellular activity.

4 Conclusion

Prior to initiation of discovery campaigns for anti-HCV agents, a track record of success in identifying and developing nucleoside and nucleotide drugs to treat other viral infections had been achieved, and a significant knowledge on chemistry, biology, pharmacology, and toxicology around this class of compounds had been accumulated. Accordingly, the search for anti-HCV agents appeared straightforward at first. The previous antiviral agents were all structural mimics of endogenous 2'-deoxynucleosides targeting DNA polymerases. Since HCV NS5B is an RNA polymerase, however, new structural elements had to be incorporated for selective recognition by the RNA polymerase. In 2003, it was reported for the first time that 2'-modified nucleoside analogs had selective anti-HCV activity. Since then, a number of new structural modifications were made in order to find a compound

with optimal properties such as potency, selectivity, and oral bioavailability. More than a dozen compounds were advanced into clinical trials. All these compounds but one were unsuccessful in advancing further due to insufficient antiviral efficacy or unacceptable drug-associated toxicity. A prodrug of 2'-fluoro-2'-C-methyluridine monophosphate PSI-7977 (GS-7977, sofosbuvir) was approved in 2013 by the US Food and Drug Administration and became a cornerstone of current treatment regimens for chronic HCV infection.

Compliance with Ethical Standards

Conflict of Interest The author is an employee of Gilead Sciences, Inc.

Ethical Approval This is a review article that does not contain any studies with human participants or animals performed by the author.

References

1. Carroll SS, Tomassini JE, Bosserman M, Getty K, Stahlhut MW, Eldrup AB, Bhat B, Hall D, Simcoe AL, LaFemina R, Rutkowski CA, Wolanski B, Yang Z, Migliaccio G, De Francesco R, Kuo LC, MacCoss M, Olsen DB (2003) Inhibition of hepatitis C virus RNA replication by 2'-modified nucleoside analogs. *J Biol Chem* 278(14):11979–11984
2. Stuyver LJ, McBrayer TR, Tharnish PM, Hassan AE, Chu CK, Pankiewicz KW, Watanabe KA, Schinazi RF, Otto MJ (2003) Dynamics of subgenomic hepatitis C virus replicon RNA levels in Huh-7 cells after exposure to nucleoside antimetabolites. *J Virol* 77(19):10689–10694
3. Stuyver LJ, McBrayer TR, Whitaker T, Tharnish PM, Ramesh M, Lostia S, Cartee L, Shi J, Hobbs A, Schinazi RF, Watanabe KA, Otto MJ (2004) Inhibition of the subgenomic hepatitis C virus replicon in huh-7 cells by 2'-deoxy-2'-fluorocytidine. *Antimicrob Agents Chemother* 48(2):651–654
4. Smith DB, Martin JA, Klumpp K, Baker SJ, Blomgren PA, Devos R, Granycome C, Hang J, Hobbs CJ, Jiang WR, Laxton C, Le Pogam S, Leveque V, Ma H, Maile G, Merrett JH, Pichota A, Sarma K, Smith M, Swallow S, Symons J, Vesey D, Najera I, Cammack N (2007) Design, synthesis, and antiviral properties of 4'-substituted ribonucleosides as inhibitors of hepatitis C virus replication: the discovery of R1479. *Bioorg Med Chem Lett* 17(9):2570–2576
5. Eldrup AB, Allerson CR, Bennett CF, Bera S, Bhat B, Bhat N, Bosserman MR, Brooks J, Burlein C, Carroll SS, Cook PD, Getty KL, MacCoss M, McMasters DR, Olsen DB, Prakash TP, Prhavic M, Song Q, Tomassini JE, Xia J (2004) Structure-activity relationship of purine ribonucleosides for inhibition of hepatitis C virus RNA-dependent RNA polymerase. *J Med Chem* 47(9):2283–2295
6. Eldrup AB, Prhavic M, Brooks J, Bhat B, Prakash TP, Song Q, Bera S, Bhat N, Dande P, Cook PD, Bennett CF, Carroll SS, Ball RG, Bosserman M, Burlein C, Colwell LF, Fay JF, Flores OA, Getty K, LaFemina RL, Leone J, MacCoss M, McMasters DR, Tomassini JE, Von Langen D, Wolanski B, Olsen DB (2004) Structure-activity relationship of heterobase-modified 2'-C-methyl ribonucleosides as inhibitors of hepatitis C virus RNA replication. *J Med Chem* 47(21):5284–5297
7. Olsen DB, Eldrup AB, Bartholomew L, Bhat B, Bosserman MR, Ceccacci A, Colwell LF, Fay JF, Flores OA, Getty KL, Grobler JA, LaFemina RL, Markel EJ, Migliaccio G, Prhavic M, Stahlhut MW, Tomassini JE, MacCoss M, Hazuda DJ, Carroll SS (2004) A 7-deaza-adenosine

- analog is a potent and selective inhibitor of hepatitis C virus replication with excellent pharmacokinetic properties. *Antimicrob Agents Chemother* 48(10):3944–3953
8. Carroll SS, Ludmerer S, Handt L, Koeplinger K, Zhang NR, Graham D, Davies ME, MacCoss M, Hazuda D, Olsen DB (2009) Robust antiviral efficacy upon administration of a nucleoside analog to hepatitis C virus-infected chimpanzees. *Antimicrob Agents Chemother* 53(3):926–934
 9. Leroy F, Chaves D, Dukhan D, Storer R, Sommadossi JP, Loi AG, Cadeddu A, Fanti M, Boscu N, Bassetti F, Liuzzi M, Gosselin G (2008) Synthesis and antiviral evaluation of 7-fluoro-7-deaza-2-aminopurine nucleoside derivatives. *Nucleic Acids Symp Ser (Oxf)* 52:595–596
 10. Di Francesco ME, Avolio S, Pompei M, Pesci S, Monteagudo E, Pucci V, Giuliano C, Fiore F, Rowley M, Summa V (2012) Synthesis and antiviral properties of novel 7-heterocyclic substituted 7-deaza-adenine nucleoside inhibitors of hepatitis C NS5B polymerase. *Bioorg Med Chem* 20(15):4801–4811
 11. Shi J, Zhou L, Zhang H, McBrayer TR, Detorio MA, Johns M, Bassit L, Powdrill MH, Whitaker T, Coats SJ, Götte M, Schinazi RF (2011) Synthesis and antiviral activity of 2'-deoxy-2'-fluoro-2'-C-methyl-7-deazapurine nucleosides, their phosphoramidate prodrugs and 5'-triphosphates. *Bioorg Med Chem Lett* 21(23):7094–7098
 12. Draffan AG, Frey B, Pool B, Gannon C, Tyndall EM, Lilly M, Francom P, Hufton R, Halim R, Jahangiri S, Bond S, Nguyen VT, Jaynes TP, Wirth V, Luttick A, Tilmanis D, Thomas JD, Pryor M, Porter K, Morton CJ, Lin B, Duan J, Kukolj G, Simoneau B, McKercher G, Lagacé L, Amad M, Bethell RC, Tucker SP (2014) Discovery and synthesis of C-nucleosides as potential new anti-HCV agents. *ACS Med Chem Lett* 5(6):679–684
 13. Kirschberg TA, Metobo S, Clarke MO, Aktoudianakis V, Babusis D, Barauskas O, Birkus G, Butler T, Byun D, Chin G, Doerffler E, Edwards TE, Fenaux M, Lee R, Lew W, Mish MR, Murakami E, Park Y, Squires NH, Tirunagari N, Wang T, Whitcomb M, Xu J, Yang H, Ye H, Zhang L, Appleby TC, Feng JY, Ray AS, Cho A, Kim CU (2017) Discovery of a 2'-fluoro-2'-C-methyl C-nucleotide HCV polymerase inhibitor and a phosphoramidate prodrug with favorable properties. *Bioorg Med Chem Lett* 27(8):1840–1847
 14. Cho A, Zhang L, Xu J, Lee R, Butler T, Metobo S, Aktoudianakis V, Lew W, Ye H, Clarke M, Doerffler E, Byun D, Wang T, Babusis D, Carey AC, German P, Sauer D, Zhong W, Rossi S, Fenaux M, McHutchison JG, Perry J, Feng J, Ray AS, Kim CU (2014) Discovery of the first C-nucleoside HCV polymerase inhibitor (GS-6620) with demonstrated antiviral response in HCV infected patients. *J Med Chem* 57(5):1812–1825
 15. McGuigan C, Gilles A, Madela K, Aljarah M, Holl S, Jones S, Vernachio J, Hutchins J, Ames B, Bryant KD, Gorovits E, Ganguly B, Hunley D, Hall A, Kolykhalov A, Liu Y, Muhammad J, Raja N, Walters R, Wang J, Chamberlain S, Henson G (2010) Phosphoramidate ProTides of 2'-C-methylguanosine as highly potent inhibitors of hepatitis C virus. Study of their in vitro and in vivo properties. *J Med Chem* 53(13):4949–4957
 16. McGuigan C, Madela K, Aljarah M, Gilles A, Brancale A, Zonta N, Chamberlain S, Vernachio J, Hutchins J, Hall A, Ames B, Gorovits E, Ganguly B, Kolykhalov A, Wang J, Muhammad J, Patti JM, Henson G (2010) Design, synthesis and evaluation of a novel double pro-drug: INX-08189. A new clinical candidate for hepatitis C virus. *Bioorg Med Chem Lett* 20(16):4850–4854
 17. Vernachio JH, Bleiman B, Bryant KD, Chamberlain S, Hunley D, Hutchins J, Ames B, Gorovits E, Ganguly B, Hall A, Kolykhalov A, Liu Y, Muhammad J, Raja N, Walters CR, Wang J, Williams K, Patti JM, Henson G, Madela K, Aljarah M, Gilles A, McGuigan C (2011) INX-08189, a phosphoramidate prodrug of 6-O-methyl-2'-C-methyl guanosine, is a potent inhibitor of hepatitis C virus replication with excellent pharmacokinetic and pharmacodynamic properties. *Antimicrob Agents Chemother* 55(5):1843–1851
 18. Gill M, Horn K, Hennan J, White R, Bounous D, Clark S, Megill JR, Janovitz E, Davies M, Sanderson T, Graziano M (2017) From the cover: investigative nonclinical cardiovascular

- safety and toxicology studies with BMS-986094, an NS5b RNA-dependent RNA polymerase inhibitor. *Toxicol Sci* 155(2):348–362
19. Sizon G, Pierra C, Peyronnet J, Badaroux E, Rabeson C, Benzaria-Prad S, Surleraux D, Loi AG, Musiu C, Liuzzi M, Seifer M, Standing D, Sommadossi JP, Gosselin G (2015) Design, synthesis and antiviral evaluation of 2'-C-methyl branched guanosine pronucleotides: the discovery of IDX184, a potent liver-targeted HCV polymerase inhibitor. *Future Med Chem* 7(13):1675–1700
 20. Lalezari J, Asmuth D, Casiró A, Vargas H, Lawrence S, Dubuc-Patrick G, Chen J, McCarville J, Pietropaolo K, Zhou XJ, Sullivan-Bólyai J, Mayers D (2012) Short-term monotherapy with IDX184, a liver-targeted nucleotide polymerase inhibitor, in patients with chronic hepatitis C virus infection. *Antimicrob Agents Chemother* 56(12):6372–6378
 21. Chang W, Bao D, Chun BK, Naduthambi D, Nagarathnam D, Rachakonda S, Reddy PG, Ross BS, Zhang HR, Bansal S, Espiritu CL, Keilman M, Lam AM, Niu C, Steuer HM, Furman PA, Otto MJ, Sofia MJ (2010) Discovery of PSI-353661, a novel purine nucleotide prodrug for the treatment of HCV infection. *ACS Med Chem Lett* 2(2):130–135
 22. Reddy PG, Bao D, Chang W, Chun BK, Du J, Nagarathnam D, Rachakonda S, Ross BS, Zhang HR, Bansal S, Espiritu CL, Keilman M, Lam AM, Niu C, Steuer HM, Furman PA, Otto MJ, Sofia MJ (2010) 2'-Deoxy-2'- α -fluoro-2'- β -C-methyl 3',5'-cyclic phosphate nucleotide prodrug analogs as inhibitors of HCV NS5B polymerase: discovery of PSI-352938. *Bioorg Med Chem Lett* 20(24):7376–7380
 23. Pierra C, Amador A, Benzaria S, Cretton-Scott E, D'Amours M, Mao J, Mathieu S, Moussa A, Bridges EG, Standing DN, Sommadossi JP, Storer R, Gosselin G (2006) Synthesis and pharmacokinetics of valopicitabine (NM283), an efficient prodrug of the potent anti-HCV agent 2'-C-methylcytidine. *J Med Chem* 49(22):6614–6620
 24. Pierra C, Benzaria S, Amador A, Moussa A, Mathieu S, Storer R, Gosselin G (2005) NM 283, an efficient prodrug of the potent anti-HCV agent 2'-C-methylcytidine. *Nucleosides Nucleotides Nucleic Acids* 24(5–7):767–770
 25. Franciscus A (2007) FDA: NM-283 on hold. *HCV Advocate* 10(8):1
 26. Roberts SK, Cooksley G, Dore GJ, Robson R, Shaw D, Berns H, Hill G, Klumpp K, Najera I, Washington C (2008) Robust antiviral activity of R1626, a novel nucleoside analog: a randomized, placebo-controlled study in patients with chronic hepatitis C. *Hepatology* 48(2):398–406
 27. Clark JL, Hollecker L, Mason JC, Stuyver LJ, Tharnish PM, Lostia S, McBrayer TR, Schinazi RF, Watanabe KA, Otto MJ, Furman PA, Stec WJ, Patterson SE, Pankiewicz KW (2005) Design, synthesis, and antiviral activity of 2'-deoxy-2'-fluoro-2'-C-methylcytidine, a potent inhibitor of hepatitis C virus replication. *J Med Chem* 48(17):5504–5508
 28. Murakami E, Bao H, Ramesh M, McBrayer TR, Whitaker T, Micolochick Steuer HM, Schinazi RF, Stuyver LJ, Obikhod A, Otto MJ, Furman PA (2007) Mechanism of activation of beta-D-2'-deoxy-2'-fluoro-2'-C-methylcytidine and inhibition of hepatitis C virus NS5B RNA polymerase. *Antimicrob Agents Chemother* 51(2):503–509
 29. Asif G, Hurwitz SJ, Shi J, Hernandez-Santiago BI, Schinazi RF (2007) Pharmacokinetics of the antiviral agent beta-D-2'-deoxy-2'-fluoro-2'-C-methylcytidine in rhesus monkeys. *Antimicrob Agents Chemother* 51(8):2877–2882
 30. Cole P, Castañer R, Bolós J (2009) R-7128: RNA-directed RNA polymerase (NS5B) inhibitor treatment of hepatitis C virus infection. *Drugs Future* 34(4):282–290
 31. Jonckers TH, Lin TI, Buyck C, Lachau-Durand S, Vandyck K, Van Hoof S, Vandekerckhove LA, Hu L, Berke JM, Vijgen L, Dillen LL, Cummings MD, de Kock H, Nilsson M, Sund C, Rydegård C, Samuelsson B, Rosenquist A, Fanning G, Van Emelen K, Simmen K, Raboisson P (2010) 2'-Deoxy-2'-spirocyclopropylcytidine revisited: a new and selective inhibitor of the hepatitis C virus NS5B polymerase. *J Med Chem* 53(22):8150–8160
 32. Nilsson M, Kalayanov G, Winqvist A, Pinho P, Sund C, Zhou XX, Wähling H, Belfrage AK, Pelcman M, Agback T, Benckestock K, Wikström K, Boothe M, Lindqvist A, Rydegård C, Jonckers TH, Vandyck K, Raboisson P, Lin TI, Lachau-Durand S, de Kock H, Smith DB, Martin JA, Klumpp K, Simmen K, Vrang L, Terelius Y, Samuelsson B, Rosenquist S,

- Johansson NG (2012) Discovery of 4'-azido-2'-deoxy-2'-C-methyl cytidine and prodrugs thereof: a potent inhibitor of hepatitis C virus replication. *Bioorg Med Chem Lett* 22 (9):3265–3268
33. Kirschberg TA, Mish M, Squires NH, Zonte S, Aktoudianakis E, Metobo S, Butler T, Ju X, Cho A, Ray AS, Kim CU (2015) Synthesis of 1'-C-cyano pyrimidine nucleosides and characterization as HCV polymerase inhibitors. *Nucleosides Nucleotides Nucleic Acids* 34 (11):763–785
34. Ma H, Jiang WR, Robledo N, Leveque V, Ali S, Lara-Jaime T, Masjedizadeh M, Smith DB, Cammack N, Klumpp K, Symons J (2007) Characterization of the metabolic activation of hepatitis C virus nucleoside inhibitor beta-D-2'-Deoxy-2'-fluoro-2'-C-methylcytidine (PSI-6130) and identification of a novel active 5'-triphosphate species. *J Biol Chem* 282 (41):29812–29820
35. Sofia MJ, Bao D, Chang W, Du J, Nagarathnam D, Rachakonda S, Reddy PG, Ross BS, Wang P, Zhang HR, Bansal S, Espiritu C, Keilman M, Lam AM, Steuer HM, Niu C, Otto MJ, Furman PA (2010) Discovery of a β -d-2'-deoxy-2'- α -fluoro-2'- β -C-methyluridine nucleotide prodrug (PSI-7977) for the treatment of hepatitis C virus. *J Med Chem* 53(19):7202–7218
36. Lam AM, Murakami E, Espiritu C, Steuer HM, Niu C, Keilman M, Bao H, Zennou V, Bourne N, Julander JG, Morrey JD, Smee DF, Frick DN, Heck JA, Wang P, Nagarathnam D, Ross BS, Sofia MJ, Otto MJ, Furman PA (2010) PSI-7851, a pronucleotide of beta-D-2'-deoxy-2'-fluoro-2'-C-methyluridine monophosphate, is a potent and pan-genotype inhibitor of hepatitis C virus replication. *Antimicrob Agents Chemother* 54(8):3187–3196
37. Smith DB, Deval J, Dyatkina N, Beigelman L, Wang G (2016) US9278990 B2
38. Deshpande M, Wiles JA, Hashimoto A, Phadke A (2014) WO2104169278 A1
39. Perrone P, Luoni GM, Kelleher MR, Daverio F, Angell A, Mulready S, Congiatu C, Rajyaguru S, Martin JA, Levêque V, Le Pogam S, Najera I, Klumpp K, Smith DB, McGuigan C (2007) Application of the phosphoramidate ProTide approach to 4'-azidouridine confers sub-micromolar potency versus hepatitis C virus on an inactive nucleoside. *J Med Chem* 50 (8):1840–1849
40. Du J, Chun BK, Mosley RT, Bansal S, Bao H, Espiritu C, Lam AM, Murakami E, Niu C, Micolochick Steuer HM, Furman PA, Sofia MJ (2014) Use of 2'-spirocyclic ethers in HCV nucleoside design. *J Med Chem* 57(5):1826–1835
41. Jonckers TH, Vandeyck K, Vandekerckhove L, Hu L, Tahri A, Van Hoof S, Lin TI, Vijgen L, Berke JM, Lachau-Durand S, Stoops B, Leclercq L, Fanning G, Samuelsson B, Nilsson M, Rosenquist Å, Simmen K, Raboisson P (2014) Nucleotide prodrugs of 2'-deoxy-2'-spirooxetane ribonucleosides as novel inhibitors of the HCV NS5B polymerase. *J Med Chem* 57(5):1836–1844
42. Jonckers TH, Tahri A, Vijgen L, Berke JM, Lachau-Durand S, Stoops B, Snoeys J, Leclercq L, Tambuyser L, Lin TI, Simmen K, Raboisson P (2016) Discovery of 1-((2R,4aR,6R,7R,7aR)-2isopropoxy-2-oxidodihydro-4H,6H-spiro[furo[3,2-d][1,3,2]dioxaphosphinine-7,2'-oxetan]-6-yl)pyrimidine-2,4(1H,3H)-dione (JNJ-54257099), a 3'-5'-cyclic phosphate ester prodrug of 2'-deoxy-2'-spirooxetane uridine triphosphate useful for HCV inhibition. *J Med Chem* 59 (12):5790–5798
43. Alexandre FR, Badaroux E, Bilello JP, Bot S2, Bouisset T, Brandt G, Cappelle S, Chapron C, Chaves D, Convard T, Counor C, Da Costa D, Dukhan D, Gay M, Gosselin G, Griffon JF, Gupta K, Hernandez-Santiago B, La Colla M, Lioure MP, Milhau J, Paporin JL, Peyronnet J, Parsy C, Pierra Rouvière C, Rahali H, Rahali R, Salanson A, Seifer M, Serra I, Standing D, Surleraux D, Dousson CB (2017) The discovery of IDX21437: design, synthesis and antiviral evaluation of 2'- α -chloro-2'- β -C-methyl branched uridine pronucleotides as potent liver-targeted HCV polymerase inhibitors. *Bioorg Med Chem Lett* 27(18):4323–4330
44. Zhou S, Mahmoud S, Liu P, Zhou L, Ehteshami M, Bassit L, Tao S, Domaol RA, Sari O, Schutter C, Amiralaei S, Khalil A, Ollinger Russell O, McBrayer T, Whitaker T, Abou-Taleb N, Amblard F, Coats SJ, Schinazi RF (2017) 2'-Chloro,2'-fluoro ribonucleotide prodrugs with potent pan-genotypic activity against hepatitis C virus replication in culture. *J Med Chem* 60 (13):5424–5437

The Discovery of Sofosbuvir: A Liver-Targeted Nucleotide Prodrug for the Treatment and Cure of HCV



Michael J. Sofia and Phillip A. Furman

Contents

1	Introduction	142
2	Discovery of a 2'-F-2'-C-Methyl Nucleoside PSI-6130	143
3	Development of a Prodrug of the Nucleoside PSI-6130	150
4	The Discovery of Sofosbuvir	151
5	Structural Understanding of the Binding of Sofosbuvir to the HCV NS5B RdRp	161
6	Sofosbuvir Clinical Development	162
	References	165

Abstract Over the last 15 years, an increase in knowledge of the structure, function, life cycle, and pathogenesis of hepatitis C virus (HCV) led to a focused effort on the discovery and development of interferon (IFN)-free therapies that are well tolerated and have increased cure rates. This chapter describes the discovery and development of sofosbuvir, the first live-targeting prodrug of a nucleotide analog, and contains a detailed overview of the synthesis, activity, mechanism of action, toxicity, and clinical studies of sofosbuvir (PSI-7977). The identification of the cytidine nucleoside analog PSI-6130, which was shown to be a potent and nontoxic inhibitor of HCV replication, is described. A summary of the mechanism of action of PSI-6130 is presented that describes the metabolic pathway to its corresponding 5'-triphosphate and to the uridine metabolite (PSI-6206) and the uridine mono-, di-, and triphosphate. Both PSI-6130 triphosphate and PSI-6206 triphosphate were shown to be potent alternative substrate inhibitors of the HCV NS5B polymerase. Because the triphosphate of PSI-6206 was a potent inhibitor of the NS5B polymerase and because it had a long intracellular half-life, the goal was to find an

M. J. Sofia (✉)
Arbutus Biopharma, Inc., Warminster, PA, USA
e-mail: msofia@arbutusbio.com

P. A. Furman
Saint Augustine, FL, USA

approach that could be used to deliver PSI-6206 monophosphate to the liver. The thought process and approach that led to the design and synthesis of various phosphoramidate prodrugs of the uridine monophosphate metabolite is presented. Of the compounds synthesized, PSI-7851 possessed the desired characteristics. PSI-7851 was a mixture of two diastereoisomers, PSI-7976 and PSI-7977. The two isomers were separated, and PSI-7977 (sofosbuvir) which showed tenfold greater activity was moved forward into clinical development. On December 6, 2013, sofosbuvir (Sovaldi[®]) was approved by the US FDA for the treatment of HCV genotype (GT) 1, 2, 3, and 4 patient populations with the combination of sofosbuvir + RBV being approved for GT 2 and 3 patient populations as the first IFN-free cure for patients infected with HCV.

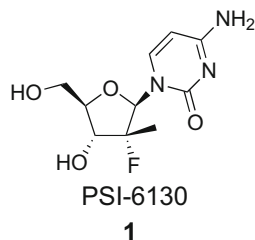
Keywords 2'-F-2'-C-methyl cytidine, 2'-F-2'-C-methyl nucleoside, 2'-F-2'-C-methyl uridine, Diphosphate, Eplclusa[®], Harvoni[®], HCV, Hepatitis C virus, Liver, Liver targeting, Mericitabine, Monophosphate, NS5B polymerase, Nucleoside, Nucleotide, Phosphoramidate, Prodrug, PSI-6130, PSI-6206, PSI-7851, PSI-7977, RdRp, Resistance, RG7128, RNA-dependent RNA polymerase, S282T, Sofosbuvir, Sovaldi[®], Triphosphate, Vosevi[®]

1 Introduction

On December 6, 2013, sofosbuvir (Sovaldi[®]) plus ribavirin became the first interferon (IFN)-free treatment and cure for patients chronically infected with the hepatitis C virus (HCV) of genotypes (GT) 1, 2, 3, and 4. This event marked a key milestone and transformational event in the history of HCV therapy. For the first time, patients could now take an oral pill once a day and within as little as 12 weeks be completely cured of HCV. Because it exhibited a high barrier to resistance and a pan-genotypic profile, sofosbuvir soon became the backbone of a number of important HCV curative therapies including the fixed-dose combination drugs Harvoni[®], Eplclusa[®], and Vosevi[®]. It was also used in combination with other approved oral direct-acting antiviral (DAA) therapies to achieve high cure rates and ward off resistance. To this date, sofosbuvir is the only approved nucleos(t)ide to treat HCV, even though in the last 13 years, over 15 different nucleos(t)ide drug candidates entered clinical development. This chapter will present the history of sofosbuvir's discovery and development and how this drug transformed the treatment of HCV.

The NS5B RNA-dependent RNA polymerase (RdRp) is one of the seven nonstructural proteins of the HCV genome. It is essential for replication of HCV, and its strong sequence homology across all six viral genotypes and a highly conserved active site made it an ideal target for the development of an HCV therapeutic [1]. In an attempt to discover small molecule DAA agents that would target the NS5B RdRp, several approaches were taken including small molecule allosteric modulators and active site-directed alternative substrate nucleoside

Fig. 1 Structure of the 2'- α -F-2'- β -C-methylcytidine nucleoside PSI-6130 (**1**)



analogs [2]. Although intrinsically potent, small molecule allosteric modulators generally suffered from having a low barrier to resistance and limited viral genotype coverage. However, the discovery of nucleoside analog NS5B inhibitors and particularly the discovery of the 2'-F-2'-C-methyl cytidine nucleoside analog PSI-6130 **1** (Fig. 1) would provide the first evidence that a nucleoside had the potential to deliver an agent that would demonstrate a high barrier to resistance, be equipotent against a broad array of viral genotypes, and also lack the safety concerns typically associated with nucleoside drugs [3].

The challenge associated with developing a nucleoside-based therapeutic begins with how to find the active agent. This is because a nucleoside must be phosphorylated at its 5'-hydroxyl group to generate the nucleoside 5'-triphosphate. It is the 5'-triphosphate that is then the substrate for, in the case of HCV, the viral NS5B polymerase ultimately resulting in the inhibition of the enzyme and cessation of viral replication. This multistep enzymatic phosphorylation process to generate the active form and subsequent requirement that the newly formed triphosphate be recognized as a substrate by the polymerase complicates the ability to identify and achieve an optimized nucleoside inhibitor. For nucleosides, standard medicinal chemistry structure activity studies become complex and difficult to interpret. This complexity arises from the fact that a nucleoside analog could fail as a substrate in any one of the four enzymatic steps required to achieve inhibition of viral replication in a cell-based system.

2 Discovery of a 2'-F-2'-C-Methyl Nucleoside PSI-6130

Even with the many challenges in finding a nucleoside inhibitor of HCV, the molecule PSI-6130 **1** was identified as an active and selective inhibitor of HCV replication in the HCV replicon assay [3, 4]. This molecule was identified by a careful exploration of structural modifications at the 2'-position of the nucleoside. Identification of the 2'- α -F and 2'- β -C-methyl combination found in PSI-6130 on the sugar portion of a nucleoside would have been completely unexpected when considering the known literature at the time. It was known that a 2'- β -methyl-2'-deoxycytidine nucleoside derivative was highly cytotoxic and that a 2'- α -F-2'-deoxycytidine nucleoside was also not particularly active and certainly not selective as an inhibitor of

HCV [2, 5]. Furthermore, the 2'-diF nucleoside, gemcitabine, was also known to be highly cytotoxic. Therefore, it was surprising that the cytidine nucleoside PSI-6130 which combined a 2'- α -F group and a 2'- β -C-methyl group was shown to be a very selective inhibitor of HCV with no apparent cytotoxicity. This observation was in contrast to the 2'- α -hydroxyl-2'- β -C-methyl class of nucleosides that were being evaluated as inhibitors of HCV replication [6]. These nucleosides were not selective inhibitors of HCV replication, and their safety profiles were not as clean when compared to the 2'- α -F-2'- β -C-methyl nucleoside class.

One of the first tasks that needed to be accomplished was development of an efficient synthesis of 2'- α -F-2'- β -C-methyl nucleosides and specifically PSI-6130 **1**. The early medicinal chemistry synthesis converted cytidine to its arabinoside analog (2'- α -C-methyl-2'- β -hydroxyl substitution) in six steps followed by fluorination with (diethylamino)sulfur trifluoride (DAST) [3]. This led to inversion of stereochemistry at the 2'-position with simultaneous introduction of the 2'-F group giving the desired 2'- α -fluoro-2'- β -C-methyl substitution. However, the yield was low, and formation of a significant amount of elimination byproduct occurred that required a difficult chromatographic separation. This need led to the development of an efficient, scalable synthesis of PSI-6130 that proceeded via a chiral lactone intermediate **4** (Fig. 2) which was then coupled with a protected cytosine base to ultimately give PSI-6130 [7]. The lactone **4** was prepared starting with the chiral reagent *D*-glyceraldehyde (Fig. 2). Addition of the remaining carbon chain using a Wittig

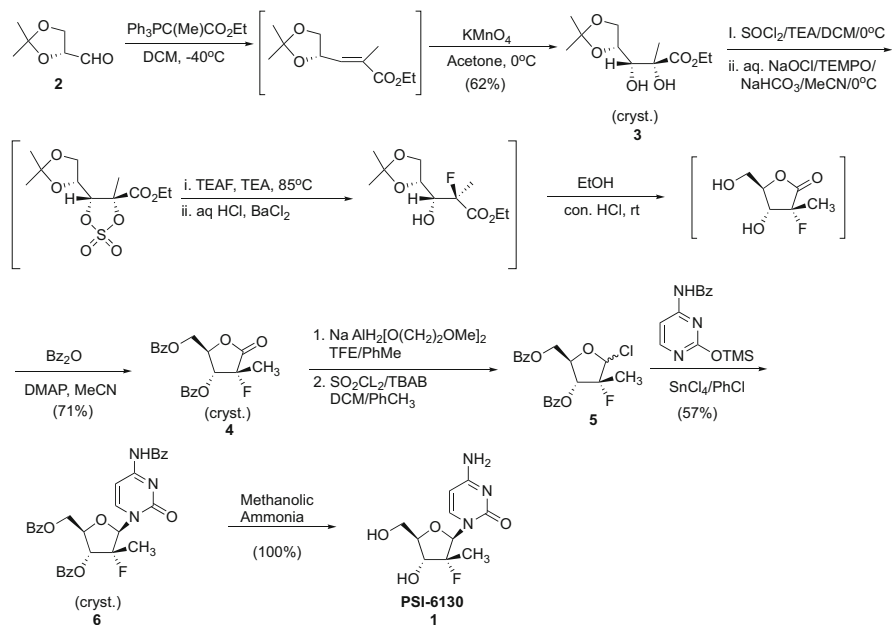


Fig. 2 Chemical synthesis scheme for the preparation of PSI-6130 (**1**), which proceeds via key intermediate lactone **4**

reaction was followed by introduction of the fluorine atom via stereoselective opening of a cyclic sulfate. Lactone **4** was subsequently useful in the preparation of multiple 2'- α -fluoro-2'- β -C-methyl nucleoside analogs.

Soon after the identification of PSI-6130, we undertook an extensive medicinal chemistry effort to see if the activity of this nucleoside analog could be improved. Using the key intermediate lactone **4**, developed in the chiral synthesis of PSI-6130, we were able to introduce numerous base analogs and also access modifications to the 3'- and 4'-positions of the ribose core. However, an exhaustive survey of nucleobase modifications and 3'- and 4'-substitutions on the ribose core of the nucleoside did not lead to identification of nucleosides that had improved potency over PSI-6130 (Fig. 3). This effort continued to support the unique characteristics of this class of nucleosides and at the time made us believe that PSI-6130 was a one-of-a-kind drug. Consequently, PSI-6130 was extensively characterized with the belief that it would progress into clinical studies.

Our early studies with PSI-6130 showed potent activity in the HCV subgenomic replicon assay with an EC₉₀ of $4.6 \pm 2.0 \mu\text{M}$ [4]. In addition, we showed that

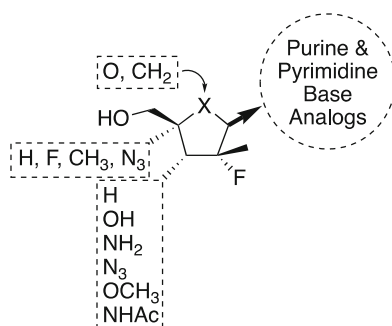


Fig. 3 Structure activity relationship study around the 2'- α -F-2'- β -C-methyl nucleoside class of molecules. Modifications at the 3' and 4' positions of the ribose sugar, construction of carbocyclic nucleoside analogs, and preparation of multiple purine and pyrimidine base analogs were investigated as inhibitors of HCV replication

Table 1 Activity of PSI-6130 **1** against HCV genotypes 1–4 (unpublished results)

HCV NS5B	GT	IC ₅₀ (μM) \pm SEM
Con1	1b	0.5 ± 0.04
RO 164	2b	0.2 ± 0.01
RO 166	3a	0.05 ± 0.1
RO 168	3a	0.6 ± 0.1
RO 169	3a	0.6 ± 0.07
RO 175	4a	0.5 ± 0.1
RO 176	4a	0.8 ± 0.2
RO 177	4a	0.5 ± 0.2
RO 181	4a	0.3 ± 0.1
RO 182	4a	0.5 ± 0.1

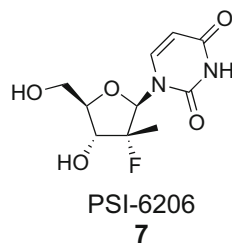
PSI-6130 gave an additive to synergistic response when tested in combination with other anti-HCV compounds of different classes. PSI-6130 showed consistent potency across HCV genotypes (Table 1), but when assayed against other members of the *Flavivirus* family, weak or no activity was observed [4]. We also tested PSI-6130 for activity against a replicon that contained the S282T amino acid change, which was an amino acid change known to confer resistance to several nucleoside analogs, and showed this amino acid change caused a 6.5-fold increase in EC₉₀ [4]. PSI-6130 showed no cytotoxicity at the highest concentration tested against a panel of various cell types, and a 6-day toxicity study performed in mice resulted in a no-effect dose of ≥ 100 mg/kg [4].

After identifying PSI-6130 as the candidate for development, detailed in vitro studies were performed to understand the metabolism of the compound and the mechanism by which it inhibited the replication of HCV [8–10]. Given that PSI-6130 was a nucleoside analog, it was likely that the compound was phosphorylated to the corresponding 5'-triphosphate by cellular enzymes that then inhibited the HCV NS5B. To determine if PSI-6130 was phosphorylated to the corresponding 5'-triphosphate (PSI-6130-TP), primary human hepatocytes were incubated with radiolabeled PSI-6130 and extracts prepared and analyzed by high-pressure liquid chromatography (HPLC) [9]. As anticipated, the 5'-monophosphate (PSI-6130-MP), 5'-diphosphate (PSI-6130-DP), and 5'-triphosphate (PSI-6130-TP) metabolites were identified in both cell types. Surprisingly however, the 5'-monophosphate, 5'-diphosphate, and 5'-triphosphate metabolites of the uridine analog PSI-6206 (7, Fig. 4) were also identified suggesting that PSI-6130 was a substrate for deamination, possibly by cytidine deaminase (CDA) (Fig. 5) [9, 10].

A time course of formation and the intracellular stability of PSI-6130-TP and PSI-6206 5'-triphosphate (PSI-6206-TP) was performed using primary human hepatocytes [9]. PSI-6130-TP was detected in primary human hepatocytes at 6 h after PSI-6130 incubation and reached steady-state levels at 24–48 h. The formation of the triphosphate of the uridine congener, PSI-6206-TP, was delayed relative to that of PSI-6130-TP. Steady-state levels of PSI-6206-TP were reached after 48–72 h of incubation. Prior to 16 h, the concentration of PSI-6206-TP was lower than that of PSI-6130-TP but was higher than the concentration of those of PSI-6130-TP after 24 h of incubation.

Following the removal of extracellular PSI-6130 from the primary human hepatocytes, the level of PSI-6130-TP remained constant up to 1 h after the removal.

Fig. 4 Structure of the 2'- α -F-2'- β -C-methyluridine nucleoside PSI-6206 (7) which is the inactive metabolite of the cytidine nucleoside PSI-6130 (1)



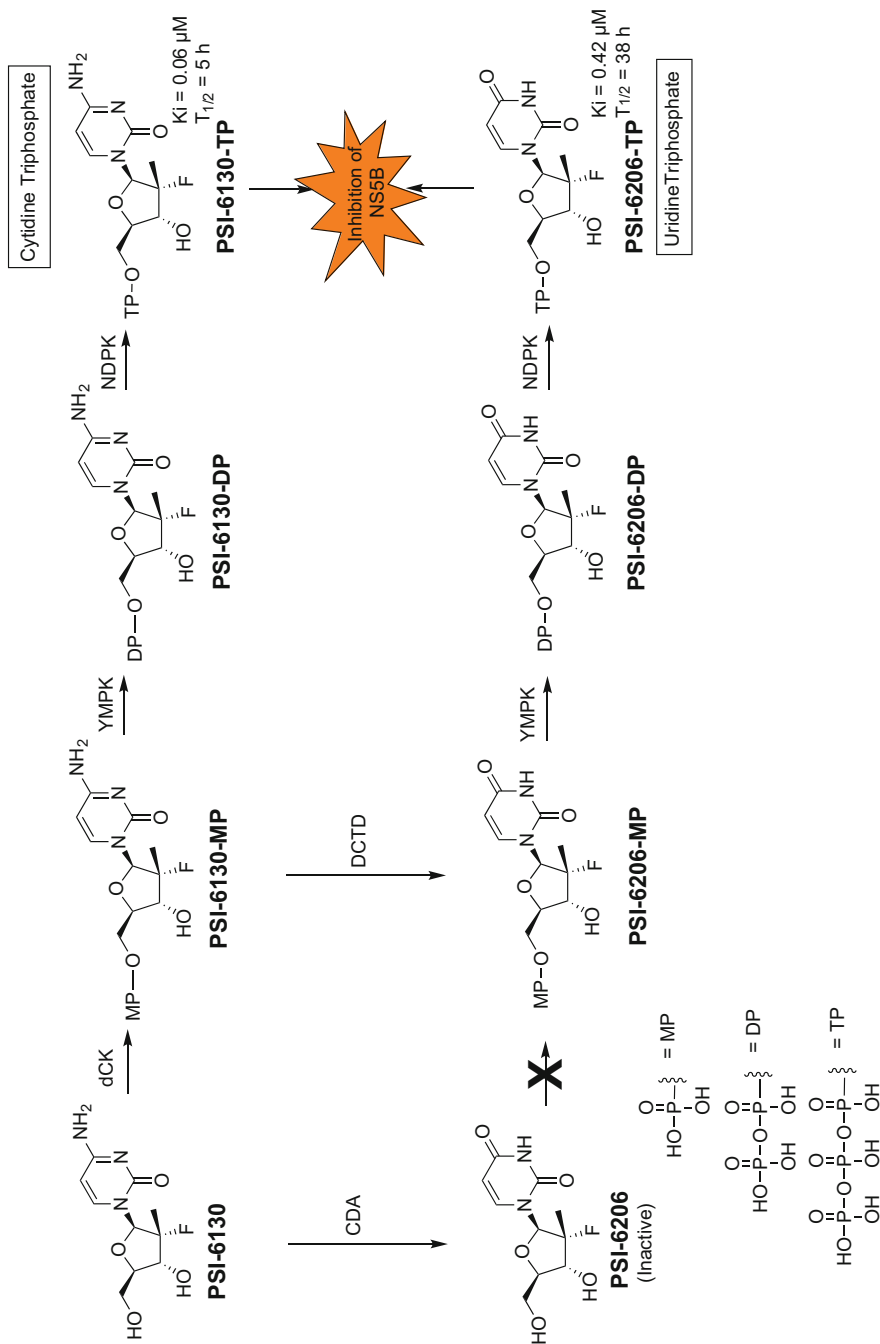


Fig. 5 Metabolic pathway of PSI-6130 (1) and PSI-6206 (7)

Thereafter, PSI-6130-TP levels decreased, and a mean half-life of 4.7 ± 0.6 h was determined. However, the level of PSI-6206-TP increased slightly and reached steady state by 1–2 h after the removal of extracellular PSI-6130. The level of PSI-6206-TP remained at steady state for up to 6 h before decreasing. A mean half-life of 38.1 ± 16.1 h was calculated for PSI-6206-TP. The unusually long half-life for PSI-6206-TP was intriguing and raised the question as to how much of a role it might play in the efficacy of PSI-6130 (Fig. 5).

To gain some insight into the mechanism of action of the compound, we assayed PSI-6130 in the replicon assay in the presence of exogenously added natural ribo- and deoxyribonucleosides [4]. Only 2'-deoxycytidine strongly inhibited the activity of PSI-6130 suggesting that deoxycytidine kinase (dCK) and not uridine-cytidine kinase was responsible for phosphorylating the compound to its corresponding 5'-monophosphate form. To better understand the activation pathway of PSI-6130, we identified the enzymes involved in the metabolism of PSI-6130 to the corresponding 5'-triphosphate (Fig. 5) [8]. As anticipated based on these results, human dCK was identified as the enzyme that catalyzed the phosphorylation of PSI-6130 to the corresponding 5'-monophosphate (PSI-6130-MP) ($k_{\text{cat}}/K_m = 1.9 \times 10^{-4} \mu\text{M}^{-1} \text{s}^{-1}$) and the subsequent phosphorylation to the 5'-diphosphate (PSI-6130-DP) was catalyzed by YMPK (UMP-CMP kinase) ($k_{\text{cat}}/K_m = 0.012 \mu\text{M}^{-1} \text{s}^{-1}$). Phosphorylation of PSI-6130-DP to the triphosphate derivative (PSI-6130-TP) was catalyzed by human nucleoside diphosphate kinase (NDPK) ($k_{\text{cat}}/K_m = 0.015 \mu\text{M}^{-1} \text{s}^{-1}$).

The enzymes involved in the second part of the metabolic pathway of PSI-6130 that led to the formation of PSI-6206-TP were also identified (Fig. 5) [10]. Indeed PSI-6130 was a weak substrate for human cytidine deaminase (CDA), which was of concern with regard to the in vivo stability of the compound given the ubiquitous nature of the enzyme. When we tested the uridine analog (PSI-6206 7 Fig. 4) in the Clone A replicon assay, we were surprised to find that the compound was inactive. This suggested to us that deamination occurred at some other point in the metabolic pathway of PSI-6130. Further studies with PSI-6206 demonstrated that the lack of activity was due to the inability of the compound to be phosphorylated to the monophosphate by any nucleoside kinase [10]. The deamination of PSI-6130 to the uridine metabolite added a distinct aspect to the understanding of how PSI-6130 might act as an inhibitor and raised questions regarding the pharmacokinetics and in vivo efficacy of the compound. Because PSI-6206 was inactive in the HCV replicon assay and the presence of the 5'-monophosphate of PSI-6206 (PSI-6206-MP) was identified in the in vitro metabolism studies, we surmised that the start of the metabolic pathway to PSI-6206-TP had to begin with the deamination of the PSI-6206-MP, presumably by deoxycytidylate deaminase (DCTD). Indeed, when steady-state kinetic studies were performed with PSI-6130-MP and purified human DCTD, PSI-6206-MP was found to be a weak substrate for the enzyme ($k_{\text{cat}}/K_m = 0.0004 \mu\text{M}^{-1} \text{s}^{-1}$) [10]. Phosphorylation of PSI-6206-MP to the corresponding 5'-diphosphate and subsequently to PSI-6206-TP was catalyzed by UMP-CMP kinase ($k_{\text{cat}}/K_m = 0.0091 \mu\text{M}^{-1} \text{s}^{-1}$) and NDPK ($k_{\text{cat}}/K_m = 0.046 \mu\text{M}^{-1} \text{s}^{-1}$), respectively [10].

To complete the mechanism of action studies, a steady-state kinetic assessment of the activity of PSI-6130-TP and PSI-6206-TP using purified recombinant HCV NS5B showed that both 5'-triphosphates functioned as alternative substrate inhibitors of the NS5B polymerase. In two separate studies, the inhibition constant (K_i value) for PSI-6206-TP was six- to sevenfold higher than the K_i for PSI-6130-TP [8–10]. Nevertheless both 5'-triphosphates were potent inhibitors of the NS5B. Furthermore, incorporation of both PSI-6130-TP and PSI-6206-TP into nascent RNA by NS5B led to chain termination indicating that both 5'-triphosphates functioned as non-obligate chain terminators.

Resistance development is a major concern in antiviral therapy, and resistance has developed to nearly all specific and effective antiviral agents. Therefore performing *in vitro* resistance studies can provide insight as to how rapidly clinical resistance might develop and what mutations might arise that could confer clinical resistance. Early resistance studies showed that the S282T amino acid change in NS5B was capable of conferring a 2.4- to 6-fold reduction in the activity of PSI-6130 in the HCV replicon assay [4]. Enzyme assays performed using recombinant NS5B containing the S282T amino acid change showed that this change resulted in a 7.5-fold reduction and a 23.7-fold reduction in the ability of PSI-6130-TP and PSI-6206-TP to inhibit the mutation-containing enzyme, respectively [10]. *In vitro* selection studies were performed with PSI-6130 using the HCV replicon system to study the emergence of replicons with reduced sensitivity and gain some insight as to what possible mutations might arise in the clinic [11]. Short-term treatment of replicon-containing cells with PSI-6130 cleared the replicon without the development of resistant variants. However, long-term exposure of the cells under selection conditions did generate the replicons that contained the S282T substitution as well as other amino acid substitutions in the NS5B polymerase. The presence of the co-selected substitutions did not result in an increase in the three- to sixfold reduction in sensitivity to PSI-6130 facilitated by the S282T amino acid substitution. The presence of these co-mutations did, however, enhance the replication fitness of replicons containing the S282T amino acid change compared to the replication fitness seen with the S282T substitution alone.

After completing the preclinical testing required by the FDA and demonstrating an excellent safety profile in the preclinical toxicology evaluation of PSI-6130, an investigational new drug application (IND) was submitted to the FDA to begin Phase I clinical trials in human volunteers. A single ascending dose study was performed at orally given doses of 500, 1,500, and 3,000 mg twice daily to assess safety and the pharmacokinetic profile of the compound [5]. Although PSI-6130 was well tolerated at all doses, significant metabolism to the inactive uridine metabolite, PSI-6206, occurred [5]. Furthermore, PSI-6130 was shown to have an oral bioavailability of only about 25%. These results called into question the further development of PSI-6130.

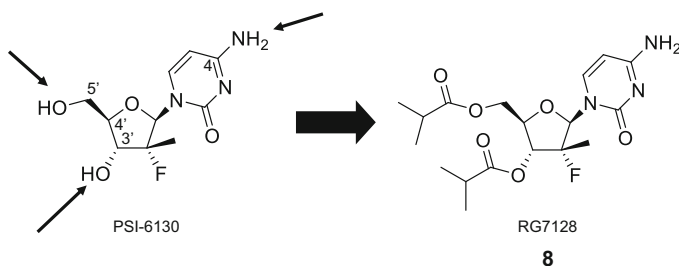


Fig. 6 Strategy for developing a prodrug of PSI-6130 that led to the 3',5'-diisobutyrate ester prodrug clinical candidate RG7128 (**8**)

3 Development of a Prodrug of the Nucleoside PSI-6130

In an attempt to circumvent the issues associated with PSI-6130, a strategy to develop a prodrug of PSI-6130 was put into place. It was hoped that a prodrug of PSI-6130 would improve the bioavailability of PSI-6130 and would help circumvent the deamination of the compound that produced the inactive uridine metabolite, PSI-6206. It was rationalized that more rapid absorption would improve plasma levels of drug and reduce the residence time in the gut, where it was believed some of the uridine metabolite was being produced. Prodrugs of the nucleoside 3'- and 5'-hydroxyl groups as well as of the C-4 amino group of the base moiety were investigated (Fig. 6). The prodrug variations included 3'- and/or 5'-esters, carbamates, and carbonates, and prodrugs of the C-4 amino group included carbamates, ureas, amides, and imines. Of all these variations, the most promising was the 3',5'-diisobutyrate ester prodrug RG7128 given the generic name mericitabine **8** (Fig. 6) [5].

Mericitabine was taken into clinical studies in HCV GT 1-infected patients and was shown to be effective at reducing serum HCV RNA levels [5]. After 14 days of monotherapy at 1,500 mg twice daily in GT 1 naïve patients, mericitabine produced a $-2.7 \log_{10}$ (IU/mL) decline in HCV RNA. Subsequently, mericitabine in combination with PEGylated interferon (PEG-IFN)/ribavirin (RBV) administered for 28 days in GT 1, 2, and 3 patients produced rapid virological response (RVR) rates of 85–90% with no adverse events or viral breakthroughs [5, 12, 13]. This was the first demonstration of pan-genotypic activity in the clinic with a direct-acting antiviral agent. Further evaluation of mericitabine, in combination with the protease inhibitor danoprevir, showed that two direct-acting antivirals when combined alone could produce significant and rapid declines in viral load (-4.9 to $-5.1 \log_{10}$ IU/mL) on par with combinations containing PEG-IFN/RBV [14].

4 The Discovery of Sofosbuvir

Even though early clinical data appeared to show that mericitabine had promise as an HCV therapeutic, we realized that this candidate carried with it a number of deficiencies that would limit its competitiveness as a clinical agent. Although implementation of a prodrug strategy did improve overall oral bioavailability, it did not solve the problem of the inactive uridine metabolite (PSI-6206) formation. In addition, the modest intrinsic activity of the parent cytidine nucleoside (PSI-6130) and the relatively short hepatic half-life of its triphosphate contributed to the need for administering a large amount of drug several times a day. It was our desire to fix these deficiencies in a next generation agent, but the question was how. We had already shown that PSI-6130 was a unique molecule and that any structural modifications we made to it did not produce a better compound. Consequently, we decided to pursue a radical redesign of our approach and began to revisit the metabolism of PSI-6130 for any possible clues on what direction we could take.

As noted earlier, a detailed assessment was done looking at the metabolism of PSI-6130 (Fig. 5). What we learned was that PSI-6130 did get extensively metabolized to the inactive uridine metabolite, and we also learned that the monophosphate, PSI-6130-MP, of the cytidine derivative, PSI-6130, was metabolized to the uridine monophosphate which went on to be further phosphorylated to give the uridine triphosphate. Interestingly, the uridine triphosphate (PSI-6206-TP) was shown in a biochemical assay to be a potent inhibitor of the HCV NS5B polymerase, and it appeared that the uridine nucleoside's inactivity was related to the fact that it was not a substrate for the first phosphorylation step and could never be converted to the triphosphate. Another important observation was that the uridine triphosphate, PSI-6206-TP, had a long half-life in hepatocytes relative to the cytidine derivative triphosphate, PSI-6130-TP. The activity of the uridine triphosphate (PSI-6206-TP) and its long half-life in hepatocytes pointed to a possible solution to developing an agent that could be dosed once daily. If one could somehow produce significant amounts of the uridine triphosphate in the liver, the possibility existed that we could achieve improved potency because of increased intracellular drug concentration, but phosphorylation was blocked at the monophosphorylation step. In addition, direct delivery of a nucleoside mono-, di-, or triphosphate was not at all practical because mono-, di-, and triphosphorylated nucleosides are extremely polar and would never penetrate biological membranes and they lack chemical and enzymatic stability. One approach to solve this problem was to try and deliver the uridine monophosphate (PSI-6206-MP, Fig. 5) by preparing a prodrug of the 5'-monophosphate group. In doing so, we would have to devise a way to mask and stabilize the phosphate group such that it would survive transit through the gut, get efficiently absorbed, be stable in serum, and ultimately get to the liver intact. The challenge was further complicated by our desire to develop an approach that would allow liver targeting of the drug and, consequently, increase exposure at the target organ and limit drug exposure elsewhere in the body. This "Trojan Horse" strategy (Fig. 7) was the approach we decided to pursue.

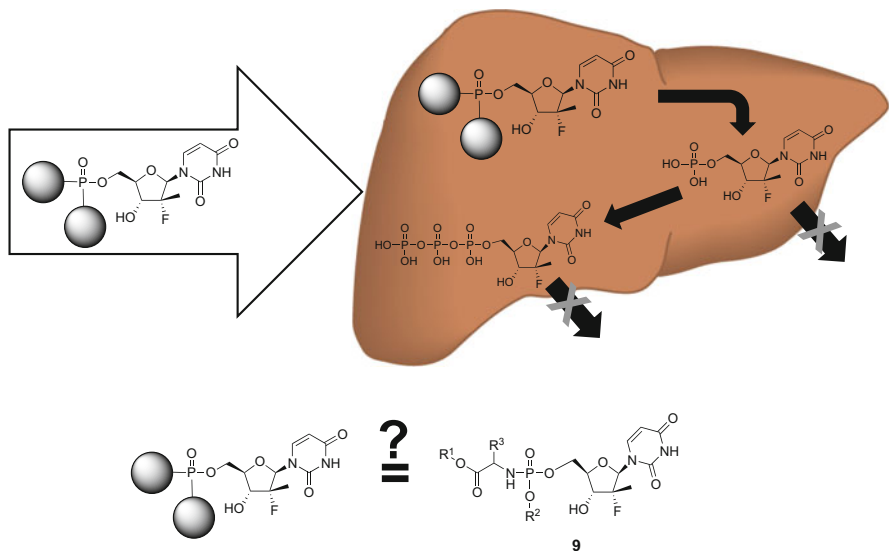


Fig. 7 The concept of using a phosphate prodrug of PSI-6206 5'-monophosphate to effect its delivery to the liver by applying the concept of liver first-pass metabolism. The phosphoramidate prodrug construct **9** to achieve liver first-pass metabolism

As we assessed the large literature on phosphate prodrugs, it was clear that the multiple objectives we hoped to achieve had little precedence [15]. There were a number of phosphate prodrugs reported in the literature over the last 15 years, but none had ever demonstrated utility in the clinic nor was liver targeting ever exemplified even in preclinical animal models. But as we contemplated a solution to these challenges, we settled on the concept of using liver first-pass metabolism as a principle to drive our choice of a prodrug construct. We concluded that if we could get an appropriately constructed prodrug of the uridine monophosphate intact into the liver, we might be able to take advantage of the liver's metabolizing capacity to deconstruct the prodrug mask and reveal the uridine monophosphate in hepatocytes (Fig. 7). But this would require that a complex sequence of events occur flawlessly. A sequence of events would include administration of a stable prodrug that would survive the gut and get absorbed intact through the gut into the portal vein where it would traffic to the liver, and once there the prodrug masking moieties would be completely metabolized off revealing the monophosphate of PSI-6206 trapped in hepatocytes. It would be at this point that the monophosphate could then be efficiently converted to its triphosphate HCV NS5B inhibitor (Fig. 7). To investigate this approach, we chose the phosphoramidate phosphate prodrug construct **9** (Fig. 7) [16]. We believed it possessed some features that might lend themselves to our liver-targeting strategy. We appreciated that the phosphoramidate moiety contained a terminal ester group that could be cleaved by esterases in the liver initiating a sequence of chemical and enzymatic events to release the desired uridine monophosphate, PSI-6206-MP (Fig. 5).

As we contemplated our prodrug design, another aspect warranted serious consideration. This had to do with the prodrug release products. With the delivery of the monophosphate into hepatocytes, pieces of the molecule that constituted the prodrug moiety would get released into the liver. We became concerned about the fate of these released molecular pieces. We realized that we needed to design a molecule that when the prodrug pieces would break away and release the monophosphate, these pieces would not complicate the safety profile of the drug by having other pharmacology or toxicity of their own. So, safety became a significant issue for us not only as it related to the administered drug itself but also as it related to all the metabolic byproducts that were formed.

To select the best molecule that would meet all of our requirements and ensure that we introduced a safe and effective agent into clinical development, we established a preclinical testing protocol that allowed us to assess as many of the key criteria as possible [16]. Consequently, the testing scheme incorporated assessments of intrinsic potency and initial cellular toxicity in the whole cell replicon assay, an extensive cytotoxicity assessment in a panel of cell lines, stability in simulated gastric and intestinal fluids, and plasma and liver S9 fraction stability. Those compounds that met the criteria of submicromolar potency in the replicon assay, lack of toxicity across multiple cell lines and prolonged stability in simulated gastric and intestinal fluid plus stability in plasma with a rapid conversion in the liver S9 fraction stability assay, would then be progressed into in vivo assessment. However, at the outset, we knew that in vivo assessment was not going to be

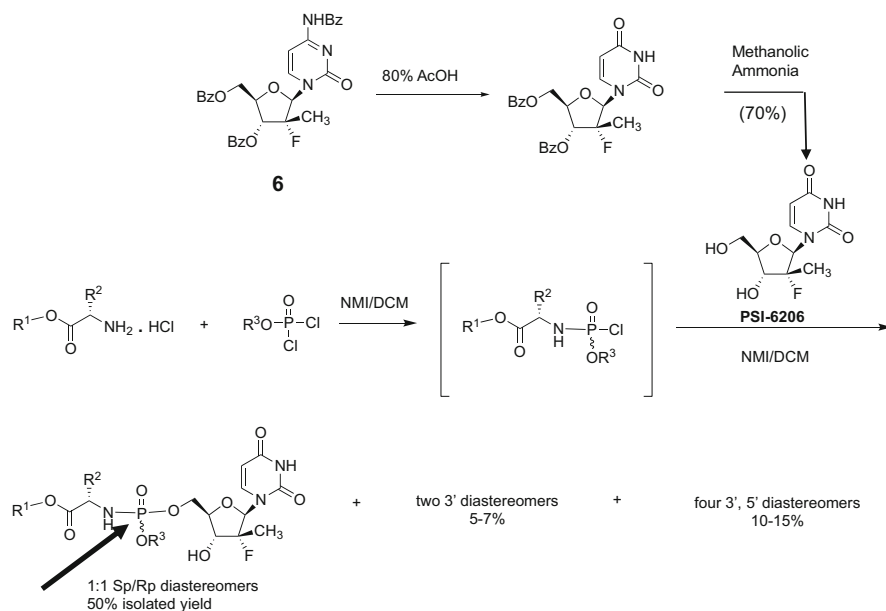


Fig. 8 The synthetic scheme to prepare phosphoramidate prodrugs of the uridine analog PSI-6206 5'-monophosphate

straightforward since the chimpanzee was the only animal model of HCV at the time and there were complications with using this system.

As we began to execute our structure activity efforts, we made a strategic decision regarding the medicinal chemistry approach. Literature reported that construction of a nucleoside phosphoramidate typically proceeds by coupling a nucleoside at the 5'-hydroxyl group with a preformed activated phosphoramidating reagent where the coupling would proceed by SN2 displacement of a leaving group on the phosphorus center of the phosphoramidating reagent (Fig. 8) [17, 18]. Because there were no methods at the time to prepare a diastereomerically pure phosphoramidating reagent, the resulting nucleotide phosphoramidate product was produced as a mixture of diastereomers at the phosphorus center. In addition, this was further complicated by the lack of convenient or reliable methods to separate the isomers and the inability to unequivocally determine the stereochemical configuration of each isomer. Consequently, we decided to proceed forward with evaluation and development of a molecule that was a mixture of diastereomers at the phosphorus center. However, we knew that this isomer issue would have to be addressed later after achieving the critical proof of concept for liver targeting and efficacy in a clinical setting.

Results of the initial phase of structure activity assessment demonstrated that small structural changes had significant effects on both intrinsic potency and cytotoxicity. What we determined from this phase of investigation was that there were preferred substituents on each of the variable sites of the phosphoramidate promoity (Fig. 9) [16]. We found that small alkyl esters (linear, branched, or cyclic) were

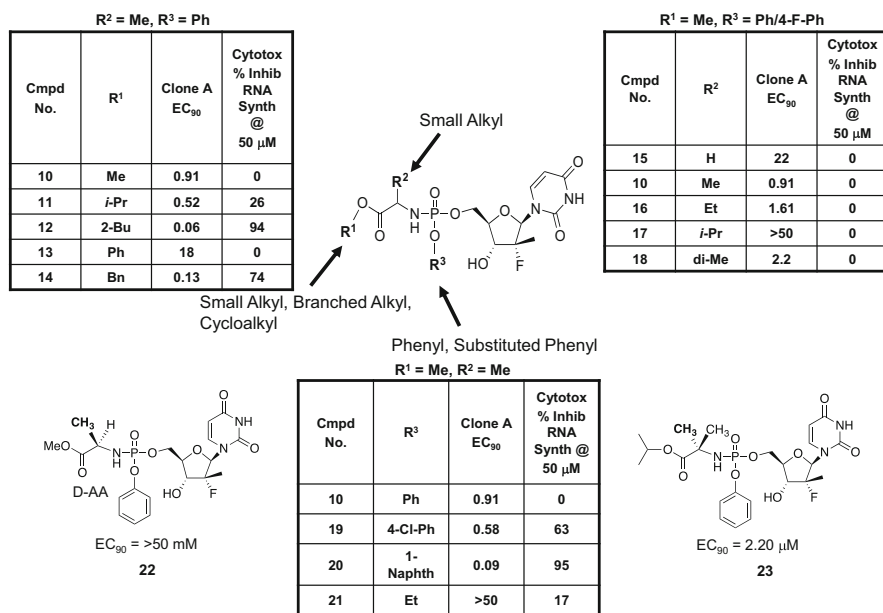


Fig. 9 Structure activity relationships around the phosphoramidate prodrug moiety of PSI-6206 5'-monophosphate

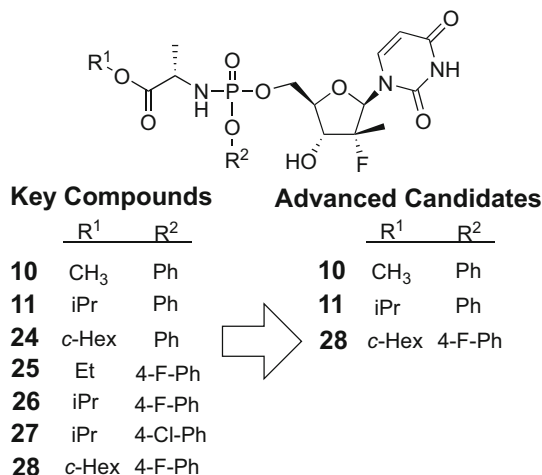



Fig. 10 Key compounds and advanced PSI-6206 monophosphate phosphoramidate prodrug candidates selected for further preclinical studies

preferred at the terminal ester of the amino acid. The *L*-configuration of the amino acid moiety was strongly preferred, and only small alkyl groups at the α -position on the amino acid unit were tolerated. It was further determined that aryl phosphoramidate phosphate esters were preferred over alkyl esters and that within these aryl esters, certain aryl groups such as naphthyl were not desired because of the toxicity they seemed to introduce into the prodrug (Fig. 9) [16]. Keeping with our objective to be fully aware of any safety concerns, we made a strategic decision to eliminate the use of any prodrug substituents that when released would have potential toxicologic issues. After evaluating over a hundred and forty compounds, seven candidates were selected and subsequently evaluated *in vitro* for cytotoxicity against a broad panel of cell lines as well as for their stability in simulated gastric fluid, simulated intestinal fluid, and liver S9 fraction [16]. This set of seven compounds (Fig. 10, Table 2) were selected to move into the *in vivo* phase of our testing scheme.

At the time, the chimpanzee was the only animal model of human HCV, but this model was impractical for our needs because of cost, accessibility, and its limited throughput for assessing multiple compounds in a rapid fashion. This left us with the decision to attempt to rethink how we were going to assess *in vivo* pharmacokinetics and efficacy. It was clear that measuring simple plasma levels of administered prodrug was not going to be adequate for determining drug exposure because if our hypothesis was correct, the liver-targeting nature of the strategy would result in trapping the drug in the liver and result in minimal plasma exposure. This led us to

Table 2 Activity, cytotoxicity, and stability assessment of seven key phosphoramidate prodrugs of PSI-6206 [16]


Cmpd No.	PSI No.	R ¹	R ²	HCV EC ₉₀	Cytotoxicity CC ₅₀ (μM)				Stability t _{1/2} (h)				
					Huh7	BxBC3	HepG2	CEM	SGF	SIF	Plasma	S9	
10	7672	Me	Ph	0.86	>100	>100	>100	>100	>100	15.5	>20	16.7	0.18
11	7851	<i>i</i> -Pr	Ph	0.31	>100	>100	>100	>100	>100	22	>24	>24	0.57
24	8028	<i>c</i> -Hex	Ph	0.13	>100	>100	>100	>100	>100	17	>20	>24	1.4
25	7950	Et	4-F-Ph	0.49	>100	>100	>100	>100	>100	17	>20	>8	0.23
26	7951	<i>i</i> -Pr	4-F-Ph	0.68	>100	>100	>100	>100	>100	>20	>20	>24	0.42
27	7994	<i>i</i> -Pr	4-Cl-Ph	0.46	>100	>100	>100	>100	>100	>20	>20	>24	0.35
28	8118	<i>c</i> -Hex	4-F-Ph	0.04	>100	>100	70	>100	>100	20	>20	>24	0.18

develop a surrogate animal model which was based on the idea that triphosphate levels in the liver were going to be directly correlated to the efficacy of the drug. Consequently, we set out to develop extensive bioanalytical methods that would allow us to measure the circulating levels of the prodrug and other key metabolites not only in the blood but also the level of key metabolites and especially the active triphosphate in the liver. With these methods in hand, we were then able to evaluate *in vivo* pharmacokinetics and liver triphosphate levels in rat, dog, and cynomolgus monkey after oral dosing [16].

The initial *in vivo* rat studies led to the selection of three advanced candidates, PSI-7672 (**10**), PSI-7851 (**11**), and PSI-8118 (**28**), that produced high liver levels of the target triphosphate (Fig. 10) [16]. However, it was evident from these early *in vivo* studies that the overall pharmacokinetic profile of PSI-7851 (**11**) was significantly better than that of PSI-7672 (**10**) and PSI-8118 (**28**). In rats dosed with PSI-7851(**11**), the level of the active triphosphate generated in the liver was twofold higher than in rats dosed with PSI-7672 (**10**) and eightfold higher than in rats dosed with PSI-8118 (**28**) [16]. Similarly, *in vivo* studies in dogs and monkeys confirmed our *in vivo* rat studies and showed that PSI-7851 (**11**) provided the better *in vivo* profile. The three advanced leads were simultaneously studied in primary human, rat, dog, and monkey hepatocytes to determine which prodrug would generate the highest level of the active PSI-6206 5'-triphosphate. When incubated with primary human hepatocytes, PSI-7851 (**11**) produced the highest level of the active 5'-triphosphate compared to the PSI-7672 (**10**) and PSI-8118 (**28**) [16]. Cumulatively, these studies supported our liver-targeting hypothesis.

Since nucleoside drugs have been historically plagued by mechanism-based bone marrow and mitochondrial toxicity, each of the advanced leads was evaluated for these potential safety issues. The three compounds demonstrated no mitochondrial toxicity, and only compound PSI-8118 (**28**) demonstrated a slight effect against bone marrow progenitor cells [16]. Studies showed that PSI-6206-TP was not a substrate or inhibitor of human DNA polymerase α , β , and γ nor was it an inhibitor of human RNA polymerases II [19, 20]. The three compounds were then compared in an acute single oral dose non-GLP study in rats at doses of 50, 300, and 1,800 mg/kg followed by a 14-day post-dose observation period. A no adverse effect level (NOAEL) of >1,800 mg/kg was established [16]. Overall PSI-7851 (**11**) outperformed PSI-7672 (**10**) and PSI-8118 (**28**) in all *in vitro* and *in vivo* evaluations. After considering all of the compiled data, prodrug PSI-7851 (**11**), which was still a mixture of diastereomers, was nominated as a clinical development candidate.

We embarked upon an extensive *in vitro* study of the metabolism of PSI-7851 that included identification of the enzymes involved in the metabolism of the prodrug portion of PSI-7851. This study provided us with a complete picture of how PSI-7851 was converted to the active triphosphate (Fig. 11) [21]. Clone A cells and primary human hepatocytes were incubated with radiolabeled PSI-7851; cell extracts were prepared and analyzed by HPLC analysis to identify and quantitate each of the metabolites. In both cell types, high levels of the amino acid intermediate PSI-352707 (**29**, Fig. 11), an alaninyl phosphate intermediate, formed rapidly. The appearance of PSI-352707 (**29**) was followed by appearance of the parent

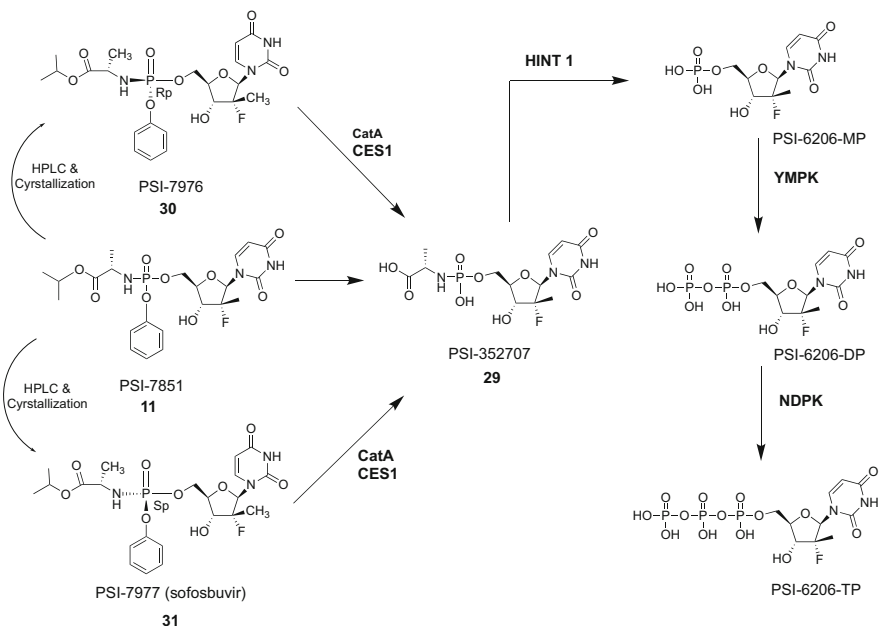


Fig. 11 Metabolic pathway of PSI-7851 (**11**) and its isolated diastereoisomers PSI-7976 (**30**) and PSI-7977 (**31**) (sofosbuvir)

5'-monophosphate and then the corresponding 5'-diphosphate and finally high levels of the active 5'-triphosphate. The level of PSI-6206-TP reached a concentration of about 100 μM in primary human hepatocytes incubated with 5 μM [^3H]-PSI-7851. After reaching steady-state levels, the intracellular concentration of PSI-6206-TP decreased slowly. The overall rate-limiting step in the metabolism of PSI-7851 to the active triphosphate appeared to be the conversion of PSI-352707 (**29**) to the parent compound PSI-6206-MP (Fig. 11).

To identify the enzyme(s) responsible for the hydrolysis of the carboxyl ester linkage, we assessed a number of human proteases, carboxylesterases, and lipases for their ability to catalyze the decarboxylation reaction [21]. Of the enzymes tested, two liver enzymes carboxylesterase 1 (CES1) and cathepsin A (CatA) were able to hydrolyze the carboxyl ester linkage of PSI-7851 (**11**) generating an alaninyl phosphate intermediate that was subsequently metabolized to the corresponding 5'-monophosphate (PSI-6206-MP) by human histidine triad nucleotide-binding protein1 (Hint1) (Fig. 11) [21]. As described above, the phosphorylation of PSI-6206-MP to the 5'-diphosphate was catalyzed by YMPK, and NDPK was responsible for phosphorylating the diphosphate to the active 5'-triphosphate PSI-6206-TP which was the inhibitor of HCV NS5B.

We performed further *in vitro* testing of PSI-7851 (**11**) against additional HCV genotypes and showed that the compound possessed pan-genotypic activity [19]. The compound also showed good anti-HCV activity in the infectious assay

[19]. PSI-7851 (**11**) demonstrated no activity *in vitro* against other viruses such as West Nile, yellow fever, influenza A, hepatitis B, and HIV-1. When tested against a genotype 1b replicon containing the S282T amino acid change in the NS5B polymerase, the presence of the S282T change caused a 14-fold decrease in sensitivity to PSI-7851 (**11**). *In vitro* resistance selection studies selected the S282T amino acid change and identified it as the primary amino acid change responsible for conferring resistance to PSI-7851 [16, 19].

PSI-7851 (**11**) entered preclinical development and successfully progressed through IND enabling safety assessment with no issues [5]. In Phase I clinical trials to assess safety and pharmacokinetics, PSI-7851 (**11**) was dose escalated to 800 mg once daily with no observed safety issues. The observed PK profile indicated that the drug was rapidly absorbed and taken up by the liver with little systemic blood levels of PSI-7851 (**11**) or the uridine 5'-monophosphate (PSI-6206-MP) [22]. All of these observations indicated that the drug was performing as hoped.

Subsequently, HCV GT 1 patients were treated with PSI-7851 (**11**) at doses of 50–400 mg once daily orally for 3 days. In these patients, it was observed that HCV RNA declined in a dose-dependent manner with mean changes from baseline of -0.49 to $-1.95 \log_{10}$ IU/mL [22]. The drug was well tolerated with no detectable preexisting or treatment-emergent mutations. These results provided proof of concept for the liver-targeted prodrug strategy and the first example of a phosphate prodrug showing clinical efficacy. The stage was now set for further development of this agent.

With clinical proof of concept achieved for PSI-7851 (**11**), it became more critical that we develop a method to access each of the diastereomers that comprised the mixture PSI-7851 (**11**) and determine which of the two isomers should move forward in development. It was our opinion that development of a single isomeric drug was preferable from a regulatory and manufacturing perspective. Through careful HPLC separation, we were able to obtain samples of the two isomers PSI-7976 (**30**) and PSI-7977 (**31**) (Fig. 11) and determine that one of the isomers, PSI-7977 (**31**), was tenfold more active than the other in the whole cell replicon assay [16, 21]. We later developed a crystallization method for PSI-7977 (**31**), and the first X-ray crystallographic structure of the molecule confirmed the absolute stereochemistry at the phosphorus center as Sp [16]. Selective crystallization of PSI-7977 (**31**) from the mixture provided pure material to move forward with clinical development of this single isomer. Ultimately, we were able to develop a

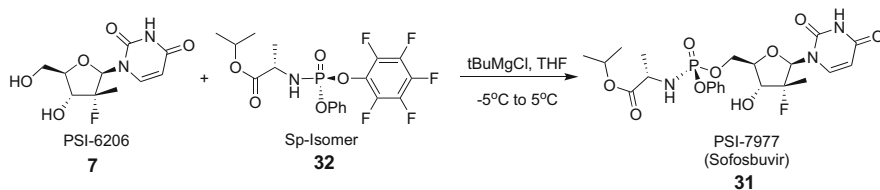


Fig. 12 Scheme showing the synthetic method used to prepare diastereomerically pure sofosbuvir from the uridine nucleoside PSI-6206 using a novel chiral phosphoramidating reagent **32**

commercially viable diastereoselective synthesis of PSI-7977 (**31**) that eliminated the need to discard 50% of the product as a result of selective crystallization from a 1:1 mixture of PSI-7977 (**31**) and PSI-7976 (**30**) (Fig. 12) [23]. The diastereoselective synthesis was achieved by developing a unique stable chiral phosphoramidating reagent (**32**) that when coupled with homochiral PSI-6206 (**7**) generated PSI-7977 (**31**) in high yield and >99.7% isomeric purity after direct crystallization from a crude reaction mixture (Fig. 12) [23]. This diastereoselective synthesis now allowed the development program for PSI-7977 to proceed unhindered. PSI-7977 (**31**) became known as sofosbuvir (SOF).

When we evaluated the two purified isomers in the Clone A replicon assay, sofosbuvir showed significantly greater activity with an $EC_{90} = 0.092 \mu\text{M}$ than did PSI-7976 (**30**) ($EC_{90} = 1.1 \mu\text{M}$) [16, 21]. Sofosbuvir also showed good activity in the infectious virus assay [24]. Of importance sofosbuvir demonstrated pan-genotypic activity across HCV GT1–6 [24]. We believed that being able to combine sofosbuvir with other direct-acting antiviral agents was an important consideration. Therefore, combination studies with PEG-IFN and a wide variety of HCV DAA agents including NS5A inhibitors, NS3/4 protease inhibitors, non-nucleoside NS5B inhibitors, and other nucleos(t)ide inhibitors were performed [25]. These studies demonstrated that additive or synergistic effects could be achieved when IFN or other direct-acting antivirals were combined with sofosbuvir.

The metabolic pathway for PSI-7976 (**30**) and sofosbuvir was investigated in an attempt to understand why sofosbuvir was the more active isomer in the Clone A replicon assay [21]. Because both isomers form the non-isomeric intermediate, PSI-352707 (**29**) (Fig. 11), we believed that the difference in activity in some way involved differences in the enzymes responsible for the metabolism of PSI-7976 (**30**) and sofosbuvir to PSI-352707 (**29**). The reason for difference in activity between PSI-7976 (**30**) and sofosbuvir in the Clone A replicon assay was found to be twofold: First, cathepsin A (CatA) preferred sofosbuvir as a substrate, and carboxylesterase 1 (CES1) preferred PSI-7976 (**30**); second, Western blot analysis showed that CatA was readily expressed in Clone A cell, whereas CES1 expression could not be detected. This difference was further demonstrated when intracellular metabolism studies were performed using Clone A cells. The intracellular concentration of PSI-6206-TP was significantly higher in cells incubated with sofosbuvir than in cells incubated with PSI-7976 (**30**). Western blot studies using primary human hepatocytes showed that both CatA and CES1 are expressed in the human liver cells and that high levels of the active triphosphate are formed [21].

Sofosbuvir presented an unusually clean safety profile for a nucleotide analog. No cytotoxicity, mitochondrial toxicity, or bone marrow toxicity was seen with sofosbuvir when dosed at high concentrations [16]. The 5'-triphosphate of sofosbuvir, PSI-6206-TP, was shown not to be an inhibitor of human DNA and RNA polymerases [19, 20]. Preclinical drug-drug interaction assessment showed that sofosbuvir and its major metabolite, the uridine nucleoside, were not substrates or inducers of CYP450 enzymes, but sofosbuvir was observed to be a substrate for P-glycoprotein and breast cancer-resistant protein (BCRP). Animal toxicology studies and preclinical animal pharmacology studies showed no significant drug-related

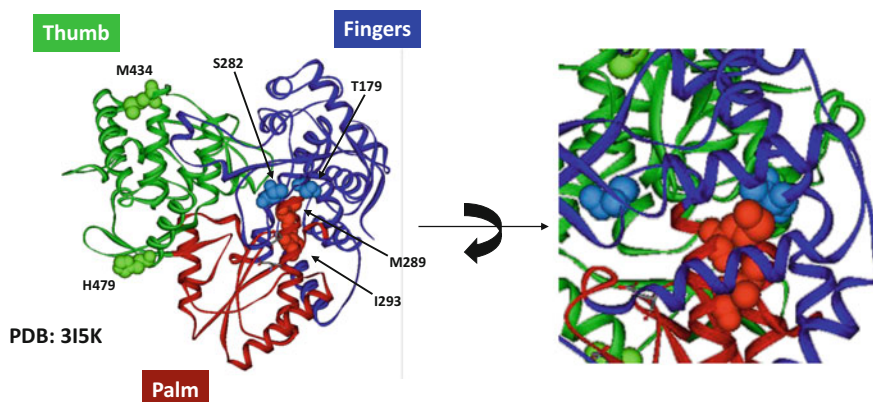


Fig. 13 Location of amino acid changes selected by sofosbuvir using JFH-1 NS5B structure (protein data bank accession number 315 K)

findings. In addition, *in vitro* or *in vivo* tests showed that sofosbuvir was not genotoxic nor did the compound affect embryo-fetal viability or fertility in rats [26].

We evaluated sofosbuvir for its ability to select for resistance using GT 1a, 1b, and 2a (JFH-1) replicon cells (Fig. 13) [19, 24]. The common mutation that was selected for all three genotypes was the S282T amino acid change. While the S282T change resulted in resistance to sofosbuvir in GT 1a and 1b, the S282T change in the JFH-1 GT 2a replicon caused only a slight shift in the EC_{50} value for sofosbuvir. Sequence analysis of the JFH-1 NS5B region revealed that additional amino acid changes, T179A, M289L, I293L, M434T, and H479P, were selected before and after the appearance of the S282T amino acid change. Residues 179, 289, and 293 are found within the finger and palm domains, whereas residues 434 and 479 are found on the surface of the thumb domain. These amino acid changes in the finger and palm domains along with S282T were needed to confer resistance to sofosbuvir. Other mutations that lay in the thumb domain enhanced the replication capacity of the S282T replicons. JFH-1 GT 2a replicons possessing changes M434T or H479P appeared to compensate for the reduce replication fitness caused by S282T.

5 Structural Understanding of the Binding of Sofosbuvir to the HCV NS5B RdRp

To gain an understanding of the recognition event between sofosbuvir and the HCV NS5B RdRp at the molecular level, efforts were undertaken to obtain X-ray crystallographic data of the ternary complex that would comprise the HCV NS5B RdRp, the RNA primer-template strand, and sofosbuvir. To accomplish this, the NS5B from the JFH-1 genotype 2 was used that contained the three mutations at S15G, C223H, and V321I along with the nucleotide diphosphate of sofosbuvir

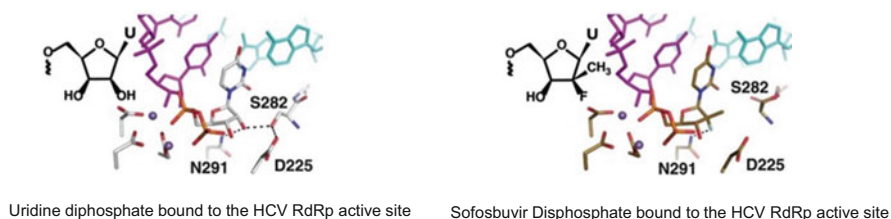


Fig. 14 Ternary co-crystal structures of the HCV NS5B RdRp triple mutant construct with uridine diphosphate and sofosbuvir diphosphate

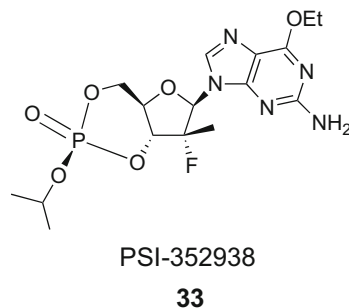
[27, 28]. This construct led to the formation of a stalled ternary complex. These crystallographic studies revealed that the hydrogen bonding network is disrupted when sofosbuvir diphosphate binds resulting in D225 being oriented away from the incoming nucleotide (Fig. 14) [28]. This is in distinct contrast to what is observed for the natural uridine diphosphate and for the 2'-hydroxyl-2'-C-methyl nucleoside class of NS5B inhibitors where a clear H-bond is formed between the 2'-OH and D225 [28]. In addition, presence of the 2'-methyl substituent in sofosbuvir results in additional H-bond disruption involving S282 (Fig. 14) [28]. Even with these H-bond network disruptions, the recognition of the 2'-F by N291 and Watson-Crick base pairing allows sofosbuvir to achieve the necessary conformation that results in substrate-like recognition and ultimate incorporation into the growing RNA chain, thus promoting non-obligate chain termination and HCV NS5B inhibition. In addition, the crystal structure provides insight into the nonclinical resistance observed with the HCV NS5B S282T amino acid change (Fig. 14) [28]. A steric clash between the 2'-methyl group of sofosbuvir and the mutant 282T residue appears to be responsible for the observed resistant phenotype.

6 Sofosbuvir Clinical Development

The first clinical evaluation of sofosbuvir was performed in a Phase IIa study [29]. In this study patients infected with HCV genotype 1 were given sofosbuvir at doses of 100, 200, and 400 mg QD in combination with PEG-IFN-RBV for 24 days. A rapid virological response was seen in 88–94% of the patients along with a 5.1–5.3 log₁₀ decrease in viral load. No virologic breakthroughs, emergence of resistance, drug-related serious adverse events, or discontinuations occurred in the study.

Following the positive results of the study with PEG-IFN, a multiple-arm combination study was performed in infected patients with sofosbuvir alone and in combination with another direct-acting antiviral, the nucleotide prodrug PSI-352938 **33** (Fig. 15) [30, 31]. Unexpectedly, the efficacy of sofosbuvir monotherapy far exceeded that of the diastereomeric mixture PSI-7851 (**11**). A 400 mg qd oral dose of sofosbuvir over 3 days produced a rapid decrease in virologic load with a maximal viral load decline of approximately a 3.9 log₁₀ IU/mL.

Fig. 15 Structure of cyclic phosphate nucleotide prodrug PSI-352938 (**33**)



A small Phase II 50-patient five-arm clinical study (Electron study) was designed to evaluate sofosbuvir monotherapy, sofosbuvir in combination with ribavirin (RBV), and sofosbuvir in combination with PEG-IFN/RBV [32]. Patients with GT 2 or GT3 HCV were dosed with their respective regimens for 12 weeks. At 12 and 24 weeks post-dosing, the patients were evaluated for a sustained virologic response (SVR). Patients receiving sofosbuvir in combination with RBV or PEG-IFN/RBV achieved a 100% SVR 12 and 24. No virologic breakthroughs occurred, and the sofosbuvir-RBV combination was well tolerated.

As part of the clinical studies, the human pharmacokinetics of sofosbuvir was evaluated. Nucleotide analog levels in liver explants from HCV-infected patients undergoing liver transplants were measured after up to 24 weeks of sofosbuvir treatment in combination with RBV. The results reflected those seen in the preclinical PK studies in rats, dogs, and monkeys. The human pharmacokinetic (PK) studies showed that in the liver, sofosbuvir was rapidly converted to the corresponding 5'-monophosphate (PSI-6206-MP) and the active 5'-triphosphate (PSI-6206-TP). Little or no sofosbuvir was detected in the systemic circulation [33, 34]. These results coupled with the results obtained in the animal PK studies supported a liver-targeting mechanism for sofosbuvir. The PK profile of sofosbuvir was unaffected by food, and evaluation of the PK of sofosbuvir in cirrhotic patients showed that liver cirrhosis had no clinically relevant effect on sofosbuvir exposure [29]. Drug-drug interactions that can result in alterations of either drug pharmacokinetics (PK) or pharmacodynamics (PD) or both can cause significant clinical effects, either by reducing therapeutic efficacy or enhancing drug toxicity. Drug-drug interaction studies did not identify any combinations that would limit the use of sofosbuvir in different populations of patients including HIV-infected patients, transplant recipients, or recovering drug addicts [35–37].

The initial Phase III registration trials were designed to evaluate sofosbuvir in combination with RBV in a GT 2 and GT 3 HCV patient population and sofosbuvir in combination with PEG-IFN/RBV in patients infected with GT 1 or GT 4 HCV [38, 39]. In a broad GT 2 patient population, sofosbuvir (400 mg, QD) in combination with RBV led to high cure rates of 92% and 94% following 12 and 16 weeks of therapy, respectively. In GT 2 treatment-naïve patients or patients that previously received PEG-IFN treatment, a 93% SVR12 was achieved. Sofosbuvir (400 mg) + RBV for 12 weeks resulted in an overall SVR12 of 93% in patients

who were not able to take PEG-IFN or who were not willing to take PEG-IFN. Treatment-experienced patients who had either relapsed or were nonresponders achieved SVR12 rates of 86%. However, when therapy was expanded to 16 weeks, cure rates improved to 94%. Whether or not GT 2 patients were treatment naïve, cirrhotic, or treatment experienced did not affect cure rates.

Patients infected with GT3 proved to be a greater challenge for the IFN-free sofosbuvir + RBV regimen [38]. GT 3 patients who were intolerant to IFN, ineligible, or not willing to take IFN experienced only a 61% SVR12 after receiving 12 weeks of sofosbuvir + RBV. And only a 30% SVR12 was attained in the treatment-experienced population. Extending treatment an additional 4 weeks increased the cure rate to 62%. Extending treatment in the treatment-naïve or previously IFN-treated patient study to a 24-week course of therapy, the cure rate was increased to 84%. Overall, in the GT 3 patient population, there was a clear difference in SVR response rates depending on patient status. Experienced GT3 patients responded less well to treatment than did treatment-naïve patients; and treatment-experienced cirrhotic patients (SVR12 60%) responded less well to treatment than did non-cirrhotic patients (SVR12 85%).

In GT 1 and GT 4 patients, sofosbuvir + RBV was not able to provide adequate cure rates. However, in this patient population, the combination of sofosbuvir + PEG-IFN/RBV for 12 weeks did provide a SVR12 of 90% (GT 1 89%, GT 4 96%) [39]. Unlike PEG-IFN/RBV, neither the IL28B status of patients or the presence or absence of cirrhosis appeared to affect the patient SVR response rates in this study. In a small cohort of GT 5 and 6 patients administered sofosbuvir + RBV, the SVR12 was reported as 100% [39].

Sofosbuvir regimens also demonstrated high cure rates in hard to treat patient population such as African-Americans, HIV co-infected, and liver transplant patients. In a study consisting of GT1 patients, mostly African-American, in different stages of liver fibrosis and having a high CT/TT IL28B allele frequency, 24 weeks of sofosbuvir + RBV delivered SVR12 rates in the 90% range [40]. HIV/HCV co-infected patients who were HIV virologically suppressed responded well to sofosbuvir + RBV with SVR12 rates of 76% (GT1, 24 weeks), 88% (GT2, 12 weeks), and 92% (GT3, 24 weeks) [36]. Liver transplant patients that had severe relapses of their HCV infection who received sofosbuvir + RBV with or without PEG-IFN achieved an overall SVR12 of 56% and showed marked clinical improvement and improved liver function tests [36, 41].

Overall, the clinical efficacy of sofosbuvir in HCV-infected patients was not limited by race, gender, age, or whether a patient was non-cirrhotic, cirrhotic, treatment-experienced, or null responders. Sofosbuvir demonstrated clinical efficacy against a range of HCV genotypes including GT 1 and 4 patients treated with sofosbuvir in combination with Peg-IFN/RBV and GT 2 and 3 patients treated with sofosbuvir in combination with RBV. Emergence of clinical resistance has always been a concern when treating patients with an antiviral agent including nucleos(t)ide analogs. To date however, resistance to sofosbuvir has not been a concern. In the laboratory, the S282T amino acid change in the HCV RdRp was identified as the primary change that conferred a 2- to 18-fold reduction in sensitivity to sofosbuvir [19]. However, this substitution also reduced viral replication fitness

by 89–99% making the mutant virus very unfit for survival. In the clinic, the S282T change has not been identified as a preemergent variant [42]. Virus that encodes for this amino acid change was observed after relapse at 4 weeks in only one instance where sofosbuvir was administered as monotherapy but was no longer detected after 12 weeks on therapy [38].

On December 6, 2013, sofosbuvir (Sovaldi[®]) was approved by the US FDA for the treatment of HCV GT1, 2, 3, and 4 patient populations with the combination of sofosbuvir + RBV being approved for GT 2 and 3 patient populations as the first IFN-free cure for patients infected with HCV. In January 2014, sofosbuvir was approved by the European regulatory authorities for the treatment and cure of HCV. In real-world clinical settings, it has been demonstrated that sofosbuvir is as effective as was demonstrated in clinical trials [43]. Sofosbuvir has gone on to become the backbone of a number of IFN-free curative therapies including the fixed-dose combination agents Harvoni[®] [44–46], Epclusa[®] [47], and Vosevi[®] [48] that produce cure rates of >95% in all patient populations. In 2015 sofosbuvir was designated an essential medicine by the World Health Organization.

Acknowledgments The discovery and development of sofosbuvir would not have been possible if not for the dedicated staff at Pharmasset, Inc. Their commitment to finding a cure for HCV made sofosbuvir a reality. Thanks also goes to the clinical development team at Gilead Sciences, Inc. for among other things, completing the Phase III clinical studies and bringing sofosbuvir to the market so that the millions of HCV patients worldwide could realize a cure for their disease.

Compliance with Ethical Standards

Conflict of Interest Author Michael J. Sofia was an employee of Pharmasset, Inc. and Gilead Sciences Inc., and he is currently an employee and Chief Scientific Officer of Arbutus Biopharma, Inc. He is also a stockholder in Arbutus Biopharma, Inc.

Author Phillip A. Furman was an employee of Pharmasset, Inc.

Ethical Approval All applicable international, national, and/or institutional guidelines for the care and use of animals were followed in the studies reported in this chapter.

All procedures performed in the studies reported in this chapter involving human participants were in accordance with the ethical standards of the institutional and/or national research committee and with the 1964 Helsinki declaration and its later amendments or comparable ethical standards.

Informed Consent Informed consent was obtained from all individual participants included in the study.

References

1. Poch O, Sauvaget I, Delarue M, Tordo N (1989) Identification of four conserved motifs among the RNA-dependent polymerase encoding elements. *EMBO J* 8(12):3867–3874
2. Sofia MJ, Chang W, Furman PA, Mosley RT, Ross BS (2012) Nucleoside, nucleotide and non-nucleoside inhibitors of hepatitis C virus NS5B RNA-dependent RNA polymerase. *J Med Chem* 55:2481–2531

3. Clark JL, Hollecker L, Mason JC, Stuyver LJ, Tharnish PM, Lostia S, McBrayer TR, Schinazi RF, Watanabe KA, Otto MJ, Furman PA, Stec WJ, Patterson SE, Pankiewicz KW (2005) Design, synthesis, and antiviral activity of 2'-Deoxy-2'-fluoro-2'-C-methylcytidine, a potent inhibitor of hepatitis C virus replication. *J Med Chem* 48(17):5504–5508
4. Stuyver LJ, McBrayer TR, Tharnish PM, Clark J, Hollecker L, Lostia S, Nachman T, Grier J, Bennett MA, Xie M-Y, Schinazi RF, Morrey JD, Julander JL, Furman PA, Otto MJ (2006) Inhibition of hepatitis C replicon RNA synthesis by beta-D-2'-deoxy-2'-fluoro-2'-C-methylcytidine: a specific inhibitor of hepatitis C virus replication. *Antivir Chem Chemother* 17(2):79–87
5. Sofia MJ, Furman PA, Symonds WT (2010) 2'-F-2'-C-methyl nucleosides and nucleotides for the treatment of hepatitis C virus: from discovery to the clinic. In: Barrish JC, Carter PH, Cheng PTW, Zahler R (eds) RSC drug discovery ser. Accounts in drug discovery, vol 4. Royal Society of Chemistry, London, pp 238–266
6. Sofia MJ (2013) Nucleotide prodrugs for the treatment of HCV infection. *Adv Pharmacol* 67:39–73. <https://doi.org/10.1016/B978-0-12-405880-4.00002-0>
7. Wang P, Ching B-K, Rachakonda S, Du J, Khan N, Shi W, Stec D, Cleary D, Sofia MJ (2009) An efficient and diastereoselective synthesis of PSI-6130: a clinically efficacious inhibitor of HCV NS5B polymerase. *J Org Chem* 74:6819–6824
8. Murakami E, Bao H, Ramesh M, McBrayer TR, Whitaker T, Micolochick SHM, Schinazi RF, Stuyver LJ, Obikhod A, Otto MJ, Furman PA (2007) Mechanism of activation of beta-D-2'-deoxy-2'-fluoro-2'-C-methylcytidine and inhibition of hepatitis C virus NS5B RNA polymerase. *Antimicrob Agents Chemother* 51(2):503–509
9. Ma H, Jiang WR, Robledo N, Leveque V, Ali S, Lara-Jaime T, Masjedizadeh M, Smith DB, Cammack N, Klumpp K, Symons J (2007) Characterization of the metabolic activation of hepatitis C virus nucleoside inhibitor beta-D-2'-Deoxy-2'-fluoro-2'-C-methylcytidine (PSI-6130) and identification of a novel active 5'-triphosphate species. *J Biol Chem* 282(41):29812–29820
10. Murakami E, Niu C, Bao H, Micolochick SHM, Whitaker T, Nachman T, Sofia MA, Wang P, Otto MJ, Furman PA (2008) The mechanism of action of beta-D-2'-deoxy-2'-fluoro-2'-C-methylcytidine involves a second metabolic pathway leading to beta-D-2'-deoxy-2'-fluoro-2'-C-methyluridine 5'-triphosphate, a potent inhibitor of the hepatitis C virus RNA-dependent RNA polymerase. *Antimicrob Agents Chemother* 52(2):458–464
11. Ali S, Leveque V, Le Pogam S, Ma H, Philipp F, Inocencio N, Smith M, Alker A, Kang H, Najera I, Klumpp K, Symons J, Cammack N, Jiang WR (2008) Selected replicon variants with low-level in vitro resistance to the hepatitis C virus NS5B polymerase inhibitor PSI-6130 lack cross-resistance with R1479. *Antimicrob Agents Chemother* 52(12):4356–4369
12. Brown NA (2009) Progress towards improving antiviral therapy for hepatitis C with hepatitis C virus polymerase inhibitors. Part I: nucleoside analogues. *Expert Opin Investig Drugs* 18(6):709–725. <https://doi.org/10.1517/13543780902854194>
13. Burton JR (2009) HCV NS5B polymerase inhibitors. *Clin Liver Dis* 13:12
14. Gane EJ, Roberts SK, Stedman CA, Angus PW, Ritchie B, Elston R, Ipe D, Morcos PN, Baher L, Najera I, Chu T, Lopatin U, Berrey MM, Bradford W, Laughlin M, Shulman NS, Smith PF (2010) Oral combination therapy with a nucleoside polymerase inhibitor (RG7128) and danoprevir for chronic hepatitis C genotype 1 infection (INFORM-1): a randomised, double-blind, placebo-controlled, dose-escalation trial. *Lancet* 376(9751):1467–1475
15. Hecker SJ, Erion MD (2008) Prodrugs of phosphates and phosphonates. *J Med Chem* 51(8):2328–2345
16. Sofia MJ, Bao D, Chang W, Du J, Nagarathnam D, Rachakonda S, Reddy PG, Ross BS, Wang P, Zhang H-R, Bansal S, Espiritu C, Keilman M, Lam AM, Steuer HMM, Niu C, Otto MJ, Furman PA (2010) Discovery of a beta-D-2'-Deoxy-2'-alpha-fluoro-2'-beta-C-methyluridine nucleotide prodrug (PSI-7977) for the treatment of hepatitis C virus. *J Med Chem* 53(19):7202–7218
17. McGuigan C, Wedgwood OM, De Clercq E, Balzarini J (1996) Phosphoramidate derivatives of 2',3'-didehydro-2',3'-dideoxyadenosine (d4A) have markedly improved anti-HIV potency and selectivity. *Bioorg Med Chem Lett* 6:2359–2362

18. McGuigan C, Cahard D, Sheeka HM, De CE, Balzarini J (1996) Phosphoramidate derivatives of d4T with improved anti-HIV efficacy retain full activity in thymidine kinase-deficient cells. *Bioorg Med Chem Lett* 6(10):1183–1186
19. Lam AM, Murakami E, Espiritu C, Steuer HM, Niu C, Keilman M, Bao H, Zennou V, Bourne N, Julander JG, Morrey JD, Smee DF, Frick DN, Heck JA, Wang P, Nagarathnam D, Ross BS, Sofia MJ, Otto MJ, Furman PA (2010) PSI-7851, a pronucleotide of beta-*D*-2'-deoxy-2'-fluoro-2'-*C*-methyluridine monophosphate, is a potent and pan-genotype inhibitor of hepatitis C virus replication. *Antimicrob Agents Chemother* 54(8):3187–3196
20. Arnold JJ, Sharma SD, Feng JY, Ray AS, Smidansky ED, Kireeva ML, Cho A, Perry J, Vela JE, Park Y, Xu Y, Tian Y, Babusis D, Barauskus O, Peterson BR, Gnatt A, Kashlev M, Zhong W, Cameron CE (2012) Sensitivity of mitochondrial transcription and resistance of RNA polymerase II dependent nuclear transcription to antiviral ribonucleosides. *PLoS Pathog* 8(11): e1003030. <https://doi.org/10.1371/journal.ppat.1003030>
21. Murakami E, Tolstykh T, Bao H, Niu C, Steuer HMM, Bao D, Chang W, Espiritu C, Bansal S, Lam AM, Otto MJ, Sofia MJ, Furman PA (2010) Mechanism of activation of PSI-7851 and its diastereoisomer PSI-7977. *J Biol Chem* 285(45):34337–34347
22. Lawitz E, Rodriguez-Torres M, Denning J, Albanis E, Compropst M, Berrey MM, Symonds WT (2013) Pharmacokinetics, pharmacodynamics, and tolerability of GS-7851 a nucleotide analog polymerase inhibitor, following multiple ascending doses in patients with chronic hepatitis C infection. *Antimicrob Agents Chemother* 57(3):1209–1217
23. Ross BS, Reddy GP, Zhang H-R, Rachakonda S, Sofia MJ (2011) Synthesis of diastereomerically pure nucleotide phosphoramidates. *J Org Chem* 76(20):8311–8319
24. Lam AM, Espiritu C, Bansal S, Micolochick Steuer HM, Niu C, Zennou V, Keilman M, Zhu Y, Lan S, Otto MJ, Furman PA (2012) Genotype and subtype profiling of PSI-7977 as a nucleotide inhibitor of hepatitis C virus. *Antimicrob Agents Chemother* 56(6):3359–3368. <https://doi.org/10.1128/AAC.00054-12>
25. Zennou V, Lam AM, Keilman M, Espiritu C, Micolochick Steuer H, Sofia MJ, Reddy PG, Chang W, Rachakonda S, Otto MJ, Furman PA (2010) Combination of two complementary nucleotide analogues, PSI-7977 and PSI-938, effectively clears wild type and NS5b:S282T HCV replicons-comparison with combinations of other antiviral compounds. In: Paper presented at the 61st annual meeting of the European Association for the Study of the Liver, Vienna, 14–18 Apr
26. Gilead Sciences (2013) Sovaldi™ [package insert]
27. Mosley RT, Edwards TE, Murakami E, Lam AM, Grice RL, Du J, Sofia MJ, Furman PA, Otto MJ (2012) Structure of hepatitis C virus polymerase in complex with primer-template RNA. *J Virol* 86(12):6503–6511
28. Appleby TC, Perry JK, Murakami E, Barauskas O, Feng J, Cho A, Fox IIIID, Wetmore DR, McGrath ME, Ray A, Sofia MJ, Swaminathan S, Edwards TE (2015) Structural basis of RNA replication by the hepatitis C virus polymerase. *Science* 347(6223):771–775
29. Rodriguez-Torres M, Lawitz E, Kowdley KV, Nelson DR, Dejesus E, McHutchison JG, Cornpropst MT, Mader M, Albanis E, Jiang D, Hebner CM, Symonds WT, Berrey MM, Lalezari J (2013) Sofosbuvir (GS-7977) plus peginterferon/ribavirin in treatment-naive patients with HCV genotype 1: a randomized, 28-day, dose-ranging trial. *J Hepatol* 58(4):663–668. <https://doi.org/10.1016/j.jhep.2012.11.018>
30. Lawitz E, Rodriguez-Torres M, Denning JM, Cornpropst MT, Clemons D, McNair L, Berrey MM, Symonds WT (2011) Once daily dual-nucleotide combination of PSI-938 and PSI-7977 provides 94% HCV RNA < LOD at day 14: first purine/pyrimidine clinical combination data (the nuclear study). In: Paper presented at the 46th annual meeting of the European Association for the Study of the Liver, Berlin, 30 Mar–3 Apr
31. Reddy PG, Bao D, Chang W, Chun B-K, Du J, Nagarathnam D, Rachakonda S, Ross BS, Zhang H-R, Bansal S, Espiritu CL, Keilman M, Lam AM, Niu C, Steuer HM, Furman PA, Otto MJ, Sofia MJ (2010) 2'-Deoxy-2'-alpha-fluoro-2'-beta-C-methyl 3',5'-cyclic phosphate nucleotide prodrug analogs as inhibitors of HCV NS5B polymerase: discovery of PSI-352938. *Bioorg Med Chem Lett* 20(24):7376–7380

32. Gane EJ, Stedman CA, Hyland R, Ding X, Svarovskaia E, Symonds WT, Hindes R, Berrey MM (2013) Nucleotide polymerase inhibitor sofosbuvir plus ribavirin for hepatitis C. *N Engl J Med* 368:34–44
33. Babusis D, Curry MP, Denning J, Park Y, Murakami E, Afdhal N, Symonds W, McHutchinson JG, Ray A (2013) Nucleotide analog levels in liver explants from HCV infected subjects undergoing liver transplantation after up to 24 weeks sofosbuvir (GS-7977) with ribavirin treatment. *Hepatology* 58(Suppl):737A
34. Martel-Laferrriere V, Dieterich DT (2012) GS-7977: a promising nucleotide analog NS5B polymerase inhibitor of HCV. *Futur Virol* 7(6):537–546
35. Karageorgopoulos DE, El-Sherif O, Bhagani S, Khoo SH (2014) Drug interactions between antivirals and new or emerging direct-acting antivirals in HIV/hepatitis C virus coinfection. *Curr Opin Infect Dis* 27(1):36–45
36. Koff RS (2014) Review article: the efficacy and safety of sofosbuvir, a novel, oral nucleotide NS5B polymerase inhibitor, in the treatment of chronic hepatitis C virus infection. *Aliment Pharmacol Ther* 39(5):478–487. <https://doi.org/10.1111/apt.12601>
37. Mathias A, Cornpropst MT, Clemons D, Denning J, Symonds W (2012) No clinically significant pharmacokinetic drug-drug interactions between sofosbuvir (GS-7977) and the immunosuppressants cyclosporine A or tacrolimus in healthy volunteers. In: Paper presented at the 63rd annual meeting of the American Association for the Study of Liver Diseases, Boston, 9–13 Nov
38. Jacobson IM, Gordon SC, Kowdley KV, Yoshida EM, Rodriguez-Torres M, Sulkowski MS, Shiffman ML, Lawitz E, Everson G, Bennett M, Schiff E, Al-Assi MT, Subramanian GM, An D, Lin M, McNally J, Brainard D, Symonds WT, McHutchinson JG, Patel K, Feld J, Pianko S, Nelson DR (2013) Sofosbuvir for hepatitis C genotype 2 or 3 in patients without treatment options. *N Engl J Med* 368(20):1867–1877. <https://doi.org/10.1056/NEJMoa1214854>
39. Lawitz E, Mangia A, Wyles D, Rodriguez-Torres M, Hassanein T, Gordon SC, Schultz M, Davis MN, Kayali Z, Reddy KR, Jacobson IM, Kowdley KV, Nyberg L, Subramanian GM, Hyland RH, Arterburn S, Jiang D, McNally J, Brainard D, Symonds WT, McHutchinson JG, Sheikh AM, Younossi Z, Gane EJ (2013) Sofosbuvir for previously untreated chronic hepatitis C infection. *N Engl J Med* 368(20):1878–1887. <https://doi.org/10.1056/NEJMoa1214853>
40. Osinusi A, Meissner EG, Lee YJ, Bon D, Heytens L, Nelson A, Sneller M, Kohli A, Barrett L, Proschan M, Herrmann E, Shivakumar B, Gu W, Kwan R, Teferi G, Talwani R, Silk R, Kotb C, Wroblewski S, Fishbein D, Dewar R, Highbarger H, Zhang X, Kleiner D, Wood BJ, Chavez J, Symonds WT, Subramanian M, McHutchinson J, Polis MA, Fauci AS, Masur H, Kottlilil S (2013) Sofosbuvir and ribavirin for hepatitis C genotype 1 in patients with unfavorable treatment characteristics: a randomized clinical trial. *JAMA* 310(8):804–811. <https://doi.org/10.1001/jama.2013.109309>
41. Charlton M, Gane E, Manns MP, Brown RS, Curry MP, Kwo P, Fontana RJ, Gilroy R, Teperman L, Muir A, McHutchinson JG, Symonds W, Denning J, McNair L, Arterburn S, Terrault N, Samuel D, Forns X (2013) Sofosbuvir and ribavirin for the treatment of established recurrent hepatitis C infection after liver transplantation: preliminary results of a prospective, multicenter study. In: Paper presented at the 64th annual meeting of the American Association for the Study of Liver Diseases, Washington, 1–5 Nov
42. Tong X, Le Pogam S, Li L, Haines K, Pisco K, Baronas V, Yan JM, So SS, Klumpp K, Najera I (2014) In vivo emergence of a novel mutant L159F/L320F in the NS5B polymerase confers low-level resistance to the HCV polymerase inhibitors mericitabine and sofosbuvir. *J Infect Dis* 209(5):668–675. <https://doi.org/10.1093/infdis/jit562>
43. Gentile I, Maracolo AE, Buonomo AR, Zappulo E, Borgia F (2015) The discovery of sofosbuvir: a revolution for therapy of chronic hepatitis C. *Expert Opin Drug Discovery* 10(12):1363–1377
44. Afdhal N, Zeuzem S, Kwo P, Chojkier M, Gitlin N, Puoti M, Romero-Gomez M, Zarski JP, Agarwai K, Buggisch P, Foster G, Brau N, Buti M, Jacobson I, Subramanian GM, Ding X, Hong M, Yang JC, Pang PS, Symonds WT, McHutchinson JG, Muir A, Mangia A, Marcellin P

- (2014) Ledipasvir and sofosbuvir for untreated HCV genotype 1 infection. *N Engl J Med* 370:1889–1898
45. Kowdley KV, Lawitz E, Poordad F, Cohen DE, Nelson DR, Zeuzem S, Everson GT, Kwo P, Foster GR, Sulkowski MS, Xie W, Pilot-Matias T, Liossis G, Larsen L, Khatri A, Podsadecki T, Bernstein B (2014) Phase 2b trial of interferon-free therapy for hepatitis C virus genotype 1. *N Engl J Med* 370(3):222–232. <https://doi.org/10.1056/NEJMoa1306227>
 46. Afdhal N, Reddy KR, Nelson DR, Lawitz E, Gordon SC, Schiff E, Nahass R, Ghalib R, Gitlin N, Herring R, Lalezari J, Younes ZH, Pockros PJ, Di Bisceglie AM, Arora S, Subramanian GM, Zhu Y, Dvory-Sobol H, Yang JC, Pang PS, Symonds WT, McHutchinson JG, Muir AJ, Sulkowski M, Kwo P, Investigators ION (2014) Ledipasvir and sofosbuvir for previously treated HCV genotype 1 infection. *N Engl J Med* 370(16):1483–1493. <https://doi.org/10.1056/NEJMoa1316366>
 47. Everson G, Towner WJ, Davis MN, Wyles D, Nahass R, Thuluvath PJ, Etkorn K, Hineostrova F, Tong M, Rabinovitz M, McNally J, Brainard DM, Han L, Doehle B, McHutchinson JG, Morgan T, Chung RT, Tran TT (2015) Sofosbuvir with velpatasvir in treatment-naïve noncirrhotic patients with genotype 1 to 6 hepatitis C virus infection: a randomized trial. *Ann Intern Med* 163(11):818–826
 48. Bourleire M, Gordon SC, Flamm SL, Cooper CL, Ramji A, Tong M, Ravendhran N, Vierling JM, Tran TT, Pianko S, Bansal MB, de Ledinghen V, Hyland R, Stamm LM, Dvory-Sobol H, Svarovskaia E, Zhang J, Huang KC, Subramanian GM, Brainard DM, McHutchinson JG, Verna EC, Buggisch P, Landis CS, Younes ZH, Curry MP, Strasser SI, Reddy KR, Manns M, Kowdley KV, Zeuzem S, Investigators P-aP (2017) Sofosbuvir, velpatasvir, and voxilaprevir for previously treated HCV infection. *N Engl J Med* 376(22):2134–2146

Evolution of HCV NS5B Non-nucleoside Inhibitors



William J. Watkins

Contents

1	Introduction	171
2	Thumb Site I Inhibitors	173
3	Thumb Site II Inhibitors	177
4	Palm Site I Inhibitors	179
5	Palm Site II Inhibitors	183
6	Perspective	186
	References	187

Abstract The HCV polymerase NS5B is susceptible to allosteric inhibition at four sites that have been exploited by compounds that have shown clinical efficacy. The history of the discovery and optimization of leads acting at each of these sites is discussed. The many clinical candidates that emerged from these efforts are described, together with their impact on emerging regimens of increasing effectiveness.

Keywords Beclabuvir, BILB 1941, BMS-929075, Dasabuvir, Deleobuvir, Filibuvir, GSK2485852, GSK625433, HCV-371, IDX375, JTK-109, Lomibuvir, MK-3281, MK-8876, Nesbuvir, NS5B, Palm, Polymerase, Radalbuvir, RG7109, SB-750330, Setrobuvir, Tegobuvir, Thumb, TMC647055, VCH-759

1 Introduction

For any virus, the polymerase enzyme lies at the very heart of the life cycle, being the means by which the genomic information is copied and multiplied inside host cells. The efficiency with which the polymerase functions, and the fidelity with which it catalyzes the formation of copies of nucleic acids, is central to the ability of the virus

W. J. Watkins (✉)
Gilead Sciences, Foster City, CA, USA
e-mail: Will.watkins@gilead.com

to propagate and to adapt under selection pressure. It is not surprising, then, that exploiting the polymerase function of viruses has proven a highly effective tactic for direct-acting antiviral approaches – either by providing false nucleotide substrates for the enzyme, leading to aberrant nucleic acid formation and chain termination, or by allosteric inhibition. Given the success of such approaches, especially in developing therapies for human immunodeficiency virus (HIV) and hepatitis B virus (HBV), the hepatitis C virus (HCV) RNA-dependent RNA polymerase NS5B was a prime early focus of attention for drug discovery efforts for treatment of chronic HCV infection following the discovery of the virus in 1989 [1]. As for the HCV protease NS3, biochemical assays using recombinant NS5B became available before the advent of cellular viral replication systems (replicons), and these were used both for nucleoside research and for screens for other modes of inhibition. The potential for the utility of allosteric inhibitors was clear from the precedent set by HIV treatment, where the combination of non-nucleoside reverse transcriptase inhibitors (NNRTIs) with nucleosides and protease inhibitors and, latterly, integrase inhibitors has delivered highly effective once-daily regimens.

In hepatocytes, NS5B functions in concert with other viral proteins in a replicase complex that is anchored in a membranous web induced by the virus. Recombinant genotype (GT) 1b NS5B in which the membrane-binding C-terminal region was deleted ($\Delta 21$) proved competent for HCV RNA synthesis [2] and became widely used for screening assays. At the time that these assays were being established, high-throughput screening using emerging compound libraries had become a routine method for identifying starting points for medicinal optimization, and so a rapid and intensive phase of new lead discovery for HCV ensued.

Unlike for HIV RT, where diverse lipophilic hits can routinely be found that bind to a single allosteric site, screening against NS5B revealed compounds that turned out to inhibit the enzyme through binding in several different locations. The discussion that follows will categorize the chemical series according to these locations, and it is appropriate before doing so to briefly summarize the structure of the protein in relation to its function.

Like other polymerases, NS5B $\Delta 21$ in the solid state resembles a right-handed baseball glove with domains that have been named the thumb, fingers, and palm (Fig. 1). The analogy is apt in that the movement of these domains during the catalytic cycle also mimics that of the human hand, with the fingers and thumb opening and closing in an orchestrated fashion to enable binding of the template RNA, priming of replication with a few complementary base pairs, and then transitioning into full replication mode. The analogy even holds for a conformation in which the tip of the forefinger is touching the thumb, creating a closed state that is involved in the initiation events. However, it breaks down insofar as there is a fourth element termed the β -loop (colored yellow in Fig. 1) whose movement is also critical for function and that in the closed state is tucked under the C-terminus. The overall picture is that of a complex protein in which the flexibility and mobility of each domain are critical to its function.

The extensive search for non-nucleoside inhibitors (NNIs) that could be used clinically to address chronic HCV infection took place over many years and in many

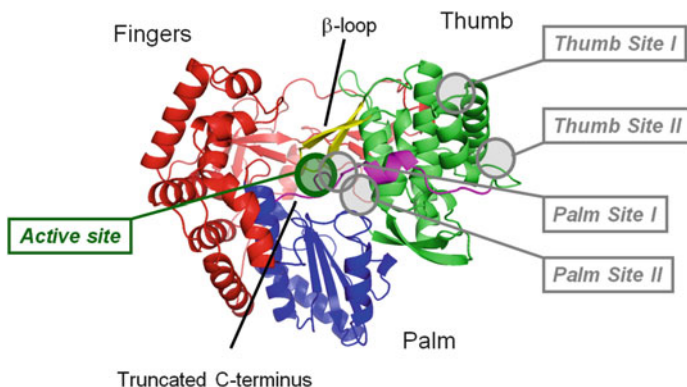


Fig. 1 Crystal structure of NS5B $\Delta 21$, with domains color coded (thumb, green; palm, blue; fingers, red; β -loop, yellow; truncated C-terminus, magenta) and the major allosteric inhibitory sites indicated. Image created within PyMOL (Schrödinger LLC) using coordinates from the Protein Data Bank entry 1C2P [3]

different research groups. In what follows, these efforts are summarized with an emphasis on the programs that led to clinical candidates, and in the figures, key compounds are displayed on an approximate timeline to facilitate comparison of the evolution of related series.

2 Thumb Site I Inhibitors

Some of the earliest hits to appear in the patent literature and subsequently in journals inhibit NS5B by binding to the tip of the thumb domain, at a site that has become known as Thumb Site I. Japan Tobacco were particularly quick to capitalize on the output of their biochemical screen [4] building on the weak activity of the amide-bearing 1-cyclopentyl benzimidazole **1** (Fig. 2), which provided 47% inhibition of replication at 10 μM [5]. They soon discovered that replacement of the amide with a carboxylic acid delivered a boost in potency, and subsequent elaboration of the benzylic tail led to *JTK-109*. This compound inhibited the activity of GT1 NS5B with an IC_{50} of 17 nM and inhibited the GT1 replicon in Huh7 cells with an EC_{50} of 320 nM [6]. Although the addition of 50% human serum in the latter assay led to a 20-fold reduction in potency, it was unclear at that time what plasma levels would be required for clinical effectiveness; furthermore, levels of drug were tenfold higher in the liver than plasma in rats. The drug entered clinical development and reached Phase 2 but was abandoned in 2003 for undisclosed reasons.

Also very early in exploiting screening hits acting at this site [7] was the Boehringer Ingelheim group based in Laval, Quebec. Their initial hit **2** (Fig. 2) (IC_{50} 14 μM) was initially optimized in the biochemical assay to deliver a dicarboxylic acid with 19 nM potency, but cellular activity was lacking. The compound was

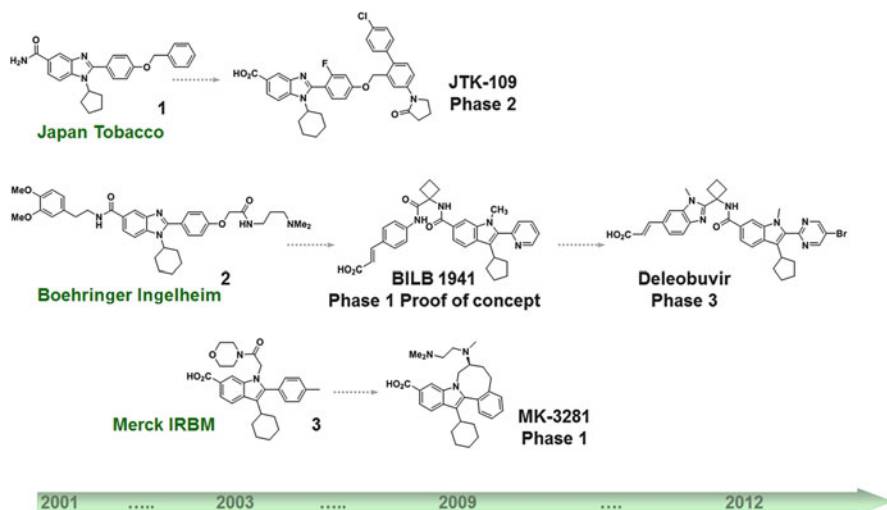


Fig. 2 Early Thumb Site I inhibitors

reengineered through the incorporation of a central spirocyclic motif that enforces the preferred conformation for binding to NS5B. The first clinical candidate from the program, *BILB 1941* [8], uses a cyclobutane for this purpose, and the interaction with Arg503 is provided for with the indole 5-carboxamide. The remaining binding interactions are predominantly lipophilic in nature. BILB 1941 displays a GT1 replicon EC_{50} of 84 nM and, like JTK-109, hepatic drug levels >10-fold higher than plasma levels in rat. This compound is notable as the first Thumb Site I inhibitor to demonstrate clinical activity: doses of 10–450 mg were administered three times daily over 5 days to GT1-infected subjects, and four of five patients in the highest dose cohort exhibited $>1 \log_{10}$ IU mL^{-1} decline in viremia [9]. Unfortunately gastrointestinal intolerance and liver enzyme elevation precluded further development, but the result certainly stimulated further discovery efforts based upon this mode of inhibition.

The Boehringer Ingelheim group assessed the roles of every structural element in BILB 1941 and used the analysis to identify rotatable bonds that might be modified to increase potency [10]. Key in this effort was the incorporation of a benzimidazole to mimic the central anilide, which also served to eliminate the genotoxicity risk presented by the embedded aniline. The result was *deleobuvir* (Fig. 2) (GT1b EC_{50} 11 nM; GT1a EC_{50} 23 nM), which progressed as far as a Phase 3 trial in which it was dosed at 600 mg BID in combination with the protease inhibitor faldaprevir (120 mg QD) and ribavirin [11].

Another research team with an early interest in this site was the Merck group based at IRBM in Rome. In 2003, they demonstrated that the Japan Tobacco and Boehringer Ingelheim leads acted as noncompetitive inhibitors with respect to nucleotide substrates, inhibiting the polymerase prior to the elongation phase. In

the emerging cellular replicon system, they further showed that escape mutations mapped to Pro495 at Thumb Site I [12]. They built upon this knowledge to formulate a proprietary series of inhibitors [13] that appended an amide motif off the central indole, as in **3** (Fig. 2) [14]. This relatively compact lead displayed a replicon EC_{50} of 0.3 μM and stimulated further optimization efforts. The newly introduced amide was intended to modulate physicochemical properties, and a further innovation was to use it to incorporate a further ring that would constrain the aryl residue at the indole 2-position (and, in turn, the neighboring cyclohexyl ring) [15, 16]. The Japan Tobacco group introduced a similar tactic, noting that the use of a basic residue off the new ring served to reduce the plasma shift for the class [17]. From IRBM, *MK-3281* emerged as a clinical candidate and demonstrated a 1.95 \log_{10} IU mL^{-1} reduction in plasma viral load in GT1 subjects when dosed at 800 mg BID over 7 days (<https://clinicaltrials.gov/ct2/show/results/NCT00635804?sect=Xh0156#outcome11>).

The discovery team at Bristol-Myers Squibb (BMS) exploited the tetracyclic motif in the form of the benzodiazepinone **4** (Fig. 3) [18]. They favored the use of an acylsulfamide as the acidic entity as it eliminated glucuronidation as a pathway for metabolism. Extensive exploration of the seven-membered ring ultimately led to the fusion with a cyclopropyl ring, thereby forcing the optimal binding conformation, and attachment of an amide. The bicyclic piperazine motif in *beclabuvir* (Fig. 3) was adopted for optimal pharmacokinetic properties and in order to mitigate the potential for drug-drug interactions resulting from PXR agonism.

Beclabuvir was advanced into clinical development in 2008, and in a Phase 1b clinical trial produced a mean 2.5 \log_{10} IU mL^{-1} decline in viral load in GT1-infected subjects after a single dose of 300 mg. As with other agents acting at this site, the activity of the compound is limited to GTs 1, 3a, 4a, and 5a, with

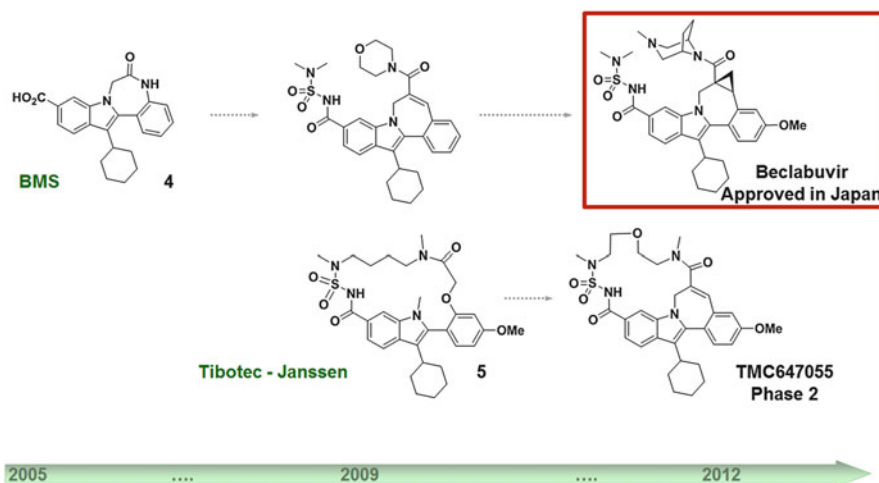


Fig. 3 Further Thumb Site I inhibitors

weaker activity against GTs 2a and 6a. As a result, the clinical development was directed toward populations where GT1 predominates, and ultimately the compound was approved in Japan in late 2016 (<http://www.genome.jp/kegg/drug/br08318.html>), co-formulated in a single tablet with the NS3 protease inhibitor asunaprevir and the NS5A inhibitor daclatasvir (Ximency™).

In a further iteration of the overall topology of Thumb Site I inhibitors, Tibotec exploited the opportunity afforded by the acylsulfamide to incorporate a macrocyclic ring linking back to the aryl residue at the indole 2-position as in **5** (Fig. 3) [19]. While demonstrating that this tactic could provide active analogs, it proved difficult to engineer acceptable pharmacokinetic properties, resulting in a redesign in which the macrocycle was instead connected to the bridging ring. This led to the discovery of *TMC647055* [20], an agent which was explored in Phase 2 studies in combination with the NS3 protease inhibitor simeprevir (and the Cyp3A4 inhibitor ritonavir, as *TMC647055* induces its own metabolism).

Overall, at least six clinical candidates emerged over approximately two decades of research into the inhibition of NS5B via this site, and one, beclabuvir, reached approval, albeit only in Japan. The structural basis for the inhibitory mode of action is very evident from the co-crystal structures that have been published over the course of this work, one of which ([21]; pdb 3q0z) is depicted in Fig. 4. The binding of the inhibitor blocks the interaction of the tip of the fingers domain and the thumb, thereby preventing the formation of the closed conformation that is necessary for initiation. The different protein sequences in this region are the reason that Thumb Site I inhibitors lack useful activity against GTs 2 and 6.

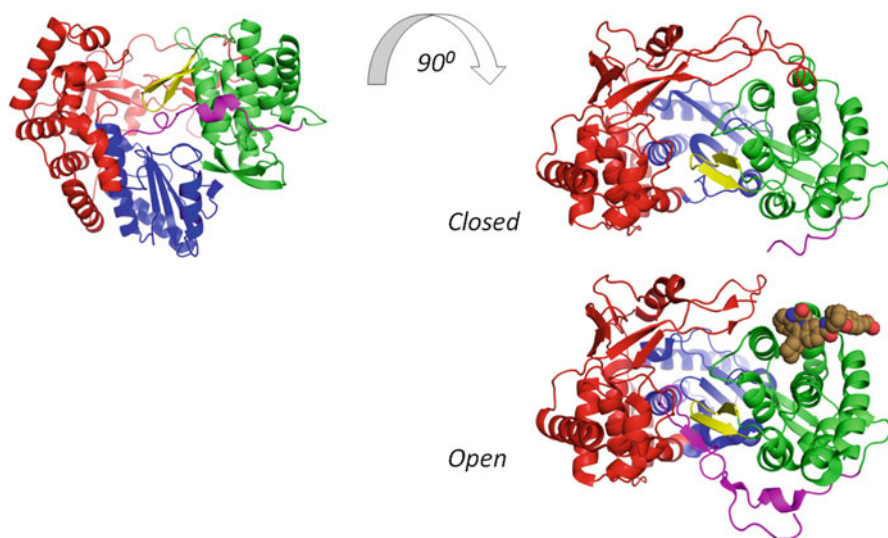


Fig. 4 Crystal structures of apo NS5B Δ21 and NS5B Δ21 with a Thumb Site I inhibitor bound

3 Thumb Site II Inhibitors

The earliest patent applications for chemical series that inhibit NS5B by binding at Thumb Site II appeared at about the same time as those for the Thumb Site I examples discussed above – doubtless because they emerged from similar biochemical screening campaigns. One of the first companies to pursue a lead to the point of entry into the clinic was ViroPharma, in a collaboration with Wyeth [22]. Analogs of the racemic screening hit **6** (Fig. 5) (IC_{50} 3 μ M) demonstrated the importance of the acid and the n-propyl substituent for activity, and the indole substituents were optimized [23]. The eutomer *HCV-371* displayed an EC_{50} of 4.8 μ M and was studied in humans but showed no activity. This finding was instrumental for the field in that it served as a useful negative control when a mouse model of chronic HCV infection was later developed [24]. The series was subsequently optimized by refining the alkyl substituent and through introduction of a tether to an extra ring to **7**, with GT1a EC_{50} 4.5 nM and GT1b EC_{50} 23 nM [25], and this compound did show some activity in the GT1a-infected scid-Alb/uPA murine model.

The screening hit **8** (Fig. 5) was discovered at Agouron [26] as a legacy of their HIV protease research, and the pursuit of the series, guided by X-ray co-crystal data, continued after Pfizer acquired the company. Replacing the aniline with heterocycles and masking the phenol, as in **9**, led to gains in cellular potency. Key to the ultimate identification of *filibuvir* was modulation of the acidity of the enol component by replacing S with CH_2 , and avoidance of CYP2D6-mediated metabolism through use of the diethylpyridine moiety [27]. Filibuvir exhibited a mean EC_{50} of 59 nM against a panel of replicon cells created using GT1 patient isolates [28] and produced a plasma viral load reduction of 2.13 \log_{10} IU mL^{-1} when dosed at 300 mg TID for 8 days [29], establishing the potential for useful clinical activity by inhibition at this

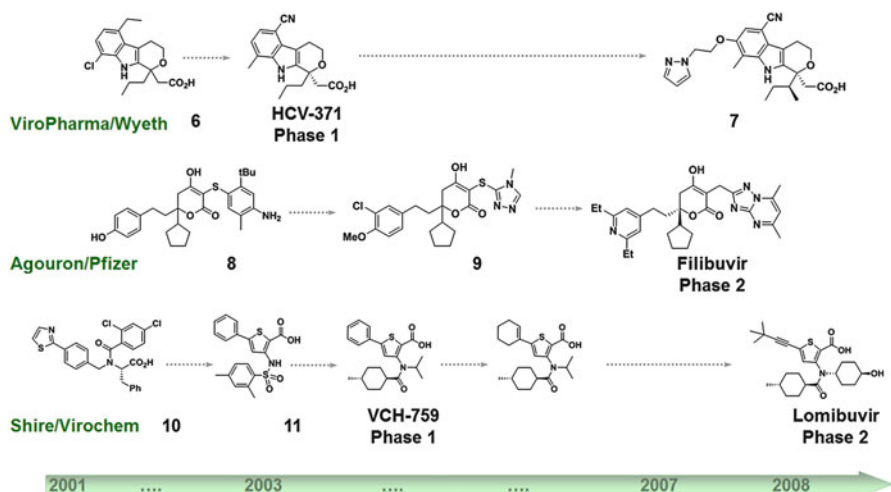


Fig. 5 Early Thumb Site II inhibitors

site. In the Phase 1 study as well as through in vitro characterization, resistance was mediated by mutations at M423, further corroborating the relevance of this region of the polymerase in the mode of action. A Phase 2 study in combination with pegylated interferon and ribavirin was conducted, but the compound was never combined with other direct-acting antivirals in the clinic.

A third series with a long history of optimization originated at Shire Biochem in Laval, Quebec – another research organization with a storied record of antiviral drug discovery. In this case, phenylalanine derivatives such as **10** (Fig. 5) [30] and thiophene-2-carboxylic acids [31] rapidly merged into leads typified by **11**. Elements of the series that were essential for activity were the carboxylic acid and a proximal lipophilic substituent, fulfilled by the benzamide in **10** and the aryl sulfonamide in **11**, reminiscent of the pharmacophore for the ViroPharma/Wyeth series. N-alkylation of **11** led to a loss in potency, but the tertiary amide motif was preferred over secondary analogs [32], and branching, as in the isopropyl case, conferred improved cellular as well as biochemical potency. A further innovation was the introduction of the *trans*-4-methylcyclohexanyl motif, and this resulted in *VCH-759*, which exhibited a GT1 replicon EC₅₀ of 0.3 μM and was advanced into clinical development where a dose of 800 mg BID reduced plasma viral load by 2.5 log₁₀ IU mL⁻¹ [33].

Other organizations later revealed related compounds: the research group at Bayer (subsequently Aicuris) explored alternative orientations of the thiophene ring (**12**, Fig. 6) [34] before reverting to the initial isomer and introducing an acetylenic substituent as the thiophene 5-substituent [35]. This latter tactic was also adopted by Virochem in the phase of their research that led to *lomibuvir*

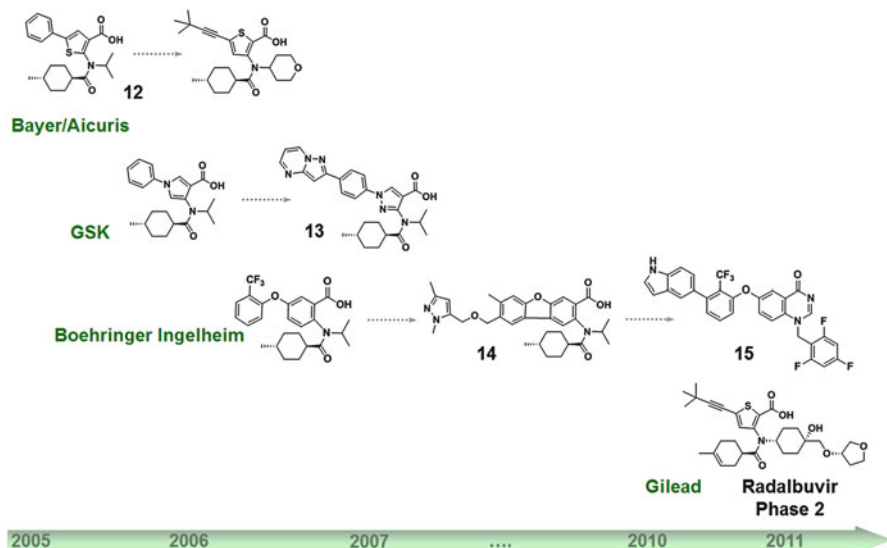


Fig. 6 Further Thumb Site II inhibitors

(Fig. 5), a compound that demonstrated an impressive $3.4 \log_{10} \text{ IU mL}^{-1}$ decline in plasma GT1 HCV RNA after dosing at 750 mg BID for 3 days (<http://investors.vrtx.com/releasedetail.cfm?releaseid=460352>). Following acquisition by Vertex, lomitubivir was studied in a Phase 2 trial in combination with the NS3 protease inhibitor telaprevir but was not developed further [36]. GlaxoSmithKline (GSK) (Fig. 6) found that pyrrole and pyrazole could serve as a central heteroaromatic scaffold [37] and that further aromatic systems could be introduced, as in **13**. Similarly, Boehringer Ingelheim adopted a phenyl ring as the central element in the form of anthranilic acid derivatives [38], and used it to append elongated motifs as in **14** and **15**. The latter is a particularly notable analog in that the canonical carboxylic acid is absent and yet sub-nanomolar replicon potency is achieved [39]. A final late entrant in this area was Gilead, who manipulated the amide substituent and refined the structure to generate *radalbuvir* [40]. This compound drove a $>3 \log_{10} \text{ IU mL}^{-1}$ decline in GT1a and GT1b plasma load after dosing at 500 mg QD for 3 days [41] and was subsequently studied in Phase 2 combination regimens.

Inhibitors binding at Thumb Site II are anchored by an interaction with the backbone amide of S476 and exploit an adjacent lipophilic pocket that is exposed upon rotation of the side chains of adjacent residues. This site is approximately 35 Å from the active site, and insight into why binding in this fashion might inhibit the polymerase activity came from a systematic study of enzyme constructs involving deletion or mutation of both the β -loop and the C-terminal tail, with activity lost in the C-terminal $\Delta 47$ and $\Delta 55$ constructs [42]. Binding at Thumb Site II stabilizes a conformation of NS5B in which the C-terminus wraps over the β -loop, preventing the adoption of the open form that is necessary for elongation (Fig. 7) [43]. Differences in residues around this pocket in GTs 2, 3, and 4 NS5B render inhibitors at this site effective only for GTs 1 and 5.

4 Palm Site I Inhibitors

The two other most explored allosteric inhibitory sites on NS5B are located very close to each other and much closer to the active site, in the palm domain of the protein. Although adjacent, discrete mutations arise from inhibitors acting at each site demonstrating that the modes of inhibition are distinct. Like the two thumb sites, both have been heavily explored for optimization for clinical use.

The earliest leads for inhibitors at Palm Site I appeared at about the same time as those for the sites already discussed, again as a result of the screening efforts with the biochemical assay. Patent applications from progenitor companies of GSK appeared in 2001 and soon thereafter relating to a series of substituted prolines [44, 45] that resulted from deconvolution of a combinatorial library [46]. While the acid at the 2-position proved essential for activity, manipulation of the 4-position enabled optimization of cellular potency and pharmacokinetic properties [47], resulting ultimately in the clinical candidate *GSK625433* (Fig. 8) – an analog that was significantly more potent against GT1b than GT1a (EC_{50} 3 nM vs 290 nM) and

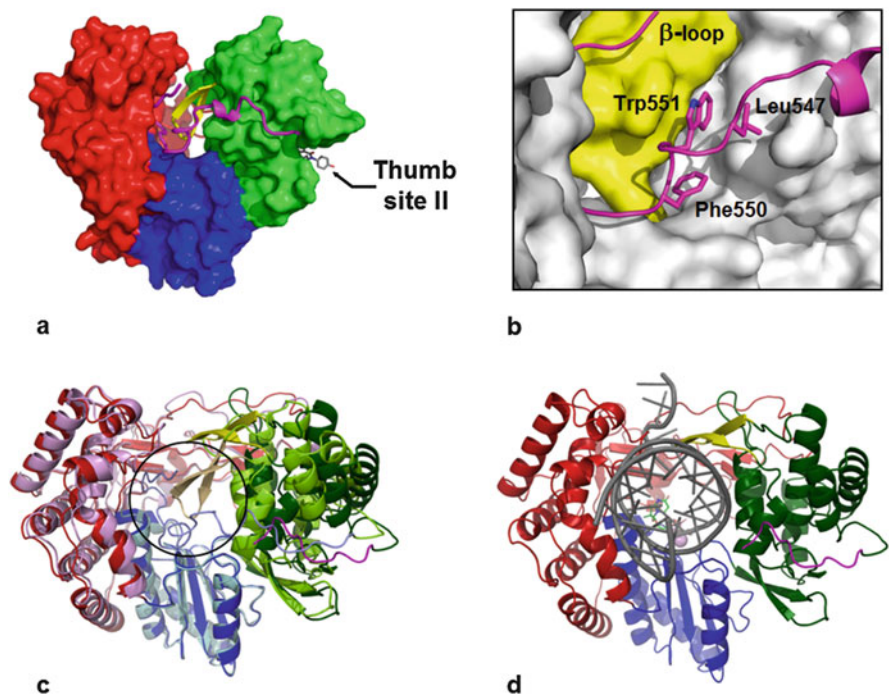


Fig. 7 Illustration of the closed conformation stabilized by Thumb Site II inhibitors. (a) Overall topography; (b) close-up of β -loop and C-terminal LWF motif; (c) closed conformation in ribbon diagram with RNA-binding region circled; (d) open form required for full elongation mode

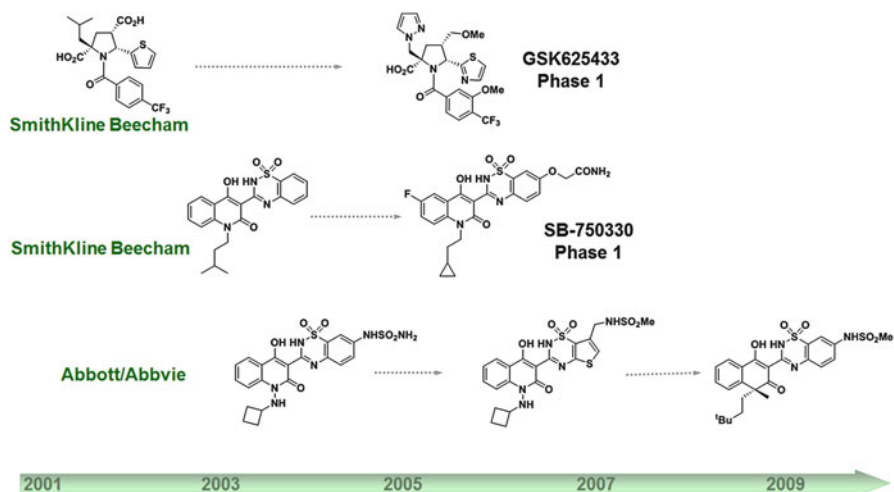


Fig. 8 Early Palm Site I inhibitors

much less active against GTs 2–4 [48]. The Phase 1 results from this compound have not been reported.

Further patent applications from SmithKline Beecham appeared in 2003 for a series of benzothiadiazines that preceded a large number of related efforts in several companies [49]. In this chemotype, the enol proved essential for potency, as did the presence of a lipophilic N-substituent. A key advance came in improvement in potency through the introduction of an amide-bearing side chain as in the clinical candidate *SB-750330* (Fig. 8), which displayed GT1b EC₅₀ of 2 nM [50]. Ultimately, however, the preferred substituent at this position became a sulfonamide, as is evident from the progression in the AbbVie series also illustrated in Fig. 8. A further innovation in this series was the demonstration that a quaternary carbon could replace the quinolone nitrogen, and these analogs demonstrated evidence of high liver concentrations relative to plasma when dosed in rats [51].

Meanwhile, Anadys were exploring monocyclic variants of the quinolone portion of the general pharmacophore as in **16** (Fig. 9). This gambit enabled the subsequent fusion of a bridged aliphatic motif onto the central ring, filling the available lipophilic pocket more effectively and resulting in *setrobuvir* [52]. This compound, with GT1b and GT1a EC₅₀ 3 nM and 18 nM, respectively, demonstrated 2.9 log₁₀ IU mL⁻¹ decline in GT1 plasma load after dosing at 800 mg BID for 3 days [53] and was advanced by Roche to Phase 2 studies in combination with pegylated interferon and ribavirin.

A second series to reach a similar stage of clinical progression originated at Idenix [54]. Like Anadys, this series exploited a monocyclic enolic motif in the form of a pyrazolone, but here the canonical benzothiadiazine was replaced with a phosphadiazine. Ultimately the pyrazolone was replaced with a tetramic acid, enabling incorporation of a *tert*-butyl motif to exploit the lipophilic pocket distal to the plane of the ring system, as in the AbbVie context. In the form of *IDX375* (Fig. 9), this resulted in a compound with EC₅₀ 6 nM and 2 nM vs GT1a and GT1b. *IDX375* advanced into a small Phase 1 trial, where in three HCV-infected subjects administered two 200 mg doses plasma viral load declined by 0.5–1.1 log₁₀

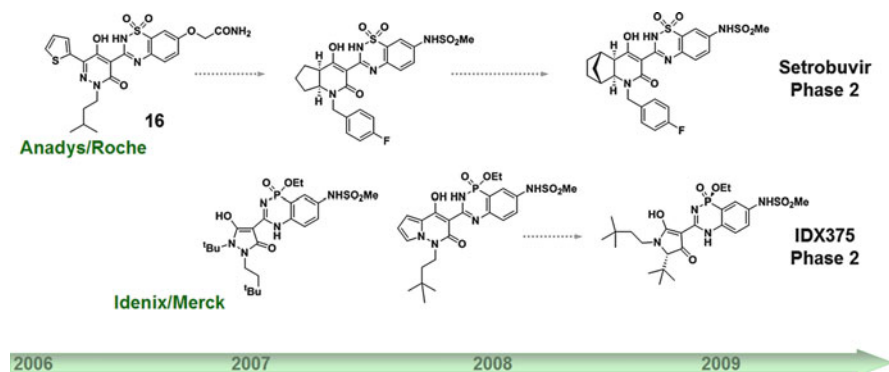


Fig. 9 Further Palm Site I inhibitors

IU mL⁻¹. In two of these subjects, slight increases in bilirubin, attributable to UGT1A1 inhibition, were observed [55].

A distinct neutral chemotype that binds at the same site as the benzothiadiazine class later emerged from high-throughput screening in the form of the dihydrouracil **17** [56, 57] (Fig. 10), with EC₅₀ 0.58 μM and 0.36 μM vs GT1a and GT1b. Although a relatively late entrant, this series matured rapidly through the incorporation of a benzenesulfonamide motif analogous to that in the benzothiazines. Initially this motif was attached to the central aryl ring via an amide, but poor pharmaceutical properties led to adoption of an olefinic link as in *ABT-072* [58] and then the naphthalene contained in *dasabuvir*. Both these compounds progressed into the clinic and were evaluated in Phase 2 studies in combination with other agents, and ultimately dasabuvir was approved in December 2014 for the treatment of GT1 patients in combination with the NS5 inhibitor ombitasvir and the NS3 protease inhibitor paritaprevir together with the pharmacokinetic boosting agent ritonavir. This series was also explored by Roche, who arrived at it from an innovative variation on a fragment-based screen [59] that demonstrated that a pyridone motif could serve as a substitute for the dihydrouracil [60], and then went on to incorporate a quinolone as a central bicyclic scaffold. This optimization effort resulted in the clinical candidate *RG7109*, whose preclinical data suggested that a dose of ca. 100 mg BID would be sufficient to reduce plasma viral load by >1.5 log₁₀ IU mL⁻¹ [61]. Clinical data has not been reported.

Palm Site I inhibitors prevent initiation of RNA synthesis and are thought to bind in a ternary complex with the enzyme and the RNA template [62], and the key interactions that define the pharmacophore are found in GT1 only.

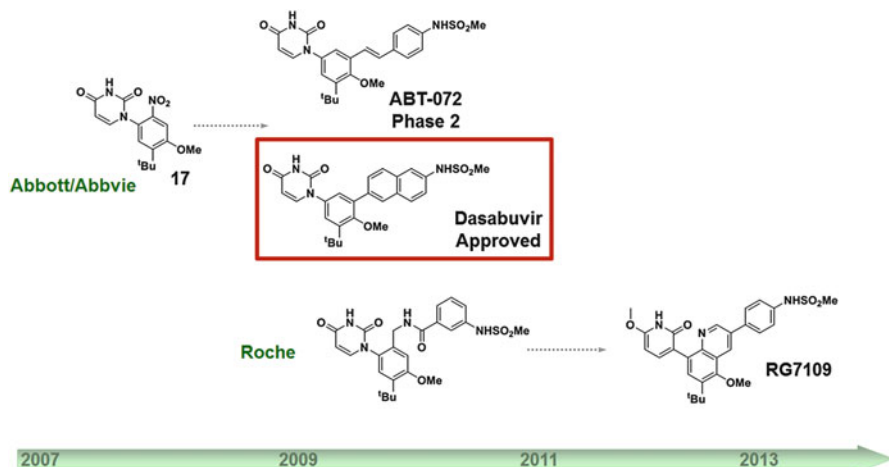


Fig. 10 Dihydrouracil Palm Site I inhibitors

5 Palm Site II Inhibitors

The fourth allosteric site that has proven valuable for clinical intervention was first exploited by ViroPharma working in collaboration with Wyeth [63]. Their series was characterized by a benzofuran core with a secondary amide at the 3-position. Other necessary elements for activity were an aryl 2-substituent and a small lipophilic group at the 5-position. The 6-substituent was used for modulation of properties in the course of pharmacokinetic optimization, resulting in *nesbuvir* (Fig. 11), with EC_{50} 5 nM and 9 nM vs GT1a and GT1b. Following confirmation of activity in the mouse model developed by this group [24], *nesbuvir* was advanced into clinical studies where it established that inhibitors binding at Palm Site II could result in viral load reductions in patients ($1.4 \log_{10}$ IU mL^{-1}), albeit at a dose of 1,500 mg BID [64]. Regrettably, when combined with pegylated interferon and ribavirin in a Phase 2 study, *nesbuvir* caused liver enzyme elevations after 8 weeks of dosing at 500 mg BID [65], and it was not developed further.

Subsequent to these efforts, and as the whole field of HCV drug development expanded to address the broader patient population infected with GTs 2–6, the unique potential of inhibitors binding at this site to result in coverage beyond GT1 stimulated exploratory efforts in several other companies (Fig. 11). The IRBM branch of Merck demonstrated the viability of a further ring fusion on the benzofuran [66], and other research groups within Merck went on to extend the 5-substituent

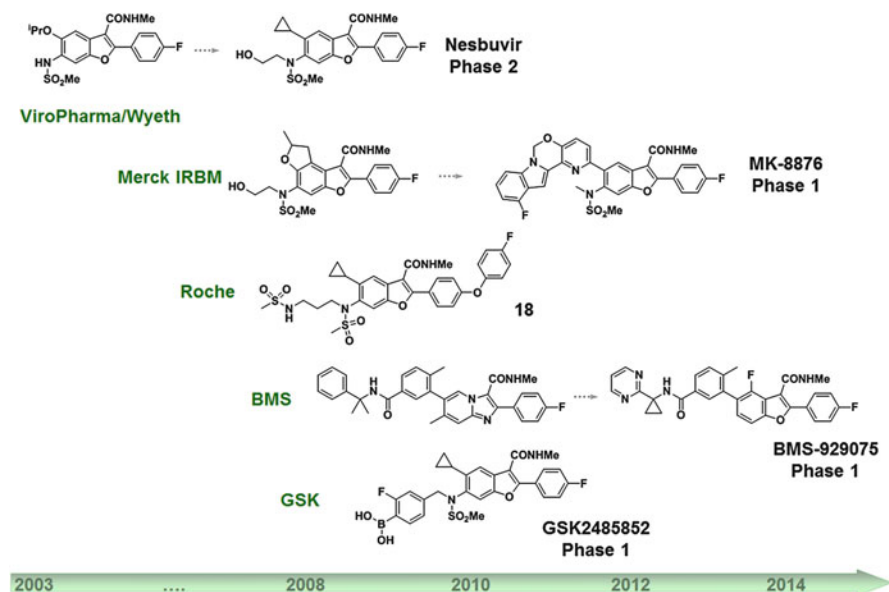


Fig. 11 Palm Site II inhibitors

considerably, noting that this region of the inhibitor enabled reaching elements of the Palm Site I pocket. The result was *MK-8876* (Fig. 11), an analog with exceptional potency and breadth of activity for a NNI (EC_{50} 1–7 nM vs GTs 1–5, with potency also retained against known relevant Palm Site II mutants) [67]. In a Phase 1 trial, this compound produced a reduction in plasma load of $3.4 \log_{10}$ IU mL⁻¹ in GT1a and $1.9 \log_{10}$ IU mL⁻¹ in GT3 patients upon dosing at 800 mg QD for 7 days (<https://clinicaltrials.gov/ct2/show/results/NCT01930058?term=MK8876&rank=1>).

The Roche group [68] established the potential for extending the aryl 2-substituent in the form of the bis-aryl ether **18** (Fig. 11). BMS found that the benzofuran core could be replaced by other 5,6-bicyclic systems [69] but chose to retain it while incorporating added interactions via the 5-substituent, exploiting the plasticity of this region of the Palm site [70]. They succeeded in discovering *BMS-929075*, an analog with balanced potency against GTs 1 and 3–6 (EC_{50} 3–20 nM, including the resistant GT1b mutant C316N), but lacking useful activity against GT2. The human pharmacokinetics of this compound suggested that a 25 mg QD dose would be sufficient to provide trough plasma concentrations tenfold above the GT1b C316N EC_{50} [71], but the intended study in patients was withdrawn in 2013 (<https://clinicaltrials.gov/ct2/show/NCT01525212?term=BMS-929075&rank=1>).

Structure-guided design featured heavily in the efforts at GSK that resulted in the identification of *GSK2485852* (Fig. 11) [72]. Here the intention was to incorporate a boronic acid substituent such that it might interfere with incoming nucleoside triphosphates. Optimization also addressed the desire for activity against the GT1b C316N mutant as well as other GTs, and the compound chosen for clinical development displayed EC_{50} s ranging from 1 nM (GT1b) to 8 (GT2a) [73]. Unfortunately the pharmacokinetic results of Phase 1 studies precluded further advancement [36].

Co-crystal structures with NS5B revealed the deep hydrophobic pocket that is induced upon binding of Palm Site II inhibitors, and biochemical studies with HCV-796 demonstrated slow-binding kinetics that were unaffected by preformation of the enzyme with RNA template [74]. *GSK2485852* exhibited a 40-fold slower dissociation rate even than HCV-796 and inhibited initiation of elongation [72]. While co-crystallographic studies in the absence of RNA template revealed no evidence of covalent bond formation to boron, superimposition of these structures with the ternary crystal structure [43] suggested that the 2'-hydroxyl of an incoming ribose unit might approach within 3 Å.

A final series of NNIs explored in clinical studies originated not in high-throughput biochemical screens for NS5B inhibition but rather in a phenotypic screen using a bovine viral diarrhea virus (BVDV) cellular assay [75]. When SAR was developed in the GT1b HCV replicon, introduction of the *o*-F substituent in **19** (Fig. 12) gave a boost in potency and served as the lead for further optimization. The result of this effort was *tegobuvir*, a GT1-specific inhibitor (GT1a and GT1b EC_{50} s 14 nM and 1 nM) [76] that reduced plasma viral load by $1.95 \log_{10}$ IU mL⁻¹ when dosed at 120 mg BID over 8 days to GT1-infected patients. In subsequent Phase

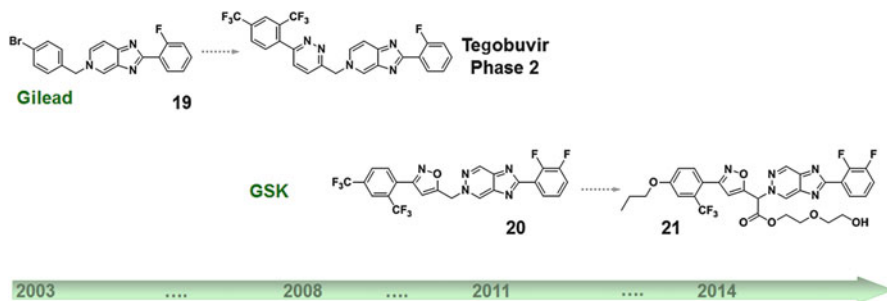


Fig. 12 Covalent NS5B inhibitors

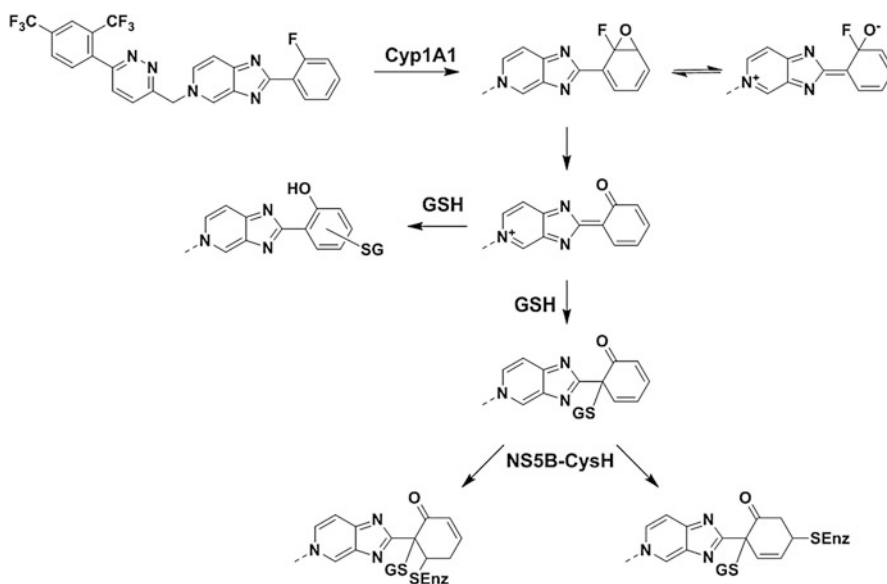


Fig. 13 Proposed activation mode for tegobuvir

2 studies, the dose was restricted to 40 mg due to concerns over potential for QT prolongation.

The mechanism of action of tegobuvir and its progenitor compounds was initially cryptic as no activity was seen in biochemical assays. However, experiments in chimeric replicon systems implicated NS5B as the protein target, with variants lacking a cysteine at position 445 exhibiting reduced susceptibility [77]. Further investigation revealed that after replicon cells were treated with tegobuvir the NS5B protein was modified, and the intensity of the modified band (with altered mobility on SDS-PAGE gel) was dependent upon cellular glutathione levels as well as CYP1A activity [78]. Figure 13 depicts a mechanism of activation and covalent attachment consistent with these data.

Mindful of the QT prolongation risk associated with tegobuvir, the research group at GSK devised a less basic imidazopyridazine core [79] that led to a series with reduced hERG channel-blocking potency (**12**, Fig. 12). In the course of their optimization efforts, assessment of substituents on the methylene group led to the surprising finding that a carboxylic acid in this position spontaneously decarboxylates in biological media to deliver the parent methylene analog. This proved especially useful as the poor solubility of the series presented challenges in achieving acceptable oral bioavailability. Ultimately the pegylated ester derivative **21** was used as a “traceless” prodrug, but unfortunately liver toxicity in preclinical experiments in dog precluded further development of the series [80].

6 Perspective

The search for non-nucleoside inhibitors of HCV NS5B began shortly after the virus was discovered, well before cellular assays for viral replication became available, and spanned over two decades of sustained effort in very many research institutions. Only two other modes of inhibition – nucleoside-based chain terminators and NS3 protease inhibitors – reflect the same early start, driven by the feasibility of biochemical screens. Together these three classes enabled early clinical experiments, directed largely at GT1 patients. NNIs played a prominent part in these efforts; an extraordinarily diverse range of chemical series emerged, spawning well over 20 clinical candidates. These compounds contributed significantly to our understanding of the extent of inhibition of replication necessary to drive reductions in plasma viral load, as well as providing valuable information on what would be required to prevent the emergence of resistant virus. As the protease inhibitors were gradually improved, and prior to the discovery of sofosbuvir as a safe and effective chain terminator, exploratory regimens containing NNIs were at the leading edge in achieving meaningful improvements in efficacy over interferon-based treatments.

The later emergence of the NS5A inhibitors, providing dramatic reductions in viral load at relatively low doses, impacted the field of HCV clinical development considerably. When combined with sofosbuvir, very high levels of SVR proved readily achievable in GT1 patients, rendering the requirement for a third agent less stringent. In regimens not containing sofosbuvir combinations containing an NNI, an NS5A inhibitor and an NS3 inhibitor proved necessary, and it was on the basis of these that both dasabuvir and beclabuvir were approved.

With high levels of SVR in GT1 achieved, the emphasis of clinical exploration shifted to coverage of other genotypes, with the ultimate goal of rendering genotyping of the patient prior to initiation of therapy unnecessary. Here the utility of NS5B NNIs became more questionable due to the heterogeneity of protein structure at the allosteric sites. Only at Palm Site II has it proved possible to identify agents approaching the desired breadth of activity, and in the meantime, advances in pan-genotypic NS5A and NS3 inhibitors, especially in combination with sofosbuvir, have delivered the desired clinical results.

A recent analysis of the overall attrition rate for research and development in HCV has estimated a 2.0% success rate, less than half the industry average (4.1%) [81], and the NNIs have seen fewer approvals than other classes. Nonetheless, the NNI discovery effort is testament to the creativity and ingenuity of thousands of researchers (many at research sites that have since been disbanded), with eventual success resulting from lessons learned collectively. Despite the attrition, highly effective and well-tolerated once-daily single-tablet regimens were introduced in a much shorter time than was the case for HIV [82], providing cures for a debilitating chronic disease.

Acknowledgment The author is grateful to Todd Appleby for assistance in the preparation of Figs. 1, 4, and 7.

Compliance with Ethical Standards

Conflict of Interest The author is an employee of Gilead Sciences and owns stock in Gilead Sciences.

Ethical Approval This article does not contain any studies with human participants or animals performed by any of the authors.

References

1. Houghton M (2009) Discovery of the hepatitis C virus. *Liver Int* 29(Suppl1):82–88
2. Yamashita T, Kaneko S, Shiota Y et al (1998) RNA-dependent RNA polymerase activity of the soluble recombinant hepatitis C virus NS5B protein truncated at the C-terminal region. *J Biol Chem* 273:15479–15486
3. Lesburg C, Cable MB, Ferrari E et al (1999) Crystal structure of the RNA-dependent RNA polymerase from hepatitis C virus reveals a fully encircled active site. *Nat Struct Biol* 6:937–943
4. Hashimoto H, Mizutani K, Yoshida A (2001) Novel fused-ring compounds useful for treating hepatitis C infection. WO-00147883
5. Ishida T, Suzuki T, Hirashima S et al (2006) Benzimidazole inhibitors of hepatitis C virus NS5B polymerase: identification of 2-[(4-diarylmethoxy)phenyl]-benzimidazole. *Bioorg Med Chem Lett* 16(7):1859–1863
6. Hirashima S, Suzuki T, Ishida T et al (2006) Benzimidazole derivatives bearing substituted biphenyls as hepatitis C virus NS5B RNA-dependent RNA polymerase inhibitors: structure-activity relationship studies and identification of a potent and highly selective inhibitor JTK-109. *J Med Chem* 49(15):4721–4736
7. Beaulieu PL, Fazal G, Gillard J et al (2002) Viral polymerase inhibitors. US-06448281
8. Beaulieu PL, Bös M, Cordingley MG et al (2012) Discovery of the first thumb pocket 1 NS5B polymerase inhibitor (BILB 1941) with demonstrated antiviral activity in patients chronically infected with genotype 1 hepatitis C virus (HCV). *J Med Chem* 55(17):7650–7666
9. Erhardt A, Deterding K, Benhamou Y et al (2009) Safety, pharmacokinetics and antiviral effect of BILB 1941, a novel hepatitis C virus RNA polymerase inhibitor, after 5 days oral treatment. *Antivir Ther* 14(1):23–32

10. LaPlante SR, Bös M, Brochu C et al (2014) Conformation-based restrictions and scaffold replacements in the design of hepatitis C virus polymerase inhibitors: discovery of delebovir (BI 207127). *J Med Chem* 57(5):1845–1854
11. Sarrazin C, Castelli F, Andreone P et al (2016) HCverso1 and 2: faldaprevir with delebovir (BI 207127) and ribavirin for treatment-naïve patients with chronic hepatitis C virus genotype-1b infection. *Clin Exp Gastroenterol* 9:351–363
12. Tomei L, Altamura S, Bartholomew L et al (2003) Mechanism of action and antiviral activity of benzimidazole-based allosteric inhibitors of the hepatitis C virus RNA-dependent RNA polymerase. *J Virol* 77(24):13225–13231
13. Avolio S, Di Filippo M, Harper S et al (2004) Indole acetamides as inhibitors of the hepatitis C virus NS5B polymerase. WO-04087714
14. Harper S, Pacini B, Avolio S et al (2005) Development and preliminary optimization of indole-N-acetamide inhibitors of hepatitis C virus NS5B polymerase. *J Med Chem* 48(5):1314–1317
15. Stansfield I, Ercolani C, Mackay A et al (2009) Tetracyclic indole inhibitors of hepatitis C virus NS5B-polymerase. *Bioorg Med Chem Lett* 19(3):627–632
16. Narjes F, Crescenzi B, Ferrara M et al (2011) Discovery of (7R)-14-cyclohexyl-7-{{[2-(dimethylamino)ethyl](methyl) amino]-7,8-dihydro-6H-indolo[1,2-e][1,5]benzoxazocine-11-carboxylic acid (MK-3281), a potent and orally bioavailable finger-loop inhibitor of the hepatitis C virus NS5B polymerase. *J Med Chem* 54(1):289–301
17. Ikegashira K, Oka T, Hirashima S et al (2006) Discovery of conformationally constrained tetracyclic compounds as potent hepatitis C virus NS5B RNA polymerase inhibitors. *J Med Chem* 49(24):6950–6953
18. Hudyma TW, Zheng X, Romine JL (2005) Inhibitors of HCV replication. US-050119318
19. McGowan DC, Vendeville SMH, Raboisson P (2010) Macrocyclic indole derivatives useful as hepatitis C virus inhibitors. WO2010018233A1
20. Cummings MD, Lin TI, Hu L et al (2014) Discovery and early development of TMC647055, a non-nucleoside inhibitor of the hepatitis C virus NS5B polymerase. *J Med Chem* 57(5):1880–1892
21. Zheng X, Hudyma TW, Martin SW et al (2011) Syntheses and initial evaluation of a series of indolo-fused heterocyclic inhibitors of the polymerase enzyme (NS5B) of the hepatitis C virus. *Bioorg Med Chem Lett* 21(10):2925–2929
22. Gopalsamy A, Collette MS, Ellingboe JW et al (2003) The use of pyranoindole derivatives as hepatitis C polymerase inhibitors. WO-03099275
23. Gopalsamy A, Lim K, Ciszewski G et al (2004) Discovery of pyrano[3,4-b]indoles as potent and selective HCV NS5B polymerase inhibitors. *J Med Chem* 47(25):6603–6608
24. Kneteman NM, Weiner AJ, O'Connell J et al (2006) Anti-HCV therapies in chimeric scid-Alb/uPA mice parallel outcomes in human clinical application. *Hepatology* 43(6):1346–1353
25. Laporte MG, Jackson RW, Draper TL et al (2008) The discovery of pyrano[3,4-b]indole-based allosteric inhibitors of HCV NS5B polymerase with in vivo activity. *ChemMedChem* 3(10):1508–1515
26. Love RA, Yu X, Diehl W, et al (2002) Hepatitis C virus (HCV) NS5B RNA polymerase and mutants thereof. EP-01256628
27. Li H, Tatlock J, Linton A et al (2009) Discovery of (R)-6-cyclopentyl-6-(2-(2,6-diethylpyridin-4-yl)ethyl)-3-((5,7-dimethyl-1,2,4-triazolo[1,5-a]pyrimidin-2-yl)methyl)-4-hydroxy-5,6-dihydropyran-2-one (PF-00868554) as a potent and orally available hepatitis C virus polymerase inhibitor. *J Med Chem* 52(5):1255–1258
28. Shi ST, Herlihy KJ, Graham JP et al (2009) Preclinical characterization of PF-00868554, a potent nonnucleoside inhibitor of the hepatitis C virus RNA-dependent RNA polymerase. *Antimicrob Agents Chemother* 53(6):2544–2552
29. Wagner F, Thompson R, Kantaridis C et al (2011) Antiviral activity of the hepatitis C virus polymerase inhibitor filibuvir in genotype 1-infected patients. *Hepatology* 54(1):50–59
30. Chan CKL, Bidard J, Das SK et al (2002) Novel biaryl compounds useful for the treatment of flavivirus infections. WO-02100846

31. Chan CKL, Bidard J, Das SK et al (2002) Novel substituted thiophene compounds useful for the treatment of flavivirus infections. WO-02100851
32. Chan L, Pereira O, Reddy TJ et al (2004) Discovery of thiophene-2-carboxylic acids as potent inhibitors of HCV NS5B polymerase and HCV subgenomic RNA replication. Part 2: tertiary amides. *Bioorg Med Chem Lett* 19(3):627–632
33. Cooper C, Lawitz EJ, Ghali P et al (2009) Evaluation of VCH-759 monotherapy in hepatitis C infection. *J Hepatol* 51(1):39–46
34. Thede K, Wunberg T, Lowinger T et al (2005) Substituted thiophenes. WO2005/063734
35. Wunberg T, Baumeister J, Gottschling D et al (2006) Alkynyl-substituted thiophenes. WO2005/072348
36. Gentile I, Buonomo AR, Zappulo E et al (2015) Discontinued drugs in 2012–2013: hepatitis C virus infection. *Expert Opin Investig Drugs* 24:239–251
37. Bravi G, Cheasty A, Corfield JA et al (2007) 4-Carboxy pyrazole derivatives as anti-viral agents. WO 2007/039146
38. Coulombe R, Goulet S, Thavonekham B et al (2008) Viral polymerase inhibitors. WO 2008/019477
39. Hucce O, Coulombe R, Bonneau P et al (2014) Molecular dynamics simulations and structure-based rational design lead to allosteric HCV NS5B polymerase thumb pocket 2 inhibitor with picomolar cellular replicon potency. *J Med Chem* 57(5):1932–1943
40. Lazerwith SE, Lew W, Zhang J et al (2014) Discovery of GS-9669, a thumb site II non-nucleoside inhibitor of NS5B for the treatment of genotype 1 chronic hepatitis C infection. *J Med Chem* 57(5):1893–1901
41. Dvory-Sobol H, Voitenleitner C, Mabery E et al (2014) Clinical and in vitro resistance to GS-9669, a thumb site II nonnucleoside inhibitor of the hepatitis C virus NS5B polymerase. *Antimicrob Agents Chemother* 58(11):6599–6606
42. Boyce SE, Tirunagari N, Niedziela-Majka A et al (2014) Structural and regulatory elements of HCV NS5B polymerase-- β -loop and C-terminal tail--are required for activity of allosteric thumb site II inhibitors. *PLoS One* 9(1):e84808
43. Appleby TC, Perry JK, Murakami E et al (2015) Viral replication. Structural basis for RNA replication by the hepatitis C virus polymerase. *Science* 347(6223):771–775
44. Dhanak D, Carr T (2001) Novel heterocyclic compounds for the treatment of hepatitis C viral infection. WO-00185720
45. Bravi G, Goodland HS, Haigh D et al (2003) 4-(5-Membered)-heteroaryl acyl pyrrolidine derivatives as HCV inhibitors. WO-03037894
46. Burton G, Ku TW, Carr TJ et al (2005) Identification of small molecule inhibitors of the hepatitis C virus RNA-dependent RNA polymerase from a pyrrolidine combinatorial mixture. *Bioorg Med Chem Lett* 15(6):1553–1556
47. Slater MJ, Amphlett EM, Andrews DM et al (2007) Optimization of novel acyl pyrrolidine inhibitors of hepatitis C virus RNA-dependent RNA polymerase leading to a development candidate. *J Med Chem* 50(5):897–900
48. Gray F, Amphlett E, Bright H et al (2007) GSK625433; a novel and highly potent inhibitor of the HCV NS5B polymerase. In: Abstract 594, 42nd annual meeting of the European Association for the Study of the Liver, Barcelona, 11–15 Apr 2007
49. Dhanak D, Duffy KJ, Sarisky RT et al (2003) Novel anti-infectives. WO-03037262
50. Shaw AN, Tedesco R, Bambal R et al (2009) Substituted benzothiadiazine inhibitors of hepatitis C virus polymerase. *Bioorg Med Chem Lett* 19(15):4350–4353
51. Randolph JT, Flentge CA, Huang PP et al (2009) Synthesis and biological characterization of B-ring amino analogues of potent benzothiadiazine hepatitis C virus polymerase inhibitors. *J Med Chem* 52(10):3174–3183
52. Ruebsam F, Murphy DE, Tran CV et al (2009) Discovery of tricyclic 5,6-dihydro-1H-pyridin-2-ones as novel, potent, and orally bioavailable inhibitors of HCV NS5B polymerase. *Bioorg Med Chem Lett* 19(22):6404–6412

53. Mallalieu NL, Rahimy MH, Crowley CA et al (2014) Pharmacokinetics and pharmacodynamics of setrobutvir, an orally administered hepatitis C virus non-nucleoside analogue inhibitor. *Clin Ther* 36(12):2047–2063
54. Dousson C, Surleraux D, Roland A et al (2009) Phosphadiazine HCV polymerase inhibitors I and II. WO 2009/032177
55. de Bruijne J, van de Wetering de Rooij J, van Vliet AA et al (2012) First-in-human study of the pharmacokinetics and antiviral activity of IDX375, a novel nonnucleoside hepatitis C virus polymerase inhibitor. *Antimicrob Agents Chemother* 56(8):4525–4528
56. Wagner R, Tufano MD, Stewart KD et al (2009) Uracil or thymine derivative for treating hepatitis C. WO 2009/039127
57. Liu Y, Lim BH, Jiang WW et al (2012) Identification of aryl dihydrouracil derivatives as palm initiation site inhibitors of HCV NS5B polymerase. *Bioorg Med Chem Lett* 22(11):3747–3750
58. Randolph JT, Krueger AC, Donner PL et al (2018) Synthesis and biological characterization of aryl uracil inhibitors of hepatitis C virus NS5B polymerase: discovery of ABT-072, a trans-Stilbene analog with good oral bioavailability. *J Med Chem* 61(3):1153–1163
59. Talamas FX, Ao-Ieong G, Brameld KA et al (2013) De novo fragment design: a medicinal chemistry approach to fragment-based lead generation. *J Med Chem* 56(7):3115–3119
60. Schoenfeld RC, Bourdet DL, Brameld KA et al (2013) Discovery of a novel series of potent non-nucleoside inhibitors of hepatitis C virus NS5B. *J Med Chem* 56(20):8163–8182
61. Talamas FX, Abbot SC, Anand S et al (2014) Discovery of N-[4-[6-tert-butyl-5-methoxy-8-(6-methoxy-2-oxo-1H-pyridin-3-yl)-3-quinolyl]phenyl]methanesulfonamide (RG7109), a potent inhibitor of the hepatitis C virus NS5B polymerase. *J Med Chem* 57(5):1914–1931
62. Gu B, Johnston VK, Gutshall LL et al (2003) Arresting initiation of hepatitis C virus RNA synthesis using heterocyclic derivatives. *J Biol Chem* 278(19):16602–16607
63. Burns CJ, Del Vecchio AM, Bailey TR et al (2004) Benzofuran compounds, compositions and methods for treatment and prophylaxis of hepatitis C viral infections and associated diseases. WO-04041201
64. Kneteman NM, Howe AY, Gao T et al (2009) HCV796: a selective nonstructural protein 5B polymerase inhibitor with potent anti-hepatitis C virus activity in vitro, in mice with chimeric human livers, and in humans infected with hepatitis C virus. *Hepatology* 49(3):745–752
65. Feldstein A, Kleiner D, Kravetz D et al (2009) Severe hepatocellular injury with apoptosis induced by a hepatitis C polymerase inhibitor. *J Clin Gastroenterol* 43(4):374–381
66. Koch U, Mackay AC, Narjes F et al (2008) Benzofuran-carboxamide derivatives as antiviral agents. WO 2008/125874
67. McComas CC, Palani A, Chang W et al (2017) Development of a new structural class of broadly acting HCV non-nucleoside inhibitors leading to the discovery of MK-8876. *ChemMedChem* 12(17):1436–1448
68. Labadie SS, Lin CJJ, Talamas FX et al (2009) Heterocyclic antiviral compounds. WO 2009/101022
69. Pracitto R, Kadow JF, Bender JA et al (2010) Compounds for the treatment of hepatitis C. US 2010/0063068
70. Yeung K-S, Parcella KE, Bender JA et al (2010) Compounds for the treatment of hepatitis C. US 2010/030592
71. Yeung K-S, Beno BR, Parcella K et al (2017) Discovery of a hepatitis C virus NS5B replicase palm site allosteric inhibitor (BMS-929075) advanced to phase I clinical studies. *J Med Chem* 60(10):4369–4385
72. Maynard A, Crosby RM, Ellis B et al (2014) Discovery of a potent boronic acid derived inhibitor of the HCV RNA-dependent RNA polymerase. *J Med Chem* 57(5):1902–1913
73. Voitenleitner C, Crosby R, Walker J et al (2013) In vitro characterization of GSK2485852, a novel hepatitis C virus polymerase inhibitor. *Antimicrob Agents Chemother* 57(11):5216–5224
74. Hang JQ, Yang Y, Harris SF et al (2009) Slow binding inhibition and mechanism of resistance of non-nucleoside polymerase inhibitors of hepatitis C virus. *J Biol Chem* 284(23):15517–15529

75. Puerstinger G, Paeshuysse J, De Clercq E et al (2007) Antiviral 2,5-disubstituted imidazo[4,5-c]pyridines: from anti-pestivirus to antihepatitis C virus activity. *Bioorg Med Chem Lett* 17(2):390–393
76. Shih I-H, Vliegen I, Peng B et al (2011) Mechanistic characterization of GS-9190 (tegobuvir), a novel nonnucleoside inhibitor of hepatitis C virus NS5B polymerase. *Antimicrob Agents Chemother* 55(9):4196–4203
77. Wong KA, Xu S, Martin R et al (2012) Tegobuvir (GS-9190) potency against HCV chimeric replicons derived from consensus NS5B sequences from genotypes 2b, 3a, 4a, 5a, and 6a. *Virology* 429(1):57–62
78. Hebner CM, Han B, Brendza KM et al (2012) The HCV non-nucleoside inhibitor tegobuvir utilizes a novel mechanism of action to inhibit NS5B polymerase function. *PLoS One* 7(6): e39163
79. Leivers M, Miller J (2011) Imidazopyridazine compounds for treating viral infections. WO 2011/026091
80. Leivers M, Miller JF, Chan SA et al (2011) Imidazopyridazine hepatitis C virus polymerase inhibitors. Structure-activity relationship studies and the discovery of a novel, traceless prodrug mechanism. *J Med Chem* 57(5):1964–1975
81. Calcoen D, Elias L, Yu X (2015) What does it take to produce a breakthrough drug? *Nat Rev Drug Discov* 14(3):161–162
82. Watkins WJ, Desai MC (2013) HCV versus HIV drug discovery: Déjà vu all over again? *Bioorg Med Chem Lett* 23(8):2281–2287

Discovery of Beclabuvir: A Potent Allosteric Inhibitor of the Hepatitis C Virus Polymerase



Robert G. Gentles

Contents

1 Introduction	194
References	224

Abstract The discovery of beclabuvir occurred through an iterative series of structure-activity relationship studies directed at the optimization of a novel class of indolobenzazepines. Within this research, a strategic decision to abandon a highly potent but physiochemically problematic series in favor of one of lower molecular weight and potency was key in the realization of the program's objectives. Subsequent cycles of analog design incorporating progressive conformational constraints successfully addressed off-target liabilities and identified compounds with improved physiochemical profiles. Ultimately, a class of alkyl-bridged piperazine carboxamides was found to be of particular interest, and from this series, beclabuvir was identified as having superior antiviral, safety, and pharmacokinetic properties. The clinical evaluation of beclabuvir in combination with both the NS5A replication complex inhibitor daclatasvir and the NS3 protease inhibitor asunaprevir in a single, fixed-dose formulation (Ximency) resulted in the approval by the Japanese Pharmaceutical and Food Safety Bureau for its use in the treatment of patients infected with genotype 1 HCV.

Keywords Asunaprevir, Beclabuvir, Daclatasvir, HCV, Hepatitis C virus, NS5B inhibitor, Polymerase inhibitor

R. G. Gentles (✉)

Department of Discovery Chemistry and Molecular Technologies, Bristol-Myers Squibb Research and Development, Wallingford, CT, USA

e-mail: robert.gentles@bms.com

1 Introduction

As part of a large multidisciplinary team at Bristol-Myers Squibb tasked with the development of effective oral treatments for hepatitis C virus (HCV) infections, we were involved in the identification of drug combinations that would target two or preferably three orthogonal viral proteins [1]. This strategy was predicated on the success of co-administration of agents of distinct mechanisms of action used to treat human immunodeficiency virus-1 (HIV-1) infections; in these instances, tertiary combinations of direct-acting antivirals (DAAs) were effective in controlling the emergence of viral resistance, a necessary feature of any therapy targeting a cure in HCV infection [2].

The focus of our specific efforts was the discovery of potent inhibitors of the HCV NS5B polymerase enzyme [3]. As polymerases of a number of viruses had been shown to be attractive targets for the development of DAA therapeutics, we embarked on this discovery with the assurance of at least some successful precedent [4]. At the inception of our research, the optimal therapy for HCV patients required extended (48 weeks) co-administration of pegylated interferon- α (Peg-IFN) and ribavirin (RBV), a regime that resulted in only 40–50% of genotype 1 patients achieving a sustained viral response (SVR), as defined as the absence of detectable viral RNA in serum 6 months after conclusion of treatment [5]. Additionally, Peg-IFN treatments are associated with severe flu-like side effects, as well as fatigue, drowsiness, and anemia. This leads to significant patient discontinuations despite the severe prognosis of the untreated disease [6]. The necessity to address the substantial unmet medical need with a well-tolerated and effective oral therapy was the compelling impetus for the initiation of our research.

HCV is a member of the *Flaviviridae* family of viruses and has a single-stranded, positive-sense RNA genome [7, 8]. Variability within the gene that encodes the polymerase enzyme, the nonstructural protein 5B (NS5B), is used to classify the virus into seven major genotypes (1–7) and five principal subclasses (a, b, c, d, and e) [9]. The genotypes vary geographically, with genotype 1 predominating in North America, Europe, and Japan, with smaller populations in these areas also infected with genotypes 2 and 3. Genotypes 4 and 5 are found almost exclusively in Africa, whereas genotype 6 is most prevalent in Asia [10, 11]. As an initial focus, and partly driven by the properties of the program's early lead compounds, targeting of genotype 1 was prioritized, with a longer-term objective being the development of pan-genotypic inhibitors.

NS5B is an RNA-dependent RNA polymerase that forms the catalytic core of the viral replicase complex [12–14]. It is essential for HCV replication, and given that no mammalian congener exists, targeting this enzyme was anticipated to have a reduced risk of unwanted side effects [15]. Additionally, priority was given to the identification of allosteric inhibitors in the belief that the developability of such compounds may be more facile than traditional active-site nucleoside-based inhibitors.

Our initial attempts at identification of viable leads through a high-throughput screening campaign proved to be frustrating; while inhibitors of the enzyme were

identified, attempts to advance these series in the context of cellular replicon assays proved to be challenging, primarily due to difficulties in achieving cellular activity without obfuscating cytotoxicity. In this review, the biochemical enzyme assays (for which IC_{50} s are reported) were performed with recombinant wild-type NS5B (genotype 1b, Con1) containing a carboxyl-terminal deletion of 18 amino acids and a resistance variant containing a single amino acid substitution, P495L. The inhibition of the incorporation of radiolabeled nucleotides in these transcriptional assays was detected using scintillation proximity assay (SPA) beads [16]. Compound inhibitory activities were also determined in replicon systems (for which we report EC_{50} s) consisting of human hepatocyte-derived cell lines (Huh-7) that constitutively express sub-genomic HCV RNA (genotypes 1b and 1a, Con1 and H77c, respectively) encoding essential cis-elements and the HCV nonstructural proteins required for RNA replication. Inhibition of viral RNA replication correlates with a decrease in HCV RNA and protein production. Reduction in HCV replication was measured indirectly by monitoring HCV NS3 protease activity using a fluorescence resonance energy transfer (FRET) assay [17–19]. The cytotoxicity of compounds in the replicon host cells was determined by measurement of the fluorescence of Alamar blue dye, an indicator of mitochondrial function and cellular metabolism.

Given the lack of success in identifying progressable leads from in-house sources, the program's focus shifted to the evaluation of reported inhibitors, and we initially attempted to characterize and investigate the indole and benzimidazole chemotypes **1** and **2** (Fig. 1) [20, 21]. While these compounds exhibited modest antiviral activity in the genotype 1b replicon assay (EC_{50} values of 400 nM and 100 nM, respectively), both displayed good cellular therapeutic indexes ($CC_{50}/EC_{50} > 20$), and it was considered that opportunities existed to address what appeared to be structural and physicochemical liabilities in these series.

Considering first compound **1**, of the many initiatives undertaken with this chemotype, one of the more productive involved a de-annulation derived from a one-carbon excision from the parent heterocycle [22]. This generated the imidazole-appended acrylate **3** shown in Fig. 2. Encouragingly, this derivative retained a significant activity and prompted the evaluation of a number of isosteric heterocycles. Unfortunately, in the case of 1,3,5-substituted pyrazoles, as exemplified by

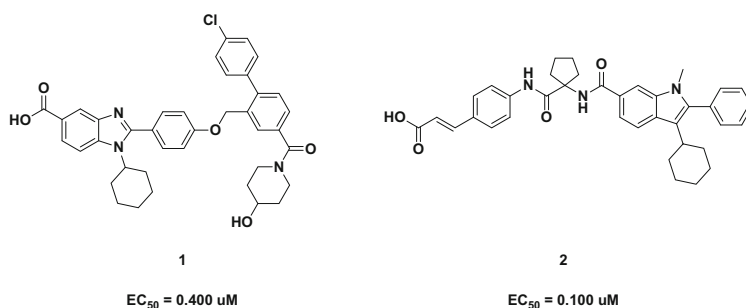


Fig. 1 Literature HCV NS5B inhibitors

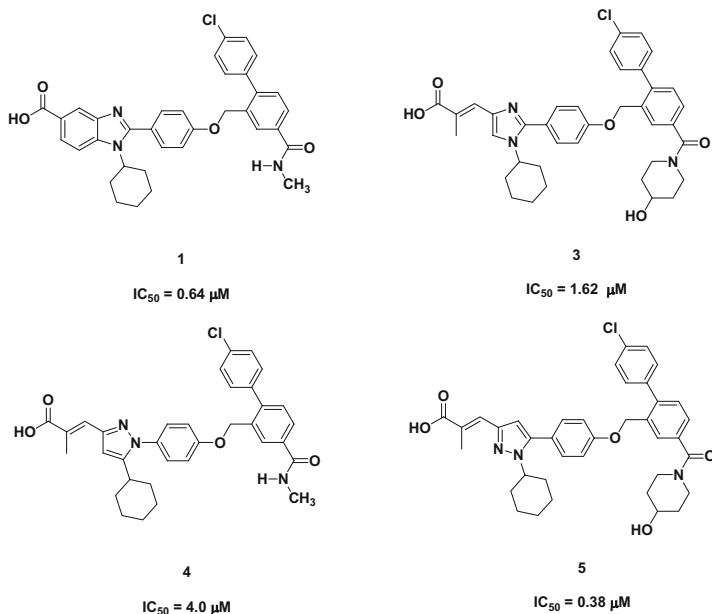


Fig. 2 Exploratory investigations on benzimidazole lead chemotype

compound **4**, it was disappointing that these proved to be less active than the parent benzimidazole. Interestingly, however, the isomeric derivative **5** was found to be essentially equipotent with the original lead; this was attributed to a reduction in allylic strain in a putative bioactive conformation [22]. In modeling studies, the differences in potencies of many of the heterocycles explored could be most comprehensively rationalized by considering subtle variations in the vectors defined by the distances between the cyclohexyl moiety and the acid functionalities of the various analogs tested. It was known that the cyclohexyl group appeared to function as an anchor, binding the ligand to NS5B; variations in the distances between this functionality and the acid moieties were projected to modulate key binding interactions between each of the ligands' carboxylate moieties and Arg503 of NS5B, and this concept could rationalize much of the potency variations observed with the analogs explored.

Given the preference for the geometry presented by compound **5**, this molecular silhouette was used in subsequent studies as a template to assess a series of derivatives represented by the generic structure shown in Fig. 3.

Using this scaffold efforts were directed at the introduction of structural diversity at the R_1 , R_2 , and Ar_3 vectors, and the attendant analog screen resulted in the identification of the piperidine carboxamide **6**, a compound that exhibited moderately potent inhibition in both the NS5B enzyme assay and in a genotype 1b replicon system, as shown in Fig. 4. The compound was determined to be relatively nontoxic ($CC_{50} = 25 \mu M$) and had a therapeutic index of >60 . Furthermore, the closely

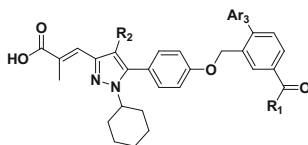


Fig. 3 Molecular template utilized in pyrazole SAR studies

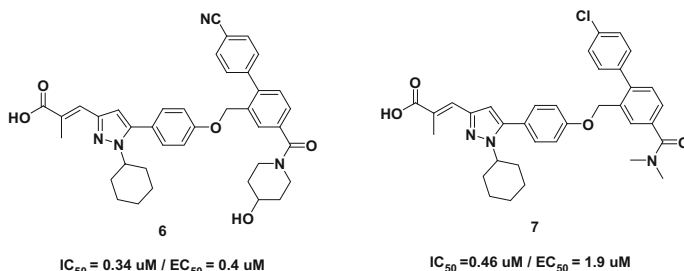


Fig. 4 Early pyrazole lead structures

related analog **7** not only exhibited similar activity but was shown to have good bioavailability in rat when dosed orally at 2 mg/kg, ($F = 69\%$, $t_{1/2} = 1.3 \pm 0.7$ h).

These activities and profiles were encouraging and some clear paths for further advancement were identified. However, more compelling opportunities were presenting themselves as a result of concurrent efforts on the indole chemotype **2** (Fig. 5), and these subsequently became the focus of attention.

The initial explorations with this chemotype contrasted with the approach that was adopted above, in that an annulation strategy was first investigated [23]. In order to address what was perceived as liabilities within the series, specifically the high molecular weight, polyamidic character, and high lipophilicity, avenues were sought, whereby increased potency could be achieved in smaller, more ligand-efficient derivatives.

It was projected that this might be achieved through the introduction of novel bridging tethers between the pendent phenyl moiety and the core indole heterocycle. In addition, it was anticipated that such a strategy would induce a degree of pre-organization through conformational constraint, as well as provide a scaffold from which additional functionality could be extended along unique vectors. In some variants of this basic concept, additional polarity was introduced into the system through the incorporation of heteroatoms and polar linking moieties within the bridging groups themselves. To explore these concepts, the simple 6-carboxylate derivatives were examined first as these would lead to lower molecular weight, non-amidic analogs. However, to fully assess the potential of the bridging elements, the related cinnamic acid conjugates were also considered. This led to the synthesis of the indolo-fused heterocycles shown in Fig. 6.

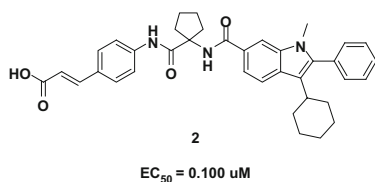


Fig. 5 Initial indole lead structure

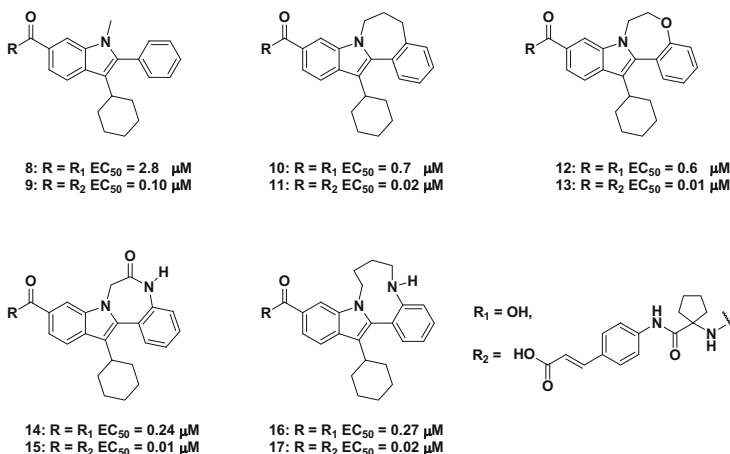


Fig. 6 Truncated and extended indolo-fused heterocyclic NS5B inhibitors

The low-energy geometries of the truncated indolo acids were explored using molecular mechanics employing an OPLS force field [24]. Optimized structures are shown in Fig. 7, and the dihedral angles between the phenyl and indole rings for each heterocycle are listed in Table 1. In the interpretation of the subsequently derived structure-activity relationships (SARs), compounds **8** and **9** were used as primary comparators.

What emerged quickly from these investigations was that all of the annulations were associated with significant (four- to tenfold) improvements in potency, in both the truncated and the extended cinnamic acid series. The optimized dihedral angles between the pendent phenyl and the indole cores did not appear to be key determinants of activity since equipotent derivatives with inclinations between these moieties of between 43° and 70° were observed. This suggested that the preferred bioactive conformations could be easily accessed in all of the ring systems explored. None of the indolo-fused heterocycles are rigid, and, correspondingly, any entropic factors positively contributing to binding may be quite modest. This, in conjunction with the observation that the introduction of polarity into various positions on the bridging elements was not only tolerated, but could be associated with further improvements in activity, as seen in analogs **12** through **16**, was supportive of the

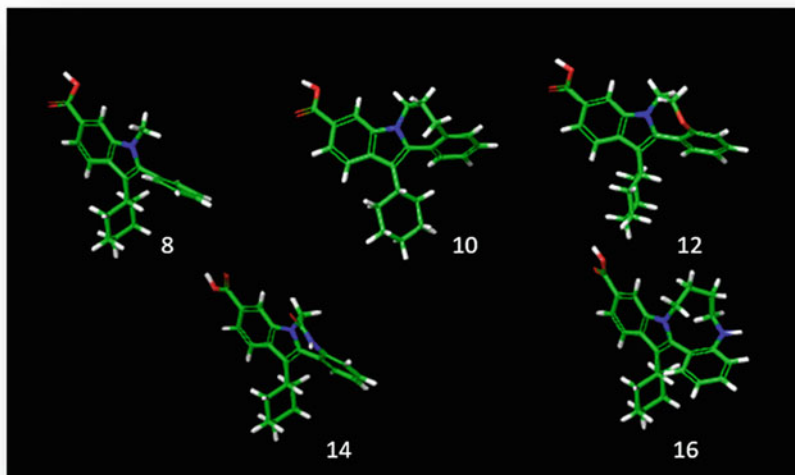


Fig. 7 Molecular mechanics (OPLS) minimized structures of the indolo-fused heterocycles [24]

Table 1 Dihedral angles of bridged indolo analogs and their related replicon activities

Compound	Dihedral angle	Replicon 1B EC ₅₀ (μM) ^a
8	66°	2.8
10	45°	0.6
12	49°	0.7
14	43°	0.2
16	71°	0.3

^aValues are means of three experiments. All analogs were equipotent with respect to replicon genotype 1a and 1b inhibition

interpretation of productive interactions between the tethering elements and the protein. Furthermore, the significant enhancement of activity noted in compounds **14** and **15** gave an early insight into the possibility of further incorporation of amidic motifs at this position on the chemotype, *vide infra*.

Within the extended cinnamate series, compound **15** was of particular note given its exquisite potency, displaying EC₅₀ values of 10 nM and 8 nM against genotypes 1a and 1b, respectively. This represented a milestone within the program since it achieved the clinical candidate potency objectives of <10 nM against both of the primary targeted viral genotypes. A co-crystal structure of this analog complexed to NS5B [1b Bartenschlager construct] was obtained and is shown in Fig. 8 [25, 26].

It can be seen in the depiction above that NS5B adopts the figurative right-hand topology typically observed with RNA polymerases. The cinnamate moiety is observed to bind in the thumb domain of the enzyme with the cyclohexyl ring

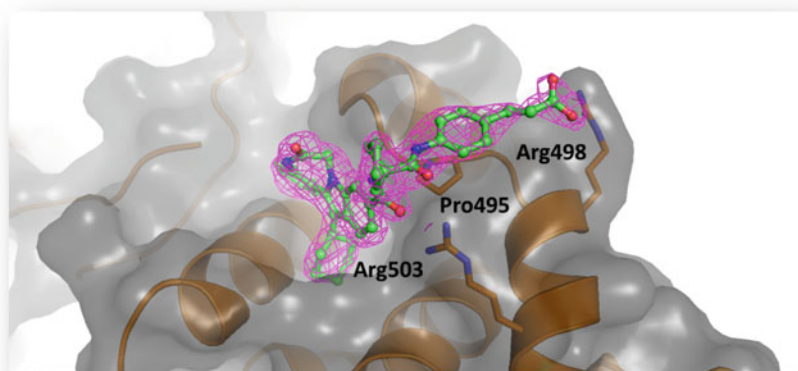


Fig. 8 Compound **8** bound to HCV genotype 1b NS5B (Bartenschlager) [25]. The protein proximal to the P495 site is represented by a surface (gray) and cartoon (orange). The side chains of Pro495, Arg498, and Arg503 are represented with sticks (orange carbon atoms), and compound **8** is depicted in ball-and-stick representation with green carbon atoms. The initial (prior to placing compound **8** in the model) 2Fo-Fc electron density is contoured at 1σ (magenta). Image created with PyMol (www.pymol.org)

occupying a small hydrophobic pocket proximal to P495 (explaining the P495L resistance profile of all of the compounds of the current discussion, *vide infra*) [23, 26]. The amidic N-H moiety of the proximal carboxamide forms a hydrogen bond with ARG 503, and the terminal carboxylate forms a salt bridge with R498. The fused, formerly pendent phenyl group lies in a hydrophobic cleft on the surface of NS5B and is inclined at an angle of $\sim 46^\circ$ relative to the indole ring. This is similar to that observed in the minimized structure of the indolobenzazepinones **14** and **15** and in these specific analogs doubtless contributes to their potency. It should be noted that in the above structure and in others that were obtained, the $\Delta 1$ finger domain of the enzyme could not be resolved due to disorder in this region of the peptide. This significantly curtailed the ability to fully adopt a rational design approach, especially in relation to modifications of the bridging tethers, and this will be elaborated on later in this account.

A number of potent leads from these efforts were advanced into a succession of rat pharmacokinetic (PK) studies, selected results from which are shown in Table 2. A striking aspect of these data was the relatively poor PK profiles exhibited by the cinnamate derivatives **11**, **15**, and **17**. All showed low bioavailability and all exhibited moderate to high clearances. This could be rationalized by recognizing that these analogs retained both the polyamidic and acidic character of the original lead. Much more interesting, however, was that the acidic polar lactam **14** exhibited significantly improved exposure despite displaying high clearance. It was quickly established that the latter was due to glucuronidation of the carboxylate moiety, an

Table 2 Rat PK results observed with select examples of the indolo-fused tetracyclic NS5B inhibitors shown in Fig. 2

Compound	F (%) ^a	AUC (μM h)	Clearance (mL/min/kg) ^b
10	6	1.3	53
11	8	0.3	250
13	5	0.8	17
14	18	2.2	35
15	3	0.7	13
17	12	3.6	9

^aOral bioavailability^bIV (dose 2 mg/kg)

issue that might be resolved given the structural information obtained from the data shown in Fig. 8, as well as that from related structures.

This proved to be a critical and pivotal point in the identification of beclabuvir: the decision was made to pursue the optimization of the truncated indolobenzodiazepine **14** rather than persist with the more potent, extended variants typified by **15**. This change in the focus of the program was driven by the realization that there was no clear path to address the issues identified with the latter compound, whereas the problems associated with the truncated version seemed more tractable, assuming that the potency of this series could be advanced sufficiently.

From this point, two interdependent avenues of research were conducted. The first attempted to establish if potency could be enhanced by further modification of the bridging element, and the second was to address the glucuronidation issue which, if resolved successfully, would result in significantly improved PK properties.

An extensive array of fused heterocycles were explored in the context of modifications of the bridging motifs, but one of the most significant resulted from a transposition of the amide from the lactam topology in **14**, to the pendent carboxamide motif, as represented by **18** in Fig. 9. This configuration retained the 6,5,7,6 ring system of the parent heterocycle, and when the transposition was coupled with concomitant introduction of unsaturation into the azepine ring, the overall topology of the precursor system was recapitulated and the introduction of a chiral center obviated. Carboxamides are ubiquitous in medicinal chemistry since they can improve the solubility of a molecule as well as provide a flexible coupling element that projects both H-bonding donor and acceptor motifs for interaction with cognate targets. The incorporation of this element in an exocyclic fashion on the indolobenzazepine ring system facilitated a rapid scan of an extensive array of amines and quickly identified what proved to be a progressable series.

While a large number of carboxamides of the general structure depicted by **18** were found that retained significant activity, it was discovered that simple morpholine carboxamides such as **19** were among the most ligand-efficient derivatives identified, and had the best overall balance of potency and targeted genotype coverage, as can be seen from Fig. 10.

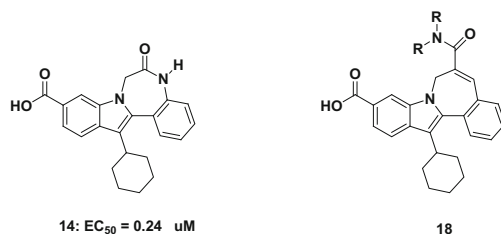


Fig. 9 Indole leads exhibiting transposition of carboxamide moieties

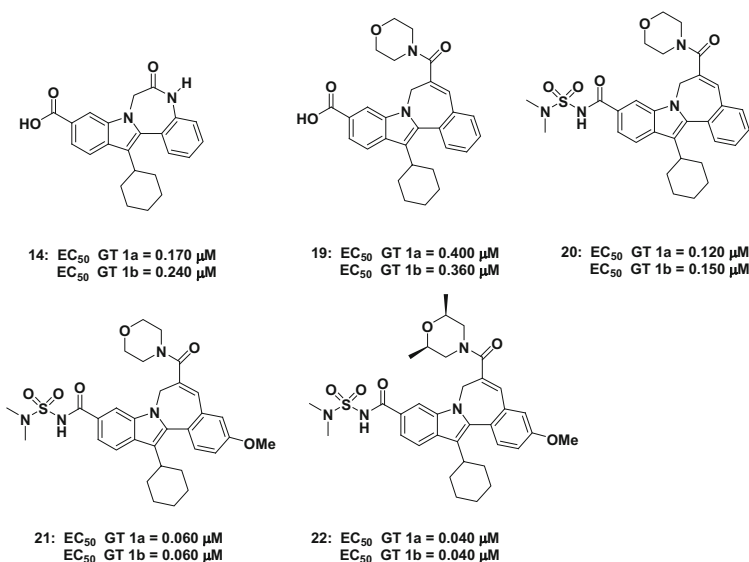


Fig. 10 Pendent morpholine and functionalized-morpholine carboxamides in lead indolobenzazepine series

However, the exposure profiles of these simple indole carboxylates following oral dosing to rats were frequently poor, as noted above. Correspondingly, a concurrent parallel effort was directed at the evaluation of acid isosteres, and a particularly productive discovery was the identification of the *N,N*-dimethylsulfamide moiety, as exhibited in analogs **20**, **21**, and **22** [27].¹ This modification not only modestly enhanced the activity of the series but was also found to obviate the glucuronidation issue noted previously. With the acylsulfamide **20**, potencies approaching 100 nM were achieved against the primary genotypes of interest with an analog with a significantly improved PK profile: Compound **20** was 30% orally bioavailable in

¹The research discussed in [27] was essentially mirrored in the earlier related studies cited in the text.

the rat at a dose of 5 mpk, and achieved liver levels of 24 μM , as determined 4 h post dose in an abbreviated PK study.

Further optimization of the chemotype was directed at identifying optimal substituents on the fused aryl moiety. The introduction of additional functionality at this position on the chemotype was challenging, given that the diversity elements had to be introduced at an early stage of the synthesis, as can be appreciated from the route depicted in Fig. 11.

Initial syntheses employed in these efforts introduced the aryl diversity element through boronate styrene derivatives of the type shown above. These were employed in a Suzuki coupling with the bromoindole **23** to give the 2-arylindoles **24** [28–31]. Subsequent Michael addition with methyl 2-(bromomethyl)acrylate afforded dienes of the type **25**, which were employed in an olefin metathesis ring closure to generate the intermediate indolobenzazepines **26**. Subsequent derivatization of the two acid moieties allowed access to the final targets [32–34]. The yields of these reactions were frequently poor, prompting the development of the alternative synthesis depicted at the bottom of Fig. 11. This latter route utilized the arylaldehydes **27** in a tandem Michael addition/Wadsworth-Horner-Emmons reaction with *tert*-butyl 2-(dimethoxyphosphoryl)acrylate to generate the differentially functionalized diester intermediates **28** [35]. The two carboxylate moieties could chemoselectively be cleaved under orthogonal conditions to provide either mixed acid ester. This additional degree of freedom in the order of subsequent derivatizations expedited ensuing SAR studies.

Using these methodologies, a significant number of analogs were prepared from which it was determined that the simple 4-methoxy-appended aryl was a preferred motif. This group significantly improved the potency of analogs into which it had been incorporated, as can be seen in compound **21**, the first analog in a non-cinnamate series that achieved potency of <100 nM in the replicon assays.

Extensive profiling of members of this series highlighted some recurrent issues, as typified by the poor solubility and human pregnane X receptor (hPXR) activation

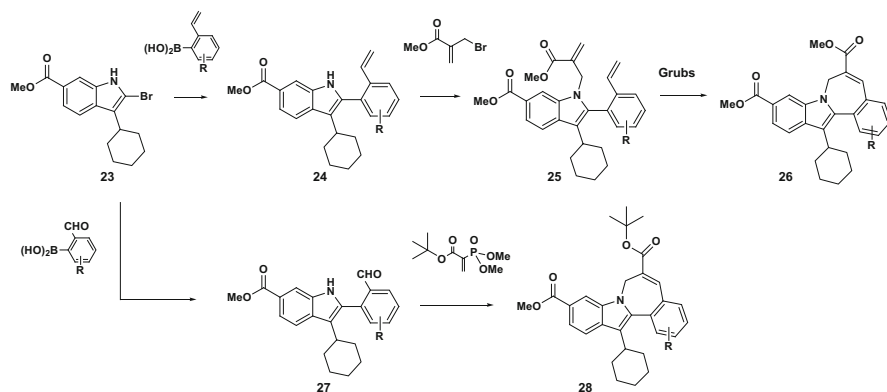


Fig. 11 Synthetic routes to access key intermediates required in the syntheses of indolobenzazepines

exhibited by compound **20**. This derivative had an amorphous aqueous solubility of $<1 \mu\text{g/mL}$ and an IC_{50} of 440 nM in the PXR assay, indicating a significant potential for induction of drug-drug interactions (DDIs) [36]. This was of concern given the anticipated use of this inhibitor as part of a multi-DAA regime. However, continued profiling of analogs in this series demonstrated that the introduction of steric bulk around the ether element of the morpholine ring could eliminate this property, and with the simple 2,6-dimethylmorpholine derivative **22**, a benchmark compound was identified that exhibited a potent and balanced genotype inhibition profile ($\text{EC}_{50 \text{ 1a/1b}} = 40/40 \text{ nM}$) and a PXR IC_{50} value of $>10 \mu\text{M}$. In rat PK studies, this compound also exhibited high liver levels of $33 \mu\text{M}$ when measured 4 h after an oral dose of 10 mg/kg .

Strongly encouraged by what had been achieved, further modifications to the bridging tethers were aggressively investigated. A particularly fruitful finding in this area involved a cyclopropanation of the olefin group in the fused benzazepine moiety of the parent heterocycle. The intentions with this manipulation were twofold: firstly, to establish a supplementary degree of conformational constraint across the ring system and, secondly, to investigate possible interactions between the polarized C-Hs of the cyclopropyl motif and the NS5B protein, this interaction being of interest from prior structural investigations [23]. Furthermore, this modification had the added advantage of removing a potential Michael acceptor (although in biotransformation studies on the parent heterocycles, this reactivity was never observed).

Racemic and enantiomerically pure forms of the cyclopropylindolobenzazepines were accessed by a number of routes. However, the chemistry depicted in Fig. 12 allowed the introduction of the amine component of the carboxamide moiety at the last step of the synthesis, thus facilitating both the rapid scanning of a variety of derivatives and efficient access to enantiomerically pure analogs.

This methodology required the hydrolysis of **23** under basic conditions followed by coupling of the resultant acid **29** with *N,N*-dimethylsulfonylurea to provide the acyl sulfamide **30** [31]. This could subsequently be coupled with 4-methoxyphenylboronic acid (**31**) using Suzuki-Miyaura conditions to produce the aromatic aldehyde **32** [28–30]. A tandem Michael addition and Horner-Wadsworth-Emmons alkylation-olefination procedure employing the dimethylphosphonate **33** provided access to the indolobenzazepine **34** [35]. The resultant embedded methyl acrylate could be efficiently converted to the racemic cyclopropyl derivative **35** under Corey-Chaykovsky conditions, and subsequent chiral resolution of the racemic **35** (achievable on a multi-gram scale) using preparative chiral HPLC provided the (–)-enantiomer **37** [37]. This intermediate was used to generate the more highly active enantiomers via hydrolysis to the enantiomerically pure acid **38** and subsequent conversion to the desired optically pure carboxamides, shown generically as **39**. The alternate (+)-enantiomer **36** could be utilized in the generation of the antipodes, and these consistently exhibited a three- to fivefold loss of inhibitory activity relative to their related enantiomers. The assignment of the absolute stereochemistry in the cyclopropyl-fused analogs was determined based on data obtained from an X-ray co-crystal structure of compound **66** (*vide infra*) bound to NS5B, data that also

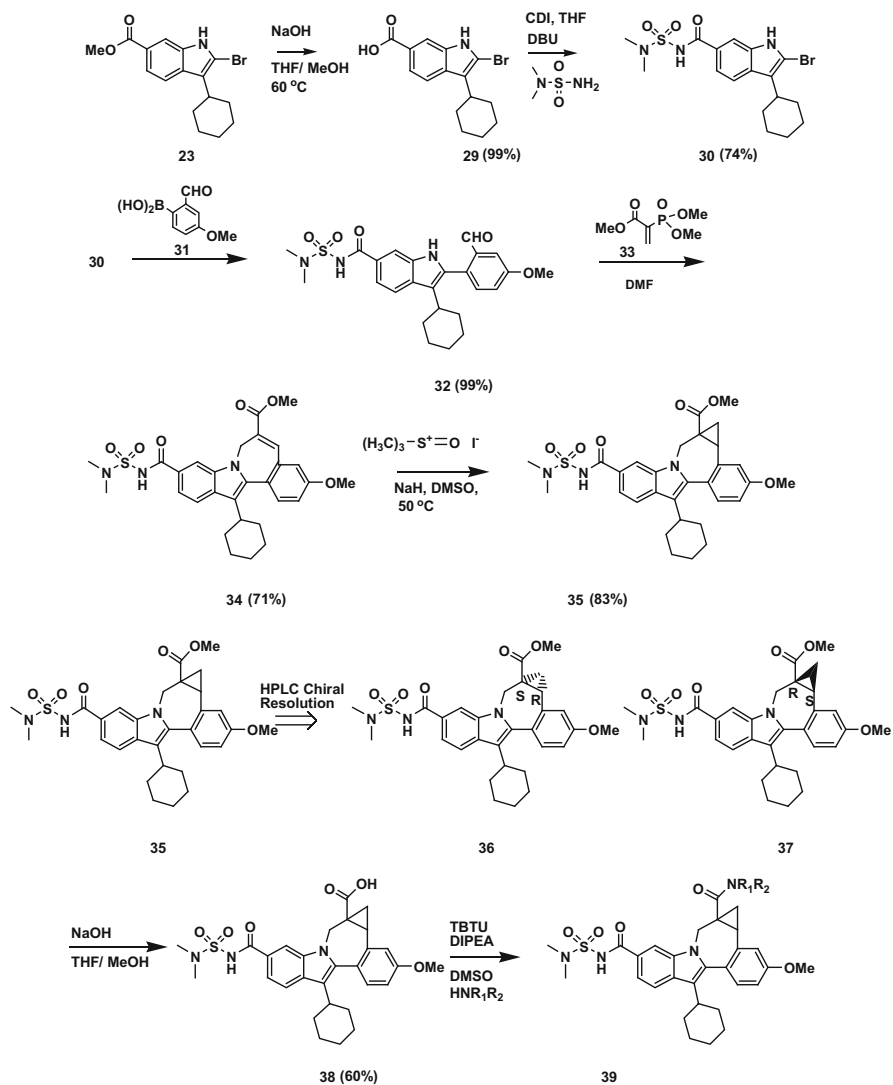


Fig. 12 Methodology utilized in accessing specific enantiomers of cyclopropyl fused indolobenzazepines

supported the idea of productive interactions between the hydrogen atoms of the cyclopropyl motif and NS5B.

As there was a significant motivation to quickly develop SAR within this chemotype, racemic materials were screened initially, and for those analogs that showed promise, a comprehensive assessment of the individual enantiomers was subsequently conducted. The data on selected key examples from this endeavor are shown in Fig. 13.

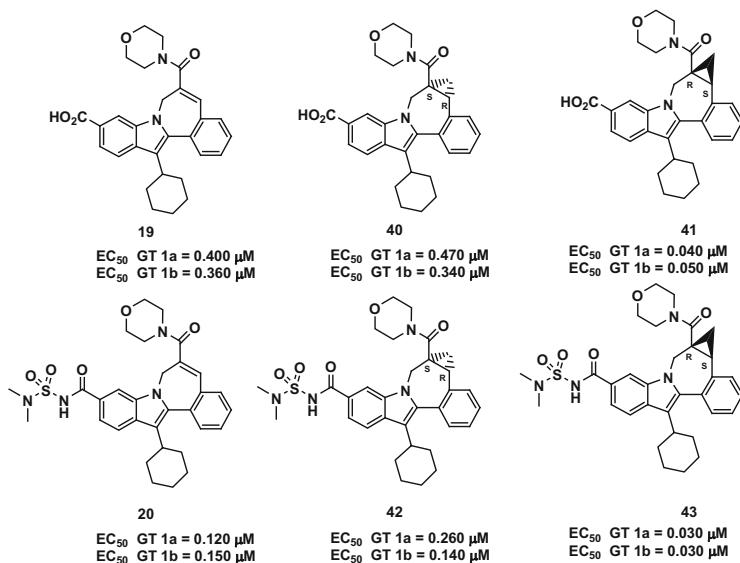


Fig. 13 Impact on potency associated with the introduction of a fused cyclopropyl moiety

In reviewing these data, what became immediately apparent was that for those enantiomers with the *R* configuration at the carboxamide-appended carbons, as in **41** and **43**, an approximately five- to tenfold enhancement of antiviral activity was observed relative to the unsaturated congeners **19** and **20**. Contrastingly, the cyclopropyl antipodes **40** and **42** were essentially equipotent with the related indolobenzazepines. Importantly, these observations confirmed a working hypothesis that the introduction of the cyclopropane modification with the correct stereochemistry might be associated with some enhancement in activity. This was predicated on modeling studies in which potential binding modes of **42** and **43** in Site I of the thumb domain of NS5B were compared, as shown in Fig. 14 [38]. In these models, both enantiomers are presented in what is calculated to be optimized conformations, and both compounds exhibit a number of redundant interactions with the enzyme. However, relative to **42**, the antipode **43** participates in additional productive contacts, most notably between elements in the morpholine moiety and the side-chain methyl group of residue T399, as well as interaction between the polarized methylene hydrogen atoms in the cyclopropyl group and the backbone carbonyl oxygen of L492. Furthermore, the carbonyl oxygen of the acylsulfamide in **43** is better positioned for optimal H-bonding with R503. This is in contrast to what is predicted with **42**, where steric impediments between the morpholine ring and the acylsulfamide reduce the latter's engagement with R503. Additionally, the disposition of the cyclopropyl moiety in **42** prevented contact of its methylene hydrogens with the carbonyl oxygen of L492. Although not apparent from these static models, it was considered reasonable to assume that the cyclopropyl moiety introduced a degree of conformational constraint within the indolobenzazepine ring system and

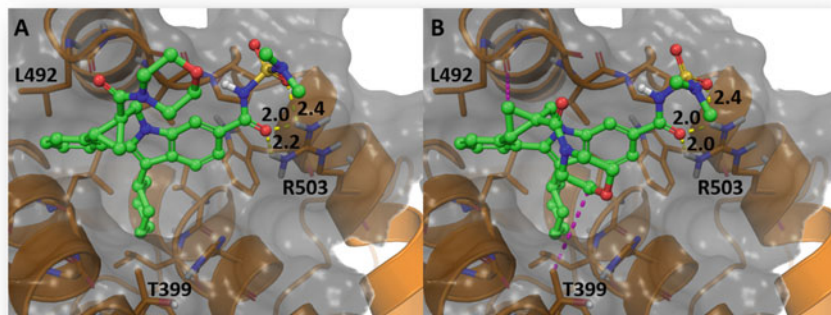


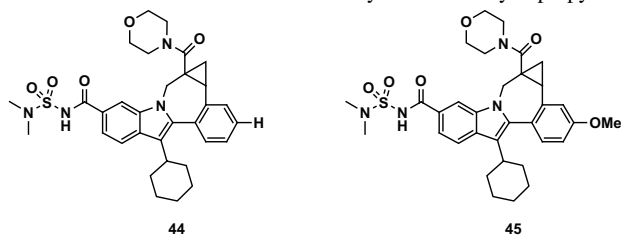
Fig. 14 Models of enantiomers **42** (a) and **43** (b) bound to the NS5B thumb site [38]. Close contacts and hydrogen bonds are depicted with magenta and yellow dashed lines, respectively, and distances are in angstroms. Images created with PyMOL (The PyMOL Molecular Graphics System, Version 2.0 Schrödinger, LLC)

that this might also contribute to the stabilization of the bound conformation shown in Fig. 14b.

As in prior studies, substitutions on the fused aryl ring were investigated and consistent with those experiences, and the 4-methoxy group was again identified as a preferred aryl substituent. Exemplified by the racemic cyclopropyl-fused analogs **44** and **45** shown in Table 3, there was a trend toward increased activity with the 4-methoxy derivatives, and the activity differential was more pronounced in the presence of 40% human serum. This effect was attributed to protein binding, and the modest right shift shown for **45** was observed with many members of this chemotype. However, with other closely related compounds, minor structural modifications were observed to result in pronounced loss of potency in the presence of serum.

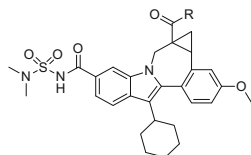
With a high degree of confidence that the southern hemisphere of the molecule had been reasonably optimized, a rigorous effort to identify the most preferred carboxamide derivatives was initiated. As noted above, this was largely an empirical exercise; the finger domains of NS5B that might reasonably be expected to interact with the carboxamide groups were unresolved in the co-crystal structures that had been obtained. This was attributed to a high degree of mobility in this region of the protein, a proposition that was consistent with extant SAR observations that a diversity of carboxamides could be accommodated at this vector.

Notwithstanding, after comprehensive scanning exercises had been completed, a preferred topology gradually emerged, first represented by the previously discussed morpholine derivative **45**. Subsequent optimization studies were directed at modulation of the properties of the series that would impact on its ability to be developed, and these initially took the form of preparing a range of closely related analogs, representative examples of which are listed in Table 4.

Table 3 SARs associated with methoxy-substituted cyclopropylindolobenzazepines

Compound	1b (FRET) EC ₅₀ (μM)	1a (FRET) EC ₅₀ (μM)	1b (FRET) + 40% human serum EC ₅₀ (μM)	P495A resistance EC ₅₀ (μM)	Toxicity CC ₅₀ (μM)
44	0.082	*0.044	0.821	*0.165	>10
45	0.061	*0.054	0.300	*0.385	>10

*EC₅₀ values marked with an asterisk are derived from a single experiment run in duplicate; other values represent the mean of >2 test occasions

Table 4 SARs associated with indolobenzazepine morpholine carboxamides

Compound	R	1b (FRET) EC ₅₀ (μM)	1a (FRET) EC ₅₀ (μM)	1b (FRET) + 40% serum EC ₅₀ (μM)	Toxicity CC ₅₀ (μM)	PXR-TA EC ₅₀ (μM)/ Y _{max}
45		0.061	*0.054	0.300	>10	ND
46		0.012	*0.006	0.036	>10	>50/12
47		0.024	*0.012	0.098	*9	#2.8
48		0.031	*0.007	0.114	>10	0.6/144

*EC₅₀ values marked with an asterisk are derived from a single experiment run in duplicate; other values represent the mean of >2 test occasions. *ND* not determined. Homochiral designates the associated data originated from a single enantiomer; #Indicates an EC₂₀ value

Of immediate note in these data was the significant enhancement of activity seen with the more highly substituted morpholine variants, as highlighted by compound **46**. This analog approached single-digit nanomolar inhibitory activity in the genotype 1b and 1a replicons and exhibited only a modest threefold reduction of potency in the presence of 40% human serum. However, enthusiasm for this finding was tempered by the observation that a number of related analogs, including **47** and **48**, exhibited a significant activity in the hPXR transactivation assay [36]. This observation occurred with sufficient frequency within the series that efforts were directed toward identifying analogs that obviated this liability.

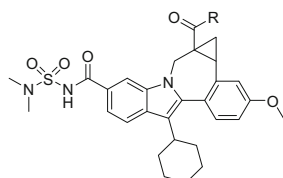
Few published SARs related to hPXR transactivation existed at the time of this work, and those that did were consistent with the characterization of the ligand-binding domain as large, mobile, and hydrophobic [39–42]. However, from these and related studies, it could be deduced that common structural features of hPXR ligands are that they possess an H-bond acceptor proximal to their core that is flanked by mostly hydrophobic moieties. As these elements are present within the analogs presented in Table 4, some directions for the further development of the series were suggested.

To resolve this issue, replacements for the morpholine moiety that would exploit more polar bioisosteres were sought. An initial effort in this area examined the use of 3-hydroxyazetidine as a morpholine surrogate. In this design, the distal Lewis base of the morpholine heterocycle was replaced by a polar H-bond donor. To temper what was considered to be a significant structural modification, substituents at the C3 position of the azetidine were introduced to function as shielding elements and also to array the hydrophobic moieties in a differentiated pattern. Select examples from this approach are shown in Table 5.

These changes proved to be highly effective at either eliminating or significantly ameliorating the hPXR liability. Less encouraging, however, was the inability to advance antiviral potency within the series. While the less sterically demanding derivatives such as **50** and **51** largely retained the activity, the introduction of larger aromatic moieties at the 3-position of the azetidine not only eroded antiviral potency but tended to exhibit greater cytotoxicity, as evidenced with **54** and **55**.

In additional profiling studies directed at determining solubility and permeability properties (Table 6), it was determined that the majority of these compounds could be categorized as Class II within the Biopharmaceutics Classification System (BCS), that is, analogs displaying high permeability ($P_c > 100$ nm/s) and low solubility [45].

In attempts to relate the data shown in Table 6 with in vivo observations, compounds **49** and **50** were advanced into abbreviated rat PK screens in which exposures were determined 4 h post-dosing. Results from these experiments are shown in Table 7. Following intravenous (IV) administration, compound **49** exhibited a high plasma clearance of 96 mL/min/kg. This was attributed to extensive extraction by the liver, a conjecture consistent with the observed high L/P ratio of >200 (observed at the 4 h time point). When dosed orally (PO), **49** displayed a low plasma AUC of 41 nM h, with liver concentrations of 8.8 μ M, indicating limited absorption and possibly high hepatic extraction. In contrast, the simple 3-methylazetidine **50** exhibited a significantly higher plasma AUC of 9,800 nM h,

Table 5 Structure-activity relationships and liability profiling associated with indolobenzazepine azetidines carboxamide derivatives

Compound	R	1b (FRET) EC ₅₀ (μM)	1a (FRET) EC ₅₀ (μM)	1b (FRET) + 40% serum EC ₅₀ (μM)	Cytotoxicity CC ₅₀ (μM)	PXR- TA EC ₅₀ (μM)/ Y _{max} (%)
49		0.038	0.045	0.059	>10	>50/ ND
50		0.020	*0.014	0.056	>10	>50/ ND
51		0.050	*0.015	0.115	>10	>3/32
52		*0.023	*<0.014	0.065	*6.5	>50/14
53		0.029	*<0.014	0.068	>10	>50/12
54		*0.16	*0.068	ND	*8	>50/10
55		*0.22	*0.054	ND	*7	>50/3

*EC₅₀ values marked with an asterisk are derived from a single experiment run in duplicate; other values represent the mean of >2 test occasions. *ND* not determined. All compounds listed were tested as racemic mixtures

higher liver levels of 9.6 μM, and a reduced clearance of 14 mL/min/kg following IV administration. However, in the oral leg of the study, the liver levels of **50** fell to 3.7 μM at the 4 h time point and were actually lower than that observed with **49** (8.8 μM). Additionally, the plasma AUC was equally disappointing. Collectively,

Table 6 Metabolic stability and profiling studies of azetidine carboxamides

Compound	PAMPA Pc (nm/s) at pH 7.4	Microsome stability % remaining human/rat	Amorphous solubility ($\mu\text{g/mL}$)
49	250	95/84	57
50	300	81/85	93
51	470	100/100	ND
52	740	72/100	ND
53	190	100/100	ND
54	390	72/100	ND
55	ND	87/100	ND

The permeability data used in this and following studies were generated using a parallel artificial membrane permeability (PAMPA) assay, and the solubilities of selected amorphous analogs were assessed in phosphate buffer at pH 6.5 [43]. Additionally, the metabolic stabilities of members of the class were initially profiled in human and rat liver microsomes, and for more advanced analogs, against a broader range of species [44]

ND not determined. All material listed were tested as racemic mixtures

Table 7 Rat PK parameters (0 to 4 h) associated with azetidine carboxamides

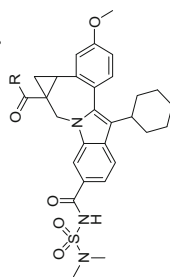
Compound	IV AUC 0–4 h (nM h)	Cl (est.) (mL/min/kg)	4 h plasma IV (nM)	4 h liver IV (nM)	PO AUC 0–4 h (nM h)	4 h plasma PO (nM)	4 h liver PO (nM)
49	1,416	96	17	5,000	41	11	8,800
50	9,800	14	29	9,600	139	25	3,700

Values are the average of the data from two animals. Vehicle, 100% PEG400. IV and PO dosing was conducted at 5 and 10 mg/kg, respectively

these data were considerably removed from what was considered necessary of a candidate for clinical evaluation.

With improved insights on the limitations of the lipophilic carboxamides that had been explored to this point, in a key decision, attention was directed toward the assessment of a more hydrophilic series of piperazine carboxamides. These retained the topology of the prior morpholine analogs but, as zwitterions, were significantly more polar and offered the possibility of evaluating a range of salt forms. Furthermore, the piperazine moiety facilitated rapid development of a systematic, progressive SAR as illustrated by the selected examples shown in Table 8.

Within this series it was found that analogs that retained a basic nitrogen, such as in **51** and **52**, were generally among the most potent derivatives identified, approaching the activity of the previously discussed ether-appended morpholine **46**. In addition, unlike the morpholine compounds, all of the piperazine carboxamides were devoid of significant effects in the hPXR transactivation assay [36]. This was true even with the basic derivatives **51** and **52**, an observation that might be rationalized by appreciating that under physiological (or assay) conditions, the distal nitrogen of the piperazine would be expected to be partly protonated, thus preventing the presentation of a Lewis base element. More disappointing, however, was the finding that the

Table 8 Structure-activity relationships associated with cyclopropylindolobenzazepine piperazine carboxamide derivatives

Compound	R	1b (FRET) EC ₅₀ (μM)	1a (FRET) EC ₅₀ (μM)	1b (FRET) serum EC ₅₀ (μM)	1b (FRET) +40% serum EC ₅₀ (μM)	CC ₅₀ (μM)	PXR-TA EC ₅₀ (μM)	PAMPA Pc (nm/s) at pH 7.4	Microsome stability % remaining human/rat	Amorphous solubility (μg/mL)
51		0.029	*0.021	0.055		15	>50	140	91/100	<1
52		0.017	*0.014	0.046		8	>50	480	88/99	34
53		0.038	*0.024	0.035		>10	>50	480	100/93	17
54		0.098	0.045	0.089		>10	>50	340	93/100	18
55		0.054	0.023	0.059		>10	>50	430	64/93	18

*EC₅₀ values marked with an asterisk are derived from a single experiment run in duplicate; other values represent the mean of >2 test occasions. *ND* not determined. All materials listed were tested as racemic mixtures

introduction of additional charged or polar groups at this vector did not generally result in improved solubility. However, as zwitterions, more complex pH-dependent solubility profiles would be expected, and, as discussed, these compounds offered the possibility of exploring alternative salt forms, a feature that was thoroughly evaluated with these and related analogs [46].

In profiling studies, the piperazines **52** and **53** exhibited a significantly enhanced metabolic stability and permeability properties. It was considered that these improvements would partly address the issues seen with the two azetidines **49** and **50**, and both were progressed into 4 h rat PK screens, the results from which are shown in Table 9.

In the case of the *N*-acetyl derivative **53**, there was no translation into an enhanced exposure profile. This, combined with an observed reduction in liver tropism, led to the deprioritization of this class. Of much greater significance, however, was the data obtained on the zwitterionic derivative **52**. This analog displayed decidedly improved plasma AUC and liver levels (PO), findings that were attributed to the improved balance of permeability (Pc 480 nM/s) and solubility (34 µg/mL). Given that this analog was also among the most potent identified, it was immediately prioritized for further investigation.

In the attendant studies, an initial design prioritized analogs that retained a basic character at the N4-position of the piperazine. In addition, novel structural elements that would induce further conformation constraints were incorporated. This revisited one of the original concepts associated with the introduction of the cyclopropyl moiety, and as it could be achieved without dramatically impacting the overall silhouette of the chemotype, priority was given to the syntheses of the analogs compiled in Table 10.

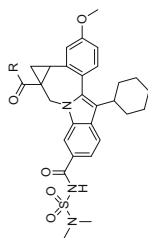
The data obtained with these derivatives proved to be of immense value. With the proximal methano- and ethano-bridged derivatives **58**, **59**, and **66**, clinically relevant potencies of <10 nM against the targeted genotypes were achieved. This was in contrast to the distally bridged congeners that were consistently less potent. Additionally, there appeared to be steric limitations associated with the N4 nitrogen of the carboxamide moieties, with larger substituents displaying reduced potencies and, in the case of aromatic functionality, a reemergence of prior hPXR issues.

While all of the bridged piperazines possessed good metabolic stability in liver microsomes, they displayed a significant variation in their permeability properties. The N4-alkylated, proximally bridged derivatives **58**, **65**, and **66** all exhibited

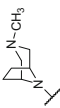
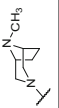

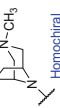
Table 9 Rat PK parameters (0 to 4 h) associated with piperazine carboxamides

Compound	IV AUC 0–4 h (nM h)	Cl (est.) (mL/min/ kg)	4 h plasma IV (nM)	4 h liver IV (nM)	PO AUC 0–4 h (nM h)	4 h plasma PO (nM)	4 h liver PO (nM)
52	4,287	29	67	1858	516	158	9,700
53	3,841	37	9	126	277	14	345

Values are the average of the data from two animals. Vehicle, 100% PEG400. IV and PO dosing was conducted at 5 and 10 mg/kg, respectively

Table 10 Structure-activity relationships of bridged piperazine carboxamides

Compound	R	1b (FRET) EC ₅₀ (μM)	1a (FRET) EC ₅₀ (μM)	1b (FRET) EC ₅₀ (μM) 40% human serum	CC ₅₀ (μM)	PXR-TA EC ₅₀ (μM)/ Y _{max} (%)	PAMPA Pc (nm/s) at pH 7.4	Microsome stability % remaining human/ rat	Amorphous solubility (μg/mL)
56		0.080	*0.023	0.094	>10	>50	60	97/100	ND
57		0.012	*0.004	0.039	*10	>50	ND	100/100	ND
58		0.005	0.006	0.028	*13	>50	430	98/ 98	760
59		*0.004	*0.004	ND	ND	>50	270	ND	450
60		0.162	0.035	ND	* >10	2/22	560	80/100	ND
61		0.032	*0.014	ND	>10	9/31	40	96/100	ND
62		0.089	*0.034	ND	>10	>50	2	100/100	ND

63		0.013	0.005	0.045	> 10	1/21	770	90/100	44
64		0.039	*0.016	0.153	* > 16	3/29	210	100/100	41
65		0.022	*0.004	0.037	* > 10	> 50	410	98/98	ND
66		0.006	0.003	0.028	* > 10	> 50	640	90/99	29

*EC₅₀ values marked with an asterisk are derived from a single experiment run in duplicate; other values represent the mean of > 2 test occasions. ND not determined. Homochiral designates the associated data originated from a single enantiomer with identical stereochemistry to analog **37**. EC₅₀ values for **66** have also been determined in luciferase-expressing reporter systems and have been previously reported. The values are similar to the FRET values

excellent membrane permeability values; this was in contrast to the permeability properties shown by the non-alkylated and distally bridged derivatives. Another source of differentiation within the series related to amorphous solubility, with the methano-bridged analogs **58** (760 µg/mL) and **59** (450 µg/mL) clearly distinguishing themselves. However, given the amorphous nature of the materials assessed in these assays, the significance of these data was challenging to interpret [47]. Nonetheless, given the overall properties of compound **58**, this analog was advanced into a 6 h rat PK study, the data from which are shown in Table 11.

Very encouragingly, **58** exhibited lower clearance, markedly higher oral and IV plasma AUCs, and improved liver levels throughout the extended 6 h time period. This, together with the collective data from Table 10, drove the further characterization of these methano analogs in an expanded set of liability assays. Selected data for compounds **58** and **59** are presented Table 12 and are representative of many of the members of this series.

Cytotoxicity in a liver Hep G2 cell line was observed but was weak, and a significant selectivity index existed with a majority of the analogs explored. In cytochrome P450 inhibition assays, only moderate, sporadic inhibitory activities against a panel of isozymes were noted, but of more concern were the variable levels of inhibitory activities observed in the ion channel screens [48]. While the majority of analogs in the bridged piperazines displayed little to no effect at the hNaV1.5 sodium channel (expressed in HEK cells), single-digit micromolar inhibition of the human ether-à-go-go (hERG) channel was observed, as can be seen with **59** above, a compound that also exhibited single-digit micromolar inhibition of the CYP3A4 enzyme [49].

Contrasting the ethano- and methano-bridged derivatives allowed a study of the effect of transposition and homologation of the bridging element. Within the ethano series, relocation of the bridge from a proximal to a distal position relative to the

Table 11 Rat PK profile of indolobenzazepine **58** (0–6 h post-dosing)

Compound	IV AUC 0–6 h (nM h)	Cl (est.) (mL/min/ kg)	6 h plasma IV (nM)	6 h liver IV (nM)	PO AUC 0–6 h (nM h)	6 h plasma PO (nM)	6 h liver PO (nM)
58	11,200	9	409	17,500	4,930	440	14,300

Values are the average of the data from two animals. Vehicle, 100% PEG400. IV and PO dosing was conducted at 5 and 10 mg/kg, respectively

Table 12 Profiling studies of cyclopropylindolobenzazepine-bridged piperazine carboxamides

Compound	Hep G2 CC50 (µM)	hERG IC ₅₀ (µM)	NACH IC ₅₀ (µM)	CYP 1A2 IC ₅₀ (µM)	CYP 2C9 IC ₅₀ (µM)	CYP 2C19 IC ₅₀ (µM)	CYP 2D6 IC ₅₀ (µM)	CYP 3A4 (BZRes) IC ₅₀ (µM)
58	25	20	30	>40	>40	>40	>40	14
59	19	6	29	>40	>40	>40	>40	9

Values are the average from at least two experiments

carboxamide nitrogen was associated with a modest reduction in potency, as can be seen by comparing **61** to **62** and **63** to **64**. Additionally, homologation of the bridging element was associated with enhanced permeability as evidenced by the higher Pc values exhibited by the ethano analogs **65** and **66** (Pc values of 410 and 640 nM/s, respectively), compared to their lower homologs **59** and **58** (Pc values of 270 vs. 430 nM/s, respectively). Furthermore, a signal in the hPXR transactivation assay associated with the racemic ethano-bridged N-methyl analog **63** was notably absent from the highly potent, resolved enantiomer **66** [36].

With many of the bridged piperazines, significant advances in both the on- and off-target profiles of the compounds had been realized. In particular, as a result of the excellent level of activity achieved with **66**, and its enhanced membrane permeability and profiling properties relative to **58**, this compound was rapidly advanced into additional profiling and PK studies, as well as efforts to further understand its broader toxicological and virological profiles.

The zwitterionic form of **66** (pKa values = 4.6 and 6.8) was amorphous and displayed pH-dependent aqueous solubility of between ~0.02 mg/mL and greater than 1.60 mg/mL. The compound was highly permeable, as determined in a PAMPA assay, but exhibited efflux ratios in a Caco-2 system that increased from 2.2 at pH = 5.5 to 8.3 at pH = 7.4 [50]. It was surmised that the lower efflux ratio expected in the gut could be accommodated, and the higher efflux ratio seen at pH = 7.4 would preclude any uptake into the central nervous system (CNS) and would therefore limit any unwanted neurological effects. The metabolic stability of this compound was also evaluated in an expanded panel of liver microsomes that included human, rat, dog, and cynomolgus monkey. Half-life values of >200 min were observed in both the rat and dog assays, while in human and monkey microsomes, the $t_{1/2}$ values were 53 and 23 min, respectively. Collectively, these data were highly supportive of the continued evaluation of **66**, which was subsequently progressed into 24 h rat PK studies, the data from which are presented in Table 13.

From these investigations the oral bioavailability of **66** was determined to be 66% when dosed as a solution in PEG-400. The compound was well distributed, having a volume of distribution of 2.7 L/kg. It exhibited low-clearance (3.5 mL/min/kg) characteristics following an IV dose as a solution in PEG-400, a finding consistent with the stability observed in rat liver microsomes. These properties led to a plasma half-life of 8.3 h and, importantly, liver levels (evaluated in a satellite study (in two rats) measured at both 4 and 24 h following oral dosing) of 24,400 nM and 1,700 nM, respectively. These represented significant multiples of the serum-adjusted replicon EC₅₀ values.

In vivo biotransformation studies showed that **66** generated one principal circulating metabolite that arose from mono-demethylation of the sulfamide moiety [51]. Profiling of this species showed that it retained a significant antiviral activity but was otherwise benign and did not constitute a liability. The overall profile exhibited by **66** was largely mirrored in other species in which it was evaluated, and with these findings, the primary criteria for nomination of a clinical candidate had been achieved.

Table 13 Preliminary rat PK study data for cyclopropylindolobenzazepine **66** (0–24 h)

Route of admin.	Dose (mg/kg)	C _{max} (μM)	t _{max} (h)	AUC (0-INF) (μM h)	t _{1/2} (h)	Cl (mL/min/kg)	Vd (L/kg)	F (%)
IV	5	12,100 (±3,400)	–	30,000 (±2,500)	11.2 (±4.9)	3.5 (±0.8)	2.7 (±0.7)	–
PO	10	3,260 (±540)	5.3 (±1.2)	39,300 (±6,700)	8.3 (±1.6)	–	–	66

Values are the average from at least two experiments, unless otherwise indicated. Std. dev. are shown in parenthesis

As the compound progressed through the above studies, additional effort was directed at more fully characterizing the virological and toxicological profiles. In relation to the former, compound **66** was evaluated against a range of HCV genotypes, in both enzyme and replicon assays, the results from which are shown in Table 14. As previously noted (*vide supra*), the primary goal was inhibition of genotypes 1a and 1b; however, it was highly encouraging that **66** displayed an activity against most genotypes tested with the exceptions of 2a, 2b, and 6a. Since genotypes 2a and 2b responded well to what was the optimal treatment for HCV at the time of these discoveries, and the fact that genotype 6 was of lower prevalence, the antiviral activity exhibited by this indolobenzazepine was considered supportive of further advancement.

In viral selectivity studies used to assess non-specificity of action, the activity of **66** was evaluated against a panel of viruses that included the HCV-related bovine viral diarrhoea virus (BVDV), as well as polio, rhino, corona, coxsackie, influenza, and human immunodeficiency viruses (HIV) [52]. In all of these assays, **66** was found to be essentially inactive (EC_{50} value $>14 \mu\text{M}$) and therefore likely to be highly specific in its mechanism of action.

Given the sporadic cytotoxicity seen with some members of the compound class, **66** was profiled in cell lines derived from a number of tissues. While effects were seen in some cells with CC_{50} values in the range of 14 to more than $48 \mu\text{M}$, given the potency of **66** in the HCV genotype 1b replicon, there existed selectivity indices in excess of 2000. It was therefore concluded that the toxicity signals observed were unlikely to be of clinical relevance.

To further characterize potential off-target effects, **66** was evaluated in a panel of receptor and ion channel binding and enzyme inhibition assays (<https://www.mdps.com/>). In these studies, there were no significant findings other than a moderate inhibition of human phosphodiesterase 4. This activity was explored in a functional assay where it was determined that **66** had an IC_{50} value in excess of $10 \mu\text{M}$. Given this moderate level of activity, coupled with a low potential for uptake into the CNS (*vide supra*), it was assessed that there was limited risk for induction of emesis [53]. In studies designed to assess cardiac liabilities, **66** was profiled in a hERG patch-clamp assay and was determined to inhibit the channel with an IC_{50} value of $12.4 \mu\text{M}$ ($n = 1$). This was considered acceptable given that the compound was highly bound (98%) to human serum, and the anticipated doses would not result in a circulating free fraction that would approach this concentration (additional studies were undertaken to confirm this hypothesis but are not reviewed here).

As **66** was designed to be administered as part of a combination therapy, it was necessary to fully assess the potential for DDIs. Correspondingly, it was profiled for CYP inhibition in a panel incorporating 1A2, 2C19, 2C9, 2D6, and 3A4 enzymes and displayed IC_{50} values of $>40 \mu\text{M}$ (based on the average of three determinations), suggesting a low probability for inducing DDIs through cytochrome P450 inhibition. In addition, when assessed in the hPXR transactivation assay, the compound displayed a minimal activity ($EC_{50} > 50 \mu\text{M}$, $Y_{\text{max}} = 8.1 \pm 1.9$ at $5.56 \mu\text{M}$), again suggesting a low potential for autoinduction of metabolism and attendant DDI potential.

Table 14 HCV genotype inhibitory activity associated with cyclopropylindolobenzazepine **66**

Compound	1a: Replicon EC ₅₀ (nM)	1b: Replicon EC ₅₀ (nM)	2a: Replicon EC ₅₀ (nM)	1a: Enzyme IC ₅₀ (nM)	1b: Enzyme IC ₅₀ (nM)	2a: Enzyme IC ₅₀ (nM)	2b: Enzyme IC ₅₀ (nM)	3a: Enzyme IC ₅₀ (nM)	4a: Enzyme IC ₅₀ (nM)	5a: Enzyme IC ₅₀ (nM)	6a: Enzyme IC ₅₀ (nM)
2	3	6	87	3	4	165	164	2	20	5	62

EC₅₀ and IC₅₀ values are the mean of ≥ 2 test occasions

Although not directly related to the clinical advancement of compound **66**, a number of structural and mechanistic studies were undertaken. These included obtaining an X-ray structure of a co-crystal of **66** bound to NS5B [54]. Consistent with prior investigations of the bridged indole chemotypes, the compound was observed to bind in Site I of the thumb domain of the polymerase, as depicted graphically in Fig. 15. Importantly, the data acquired in these experiments were used to assign the absolute stereochemistry of **66** and, by extension, that of the other cyclopropylindolobenzazepines presented here.

From these data, **66** can be seen to occupy a largely hydrophobic binding site, with the polar elements of the molecule mostly protruding into an aqueous-accessible compartment. The primary drivers of binding are interactions between the cyclohexyl, phenyl, and indole elements of the molecule with hydrophobic amino acid side chains in the binding site, in combination with H-bonds between the sulfamide moiety and R503. Additional contacts between the methylene moiety of the cyclopropyl ring and the ethano-bridged N-methyl piperazine group and the proximal L492, T399, and A400 residues also contribute to binding affinity. Significantly, P495 is seen to make multiple contacts with the indole ligand, explaining the reduced activity of **66** in assays utilizing the P495A and P495L mutant NS5B proteins (e.g., IC_{50} WT 1b/P495L = 0.02/0.19 μ M). Returning to a point made first when introducing the bridged indole chemotype, the dihedral angle between the fused methoxyaryl moiety and the indole ring in **66** is 44° ; this approximates that seen for the same dihedral (43°) in compound **14**, the analog that was the essential precursor for most of the work that was described subsequently [23].

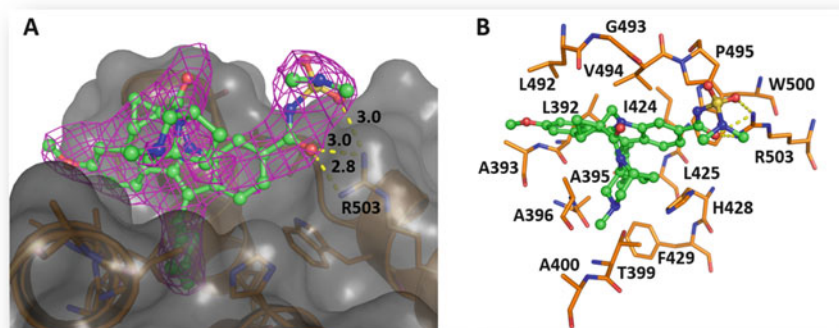


Fig. 15 (a) The Connolly surface of NS5B with compound **66** bound in Site I [55]. (b) Detailed view of residues (stick representation, orange carbon atoms) proximal to bound **66** (ball-and-stick representation, green carbon atoms). Data derived from the co-crystal structure of the ternary complex of **66** (thumb site, shown), a palm site inhibitor (not shown), and NS5B determined to 2.75 Å resolution. Hydrogen bonds are denoted with dashed yellow lines, and the initial 2Fo-Fc electron density for **66** is shown as a magenta mesh, contoured at 1 rmsd. All distances are in angstroms. Images created with PyMOL (The PyMOL Molecular Graphics System, Version 2.0 Schrödinger, LLC)

The mode of binding observed with **66** suggests an explanation for its probable mechanism of action, where occupation of a lipophilic pocket in the thumb domain of NS5B is believed to prevent the enzyme from adopting a transcriptionally active conformation, as outlined below [56].

This putative inhibition mechanism is depicted graphically in Fig. 16. In the apo structure shown in Panel A, Leu-30 of the $\Delta 1$ loop of NS5B is observed to occupy the same pocket into which the cyclohexyl moiety of **66** inserts when it binds to the enzyme, as shown in Panel B. It is thought that Leu-30 occupies this pocket during transcription of the viral genome and that this interaction contributes to the stabilization of the transcriptionally active, “closed” conformation. However, when this residue is displaced by the binding of compound **66**, the enzyme can no longer adopt this conformation, and viral replication is prevented. Consistent with this hypothesis, kinetic studies indicate that the $\Delta 1$ finger domains interact dynamically with Site I in the thumb domain and appear to compete with **66** during its initial binding to NS5B [56].

To conclude the discussion of the preclinical characterization of compound **66**, the data reviewed above met or exceeded the goals for nomination of a clinical candidate, and **66**, also known as BMS-791325, was accepted for advancement into early development during which time it acquired its generic nomenclature of beclabuvir (BCV).

In Phase I clinical studies, the pharmacokinetics, safety, and antiviral profiles of **66** were assessed in a double-blind, placebo-controlled, single-ascending-dose (SAD) study [57]. Twenty-four patients with chronic HCV genotype 1 infection,

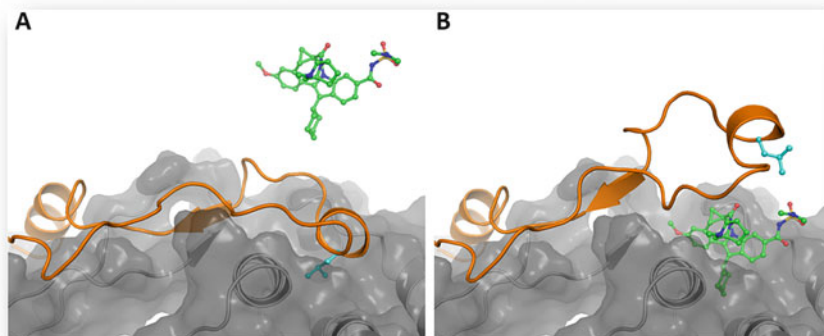
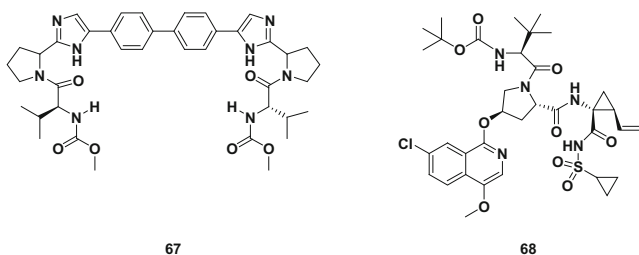


Fig. 16 Possible mechanism of inhibition of NS5B by compound **66**. In both figures the indolobenzazepine ligand and residue Leu-30 of NS5B are shown in ball-and-stick representations with green- and cyan-colored carbon atoms, respectively. Residues 1–53 of NS5B are depicted in orange, and the remainder of the protein is shown with gray schematic and surface representations. Panel (a) shows the apo crystal structure of NS5B (Protein Data Bank code 1C2P) together with unbound **66**. Panel (b) the conformation shown for residues 1–53 (orange) of NS5B is for illustrative purposes only. Compound **66** is shown in its correct bound pose. Images created with PyMOL (The PyMOL Molecular Graphics System, Version 2.0 Schrödinger, LLC)

including both INF-naïve and INF-experienced groups, were randomized to receive ascending doses of 100, 300, 600, and 900 mg of **66** or placebo. Antiviral activity was observed in all dose groups, with those patients receiving the 300 mg dose exhibiting an approximately $2.5 \log_{10}$ IU/mL decline in viral load measured 24 h post-dosing. Single doses of **66** exhibited dose-related increases in exposure, demonstrated rapid and exposure-related antiviral activity, and were well tolerated. The established pharmacokinetic profiles were supportive of once- or twice-daily dosing.

As noted in the introduction to this chapter, the intended use of an NS5B inhibitor was in combination with other DAAs of unrelated mechanisms of action. To that end, **66** was investigated in a fixed-dose combination (termed DCV-TRIO) with the NS5A inhibitor daclatasvir (DCV) (**67**) and the NS3 protease inhibitor asunaprevir (ASV) (**68**) [58–60] in a clinical program designated UNITY. The Phase 3 studies [61] investigated the use of DCV-TRIO in both cirrhotic and non-cirrhotic patients infected with HCV genotype 1 for a period of 12 weeks.



In the open-label UNITY-1 study, DCV-TRIO was dosed without ribavirin in both treatment-naïve and treatment-experienced non-cirrhotic patients. The treatment-naïve group ($n = 312$) and the treatment-experienced patients ($n = 103$) received one pill twice daily for 12 weeks with 24 weeks of follow-up. SVR12 was achieved by 91% of all treated patients.

In the UNITY-2 study, treatment-naïve and treatment-experienced patients with cirrhosis received the DCV-TRIO fixed-dose combination, one arm without ribavirin ($n = 102$) and the other with ribavirin ($n = 100$). SVR12 rates of 96% or 90% were achieved by patients treated with DCV-TRIO with or without ribavirin, respectively [62].

In these studies the DCV-TRIO fixed-dose combination was well tolerated with very low rates of both adverse events (AEs) and serious adverse events (SAEs) reported. Only in the UNITY-2 study were there treatment-related AEs (4) and SAEs (3) that subsequently led to treatment discontinuations.

In relation to BCV and its development as a component of the DCV-TRIO formulation, later termed Ximency, clinical trials were directed at gaining approval in Japan. These included a Japanese Phase 3 study (AI443117) [63], a global Phase 1 study (AI443006) [64] in healthy Japanese subjects, a Phase 1 study (AI443112) [65] on the effect on QT interval, and a proof-of-concept study (AI443014)

[66, 67]. These were used as to support a Japanese new drug application that was subsequently approved by the Japanese Pharmaceutical and Food Safety Bureau in December 2016.

Acknowledgments The following individuals made invaluable contributions to the work described above: Min Ding, John Bender, Carl P. Bergstrom, Katherine Grant-Young, Piyasena Hewawasam, Thomas Hudyma, Scott Martin, Andrew Nickel, Alicia Regueiro-Ren, Yong Tu, Zhong Yang, Kap-Sun Yeung, Xiaofan Zheng, Sam Chao, Jung-Hui Sun, Brett R. Beno, Dan Camac, Chong-Hwan Chang, Mian Gao, Paul Morin, Steven Sheriff, Jeff Tredup, John Wan, Mark Witmer, Dianlin Xie, Umesh Hanumegowda, Jay Knipe, Kathy Mosure, Kenneth S. Santone, Dawn D. Parker, Xiaoliang Zhuo, Julie Lemm, Mengping Liu, Lenore Pelosi, Karen Rigat, Stacey Voss, Yi Wang, Ying-Kai Wang, Richard C. Colonna, Min Gao, Susan B. Roberts, Qi Gao, Alicia Ng, Nicholas A Meanwell, and John F. Kadow.

The author also thanks the following: Arvind Mathur and Bang-Chi Chen for their participation in multiple synthesis campaigns that enabled many of the above studies; Richard Rampulla and the chemists at Syngene International for synthesizing and providing numerous intermediates that greatly expedited much of the research reviewed; Brett Beno for his provision of several of the figures shown above; and Nicholas A. Meanwell, Fiona McPhee, and Richard Olson for proof-reading this manuscript and for their many helpful suggestions.

Compliance with Ethical Standards

Funding The work described herein was funded by Bristol Myers Squibb as part of its routine business operations.

Conflict of Interest The author declares that he has no conflict of interest.

Ethical Approval This article does not contain any studies with human participants or animals performed by the author.

However, the work described does refer to a number of animal studies and subsequent human clinical studies conducted by others. With respect to those studies, all applicable international, national, and/or institutional guidelines for the care and use of animals were followed, and with respect to clinical studies, all were conducted in accordance with the ethical standards of the institutional and/or national research committee and with the 1964 Helsinki declaration and its later amendments or comparable ethical standards.

References

1. Meanwell NA (2016) 2015 Philip S. Portoghese Medicinal Chemistry Lectureship. Curing hepatitis C virus infection with direct-acting antiviral agents: the arc of a medicinal chemistry triumph. *J Med Chem* 59:7311–7351
2. Looney D, Ma AI, Johns S (2015) HIV therapy – the state of ART. *Curr Top Microbiol Immunol* 389:1–29
3. Borgia G, Maraolo AE, Nappa S, Gentile I, Buonomo AR (2018) NS5B polymerase inhibitors in phase II clinical trials for HCV infection. *Expert Opin Investig Drugs* 27(3):243–250
4. Tsai CH, Lee PY, Stollar V, Li ML (2006) *Curr Pharm Des* 12(11):1339–1355

5. Dogan UB, Atabay A, Akin MS, Yalaki S (2013) The comparison of the efficacy of pegylated interferon α -2a and α -2b in chronic hepatitis C patients with genotype 1. *Eur J Gastroenterol Hepatol* 25:1082–1085
6. Fontaine H, Pol S (2001) Side effects of interferon- α in treating hepatitis C virus infection. *Transplant Proc* 33:2327–2329
7. Shukla DD, Hoyne PA, Ward CW (1995) Evaluation of complete genome sequences and sequences of individual gene products for the classification of hepatitis C viruses. *Arch Virol* 140:1747–1761
8. Thurner C, Witwer C, Hofacker Ivo L, Stadler PF (2004) Conserved RNA secondary structures in Flaviviridae genomes. *J Gen Virol* 85:1113–1124
9. Sandres-Saune K, Deny P, Pasquier C, Thibaut V, Duverlie G, Izopet J (2003) Determining hepatitis C genotype by analyzing the sequence of the NS5b region. *J Virol Methods* 109:187–193
10. Davis GL (1999) Hepatitis C virus genotypes and quasispecies. *Am J Med* 107:21S–26S
11. Nolte FS (2001) Hepatitis C virus genotyping: clinical implications and methods. *Mol Diagn* 6:265–277
12. Rosenberg S (2001) Recent advances in the molecular biology of hepatitis C virus. *J Mol Biol* 313:451–464
13. Bressanelli S, Tomei L, Roussel A, Incitti I, Vitale RL, Mathieu M, De Francesco R, Rey FA (1999) Crystal structure of the RNA-dependent RNA polymerase of hepatitis C virus. *Proc Natl Acad Sci U S A* 96:13034–13039
14. Simister P, Schmitt M, Geitmann M, Wicht O, Danielson UH, Klein R, Bressanelli S, Lohmann V (2009) Structural and functional analysis of hepatitis C virus strain JFH1 polymerase. *J Virol* 83:11926–11939
15. Patil VM, Gupta SP, Samanta S, Masand N (2011) Current perspective of HCV NS5B inhibitors: a review. *Curr Med Chem* 18:5564–5597
16. Wang Y-K, Rigat KL, Roberts SB, Gao M (2006) A homogeneous, solid-phase assay for hepatitis C virus RNA-dependent RNA polymerase. *Anal Biochem* 359:106–111
17. Lemm JA, O'Boyle II D, Liu M, Nower PT, Colonna R, Deshpande MS, Snyder LB, Martin SW, St. Laurent DR, Serrano-Wu MH, Romine JL, Meanwell NA, Gao M (2009) Identification of hepatitis C virus NS5A inhibitors. *J Virol* 84:482–491
18. O'Boyle II DR, Nower PT, Lemm JA, Valera L, Sun J-H, Rigat K, Colonna R, Gao M (2005) Development of a cell-based high-throughput specificity screen using a hepatitis C virus-bovine viral diarrhea virus dual replicon assay. *Antimicrob Agents Chemother* 49:1346–1353
19. Pelosi LA, Voss S, Liu M, Gao M, Lemm JA (2012) Effect on hepatitis C virus replication of combinations of direct-acting antivirals, including NS5A inhibitor daclatasvir. *Antimicrob Agents Chemother* 56:5230–5239
20. Hashimoto H, Mizutani K, Yoshida A (2001) PCT Int Appl. WO 2001047883 A1 20010705
21. Beaulieu PL, Fazal G, Goulet S, Kukolj G, Poirier M, Tsantrizos YS, Jolicoeur E, Gillard J, Poupart MA, Rancourt J (2003) PCT Int Appl. WO 2003010141 A2 20030206
22. Martin SW, Glunz P, Beno BR, Bergstrom C, Romine JL, Scott PE, Newman M, Gao M, Roberts S, Rigat K, Robert F, Dike Q, Galina K, Ying-Kai W (2011) The synthesis and evaluation of a novel class of (E)-3-(1-cyclohexyl-1H-pyrazol-3-yl)-2-methylacrylic acid Hepatitis C virus polymerase NS5B inhibitors. *Bioorg Med Chem Lett* 21(10):2869–2872
23. Zheng X, Hudyma TW, Martin SW, Bergstrom C, Ding M, He F, Romine J, Poss MA, Kadow JF, Chang C, Wan J, Witmer MR, Morin P, Camac DM, Sheriff S, Beno BR, Rigat KL, Want YK, Fridell R, Lemm J, Qui D, Liu M, Voss S, Pelosi L, Roberts SB, Gao M, Knipe J, Gentles RG (2011) Syntheses and initial evaluation of a series of indolo-fused heterocyclic inhibitors of the polymerase enzyme (NS5B) of the hepatitis C virus. *Bioorg Med Chem Lett* 21(10):2925–2929
24. Harder E, Damm W, Maple J, Wu C, Reboul M, Xiang JY, Wang L, Lupyan D, Dahlgren MK, Knight JL et al (2016) OPLS3: a force field providing broad coverage of drug-like small molecules and proteins. *J Chem Theory Comput* 12(1):281–296
25. Lohmann V, Korner F, Koch J, Herian U, Theilmann L, Bartenschlager R (1999) Replication of subgenomic hepatitis C virus RNAs in a hepatoma cell line. *Science* 285(5424):110–113

26. PDB 3Q0Z at 2.29 angstrom resolution with R-work = 0.200 and R-free = 0.224
27. Hewawasam P, Tu Y, Gao M, Hanumegowda U, Knipe J, Lemm JA, Parker DD, Rigat KL, Roberts SB, Meanwell NA, Kadow JF (2016) Discovery and preclinical evaluation of potent, orally bioavailable, metabolically stable cyclopropylindolobenzazepine acylsulfonamides as thumb site 1 inhibitors of the hepatitis c virus NS5B RNA-dependent, RNA polymerase. *Bioorg Med Chem Lett* 26(3):936–940
28. Martin AR, Yang Y (1993) Palladium-catalyzed cross-coupling reactions of organoboronic acids with organic electrophiles. *Acta Chem Scand* 47:221–230
29. Suzuki A (1999) Recent advances in the cross-coupling reactions of organoboron derivatives with organic electrophiles, 1995–1998. *J Organomet Chem* 576:147–168
30. Suzuki A (2002) Cross-coupling reactions via organoboranes. *J Organomet Chem* 653:83–90
31. Beaulieu PL, Gillard J, Bykowski D, Brochu C, Dansereau N, Duceppe J-S, Hache B, Jakalian A, Lagace L, LaPlante S, McKercher G, Moreau E, Perreault S, Stammers T, Thauvette L, Warrington J, Kukolj G (2006) Improved replicon cellular activity of non-nucleoside allosteric inhibitors of HCV NS5B polymerase: From benzimidazole to indole scaffolds. *Bioorg Med Chem Lett* 16:4987–4993
32. Hudyma TW, Zheng X, He F, Ding M, Bergstrom CP, Hewawasam P, Martin SW, Gentles RG (2006) Preparation of indolecarboxylic acid derivatives as inhibitors of HCV replication. *PCT Int Appl. WO 2006020082 A1 2006022*
33. Grubbs RH (2003) *Handbook of metathesis*. Wiley-VCH, Weinheim
34. Furstner A (2000) *Angew Chem Int Ed* 39:3012
35. Hewawasam P, Tu Y, Hudyma TW, Zhang X, Gentles RG, Kadow JF, Meanwell NA (2014) A practical and efficient synthesis of 6-carboalkoxy-13-cycloalkyl-5H-indolo[2,1-a][2] benzazepine-10-carboxylic acid derivatives. *Tetrahedron Lett* 55(6):1148–1153
36. Herbst J, Anthony M, Stewart J, Connors D, Chen T, Banks M, Petrillo EW, Agler M (2009) Multiplexing a high-throughput liability assay to leverage efficiencies. *Assay Drug Dev Technol* 7:294–303
37. Trost BM, Melvin LS Jr (1975) *Organic chemistry. Sulfur ylides, emerging synthetic intermediates*, vol 31. Academic Press, New York, 346 pp
38. Gentles RG, Ding M, Bender JA, Bergstrom CP, Grant-Young K, Hewawasam P, Hudyma T, Martin S, Nickel A, Regueiro-Ren A et al (2014) Discovery and preclinical characterization of the cyclopropylindolobenzazepine BMS-791325, a potent allosteric inhibitor of the hepatitis C virus NS5B polymerase. *J Med Chem* 57(5):1855–1879
39. Chen C-N, Shih Y-H, Ding Y-L, Leong MK (2011) Predicting activation of the promiscuous human pregnane X receptor by pharmacophore ensemble/support vector machine approach. *Chem Res Toxicol* 24:1765–1778
40. Ekins S, Kortagere S, Iyer M, Reschly EJ, Lill MA, Redinbo MR, Krasowski MD (2009) Challenges predicting ligand-receptor interactions of promiscuous proteins: the nuclear receptor PXR. *PLoS Comput Biol* 5
41. Wallace BD, Betts L, Talmage G, Pollet RM, Holman NS, Redinbo MR (2013) Structural and functional analysis of the human nuclear xenobiotic receptor PXR in complex with RXR α . *J Mol Biol* 425:2561–2577
42. Wu B, Li S, Dong D (2013) 3D structures and ligand specificities of nuclear xenobiotic receptors CAR, PXR and VDR. *Drug Discov Today* 18:574–581
43. Kansy M, Senner F, Gubernator K (1998) Physicochemical high throughput screening: parallel artificial membrane permeation assay in the description of passive absorption processes. *J Med Chem* 41:1007–1010
44. Tran A, Rey E, Pons G, Rousseau M, d'Athis P, Olive G, Mather GG, Bishop FE, Wurden CJ, Labrou R, Trager WF, Kunze KL, Thummel KE, Vincent JC, Gillardin J-M, Lepage F, Levy RH (1997) Influence of stiripentol on cytochrome P450-mediated metabolic pathways in humans: in vitro and in vivo comparison and calculation of in vivo inhibition constants. *Clin Pharmacol Ther (St Louis)* 62:490–504

45. Wu C-Y, Benet LZ (2005) Predicting drug disposition via application of BCS: transport/absorption/elimination interplay and development of a biopharmaceutics drug disposition classification system. *Pharm Res* 22:11–23
46. Shoghi E, Fuguet E, Bosch E, Rafols C (2013) Solubility-pH profiles of some acidic, basic and amphoteric drugs. *Eur J Pharm Sci* 48(1–2):291–300
47. Paus R, Ji Y, Vahle L, Sadowski G (2015) Predicting the solubility advantage of amorphous pharmaceuticals: a novel thermodynamic approach. *Mol Pharm* 12(8):2823–2833
48. Zvyaga T, Chang S-Y, Chen C, Yang Z, Vuppugalla R, Hurley J, Thorndike D, Wagner A, Chimalakonda A, Rodrigues AD (2012) Evaluation of six proton pump inhibitors as inhibitors of various human cytochromes P450: focus on cytochrome P450 2C19. *Drug Metab Dispos* 40:1698–1711
49. Weaver CD, Harden D, Dworetzky SI, Robertson B, Knox RJ (2004) A thallium-sensitive, fluorescence-based assay for detecting and characterizing potassium channel modulators in mammalian cells. *J Biomol Screen* 9:671–677
50. Cai X, Walker A, Cheng C, Paiva A, Li Y, Kolb J, Herbst J, Shou W, Weller H (2012) Approach to improve compound recovery in a high-throughput Caco-2 permeability assay supported by liquid chromatography-tandem mass spectrometry. *J Pharm Sci* 101:2755–2762
51. Jiang H, Demers R, Kandoussi H, Burrell R, Eley T, Kadiyala P, Cojocar L, Baker C, Ryan J, Aubry AF et al (2015) Sensitive and accurate liquid chromatography-tandem mass spectrometry methods for quantitative determination of a novel hepatitis C NS5B inhibitor BMS-791325 and its active metabolite in human plasma and urine. *J Pharm Biomed Anal* 107:17–23
52. Obha K, Mizokami M, Lau JYN, Orito E, Ikeo K, Gojobori T (1996) Evolutionary relationship of hepatitis C, pesti-, flavi-, plantviruses, and newly discovered GB hepatitis agents. *FEBS Lett* 378:232–223
53. Gurney ME, Burgin AB, Magnusson OT, Stewart LJ (2011) Small molecule allosteric modulators of phosphodiesterase 4. *Handb Exp Pharmacol* 204:167–192
54. PDB ID is 4NLD
55. Connolly ML (1983) Solvent-accessible surfaces of proteins and nucleic acids. *Science* 221:709–713
56. Rigat KL, Lu H, Wang Y, Argyrou A, Fanslau C, Beno B, Wang Y, Marcinkeviciene J, Ding M, Gentles RG et al (2014) Mechanism of inhibition for BMS-791325, a novel non-nucleoside inhibitor of hepatitis C virus NS5B polymerase. *J Biol Chem* 289(48):33456–33289
57. Sims KD, Lemm J, Eley T, Liu M, Berglund A, Sherman D, Lawitz E, Vutikullird AB, Tebas P, Gao M, Pasquinelli C, Grasela DM (2014) Randomized, placebo-controlled, single-ascending-dose study of BMS-791325, a hepatitis C virus (HCV) NS5B polymerase inhibitor, in HCV genotype 1 infection. *Antimicrob Agents Chemother* 58:3496–3503
58. Belema M, Nguyen VN, Bachand C, Deon DH, Goodrich JT, James CA, Lavoie R, Lopez OD, Martel A, Romine JL et al (2014) Hepatitis C virus NS5A replication complex inhibitors: the discovery of daclatasvir. *J Med Chem* 57(5):2013–2032
59. Belema M, Meanwell NA (2014) Discovery of daclatasvir, a pan-genotypic hepatitis C virus NS5A replication complex inhibitor with potent clinical effect. *J Med Chem* 57(12):5057–5071
60. Scola PM, Sun L, Wang AX, Chen J, Sin N, Venables BL, Sit S, Chen Y, Cocuzza A, Bilder DM et al (2014) The discovery of asunaprevir (BMS-650032), an orally efficacious NS3 protease inhibitor for the treatment of hepatitis C virus infection. *J Med Chem* 57(5):1730–1752
61. Kao J-H, Yu M-L, Peng C-Y, Heo J, Chu C-J, Chang T-T, Lee Y-J, Hu T-H, Yoon KT, Paik SW, Lim Y, Lim S, Ahn SH, Isakov V, McPhee F, Hu W, Swenson ES, Yin PD, Treitel M (2017) Daclatasvir/asunaprevir/beclabuvir, all-oral, fixed-dose combination for patients with chronic hepatitis C virus genotype 1. *J Gastroenterol Hepatol* 32(12):1998–2005
62. Muir AJ, Poordad F, Lalezari J, Everson G, Dore GJ, Herring R, Sheikh A, Kwo P, Hézode C, Pockros PJ, Tran A, Yozviak J, Reau N, Ramji A, Stuart K, Thompson AJ, Vierling J, Freilich B, Cooper J, Ghesquiere W, Yang R, McPhee F, Hughes EA, Swenson ES, Yin PD

- (2015) Daclatasvir in combination with asunaprevir and beclabuvir for hepatitis C virus genotype 1 infection with compensated cirrhosis. *J Am Med Assoc* 313(17):1736–1744
63. Toyota J, Karino Y, Suzuki F, Ikeda F, Ido A, Tanaka K, Takaguchi K, Naganuma A, Tomita E, Chayama K, Fujiyama S, Inada Y, Yoshiji H, Watanabe H, Ishikawa H, Hu W, McPhee F, Linaberry M, Yin PD, Swenson ES, Kumada H (2017) Daclatasvir/asunaprevir/beclabuvir fixed-dose combination in Japanese patients with HCV genotype 1 infection. *J Gastroenterol* 52(3):385–395
64. AbuTarif M, He B, Ding Y, Sims K, Zhu K, Rege B, Pursley J, Wind-Rotolo M, Li W, Bertz RJ (2014) The effect of steady-state BMS-791325, a non-nucleoside HCV NS5B polymerase inhibitor, on the pharmacokinetics of midazolam in healthy Japanese and Caucasian males. 15th international workshop on clinical pharmacology of HIV and hepatitis therapy. Washington DC, May 19–21
65. Tatum H, Thuluvath PJ, Lawitz E, Martorell C, DeMicco M, Cohen S, Rustgi V, Ravendhran N, Ghalib R, Hanson J, Zamparo J, Zhao J, Cooney E, Treitel M, Hughes E (2015) A randomized, placebo-controlled study of the NS5B inhibitor beclabuvir with peginterferon/ribavirin for HCV genotype 1. *J Viral Hepatol* 22(8):658–664
66. Everson GT, Sims KD, Rodriguez-Torres M, Hézode C, Lawitz E, Bourlière M, Loustaud-Ratti V, Rustgi V, Schwartz H, Tatum H, Marcellin P, Pol S, Thuluvath PJ, Eley T, Wang X, Huang SP, McPhee F, Wind-Rotolo M, Chung E, Pasquinnelli C, Grasela DM, Gardiner DF (2014) Efficacy of an interferon- and ribavirin-free regimen of daclatasvir, asunaprevir, and BMS-791325 in treatment-naive patients with HCV genotype 1 infection. *Gastroenterology* 146(2):420–429
67. Hassanein T, Sims KD, Bennett M, Gitlin N, Lawitz E, Nguyen T, Webster L, Younossi Z, Schwartz H, Thuluvath PA, Zhou H, Raga B, McPhee F, Zhou N, Wind-Retools M, Chung E, Griffies A, Grasela DM, Gardiner DF (2015) A randomized trial of daclatasvir in combination with asunaprevir and beclabuvir in patients with chronic hepatitis C virus genotype 4 infection. *J Hepatol* 62(5):1204–1206

Part III
HCV NS3/4a Protease Inhibitors

Evolution of HCV NS3/4a Protease Inhibitors



Nigel J. Liverton

Contents

1	Introduction	232
2	Product-Based Inhibition as a Starting Point for Medicinal Chemistry	232
3	Peptide Optimization and Replacement of P1 Cysteine	234
4	Serine Trap Compounds: Slowly Reversible Covalent Inhibitors	237
5	Acyclic Reversible NS3/4a Inhibitors	240
6	P1–P3 Macrocyclic NS3/4a Inhibitors	243
7	P2–P4 Macrocyclic NS3/4a Inhibitors	247
8	Bismacrocyclic Inhibitors	251
9	Conclusions	252
	References	254

Abstract HCV NS3/4a protease was identified as a target for drug discovery over 20 years ago. Cleavage products from substrate-based peptides provided the starting point for medicinal chemistry. However, their less-than-ideal properties as leads would make the path to orally bioavailable inhibitors a highly challenging one. Extensive optimization efforts by multiple groups led to inhibitors with reduced peptidic character in both reversible and slowly reversible covalent classes. Ten NS3/4a inhibitors have received regulatory approval to date starting with slowly reversible ketoamides boceprevir and telaprevir in 2011 for use in combination with interferon and ribavirin. Subsequently, reversible inhibitors that advanced into clinical studies from acyclic, P1–P3 macrocyclic, P2–P4 macrocyclic, and P1–P3/P2–P4 bismacrocyclic structural classes yielded seven approved drugs to date. The most recent approvals include multiple third-generation cross-genotype active compounds that also have improved activity against key NS3/4a resistance mutations at A156, R155, and D168. These compounds, including grazoprevir, glecaprevir, and

N. J. Liverton (✉)
Tri-Institutional Therapeutics Discovery Institute, New York, NY, USA
e-mail: nliverton@tritdi.org

voxilaprevir, can be used in interferon/ribavirin-free, direct-acting antiviral combinations with cure rates approaching 100% coupled with reduced duration of treatment. The evolution of inhibitor design leading to this successful outcome is discussed.

Keywords Asunaprevir, Boceprevir, Ciluprevir, Danoprevir, Faldaprevir, Glecaprevir, Grazoprevir, HCV protease, Interferon-free, Macrocyclic inhibitors, Narlaprevir, Paritaprevir, Ribavirin-free, Simeprevir, Sovaprevir, Telaprevir, Vaniprevir, Vedoprevir, Voxilaprevir

1 Introduction

HCV NS3/4a protease is a member of the chymotrypsin superfamily of serine proteases [1] and plays a critical role in HCV replication. It is responsible for cleavage of a viral polypeptide at four sites (NS3-NS4a, NS4a-NS4b, NS4b-NS5a, and NS5a-NS5b) to release nonstructural proteins possessing activities essential for viral replication [2]. HCV also evades the host immune response via multiple mechanisms including NS3/4a-mediated cleavage of key proteins involved in the immune system signaling pathways [3]. NS3/4a protease is composed of two separate domains, a smaller 1–180 serine protease domain and a larger helicase domain [4], and the NS4A cofactor is required for activity [5].

The starting point for medicinal chemistry efforts to identify NS3/4a protease inhibitors was observations of product-based inhibition by substrate cleavage products made by multiple groups.

2 Product-Based Inhibition as a Starting Point for Medicinal Chemistry

The IRBM group found that a P6–P7' [6] peptide substrate **1** based on the NS4a-NS4b cleavage sequence led to a product-based inhibitor with a calculated K_i of 0.7 μM (Fig. 1) [7]. Additional experiments showed that the N-terminal cleavage product **3** was responsible for inhibition (K_i 0.6 μM), while the C-terminal cleavage product **2** showed no activity ($K_i > 500 \mu\text{M}$). Substrates based on other cleavage sites (NS5a-NS5b (**4**), NS4b-NS5a (**6**), and NS3-NS4a (**8**)) were also evaluated. In all cases the C-terminal products were inactive, and while the N-terminal products **5** and **7** were inhibitors (K_i 1.4 μM and 180 μM , respectively), the NS3-NS4a N-terminal cleavage product **9** was inactive.

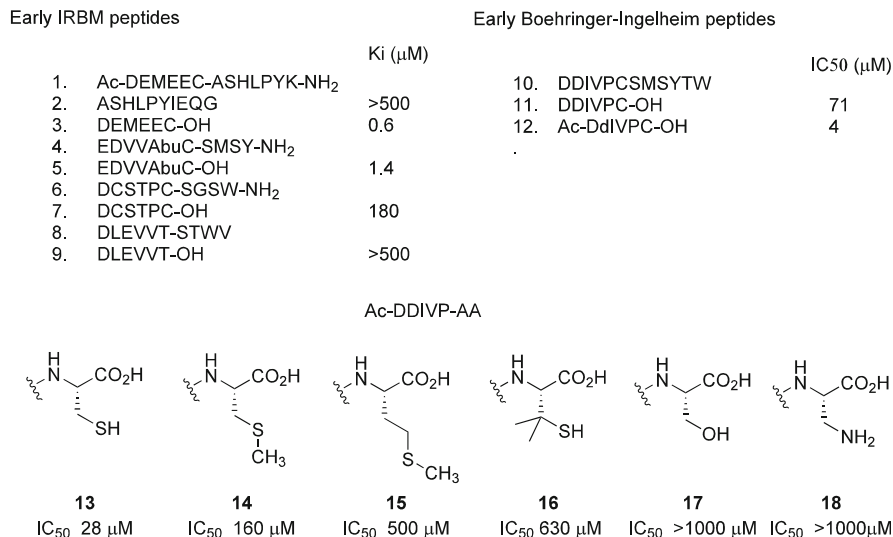


Fig. 1 Early product-based peptide inhibitors

Concurrently, the Boehringer Ingelheim group made similar observations using a related substrate **10** also derived from the NS5A-NS5B cleavage site [8]. The N-terminal hexapeptide product **11** inhibited cleavage with IC₅₀ 71 μM. An alanine scan across hexapeptide **11** did not lead to more potent compounds. In contrast, a D-amino acid scan yielded a single more potent compound when P5 Asp was inverted, leading to hexapeptide **12** (IC₅₀ 4 μM), a competitive inhibitor of NS3/4a protease with K_i 0.6 μM.

These early observations formed a critical starting point for medicinal chemistry efforts although the journey to multiple marketed NS3/4a inhibitors presented formidable obstacles. These included the well-known issues of transforming peptide leads into orally bioavailable drugs as well as specific hurdles to overcome related to the unique structure of NS3/4a protease relative to other related serine proteases. Crystal structures [9–12] revealed that NS3/4a differed from other proteases in the chymotrypsin family with multiple loops connecting the β-strands of the N-terminal domain being significantly shorter in NS3/4a. The net result of these changes is a shallow, solvent-exposed substrate-binding channel in NS3/4a lacking deep binding pockets, further complicating the design of orally bioavailable inhibitors. The presence of a P1 cysteine in these early product-based inhibitors only served to add to the medicinal chemistry challenges, particularly in light of initial studies evaluating replacements (**14–17**) in Cys-containing peptide **13**, which demonstrated at best weak inhibitory activity [8].

3 Peptide Optimization and Replacement of P1 Cysteine

The IRBM group tackled optimization of hexapeptide **3** through both single changes and combinatorial libraries [13]. Key binding elements were confirmed to be the P1 Cys and the P5–P6 acidic residue pair. Lipophilic P4 substituents improved activity with peptide **19** (Fig. 2) possessing the 3,3-diphenylalanine showing the most potent activity (K_i 40 nM).

Recognizing that the P1 Cys would be incompatible with the goal of developing chemically stable and orally bioavailable drugs, the group turned attention to thiol replacement. Using a computational chemistry approach, CHF₂ appeared to mimic the SH group both in terms of volume and molecular electrostatic potential [14]. Incorporation of this modified P1 amino acid into hexapeptide **19** (K_i 40 nM, Fig. 2) led to **20** (K_i 30 nM) providing an entry point into a chemically stable series of

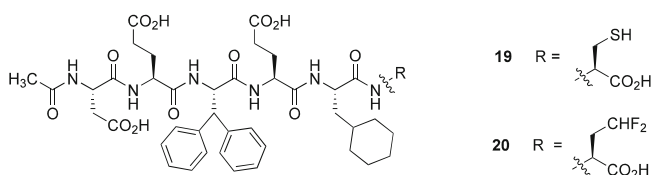


Fig. 2 P1 Cys replacement

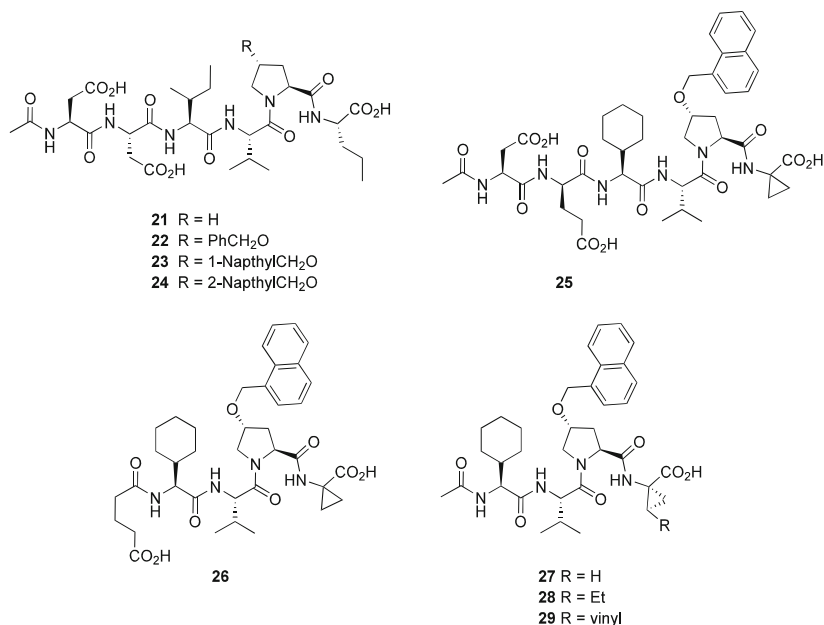


Fig. 3 Boehringer Ingelheim peptide evolution

inhibitors but still contained two acidic P5–P6 amino acids making oral bioavailability unlikely.

The Boehringer Ingelheim group utilized hexapeptide **21** (IC_{50} 150 μ M, Fig. 3) as a starting point for lead development with the goal of reducing overall size and peptidic character. One of the key differences between this and the IRBM peptide lead was the P2 proline which became a key focus for SAR studies after initial substitution with (R)-benzyloxy at the proline 4-position yielded inhibitor **22** (IC_{50} 7 μ M) [15]. Compound **22** was shown by NMR studies to bind to NS3/4a protease in a well-defined extended conformation with the benzyloxy substituent in direct contact with the protease [16]. The improved activity was limited to (R)-stereochemistry and could be further optimized with larger naphthyl groups to give submicromolar analogs **23** and **24** (IC_{50} 0.39 μ M, 0.71 μ M, respectively).

Other modifications associated with improving activity included cyclopropylglycine for norvaline at P1, cyclohexylglycine for isoleucine at P4, and D-glutamic acid for aspartic acid at P5. Combining the different changes afforded **25** (K_i 0.013 μ M) which showed >10,000-fold selectivity over representative serine proteases (human leucocyte elastase, human pancreatic elastase, α -chymotrypsin, and cathepsin B). In an important development for the field, this potent inhibitor provided the entry point for reducing lead size first to pentapeptide **26** (IC_{50} 0.9 μ M) and subsequently tetrapeptide **27** (IC_{50} 3.5 μ M), removing two carboxylate-containing amino acids.

Further optimization of the shortened peptide **27** was carried out via a series of elegant SAR investigations. Substitution on the cyclopropyl ring in **27** with ethyl yielded a modest threefold improvement in activity (**28** IC_{50} 4.8 μ M) [17]. Vinyl substitution yielded a more significant ~20-fold enhancement in activity (**28** IC_{50} 0.63 μ M), and this P1 moiety is found in multiple HCV protease inhibitors that entered clinical trials. Using NMR and computational chemistry to guide inhibitor design; the naphthyl substituent on P2 proline was modified to the phenylquinoline analogs **30** and **31** [18] (Fig. 4). Hexapeptide analog **30** showed subnanomolar potency against NS3/4a (IC_{50} < 0.5 nM); however, cell-based activity as measured in a subgenomic replicon assay showed a dramatic shift (EC_{50} 1,900 nM) [20]. Tetrapeptide **31** while showing reduced enzyme inhibition activity (IC_{50} 13 nM) nonetheless represented a landmark activity for a reversible tetrapeptide inhibitor.

With potent NS3/4a inhibitors in hand, identifying further modified analogs that could enhance cell-based assay activity became an important objective. X-ray structural data showing the close proximity of the terminal P3 methyl and the P1 α -hydrogen in hexapeptide **30** when docked into the active site of NS3/4a [19] provided the basis for design of P1–P3 macrocycles. Macrocycle **32** (IC_{50} 11 nM, EC_{50} 77 nM) was obtained by incorporating a 15-membered macrocyclic ring into the tetrapeptide inhibitor series. This not only addressed the large shift in potency going from enzyme inhibition to cell-based assay, but **32** and more particularly the reduced analog **33** (IC_{50} 28 nM, EC_{50} 120 nM) showed oral bioavailability in rat PK studies (F 2% and 20%, respectively). Having demonstrated oral bioavailability, the stage was set for an end game in which the P4 capping carbamate and P2 quinoline

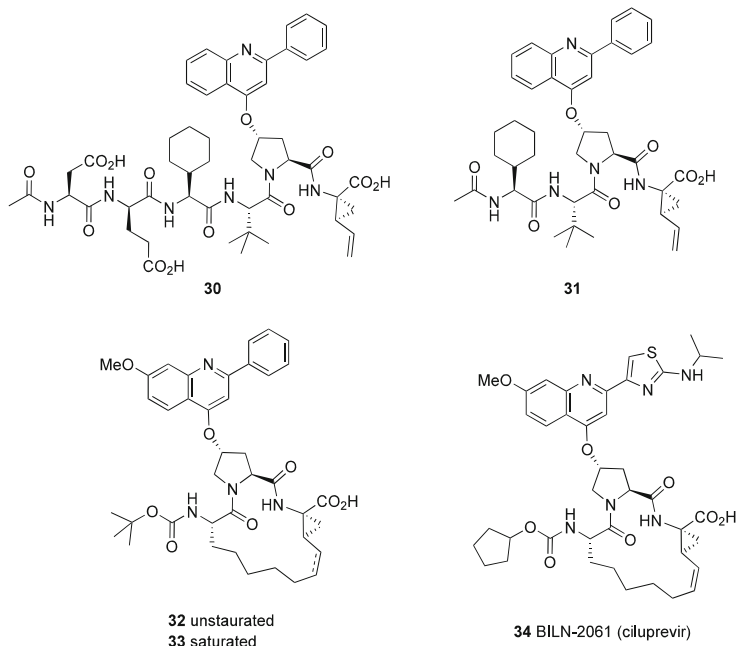


Fig. 4 Boehringer Ingelheim late-stage optimization leading to ciluprevir

substituents were optimized to lead to **34** (BILN-2061, ciluprevir) (IC_{50} 3 nM, EC_{50} 1.2 nM) [20]. Proof-of-concept antiviral activity was observed in Phase 1b studies with BILN-2061 [21], the first NS3/4 inhibitor dosed to patients. While development of BILN-2061 was ultimately discontinued [22] due to cardiac toxicity in rhesus monkey [23], it remains a seminal contribution in the field of NS3/4a inhibitor research. Additionally the process development research on BILN-2061 demonstrated the viability of a ring closing metathesis approach to these macrocycles on large scale [24–26].

In vitro resistance selection studies with BILN-2061 identified R155, A156, and D168 as key residues that confer reduced sensitivity to inhibitor [27, 28], a pattern that would be replicated across most of the reversible inhibitors. While many key questions remained unanswered in 2004, including maximum SVR rates that could be achieved, breadth of genotype coverage, impact of resistance mutations, appropriate combination dosing and treatment duration, the clinical data with BILN-2061 provided human validation for NS3/4a protease as a target and led different groups to take many shots on goal with, ultimately, multiple successful outcomes.

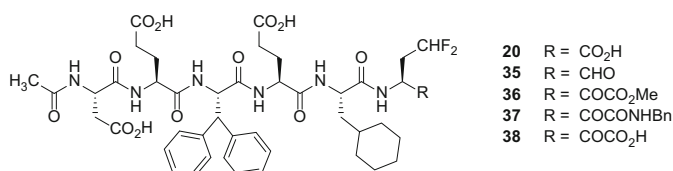
4 Serine Trap Compounds: Slowly Reversible Covalent Inhibitors

In parallel with efforts to optimize reversible inhibitors, several groups took the alternative path of developing compounds with warheads capable of forming covalent adducts with the active site serine. This approach has been used with other serine proteases [29, 30], and the warhead group can result in either a fully covalently bound (e.g., fluoromethylketone) or slowly reversible inhibitor (aldehyde, α -ketoacid, α -ketoamide, or boronic acid), the latter having potential advantages.

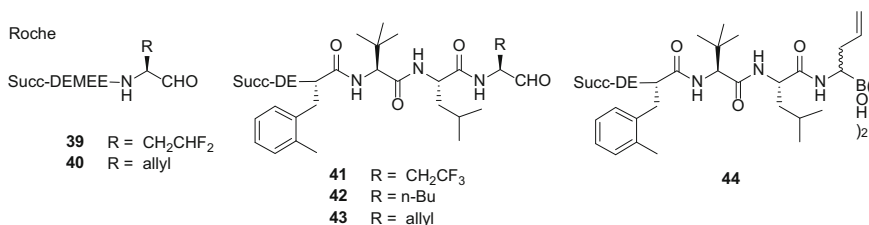
The IRBM group introduced a number of these functionalities into the reversible hexapeptide **20** (K_i 30 nM) described above. Aldehyde **35** (Fig. 5, K_i 0.5 nM), keto ester **36** (K_i 2 nM), and ketoamide **37** (K_i 1.5 nM) all proved more potent than **20**. The ketoacid **38** proved to be an exceptionally potent inhibitor of NS3/4a protease (K_i 0.01 nM) [14].

The Roche group also developed a series of aldehyde-based inhibitors using substrate cleavage rates to design P1 cysteine replacements. Initial compounds such as **39** and **40** possessing difluoroethyl and allyl P1 side chains showed modest

IRBM



Roche



Vertex

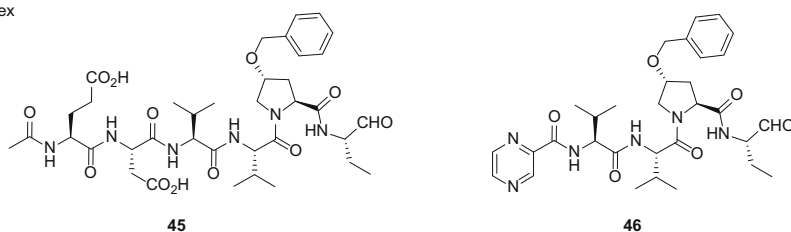


Fig. 5 Early covalent inhibitors

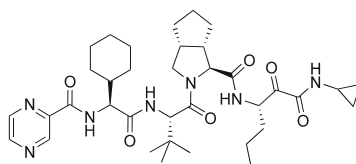
potency (IC_{50} 22 μ M and 20 μ M, respectively) [31]. After a process of P2, P3, and P4 optimization, aldehydes with ~1,000-fold improvement in potency were obtained with P1 trifluoroethyl (**41** IC_{50} 64 nM), *n*-butyl (**42**, IC_{50} 65 nM), and allyl (**43**, IC_{50} 90 nM).

Recognizing that aldehydes would not be viable drug candidates and with boronic acids having previously shown potent serine protease activity in vitro [32] and in vivo [33], analogs in this hexapeptide system were synthesized. The boronic acid analog **44** (IC_{50} 34 nM) of aldehyde **43** improved potency approximately twofold.

The Vertex group also used an aldehyde warhead to develop early SAR, using a Boehringer Ingelheim-related hexapeptide **45** (K_i 0.89 μ M) as the starting point (Fig. 5). Removing the P5 and P6 substituents in **45** and capping with the pyrazine amide afforded aldehyde **46** which showed a relatively modest drop in activity (K_i 12 μ M) relative to the effect of truncation of the two acidic residues in reversible peptide scaffolds. An extensive optimization program [34, 35] then led to bicyclic proline derivatives [36–38] ultimately affording **47** (Fig. 6, VX-950, L-570310, telaprevir). Further advancement of VX-950 was carried out within Vertex after a 2003 restructuring of the Lilly-Vertex collaboration to give Vertex worldwide rights to compounds discovered under the collaboration in return for royalties [39].

The Schering–Plough group was also working on ketoamide inhibitors of NS3/4a, although taking a somewhat different approach. The IRBM and Vertex/Lilly efforts focused on substrate cleavage product peptides as starting points. In contrast, Schering–Plough started with a P6–P5' undecapeptide substrate analog **48** (Fig. 7, K_i 1.9 nM) that already incorporated the ketoamide functionality in place of the scissile bond [40]. Removal of the P2' to P5' fragment provided a good trade-off in terms of activity lost vs. MWt decrease of almost 50% to give heptapeptide **49** (K_i 43 nM) spanning P6–P1'. As in the optimization process of other groups, identifying changes that permitted deletion of the P5, P6 was a key objective to deliver cell-based activity and provide opportunities to build in oral bioavailability. Schering–Plough accomplished this with pentapeptide derivative **50** (K_i 66 nM) which provided an entry point into SAR optimization studies that ultimately delivered **51** (SCH503034, boceprevir) (K_i 14 nM, EC_{90} 350 nM).

Boceprevir and telaprevir were both approved by the FDA in May 2011 for treatment of genotype 1 (Gt1) HCV infected patients in combination with pegylated interferon (PEG-IFN) and ribavirin (RBV). As the first NS3/4a protease inhibitors



47 VX-950 (telaprevir)

Fig. 6 Telaprevir

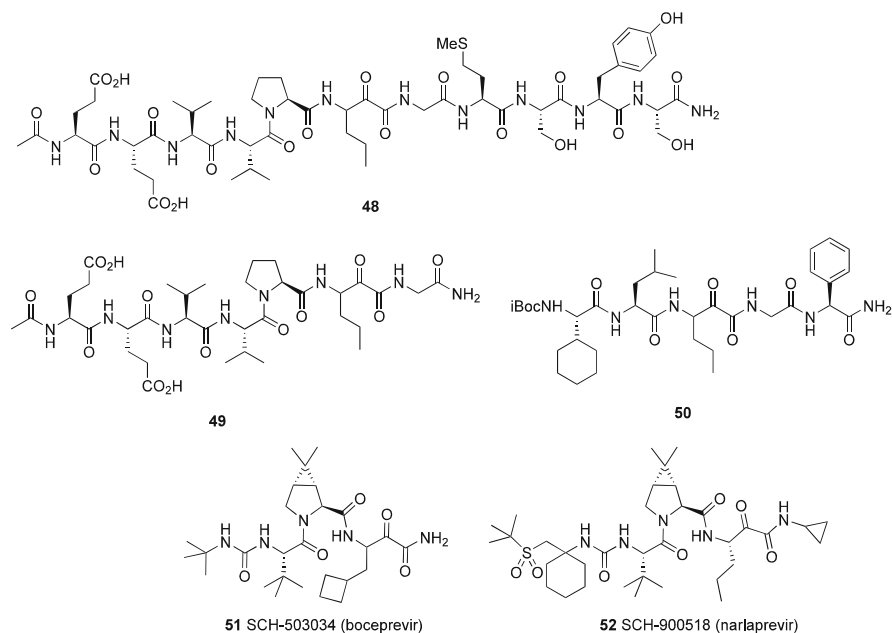


Fig. 7 Schering–Plough covalent inhibitor evolution

and indeed the first direct-acting antiviral drugs approved to treat hepatitis C, this marked the start of a new era in treatment paradigms. SVR rates in Gt1 patients were significantly improved from ~40 to ~70–80%. With warehousing of patients having occurred widely in anticipation of new treatment options becoming available, rapid adoption of these new treatment options led to telaprevir becoming the fastest drug to reach \$1B in cumulative sales in just over 6 months.

While a major step forward, these first-generation inhibitors were not without issues. The need to dose in combination with PEG-IFN/RBV meant the AEs associated with those agents – primarily flu-like symptoms and anemia were added to the protease inhibitor side-effect profiles. In addition, dosing frequency was significantly less than ideal with t.i.d required for boceprevir and t.i.d (or b.i.d with a high fat meal) for telaprevir. Both of these first-generation inhibitors presented a relatively low barrier to resistance with V36, T54, R155, and A156 mutations identified in clinical studies. Thus, while these two initial drugs showed very rapid uptake, they proved vulnerable as new direct-acting agents (DAAs) were approved. The first of these, sofosbuvir, approved by the FDA in December 2013 (an NS5B polymerase nucleotide inhibitor rather than NS3/4a inhibitor) provided a more compelling profile – once-a-day dosing coupled with the high genetic barrier to resistance associated with nucleotides. Reduced duration of treatment (12–24 weeks) and the removal of PEG-IFN for treatment of genotypes 2 and 3 and possibly genotype 1 proved highly attractive to prescribing physicians. Together with other emerging treatments, this led to rapidly declining sales for both telaprevir and

boceprevir and ultimately their discontinuation in October 2014 and December 2015, respectively.

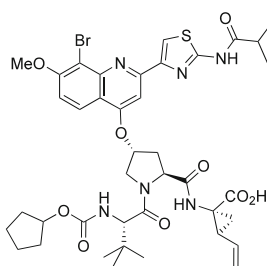
Schering–Plough continued to work on ketoamide-based inhibitors with optimization directed toward improved in vitro potency and PK. While SAR of P4 carbamate, ketone, ester, imide, and sulfonamide caps could improve cell-based activity and rat PK, improvements in primate PK were more challenging [41–43]. Sulfone-based capping groups in combination with P1 and P1' re-optimization succeeded in delivering improved in vitro potency coupled with improved PK including in monkey ($F = 46\%$) in **52** (SCH-900518, narlaprevir) [44]. Resistance selection studies in replicon cells indicated cross resistance to mutations conferring resistance to boceprevir and telaprevir, although the higher intrinsic potency (~tenfold in replicon) offered potentially improved coverage of resistant mutants [45].

Following the Schering–Plough–Merck merger, narlaprevir was licensed to the Russian company R-Pharm in 2012. Following additional clinical studies [46], a Russian Federation registration certificate was granted for narlaprevir (Arlansa) in May 2016 for treatment of naïve and treatment-experienced genotype 1b infected patients in combination with PEG-IFN/RBV.

5 Acyclic Reversible NS3/4a Inhibitors

In their early studies, Boehringer Ingelheim showed that acyclic analogs on the optimization path to ciluprevir had poor pharmacokinetics relative to closely related P1–P3 macrocycles. Further optimization in the acyclic series both in their group and others led to acyclic compounds with improved preclinical PK profiles.

Re-optimization of the acyclic series by modifying the ciluprevir P2 quinoline with introduction of a bromo substituent and an amide substituent rather than amine substituent on the thiazole led to discovery of second-generation inhibitor BI 201335 **53** (faldaprevir) (Fig. 8) with potent enzyme (IC_{50} 3 nM) and cell-based activity (EC_{50} 3 nM) [47]. In testing across a broader panel of protease genotypes, it showed



53 BI 201335 (faldaprevir)

Fig. 8 Faldaprevir

broadly comparable activity against Gt4a, 5a, and 6a. As is typical of NS3/4a protease inhibitors, Gt3 activity displays the greatest shift (~100-fold), although Gt2a/2b shifts were also significant (~10–25-fold). BI 201335 showed good oral exposure after dosing to rat, dog, and monkey, with partitioning into liver evident from rat studies (liver/plasma 42-fold within 1 h) and maintained over 8 h [48].

The compound advanced into Phase 3 clinical studies with PEG-IFN/RBV (120 or 240 mg qd 12–24 weeks and additional PEG-IFN for 12–36 weeks) [49] leading to 73% SVR rate. In an effort to move toward PRG-IFN-free combinations, faldaprevir was studied in combination with deleobuvir (NS5b non-nucleoside inhibitor) and RBV [50, 51], but these trials showed significantly lower efficacy in Gt1a vs. Gt1b patients. In light of the rapidly advancing treatment landscape, Boehringer Ingelheim announced in June 2014 that it was withdrawing all marketing applications for faldaprevir/PEG-IFN-based treatments and exiting the HCV therapeutic area.

The BMS group made a key contribution to the field through synthesis of reversible inhibitors that could make additional P1' binding interactions by replacement of the carboxylic acid with an acyl sulfonamide moiety [52]. The simplest methyl analog **55** (Fig. 9) showed activity (IC_{50} 36 nM, EC_{50} 600 nM) comparable to the carboxylic acid starting point **54** (IC_{50} 54 nM, EC_{50} 550 nM). Guided by modeling, SAR around the methyl was extended leading to the cyclopropyl acylsulfonamide **56** (IC_{50} 1 nM, EC_{50} 4 nM), with minor modifications of cyclopropyl leading to a dramatic falloff in activity. Adopting an isoquinoline P2 substituent combined with the cyclopropyl acylsulfonamide led, after optimization, to **57** (BMS-605339) as a compound that balanced potent in vitro activity (Gt1a IC_{50} 2 nM, Gt1b EC_{50} 12 nM) with a good preclinical PK profile. As observed by other groups, the PK parameters of very closely related analogs showed significant differences, suggesting potential involvement of transporters in distribution of compound in vivo. BMS-605339 advanced into Phase 1 clinical studies in healthy

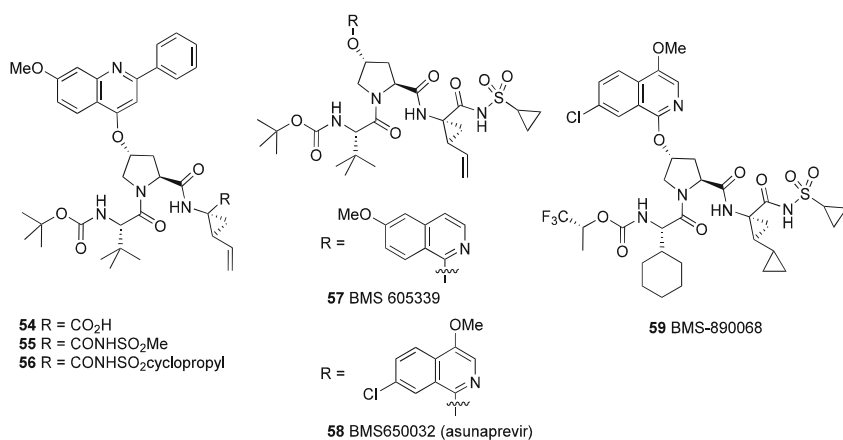


Fig. 9 BMS acyclic inhibitors

subjects and Gt1 infected patients in which significant drops in viral load (average 1.8 \log_{10} reductions at 120 mg dose) were observed. Development of BMS-605339 was discontinued after observation of ECG changes in Phase 1.

To guide the development of compounds that would circumvent this issue, the BMS group developed an ex vivo model with predictive value for cardiovascular effects. Careful modification of the isoquinoline P2 substituent eliminated the cardiovascular effects while maintaining an attractive in vitro profile in **58** (BMS-650032, asunaprevir) (IC_{50} Gt1a 1 nM, EC_{50} Gt1b 6 nM) [53]. This was coupled with oral bioavailability (rat $F = 12\%$) and liver exposure (15.2 μM @ 24 h after 15 mpk dose) [54]. Asunaprevir in combination with NS5a inhibitor daclatasvir led to >90% SVR rate in Asian Gt1b infected patients [55–57].

In July 2014 Japan approved the combination of asunaprevir and daclatasvir as the first all-oral PEG-IFN/RBV-free treatment available in Japan for Gt1b infected patients with a treatment duration of 24 weeks.

Continued work on this series led to identification of backup analog BMS-890068 **59** [58] that represented additional optimization of the P3 capping group in combination with cyclopropyl-substituted P1 amino acid in place of the more typical vinyl or ethyl substituents.

The vinyl acylsulfonamide P1 fragment was ultimately incorporated into multiple NS3/4a clinical candidates and approved drugs.

Achillion identified an acyclic analog **60** (ACH-1625, sovalprevir) (Fig. 10) that differed in using a substituted succinic diamide scaffold in P3 instead of the typically used amino acids. The compound was potent in vitro vs. both Gt1a and 1b ($IC_{50} < 1$ nM) [59] and a Gt1b replicon assay (EC_{50} 11 nM) [60]. Clinical proof of concept was obtained with the compound in a 4-day monotherapy study with additional Phase 2 studies either in combination with PEG-IFN/RBV or in a separate trial, with ACH-3102 (NS5a inhibitor) showing impressive SVR rates (~90%). However the compound was placed on clinical hold in early 2013 due to liver enzyme elevations seen in a DDI study with atazanavir. That clinical hold was lifted in mid-2014, although further development activities have not been reported.

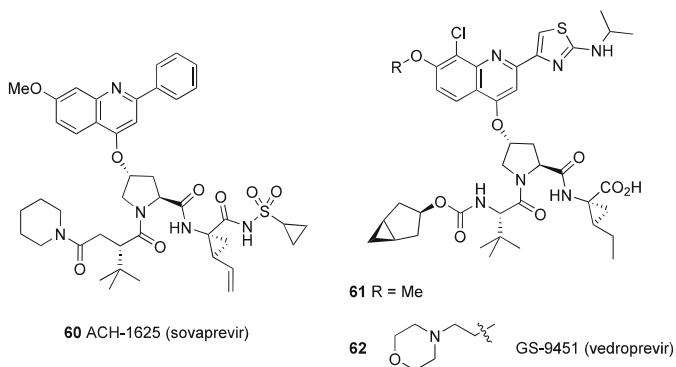


Fig. 10 Achillion and Gilead acyclic inhibitors

The Gilead group also optimized SAR in the P2 quinoline acyclic series. After saturating the P1 vinyl cyclopropyl group to ethylcyclopropyl, introduction of cis-fused cyclopropyl on the P3 capping cyclopentyl carbamate afforded **61** with good in vitro activity (IC_{50} 1.4 nM, EC_{50} 9 nM) [61]. The methyl ether on the quinoline was replaced by ether-linked amines with the morpholinoethyl analog **62** (GS-9451, vedoprevir) resulting in improved cell-based activity (IC_{50} 3.2 nM, EC_{50} 2.0 nM) together with greatly improved solubility at low pH. GS-9451 had an attractive PK profile in rat, dog, and cynomolgous monkey coupled with significant liver partitioning in rats (~40-fold liver: plasma after a 1 mpk IV dose) [62]. However, in vitro activity was significantly weaker vs. Gt2a (EC_{50} 251–316 nM). Vedoprevir progressed into Phase 2 clinical studies but no longer appeared in Gilead pipeline updates from 2015, and development was likely discontinued as a result of more attractive profiles of other all-oral DAA combinations that Gilead was advancing.

A number of these acyclic analogs emerged from relatively early discovery efforts when the primary focus was on agents that could be combined with PEG-IFN/RBV targeting primarily genotype 1 infections which were the hardest to treat with PEG-IFN/RBV alone. As discovery efforts advanced in both the acyclic and macrocyclic inhibitor series, the confirmation of key resistance mutations at residues R155, A156, and D168 in other reversible inhibitors provided additional goals for compound profile optimization. As indicated, a number of the compounds described in this section were discontinued not for clinical failure but rather as part of strategic decisions based on the rapidly evolving treatment options that continually raised the bar on the clinical profile required to be a commercially competitive compound. Asunaprevir, a second-generation inhibitor, is the only reversible acyclic inhibitor to have been approved in a major market.

6 P1–P3 Macrocyclic NS3/4a Inhibitors

Ciluprevir was the prototypical P1–P3 macrocyclic inhibitor, but as described above, it was discontinued as a result of preclinical toxicity. Subsequently multiple groups entered into the P1–P3 macrocycle arena which ultimately yielded a number of marketed NS3/4a protease inhibitors from this structural class.

In analogs **63** (K_i 22 nM) and **64** (K_i 1.3 nM) [63] (Fig. 11), the Medivir/Janssen group made an early decision to change the proline ring at P2 to carbocyclic cyclopentyl or cyclopentenyl scaffolds. They were then able to utilize these proline replacements in conjunction with other key advances including P2 substituents, P1–P3 macrocyclization [64] and the P1–P1' acylsulfonamide group [65]. Extensive optimization led to identification of **65** (TMC-435, simeprevir) [66]. It is noteworthy that the P4 substituent in this scaffold has been successfully minimized to a methyl group, significantly smaller than present in most other inhibitors. Clinical development led to approval of simeprevir in November 2013 for treatment of Gt1 infected patients, in combination with PEG-IFN/RBV for 12 weeks followed by either 24 or

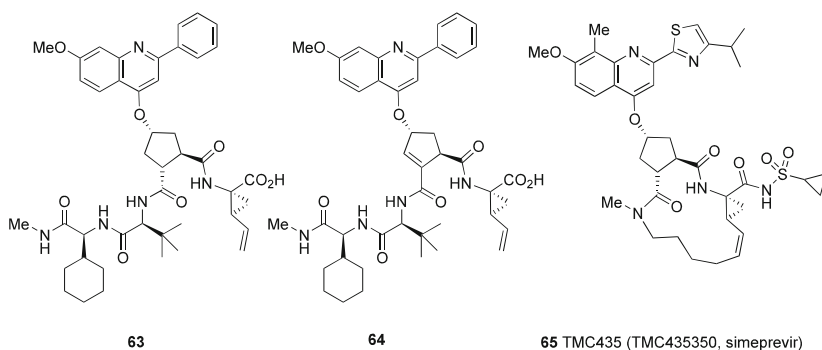


Fig. 11 Medivir/Janssen P1-P3 macrocycles

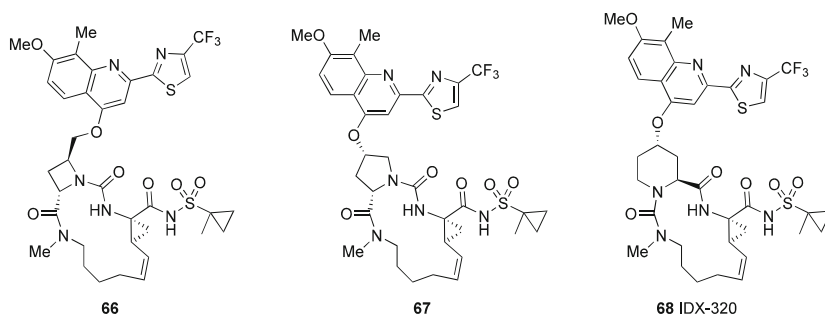


Fig. 12 Idenix P1-P3 macrocyclic inhibitors

48 weeks of PEG-IFN/RBV [67]. An extensive clinical development program was undertaken evaluating simeprevir in combination with other DAAs as it was becoming clearer that the era of PEG-IFN/RBV containing treatment paradigms was drawing to a close. One of the combinations studied, simeprevir + sofosbuvir, was approved for use in Gt1 patients in November 2014. This represented the first approval for an all-oral DAA combination containing an NS3/4a protease inhibitor and led to >90% SVR rates after 12/24-week treatment, although the high cost of combining drugs from different companies leading to 12/24-week treatment price of \$150,000/\$300,000 represents a disadvantage of this approach. Clinical studies combining simeprevir with other Janssen DAAs, odalasvir (NS5a inhibitor) and AL-335 (NS5b nucleotide prodrug inhibitor), advanced to Phase 2, but further clinical development was discontinued in 2017 “in light of the increasing availability of a number of highly effective therapies addressing the medical need in hepatitis C.”

The Idenix group also pursued alternatives to the P2 proline amino acid. Initial exploration of a series of disubstituted azetidine urea derivatives led to good in vitro activity (e.g., **66** IC₅₀ 2.1 nM) [68] (Fig. 12); however, high microsomal clearance/short half-life across species led to a focus on “reverse” proline derivatives with the

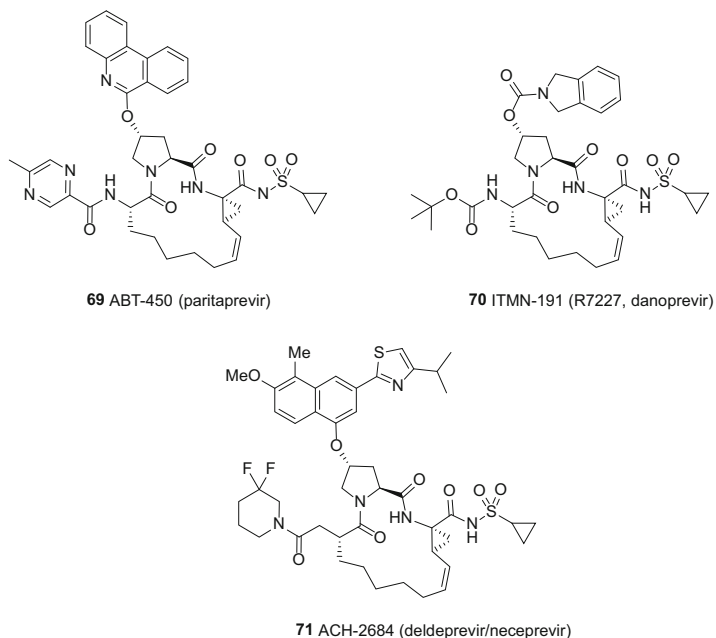


Fig. 13 AbbVie, InterMune, and Achillion P1–P3 macrocyclic inhibitors

nitrogen migrated to generate a urea link to P1. This modification yielded highly potent compounds such as **67** (IC_{50} 0.5 nM, EC_{50} 13 nM), and a bound X-ray structure of an analog related to **67** provided the design basis for incorporating a pipecolic acid scaffold in place of the proline urea. Optimization in this new series afforded **68** (IDX-320) [69] which maintained potent enzyme activity (IC_{50} 0.6 nM) coupled with a significant gain in cell-based activity (EC_{50} 0.2 nM). While proline derivative **67** showed lower clearance than pipecolic acid derivative **68**, the oral bioavailability of the latter was better (45% vs. 18%), and **68** showed drug levels in the liver at 24 h, while **67** did not. IDX-320 inhibited NS3/4a proteases across genotypes 1a, 1b, 2a, and 4a with IC_{50} 0.8–1.9 nM; as typically observed, activity was weaker against Gt3a (IC_{50} 23 nM). IDX-320 entered clinical development but was discontinued after DDI studies with nucleoside NS5b inhibitor IDX-184 in healthy subjects led to significant AEs (elevated liver function tests) which were attributed to IDX-320.

The Enanata/AbbVie group discovered **69** (Fig. 13, ABT-450 paritaprevir) based around the more typical proline-based P2, substituted with a novel tricyclic phenanthridine, and combined with the cyclopropyl acylsulfonamide. Interestingly, it incorporates a P4 pyrazine amide group similar to that present in telaprevir. Ritonavir boosting increased paritaprevir AUC and $T_{1/2}$ allowing it to be dosed qd. In December 2014, paritaprevir received FDA approval for use with ombitasvir/ritonavir/dasabuvir in a 12-week treatment for Gt1b and with RBV added for Gt1a

patients. In 2015 paritaprevir was approved for use in Gt4 patients in combination with ombitasvir (NS5a inhibitor), ritonavir, and RBV.

InterMune/Roche efforts in this area led to an isoindoline substituent on the P2 proline attached through a carbamate, a linker also evaluated by Vertex in the slowly reversible inhibitor series. Combination of the 15-membered P1–P3 macrocycle with cyclopropyl acylsulfonamide and the isoindoline moiety led to **70** (ITMN-191, R7227, danoprevir) (Gt1b K_i 0.23 nM) (Fig. 13) [70]. In vitro activity was potent against all genotypes including relatively modest shifts (~8- and ~12-fold, respectively) vs. Gt2b/3a. Danoprevir also partitioned into the liver in rat (liver:plasma 12-fold) and monkey (liver:plasma 116-fold).

Clinical development initially followed the standard approach at the time, in combination with PEG-IFN/RBV. A development path to a PEG-IFN-free combination with ritonavir and mericitabine (NS5B nucleoside inhibitor) advanced into Phase 2 studies [71]. Development of mericitabine was subsequently discontinued. In 2016 Roche licensed danoprevir to China-based Ascleitis with the goal of developing a PEG-IFN-free hepatitis C treatment for China. Combination studies of ritonavir-boosted danoprevir in combination with NS5A inhibitor ravidasvir and RBV for 12 weeks led to 100% SVR in a 38-patient trial, and danoprevir was approved by the CFDA in June 2018.

Achillion developed **71** (ACH-2684, deldeprevir, neceprevir) (Fig. 13) by adapting the succinamide scaffold present in acyclic inhibitor ACH-1625 to a P1–P3 macrocycle together with a simeprevir P2 isoquinoline. ACH-2684 has potent pan-genotypic activity in vitro [72] and showed efficacy in both Gt1 (max 4.63 log₁₀ drop) and Gt3 infected patients (2.03 log₁₀ drop). No recent development activities have been reported for deldeprevir.

All of the P1–P3 macrocycles described above have either the carboxyl or acylsulfonamide group as the P1 acidic functionality. The possibility of replacement with a phosphonic acid or phosphinic acid functionality has been investigated in P2–P4 macrocycles by the IRBM/Merck group [73]. Gilead also evaluated replacement of carboxylic acid with phosphonic acid in an acyclic tripeptide scaffold [74]. Extension of this work into the P1–P3 macrocycle series led to **72** (Fig. 14), a potent in vitro inhibitor of NS3/4a (IC₅₀ 1 nM, EC₅₀ 5 nM) [75]. While bioavailability of the macrocyclic phosphonic acid was not reported, the corresponding acyclic peptide analog had poor bioavailability which was believed to be due to the low pK_a of the phosphonic acid. After an initial study of phosphinic acids in the acyclic series, which showed that benzyl phosphinates were significantly more bioavailable than alkyl phosphinates, macrocyclic benzyl phosphinates were prepared [76]. Interestingly and unusually for these macrocyclic inhibitors, the saturated macrocycle **73** (IC₅₀ 6 nM, EC₅₀ 5 nM) (Fig. 14) was slightly more potent in the cell-based assay than the unsaturated analog **74** (IC₅₀ 3 nM, EC₅₀ 10 nM) and also had reduced clearance in dog PK (0.36 L/h/kg vs. 0.56 L/kg/h, respectively). This set the stage for an end-game optimization of a solvent-exposed benzylphosphinate and the P2 substituent to modulate oral bioavailability [77]. 2,6-Difluoro substitution on the benzyl group was found to improve Caco-2 permeability in the acyclic series and was incorporated into the macrocycle series to give **75** (IC₅₀ 4 nM, EC₅₀ 10 nM).

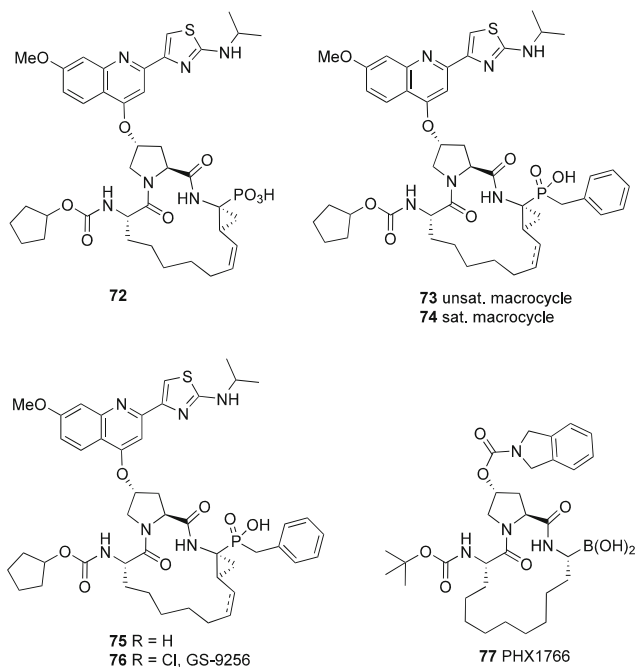


Fig. 14 P1–P3 macrocycles with alternative P1 acidic groups

Replacement of H on the P-2 substituent with Cl led to **76** (GS-9256) (IC_{50} 4 nM, EC_{50} 20 nM) which demonstrated a 7.5-fold increase in dog oral bioavailability (**75**, 2.9%, **76**, 21%). GS-9256 advanced into Phase 2 clinical studies but was ultimately discontinued in favor of GS-9451, a P2–P4 macrocycle described below which was being developed concurrently.

Limited work has been done in the P1–P3 macrocycle series with slowly reversible or irreversible inhibitors. The boronic acid-based inhibitor **77** (PHX-1766) (Fig. 14) was developed by Phenomex that uses a similar scaffold to ITMN-191 lacking the cyclopropyl constraint at P1 [78]. PHX-1766 advanced into 7-day proof-of-concept monotherapy clinical studies. Modest antiviral effects (maximum of ~2.2 log₁₀ drop at 800 mg b.i.d) led to development being discontinued.

7 P2–P4 Macrocylic NS3/4a Inhibitors

The potential to form an alternative macrocyclic linkage from P2 to P4 was first explored by the IRBM group through synthesis of biaryl ether analogs **77** and **78** (Fig. 15) related to an early peptide lead **76**, although biological data was not reported for the macrocycles [79].

IRBM

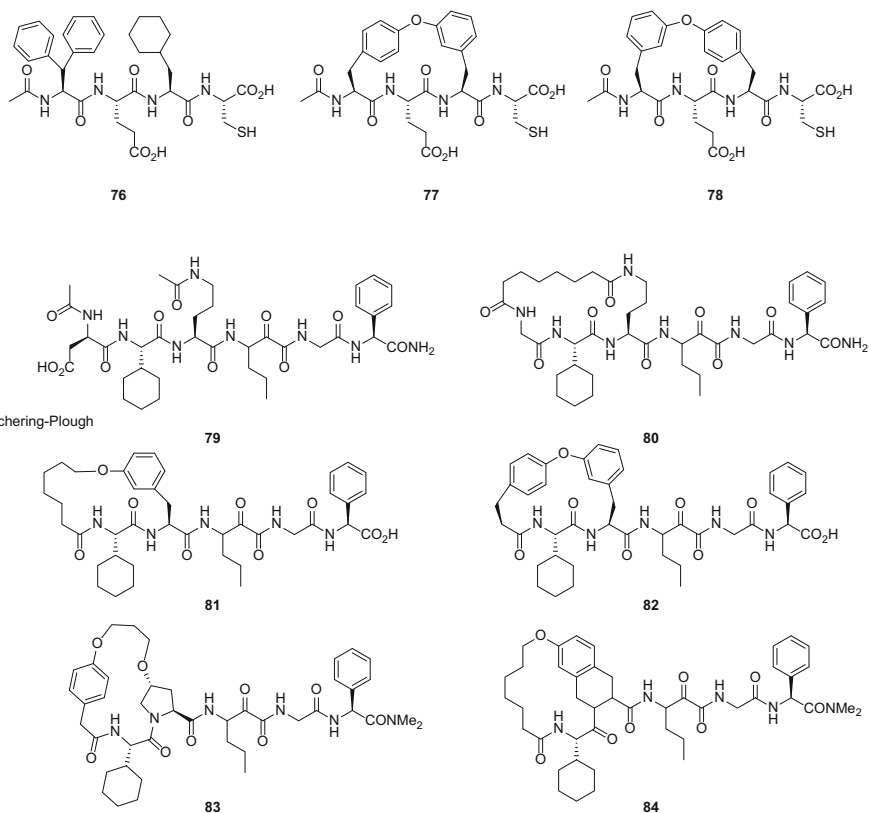


Fig. 15 Early IRBM and Schering–Plough P2–P4 macrocycles

The Schering–Plough group was also active in this arena (Fig. 15), exploring a number of P2–P4 macrocyclic constructs that incorporated the slowly reversible ketoamide warhead using acyclic peptide **79** (K_i 11 μM) as a starting point [80]. Initial compounds used a P2 lysine and an α,ω -diacid linker to afford significantly more potent compounds such as **80** (K_i 0.44 μM). Using either a tyrosine ether [**81**] (**81** K_i 0.16 μM) or a diaryl ether analogous to the IRBM constraint such as **82** (K_i 0.11 μM) [82] afforded small incremental improvements in activity. Incorporating a P2 proline into the macrocycle gave more significant improvement in potency, for example, **83** (K_i 8 nM) [83]. The Schering–Plough scaffold design also included a unique tetrahydroisoquinoline-based series exemplified by **84** (K_i 15 nM) [84]. While a number of innovative and potent in vitro P2–P4 macrocycles were identified from these efforts, PK where obtained appeared to be poor which may be associated with the extended P1'–P2' residues, and no compounds from these series appear to have advanced into development.

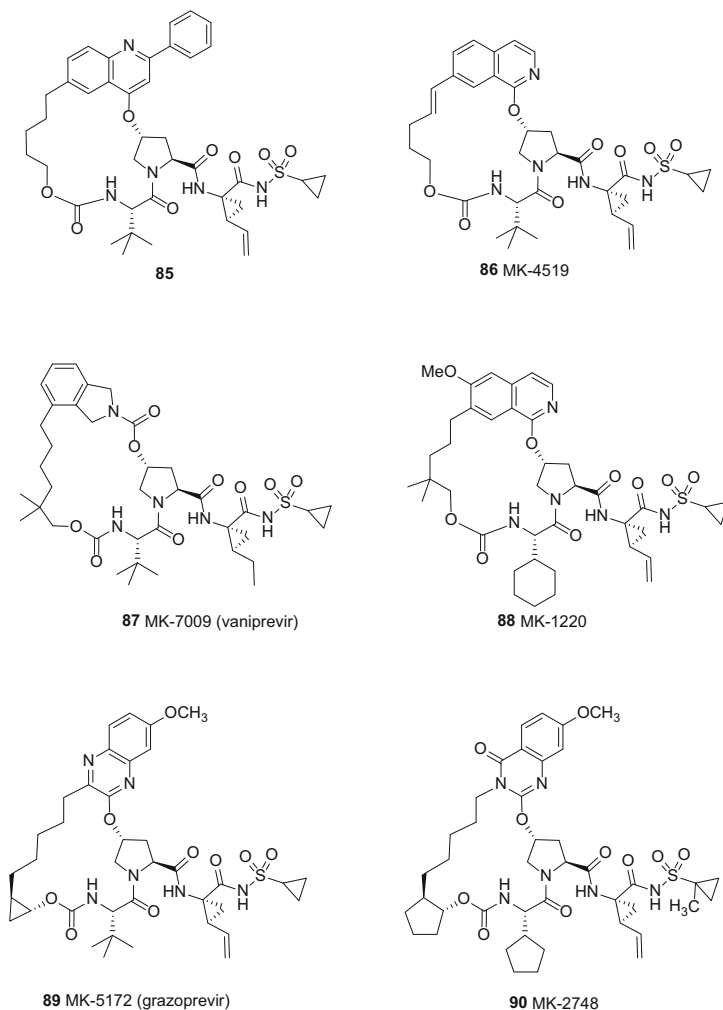


Fig. 16 Merck P2–P4 macrocyclic inhibitors

The Merck group took a different approach by modeling BILN-2061 bound to the full-length NS3/4a protease that included the helicase domain, rather than the 1–180 protease domain alone. This revealed the potential for additional interactions with the helicase domain and provided the design basis for novel reversible P2–P4 macrocycles [85]. Initial optimization of the macrocycle formed using a phenylquinoline P2 led to compounds such as **85** (Fig. 16) that combined potent in vitro activity (K_i 0.07 nM, EC_{50} 4.5 nM) with good liver exposure after oral dosing, thereby demonstrating the potential of the series. Changing the quinoline P2 substituent to an isoquinoline afforded **86** (MK-4519) (Gt1b K_i 0.07 nM, Gt1b EC_{50}

4.5 nM) that partitioned effectively into rat liver (18.6 μM @ 4 h post 5 mpk dose) [86].

Optimization of an isoindoline carbamate P2 series (Fig. 16) that included varied linker lengths and substitution on the linker resulted in the identification of **87** (MK-7009, vaniprevir) which combined potent in vitro activity (Gt1b K_i 0.04 nM, Gt1b replicon EC_{50} 4.5 nM) with high liver exposure (9.9 μM @ 4 h after 5 mpk PO in rat) [87]. With an attractive preclinical profile [88], clinical development of vaniprevir was undertaken leading to approval in Japan in 2014 for treatment of Gt1 infected patients in combination with PEG-IFN/RBV.

Additional work was done in the P2–P4 macrocycle space at Merck (Fig. 16) with an initial goal of improving plasma exposure in preclinical species relative to MK-7009. Optimization of MK-4519 in terms of linker length, linker substitution, and isoquinoline substitution led to MK-1220 which maintained potent in vitro activity (Gt1b K_i 0.02 nM, Gt1b replicon EC_{50} 4 nM), with the desired improved preclinical PK profile (5 mpk PO rat AUC 11.8 $\mu\text{M}^*\text{h}$, 4 h liver 23 μm) relative to MK-7009, particularly in terms of plasma exposure [89].

The P2–P4 macrocycle approach was further developed at Merck (Fig. 16) with the objective of developing third-generation compounds that would show both cross-genotype activity and improved activity against clinically relevant Gt1 mutations associated with the reversible inhibitors (D168, R155, and A156). Compounds were designed with a P2 quinoline and later quinoxaline. An extensive optimization program led to the discovery of **89** (MK-5172, grazoprevir) (Gt1b K_i 0.02 nM, Gt1b replicon EC_{50} 7.4 nM) which also had subnanomolar Gt3a activity (K_i 0.7 nM) [90]. The P2 quinoxaline was found to bind in a different manner from previous P2–P4 macrocycles with the substituent stacking against the highly conserved catalytic triad [91]. This modified binding mode helps explain the cross-genotypic activity observed with MK-5172 and the potent activity against R155K (K_i 0.07 nM) and D168 (K_i 0.14 nM) mutants as they are no longer in close contact with the P2 substituent. Shifts were larger against A156T (K_i 5.3 nM) and A156V (K_i 12 nM), although this may be mitigated in part by the significantly reduced replication fitness conferred upon the virus by these mutations in vitro [92]. Exhibiting a favorable preclinical profile including liver exposure (5 mpk PO rat 4 h liver 23 μm) [93], grazoprevir entered clinical development and was approved in January 2016 for use in combination with NS5a inhibitor elbasvir to treat Gt1 and Gt4 infected patients in as short as 12 weeks (16 weeks with RBV added for PEG-IFN/RBV experienced patients or patients possessing baseline NS5a polymorphisms). The combination was shown to have a high genetic barrier to resistance in Gt1a replicons [94].

Continued evolution of related scaffolds at Merck identified a quinazolinone P2 substituent that potentially took advantage of an ordered water molecule observed in the X-ray crystal structure of MK-5172 bound to NS3/4a protease. Re-optimization of the P2–P4 linker along with P3 amino acid and the P1 acylsulfonamide afforded **90** (MK-2748) (Fig. 16) which demonstrated potent activity, including against Gt3a (K_i 1.2 nM) and key mutants R155K, D168Y, A156T, and A156V (K_i 0.03, 0.06, 2.5, 2.8 nM, respectively) along with good liver exposure in multiple preclinical species [95].

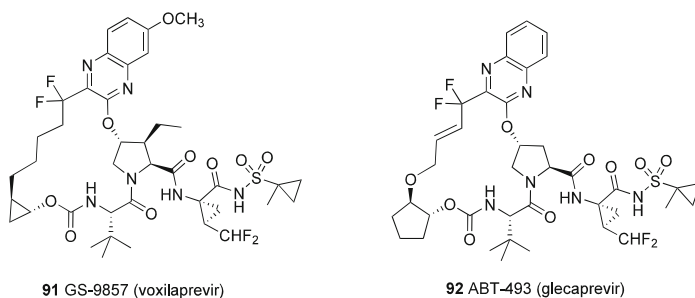


Fig. 17 Difluoromethyl cyclopropyl P1 containing P2–P4 macrocyclic inhibitors

Gilead synthesized **91** (GS-9587, voxilaprevir) (Fig. 17), a compound that brought together the MK-5172 quinoxaline P2 with a P1 difluoromethyl cyclopropyl group as a replacement for the vinyl cyclopropyl moiety in MK-5172 and many of the other reversible NS3/4a inhibitors [96]. This P1 fragment was based on an IRBM peptide containing a difluoroethyl P1 substituent. The hydrogen bond between the CHF₂ group and Leu 135 in the conformationally flexible IRBM analog was also observed in an X-ray crystal structure of this more constrained analog [97]. The combination of voxilaprevir with sofosbuvir and velpatasvir was approved in June 2017 for Gt1–6 with a 12-week treatment duration in patients who previously failed a combination including an NS5A inhibitor.

Similarly, Enanta/AbbVie utilized a quinoxaline-based P2 substituent in combination with the P1 difluoromethyl cyclopropyl moiety to identify **92** (ABT-493, glecaprevir) (Fig. 17) [98]. Glecaprevir inhibited Gt1–6 NS3/4a *in vitro* with an IC₅₀ range of 3.5–11.3 nM. In common with MK-5172, Gt1b mutations in R155K (EC₅₀ 0.27 nM) and D168V (EC₅₀ 1.5 nM) led to relatively modest shifts, while A156T (EC₅₀ 301 nM) and A156V (EC₅₀ 839 nM) led to more dramatic shifts. The combination of glecaprevir and NS5a inhibitor pibrentasvir was approved in August 2017 for treatment of Gt1–6 infected patients with reduced treatment duration of 8 weeks in treatment-naïve non-cirrhotic patients.

8 Bismacrocyclic Inhibitors

As part of the initial design strategy to develop P2–P4 macrocyclic inhibitors, Merck opened the P1–P3 macrocycle to facilitate synthetic access and rapidly test the modeling hypothesis. Later, a P1–P3 macrocycle was reintroduced into a P2–P4 macrocyclic inhibitor resulting in the discovery of a series of unique bismacrocyclic inhibitors [99]. Optimization of the series led to **93** (MK-6325) (Fig. 18) which exhibited potent *in vitro* activity against Gt3a (*K_i* 0.26 nM). Incorporation of the second macrocyclic ring also provided significantly improved subnanomolar potency against A156T (*K_i* 0.42 nM) and A156V (*K_i* 0.57 nM) resistance mutations. Coupled with an attractive preclinical PK profile, MK-6325 moved into clinical

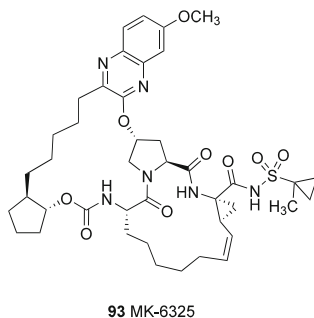


Fig. 18 Bismacrocylic inhibitor MK-6325

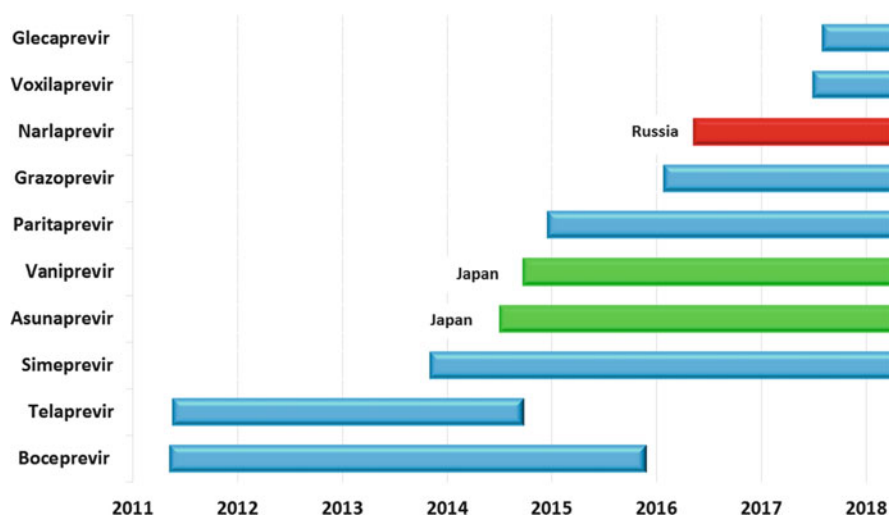


Fig. 19 Regulatory approval timeline for NS3/4a inhibitors

studies. The original chemistry approach to the 18/15-membered bismacrocylic scaffold utilized a bis ring-closing metathesis to generate these complex targets, but a modified approach was used to prepare multi-kg quantities for clinical studies [100].

9 Conclusions

The development of HCV NS3/4a inhibitors as orally bioavailable drugs presented as an extremely challenging problem based on structural features of the enzyme and the initial product-based peptide inhibitor leads. Evolution to the present situation with 10 NS3/4a inhibitors having received regulatory approval (Fig. 19) reflects a tremendous accomplishment for medicinal chemistry discovery efforts by many

Table 1 Molecular weights of approved NS3/4a inhibitors

Drug	MWt.
Boceprevir	519.7
Telaprevir	679.8
Narlaprevir	708.0
Asunaprevir	748.3
Simeprevir	749.9
Vaniprevir	755.9
Paritaprevir	765.9
Grazoprevir	766.9
Glecaprevir	838.9
Voxilaprevir	868.9

groups. Most importantly, these approved drugs provide improved treatment options for HCV infected patients.

The properties of most of the marketed NS3/4a protease inhibitors fall considerably outside of traditional drug-like space, and the molecular weight in particular has continued to increase with newer agents (Table 1). Uptake by transporter mechanisms as noted by multiple groups may at least in part explain the ability to obtain compounds with oral bioavailability in this chemical space and also contribute to liver partitioning.

The evolution of treatment paradigms with combinations of DAAs has been dramatic and rapid. Initially approved first-generation inhibitors telaprevir and boceprevir were dosed in combination with PEG-IFN and/or RBV leading to improved SVR rates (~70–80%) relative to PEG-IFN/RBV alone and offered potential for reduced treatment duration from 48 weeks to 24 weeks in some patient subgroups. At that point in time, the potential for removing PEG-IFN and RBV to provide combinations of DAAs was unclear as was the breadth of genotype coverage and extent to which treatment duration could be reduced. The number of DAAs required for an effective combination capable of suppressing emergence of resistance mutations was also the subject of vigorous debate.

Next to be approved were the second-generation reversible NS3/4a inhibitors including simeprevir, vaniprevir, and paritaprevir for Gt1 infected patients.

Third-generation NS3/4a protease inhibitors, grazoprevir, glecaprevir, and voxilaprevir, all share a quinoxaline-based P2 substituent that imparts unique cross genotype and resistance mutation profiles. They have each been approved as part of DAA combinations with either one or two additional agents allowing PEG-IFN/RBV-free treatment options for at least some patient populations. Zepatier™ (grazoprevir + elbasvir) is approved for Gt1 and Gt4 patients with 12-week treatment duration in treatment-naïve patients. Vosevi™ (sofosbuvir + velpatasvir + voxilaprevir) is approved for Gt1–6 infected patients with a 12-week treatment duration in patients who previously failed a combination including an NS5A inhibitor. Most recently, Mavyret™, a combination of glecaprevir and pibrentasvir, was approved for an 8-week treatment of Gt1–6 non-cirrhotic patients.

The NS3/4a inhibitor specifically and DAA arena more broadly have evolved so rapidly that the first-approved inhibitors, telaprevir and boceprevir, were discontinued. With the third-generation NS3/4a containing DAA combinations along with others, the treatment burden for patients has been greatly reduced with SVR rates >90% attainable for most patient populations.

With multiple highly effective DAA combinations now available, the question is: How many additional combinations will be taken through clinical trials given the high bar set by currently available options? The answer in part has been delivered with multiple companies making the decision to discontinue basic research and clinical development programs in the HCV field. The greater challenge moving forward may lie in making these newer treatments widely available in developing countries where, despite the reduced prices of recently approved DAA combinations, cost still represents a significant hurdle to universal treatment for millions of patients.

Compliance with Ethical Standards

Conflict of Interest Author declares that he has no conflict of interest.

Ethical Approval This article does not contain any studies with human participants or animals performed by the author.

References

1. Hahn B, Han DS, Back SH et al (1995) NS3-4A of hepatitis C virus is a chymotrypsin-like protease. *J Virol* 69:2534–2539
2. Kolykhalov AA, Mihalik K, Feinstone SM et al (2000) Hepatitis C virus encoded enzymatic activities and conserved RNA elements in the 3' nontranslated region are essential for virus replication in vivo. *J Virol* 74:2046–2051
3. Gale Jr M, Foy EM (2005) Evasion of intracellular host defence by hepatitis C virus. *Nature* 436:939–945
4. Yao N, Reichert P, Taremi SS et al (1999) Molecular views of viral polyprotein processing revealed by the crystal structure of the hepatitis C virus bifunctional protease–helicase. *Structure* 7:1353–1363
5. Failla C, Tomei L, De Francesco R (1994) Both NS3 and NS4A are required for proteolytic processing of hepatitis C virus nonstructural proteins. *J Virol* 68:3753–3760
6. Schechter I, Berger A (1967). *Biochem Biophys Res Commun* 27:57–62
7. Steinkuhler C, Biasiol G, Brunetti M et al (1998) Product inhibition of the hepatitis C virus NS3 protease. *Biochemistry* 37:8899–8905
8. Llinas-Brunet M, Bailey M, Fazal G et al (1998) Peptide-based inhibitors of the hepatitis C virus serine protease. *Bioorg Med Chem Lett* 8:1713–1718
9. Love RA, Parge HE, Wickersham JA et al (1996) The crystal structure of hepatitis C virus NS3 proteinase reveals a trypsin-like fold and a structural zinc binding site. *Cell* 87:331–342
10. Kim JL, Morgenstern KA, Lin C et al (1996) Crystal structure of the hepatitis C virus NS3 protease domain complexed with a synthetic NS4A cofactor peptide. *Cell* 87:343–355
11. Yah Y, Li Y, Munshi S et al (1998) Complex of NS3 protease and NS4A peptide of BK strain hepatitis C virus: a 2.2 Å resolution structure in a hexagonal crystal form. *Protein Sci* 7:837–847

12. Barbato G, Cicero DO, Nardi MC et al (1999). *J Mol Biol* 289:371–384
13. Ingallinella P, Altamura S, Bianchi E et al (1998) Potent peptide inhibitors of human hepatitis C virus NS3 protease are obtained by optimizing the cleavage products. *Biochemistry* 37:8906–8914
14. Narjes F, Koehler KF, Koch U et al (2002) A designed P(1) cysteine mimetic for covalent and non-covalent inhibitors of HCV NS3 protease. *Bioorg Med Chem Lett* 12:701–704
15. Llinas-Brunet M, Bailey M, Fazal G et al (2000) Highly potent and selective peptide-based inhibitors of the hepatitis C virus serine protease; towards smaller inhibitors. *Bioorg Med Chem Lett* 10:2267–2270
16. LaPlante S, Cameron DR, Aubry N et al (1999) Solution structure of substrate-based ligands when bound to hepatitis C virus NS3 protease domain. *J Biol Chem* 274:18618–18624
17. Rancourt J, Cameron D, Gorys V et al (2004) Peptide-based inhibitors of the hepatitis C virus NS3 protease: structure-activity relationship at the C-terminal position. *J Med Chem* 47:2511–2522
18. Goudreau N, Cameron DR, Bonneau P et al (2004) NMR structural characterization of peptide inhibitors bound to the HCV NS3 protease: design of a new P2 substituent. *J Med Chem* 47:123–132
19. Tsantrizos YS, Bolger G, Bonneau P et al (2003) Macrocyclic inhibitors of the NS3 protease as potential therapeutic agents of hepatitis C virus infection. *Angew Chem Int Ed* 42:1356–1360
20. Llinas-Brunet M, Bailey MD, Bolger G et al (2004) Structure-activity study on a novel series of macrocyclic inhibitors of the hepatitis C virus NS3 protease leading to the discovery of BILN-2061. *J Med Chem* 47:1605–1608
21. Lamarre D, Anderson PC, Bailey M et al (2003) An NS3 protease inhibitor with antiviral effects in humans infected with hepatitis C virus. *Nature* 426:186–189
22. Reiser M, Hinrichsen H, Benhamou Y, Reesink HW et al (2005) Antiviral efficacy of NS3-serine protease inhibitor BILN-2061 in patients with chronic genotype 2 and 3 hepatitis C. *Hepatology* 41:832–835
23. Stoltz JH, Stern JO, Huang Q et al (2011) A 28-day mechanistic time course study in the rhesus monkey with hepatitis C virus protease inhibitor BILN 2061. *Toxicol Pathol* 39:496–501
24. Yee NK, Farina V, Houpiis IN et al (2006) Efficient large-scale synthesis of BILN 2061, a potent HCV protease inhibitor, by a convergent approach based on ring-closing metathesis. *J Org Chem* 71:7133–7145
25. Nicola T, Brenner M, Donsbach K et al (2005) First scale-up to production scale of a ring closing metathesis reaction forming a 15-membered macrocycle as a precursor of an active pharmaceutical ingredient. *Org Process Res Dev* 9:513–515
26. Farina V, Shu C, Zeng X et al (2009) Second-generation process for the HCV protease inhibitor BILN 2061: a greener approach to Ru catalyzed ring-closing metathesis. *Org Process Res Dev* 13:250–254
27. Lin C, Lin K, Luong Y-P (2004) In vitro resistance studies of hepatitis C virus serine protease inhibitors, VX-950 and BILN 2061: structural analysis indicates different resistance mechanisms. *J Biol Chem* 279:17508–17514
28. Lu L, Pilot-Matias TJ, Stewart KD (2004) Mutations conferring resistance to a potent hepatitis C virus serine protease inhibitor in vitro. *Antimicrob Agents Chemother* 48:2260–2266
29. Powers JC, Asgian JL, Ekici OD et al (2002) Irreversible inhibitors of serine, cysteine, and threonine proteases. *Chem Rev* 102:4639–4750
30. Johnson DS, Weerapana E, Cravatt BF (2010) Strategies for discovering and derisking covalent, irreversible enzyme inhibitors. *Future Med Chem* 2:949–964
31. Attwood MR, Bennett JM, Campbell AD et al (1999) The design and synthesis of potent inhibitors of hepatitis C virus NS3-4A proteinase. *Antivir Chem Chemother* 10:259–273
32. Kettner CA, Shenvi AB (1984) Inhibition of the serine proteases leukocyte elastase, pancreatic elastase, cathepsin G and chymotrypsin by peptide boronic acids. *J Biol Chem* 259:15106–15112

33. Kinder DH, Elstad CA, Meadows GG et al (1992) Antimetastatic activity of boro-amino acid analog protease inhibitors against B16BL6 melanoma in vivo. *Invasion Metastasis* 12:309–319
34. Perni RB, Pitlik J, Britt SD et al (2004) Inhibitors of hepatitis C virus NS3.4A protease 2. Warhead SAR and optimization. *Bioorg Med Chem Lett* 14:1441–1446
35. Perni RB, Farmer LJ, Cottrell KM et al (2004) Inhibitors of hepatitis C virus NS3.4A protease. Part 3: P2 proline variants. *Bioorg Med Chem Lett* 14:1939–1942
36. Yip Y, Victor F, Lamar J et al (2004) Discovery of a novel bicycloproline P2 bearing peptidyl α -ketoamide LY514962 as HCV protease inhibitor. *Bioorg Med Chem Lett* 14:251–256
37. Victor F, Lamar J, Snyder N et al (2004) P1 and P3 optimization of novel bicycloproline P2 bearing tetrapeptidyl α -ketoamide based HCV protease inhibitors. *Bioorg Med Chem Lett* 14:257–261
38. Chen S-H, Lamar J, Yip Y et al (2005) P1 and P1; optimization of [3,4]-bicycloproline P2 incorporated tetrapeptidyl α -ketoamide based HCV protease inhibitors. *Lett Drug Des Disc* 2:118–123
39. Drugs RD (2010) Telaprevir. *Drugs R D* 10:179–202
40. Venkatraman S, Bogen SL, Arassappan A et al (2006) Discovery of (1R,5S)-N-[3-amino-1-(cyclobutylmethyl)-2,3-dioxopropyl]-3-[2(S)-[[[(1,1-dimethylethyl)amino]carbonyl]amino]-3,3-dimethyl-1-oxobutyl]-6,6-dimethyl-3-azabicyclo[3.1.0]hexan-2(S)-carboxamide (SCH 503034), a selective, potent, orally bioavailable HCV NS3 protease inhibitor: a potential therapeutic agent for the treatment of hepatitis C infection. *J Med Chem* 49:6074–6086
41. Arasappan A, Padilla AI, Jao E et al (2009) Toward second generation hepatitis C virus NS3 serine protease inhibitors: discovery of novel P4 modified analogues with improved potency and pharmacokinetic profile. *J Med Chem* 52:2806–2817
42. Bogen SL, Pan W, Ruan S et al (2009) Toward the back-up of boceprevir (SCH 503034): discovery of new extended P4-capped ketoamide inhibitors of hepatitis C virus NS3 serine protease with improved potency and pharmacokinetic profiles. *J Med Chem* 52:3679–3688
43. Venkatraman S, Blackman M, Wu W et al (2009) Discovery of novel P3 sulfonamide-capped inhibitors of HCV NS3 protease. Inhibitors with improved cellular potencies. *Bioorg Med Chem* 17:4486–4495
44. Arasappan AF, Bennett SL, Bogen S et al (2010) Discovery of narlaprevir (SCH 900518): a potent, second generation HCV NS3 serine protease inhibitor. *ACS Med Chem Lett* 1:64–69
45. Tong X, Arasappan A, Bennett F et al (2010) Preclinical characterization of the antiviral activity of SCH 900518 (narlaprevir), a novel mechanism-based inhibitor of hepatitis C virus NS3 protease. *Antimicrob Agents Chemother* 54:2365–2370
46. Isakov V, Koloda D, Tikhonova N et al (2016) Pharmacokinetics of the new hepatitis C virus NS3 protease inhibitor narlaprevir following single-dose use with or without ritonavir in patients with liver cirrhosis. *Antimicrob Agents Chemother* 60:7098–7104
47. Llinas-Brunet M, Bailey MD, Goudreau N et al (2010) Discovery of a potent and selective noncovalent linear inhibitor of the hepatitis C virus NS3protease (BI 201335). *J Med Chem* 53:6466–6476
48. White PW, Llinàs-Brunet M, Amad M et al (2010) Preclinical characterization of BI 201335, a C-terminal carboxylic acid inhibitor of the hepatitis C virus NS3-NS4A protease. *Antimicrob Agents Chemother* 54:4611
49. Jensen DM, Asselah T, Dieterich D et al (2016) Faldaprevir, pegylated interferon, and ribavirin for treatment-naïve HCV genotype-1: pooled analysis of two phase 3 trials. *Ann Hepatol* 15:333–349
50. Zeuzem S, Soriano V, Asselah T et al (2015) Efficacy and safety of faldaprevir, deleobuvir, and ribavirin in treatment-naive patients with chronic hepatitis C virus infection and advanced liver fibrosis or cirrhosis. *Antimicrob Agents Chemother* 59:1282–1291
51. Zeuzem S, Dufour J-F, Buti M et al (2015) Interferon-free treatment of chronic hepatitis C with faldaprevir, deleobuvir and ribavirin: SOUND-C3, a phase 2b study. *Liver Int* 35:417–421

52. Scola PM, Wang A, Good AC et al (2014) Discovery and early clinical evaluation of BMS-605339, a potent and orally efficacious tripeptidic acylsulfonamide NS3 protease inhibitor for the treatment of hepatitis C virus infection. *J Med Chem* 57:1730–1755
53. Scola PM, Sun L-Q, Wang AX et al (2014) The discovery of asunaprevir (BMS-650032), an orally efficacious NS3 protease inhibitor for the treatment of hepatitis C virus infection. *J Med Chem* 57:1730–1752
54. McPhee F, Sheaffer AK, Friborg J et al (2012) Preclinical profile and characterization of the hepatitis C virus NS3 protease inhibitor asunaprevir (BMS-650032). *Antimicrob Agents Chemother* 56:5387–5396
55. Wei L, Zhang M, Xu M et al (2016) Phase 3, open-label study of daclatasvir plus asunaprevir in Asian patients with chronic hepatitis C virus genotype 1b infection who are ineligible for or intolerant to interferon alfa therapies with or without ribavirin. *J Gastroenterol Hepatol* 31:1860–1867
56. Suzuki Y, Ikeda K, Suzuki F et al (2013) Dual oral therapy with daclatasvir and asunaprevir for patients with HCV genotype 1b infection and limited treatment options. *J Hepatol* 58:655–662
57. Kumada H, Suzuki Y, Ikeda K et al (2014) Daclatasvir plus asunaprevir for chronic HCV genotype 1b infection. *Hepatology* 59:2083–2091
58. Sun L-Q, Mull E, Zheng B et al (2016) Discovery of a potent acyclic, tripeptidic, acyl sulfonamide inhibitor of hepatitis C virus NS3 protease as a back-up to asunaprevir with the potential for once-daily dosing. *J Med Chem* 59:8042–8060
59. Huang M, Fabrycki J, Patel D et al (2010) Antiviral activity, combination and resistance of ACH-1625, a potent, clinical stage HCV NS3 protease inhibitor. *J Hepatol* 52:S254
60. Agarwal A, Zhang B, Olek E et al (2012) Rapid and sharp decline in HCV upon monotherapy with NS3 protease inhibitor, ACH-1625. *Antivir Ther* 17:1533–1539
61. Sheng XC, Appleby T, Butler T et al (2012) Discovery of GS-9451: an acid inhibitor of the hepatitis C virus NS3/4A protease. *Bioorg Med Chem Lett* 22:2629–2634
62. Yang H, Robinson M, Corsa AC et al (2014) IV preclinical characterization of the novel hepatitis C virus NS3 protease inhibitor GS-9451. *Antimicrob Agents Chemother* 58:647–653
63. Johansson PO, Back M, Kvarnstrom I et al (2006) Potent inhibitors of the hepatitis C virus NS3 protease: use of a novel P2 cyclopentane-derived template. *Bioorg Med Chem* 14:5136–5151
64. Thorstensson F, Wangsell F, Kvarnstrom I et al (2007) Synthesis of novel potent hepatitis C virus NS3 protease inhibitors: discovery of 4-hydroxy-cyclopent-2-ene-1,2-dicarboxylic acid as an acyl-L-hydroxyproline bioisostere. *Bioorg Med Chem* 15:827–838
65. Back M, Johansson PO, Wangsell F et al (2007) Novel potent macrocyclic inhibitors of the hepatitis C virus NS3 protease: use of cyclopentane and cyclopentene P2-motifs. *Bioorg Med Chem* 15:7184–7202
66. Raboisson P, de Kock H, Rosenquist A et al (2008) Structure–activity relationship study on a novel series of cyclopentane-containing macrocyclic inhibitors of the hepatitis C virus NS3/4A protease leading to the discovery of TMC435350. *Bioorg Med Chem Lett* 18:4853–4858
67. Rosenquist Å, Samuelsson B, Johansson P-O et al (2014) Discovery and development of simeprevir (TMC435), a HCV NS3/4A protease inhibitor. *J Med Chem* 57:1673–1693
68. Parsy C, Alexandre F-R, Brandt G et al (2014) Structure-based design of a novel series of azetidine inhibitors of the hepatitis C virus NS3/4A serine protease. *Bioorg Med Chem Lett* 24:4444–4449
69. Parsy CC, Alexandre F-R, Bidau V et al (2015) Discovery and structural diversity of the hepatitis C virus NS3/4A serine protease inhibitor series leading to clinical candidate IDX320. *Bioorg Med Chem Lett* 25:5427–5436
70. Seiwert SD, Andrews SW, Jiang Y et al (2008) Preclinical characteristics of the hepatitis C virus NS3/4A protease inhibitor ITMN-191 (R7227). *Antimicrob Agents Chemother* 52:4432–4441

71. Jensen DM, Brunda M, Elston R et al (2016) Interferon-free regimens containing sofosbuvir for patients with genotype 1 chronic hepatitis C: a randomized, multicenter study. *Liver Int* 36:505–514
72. Huang M, Podos S, Patel D et al (2010) ACH-2684: HCV NS3 protease inhibitor with potent activity against multiple genotypes and known resistant variants. *Hepatology* 52(S1):1204A
73. Pompei M, Di Francesco ME, Koch U et al (2009) Phosphorous acid analogs of novel P2–P4 macrocycles as inhibitors of HCV–NS3 protease. *Bioorg Med Chem Lett* 19:2574–2578
74. Pyun H-J, Chaudhary K, Somoza JR et al (2009) Synthesis and resolution of diethyl (1S,2S)-1-amino-2-vinylcyclopropane-1-phosphonate for HCV NS3 protease inhibitors. *Tetrahedron Lett* 50:3833–3835
75. Sheng XC, Pyun H-J, Chaudhary K et al (2009) Discovery of novel phosphonate derivatives as hepatitis C virus NS3 protease inhibitors. *Bioorg Med Chem Lett* 19:3453–3457
76. Clarke MO, Chen X, Cho A et al (2011) Novel, potent, and orally bioavailable phosphinic acid inhibitors of the hepatitis C virus NS3 protease. *Bioorg Med Chem Lett* 21:3568–3572
77. Sheng XC, Casarez A, Cai R et al (2012) Discovery of GS-9256: a novel phosphinic acid derived inhibitor of the hepatitis C virus NS3/4A protease with potent clinical activity. *Bioorg Med Chem Lett* 22:1394–1396
78. Hotho DM, de Bruijne J, O'Farrell AM et al (2012) Pharmacokinetics and antiviral activity of PHX1766, a novel HCV protease inhibitor, using an accelerated phase I study design. *Antivir Ther* 17:365–375
79. Marchetti A, Ontoria JM, Matassa VG (1999) Synthesis of two novel cyclic biphenyl ether analogs of an inhibitor of HCV NS3 protease. *Synlett* S1:1000–1002
80. Venkatram S, Njoroge FG (2007) Macrocyclic inhibitors of HCV NS3-4A protease: design and structure activity relationship. *Curr Top Med Chem* 7:1290–1301
81. Chen KX, Njoroge FG, Pichardo J et al (2005) Design, synthesis, and biological activity of m-tyrosine-based 16- and 17-membered macrocyclic inhibitors of hepatitis C virus NS3 serine protease. *J Med Chem* 48:6229–6235
82. Venkatraman S, Njoroge FG, Girijavallabhan VM et al (2005) Design and synthesis of depeptidized macrocyclic inhibitors of hepatitis C NS3-4A protease using structure-based drug design. *J Med Chem* 48:5088–5091
83. Chen KX, Njoroge FG, Arasappan A et al (2006) Novel potent hepatitis C virus NS3 serine protease inhibitors derived from proline-based macrocycles. *J Med Chem* 49:995–1005
84. Chen KX, Njoroge FG, Pichardo J et al (2006) Potent 7-hydroxy-1,2,3,4-tetrahydroisoquinoline-3-carboxylic acid-based macrocyclic inhibitors of hepatitis C virus NS3 protease. *J Med Chem* 49:567–574
85. Liverton NJ, Holloway MK, McCauley JA et al (2008) Molecular modeling based approach to potent P2–P4 macrocyclic inhibitors of hepatitis C NS3/4A protease. *J Am Chem Soc* 130:4607–4609
86. Brown AN, McSharry JJ, Adams JR et al (2016) Pharmacodynamic analysis of a serine protease inhibitor, MK-4519, against hepatitis C virus using a novel in vitro pharmacodynamic system. *Antimicrob Agents Chemother* 56:1170–1181
87. McCauley JA, McIntyre CJ, Rudd MT et al (2010) Discovery of vaniprevir (MK-7009), a macrocyclic hepatitis C virus NS3/4A protease inhibitor. *J Med Chem* 53:2443–2463
88. Liverton NJ, Carroll SS, Di Muzio J et al (2010) MK-7009, a potent and selective inhibitor of hepatitis C virus NS3/4A protease. *Antimicrob Agents Chemother* 54:305–311
89. Rudd MT, McCauley JA, Butcher JW et al (2011) Discovery of MK-1220: a macrocyclic inhibitor of hepatitis C virus NS3/4a protease with improved preclinical plasma exposure. *ACS Med Chem Lett* 2:207–212
90. Harper S, McCauley JA, Rudd MT et al (2012) Discovery of MK-5172, a macrocyclic hepatitis C virus NS3/4a protease inhibitor. *ACS Med Chem Lett* 3:332–336
91. Romano KP, Ali A, Aydin C et al (2012) The molecular basis of drug resistance against hepatitis C virus NS3/4A protease inhibitors. *PLoS Pathog* 8:e1002832

92. Shimakami T, Welsch C, Yamane D (2011) Protease inhibitor-resistant hepatitis C virus mutants with reduced fitness from impaired production of infectious virus. *Gastroenterology* 140:667–675
93. Summa V, Ludmerer SW, McCauley JA et al (2012) MK-5172, a selective inhibitor of hepatitis C virus NS3/4a protease with broad activity across genotypes and resistant variants. *Antimicrob Agents Chemother* 56:4161–4167
94. Lahser FC, Bystol K, Curry S, et al (2016) The combination of grazoprevir, a hepatitis C virus (HCV) NS3/4A protease inhibitor, and elbasvir, an HCV NS5A inhibitor, demonstrates a high genetic barrier to resistance in HCV genotype 1a replicons. *Antimicrob Agents Chemother* 60:2954–2964
95. Rudd MT, Butcher JW, Nguyen KT et al (2015) P2-quinazolinones and bis-macrocycles as new templates for next-generation hepatitis C virus NS3/4a protease inhibitors: discovery of MK-2748 and MK-6325. *ChemMedChem* 10:727–735
96. Voaklander R, Jacobson IM (2017) Sofosbuvir, velpatasvir and voxilaprevir combination for the treatment of hepatitis C. *Expert Rev Gastroenterol Hepatol* 11:789–795
97. Zheng B, D'Andrea SV, Sun L-Q et al (2018) Potent inhibitors of hepatitis C virus NS3 protease: employment of a difluoromethyl group as a hydrogen-bond donor. *ACS Med Chem Lett* 9:143. <https://doi.org/10.1021/acsmchemlett.7b00503>
98. Ng T, Tripathi R, Reisch T et al (2018) In vitro antiviral activity and resistance profile of the next-generation hepatitis C virus NS3/4A protease inhibitor glecaprevir. *Antimicrob Agents Chemother* 62:1–16
99. McCauley JA, Rudd MT, Nguyen KT et al (2008) Bismacrocyclic inhibitors of hepatitis C NS3/4a protease. *Angew Chem Int Ed* 47:9104–9107
100. Li H, Scott JP, Chen C-Y et al (2015) Synthesis of bis-macrocyclic HCV protease inhibitor MK-6325 via intramolecular sp²–sp³ Suzuki–Miyaura coupling and ring closing metathesis. *Org Lett* 17:1533–1536

Development and Marketing of INCIVEK (Telaprevir; VX-950): A First-Generation HCV Protease Inhibitor, in Combination with PEGylated Interferon and Ribavirin



Ann D. Kwong, Robert B. Perni, and Camilla S. Graham

Contents

1	Introduction	263
2	Telaprevir Preclinical Development	263
2.1	HCV Protease Structure and Function	264
2.2	Medicinal Chemistry Strategy	265
2.3	Preclinical Characterization of Telaprevir	267
2.4	Clinical Proof of Concept Is Obtained by Boehringer Ingelheim with BILN 2061; The Telaprevir Program Is Shutdown	268
2.5	Data from Two “Midnight Projects” Rescued the Telaprevir Program	269
3	Telaprevir Development	272
3.1	Get Out of Jail but Find Your Own Clinical Development Funding	272
3.2	Mitsubishi Pharma Saw the Data in Ways Others Did Not and Was Able to Act Upon It	273
3.3	CMC Development	273
3.4	Clinical Development	273
3.5	Phase 1 Clinical Studies	274
3.6	Phase 2 Safety and Efficacy	274
3.7	Phase 3 Safety and Efficacy	275
3.8	Characterization of Telaprevir-Resistant Variants	275
3.9	Telaprevir Approval as INCIVEK	276
3.10	Lessons Learned from the Discovery and Development of Telaprevir	276
4	Telaprevir Medical Affairs and Commercialization	277
4.1	Management of Adverse Events	279
4.2	Rash	279

A. D. Kwong (✉)
Kwong Pharma Consulting, LLC, Pepperell, MA, USA
e-mail: Ann.Kwong@KwongPharmaConsulting.com

R. B. Perni
JMD Pharma Creativity LLC, Marlborough, MA, USA
e-mail: robertperni@comcast.net

C. S. Graham
Beth Israel Deaconess Medical Center, Boston, MA, USA
e-mail: cgraham@bidmc.harvard.edu

4.3	Anemia	280
4.4	Anorectal Signs and Symptoms	280
4.5	Resistance	281
5	Examining Perceptions of Hepatitis C	282
5.1	General Public	282
5.2	Patients Living with HCV	282
5.3	Primary Care Providers	283
5.4	HCV Specialists	283
5.5	Addressing Stigma	283
5.6	Increasing Awareness	283
6	The Billion Dollar Question: Why Did INCIVEK Sell More than VICTRELIS?	285
7	Lessons for Today	286
8	Summary	287
	References	288

Abstract In the years before the development of direct-acting antiviral (DAA) drugs, patients were treated with a toxic combination of PEGylated interferon (P) and ribavirin (R) which was associated with a low success rate in patients with the most common genotype 1 hepatitis C virus (HCV) infection (40–50%), significant treatment-limiting side effects, and a long (48-week) duration of treatment. The HCV protease inhibitor telaprevir (VX-950) was discovered as part of a research collaboration between Vertex and Eli Lilly scientists. Clinical development of telaprevir in combination with PEGylated interferon alfa plus ribavirin (PR) was in collaboration with Tibotec (Janssen) and Mitsubishi Tanabe Pharma. INCIVEK (telaprevir) in combination with PR was approved in 2011, 10 days after the approval of Schering-Plough/Merck’s HCV protease inhibitor VICTRELIS (boceprevir), also in combination with PR. Both INCIVEK and VICTRELIS had similar safety and tolerability concerns, similar efficacy, three times daily dosing, and similarly complex treatment plans requiring significant attention by medical personnel. INCIVEK’s list price was higher than VICTRELIS, and INCIVEK was Vertex’s first launch, whereas Schering-Plough had been a HCV market leader with sales of Peg-INTRON/Rebetron. This chapter will briefly review the scientific challenges faced in the development of telaprevir and INCIVEK, as this story has been the subject of numerous review articles and book chapters. More emphasis will be given to the lesser-known story of how Vertex worked to prepare the HCV market, and we will unpack the variables contributing to the conundrum of why, despite being similar drugs, INCIVEK significantly outsold VICTRELIS.

Keywords Boceprevir, HCV, HCV protease, INCIVEK, PI, Telaprevir, VICTRELIS, VX-950

1 Introduction

The publication by scientists at Chiron of the identification and genome sequence of hepatitis C virus (HCV) (see review by [1]) sparked a worldwide rush to discover and develop direct-acting antiviral (DAA) drugs that was inspired in part by DAA drugs developed to treat HIV infection. HCV is currently the only chronic viral infection that can be cured with drugs, and the current standard of care consists of combinations of HCV antiviral drugs targeting different mechanisms of action (for a review of the HCV lifecycle, see [2]). Different combinations of the four major classes of HCV antiviral drugs are combined in approved HCV regimens: (1) HCV NS3 protease inhibitors (PI), (2) active site nucleotide inhibitors of HCV polymerase (NUC), (3) allosteric (non-nucleotide) inhibitors of the HCV polymerase (NNI), and (4) NS5A inhibitors. In the early days, there were no HCV replicon or HCV infectious virus assays, and viral targets such as the polymerase, protease, and helicase were identified by conserved sequence homology to known proteins. The development of the HCV replicon system [3] led to identification of NS5A inhibitors [4].

The HCV protease inhibitor telaprevir (VX-950) was discovered as part of a research collaboration that was begun in 1997 between Vertex and Eli Lilly scientists. Clinical development of telaprevir began in 2004 in collaboration with Tibotec (Janssen) and Mitsubishi Tanabe Pharma. The combination of telaprevir (INCIVEK) plus PR was approved in 2011 in the USA, followed by Canada, Europe, and Japan.

2 Telaprevir Preclinical Development

In the late 1990s, industry-wide efforts to develop HCV protease inhibitors were challenged by several adverse circumstances. From a commercial perspective, the HCV market was perceived to be too small, only a fraction of infected individuals had been screened and diagnosed [5, 6], and the market was expected to shrink as the incidence of new HCV infections had peaked in the 1960s–1980s [7]. From a drug discovery perspective, the major risk was the lack of validation of HCV protease inhibition as a mechanism of viral inhibition *in vivo* and in the clinic. It was only by analogy with HIV protease inhibitors that scientists believed a HCV protease inhibitor might represent a viable clinical approach. However, in many ways this was a misleading and false analogy, as the HCV protease inhibitor binding site was a less “druggable” target than HIV protease. As shown in Fig. 1, in contrast to the co-crystal structure of HIV protease with Agenerase, the major HCV protease binding pocket is extremely hydrophobic and flat, with few features for an inhibitor to grab on to. As Vertex’s HCV protease chemistry and project leader, Bob Perni famously described, trying to design an inhibitor to bind to the HCV protease domain as akin to trying to land a plane on a piece of cold pizza: it’s flat, greasy, and slides right off!

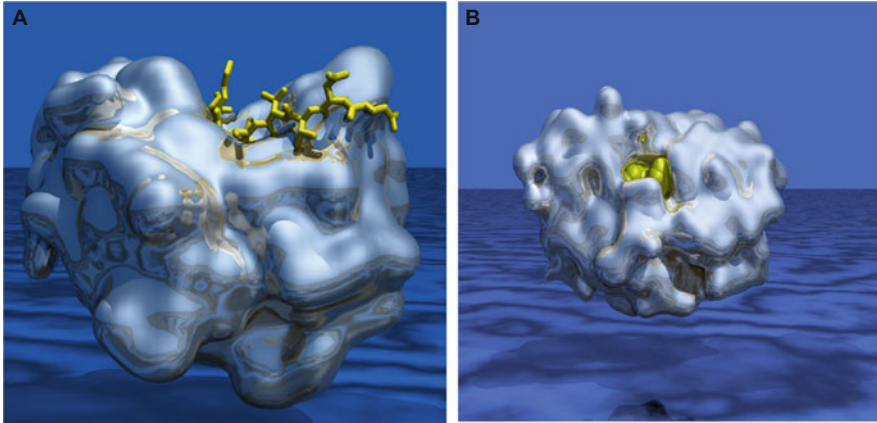


Fig. 1 Comparison of the HIV and HCV protease binding pocket. (a) HCV NS3-4A protease co-complexed with NS5A-5B substrate. (b) HIV protease co-complexed with Agenerase[®]

2.1 HCV Protease Structure and Function

HCV protease forms a dimer between the 631-amino acid NS3 protease-helicase polypeptide and a 54-amino acid peptide cofactor, NS4A. NS3 is a bifunctional protein with an N-terminal serine protease and a C-terminal NTPase/helicase domain. NS4A forms a tight complex with NS3, is essential for optimal activity [8]; and is reviewed in [9]. In 1996, the structure of the functional NS3 protease domain co-complexed with a NS4A peptide was published by Vertex [10]. These results revealed that the molecular complex adopts a chymotrypsin-like fold with the catalytic triad (Ser139-His57-Asp81) located in a cleft between two β -barrels. In a crystal structure of a NS4A fusion with full-length NS3, the helicase domain is separated from the protease domain by a flexible polypeptide linker and may form the roof of the HCV protease substrate-binding pocket [11–13]. Examination of the crystal structure revealed that the protease active site is extremely hydrophobic, flat, and solvent-exposed, with few pockets to increase the affinity for an inhibitor to bind [10].

There are multiple host and viral proteases that cleave the HCV polyprotein. The NS3/4A protease is responsible for the cleavage of the HCV polyprotein between NS3 and NS4A to form the active protease, between NS4A and NS5A to release the NS5A replication protein, and between NS5A and the NS5B to release the viral polymerase. HCV protease inhibitors work upstream of viral replication by blocking the release of proteins to form the viral replicase, which is essential for HCV replication.

2.2 Medicinal Chemistry Strategy

Telaprevir was synthesized in 2000 in a joint program between Eli Lilly and Vertex. Detailed description of the optimization of inhibitor binding to different pockets of the substrate binding site has been extensively reviewed and described [14–20].

Structure-based SAR development evolved from a decamer peptide inhibitor derived from the natural NS5A-5B substrate. This decamer was identified through a truncation study by Landro [21]. Simple deletion of two amino acid at the N-terminal and C-terminal end resulted in a 230-fold and 80-fold loss in potency, respectively (Fig. 2). This suggested that the HCV protease ligand interactions are spread over a large area and that a rather large inhibitor would be needed. Also, tellingly the loss of only twofold activity by truncation of the prime side, Ser and Nle, suggested that there were relatively small contributions to binding being generated by prime side residues close to the active site. This allowed the medicinal chemistry team to focus design efforts on the non-prime side of the peptide. Drug design was further aided by the demonstration that HCV protease could be inhibited by its own cleavage products [22, 23].

A defining feature of the medicinal chemistry effort was to design the inhibitors in such a way as to target the drug to the liver. This is in stark contrast to most drug discovery programs, since hepatic toxicity is always a concern. Early in the program, Perni and colleagues made the conscious decision to develop reversible covalent HCV protease inhibitors and to enrich inhibitor concentrations in the liver by incorporating the measurement of liver and plasma compound levels in rodents into the drug design cycle. The HCV replicon assay and liver-plasma pharmacokinetic profiling were used to drive the preclinical program [24]. Raj Kalkeri and Ann Kwong also developed an HCV protease animal model to measure the pharmacokinetic and pharmacodynamic (PK/PD) effect of an oral inhibitor on HCV protease activity in the liver of a mouse [25].

The desire to utilize a reversible covalent warhead to anchor the inhibitor to the protease active site led to the use, initially, of an aldehyde terminus. While it was realized that an aliphatic aldehyde was likely not practical as a component of a successful drug, its ease of synthesis and high reactivity in the active site made it a

Peptide Sequence	K _i (μM)
H-Glu-Asp-Val-Val-Leu-Cys-Tic-Nle-Ser-Tyr-OH	0.34
H-Glu-Asp-Val-Val-Leu-Cys-Tic-Nle-Ser-OH	27
H-Glu-Asp-Val-Val-Leu-Cys-Tic-Nle-OH	17
H-Glu-Asp-Val-Val-Leu-Cys-Tic-OH	14
H-Asp-Val-Val-Leu-Cys-Tic-Nle-Ser-Tyr-OH	4.4
H-Val-Val-Leu-Cys-Tic-Nle-Ser-Tyr-OH	79
H-Val-Leu-Cys-Tic-Nle-Ser-Tyr-OH	500
H-Leu-Cys-Tic-Nle-Ser-Tyr-OH	2000

Diagram illustrating the effect of truncation on a decamer peptide on the K_i for HCV protease. The table shows the K_i (μM) for various peptide sequences. A 230X increase in K_i is indicated for the sequence H-Val-Val-Leu-Cys-Tic-Nle-Ser-Tyr-OH compared to the full decamer. An 80X increase in K_i is indicated for the sequence H-Glu-Asp-Val-Val-Leu-Cys-Tic-Nle-Ser-OH compared to the full decamer.

Fig. 2 Effect of truncation on a decamer peptide on the K_i for HCV protease

useful model system to allow the optimization of the P1-P4 subsites. The prototype aldehyde is shown in Fig. 3 [15].

Replacing the aldehyde terminus with a more chemically stable group turned out to be a significant challenge. The more conventional covalent warhead groups (e.g., trifluoromethyl ketones, chloromethyl ketones) generally demonstrated poor affinity. When we turned to the less conventional groups such as keto amides and diketones, we found these to provide potent inhibition. The ketoamide group ultimately proved to be optimal (Fig. 4). It was subsequently shown that the high

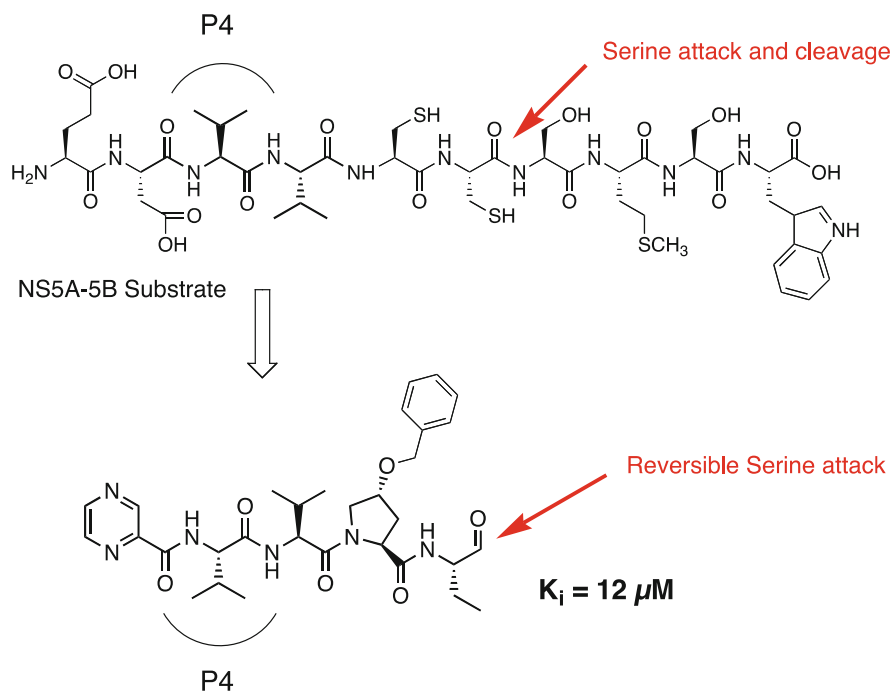


Fig. 3 Derivation of tetrapeptide scaffold

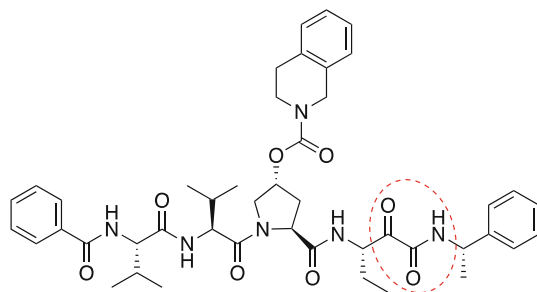


Fig. 4 Example of ketoamide-based inhibitor (ketoamide group circled)

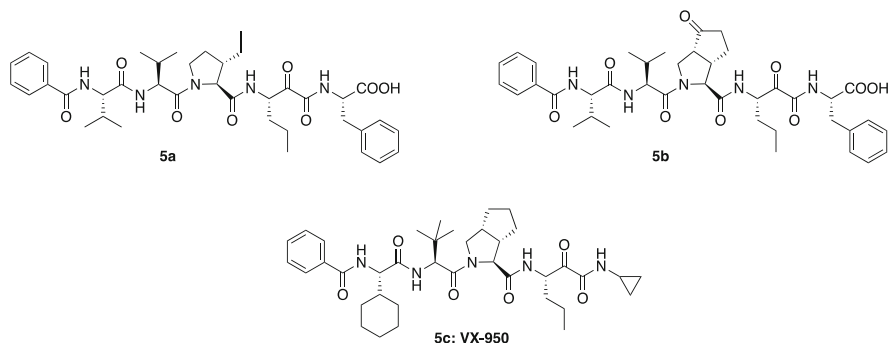


Fig. 5 Derivation of the bicyclic proline group

affinity of these warheads was due to a rearrangement of the active site and an additional, unexpected interaction being generated by the amide carbonyl [20].

A major challenge the team confronted was that the HCV protease changes conformation with different inhibitors, much like a water bed which will change shape in response to pressure, making it difficult to optimize one subsite at a time, and “lock it down”. Although simultaneous multigroup optimization can be challenging, the P3 and P4 positions were adequately optimized by brute force. A plethora of hydrophobic groups was examined at P3 and P4, to fill hydrophobic pockets while trying to keep the overall lipophilicity of the molecule as low as possible. The team eventually settled on a t-butyl group at P3 and a cyclohexyl at P4 [26, 27].

Through modeling efforts, it was shown that the P2 proline benzyl ether was not required for a potent inhibitor. Indeed, a simple ethyl group was found to be suitable (Fig. 5a) [18]. Chemists at Eli Lilly collaborating on the project had in hand from a previous project a bicyclic proline synthon that essentially represented a tied back ethyl group. It was the incorporation of this bicyclic keto-proline (Fig. 5b) [26, 27] that evolved into the saturated bicyclic proline derivative in VX-950 (Fig. 5c) [25].

2.3 Preclinical Characterization of Telaprevir

A detailed summary of the preclinical profile of telaprevir has been published [24, 25]. As shown in Fig. 6, telaprevir had a 50% inhibitory concentration (IC_{50}) of 354 nM and a 50% cytotoxicity concentration (CC_{50}) of 83 μ M in a GT1b HCV replicon assay and an IC_{50} of 280 nM in a GT 1a infectious virus assay with excellent selectivity against cellular serine proteases.

Combination studies revealed that telaprevir is additive to moderately synergistic with interferon- α and additive with ribavirin, in a genotype 1b HCV replicon assay [28]. Based on its potency in the replicon assay and its liver exposure in several animal species, telaprevir was selected as a clinical development candidate by Lilly and Vertex in 2000. The structure of telaprevir and a co-complex crystal structure with the HCV protease domain are shown in Fig. 7.

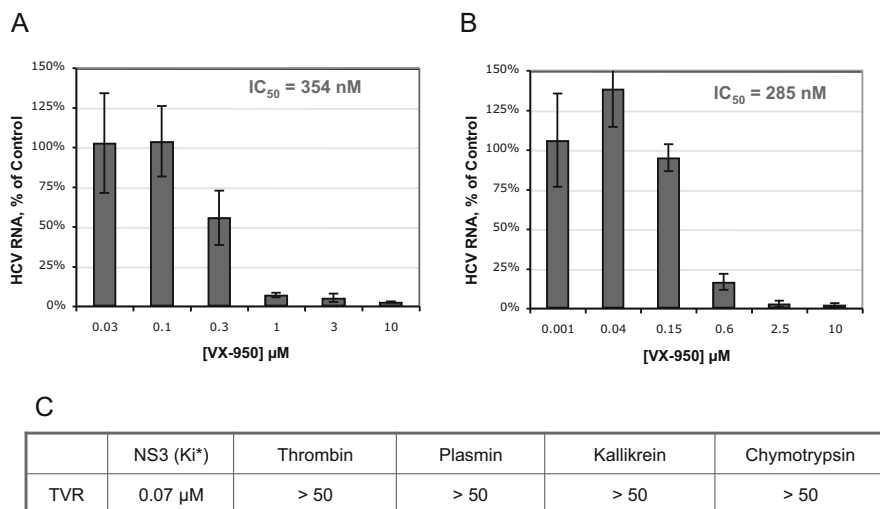


Fig. 6 Telaprevir activity in the HCV replicon and infectious virus assays and host selectivity. (a) GT1b HCV replicon assay. (b) GT1a infectious virus assay. (c) Enzyme selectivity (x -fold of NS3 Ki)

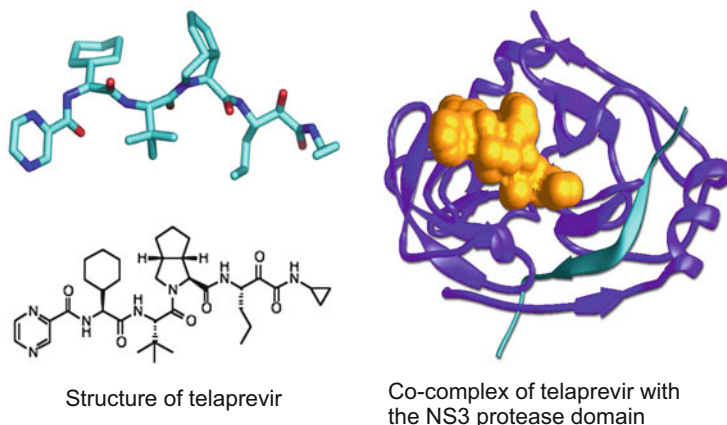


Fig. 7 Structure of telaprevir and co-complex with HCV protease domain

2.4 Clinical Proof of Concept Is Obtained by Boehringer Ingelheim with BILN 2061; The Telaprevir Program Is Shutdown

In 2002, Boehringer Ingelheim's BILN 2061 [29] became the first protease inhibitor to demonstrate clinical proof-of-concept for HCV when it demonstrated a reduction in HCV RNA after oral dosing [30, 31]. This dramatic result energized the field and

provided impetus to move HCV protease inhibitors into clinical development. Unfortunately, the IC_{50} for BILN 2061 was 300-fold higher than telaprevir in an HCV replicon assay and Vertex decided to discontinue telaprevir development and to shut down antiviral drug discovery.

2.5 *Data from Two “Midnight Projects” Rescued the Telaprevir Program*

As head of the infectious diseases group at Vertex, Ann Kwong had always negotiated for 20% of her team’s time to work on “midnight projects,” a.k.a. “skunk works,” and her team continued to work on telaprevir under these auspices. Within Vertex, data from two sets of “midnight projects” – a cell-based assay and a HCV protease animal model – provided the basis for Vertex to allow the telaprevir project team to raise funds from a strategic partner that would enable telaprevir to move forward into the clinic.

The goal of HCV inhibitors in the clinic is to drive the patient’s viral load from, typically, 1–10 million IU/mL to below the limit of detection, and to maintain undetectable viral loads for 12 weeks after drug is removed (e.g., to generate a sustained viral response 12 weeks after stopping treatment (SVR12), considered a virologic cure). For a patient, a twofold decrease which is a 50% decrease or the equivalent of an IC_{50} measurement is not meaningful. The central question asked in the first midnight project experiment is described in Fig. 8 and has to do with the relationship between a twofold drop in viral load (i.e., an IC_{50} measurement) and a multi-log drop in viral load.

In this pivotal study, Kai Lin and Ann Kwong compared the amount of telaprevir or BILN 2061 (the gold standard because it had clinical proof of concept) required for an IC_{50} assay (twofold reduction) to the amounts required in a multiple log reduction assay. The results of this experiment are shown in Fig. 9 [25]. The experiment reproduced previous results in a standard replicon IC_{50} assay that

Which assay is more relevant to clinical efficacy?

- **IC_{50} HCV replicon assay**
 - Short term (2-3 days)
 - Measure 50% (2-fold) drop in HCV replicon RNA or HCV viral RNA
- **Multi-log drop viral clearance (VC) HCV replicon assay**
 - Long term assay (> 9 days)
 - Measure drop in HCV replicon RNA to below the limit of detection (10,000-fold)
 - Measure viral rebound after drug withdrawal
 - Evaluate viral resistance after drug selection

Fig. 8 What is the relationship between an IC_{50} and multi-log elimination of virus replication?

Telaprevir and BILN 2061 have similar 3.5 log₁₀ drop

in the HCV replicon multi-log drop assay

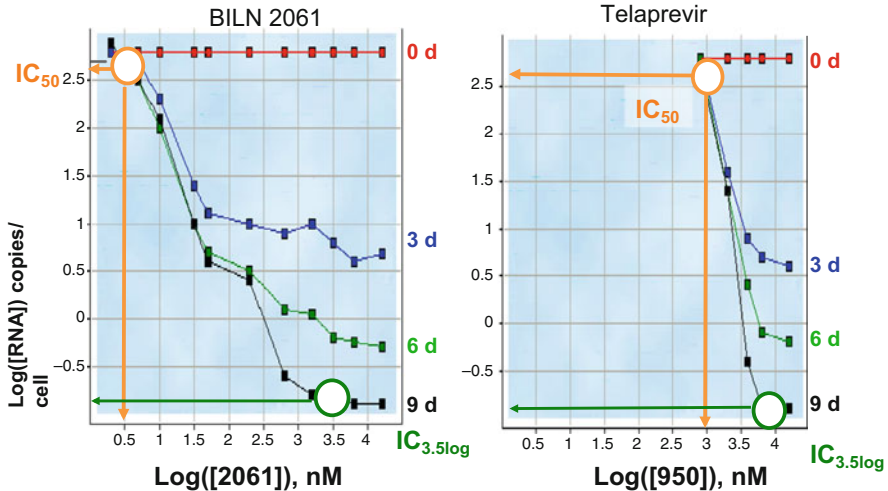


Fig. 9 Comparison of telaprevir and BILN 2061 in a multi-log drop HCV replicon assay

telaprevir was 350-fold less potent than BILN 2061 (IC_{50} is highlighted in orange circles in Fig. 9). In contrast, telaprevir had similar potency to BILN 2061 in reducing HCV replicon RNA levels by 3.5 logs ($IC_{3.5 \log}$ is highlighted in green circles in Fig. 9).

Further enzymatic investigation of the difference in kinetics between telaprevir and BILN 2061 by Cindy Gates at Vertex revealed two different mechanisms of action with a longer half-life for the reversible covalent interaction of telaprevir with the HCV protease active site (to form EI*) [25] as shown in Fig. 10.

The second “midnight project” experiment compared the ability of telaprevir and BILN 2061 to inhibit HCV protease activity in the HCV protease animal model after oral dosing [14, 25, 32]. This had been a long-term midnight project of Ann Kwong, and she and Raj Kalker were close to the proof-of-concept stage when the telaprevir program was shut down and Raj was laid off. Raj contributed 6 months of his own time and money to complete the HCV protease animal model at Vertex that is schematically described in Fig. 11.

Up until this point, the only HCV animal model that was available was chronically infected chimpanzees. These animals are known to be able to spontaneously clear their HCV infections, their use was extremely expensive resulting in tiny experimental numbers, and using chimpanzees was fraught with ethical problems. The ability to get significant statistical numbers in pharmacology experiments was one of the reasons we decided to develop a mouse model. Using the HCV protease mouse model, we were able to deliver real-time pharmacokinetic and pharmacodynamics data after oral dosing (Fig. 12).

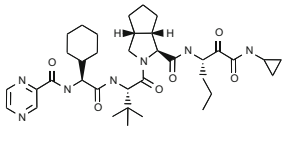
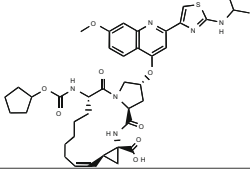
	Telaprevir	BILN-2061
Structure		
IC ₅₀	350 nM	1 nM
Enzyme kinetics	$E+I \xrightleftharpoons[k_2]{k_1} EI \xrightleftharpoons[k_4]{k_3} EI^*$ <p>FAST slow</p>	$E+I \xrightleftharpoons[k_2]{k_1} EI$ <p>FAST</p>
Half-life of complex	1 hr	seconds

Fig. 10 Comparison of telaprevir and BILN 2061 in vitro potency and mechanism of action

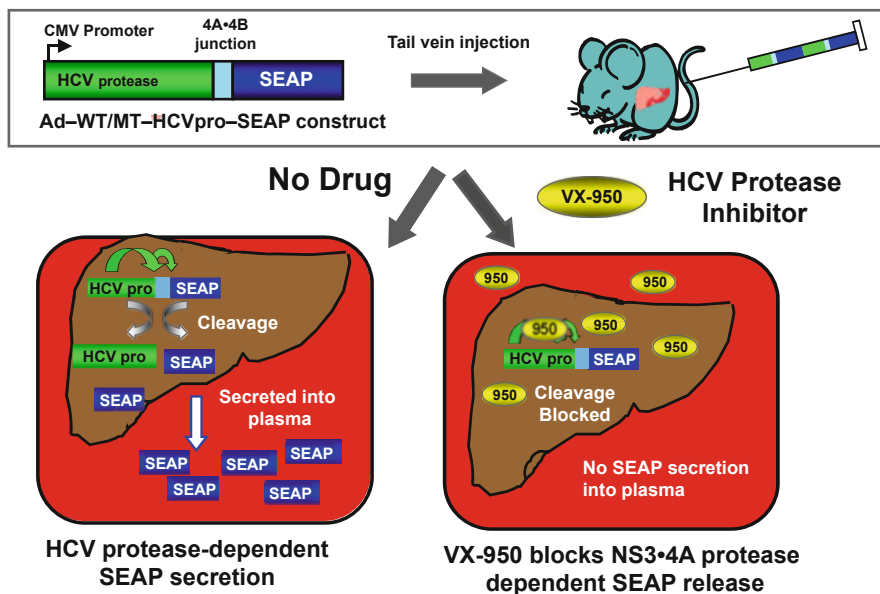


Fig. 11 Schematic illustration of the development of a HCV protease mouse model

The results of this experiment are shown in Fig. 13 and revealed that both telaprevir and BILN 2061 had similar potency in inhibiting HCV protease activity in the liver of a mouse after oral administration.

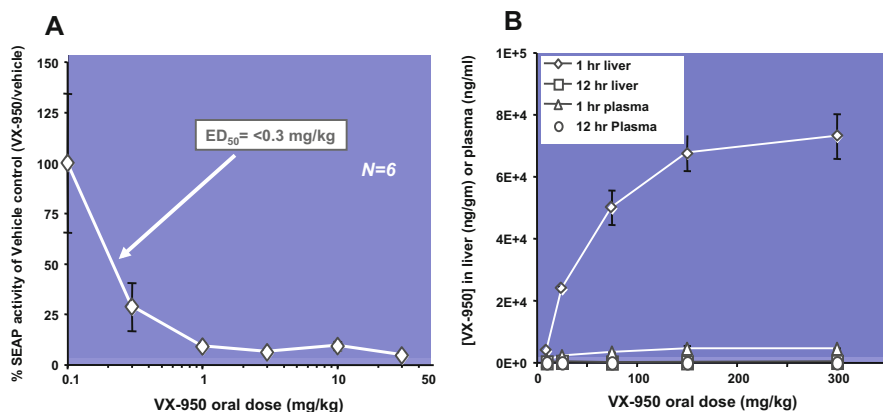


Fig. 12 PK/PD of telaprevir in the HCV protease mouse model. (a) HCV protease pharmacodynamics (PD) activity in the mouse liver as a function of SEAP activity. (b) Pharmacokinetic (PK) assessment of telaprevir concentrations in the liver and plasma

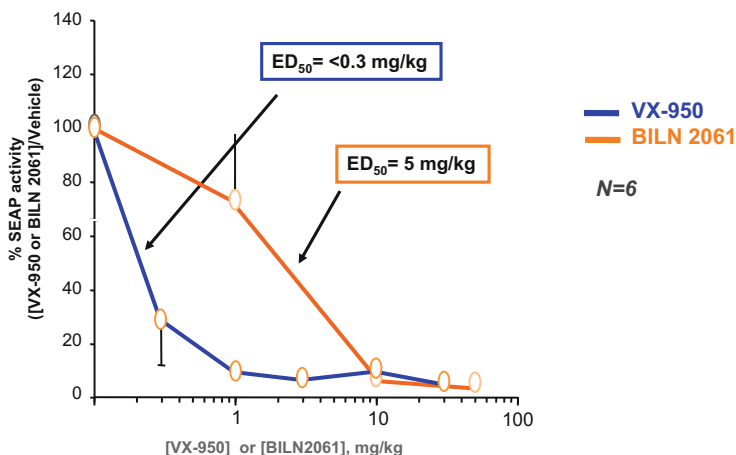


Fig. 13 VX-950 (telaprevir) and BILN-2061 activity in the HCV protease mouse model

3 Telaprevir Development

3.1 *Get Out of Jail but Find Your Own Clinical Development Funding*

The positive results from the multi-log drop assay and HCV protease animal model comparing telaprevir and the gold standard BILN 2061 played a crucial role in Vertex's decision to allow the telaprevir team to take the drug into the clinic, if they

could find a strategic partner to help pay for clinical studies. The Vertex business development team visited every major pharmaceutical company in the USA, Europe, and Japan who would listen to our pitch on why telaprevir should be tested in the clinic. In all but one case, companies refused to partner with Vertex because of the 350-fold difference in potency in the HCV replicon IC_{50} assay between BILN-2061 and telaprevir, ignoring the results of the HCV replicon multi-log drop assay and the HCV protease animal model.

3.2 Mitsubishi Pharma Saw the Data in Ways Others Did Not and Was Able to Act Upon It

In 2004, Mitsubishi Pharma Corp. of Tokyo signed a deal with Vertex to develop and commercialize telaprevir for the treatment of HCV in Japan and certain Far East countries. As part of the agreement, Mitsubishi would make pre-commercial payments to Vertex of \$33 million to support clinical development of telaprevir [33].

3.3 CMC Development

Telaprevir is a crystalline drug substance and is famously “less soluble in water than marble”; this posed tremendous chemistry, manufacturing, and control (CMC) challenges that were overcome by Patricia Hurter and her team at Vertex [34]. Because telaprevir was the first drug that Vertex brought to market, a strategic decision was made to build an in-house pharmaceutical development group and to set up a virtual global manufacturing network. The medicinal chemistry route for telaprevir had 20 steps with low overall yield. Hurter and colleagues were able to optimize the Med Chem route to a commercial route with 14 steps and high overall yield and used a quality by design (QbD) approach for the CMC development of telaprevir to significantly improve product and process understanding to improve manufacturing.

3.4 Clinical Development

The goals of the telaprevir development program were to significantly improve efficacy and to shorten the duration of treatment, compared to the standard of care, PEGylated interferon alfa-2a plus ribavirin (PR).

3.5 Phase 1 Clinical Studies

In 2004, Vertex executed a Phase 1b 14-day viral kinetic study comparing telaprevir monotherapy with placebo in patients with chronic genotype 1 HCV infection, many of whom had failed prior treatment with PEGylated interferon and ribavirin. In this study, a profound and rapid reduction in plasma HCV RNA ($\geq 4 \log_{10}$) was observed with all telaprevir-dosed patients, while no notable decline in HCV RNA was observed in patients receiving placebo [35]. The results are shown in Fig. 14 and compared favorably with the $\sim 2.5 \log_{10}$ reduction in HCV RNA obtained by BILN 2061 in the first clinical proof-of-concept study for a HCV protease inhibitor [31]. Interestingly, even in the face of these clinical data, a number of pharmaceutical companies declined to partner with Vertex based on the old IC_{50} replicon comparison to BILN 2061.

3.6 Phase 2 Safety and Efficacy

Vertex conducted two Phase 2b, randomized, placebo-controlled clinical studies in treatment-naïve patients (PROVE1 [36] and PROVE2 [37]) and one study in treatment-experienced patients (PROVE3 [38, 39]) to characterize the duration of telaprevir (12 vs 24 weeks) and PR (12, 24, or 48 weeks) and to determine the effect of the presence or absence of ribavirin on the efficacy and safety of a variety of telaprevir-based regimens. Rash and anemia were identified in Phase 2 trials as the

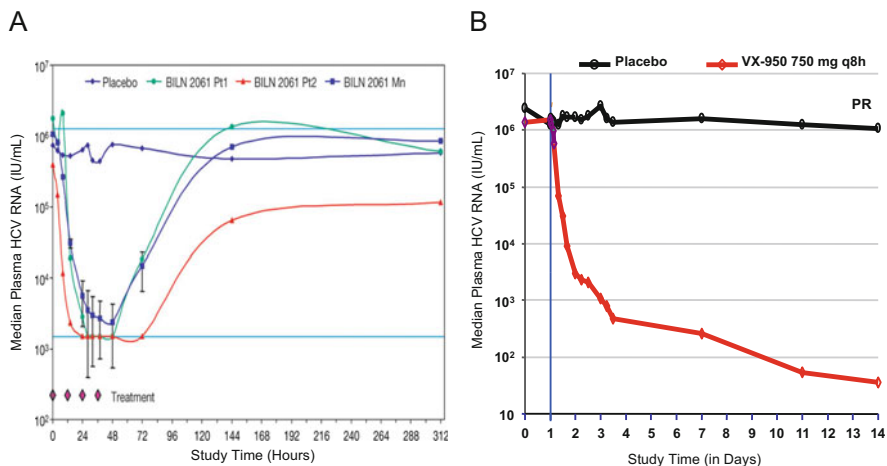


Fig. 14 Comparison of telaprevir and BILN-2061 monotherapy results from separate viral kinetic Phase 1b clinical studies. **(a)** BILN 2061 achieved clinical POC with $\sim 2.5 \text{ Log}_{10}$ viral RNA reduction in 2 days. **(b)** Telaprevir achieved 4.4 Log_{10} viral RNA reduction in 14 days

most clinically significant adverse events (AEs) associated with telaprevir, and all AEs were reversible upon cessation of treatment. In PROVE1 and PROVE2, the SVR rate was 61% and 69%, respectively, which was significantly higher as compared with 41% and 46%, respectively, for the PR48 control arms. In prior PR treatment-experienced patients treated with T12PR24 or 24-week telaprevir in combination with 48 weeks PR (referred to as T24PR48) in PROVE3, the SVR rate was 51% and 53%, respectively, compared to 14% in the PR48 arm.

3.7 Phase 3 Safety and Efficacy

Vertex conducted three Phase 3 studies (ADVANCE [40], ILLUMINATE [41], and REALIZE [42]). The most common AEs reported more frequently for telaprevir combination therapy compared to PR alone were rash, fatigue, itching, nausea, and anemia [43]. In the overall Phase 3 program, 14% of patients discontinued telaprevir due to an AE²⁹. Adverse events were generally manageable and reversible upon cessation of treatment, with rash resolving over a few weeks. Stopping rules were employed to prevent patients who were unlikely to respond to therapy from unnecessary exposure to telaprevir (while continuing PR) and to decrease the potential for the selection for more fit telaprevir-resistant variants. Futility rules were similar to those employed with PR alone in which all drugs were stopped if a patient had detectable virus after 24 weeks of treatment. An analysis of all patients in ADVANCE who had received at least one dose of study drugs (intention-to-treat) showed that 79% (T12PR) and 72% (T8PR) of telaprevir patients achieved SVR compared to 46% of patients who received PR alone. ILLUMINATE tested the hypothesis that patients who achieved an eRVR (HCV RNA undetectable 4 weeks after starting treatment) could shorten the total duration of treatment using response guided therapy (RGT). The SVR rate in patients with eRVR who were treated with 24 weeks total therapy (T12PR24) was 92% and not inferior to the SVR rate (90%) in patients treated with 48 weeks total therapy (T12PR48). The overall SVR rate in ILLUMINATE was 74%, similar to that observed in the T12PR arm of ADVANCE. SVR rates were significantly higher in the pooled telaprevir arms than in the control arm regardless of prior PR response: 86% vs 22% in prior relapsers, 59% vs 15% in partial responders, and 32% vs 5% in prior null responders.

3.8 Characterization of Telaprevir-Resistant Variants

Due to high viral replication and an error-prone RNA polymerase, HCV exists as a population of genetically distinct but closely related virus quaspecies. Resistant variants to DAAs naturally exist at baseline (before treatment), and their frequency in the population is governed by the replicative fitness of the variant. At Vertex, Tara Kieffer and colleagues developed a sensitive clonal sequencing methodology

to detect variants present at $\geq 5\%$ of the population. Although the entire sequence encoding the full-length NS3•4A protein was analyzed, all amino acid changes associated with decreased sensitivity to telaprevir mapped to 4 canonical sites in the HCV protease catalytic domain. Changes at residues 36, 54 and 155 conferred lower-level resistance (< 25 -fold decrease in sensitivity to telaprevir) and changes at position 156 plus the double mutant R155K+V36M conferred higher-level resistance (> 25 -fold change) to telaprevir [44–46].

3.9 Telaprevir Approval as INCIVEK

After filing a new drug application in the USA at the end of 2010, telaprevir was granted priority review and received FDA approval in May 2011. Telaprevir combination treatment (a.k.a. INCIVEK plus PR) represented a paradigm shift in HCV therapy by offering both treatment-naïve and treatment-experienced patients improved SVR rates and the possibility of shortened treatment duration, while increasing the occurrence of certain adverse events, compared to PR therapy alone. Just as importantly, telaprevir-based therapy provided patients who had an historically low rate of achieving SVR using peginterferon/ribavirin alone, such as people with high viral load, high body mass index, cirrhosis, and Black/African Americans, a greatly improved chance of achieving a viral cure.

Although INCIVEK plus PR represented a major advancement in HCV therapy compared to peginterferon/ribavirin therapy alone, the toxic side effects of PR therapy limited the usefulness of INCIVEK in a wide range of patients including patients who were unable to tolerate a peginterferon-based regimen, patients coinfecting with HIV/HCV, patients with decompensated cirrhosis, and patients pre- and post-liver transplant.

3.10 Lessons Learned from the Discovery and Development of Telaprevir

It has been said by many people experienced in pharmaceutical development that the road from a discovery program to an approved drug is long and arduous, marked by pot holes, road blocks, and many side ventures. The path for a truly innovative drug that is a new mechanism of action is even more difficult. Most truly innovative drugs die along the way, and those that survive are kept alive by scientists who just wouldn't give up, and many times were dismissed for continuing to work on their passion, even though their efforts result in a block buster drug many years later. Telaprevir was no different. It took 16 years from the start of the structure-based drug design program at Vertex in 1995 to FDA approval in combination with PR in 2011.

When Boehringer Ingelheim's groundbreaking work with BILN 2061 demonstrating clinical proof-of-concept for HCV protease inhibitors became public knowledge, Vertex and Lilly both terminated telaprevir development. The virology team generated two sets of innovative cell-based and animal model data to characterize properties that we thought were more illuminating and predictive of clinical success than a simple HCV replicon IC_{50} inhibition curve. Lessons learned from the rescue of the telaprevir program include: (i) the need for discovery scientist to determine which properties a drug will need to possess in order to be successful clinically and commercially, and (ii) develop assays that assess whether the compounds selected to move forward have those properties. The role of preclinical discovery is to reduce the risk of failure in the clinic and in the marketplace. To succeed, one must be able to work collaboratively with clinical, commercial, and key opinion leaders to identify criteria for critical assays and experiments to screen and characterize compounds moving forward that correlate with success in the clinic or in the marketplace. However, it is not enough to have good data – in truly innovative drug development programs, pharmaceutical managers and investors must be willing to look at the data and go out on a limb because there is no well-trodden road map to success. It cannot be emphasized enough that scientists need champions both internally and externally to help shepherd a new drug to approval successfully. The telaprevir program team was extremely fortunate that Vertex management decided to give it the opportunity to seek external funding for the program based on the unconventional data generated by their scientists.

4 Telaprevir Medical Affairs and Commercialization

A detailed comparison of boceprevir and telaprevir in the context of management of HCV-infected patients was published in *Clinical Infectious Diseases* less than a year after launch [47]. Telaprevir and boceprevir had fairly similar, though not identical properties, highlights of which are taken from the FDA product labels [48, 49] and are shown in Fig. 15.

Figure 16 shows a compilation of sales for HCV drugs and combinations gleaned from company financial reports which can be grouped into three categories: (1) DAAs such as telaprevir and boceprevir that were used in combination with PR; (2) DAAs that were used in combination with other DAAs, primarily sofosbuvir (SOVALDI); and (3) DAAs that were launched as all DAA combinations. Even though Merck's VICTRELIS was approved 10 days before Vertex's INCIVEK in May 2011, Vertex sales quickly took off, bringing in \$951 million in revenue in a little over 6 months, compared to \$140 million for Merck. During the first quarter of 2012, Vertex would go on to become the fastest drug ever to reach \$1 billion in sales from its launch and ultimately outsold Merck by ~2.5-fold over the first 3 years.

INCIVEK and VICTRELIS were pulled from the market by Vertex and Merck when their sales were significantly decreased by warehousing of patients waiting for all-oral DAA combinations shortly after the approval of SOVALDI and OLYSIO.

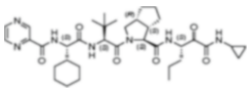
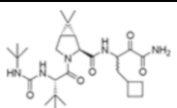
Properties	INCIVEK	VICTRELIS
Structure		
In vitro potency	Similar	Similar
HCV GT1 efficacy (% SVR)		
Treatment naïve	79	63-66
Prior PR relapse	86	70-75
Prior PR partial responder	59	40-52
Prior PR null responder	32	Not tested
Safety profile	Serious skin conditions, rash, anemia, anal symptoms	Anemia, leukopenia/neutropenia
Dosing regimen	Simpler, fewer pills, TID>>BID	More complex, more pills, TID
Food requirements	Takes with at least 20 gm fat	Take with food
May 2011 launch list price (not including PR)	US\$ 49,200	US\$ 26,400-\$48,400

Fig. 15 Properties of INCIVEK (telaprevir) and VICTRELIS (boceprevir) in combination with PR

HCV annual sales (in US\$ millions)

Type of HCV DAA treatment	Company (HCV drugs or regimen(s))	2011	2012	2013	2014	2015	2016	2017	Total
DAA used with PR	Merck (VICTRELIS)	140	502	428					1,070
	Vertex (INCIVEK)	951	1,160	466					2,577
DAAs used with SOVALDI	Johnson & Johnson (OLYSIO)			23	2,302	621	106		3,052
	BMS (DAKLYNZA)				207	458	226	59	950
All DAA combinations	Gilead (SOVALDI, HARVONI, EPCLUSA, VOSEVI)			139	12,410	19,410	14,434	9,137	55,530
	AbbVie (VIEKIRA PAK, TECHNIVIE, MAVYRET)				48	1,639	1,522	1,274	4,483
	Merck (ZEPATIER)						555	1,660	2,215
Total		1091	1662	1056	12,458	21,049	16,511	12,071	65,898

Fig. 16 Annual sales in the age of HCV DAAs

The launch of individual and DAA combinations in late 2013 increased the hepatitis C treatment market to over \$12 billion annually and a high of \$21 billion in 2015.

Although telaprevir sales were quickly eclipsed by all-oral DAA launches, the rapidity of initial uptake and sales in comparison to boceprevir is still quite remarkable. The remainder of the chapter will discuss some of the potential factors that contributed to telaprevir's brief success in the market.

The Vertex medical affairs, government affairs, and commercial teams worked closely to understand the hepatitis C landscape, and we believe the work that came out of these collaborations was critical to the commercial success of telaprevir.

Vertex recognized that telaprevir would only succeed if external barriers within the HCV care continuum were also addressed. It was not enough to just recognize these barriers – we had to work to change the existing reality. Internally, medical affairs worked closely with clinical development and clinical virology to identify scientific barriers to acceptability of telaprevir and how to address these through education. Key insights and programs are described.

As the Phase 2b clinical data for telaprevir were emerging in 2007, it was clear that telaprevir plus PR would be able to nearly double cure rates compared to the standard of care (SOC) of PR alone in patients with genotype 1 HCV infection. It was also apparent that the addition of telaprevir increased the adverse effects associated with treatment, so treatment-associated barriers found with respect to PR would still be a concern. In addition, subjects who were not cured with telaprevir had viral substitutions that conferred resistance to telaprevir. Since PR acted by modifying the host immune responses to increase clearance of virus, most hepatology and gastroenterology health professionals who were the primary HCV treaters had no experience in using DAA drugs and addressing resistance to HCV drugs. Phase 3 studies needed to be designed in a manner that simplified the treatment algorithm, provided guidance into how to manage common adverse events, and improve understanding of the importance of HCV resistance, while generating the efficacy and safety data required to achieve regulatory approval. The goal was to generate a label that maximized ease of use while providing all-important scientific data.

4.1 Management of Adverse Events

By Phase 2b, data demonstrated that all adverse events associated with PR were present in telaprevir plus PR combination studies, but two effects, rash and anemia, were more prominent in patients who also received telaprevir. In addition, a unique effect, anorectal discomfort, burning, or itching, was also present in subjects treated with telaprevir. Vertex knew that inadequate attention to these issues could reduce provider willingness to use telaprevir and/or cause unnecessary harm to patients, and medical education would be critical.

4.2 Rash

Rashes had been seen with PR but with the addition of telaprevir, over 50% of subjects had rash events and trials showed an increase in serious skin reactions such as DRESS (drug reaction with eosinophilia and systemic symptoms) and Stevens-Johnson syndrome, which are severe, potentially life-threatening, idiosyncratic reactions to a drug. These serious rashes (occurring in about 1% of subjects) had to be distinguished from annoying, but not life-threatening rashes that were also seen with PR. An external advisory panel of dermatology experts worked with

Vertex to help distinguish serious from less severe rashes, define which patients required discontinuation of telaprevir or all drugs, and provide suggestions for the management of less severe rashes so that antiviral treatment could be continued. In addition, all rashes were adjudicated by this expert panel, which was required for the safety section and regulatory authorities. Not all management strategies were built into the Phase 3 program, which posed challenges as Vertex tried to devise educational materials that would remain within the product label.

Rashes were divided into mild, moderate, severe, and serious based on rash characteristics, the quality, and extent of skin involvement and whether systemic symptoms were present. One challenge Vertex faced was the knowledge that most HCV providers were not rash experts and needed clear guidance as to when to provide symptomatic relief (such as topical steroids and antihistamines) and when to stop telaprevir or all medications. The medical affairs and clinical development teams worked closely with clinical trial investigators and made certain that physicians and nurse practitioners and physician assistants were included to provide insight into rash management. We developed a pamphlet with images of rashes, human body outlines to demonstrate the extent of rash, and suggestions for good skin care to reduce the discomfort of rash, as well as instructions on when to stop various components of the regimen. Feedback from prescribers confirmed that addressing this issue up front helped improve their confidence that rash was a manageable adverse effect.

4.3 Anemia

Anemia was a common event associated with PR, but the decrease in hemoglobin was more pronounced in patients who also received telaprevir. In the clinical trials, anemia was managed by reducing the dose of ribavirin. The challenge Vertex faced in translating this approach to usual clinical practice was that at that time, it was believed that maintaining the full ribavirin dose was critical to maximize cure rates and often patients were treated with erythropoietin products (an off-label indication). The data had to be shown and analyzed in a way that represented how providers actually practiced. Once we were able to show providers that reducing ribavirin in the setting of anemia did not reduce cure rates, ribavirin dose reduction was gradually accepted.

4.4 Anorectal Signs and Symptoms

It was unclear why about a third of patients developed some degree of anorectal symptoms, but in clinical trials, fewer than 1% discontinued treatment because of these symptoms. We suspected that excipients or metabolites of telaprevir may

be involved, and certain investigators performed endoscopy to look for inflammation or other lesions; none were found. This syndrome became known outside Vertex as “fire-arrhea” and could have led to a commercial disaster. Medical affairs did not have any specific interventions that were included in the clinical trials to draw upon. Here, investigators shared their experiences managing these symptoms with providers who had not had previous experience with telaprevir, and this approach proved invaluable.

There were many internal debates about how to share the negative findings from clinical trials in a way that would help keep patients safe once telaprevir was approved. Constraints included how to educate on potential symptom management options when these were not specifically studied in the clinical trials and fear of competitors taking educational materials and using them to shape a negative narrative about Vertex and telaprevir. The legal and regulatory teams were willing to hear what we were trying to achieve and to help us develop solutions that fit within regulatory guidelines. Our goal was to be as transparent as possible about the good and bad of telaprevir, and the HCV providers and patients seemed to appreciate this honesty.

4.5 Resistance

Drug resistance is often understood in the context of HIV therapies. Resistance in HIV can limit drug options, and patients can die from highly resistant, untreatable infection. Infectious disease providers brought their concerns about HIV resistance to their understanding of HCV drug resistance. A multidisciplinary team led by clinical virology had to come to an understanding about HCV resistance, how it was different from HIV resistance, and create a framework for how everyone should be thinking about HCV resistance. One challenge was that the FDA was simultaneously determining how to address this issue. In addition, outside Vertex, HCV resistance was being termed a “telaprevir problem,” when in reality, all direct-acting antiviral drugs that were able to create sufficient drug pressure, yet did not clear HCV, would be associated with resistance.

This work on resistance capitalized on the rigorous virology data being generated by Vertex and innovative collaborations in the precompetitive space with the HCV Drug Development Advisory Group (HCV DrAG) between regulatory agencies, pharmaceutical companies, academia, and patient community representatives that served to enable the development and approval of new HCV treatment regimens with unprecedented speed [50].

Medical affairs and clinical virology collaborated on additional educational materials, scientific presentations, and approaches to discuss resistance with HCV providers. This work helped us establish Vertex as the “high science” company that could be trusted to thoroughly examine data and share it in an understandable way.

5 Examining Perceptions of Hepatitis C

Key challenges Vertex faced in expanding the HCV market included the fact that 75% of people living with HCV had not been diagnosed, and many patients who had been diagnosed were not being treated. Vertex explored these external challenges to the use of telaprevir through market research during the Phase 2 and 3 clinical program with thousands of people, including the general public, patients living with hepatitis C, primary care providers, HCV specialists (gastroenterologists, hepatologists, infectious disease physicians, and internal medicine physicians with a specialization in HCV), and payers. We found several main themes: (1) the prevalence of hepatitis C was poorly understood; (2) the main risk factor associated with HCV was injection drug use; and (3) it was not urgent to treat most patients with HCV. Below are some key insights that were used to shape Vertex programs.

5.1 *General Public*

The public had very little knowledge about HCV and often confused it with hepatitis A or B. They were not sure what cirrhosis was or assumed that cirrhosis is caused by alcohol. In general, lay people had little “baggage” around HCV. People who had injected drugs at some point in their lives saw campaigns to encourage HCV testing of people who inject drugs as reminders of a shameful period of their lives and were likely to avoid testing or discussions with health providers.

5.2 *Patients Living with HCV*

The key finding was one of suffering and psychological distress. Many patients felt shame about the diagnosis, felt judged by others (especially within the healthcare system), worried about infecting people close to them (intimate partners or household members), were scared of complications associated with HCV even though they were not always clear what these might be, were worried about becoming more sick and being a burden on their loved ones, and were scared of undergoing evaluation for HCV (fear of bad news, liver biopsy) and fear of the adverse effects associated with PR. The idea of being cured of HCV was associated with redemption or a chance to start over with a clean slate. The stigma associated with having HCV infection was present in people who had a past history of injection drug use as well as those who were infected through medical procedures or other routes.

5.3 Primary Care Providers

This group had little knowledge about HCV. They found recommendations on who should be tested for HCV burdensome and difficult to decipher, they were concerned that if they asked about injection drug use they might offend patients, and they perceived specialists as performing liver tests each year on patients with HCV infection and not much else, which discouraged them from referring all of their HCV patients to specialists.

5.4 HCV Specialists

There was a group of “champions” who were interested in helping patients with HCV infection through treatment and addressing substance use and psychiatric comorbidity. There were others who were willing to treat patients that seemed reliable, attentive, and compliant but were judging and sometimes hostile to patients that they perceived as having substance use and/or psychiatric issues.

5.5 Addressing Stigma

It became clear that Vertex would not achieve its goal of telaprevir being used to treat appropriate patients if we did not address the issue of stigma around HCV. Even though a history of injection drug use was clearly the most important predictor of HCV infection, it was also the most stigmatizing. So we started looking for other predictors. We contracted with an actuarial firm, Milliman, who had access to large medical databases and expertise in analyzing trends in medical data. They searched for any predictors that were associated with a higher likelihood of having HCV. Remarkably, they came up with a surprisingly straightforward predictor: People who were born from 1946 through 1964 had a fivefold increased likelihood of having HCV than people outside this birth cohort. Another way of looking at it was that about one out of 30 people in this “baby boomer” cohort had HCV. Now we had a predictor that was easy to identify (everyone has year of birth recorded in their medical record) and was destigmatizing – nobody can help what year they were born in.

5.6 Increasing Awareness

A key question was how to increase awareness about this risk factor. We spoke with large health systems like Kaiser Permanente who had comprehensive medical records and had changed disease guidelines through previous analyses. We then

decided to approach the Centers for Disease Control and Prevention (CDC) since they are entrusted with the public health of the nation and create testing guidelines. We were very sensitive to the fact that an agency like the CDC can never be perceived as being influenced by pharmaceutical companies since that would erode the trust the public has in any future recommendations. On the other hand, we had invested several million dollars in our market research, and we believed that sharing these findings could help the general public if the CDC confirmed them. The CDC Foundation was an appropriate intermediary that helped “fire wall” the sharing of data and insights from any future support. We shared key data with various teams at the CDC. For the education team, we noted that campaigns that depicted people actively injecting drugs did grab peoples’ attention but often made them more reluctant to seek HCV testing. Campaigns that were more positive and hopeful would likely be more successful. We also discussed the Milliman findings.

The CDC was aware that testing rates for HCV were unacceptably low and were open to considering new approaches. The CDC Foundation reached out to a number of pharmaceutical companies, including Vertex, to seek financial support for three key CDC initiatives: (1) a study of the feasibility of HCV birth cohort testing (termed BEST-C), (2) an observational study of the natural history of hepatitis C and hepatitis B (termed CHeCS), and (3) a study of educational campaigns that would increase awareness and testing of HCV (termed KNOW More Hepatitis). No pharmaceutical company was allowed to have any influence on the conduct of the studies, the interpretation of the data, or the implementation of programs that may have resulted from these data.

The CDC had access to additional national health data and determined that recommending testing of the 1945–1965 birth cohort would be an important complement to the already existing risk-based testing recommendations. This recommendation was added to CDC HCV testing guidelines and was subsequently adopted by the US Preventive Services Task Force and Medicare [51, 52]. The CHeCS cohort has resulted in landmark publications that have shaped our understanding of the severity of diseases associated with HCV, determinants of who is treated, and outcomes after HCV treatment [53]. The KNOW More Hepatitis campaign resulted in multimedia outreach, online testing tools, posters in clinical waiting rooms, and important collaborations with HCV advocates [54]. Transforming HCV into a baby boomer epidemic began to change attitudes about people living with this infection [55].

Vertex developed our own educational and support campaigns based on our market research. One finding was that HCV providers looked for behaviors that they associated with inability to successfully complete HCV treatment. If a patient was perceived as being at risk for not completing treatment, they would be considered “not a treatment candidate.” Behaviors such as being distracted or not being respectful of the provider were seen as predictors of poorer outcomes. Interestingly, race, sex, and perceived socioeconomic status did not seem to

influence providers' decisions about who could be a successful treatment candidate. Vertex developed support materials for patient navigators, case managers, and other personnel to increase the likelihood that patients would be perceived to be good treatment candidates.

6 The Billion Dollar Question: Why Did INCIVEK Sell More than VICTRELIS?

The answer to the question of why Vertex, a newcomer in marketing and launching drugs, did so well in comparison to VICTRELIS, which was marketed by Schering-Plough/Merck in collaboration with Roche, another HCV behemoth [56], has a Rashomon aura about it, which is to say, the answer given varies widely depending on the answerer's experience and their role in the HCV treatment or discovery space. Here are some of the ideas that people close to the telaprevir and boceprevir stories have advanced to explain the difference in sales. They are not presented in order of likelihood or importance:

- Key opinion leaders (KOLs) and treaters on the front lines of patient management tend to answer that INCIVEK had a less complicated treatment paradigm and was easier to manage. For example, VICTRELIS had a 1 month PR lead in whereas INCIVEK-treated patients got the HCV protease inhibitor right from the start and were able to get the positive feedback of a significant drop in viral load faster.
- Although differences in efficacy in specific subpopulations of patients were minor, and no head-to-head trials were ever conducted, the net perception was that INCIVEK was modestly more efficacious than VICTRELIS.
- Although Vertex did not get initial approval for BID dosing, a Phase 2b study had been performed which demonstrated similar results with BID and TID dosing, and some people believed this had a significant effect on sales.
- Schering-Plough/Merck lost many of their internal HCV experts in the merger, leaving the boceprevir program without strong in-house advocates. In contrast, Vertex capitalized on the strong discovery story of loss of support and redemption through midnight projects and internal and external champions to share with the HCV treatment community. This more scientific and less blatantly commercial sales approach was viewed favorably.
- Vertex spent a lot of time and effort prior to the launch of INCIVEK working with KOLs, the CDC, community activists, etc. on treatment awareness and reducing the stigma of diagnosis and treatment of HCV.
- Vertex had multifunctional team discussions on how to design the pivotal trials. The team's goal was to have as clean and simple a package insert as possible, so there was a huge push to simplify testing at many different time points which can be more easily performed in a clinical trial than in clinical practice.

7 Lessons for Today

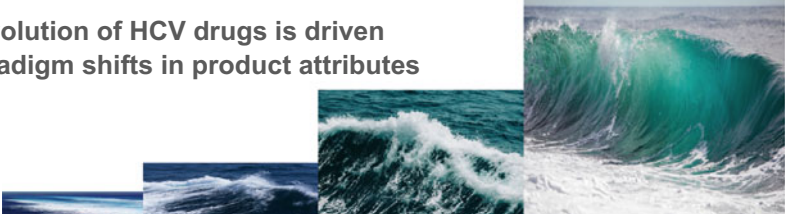
INCIVEK was quickly supplanted by SOVALDI (sofosbuvir), and the advent of all-oral DAA treatment and Vertex stopped US commercialization a little over 3 years after launch in 2014 [57]. Vertex decided it was too late to enter the all-oral DAA, premium-pricing market, and decided to focus on developing drugs for cystic fibrosis. The introduction of an off-label combination of SOVALDI plus OLYSIO (simeprevir) in late 2013, followed by Gilead's sofosbuvir/ledipasvir (Harvoni) and paritaprevir/ritonavir/ombitasvir plus dasabuvir (Viekira Pak) in 2014 ushered in an era of virologic cure rates of greater than 95% in most patient groups, highly tolerable regimens, and treatment duration of 8 to 12 weeks (Fig. 16).

However, a new toxicity emerged in higher-income countries including the USA – financial toxicity – as payers rebelled against the cumulative cost of treating large numbers HCV patients. By 2014, providers and patients in the USA were confronting severe rationing of these curative and highly effective treatments in a way never seen before in US healthcare. Payers created relatively arbitrary restrictions on access such as mandating the presence of advanced liver fibrosis even though data showed clinical benefits for those with less severe liver damage; required periods of abstinence from alcohol or illicit drugs, even though there were no data supporting worse outcomes in these groups; and limited prescribing to certain specialists, even though this severely restricted access in rural communities. These restrictions ran up against a global movement for HCV elimination, led by the World Health Organization and complemented by country-level strategies.

In contrast, both Gilead and Bristol Myers Squibb modeled access programs in low-income countries on those for HIV regimens. Generic manufacturers were permitted to sell regimens in 101 low-income countries for \$200 to \$600 for a 12-week course of treatment. Challenges in many of these countries include a lack of sufficient trained providers, lack of public awareness about HCV, and the high expense of diagnostics. In many countries, the cost of HCV RNA tests to diagnose current infection and confirm virologic cure 12 weeks after completion of antiviral treatment can cost as much as the DAA regimens themselves [58].

In response to the crisis of rationing of DAA regimens in high- and middle-income countries, Trek Therapeutics was founded to develop affordable and accessible drugs for infectious diseases, including against HCV infection. Time will tell how successful this endeavor is, but it is clear that the experience in HCV is a microcosm of the unsustainable nature of high drug prices in many higher-income countries. The next wave in drug development might better balance the cost and risk of developing innovative drugs with the moral obligation to provide important therapies to more patients in need (Fig. 17). In the absence of support to eradicate HCV through the use of anti-HCV DAAs, it may well be that the only way to achieve cost-effective global eradication and elimination of the cancer risk associated with HCV infection is through the development of a vaccine [59].

The evolution of HCV drugs is driven by paradigm shifts in product attributes



Wave	1st wave: IFN-based Poor efficacy & safety	2nd wave: Peg-IFN + RBV+DAA Improved efficacy, poor tolerability	3rd wave: ALL ORAL DAA COMBOs Excellent efficacy, safety & tolerability	4th wave: AFFORDABLE & ACCESSIBLE EVERYWHERE Efficacy & safety comparable or better than standard of care
Driver	Efficacy	Efficacy & duration	Efficacy, safety & tolerability	Convenient, affordable and available
Approval	1991, 1996, 1997, 1998, 2001, 2002	2011, 2013	2014, 2015, 2016, 2017	
Profile	≤ 40% SVR	75-80% SVR	95-99% SVR	>97% SVR
Company	Schering-Plough, Roche, Amgen	Vertex, Merck	Gilead, AbbVie, Merck, Johnson & Johnson (J&J), Bristol Meyers Squibb (BMS)	Gilead, BMS & J&J are providing access to generic drug pricing in very low-income countries

Fig. 17 Evolution of HCV drugs

8 Summary

While we suspect that the real reason for Vertex's success is multifactorial, this case study serves to illustrate a larger and important point that great care should be given to considering the commercialization of a drug throughout the entire discovery and development process. Sometimes the same old, tried, and true approach by market leaders can be truly upended by an innovative newcomer.

Lessons learned from telaprevir drug development and commercialization include the following:

- Innovative drugs need innovative metrics to succeed.
- Start from the desired clinical outcome to design preclinical properties and assays to select compounds with a higher chance of success.
- It is not enough to have great data, you need internal and external champions to succeed.

We believe the success of telaprevir offers great hope to new companies and new ideas trying to enter the pharmaceutical drug approval space that they can make a significant impact on patient lives and simultaneously generate strong financial returns.

Compliance with Ethical Standards

Conflict of Interest Robert B. Perni, Camilla S. Graham, and Ann D. Kwong were employees of Vertex Pharmaceuticals.

Ethical Approval All applicable international, national, and/or institutional guidelines for the care and use of animals were followed.

All procedures performed in studies involving human participants were in accordance with the ethical standards of the institutional and/or national research committee and with the 1964 Helsinki declaration and its later amendments or comparable ethical standards.

Informed Consent Informed consent was obtained from all patients who participated in the studies.

References

1. Houghton M (2009) The long and winding road leading to the identification of the hepatitis C virus. *J Hepatol* 51(5):939–948
2. Lindenbach BD, Rice CM (2005) Unravelling hepatitis C virus replication: from genome to function. *Nature* 436:933–938
3. Lohmann V, Korner F, Koch J-O, Herian U, Theilmann L, Bartenschlager R (1999) Replication of subgenomic hepatitis C virus RNAs in a hepatoma cell line. *Science* 285:110–113
4. Gao M, Nettles RE, Belema M, Snyder LB, Nguyen VN, Fridell RA, Serrano-Wu MH, Langley DR, Sun JH, O’Boyle 2nd DR, Lemm JA, Wang C, Knipe JO, Chien C, Colonno RJ, Grasela DM, Meanwell NA, Hamann LG (2010) Chemical genetics strategy identifies an HCV NS5A inhibitor with a potent clinical effect. *Nature* 465(7294):96–100
5. Pyenson B, Fitch K, Iwasaki K (2009) Consequences of hepatitis C virus (HCV): costs of a baby boomer epidemic of liver disease. Milliman Inc., New York. This report was commissioned by Vertex Pharmaceuticals, Inc
6. Shatin D, Schech SD, Patel K, McHutchison JG (2004) Population-based hepatitis C surveillance and treatment in a national managed care organization. *Am J Manag Care* 10:250–256
7. Davis GL, Alter MJ, El-Serag H, Poynard T, Jennings LW (2010) Aging of hepatitis C virus (HCV)-infected persons in the United States: a multiple cohort model of HCV prevalence and disease progression. *Gastroenterology* 138:513–521
8. Bartenschlager R, Ahlborn-Laake L, Yasargil K, Mous J, Jacobsen H (1995) Substrate determinants for cleavage in cis and in trans by the hepatitis C virus NS3 proteinase. *J Virol* 69(1):198–205
9. Kwong AD, Kim JL, Rao G, Lipovsek D, Raybuck SA (1999) Hepatitis C virus NS3/4A protease. *Antivir Res* 41:67–84
10. Kim JL, Morgenstern KA, Lin C, Fox T, Dwyer MD, Landro JA, Chambers SP, Markland W, Lepre CA, O’Malley ET, Harbeson SL, Rice CM, Murcko MA, Caron PR, Thomson JA (1996) Crystal structure of the hepatitis C virus NS3 protease domain complexed with a synthetic NS4A cofactor peptide. *Cell* 87:343–355
11. Pasquo A, Nardi MC, Dimasi N, Tomei L, Steinkuhler C, Delmastro P, Tramontano A, De Francesco R (1998) Rational design and functional expression of a constitutively active single-chain NS4A-NS3 proteinase. *Fold Des* 3(6):433–441
12. Taremi SS, Beyer B, Maher M, Yao N, Prosis W, Weber PC, Malcolm BA (1998) Construction, expression, and characterization of a novel fully activated recombinant single-chain hepatitis C virus protease. *Protein Sci* 7(10):2143–2149

13. Yao N, Reichert P, Taremi SS, Prosis WW, Weber PC (1999) Molecular views of the viral polyprotein processing revealed by the crystal structure of the hepatitis C virus bifunctional protease-helicase. *Structure* 7:1353–1363
14. Lin C, Kwong AD, Perni RB (2006) Discovery and development of VX-950, a novel, covalent, and reversible inhibitor of hepatitis C virus NS3.4A serine protease. *Infect Disord Drug Targets* 6(1):3–16
15. Perni RB, Britt SD, Court JJ, Courtney LF, Deininger DD, Farmer LJ, Gates CA, Harbeson SL, Kim JL, Landro JA, Levin RB, Luong YP, O'Malley ET, Pitlik J, Rao BG, Schairer WC, Thomson JA, Tung RD, Van Drie JH, Wei Y (2003) Inhibitors of hepatitis C virus NS3.4A protease 1. Non-charged tetrapeptide variants. *Bioorg Med Chem Lett* 13(22):4059–4063
16. Perni RB, Chandorkar G, Chaturvedi PR, Courtney LF, Decker CJ, Gates CA, Harbeson SL, Kwong AD, Lin C, Luong YP, Markland W, Rao BG, Tung RD, Thomson JA (2003) VX-950: the discovery of an inhibitor of the hepatitis C virus NS3.4A protease and a potential hepatitis C virus therapeutic. *Hepatology* 38:624
17. Perni RB, Chandorkar G, Cottrell KM, Gates CA, Lin C, Lin K, Luong YP, Maxwell JP, Murcko MA, Pitlik J, Rao G, Schairer WC, Van Drie J, Wei Y (2007) Inhibitors of hepatitis C virus NS3.4A protease. Effect of P4 capping groups on inhibitory potency and pharmacokinetics. *Bioorg Med Chem Lett* 17(12):3406–3411
18. Perni RB, Farmer LJ, Cottrell KM, Court JJ, Courtney LF, Deininger DD, Gates CA, Harbeson SL, Kim JL, Lin C, Lin K, Luong Y-P, Maxwell JP, Murcko MA, Pitlik J, Rao BG, Schairer WC, Tung RD, Van Drie JH, Wilson K, Thomson JA (2004) Inhibitors of hepatitis C virus NS3.4A protease 3. P2 proline variants. *Bioorg Med Chem Lett* 14(8):1939–1942
19. Perni RB, Kwong AD (2002) Inhibitors of hepatitis C virus NS3.4A protease: an overdue line of therapy. *Prog Med Chem* 39:215–255
20. Perni RB, Pitlik J, Britt SD, Court JJ, Courtney LF, Deininger DD, Farmer LJ, Gates CA, Harbeson SL, Levin RB, Lin C, Lin K, Moon Y-C, Luong Y-P, O'Malley ET, Rao BG, Thomson JA, Tung RD, Van Drie JH, Wei Y (2004) Inhibitors of hepatitis C virus NS3.4A protease 2. Warhead SAR and optimization. *Bioorg Med Chem Lett* 14(6):1441–1446
21. Landro JA, Raybuck SA, Luong YP, O'Malley ET, Harbeson SL, Morgenstern KA, Rao G, Livingston DJ (1997) Mechanistic role of an NS4A peptide cofactor with the truncated NS3 protease of hepatitis C virus: elucidation of the NS4A stimulatory effect via kinetic analysis and inhibitor mapping. *Biochemistry* 36(31):9340–9348
22. Llinas-Brunet M, Bailey M, Fazal G, Goulet S, Halmos T, Laplante S, Maurice R, Poirier M, Poupart MA, Thibeault D, Wernic D, Lamarre D (1998) Peptide-based inhibitors of the hepatitis C virus serine protease. *Bioorg Med Chem Lett* 8(13):1713–1718
23. Steinkühler C, Biasiol G, Brunetti M, Urbani A, Koch U, Cortese R, Pessi A, De Francesco R (1998) Product inhibition of the hepatitis C virus NS3 protease. *Biochemistry* 37(25):8899–8905
24. Grillot AL, Farmer L, Rao B, Taylor W, Weisberg I, Jacobson I, Perni R, Kwong A (2011) Telaprevir. In: Kakzmierski W (ed) *Antiviral drugs from basic discovery through clinical trials*. Wiley-VCH, Weinheim
25. Perni RB, Almqvist SJ, Byrn RA, Chandorkar G, Chaturvedi PR, Courtney LF, Decker CJ, Dinehart K, Gates CA, Harbeson SL, Heiser A, Kalkeri G, Kolaczowski E, Lin K, Luong YP, Rao BG, Taylor WP, Thomson JA, Tung RD, Wei Y, Kwong AD, Lin C (2006) Preclinical profile of VX-950, a potent, selective, and orally bioavailable inhibitor of hepatitis C virus NS3.4A serine protease. *Antimicrob Agents Chemother* 50(3):899–909
26. Yip Y, Victor F, Lamar J, Johnson R, Wang QM, Barket D, Glass J, Jin L, Liu L, Venable D, Wakulchik M, Xie C, Heinz B, Villarreal E, Colacino J, Yumibe N, Tebbe M, Munroe J, Chen SH (2004) Discovery of a novel bicycloproline P2 bearing peptidyl alpha-ketoamide LY514962 as HCV protease inhibitor. *Bioorg Med Chem Lett* 14(1):251–256
27. Yip Y, Victor F, Lamar J, Johnson R, Wang QM, Glass JI, Yumibe N, Wakulchik M, Munroe J, Chen SH (2004) P4 and P1' optimization of bicycloproline P2 bearing tetrapeptidyl alpha-ketoamides as HCV protease inhibitors. *Bioorg Med Chem Lett* 14(19):5007–5011

28. Lin K, Kwong AD, Lin C (2004) Combination of a hepatitis C virus NS3-NS4A protease inhibitor and alpha interferon synergistically inhibits viral RNA replication and facilitates viral RNA clearance in replicon cells. *Antimicrob Agents Chemother* 48(12):4784–4792
29. Tzantrizos YS, Bolger G, Bonneau P, Cameron DR, Goudreau N, Kukolj G, LaPlante SR, Llinas-Brunet M, Nar H, Lamarre D (2003) Macrocyclic inhibitors of the NS3 protease as potential therapeutic agents of hepatitis C virus infection. *Angew Chem* 42:1355–1360
30. Hinrichsen H, Benhamou Y, Wedemeyer H, Reiser M, Sentjens RE, Calleja JL, Forns X, Erhardt A, Cronlein J, Chaves RL, Yong CL, Nehmiz G, Steinmann GG (2004) Short-term antiviral efficacy of BILN 2061, a hepatitis C virus serine protease inhibitor, in hepatitis C genotype 1 patients. *Gastroenterology* 127(5):1347–1355
31. Lamarre D, Anderson PC, Bailey M, Beaulieu P, Bolger G, Bonneau P, Bos M, Cameron DR, Cartier M, Cordingley MG, Faucher AM, Goudreau N, Kawai SH, Kukolj G, Lagace L, LaPlante SR, Narjes H, Poupart MA, Rancourt J, Sentjens RE, George RS, Simoneau B, Steinmann G, Thibeault D, Tzantrizos YS, Weldon SM, Yong CL, Llinas-Brunet M (2003) An NS3 protease inhibitor with antiviral effects in humans infected with hepatitis C virus. *Nature* 426(6963):186–189
32. Lin K, Perni RB, Kwong AD, Lin C (2006) VX-950, a novel hepatitis C virus (HCV) NS3-4A protease inhibitor, exhibits potent antiviral activities in HCV replicon cells. *Antimicrob Agents Chemother* 50(5):1813–1822
33. Vertex Pharmaceuticals Incorporated (2004) Vertex Pharmaceuticals and Mitsubishi Pharma sign agreement for development and commercialization of the oral HCV protease inhibitor VX-950 in Japan and Far East Countries
34. Kwong A, Kauffman R, Hurter P, Mueller P (2011) Discovery and development of telaprevir: an NS3-4a protease inhibitor for treating genotype 1 chronic hepatitis C virus. *Nat Biotechnol* 29(w11):993–1003
35. Reesink HW, Zeuzem S, Weegink CJ, Forestier N, van Vliet A, van de Wetering de Rooij J, McNair L, Purdy S, Kauffman R, Alam J, Jansen PL (2006) Rapid decline of viral RNA in hepatitis C patients treated with VX-950: a phase Ib, placebo-controlled, randomized study. *Gastroenterology* 131(4):997–1002
36. McHutchison JG, Everson GT, Gordon SC, Jacobson I, Kauffman R, McNair L, Muir A (2008) PROVE1: results from a phase 2 study of telaprevir with peginterferon alfa-2a and ribavirin in treatment-naive subjects with hepatitis C. In: Proceedings of 43rd annual meeting of the European Society for the Study of the Liver (EASL), Milan, Italy, *Journal of Hepatology*
37. Hezode C, Forestier N, Dusheiko G, Ferenci P, Pol S, Goeser T, Bronowicki JP, Bourliere M, Gharakhanian S, Bengtsson L, McNair L, George S, Kieffer T, Kwong A, Kauffman RS, Alam J, Pawlotsky JM, Zeuzem S (2009) Telaprevir and peginterferon with or without ribavirin for chronic HCV infection. *N Engl J Med* 360(18):1839–1850
38. McHutchison J, Manns M, Muir A, Terrault N, Jacobson IM et al (2010) Telaprevir for previously treated chronic HCV infection. *N Engl J Med* 362:1292–1303 [Erratum in: *N Engl J Med*. 2010, 1362:1647]
39. McHutchison J, Manns M, Muir A et al (2010) Retreatment with telaprevir, peginterferon, and ribavirin for chronic HCV infection. *N Engl J Med* 362(14):30–41
40. Jacobson IM, McHutchison JG, Dusheiko G, Di Bisceglie AM, Reddy KR, Bzowej NH, Marcellin P, Muir AJ, Ferenci P, Flisiak R, George J, Rizzetto M, Shouval D, Sola R, Terg RA, Yoshida EM, Adda N, Bengtsson L, Sankoh AJ, Kieffer TL, George S, Kauffman RS, Zeuzem S (2011) Telaprevir for previously untreated chronic hepatitis C virus infection. *N Engl J Med* 364:2405–2516
41. Sherman KE, Flamm SL, Afdhal NH, Nelson DR, Sulkowski MS, Everson GT, Fried MW, Adler M, Reesink HW, Martin M, Sankoh AJ, Adda N, Kauffman RS, George S, Wright CI, Poordad F (2011) Response-guided telaprevir combination treatment for hepatitis C virus infection. *N Engl J Med* 365(11):1014–1024
42. Zeuzem S, Andreone P, Pol S, Lawitz E, Diago M, Roberts S, Focaccia R, Younossi Z, Foster G, Horban A, Ferenci P, Nevens F, Müllhaupt B, Pockros P, Terg R, Shouval D,

- van Hoek B, Weiland O, Heeswijk R, De Meyer S, Luo D, Boogaerts G, Polo R, Picchio P, Beumont M, REALIZE Study Team (2011) Telaprevir for retreatment of HCV infection. *N Engl J Med* 364:2417–2428
43. Vertex Pharmaceuticals Incorporated (2011) INCIVEK [US product insert] vertex website. Vertex Pharmaceuticals Incorporated, Cambridge
 44. Kieffer T, Kwong A, Picchio G (2009) Viral resistance to specifically targeted antiviral therapies for hepatitis C (STAT-Cs). *J Antimicrob Chemother* 65:202–212
 45. Kieffer TL, Sarrazin C, Miller JS, Welker MW, Forestier N, Reesink HW, Kwong AD, Zeuzem S (2007) Telaprevir and pegylated interferon-alpha-2a inhibit wild-type and resistant genotype 1 hepatitis C virus replication in patients. *Hepatology* 46(3):631–639
 46. Sarrazin C, Kieffer TL, Bartels D, Hanzelka B, Muh U, Welker M, Wincheringer D, Zhou Y, Chu HM, Lin C, Weegink C, Reesink H, Zeuzem S, Kwong AD (2007) Dynamic hepatitis C virus genotypic and phenotypic changes in patients treated with the protease inhibitor telaprevir. *Gastroenterology* 132(5):1767–1777
 47. Butt AA, Kanwal F (2012) Boceprevir and telaprevir in the management of hepatitis C virus-infected patients. *Clin Infect Dis* 54(1):96–104
 48. FDA (2011) INCIVEK (telaprevir) highlights of prescribing information. FDA. [accessdata.fda.gov](https://www.accessdata.fda.gov)
 49. FDA (2011) VICTRELIS (boceprevir) highlights of prescribing information. [accessdata.fda.gov](https://www.accessdata.fda.gov)
 50. Hutchison C, Kwong A, Ray S, Struble K, Swan T, Miller V (2014) Accelerating drug development through collaboration: the hepatitis C drug development advisory group. *Clin Pharmacol Ther* 96(2):162–165
 51. Smith B, Morgan R, Beckett G, Falck-Ytter Y, Holtzman D, Teo C-G, Jewett A, Baack B, Rein D, Patel N, Alter M, Yartel A, Ward J (2012) Recommendations for the identification of chronic hepatitis C virus infection among persons born during 1945–1965. *MMWR Recomm Rep* 61(RR04):1–18
 52. USPSTF (2013) Hepatitis C: screening, published final recommendations. USPSTF, Rockville
 53. Moorman AC, Rupp LB, Gordon SC, Zhong Y, Xing J, Lu M, Boscarino JA, Schmidt MA, Daida YG, Teshale EH, Spradling PR, Holmberg SD, Investigators CH (2018) Long-term liver disease, treatment, and mortality outcomes among 17,000 persons diagnosed with chronic hepatitis C virus infection: current chronic hepatitis cohort study status and review of findings. *Infect Dis Clin N Am* 32(2):253–268
 54. CDC (2015) Know more hepatitis. V. H. Division of Viral Hepatitis and National Center for HIV/AIDS, STD, and TB Prevention
 55. Valeii K (2017) Why are baby boomers more prone to Hep C? Connection, risk factors, and more
 56. Merck Sharp & Dohme Corp (2011) Merck and Roche expand agreement in fight against chronic hepatitis C. <https://www.merck.com/licensing/our-partnership/Roche-expandagree-partnership.html>
 57. Weissman R (2014) Vertex to stop selling hepatitis C drug Incivek. *Boston Globe*, Boston <https://www.bostonglobe.com/business/2014/08/12/vertex-stop-selling-hepatitis-drug-incivek/EI0jtOpH9H1CaIqQpSUKWO/story.html>
 58. Unitaid (2018) HCV diagnostics market intelligence report 2017 first report on screening and diagnosis market growth. https://www.finddx.org/wp-content/uploads/2018/04/HCV-Diagnostics-Market-Intelligence-Report_18APR2018.pdf
 59. Bartenschlager R, Baumert TF, Bukh J, Houghton M, Lemon SM, Lindenbach BD, Lohmann V, Moradpour D, Pietschmann T, Rice CM, Thimme R, Wakita T (2018) Critical challenges and emerging opportunities in hepatitis C virus research in an era of potent antiviral therapy: considerations for scientists and funding agencies. *Virus Res* 248:53–62

Discovery of Boceprevir, a Ketoamide-Derived HCV NS3 Protease Inhibitor, for Treatment of Genotype 1 Infections



Srikanth Venkatraman

Contents

1 Introduction	294
2 Conclusion	311
References	313

Abstract Blood-borne hepatitis C infections are the primary cause for liver cirrhosis and hepatocellular carcinoma. Prior to the discovery of direct-acting antiviral agents, the only treatment option was a regimen of interferon and ribavirin. It was modestly effective with only ~40% of genotype 1 patients demonstrating sustained virologic response. It was also accompanied with severe side effects with flu-like symptoms and increased suicidal tendencies during treatment. Advances in understanding the life cycle of the virus identified many potential novel drug targets that could be inhibited with small-molecule inhibitors. HCV NS3 protease, a serine enzyme, was identified as an important target for development of inhibitors because it was involved in processing of HCV-encoded polypeptide at multiple sites. The team resorted to a structure-based design because high-throughput screening with multiple compound libraries did not result in any starting point for SAR optimization. Introduction of electrophilic traps to natural substrate of the enzyme identified a ketoamide-derived undecapeptide lead. It was optimized to identify the first ketoamide-derived direct-acting antiviral agent for the treatment of HCV gt-1 infections approved by FDA. The following chapter describes the discovery of the undecapeptide lead and optimization of the scaffold to discover boceprevir for the treatment of HCV gt-1 infections.

Keywords Boceprevir, Cirrhosis, Electrophilic trap, HCV, HCV protease, Hepatitis C, Hepatocellular carcinoma, Ketoamide, NS3 protease, Replicon, Serine protease, Undecapeptide lead, Victrelis

S. Venkatraman (✉)
Disc Medicine, Cambridge, MA, USA
e-mail: vxsrkanth@gmail.com

1 Introduction

Hepatitis C virus infections are the leading causes of liver cirrhosis and hepatocellular carcinoma [1]. More than 80% of HCV infections turn chronic being the primary causes for liver transplantation. Prior to the discovery of direct-acting antiviral agents, the primary treatment option for HCV infections was a regimen of interferon for 52 weeks in combination with ribavirin [2, 3]. Treatment with interferon and ribavirin was suboptimal and plagued with serious adverse effects. The treatment was very poorly tolerated with many patients having serious side effects such as neutropenia, flu-like symptoms, and suicidal tendencies. The efficacy of Peg-interferon was also suboptimal with less than 40% of genotype 1 patients demonstrating sustained virologic response (SVR) or cure. The cure rates in genotypes 2 and 3 were significantly improved with SVRs reaching as high as 80%. The poor tolerability of interferon led to compliance issues with significant number of patients discontinuing therapy. With more than 200 million people infected worldwide, it was a health epidemic and clear that novel and improved treatments were required to treat hepatitis C infections. Even though efficient blood screening has reduced many new infection, most newer infections were primarily caused by sharing infected needles and blood products.

There are six major genotypes (gt 1–6) with multiple subtypes and quasi species. The rapid mutation of the virus results in a pool that is highly heterogenous with multiple variants. The discovery and characterization of the virus in 1983 [4, 5] led to the understanding of the life cycle of the virus resulting in the identification of many potential novel targets for drug development. The lessons learned from success of developing antiviral agents against HIV could be applied to these new targets to develop novel direct-acting agents that interfere with the synthesis of key proteins required for survival and replication of HCV. This strategy has been greatly productive with development of many drugs revolutionizing the treatment of the disease. Cure rates with greater than 99% have made HCV a highly manageable disease which can be readily cured for all genotypes. The following chapter describes the identification of Victrelis (boceprevir), the first direct-acting HCV antiviral approved for the treatment of HCV genotype 1 infections.

Hepatitis C virus is a single positive strand RNA virus of ~9,000 kb belonging to *Flaviviridae* family that primarily infects hepatocytes. The virus attaches to the cell and undergoes endocytosis, followed by uncoating to release the (+) strand RNA into the cell. The viral RNA utilizes the host cell machinery to form a (–) strand RNA and further multiply. This codes for a single polypeptide chain of ~3,000 amino acids that contain all the structural and functional proteins required for replication of the virus (Fig. 1) [6]. These encoded proteins facilitate the synthesis of new viral particles resulting in slow progression to liver cirrhosis and hepatocellular carcinoma.

The single polypeptide encoded by the virus contains all the structural proteins such as core and envelop proteins and nonstructural proteins essential for viral replication and survival. Key among them are nonstructural proteins 2, 3, 4A, 4B,

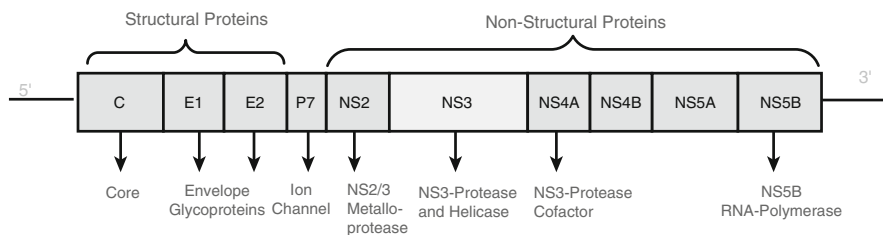


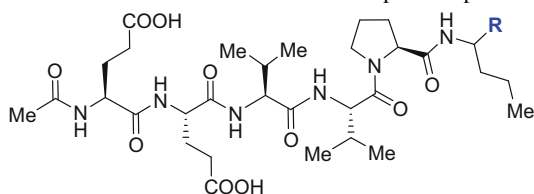
Fig. 1 Genome of HCV NS3 protease

5A, and 5B. Nonstructural protein 3 (NS3), a serine protease, plays a vital role in the posttranslational processing of the polypeptide to enable the replication of virus [7]. The encoded protein initially undergoes an autocatalytic cleavage at the NS2-NS3 site which is followed by a *trans* cleavage at NS3-NS4A, NS4A-NS4B, NS4B-NS5A, and NS5A-NS5B junctions catalyzed by NS3 protease to generate functionally active enzyme required for viral replication. This central role played by NS3 protease made it the primary target attractive for developing small-molecule inhibitors to target HCV. Coupled with success in targeting HIV proteases and polymerases, the primary focus for drug development was on HCV NS3 protease and NS5B polymerase.

HCV NS3, a serine protease, has a shallow active site located on the surface of the enzyme [8–10]. The X-ray structure of the enzyme shows a chymotrypsin-like fold with the catalytic site located between two β -barrels. The natural substrate of the enzyme makes a series of hydrogen bonds with the protease to make its interaction specific. The natural substrate contains a P1 cysteine residue [11, 12]. Cis-cleavage events have a threonine residue at P1, whereas the trans cleavage events have cysteine as the P1 residue. The natural substrate of the enzyme contains polar residues at P5 and P6 such as aspartic and glutamic acids and hydrophobic groups such as valine, proline, and cysteine at P3, P2, and P1 positions. NS4A, a 54-amino acid cofactor, is essential for the enzymatic activity, and in the absence of it, the activity is greatly diminished.

Just as any traditional medicinal chemistry program, the discovery program of HCV NS3 protease was initiated with high-throughput screening. Many compound libraries and directed synthetic libraries were screened to only discover not even a single compound could be found as a suitable starting compound that inhibited the enzyme at a micromolar concentration. We therefore decided to use structure-based drug discovery and the natural substrate as the starting point. To facilitate better binding of the ligands, we evaluated the introduction of various electrophilic traps to the peptide sequence. An undecapeptide derivative containing various electrophilic traps such as ketoamides, boronic acids, difluoro ketones, and acyl-thiazoles was synthesized and evaluated for the inhibition of the enzyme [13] (Table 1).

Introduction of electrophilic traps had only moderate effect on activity. The introduction of a ketothiazole moiety resulted in analog **1** ($K_i^* = 2.0 \mu\text{M}$) which was similar to the triketone analog **2** ($K_i^* = 1.3 \mu\text{M}$) and difluoroketone derivative

Table 1 Effect of introduction of electrophilic traps on inhibition of NS3 protease

Compound	R	K_i^* (μM)
1		2.0
2		1.3
3		1.9
4		>2.0
5		0.92

3 ($K_i^* = 1.9 \mu\text{M}$). Introduction of a boronic acid resulted in modest improvement with analog **5** ($K_i^* = 0.92 \mu\text{M}$) demonstrating a twofold improvement in activity compared to ketothiazole analog **1**. However, introduction of a ketoamide into the inhibitor that spanned from P6 to P5 had a profound improvement in potency with the ketoamide derivative **6** demonstrating a much-improved enzyme activity ($K_i^* = 1.9 \text{ nM}$, Fig. 2).

A quick analysis of the lead **6** clearly showed that it had none of the desired drug-like properties. It was peptidic and had a high molecular weight of 1,265 which made it unfavorable for oral absorption. Moreover, the compound contained primarily natural amino acids, and it would be metabolically unstable probably resulting in rapid hydrolysis in plasma. We chose human neutrophil elastase (HNE) as a comparator for selectivity because HNE shared significant similarities with the HCV protease. The HNE/HCV selectivity was low and needed significant improvement. Nevertheless, it was the only lead that inhibited the enzyme in desirable nM region. We therefore decided to optimize this molecule.

Our initial approach to optimization was to remove undesired functional groups and reduce the molecular weight. A conscious decision was made to remove acidic

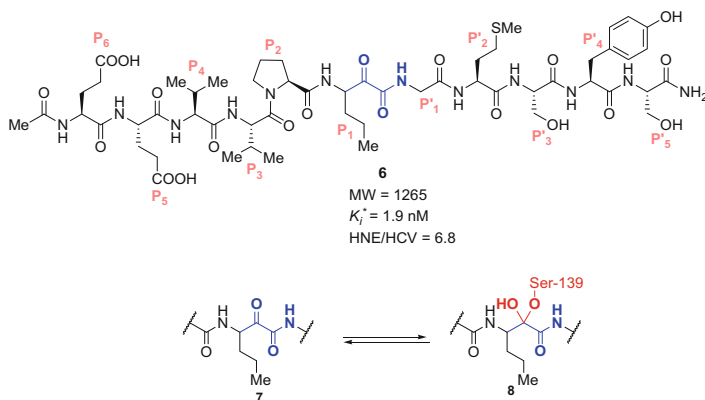
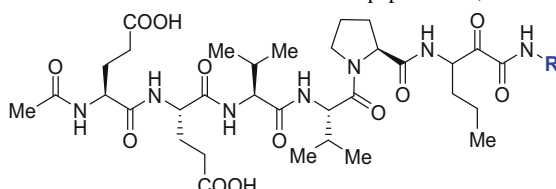


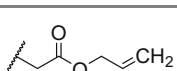
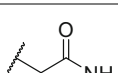
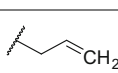
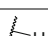
Fig. 2 Undeca-peptide ketoamide lead of HCV NS3 protease

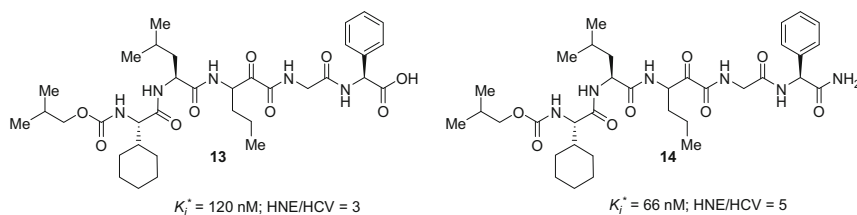
groups at the P6 and P5 positions. We capped our molecules at the P3 amino acid where the P3 capping group served as the P4 residue and occupied the S4 pocket. To further improve stability, we systematically modified various amino acids to incorporate non-proteinogenic amino acids that could potentially impart stability to serum proteases. Table 2 describes our efforts in truncation at the P1' position.

Truncation of **6** at the P1' site was well tolerated. The removal of P1'–P5' resulted in loss in potency; however, it did not result in analogs that were inactive. Replacement of the P1'–P5' segment with glycine allyl ester resulted in compound **9** with ($K_i^* = 57$ nM), a 28-fold loss in activity compared to **6**. Replacement with a glycine primary amide resulted in inhibitor **10** with potency of $K_i^* = 43$ nM. Direct truncation at P1 was also tolerated with ketoamide allyl ester **11** demonstrating a potency of $K_i^* = 270$ nM, clearly suggesting that a compound spanning from P6 to P1 had acceptable potency. However, directly capping inhibitor **6** at P1 resulted in 400-fold loss with analog **12** showing a potency of $K_i^* = 760$ nM. The lesson from these early truncation studies showed that the compounds could be readily truncated without complete loss in potency. Our next investigation was directed toward truncating the compound at P3 position. This investigation identified P3 cyclohexyl glycine as a potential replacement for valine which improved potency. Amino acid replacement studies also identified P2 isoleucine as a replacement for proline that improved activity (Fig. 3).

Analog **13** spanning from P3 to P2' containing P3 cyclohexylglycine and P2 isoleucine demonstrated a binding of $K_i^* = 120$ nM and HNE/HCV selectivity of 3. Replacement of P2' phenyl glycine acid with phenyl glycine amide showed a twofold improvement with analog **14** demonstrating a $K_i^* = 66$ nM and similar activity as **13**. Even though these compounds had significantly reduced activity compared to the lead **6**, they were neutral molecules with lower molecular weights and contained non-proteinogenic amino acids that made them potentially metabolically more stable. We therefore decided to further investigate these compounds for SAR analysis. Analysis of X-ray co-crystal structures with the NS3 protease of one

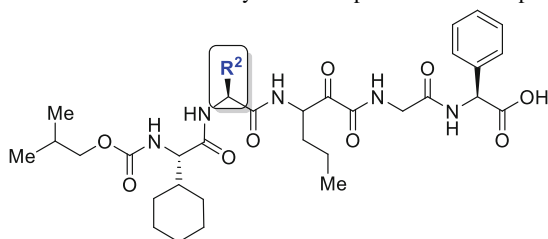
Table 2 Effect of truncation of undecapeptide lead, SAR at P1' site


Compound	R	K_i^* (nM)
9		57
10		43
11		270
12		760

**Fig. 3** Effect of truncation at P3 positions

of the leucine derivatives revealed the leucine methyl groups made key lipophilic interactions with alanine-156, an interaction that would be significantly exploited in the future designs. Our next SAR investigation focused on modifying the P2 residue.

Replacement of P2 isoleucine in **13** with five- and six-membered acetals resulted in a loss in potency compared to the parent leucine derivative (Table 3). The five-membered thioacetal derivative **15** had a $K_i^* = 90$ nM similar to leucine derivative **13**, whereas the six-membered derivative **16** had a threefold loss in potency. Similarly, the introduction of five- and six-membered acetals resulted in analogs **17** ($K_i^* = 300$ nM) and **18** ($K_i^* = 430$ nM) with a three- to fourfold loss in activity. Failing to introduce polar residues at P2, we next introduced nonpolar residues such as pentyl glycine, cyclobutyl alanine, and cyclopropyl alanine. The introduction of pentylglycine resulted in a threefold loss in activity with analog **19** having a $K_i^* = 300$ nM. The cyclobutyl alanine analog **21** had a similar potency ($K_i^* = 140$ nM) to the isoleucine derivative, and the cyclopropyl analog resulted in compound **20** with a $K_i^* = 50$ nM, a twofold improved potency compared to analog **13**.

Table 3 Structure-activity relationship on P2 leucine replacements

Compound	R ²	K _i [*] (nM)
15		90
16		250
17		300
18		430
19	C ₄ H ₉ 	300
20		50
21		140

Based on the improved activity of **20**, we further modified the compound changing the P1 residue. Replacement of P1 norvaline in **20** with cyclopropyl alanine had a profound effect on potency. This replacement resulted in compound **22** with $K_i^* = 15$ nM resulting in a threefold improvement compared to norvaline analog **20**. Excited by the improved activity of this analog, we further decided to evaluate the compound in a cellular assay [14]. The cellular activity was disappointing with the compound showing an $EC_{90} > 5$ μ M (Fig. 4). We attributed the poor cellular potency to the polar nature of the molecule mostly contributed by the carboxylic acid and the number of hydrogen bond donors and acceptors.

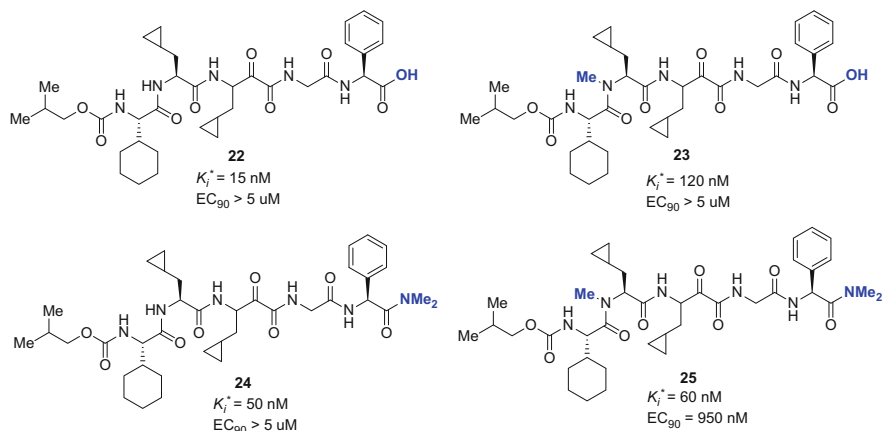


Fig. 4 Effect on functionalizing P2 nitrogen and P2' carboxylic acid on cellular activity

In an attempt to reduce the polarity of analogs of type **22**, we explored modification of the carboxylic acid at P2' to amides and reduction of the number of hydrogen bond donors. We systematically blocked each nitrogen with a methyl group. This SAR had a dramatic effect on the cellular potency (Fig. 4). Introduction of a dimethyl amide at the P2 phenyl glycine resulted in analog **24** with a modest loss in activity ($K_i^* = 50 \text{ nM}$); however, its cellular activity did not improve and still had a $EC_{90} > 5 \text{ }\mu\text{M}$. Similarly, introduction of a methyl group at the P2 amide nitrogen resulted in analog **23** with a sevenfold loss in potency ($K_i^* = 120 \text{ nM}$) and a cellular $EC_{90} > 5 \text{ }\mu\text{M}$. However, the introduction of both a methyl group and an amide at P2' together had a positive effect on the potency and cellular activity. The resultant analog **25** had a potency of $K_i^* = 60 \text{ nM}$ and a sub-micromolar cellular activity ($EC_{90} = 950 \text{ nM}$). This was the first compound to demonstrate a cellular potency below one micromolar.

It was clear from the SAR described in Fig. 4 that for compounds to demonstrate cellular potency, both the P2 nitrogen and the P2' carboxylic acid must be masked. This ensures permeability of compounds into cells. It was immediately clear looking at structures of type **25** that cyclization of the *N*-methyl group to the P2 cyclopropyl alanine would result in analogs derived from prolines. We therefore decided to synthesize and evaluate analogs derived from proline derivatives. Figure 5 summarizes these efforts and the SAR around proline derivatives.

The introduction of 4-*tert*-butoxy proline at P2 resulted in analog **26** with a $K_i^* = 19 \text{ nM}$ and having cellular activity with an $EC_{90} = 2 \text{ }\mu\text{M}$. It was selective against HNE with a HNE/HCV selectivity = 161. Cyclization of *tert*-butyl group onto the proline resulted in the five-membered fused proline derivative **27** with $K_i^* = 5 \text{ nM}$ and $EC_{90} = 400 \text{ nM}$, a fourfold improvement in potency and cellular activity compared to the 4-*tert*-butoxy analog **26**. With the observation that cyclization had a positive effect on potency, we designed compound **28** which was a hybrid of **25** and **27**. The dimethyl cyclopropyl-fused proline [15] analog with norvaline at P1

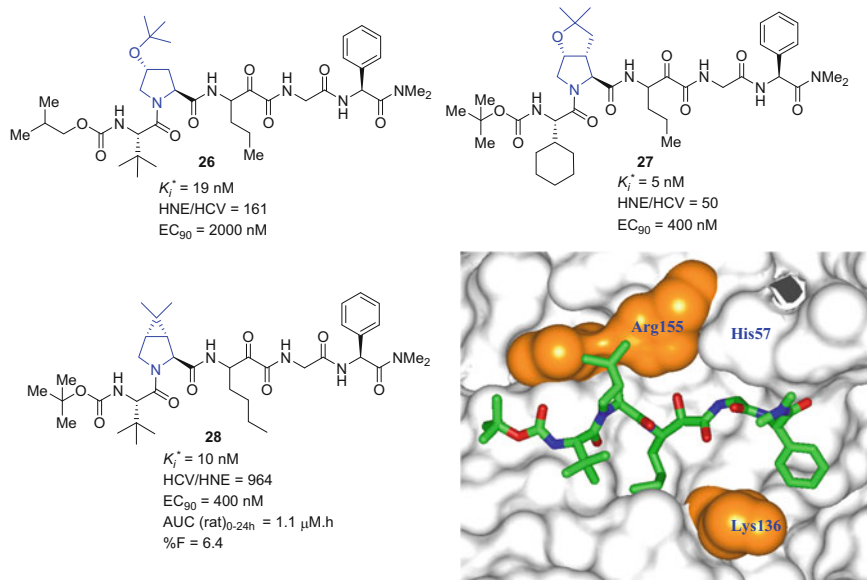


Fig. 5 Structure-activity relationship of cyclic P2 residues

demonstrated improved potency and selectivity with **28** demonstrating a $K_i^* = 10 \text{ nM}$ and a cellular $EC_{90} = 400 \text{ nM}$. It was also very reassuring to see that the HNE/HCV selectivity of **28** was much improved with HNE/HCV selectivity = 964 [16]. Having accomplished acceptable binding and selectivity, we decided to evaluate these analogs for PK in rats. Oral PK of compound **28** in rats showed it was poorly absorbed with an $AUC = 1.1 \text{ } \mu\text{M}\cdot\text{h}$ when dosed at 10 mpk and a low bioavailability. It was clear the low bioavailability was a result of poor absorption, and we decided to design future analogs with lower molecular weights and reduced number of hydrogen bond donors and acceptors.

X-ray crystal structure of **28** with HCV NS3 protease revealed key interactions that resulted in improved binding. It was clear that one of the methyl groups of the P2 proline residue made a key interaction with Arg-155 and the other made key lipophilic interaction with the methyl group of Ala-156. The P1'-P2' glycine-phenylglycine segment made a "C-clamp" conformation which overlaid on the alkyl chain of Lys-136 locking the lysine in position. Having discovered a novel P2 group which improved binding and cellular activity, we next decided to address the PK issue by reducing molecular weights and the number of amide bonds. We once again decided to truncate our molecule at P1' and P1 ketoamide group. The truncation results are summarized in Fig. 6.

Replacement of the P2 phenylglycine amide with a (*S*)-methylbenzyl amide resulted in compound **29** with $K_i^* = 55 \text{ nM}$. Evaluation of oral PK of the compound resulted in much improved exposure in a rapid rat assay [17] with an $AUC_{0-6 \text{ h}} = 2.66 \text{ } \mu\text{M}\cdot\text{h}$. It was very reassuring to note that removal of a

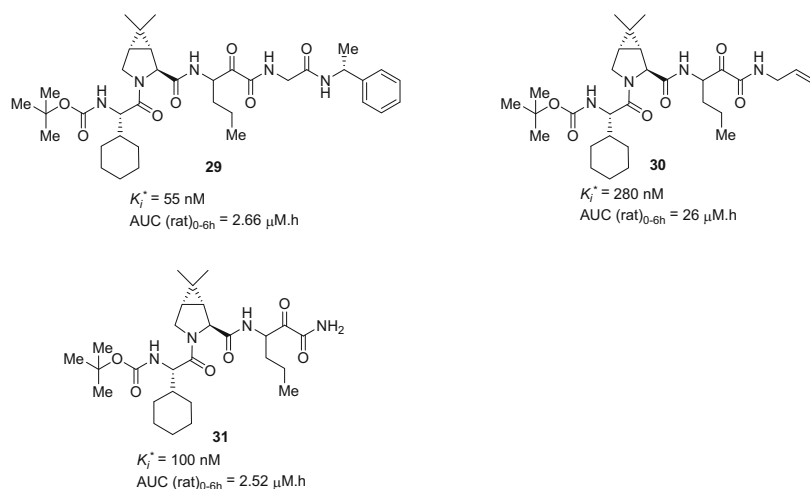
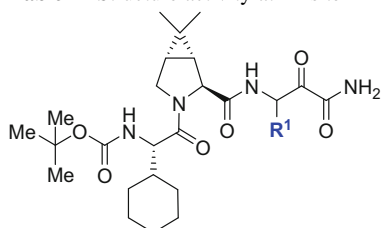


Fig. 6 Structure-activity relation at P2'. Effect on oral pharmacokinetics

single amide bond from **28** had significant improvement in oral absorption. More profound improvement in oral PK was observed when the P1'-P2' glycine-phenylglycine segment was removed and replaced with an allyl amide. Allyl amide analog **30** had a significantly reduced molecular weight compared to **28** but markedly improved oral exposure with an $\text{AUC}_{0-6 \text{ h}} = 26 \text{ }\mu\text{M h}$, when dosed at 10 mpk. However, the compound lost significant potency compared to compound **28** with $K_i^* = 280 \text{ nM}$. The primary ketoamide analog **31** ($K_i^* = 100 \text{ nM}$) had threefold improved activity compared to **30** and an exposure in rat with an $\text{AUC}_{0-6 \text{ h}} = 2.52 \text{ }\mu\text{M h}$. Thought not very surprising, from this exercise, it was clear that reducing the number of amide bonds and the molecular weight had a profound effect on oral absorption. We therefore decided to limit the molecular weight and truncate our compound at the P1 position. We decided to improve the potency of analogs of types **30** and **31** by improving the binding efficiency of the side chains. We also reasoned that the reduced molecular weight would have a positive effect on cellular activity by improving permeability of the resultant inhibitors.

We decided to do a systematic SAR evaluation of the various groups in **31** to improve the potency of the compound. Replacement of P1 norvaline with small alkyl groups was first investigated. The effect of these modifications is outlined in the Table 4. Replacement of P1 norvaline with a one carbon shorter derivative resulted in aminobutyric acid analog **32** with a sevenfold loss in activity. Extension of P1 group to form a butenylglycine derivative resulted in analog **33** with similar potency to **31** ($K_i^* = 150 \text{ nM}$). We next evaluated the effect of branching substitution at P1. Introduction of an isobutyl group was not tolerated with the resulting analog **34** ($K_i^* = 400 \text{ nM}$) losing potency by fourfold compared to **31**. Despite this there was a modest increase in selectivity with **34** showing a HNE/HCV selectivity of 9 compared to **31** which had a selectivity ratio of 3. Analysis of the co-crystal

Table 4 Structure activity at P1 site

Compound	R ¹	K _i [*] (nM)	HNE/HCV	EC ₉₀ (nM)
31		100	3	NA
32		740	NA	NA
33		150	2	NA
34		400	9	NA
35		25	23	400
36		8	138	700
37		150	370	NA
38		>12,000	NA	NA

Effect on potency, selectivity, and cellular activity

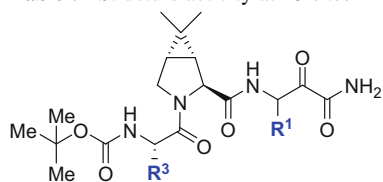
X-ray structure of the analogs suggested that the S1 pocket was narrow and the isobutyl group possibly was too big. We therefore decided to evaluate small cyclic moieties such as methyl cyclopropyl and methyl cyclobutyl groups. Incorporation of cyclopropyl methyl moiety had a beneficial effect on the potency with corresponding analog **35** demonstrating a fourfold improved activity and significantly improved

HNE/HCV selectivity. Thus, the cyclopropyl analog **35** had a $K_i^* = 25$ nM with an HNE/HCV selectivity of 23. It also showed improved cellular activity with an $EC_{90} = 400$ nM. Encouraged by this result, we expanded the ring to give the cyclobutyl analog which was also well tolerated, further improving the potency and selectivity. Thus, the cyclobutyl analog **36** had a potency of $K_i^* = 8$ nM and HNE/HCV = 138. It was less potent in the cellular assay compared to the cyclopropyl analog with an $EC_{90} = 700$ nM. Further expansion of the ring was not well tolerated and resulted in a loss in potency, with the cyclopentyl derivative **37** and cyclohexyl derivative **38** showing diminished potency clearly indicating that the cyclobutyl and cyclopropyl groups were optimal.

Having established cyclobutyl and cyclopropyl groups as desired P1 residues, we next evaluated the effect of modification of P3 moieties. These modifications are shown in Table 5. The introduction of valine in the place of P3 cyclohexyl glycine in **35** resulted in a significant loss in potency with the analog **39** showing a $K_i^* = 210$ nM and HNE/HCV selectivity 19. This was an eightfold loss in activity compared to compound **35**. The substitution of the six-membered cyclohexylglycine with the five-membered cyclopentylglycine resulted in compound **40** which demonstrated a fourfold loss in activity ($K_i^* = 100$ nM). The replacement of P3 with indanylglycine resulted in similar activity to the cyclopentyl analog suggesting that the fused phenyl ring in indanyl glycine made no contact with the enzyme. The P1 cyclopropyl analog **41** was threefold less active compared to cyclohexyl analog, whereas the cyclobutyl analog resulted in greater than 20-fold loss in potency. The introduction of *tert*-butylglycine at P3 resulted in analogs **43** ($K_i^* = 57$ nM; HNE/HCV = 112) and **44** ($K_i^* = 76$ nM; HNE/HCV = 684), a loss in activity compared to their corresponding P3 cyclohexyl derivative. However, it was interesting to note that the HNE/HCV ratio was much improved. The cellular potencies of these analogs were similar to the cyclohexyl derivative. Constraining the methyl groups of P3 *tert*-butylglycine into a methyl cyclopropyl group reduced potency significantly as shown with analogs **45** and **46** ($K_i^* = 300$ – 700 nM). Attempts to incorporate polarity at P3 were also not very well tolerated. The *tert*-hydroxy derivative **47** demonstrated lower activity reaffirming out previous analysis that this pocket was mostly hydrophobic.

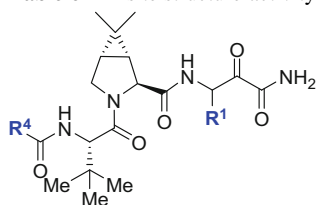
It was clear from the SAR at the P3 site that the cyclohexyl and *tert*-butyl groups were the most preferred residues. The *tert*-butyl group though produced a lower potency compared to the cyclohexyl moiety, and it was more selective against human neutrophil elastase. However, they were similar in activity in the replicon-based cellular assays. Therefore, we chose these P3 groups to further investigate SAR at the P4 site. We decided to vary the P4 site with various carbamates and ureas to see the effect of these variations on the enzyme activity (Table 6).

Replacement of P4 Boc carbamate in **35** ($K_i^* = 25$ nM) with isopropyl carbamate resulted in significant loss in activity with the resulting analog **48** having $K_i^* = 150$ nM. Neither was replacement of the *tert*-butyl carbamate with a cyclopropyl carbamate well tolerated resulting in further loss in potency showing a $K_i^* = 300$ nM, a 12-fold loss in activity compared to the Boc derivative **35**. The isobutyl carbamate substitution was tolerated with the resulting analog **50** demonstrating a $K_i^* = 70$ nM and a HNE/HCV selectivity = 160. The introduction of a

Table 5 Structure activity at P3 sites

Compound	R ³	R ¹	K _i [*] (nM)	HNE/HCV	EC ₉₀ (nM)
39			210	19	NA
40			100	11	NA
41			82	49	>1,000
42			470	NA	2000
43			57	112	600
44			76	684	800
45			300	NA	NA
46			700	NA	NA
47			220	55	NA

Effect on potency and selectivity

Table 6 P4 site structure-activity relationship

Compound	R ⁴	R ¹	K _i [*] (nM)	HNE/HCV	EC ₉₀ (nM)
48			150	100	NA
49			300	NA	NA
50			70	160	NA
51			16	4,200	700
52			13	369	400
53			14	2,200	350

Effect of P3 capping groups on selectivity

urea had a profound effect on potency and selectivity. The introduction of isopropyl urea with P1 cyclobutyl alanine resulted in analog **51** showing improvement both in potency ($K_i^* = 16$ nM) and selectivity HNE/HCV = 4,200. It was also active in the cellular assay with the EC₉₀ = 700 nM. The replacement of Boc with *tert*-butyl urea was also well tolerated with the corresponding P1 cyclopropyl alanine derivative (**53**) showing a $K_i^* = 13$ nM and HNE/HCV selectivity = 369. The cyclobutyl analog was equipotent with a $K_i^* = 14$ nM and HNE/HCV selectivity 2,200. It was very reassuring to see that the cyclobutyl analog was potent, had a good HNE/HCV selectivity, and was also active in the cellular assay with an EC₉₀ = 350 nM. Having identified a selective and potent compound analog **53**, it was further profiled in PK [18, 19].

Analog **53** with acceptable enzyme activity and selectivity was further evaluated in rat and dog PK [20]. The exposure and PK parameters are summarized in Table 7.

Table 7 PK properties of compound **53**

Parameter (units)	Rat	Dog	Monkey
Number of individual (N)	3	3	3
Dose (mg/kg)	10	3	3
AUC _{0–24 h} (μM h)	1.52	3.2	0.12
Bioavailability (%)	26	30	4
Mean residence time (h)	2.1	1.2	2.2
Mean absorption time (h)	1.4	0.5	1.4
Oral C _{max} (μM)	0.65	2.27	0.09
T _{max} (h)	0.9	0.4	0.33
Fraction of oral absorption (%)	37	31	12

Dosing rats orally with 10 mpk of compound **53** in 0.4% methyl cellulose resulted in an AUC = 1.52 μM h with acceptable oral bioavailability of 26%. It had a high clearance and moderate half-life of 4.2 h. The compound had similar absorption and bioavailability in dogs with an oral AUC = 3.1 μM h when dosed at 3 mpk with a bioavailability of 30%. The half-life in dogs was shorter with $t_{1/2}$ = 1.1 h. The compound had a poor absorption and rapid clearance in monkeys with analog **53** demonstrating variable oral bioavailability of 4–11%. We attributed this poor PK to higher CYP activity and rapid metabolism in monkeys. Administration of **53** in mouse also demonstrated acceptable pharmacokinetics with a bioavailability of 30% and half-life of 1.7 h. Based on the overall profile of **53**, we decided to progress the compound further to evaluate the proof of concept in humans. Compound **53** became known as boceprevir.

Boceprevir exists as a mixture of isomers at P1 ketoamide center. It rapidly isomerizes to a ratio of ~2:1 in plasma. Separation of the individual isomers (**54** and **55**, Fig. 7) and incubation in plasma resulted in rapid equilibrium back to a *S,R* mixture. We therefore decided to develop the compound as a mixture of diastereomers. In addition to the rapid equilibration, the ketoamide group was readily hydrated in aqueous medium. The two hydrated forms **56** and **57** rapidly reverted back to ketoamide on drying. This dynamic equilibrium of various forms of boceprevir posed many challenges for development. Many attempts to crystallize the mixture for purification did not result in success. It was therefore developed as an amorphous mixture which made the commercial purification and storage a considerable challenge. The ready hydration of boceprevir, though it posed a significant developmental challenge, helped in solubility with the parent compound having an aqueous solubility of ~350 μM.

An excellent synthetic route was developed for the commercial synthesis of boceprevir by the process group, and a novel method of purification was employed to assure specification for first in human trials. Scheme 1 outlines the synthetic route developed to supply material for initial preclinical studies. Alkylation of diphyllimine protected glycine ethyl ester **58** with cyclobutyl bromide followed by hydrolysis with aq. HCl resulted in amino ester **59**. The nitrogen of **59** was further protected with a Boc group, and the ethyl ester was hydrolyzed using aqueous LiOH. The resultant acid **60** was later converted to the Weinreb amide and reduced with

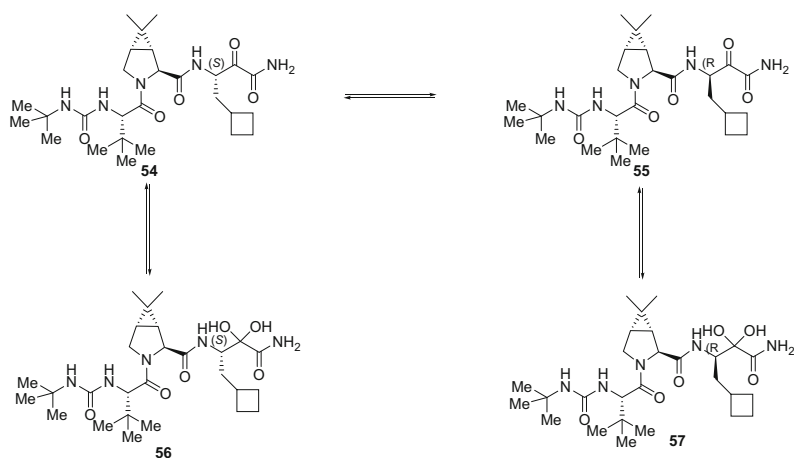
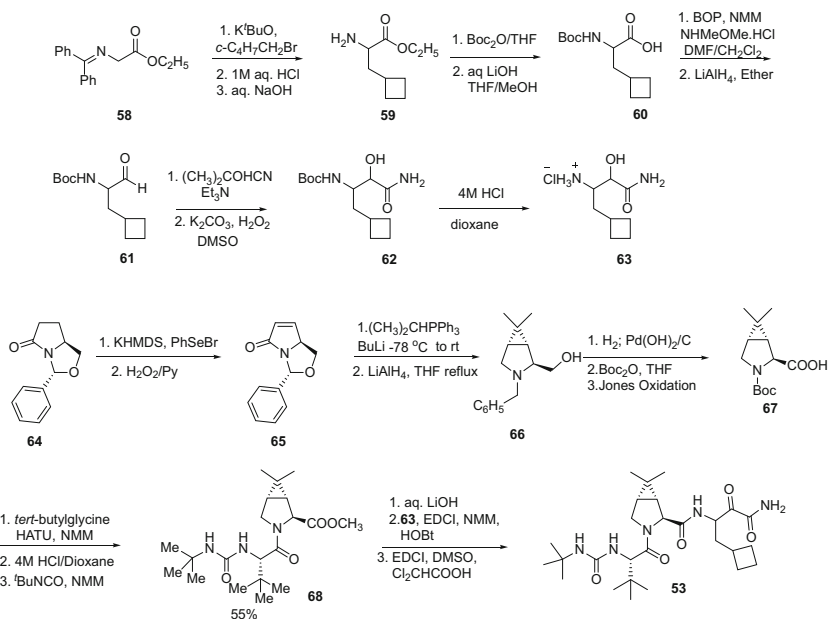


Fig. 7 Hydration and P1 isomerization of ketoamide of boceprevir



Scheme 1 Synthesis of boceprevir

$LiAlH_4$ to provide aldehyde **61** which was converted to the hydroxy amide **63** by treatment with acetone cyanohydrin followed by hydrolysis with basic hydrogen peroxide. The Boc-amine **62** was further deprotected using 4 M HCl in dioxane.

The synthesis of the non-proteinogenic P2 piece was initiated with protected pyroglutamic acid derivative **64**. Oxidation of **64** with phenyl selenium bromide

resulted in alkene **65**. Dimethyl cyclopropanation of **65** with isopropylphosphonium ylide followed by reduction with lithium aluminum hydride resulted in *N*-benzyl prolinol **66** which was oxidized to proline using Jones reagent. Deprotection and coupling with Boc *tert*-butyl glycine followed by formation of *tert*-butyl urea resulted in left-hand side intermediate **68**. Coupling of intermediate **68** with hydroxy amide fragment **63** followed by oxidation with Dess-Martin reagent resulted in boceprevir **53**.

Boceprevir was evaluated for activity against other proteases in a CEREP panel and was found to be mostly selective against various enzymes. It was clean in inhibition against cytochrome P450s with $IC_{50} > 30 \mu M$ against 3A4, 2D6, and 2C9. It was clean in PXR and other enzyme induction studies. Analysis of hERG and sodium channel inhibition showed a low potential for cardiovascular risk. It was clean in the AMES test for potential mutagenicity. On dosing boceprevir in rat at 10 mpk showed a low exposure in the brain and a significant higher exposure in the liver with a liver/plasma ratio of 30. This was very encouraging because the compound had significant target organ exposure.

Hepatitis C virus exists in six genotypes 1–6 and multiple quasi species. Evaluation of the activity of boceprevir against HCV NS3 proteases of various genotypes showed that it retained inhibitory activity against most of these enzymes. Table 8 shows the activity of the compound against different genotypes. It was equipotent against genotypes 1, 2, and 3 in the enzyme assay and less active against genotype 4 with a $K_i^* = 104 \text{ nM}$ a four- to fivefold loss in activity compared to genotypes 1 and 2. It was also potent against various genotypes in the replicon-based cellular assays with the potency ranging from $EC_{50} = 159\text{--}283 \text{ nM}$.

Resistance mutations were developed by replicon cells to boceprevir [21–23]. The observed primary mutations were arginine 155 replaced with lysine and alanine 156 replaced to serine and threonine. Also, the mutation of aspartic acid 156 to glutamic acid conferred significant loss in activity. Mutations developed in vitro in the replicon system translated well into the clinic with both Arg155 mutation and Asp168 mutation seen in patients [24].

X-ray crystal structure of boceprevir bound to HCV NS3 protease was solved, and key characteristic interactions were identified (Fig. 8). Analysis of the X-ray structure showed the catalytic serine 139 making a covalent interaction with ketoamide forming a tetrahedral intermediate. The hydrogens on the nitrogen of the primary ketoamide were involved with hydrogen bonding with glutamine 41 and glycine 137. The P2 amide nitrogen interacted through a hydrogen bond with arginine 155, and the urea nitrogens made a pair of hydrogen bonds with alanine 157. Along with a series of hydrogen bonds, boceprevir made a series of lipophilic interactions which contributed to further interactions with enzyme enhancing potency. The primary lipophilic interactions involved the overlap of P4 *tert*-butyl

Table 8 Pan-genotypic activity of boceprevir

	gt1a	gt1b	gt2a	gt3a	gt4	gt5a
K_i^* (nM)	21	23	11	17	104	53
EC_{50} (nM)	233	220	283	159	–	251

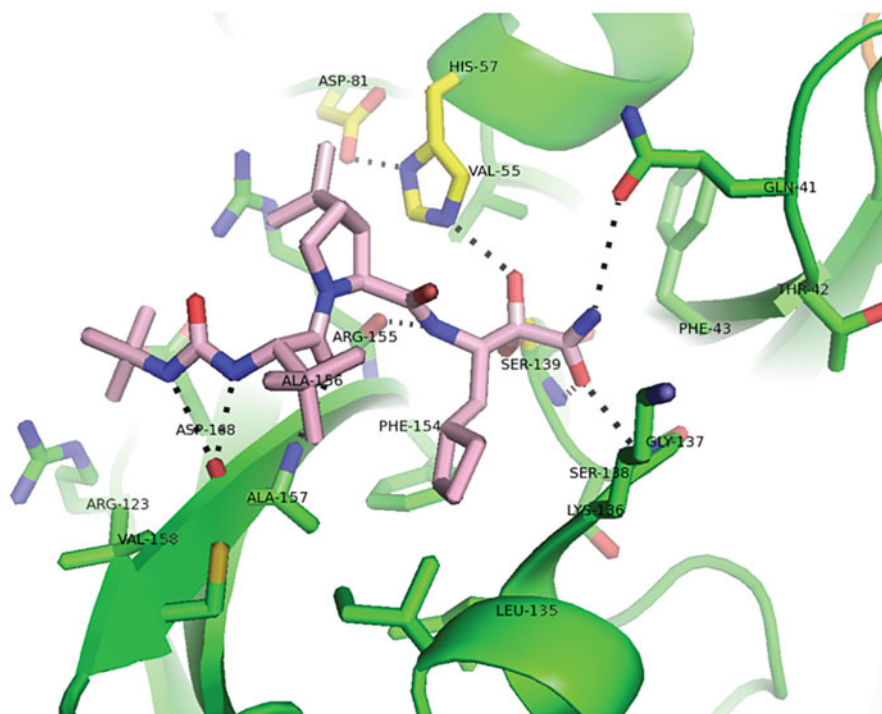


Fig. 8 X-ray structure of boceprevir bound to the active site of HCV NS3 protease

urea into the hydrophobic S4 pocket. One of the methyl groups of P3 *tert*-butyl glycine made key interactions with the surface of enzyme. The P2 proline overlapped on the alanine156 with one of the methyl groups of the dimethyl cyclopropyl proline making a key interaction with the methyl group of alanine 156. The other methyl group distal to the ring made interactions with arginine 155 enhancing potency and selectivity. The shallow S1 pocket was occupied by the cyclobutyl group which adapted a puckered conformation and making lipophilic interactions with the hydrophobic S1 pocket [25].

A computational effort was undertaken to determine the contribution of various residues to the overall binding of boceprevir to the HCV protease. Table 9 summarizes the results of these interactions. As it is clear from the table, the major contributors to the potency are the P1 cyclobutyl alanine and the covalent interaction with the serine. The P1 cyclobutyl alanine is deeply buried in the S1 pocket with a contact surface area of 59 \AA^2 and contributing up to 93-fold to the overall improvement in activity. Similarly, the formation of a covalent interaction with serine 139 results in marked improvement with a 100-fold improvement in activity. The P2, P3, and P4 groups though indispensable make key interactions with the enzyme and contributed only 7- to 16-fold improvement in activity. These residues make only partial contact with the surface, and only a small portion of the total surface area of the

Table 9 Contribution of various groups to the binding of boceprevir (**53**) to HCV NS3/4A protease

Group	Contact surface area (Å ²)	% of compound 53 surface area in contact with protein	Fold increase in affinity
<i>Tert</i> -butyl urea (P3 cap)	26	36	7
<i>Tert</i> -butyl glycine (P3)	27	40	8
Dimethylcyclopropyl proline (P2)	36	40	16
Cyclobutyl alanine (P1)	59	80	93
Subtotal	148	49	87,000
H-bonds			30
Covalent bond			100
Total fold increase			2.6×10^8

residue contribute to meaningful improvement in potency. This clearly reflects the challenges of designing an inhibitor for an enzyme with the active site on the surface. In addition to these lipophilic interactions, the directed hydrogen bonds provide an additional 30-fold improvement making boceprevir overall a nanomolar inhibitor.

Based on these positive attributes of boceprevir (**53**), the compound was progressed to first in human Phase 1 clinical studies to evaluate PK and safety in healthy volunteers. With an acceptable safety profile, it was progressed to Phase 2 and Phase 3 studies to evaluate efficacy and tolerability in combination with Peg-interferon and ribavirin in HCV gt-1-infected patients both treatment naive and nonresponders [26, 27]. In a randomized Phase 3 trials, SPRINT-2 [28] patients treated with boceprevir over standard of care demonstrated improved cure rates (SVR) than standard of care alone (Fig. 9). In addition to the beneficial effect on viral load, the number of patients relapsing was significantly reduced. With this outcome boceprevir was the first direct-acting antiviral approved by the FDA for the treatment of HCV gt-1 infections in combination with Peg-interferon and ribavirin.

2 Conclusion

With advances in virology and biology of hepatitis C virus replication, HCV NS3 protease was identified as an excellent target for drug development. It was hypothesized based on the central role of HCV NS3 protease that the identification and development of small-molecule inhibitor would pave the way to treat HCV infections particularly gt-1 infections with the greatest unmet need. Toward this end we embarked on a goal to discover small-molecule protease inhibitors. Based on the structure of the HCV protease, it was immediately evident that the task ahead would be arduous and challenging. Despite screening numerous compound libraries, we

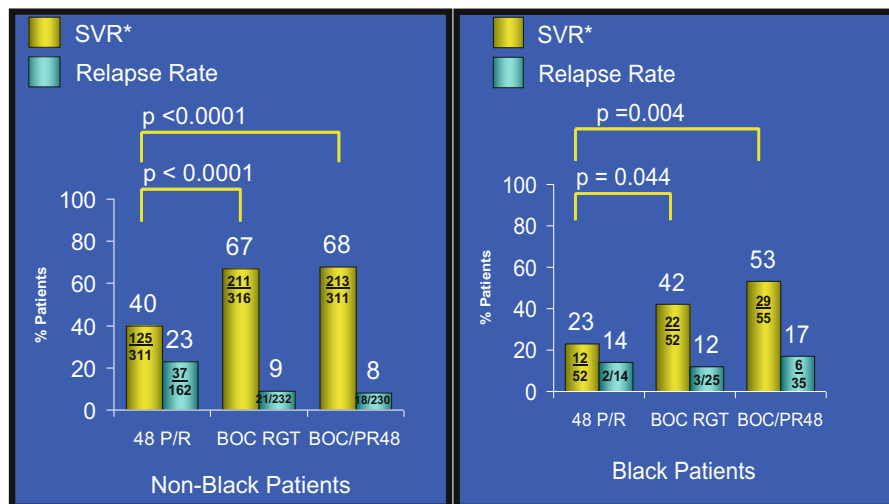


Fig. 9 Response of gt-1 HCV-infected patients treated with boceprevir in a Phase 3 SPRINT-2 trial in combination with Peg-interferon and ribavirin

failed to identify a lead for structure activity optimization. A structure-based design from the natural substrate of the enzyme with an electrophilic trap was designed resulting in analog **6** which inhibited the enzyme with a $K_i^* = 1.9$ nM. However, it was unselective toward other proteases and had none of the drug-like properties for further development. We therefore embarked on a SAR campaign to optimize this by reducing the molecular weights and improving ligand efficiencies, potency, and selectivity. The discovery of a novel dimethylcyclopropyl-fused proline P2 and phenyl glycine at P2' resulted in the identification of pentapeptide inhibitor **28** which had excellent enzyme inhibition, selectivity, and acceptable cellular activity. However, we quickly learned that the compound had very poor absorption and a poor oral PK profile. This analog was further truncated modifying the P1 residue and improving ligand efficiency to identify boceprevir (**53**), a potent inhibitor of HCV containing all non-proteinogenic amino acids, with acceptable cellular activity, selectivity, and oral PK across animals. It was moved to clinical studies and approved as the first direct-acting antiviral for the treatment of HCV genotype 1 infections. The journey from **6** to **53** (Fig. 10) was arduous with many roadblocks, wrong turns, and disappointments. With a team of highly dedicated scientists, all these were overcome leading to the discovery of boceprevir, the first direct-acting antiviral approved by the FDA for the treatment of HCV gt-1 infections.

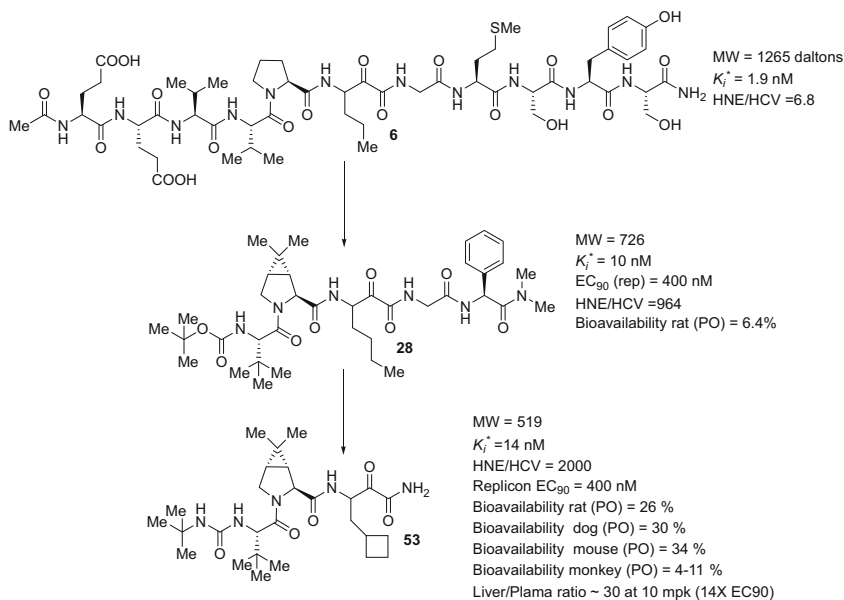


Fig. 10 Key steps leading to the discovery of boceprevir

Compliance with Ethical Standards

Conflict of Interest: Dr. Srikanth worked for Schering /Merck.

Ethical Approval: This article does not contain any studies with human participants or animals performed by any of the authors.

References

- Freeman AJ, Dore GJ, Law MG, Thorpe M, Overbeck JV, Llyods AR, Marinos G, Kaldor JM (2001) Estimating progression to cirrhosis in chronic hepatitis C infection. *Hepatology* 34:809–816
- Manns MP, McHutchison JG, Gordon SC, Rustgi VK, Shiffman M, Reindollar R, Goodman ZD, Koury K, Ling M-H, Albrecht JK, International Hepatitis Interventional Therapy Group (2001) Peginterferon alfa-2b plus ribavirin compared with interferon alfa-2b plus ribavirin for initial treatment of chronic hepatitis C: a randomized trial. *Lancet* 358:958–965
- Zeuzem S, Feinman SV, Rasenack J, Heathcote EJ, Lai M-Y, Gane E, O’Grady J, Reichen J, Diago M, Lin A, Hoffman J, Brunda MJ (2000) Peginterferon alfa-2a in patients with chronic hepatitis C. *N Engl J Med* 343(23):1666–1172
- Choo QL, Kuo G, Weiner AJ, Overby LR, Bradley DW, Houghton M (1989) Isolation of a cDNA clone derived from a blood-borne non-A, non-B viral hepatitis genome. *Science* 244:359–362
- Kuo G, Choo QL, Alter HJ, Gitnick GL, Redeker AG, Purcell RH, Miyamura T, Dienstag JL, Alter MJ, Stevens CE, Tegtmeier GE, Bonino F, Colombo M, Lee W-S, Kuo C, Berger K,

- Shuster JR, Overby LR, Bradley W, Houghton M (1989) An assay for circulating antibodies to a major etiologic virus of human non-A, non-B hepatitis. *Science* 244:362–364
6. Bartenschlager R (1999) The NS3/4A proteinase of the hepatitis C virus: unraveling structure and function of an unusual enzyme and a prime target for antiviral therapy. *J Virol Hepatitis* 6:165–181
 7. Bartenschlager R, Ahlborn-Laake L, Mous J, Jacobsen H (1993) Nonstructural protein 3 of the hepatitis C virus encodes a serine-type proteinase required for cleavage at the NS3/4 and NS4/5 junctions. *J Virol* 67:3835–3844
 8. Yan Y, Li Y, Munshi S, Sardana V, Cole JL, Sardana M, Steinkuehler C, Tomei L, De-Francesco R, Kuo LC, Chen Z (1998) Complex of NS3 protease and NS4A peptide of BK strain hepatitis C virus: a 2.2 Å resolution structure in a hexagonal crystal form. *Protein Sci* 7:837–847
 9. Love RA, Parge HE, Wickersham JA, Hostomsky Z, Habuka N, Moomaw EW, Adachi T, Hostomska Z (1996) The crystal structure of hepatitis C virus NS3 proteinase reveals a trypsin-like fold and a structural zinc binding site. *Cell* 87:331–342
 10. Kim JL, Morgenstern KA, Griffith JP, Dweyer MD, Thomson JA, Murcko MA, Lin C, Caron PR (1998) Hepatitis C virus NS3 RNA helicase domain with a bound oligonucleotide: the crystal structure provides insights into the mode of unwinding. *Structure* 6:89–100
 11. Urbani A, Bianchi E, Narjes F, Tramontano A, De Francesco R, Steinkuehler C, Pessi A (1997) Substrate specificity of the hepatitis C virus serine protease NS3. *J Biol Chem* 272:9204–9209
 12. Kolykhalov AA, Agapov EV, Rice CM (1994) Specificity of the hepatitis C virus NS3 serine protease: effects of substitutions at the 3/4A, 4A/4B, 4B/5A, and 5A/5B cleavage sites on polyprotein processing. *J Virol* 68:7525–7533
 13. Zhang R, Beyer BM, Durkin J, Ingram R, Njoroge FG, Windsor WT, Malcolm BA (1999) A continuous spectrophotometric assay for the hepatitis C virus serine protease. *Anal Biochem* 270:268–275
 14. Lohmann V, Körner F, Koch J-O, Herian U, Theilmann L, Bartenschlager R (1999) Replication of subgenomic hepatitis C virus RNAs in a hepatoma cell line. *Science* 285:110–113
 15. Mamai A, Zhang R, Natarajan A, Madalengoitia JS (2001) Poly-L-proline type-II peptide mimics based on the 3-azabicyclo[3.1.0]hexane system. *J Org Chem* 66:455–460
 16. Bogen SL, Arasappan A, Bennett F, Chen K, Jao E, Liu Y-T, Lovey R, Venkatraman S, Pan W, Parekh T, Pike RE, Ruan S, Liu R, Baroudy B, Agrawal S, Chase R, Ingravallo P, Pichardo J, Prongay A, Brisson J-M, Hsieh TY, Cheng K-C, Kemp SJ, Levy OE, Lim-Wilby M, Tamura SY, Saksena AK, Girijavallabhan V, Njoroge FG (2006) Discovery of SCH446211 (SCH6): a new ketoamide inhibitor of the HCV NS3 serine protease and HCV subgenomic RNA replication. *J Med Chem* 49:2750–2757
 17. Cox KA, Dunn-Meynell K, Korfmacher W, Broske L, Nomeir AA, Lin CC, Cayen MN, Barr WH (1999) Novel in vivo procedure for rapid pharmacokinetic screening of discovery compounds in rats. *Drug Discov Today* 4:232–237
 18. Venkatraman S, Bogen SL, Arasappan A, Bennett F, Chen K, Jao E, Liu Y-T, Lovey R, Hendrata S, Huang Y, Pan W, Parekh T, Pinto P, Popov V, Pike R, Ruan S, Santhanam B, Vibulbhan B, Wu W, Yang W, Kong J, Liang X, Wong J, Liu R, Butkiewicz N, Chase R, Hart A, Agarwal S, Ingravallo P, Pichardo J, Kong R, Baroudy B, Malcolm B, Guo Z, Prongay A, Madision BL, Cui X, Cheng K-C, Hsieh TY, Brisson J-M, Prelusky D, Kormacher W, White R, Bogonowich-Knipp S, Pavlovsky A, Prudence B, Saksena AK, Ganguly A, Piwinski J, Girijavallabhan V, Njoroge FG (2006) Discovery of (1*R*, 5*S*)-*N*-[3-amino-1-(cyclobutylmethyl)-2-3-dioxopropyl]-3-[2(*S*)-[[[1,1-dimethylethyl]-amino]carbonyl]amio]-3,3-dimethyl-1-oxobutyl]-6,6-dimethyl-3-azabicyclo[3.1.0]hexan-2(*S*)-carboxamide (SCH 503034), a selective, potent, orally bioavailable, hepatitis C virus NS3 protease inhibitor: a potential therapeutic agent for the treatment of hepatitis C infection. *J Med Chem* 49:6074–6086
 19. Malcolm BA, Liu R, Lahser F, Agrawal D, Belanger B, Butkiewicz N, Chase R, Gheyas F, Hart A, Hesk D, Ingravallo P, Jiang C, Kong R, Lu J, Pichardo J, Prongay A, Skelton A,

- Tong X, Venkatraman S, Xia E, Girijavallabhan V, Njoroge FG (2006) Sch 503034, a mechanism-based inhibitor of hepatitis C virus NS3 protease, suppresses polyprotein maturation and enhances the antiviral activity of alpha interferon in replicon cells. *Antimicrob Agents Chemother* 50:1013–1020
20. Cheng K-C, Li C, Liu T, Wang G, Hsieh Y, Pavlovsky A, Broske L, Prelusky D, Chen J, Liu R, Uss AS, White RE, Gupta S, Njoroge FG (2009) Use of preclinical invitro and in vivo pharmacokinetics for selection of potent hepatitis C protease inhibitor, Boceprevir for clinical development. *Lett Drug Des Discov* 6:312–218
 21. Tong X, Guo Z, Wright-Minogue J, Xia E, Prongay A, Madison V, Qiu P, Venkatraman S, Velazquez F, Njoroge FG, Malcolm BA (2006) Impact of naturally occurring variants of HCV protease on the binding of different classes of protease inhibitors. *Biochem J* 45:1353
 22. Guo Z, Prongay A, Tong X, Thierry F, Bogen S, Velazquez F, Venkatraman S, Njoroge FG, Madison V (2006) Computational study of the effects of mutations A156T, D168V, and D168Q on the binding of HCV protease inhibitors. *J Comput Chem* 2:1657
 23. Tong X, Chase R, Skelton A, Chen T, Wright-Minogue J, Malcolm BA (2006) Identification and analysis of fitness of resistance mutations against the HCV protease inhibitor SCH 503034. *Antiviral Res* 70:28–38
 24. Barnard RJ, Howe JA, Ogert RA, Zeuzem S, Poordad F, Gordon SC, Ralston R, Tong X, Sniukiene V, Strizki J, Ryan D, Long J, Qiu P, Brass CA, Albrecht J, Burroughs M, Vuocolo S, Hazuda DJ (2013) Analysis of boceprevir resistance associated amino acid variants (RAVs) in two phase 3 boceprevir clinical studies. *Virology* 444:329–336
 25. Prongay AJ, Guo Z, Yao N, Pichardo J, Fischmann T, Strickland C, Myers J Jr, Weber PC, Beyer BM, Ingram R, Hong Z, Prosis WW, Ramanathan L, Taremi SS, Yarosh-Tomaine T, Zhang R, Senior M, Yang RS, Malcolm B, Arasappan A, Bennett F, Bogen SL, Chen K, Jao E, Liu Y-T, Lovey RG, Saksena AK, Venkatraman S, Girijavallabhan V, Njoroge FG, Madison V (2007) Discovery of the HCV NS3/4A protease inhibitor (1R,5S)-N-[3-amino-1-(cyclobutylmethyl)-2,3-dioxopropyl]-3-[2(S)-[[[(1,1-dimethylethyl)amino]carbonyl]amino]-3,3-dimethyl-1-oxobutyl]-6,6-dimethyl-3-azabicyclo[3.1.0]hexan-2(S)-carboxamide (Sch 503034). Key steps in structure-based optimization. *J Med Chem* 50:2310–2318
 26. Bacon B, Gordon SC, Lawitz E, Marcellin P, Vierling J, Zeuzem S, Poordad F, Goodman ZD, Sings HL, Boparai N, Burroughs M, Brass CA, Albrecht JK, Esteban R (2011) For the HCV RESPOND-2 investigators. Boceprevir for previously treated chronic HCV genotype 1 infection. *N Engl J Med* 364(13):1207–1217
 27. Kwo PY, Lawitz EJ, McCone J, Schiff ER, Vierling JM, Pound D, Davis MN, Galati JS, Gordon SC, Ravendhran N, Rossaro L, Anderson FH, Jacobson IM, Rubin R, Koury K, Pedicone LD, Brass CA, Chaudhri E, Albrecht JK, On Behalf of the SPRINT-1 Investigators (2010) Efficacy of boceprevir, an NS3 protease inhibitor, in combination with peginterferon alfa-2b and ribavirin in treatment-naïve patients with genotype 1 hepatitis C infection (SPRINT-1): an open-label, randomized, multicenter phase 2 trial. *Lancet* 376:705–716
 28. Poordad F, McCone J Jr, Bacon BR, Bruno S, Manns MP, Sulkowski MS, Jacobson IM, Reddy KR, Goodman ZD, Boparai N, DiNubile MJ, Sniukiene V, Brass CA, Albrecht JK, Bronowicki J-P (2011) For the SPRINT-2 investigators. Boceprevir for untreated chronic HCV genotype 1 infection. *N Engl J Med* 364(13):1195–1206

The Discovery and Early Clinical Evaluation of the HCV NS3/4A Protease Inhibitor Asunaprevir (BMS-650032)



Nicholas A. Meanwell, Ramkumar Rajamani, Paul M. Scola,
and Li-Qiang Sun

Contents

1	Introduction	318
2	The Discovery of the First Clinical Candidate, BMS-605339	321
3	The Discovery of Asunaprevir (BMS-650032)	333
4	Clinical Studies with Asunaprevir	342
5	Conclusion	347
	References	348

Abstract The discovery of asunaprevir (**1**) began with the concept of engaging the small and well-defined S_1' pocket of the hepatitis C virus (HCV) NS3/4A protease that was explored in the context of tripeptide carboxylic acid-based inhibitors. A cyclopropyl-acyl sulfonamide moiety was found to be the optimal element at the P_1 - P_1' interface enhancing the potency of carboxylic acid-based prototypes by 10- to >100-fold, dependent upon the specific background. Optimization for oral bioavailability identified a 1-substituted isoquinoline-based P_2^* element that conferred a significant exposure advantage in rats compared to the matched 4-substituted quinoline isomer. BMS-605339 (**30**) was the first cyclopropyl-acyl sulfonamide derivative advanced into clinical trials that demonstrated dose-related reductions in plasma viral RNA in HCV-infected patients. However, **30** was

N. A. Meanwell (✉) and L.-Q. Sun
Department of Discovery Chemistry, Bristol-Myers Squibb Research and Development,
Princeton, NJ, USA
e-mail: nicholas.meanwell@bms.com

R. Rajamani
Department of Computer-Aided Drug Design and Molecular Analytics, Bristol-Myers Squibb
Research and Development, Waltham, MA, USA

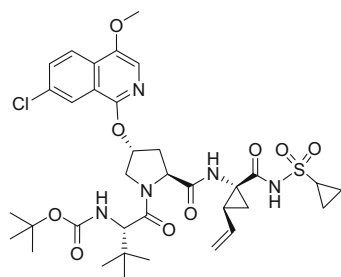
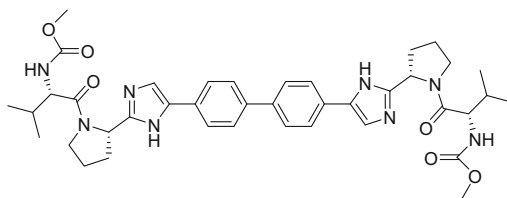
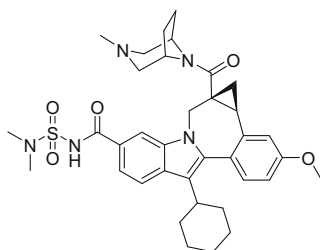
P. M. Scola
Department of Discovery Chemistry, Bristol-Myers Squibb Research and Development,
Cambridge, MA, USA

associated with cardiac events observed in a normal healthy volunteer (NHV) and an HCV-infected patient that led to the suspension of the development program. Using a Langendorff rabbit heart model, a limited structure-cardiac liability relationship was quickly established that led to the discovery of **1**. This compound, which differs from **30** only by changes in the substitution pattern of the P₂* isoquinoline heterocycle and the addition of a single chlorine atom to the molecular formula, gave a dose-dependent reduction in plasma viral RNA following oral administration to HCV-infected patients without the burden of the cardiac events that had been observed with **30**. A small clinical trial of the combination of **1** with the HCV NS5A inhibitor daclatasvir (**2**) established for the first time that a chronic genotype 1 (GT-1) HCV infection could be cured by therapy with two direct-acting antiviral agents in the absence of exogenous immune-stimulating agents. Development of the combination of **1** and **2** was initially focused on Japan where the patient population is predominantly infected with GT-1b virus, culminating in marketing approval which was granted on July 4, 2014. In order to broaden therapy to include GT-1a infections, a fixed dose triple combination of **1**, **2**, and the allosteric NS5B inhibitor beclabuvir (**3**) was developed, approved by the Japanese health authorities for the treatment of HCV GT-1 infection on December 20, 2016 and marketed as Ximency[®].

Keywords Acyl sulfonamide, Asunaprevir, Beclabuvir, Daclatasvir, HCV NS3/4A protease inhibitor, Hepatitis C virus, Pegylated interferon- α , Ribavirin

1 Introduction

Asunaprevir (BMS-650032, **1**) is a tripeptidic acyl sulfonamide derivative that has been approved in 17 countries for the treatment of chronic hepatitis C virus (HCV) infection and is marketed as Sunvepra[®] [1–7]. Asunaprevir (**1**) is a potent inhibitor of the HCV NS3/4A protease and is approved for clinical use either in combination with the HCV NS5A inhibitor daclatasvir (**2**, Daklinza[®]) or as part of a triple therapeutic regimen that includes **2** and the HCV NS5B inhibitor beclabuvir (**3**), a fixed dose combination marketed as Ximency[®] [8–15]. The dual combination provides a highly effective treatment for patients infected with hepatitis C genotype 1b (GT-1b) virus, while the triple combination extends therapy to include the GT-1a variant that is prevalent in the United States and Europe [3–10, 15]. Notably, early clinical studies with **1** and **2** provided proof of concept that a chronic HCV infection could be cured with direct-acting antiviral agents (DAAs) in the absence of the exogenous immune stimulation provided by pegylated-interferon- α (PEG-IFN- α), a component of the standard of care therapy for HCV infection prior to the advent of DAAs [16, 17]. This clinical result was described as a “watershed moment in the treatment of HCV” since it provided a clear clinical path to the orally administered, DAA drug regimens that are available today and which are capable of curing a chronic HCV infection after just 8–12 weeks of therapy [18–24].

**1** (asunaprevir, BMS-650032)**2** (daclatasvir)**3** (beclabuvir)

The discovery of **1** began with an evaluation of the hexapeptide derivative **4**, a compound that had been described in the literature as a modestly potent inhibitor of the HCV NS3/4A enzyme [25–27]. An X-ray co-crystal structure of **4** bound to an engineered NS3/4A complex (Fig. 1) provided key insights into the nonbonding interactions governing the ligand-protein complex. Of particular interest were the touchpoints between the terminal carboxylic acid functionality of this product-based enzyme inhibitor and the catalytic triad of the NS3 protease, which were essential for potent enzyme inhibitory activity [27–29]. These critical interactions included a salt bridge between the oxygen-centered anion of acid **4** and the imidazole ring of the catalytic histidine (His57) as well as hydrogen-bonding interactions between the carbonyl moiety and the backbone N-H of Gly139 that contributes to the oxyanion hole of the enzyme. As part of an effort to design more potent inhibitors, consideration was given to the introduction of structural motifs that would maintain the key interactions between the carboxylic acid moiety and the catalytic site elements while allowing an extension of functionality into the small and well-defined S_1' sub-pocket [30]. As illustrated in Fig. 2, the S_1' site is a shallow pocket that is contiguous with the oxyanion hole of the enzyme whose boundaries are defined by the side chains of Phe43, Val55, and Gly58. An acyl sulfonamide was selected as a potential structural motif with which to replace the terminal carboxylic acid moiety since it appeared to fulfill the targeted criteria [31–33]. Modeling studies provided support for the design concept which preserves an acidic element while projecting

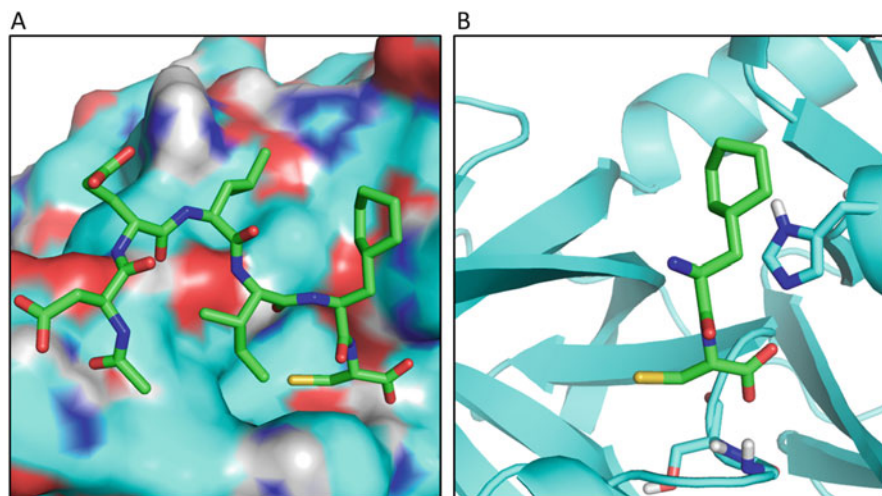


Fig. 1 Details of the binding interactions of peptide inhibitor **4** bound to an engineered HCV NS3/4A protease complex. (a) View of the hexapeptide **4** bound to HCV NS3/4A. (b) Close-up view of the P₁ element of **4** bound to HCV NS3/4A showing His157

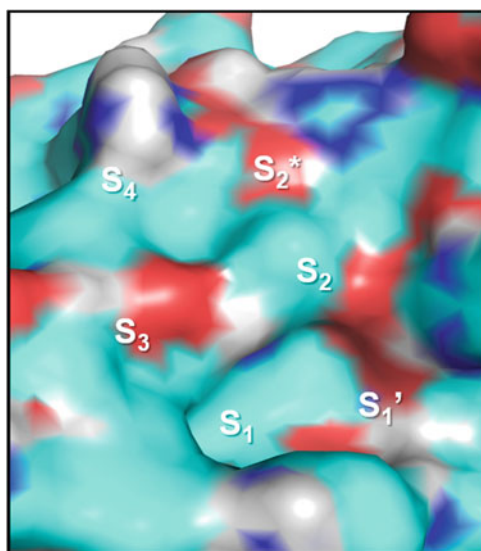
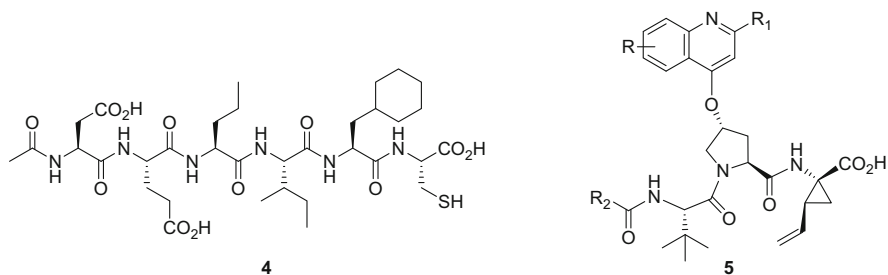


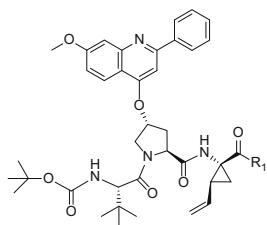
Fig. 2 Surface of the HCV NS3/4A enzyme illustrating the S₁ and S₁' subsites

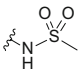
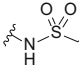
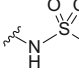
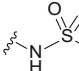
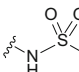
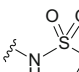
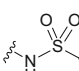
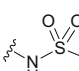
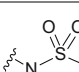
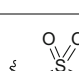
the sulfone substituent toward the S₁' pocket. The contemporaneous disclosure of the tripeptidic carboxylic acid-based inhibitors of the NS3/4A protease represented generically by **5** provided a more compelling vehicle with which to explore this design proposal, and an exploratory discovery effort was initiated [1, 25, 26, 34, 35].



2 The Discovery of the First Clinical Candidate, BMS-605339

The carboxylic acid **6** was exploited as the vehicle with which to explore the acyl sulfonamide design concept based on its potent GT-1a NS3/4A enzyme inhibition, $IC_{50} = 54$ nM, and efficacy in a GT-1b replicon assay where the EC_{50} value was 550 nM. The prototypical acyl sulfonamide, the methyl derivative **7**, exhibited enzyme and replicon inhibitory activities that were comparable to **6**, validating the design principle and encouraging further molecular editing (Table 1) [26]. Modeling studies suggested that the cyclopropyl ring deployed in **11** would be the optimal element with which to fill the S_1' pocket and the preparation of this compound was, accordingly, given priority. In vitro evaluation of **11** revealed it to be a potent inhibitor of the GT-1a NS3/4A enzyme with an IC_{50} value of 1 nM, a 54-fold advantage over **6** that extended to the GT-1b replicon where sub-genomic virus replication was half-maximally inhibited at a concentration of 4 nM. These in vitro potency values met the criteria of <10 nM that we had set as the standard for a clinical candidate for all of our HCV inhibitor programs, and the results fostered additional study of the acyl sulfonamide chemotype. Confirmation that **11** represented the optimal P_1' element came from the systematic analysis of the structure-activity relationship (SAR) studies that are summarized in Table 1. The ethyl homologue **8** offered sixfold increased potency over the methyl prototype **7**, while the propyl analogue **9** was twofold more potent than **7**. The *isopropyl* derivative **10** is the ring-opened analogue of **11**, and remarkably, the addition of just two hydrogen atoms to **11** is associated with a 20-fold reduction in potency in both the enzyme and cell-based assays, reflecting the precise demands associated with filling the NS3/4A S_1' pocket [26]. Interestingly, methyl substitution of the cyclopropyl ring proximal to the sulfone, as in **12**, was tolerated, with only a modest effect on antiviral potency. However, potency decreased progressively in both in vitro assays as the size of the ring was increased, as exemplified by compounds **13–15**, although in this series, the phenyl derivative **16** was an order of magnitude more potent than the cyclohexyl analogue **15** [36]. This SAR point was attributed to the flexibility of the Gln41 side chain of the enzyme allowing accommodation

Table 1 HCV NS3/4A protease and GT-1b replicon inhibitory profile of the tripeptide carboxylic acid **6** and acyl sulfonamide derivatives **7–16**

Compound	R ₁	IC ₅₀ inhibition of HCV NS3/4A GT-1a enzyme activity, IC ₅₀ (nM)	Inhibition of HCV GT-1b replicon activity, EC ₅₀ (nM)
6	OH	54	550
7		36	600
8		6	133
9		14	93
10		19	97
11		1	4
12		5	8
13		7	29
14		71	170
15		149	210
16		8	20

of larger P_1' structural elements. Modeling studies suggested that the key drug-target interactions of **11** revolved around the acidic acyl sulfonamide moiety engaging the imidazole of the catalytic His57 via the nitrogen rather than the carbonyl oxygen atom (Fig. 3). This contention was supported by calculations of the electrostatic

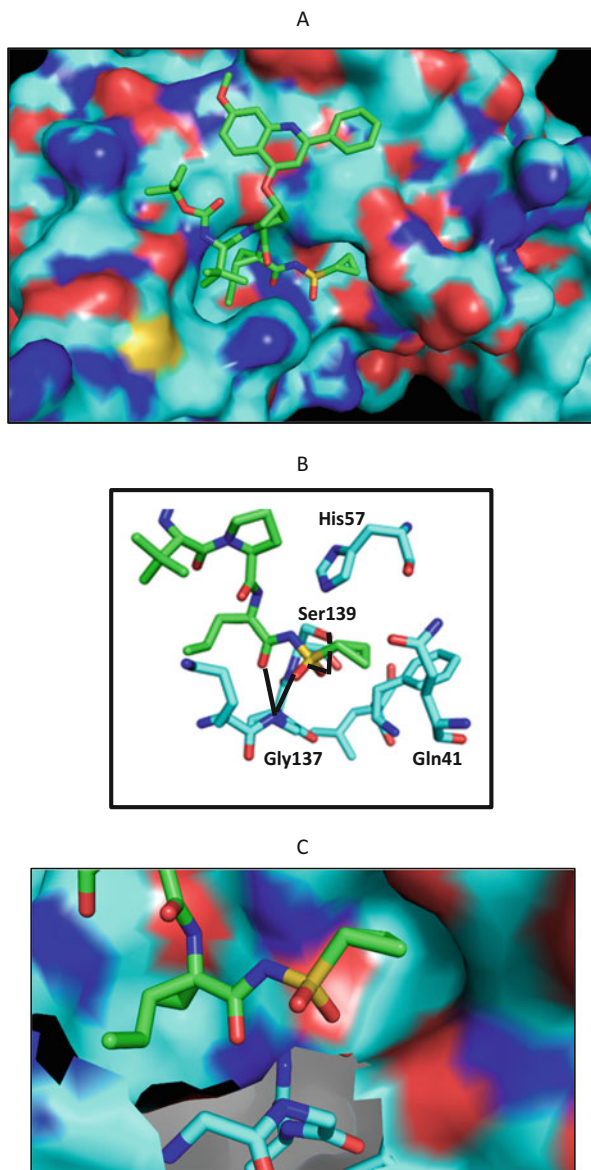
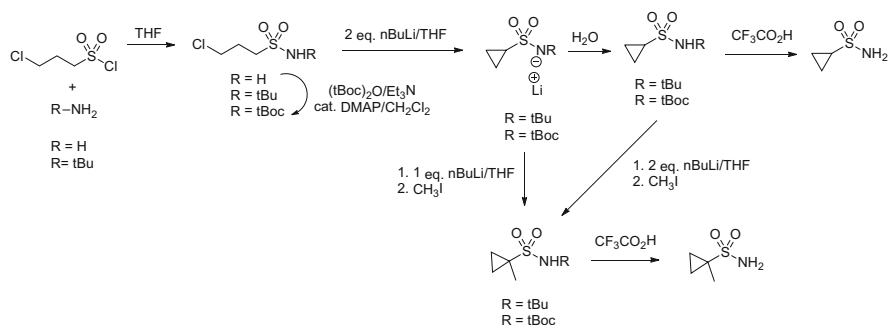


Fig. 3 (a) Model of the acyl sulfonamide moiety of **11** bound to the NS3/4A protease enzyme construct. (b) Key interactions between the acyl sulfonamide moiety and the NS3/4A protein. (c) Model of the cyclopropyl moiety bound to the S_1' pocket

potential of acyl sulfonamide derivatives and solid-state data for this structural motif [26]. This scenario anticipated that the carbonyl oxygen atom of the acyl sulfonamide would accept a H-bond from the backbone N-H of Gly137 in the oxyanion hole. These predictions were ultimately confirmed by X-ray co-crystal structures of inhibitors with the NS3/4A construct which also revealed that one of the sulfone oxygen atoms engaged in a H-bonding interaction with the side chain OH of the catalytic Ser139, while the other oxygen atom coordinated with the N-H of Gly137, resulting in this N-H engaging in a bifurcated interaction (Fig. 3).

With the identification of the cyclopropyl-acyl sulfonamide as the optimal P_1' moiety, this motif was adopted as a key structural element for further studies, stimulating the development of the synthetic methodologies to prepare cyclopropanesulfonamide and its derivatives that are summarized in Scheme 1 [37]. Commercially available 3-chloropropane-1-sulfonyl chloride was reacted with ammonia or *tert*-butylamine to afford the corresponding sulfonamide, with the primary sulfonamide converted to the *N*-*t*-Boc derivative by exposure to Boc anhydride in CH_2Cl_2 in the presence of Et_3N and a catalytic amount of DMAP. Reaction of the *tert*-butyl or *N*-Boc sulfonamides with two equivalents of *n*-BuLi in THF effected an intramolecular alkylative ring closure to afford the anions of *N*-(*tert*-butyl)cyclopropanesulfonamide or *tert*-butyl (cyclopropylsulfonyl)carbamate, respectively, in situ. These products could be quenched with H_2O and then exposed to $\text{CF}_3\text{CO}_2\text{H}$ to deprotect the nitrogen atom to afford cyclopropanesulfonamide. Alternatively, the anions could be treated with an equivalent of *n*-BuLi in situ to generate dianions that were alkylated with CH_3I to afford, after deprotection of the products by exposure to $\text{CF}_3\text{CO}_2\text{H}$, the methylated derivative explored in the context of **12**. The dianionic species could also be generated directly from *N*-(*tert*-butyl)cyclopropanesulfonamide or *tert*-butyl (cyclopropylsulfonyl)carbamate by treatment with two equivalents of *n*-BuLi in THF [37].

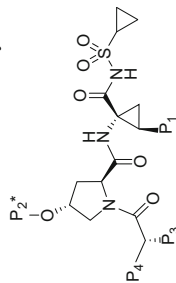
The promising potency of **11** led to an evaluation of its pharmacokinetic (PK) profile in a rat snapshot experiment which captured plasma levels of the compound over a 4-h period and liver levels at the termination of the experiment following oral dosing. After the administration of a dose of 20 mpk of **11**, the plasma



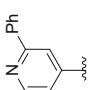
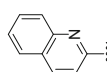
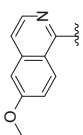
Scheme 1 Synthetic approaches developed to access cyclopropanesulfonamide derivatives

AUC was 0.73 $\mu\text{M}\cdot\text{h}$, while IV administration at a dose of 5 mpk provided information on clearance (55 mL/min/kg) and half-life (1 h), data that translated into an oral bioavailability of 9% [26]. However, liver levels of **11** at the end of the experiment (4-h post-dose) were 5.8 μM , tenfold higher than the concentration of 0.58 μM measured in plasma at the same time point. In a separate experiment, the liver levels at 8-h post-dose were 0.6 μM , while plasma levels were 0.004 μM , a 150-fold differential. In rat liver microsomes (RLMs), **11** demonstrated a $t_{1/2}$ value of 162 min, a level of metabolic stability that indicated that the clearance pathways in vivo were not simply a function of metabolic modification and suggested the potential for the involvement of transporter-mediated liver uptake. The PK profile of **11** in the dog was similar to that observed in the rat, with a $t_{1/2}$ value of 170 min in dog LMs, a plasma AUC of 2.0 $\mu\text{M}\cdot\text{h}$ and bioavailability of 20% following an oral dose of 3 mpk, while the clearance after IV dosing of the compound was 16 mL/min/kg, translating into a plasma half-life of 0.6 h.

The hepatotropic disposition of **11** in the rat and, particularly, the sustained exposure in the liver were considered to be a favorable attribute since this is the organ where HCV predominantly replicates. In order to expedite in vivo studies as the program evolved, test compounds were dosed intraduodenally (ID) to surgically prepared rats and plasma levels monitored for 4-h post-drug administration, with the liver concentration of a test compound determined at the end of the study. In this phase of the program, structural manipulation of **11** was broad-based in nature and directed toward developing a detailed understanding of SARs associated with the P₁, P₃, and P₄ elements of the molecule. In addition, modifications to the substituted quinoline heterocycle attached to C-4 of the P₂ proline residue, a motif that bound to the protease outside of the substrate-binding groove and which was therefore designated as the P₂* element, were explored. This approach recognized the importance of the backbone H-bond donors and acceptors in molecular recognition, while the side chains and the P₄ moiety established van der Waals contacts with their respective pockets in the enzyme. This SAR survey also acknowledged the high molecular weight of **11** (789 Da) and its potential impact on PK parameters to the extent that pruning elements of the molecule was considered an important part of the design strategy. The data presented in Table 2 summarize the key informative discoveries that emerged from this line of inquiry and which shaped the remainder of the program ultimately leading to the discovery of **1**. Truncating the P₁ and P₃ elements by removal of the vinyl and *tert*-butyl substituents (**17** and **18**, respectively) resulted in a greater than tenfold reduction in intrinsic enzyme inhibitory potency that translated into a more severe loss of antiviral activity in the replicon assay. Removal of the *t*-Boc moiety at P₄ (**19**) also eroded potency significantly, but replacing this element with a methoxycarbonyl (**20**) was more readily tolerated. However, this reduction in molecular weight resulted in an inferior in vivo profile, with both the plasma and, particularly, the liver exposure significantly reduced after ID dosing compared to **11**. Further molecular modification of P₄ in the context of the urea **21**, reverse carbamate **22**, the *isopropyl* carbamate **23**, and the cyclopentyl carbamate **24** led to additional insightful and interesting SAR points, but none provided the kind of in vivo profile that was considered to be promising, with plasma and liver exposures in the 4-h rat experiment less than that observed for **11** [26, 38].

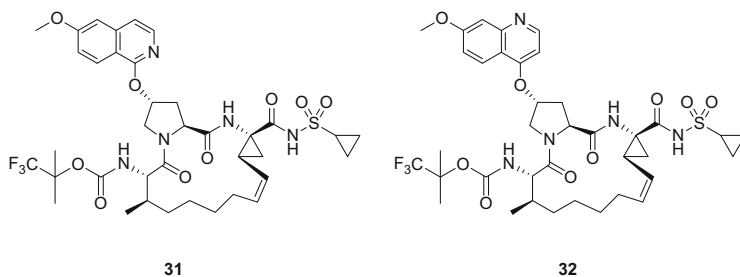
Table 2 Structure-activity relationships and PK parameters associated with a series of tripeptidic, cyclopropyl-acyl sulfonamide-based HCV NS3/4A inhibitors

Compound	P ₁	P ₂ ^a	P ₃	P ₄	GT-1a IC ₅₀ (nM)	GT-1b EC ₅₀ (nM)	AUC over 4 h (μM h)	Liver level at 4 h (ng/g)
11	Vinyl		<i>t</i> Bu	<i>t</i> BuOCO.NH	1	4	0.077	7,850
17	H				12	437		
18	vinyl		H		16	893		
19			<i>t</i> Bu	NH ₂	30	860		
20			<i>t</i> Bu	MeOCO.NH	1	32	0.009	156
21				<i>t</i> BuNHCO.NH	4.6	10	17 ng·h/mL	72
22				<i>t</i> BuNHCO.O	13	42	82 ng·h/mL	3,772
23				<i>t</i> PrOCO.NH	12	85	ND ^a	430
24				cC ₅ H ₉ OCO.NH	11	30	95 ng·h/mL	3,431
25				<i>t</i> Bu	<i>t</i> BuOCO.NH	5	26	0.015
26			<i>t</i> Bu		84	25,000		
27					10	267	ND	319

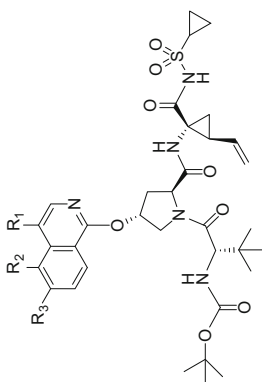
28					23	268	0.279	52,094
29					7	60	0.75 ^a	28,094
30					2	12	10.4	64,710

^aThis compound was dosed as a mixture of diastereomers at the C2 position of the P₁ cyclopropyl ring

However, modifications to the P₂* element proved to be a more promising avenue of study, with the removal of the C-3 phenyl substituent associated with only a modest reduction in both intrinsic and replicon potency, as exemplified by **25**. Unfortunately, the reduction in molecular weight was not helpful with respect to improving the in vivo exposure. A more severe truncation of the quinoline heterocycle at P₂* to the pyridine ring found in **26** defined the structural requirements at this site for potency which was enhanced by the introduction of the C-3 phenyl substituent in **27**, although with no benefit to the in vivo properties. However, configuration of the quinoline moiety as the 2-substituted topology represented in **28** was not only tolerated with some facility in the in vitro assays, but the in vivo profile of this compound in the rat was illuminating, revealing that changes at the P₂* moiety could significantly affect PK parameters. The plasma exposure of **28** offered a threefold advantage over that of **11**, while the 4-h liver levels were sixfold higher. The installation of a 1-substituted isoquinoline at P₂* gave a compound **29** that preserved much of the intrinsic enzyme inhibitory potency of **11** but, more importantly, offered an improved in vivo PK profile, with tenfold higher plasma exposure and almost fourfold higher liver levels at 4 h [26]. The oral bioavailability of **29** in the rat was 20%, with IV clearance measured as 19 mL/min/kg and a plasma *t*_{1/2} of 2.2 h. The introduction of a 6-methoxy substituent to the isoquinoline of **29** gave **30**, a compound with improved potency in both assays while further boosting the PK profile in the rat ID experiment. In the rat, the oral bioavailability of **30** was 18%, with IV clearance lower than for **29** at 4.4 mL/min/kg and a longer plasma *t*_{1/2} of 4.4 h. Comparison of the profile of **30** with that of its 4-substituted quinoline isomer **25** provides a remarkable example of the effect of a subtle structural modification on the properties in different biological systems against the structural backdrop of a large molecule (MW = 713) [39]. While the antiviral effects of the two compounds are similar, the PK profiles are quite disparate, with the plasma exposure of **30** almost 700-fold higher than that of **25**, while the 4-h liver levels are 100-fold higher, an observation amplified in the comparison with the matched pair of macrocyclic inhibitors **31** and **32** where the AUC and liver levels of the former compound exceed those of the latter by 28,000- and 1,500-fold, respectively [40].



The preliminary in vitro and in vivo profiling of **30**, which was designated as BMS-605339, indicated that this was a promising compound, with antiviral potency

Table 3 Antiviral and PK profiles of analogues of **30**

Compound #	R ₁	R ₂	R ₃	GT-1a IC ₅₀ (nM)	GT-1b EC ₅₀ (nM)	AUC over 4 h (μM·h)	Liver level at 4 h (ng/g)	F (rat)	Cl (mL/min/kg)	t _{1/2} (h)
33	OCH ₃	H	H	2	19	0.28	232,200	20%	182	9.8
34	H	OCH ₃	H	1	25	2.36	51,260	9%	6	2.2
35	H	Cl	H	1	25	5.50	36,160	6%	7	6.6
36	H	H	OCH ₂ CH ₃	3	12	1.83	14,630	NT	NT	NT
37	H	H	CH ₃	4	100	NT	NT	NT	NT	NT
38	H	H	F	87	117	1.46	69,560	NT	NT	NT
39	H	H	Cl	36	833	NT	NT	NT	NT	NT
40	H	H	<i>t</i> -Bu	31	209	NT	NT	NT	NT	NT
41	H	H	CN	4	586	NT	NT	NT	NT	NT

that met the criteria for advancement. An extensive survey of the SARs associated with substitution of the isoquinoline heterocycle of **30** confirmed its candidacy, with the compounds that provided seminal insights into SAR and PK profiles captured in Table 3. In the X-ray co-crystal structure of **30** with the NS3/4A construct, the isoquinoline ring is positioned over the side chain of Arg155 which forms a salt bridge with Asp168 (Fig. 4). The SARs associated with substitution of the isoquinoline ring of **30** were interpreted in the context of the effect on the electrostatic potential of the heterocycle that modulates a π -cation interaction with Arg155. However, the C-6-substituted nitrile **41** is an outlier, explained by modeling studies that suggested the potential for the electron-rich tip of the nitrile substituent to engage the positively charged center of the guanidine moiety of Arg155 [26]. Hence, the interaction of the isoquinoline ring with the NS3/4A protease and the effect of the C-6 substituent appear to take advantage of two distinct modes of engagement with the enzyme surface and, particularly, Arg155 that is sensitive to the substitution pattern (Table 4).

The results of antiviral and rat PK screening identified **30** and **33** as compounds of interest for more detailed studies. Full PK profiling of **33** in the rat revealed that while the oral bioavailability was an encouraging 20% following a dose of 15 mpk, the compound could not be detected in plasma 24-h post-dose, although liver levels at this time point were high at 4.2 μ M. This observation was concordant with IV PK parameters, with **33** cleared rapidly from plasma but partitioning readily into the liver, where drug concentration was measured as 8.0 μ M at 24 h following administration of a 5 mpk dose. This profile was not considered suitable for further progression of **33**, and attention was focused on the regioisomer **30** which, although displaying lower oral bioavailability in the rat, exhibited a less hepatotropic disposition in vivo [39]. After dosing of **30** to rats as a solution formulation, the oral bioavailability ranged from 5 to 18%, with plasma exposure of 14.1 μ M-h over a 24-h period following a 20 mpk dose [39]. Plasma levels of 24-h post-dose were 8 nM, with the liver concentration almost 100-fold higher at 730 nM. In the rat, **30** is

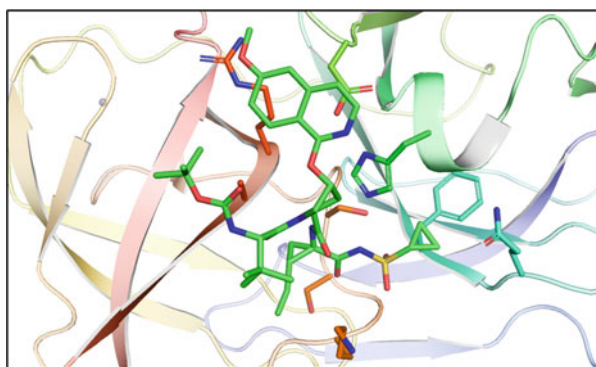


Fig. 4 X-ray co-crystal structure of **30** bound to a HCV NS3/4A protein

Table 4 PK profiles of **30** in the mouse, rat, dog, and cynomolgus monkey following IV and PO dosing

Species	Route	Dose (mpk)	t_{\max} (h)	C_{\max} (μM)	AUC_{0-t} ($\mu\text{M}\cdot\text{h}$)	Clearance (mL/min/kg)	$t_{1/2}$ (h)	V_{ss} (L/kg)	%F
Mouse	IV	4.4			2.31	46.6	1.61	1.37	
	PO	30	0.5	1.41	1.65				11
Rat	IV	2			9.03	5.3	4.7	0.4	
	IV	10			53.8	4.4	4.4	0.4	
	PO	20	1.4	5.26	14.1				13
Dog	IV	1			1.33	17.6	0.6	0.40	
	IV	4			13.9	7.4	5.1	0.33	
	PO	3	0.75	1.85	2.15				51
Cynomolgus monkey	IV	1			1.37	17.4	0.8	0.26	
	IV	3			3.91	17.9	3.7	0.60	
	PO	3	2	0.04	0.03				<1

classified as a low clearance compound, with values of 4.7 and 4.4 mL/min/kg after IV administration of doses of 2 and 10 mpk, respectively (Table 4).

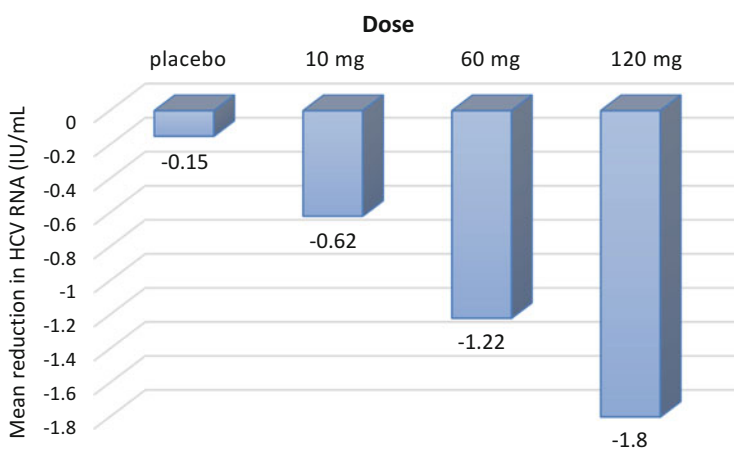
In the dog, the plasma clearance of **30** was classified as moderate, with a moderate V_{ss} and a short $t_{1/2}$ of 0.6 h following a 1 mpk IV dose. However, the AUC increased in a greater than dose-proportional fashion following a 4 mpk dose of **30**, with lower clearance and a longer $t_{1/2}$ of 5.1 h, suggesting that the drug elimination pathways were subject to saturation. In PO dosing experiments, the absorption of **30** was rapid at all doses examined, but oral bioavailability increased with exposure, rising from 23% at 1 mpk to 51% at 3 mpk. Similar to observations in the rat, the oral bioavailability of **30** in the dog was lower following administration of a suspension of the drug compared to a solution formulation, indicative of solubility- or dissolution-limited absorption. Liver levels in the dog were considerably higher than in plasma, with ratios ranging from 51 to 64 that remained constant over time (2, 8, and 24 h), consistent with parallel elimination rates from both compartments [39]. While IV clearance was moderate in the cynomolgus monkey, volume of distribution (V_{ss}) was low, and the $t_{1/2}$ value was 0.8 h after administration of a 1 mpk dose and 3.7 h following a dose of 3 mpk. The oral bioavailability of **30** in the cynomolgus monkey was poor at just 1%, attributed to rapid metabolism that was reflective of the high turnover observed in cynomolgus monkey LMs.

The HCV NS3 protease and replicon inhibitory spectrum of **30** is summarized in Table 5. In vitro analyses indicated excellent selectivity of **30** for HCV NS3/4A protease with IC_{50} values >1,000-fold higher for a panel of mammalian serine and cysteine proteases and the phylogenetically closest relative, the GBV-B NS3 protease. Compound **30** was inactive in cell culture replication assays for bovine viral diarrhea virus, canine parainfluenza virus, and HIV-1, and additional liability profiling of **30** confirmed its suitability for advancement into clinical trials [26].

After successfully completing IND toxicology studies, **30** was advanced into clinical trials following a protocol that comprised of a single ascending dose (SAD)

Table 5 Antiviral profile of **30**

Virus genotype	HCV NS3/4A protease IC ₅₀ (nM)	Replicon EC ₅₀ (nM)
1a	2	8.3
1b	0.7	2.8
2a	14	470
2b	169	ND
3a	85	1,000
4a	1.6	ND
5a	2.2	ND
6a	0.9	ND

**Fig. 5** Mean maximal reductions in plasma HCV levels following the administration of single oral doses of **30** to HCV-infected subjects. Maximal reductions at each dose occurred 12 h after drug administration

study (10, 30, 60, and 120 mg) conducted in normal healthy volunteers (NHVs) and a subsequent SAD study conducted in HCV-infected patients [26]. In the NHV study, plasma levels of **30** increased with dose, although not in a dose-proportional fashion, with a t_{\max} of ~ 1.5 h indicative of relatively rapid absorption. The terminal $t_{1/2}$ was 4–8 h, and **30** was detectable in plasma at 24-h post-drug administration. The SAD in patients infected with GT-1 HCV assessed doses of 10, 60, and 120 mg, selected based on the PK parameters determined in NHVs, with the effect of **30** on plasma viral load compared with those of a placebo control. Plasma viral RNA levels were monitored closely for 24 h and at 48, 72 and 144 h post-dose. A dose-dependent reduction in viral load was observed following administration of **30**, with the 120 mg dose associated with a mean decline of 1.8 log₁₀ international units per mL (IU/mL) measured at 12-h post-dose [26]. The dose-response data are compiled in Fig. 5.

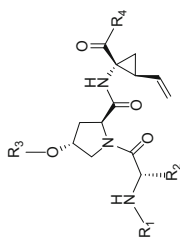
3 The Discovery of Asunaprevir (BMS-650032)

While the antiviral efficacy observed with **30** offered considerable promise, enthusiasm was tempered by the occurrence of clinically relevant electrocardiographic changes in one NHV and one HCV-infected patient following a dose of 120 mg of the drug. The effects of **30** on cardiac function were manifested as transient mild bradycardia, PR interval prolongation, and junctional rhythm disturbances that, although asymptomatic in presentation, were considered to represent an unacceptable safety risk for further clinical study, and clinical development of **30** was ended [26].

The C_{\max} value of **30** in the NHV who experienced cardiac effects was 113 nM, while in the HCV-infected patient, the C_{\max} was 206 nM, and, in each case, the effects were observed at 1-h post-dose. In preclinical studies conducted in conscious telemeterized dogs administered two 15 mpk doses of **30**, the observed cardiovascular effects were a reduction in heart rate and prolongation of the PR interval. While these general electrophysiological effects had some similarity with the observations in humans, they occurred at plasma exposures estimated to be approximately 12 μM based on studies conducted in non-telemeterized animals [1]. Since the affinity of **30** for plasma proteins was similar in dogs (98.2%) and humans (99.1%), it was concluded that humans were considerably more sensitive to the CV effects of **30** than preclinical species. In an effort to identify a predictive preclinical model, the CV effects of **30** in rabbits were investigated following IV administration of the drug to anesthetized animals. Heart rate (HR), blood pressure, and sinus node recovery time (SNRT) were monitored following incrementally increasing doses of 1, 3, and 10 mpk of **30**, with each dose infused over a 5-min period. A mild 32 beats per minute (bpm) decline in HR was noted in this experiment along with a modest reduction in blood pressure amounting to 14–23 mmHg from the baseline value; however, only the heart rate decline was drug related since changes in blood pressure were also observed in control animals infused with vehicle. The plasma concentration of **30** in this experiment peaked at 27 μM and by 60 min after the last infusion had fallen to 1.65 μM when drug concentration in cardiac tissue was 0.25 μM . The results of this study indicated that an *in vivo* rabbit evaluation protocol would not be a useful approach to identifying compounds predicted to offer reduced CV effects in humans. Evaluation of **30** in a battery of *in vitro* cardiac ion channel and receptor screens failed to identify a biochemical target, and so a Langendorff isolated rabbit heart model was investigated in an effort to more precisely understand the effects of **30** on cardiac function [1, 41]. In this model, the isolated rabbit hearts were perfused with Krebs-Henseleit solution containing **30** at concentrations of 0.3, 1, 3, and 10 μM for a period of \sim 12 min, while HR and SNRT were monitored. Declines in HR were observed at concentrations of 3 μM (–15 bpm) and 10 μM (–23 bpm) of **30** with an increase in SNRT of \geq 425 ms, effects that continued to increase during the 10 min washout period following drug perfusion. However, no effects on atrioventricular conduction time or QRS interval were observed. When rabbit hearts were perfused for 60 min at a single concentration of **30**, effects on HR

and SNRT were observed when drug was perfused at a concentration of 1 μM , but the effects were attenuated at a lower perfusion concentration of 0.3 μM and absent at 0.1 μM . These data suggested that the cardiac effects of **30** were due to a direct action of the drug on the SA node which acts as the cardiac pacemaker. Although the rabbit heart was less sensitive to the effects of **30** than humans, the Langendorff model was adopted as an in vitro liability screen since test compounds could be evaluated at high, protein-free drug concentrations, with a perfusion concentration of 10 μM selected to profile test compounds. However, the Langendorff model is a complex assay with limited throughput, necessitating a careful selection of compounds for evaluation, which sought to develop an understanding of the structure-liability relationships by evaluating systematic structural changes to **30** [1].

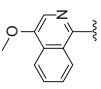
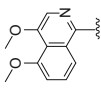
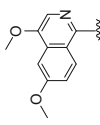
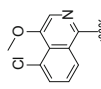
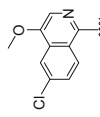
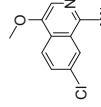
The data presented in Table 6 provided key insights into effect of molecular editing on cardiac parameters in the rabbit model. The observation of heart rate and SNRT changes associated with the carboxylic acid analogue **42** that were milder in severity than **30** was considered to absolve the cyclopropyl-acyl sulfonamide moiety as causative. This was important since the value of the cyclopropyl-acyl sulfonamide is clearly exemplified by the 100-fold compromised antiviral activity associated with **42** compared to **30**. Compounds with modifications at P₃ (**43**), P₄ (**44**), and P₂* (**45** and **46**) also exhibited significant effects on the measured rabbit heart parameters, results that indicated that identifying a compound containing potent antiviral activity with the targeted PK profile while exhibiting reduced CV effects would require considerable experimentation [1]. This consideration, coupled with the knowledge base that had been generated around the P₂* element and its effects on antiviral potency and PK, focused the attention on assessing the effects of isoquinoline substitution pattern on CV parameters, with results for the salient compounds **33**, **47–51**, and **1** compiled in Table 6. All seven of these compounds are potent GT-1a enzyme inhibitors with EC₅₀ values in the GT-1b replicon that, with the exception of **33** and **47**, are ≤ 10 nM. However, the CV effects in the Langendorff assay show a marked dependence on substitution pattern, with early structure-liability studies implicating the C-6 methoxy substituent as a contributing element. Consistent with this observation, the CV effects were moderated when the methoxy substituent was installed at the 5-position (**47**) or the 4-position (**33**) or at both the 4- and 5-position (**48**) when compared to **30**. The PK profile of **33** offered promise, with oral bioavailability of 19%, an AUC of 0.37 $\mu\text{M}\cdot\text{h}$, low clearance (9.8 mL/min/kg), and a $t_{1/2}$ of 4.3 h following a 30 mpk dose, while for **47** the oral F was 9%, the AUC was 2.7 $\mu\text{M}\cdot\text{h}$, clearance was low at 6.0 mL/min/kg, and the $t_{1/2}$ was 2.2 h. However, **33** and **47** were not progressed because of the modest potency in the GT-1b replicon with EC₅₀ values of 25 and 19 nM, respectively, that exceeded the target of ≤ 10 nM. The PK profile of **48** was less than optimal, with a short $t_{1/2}$ in the rat of 0.3 h. Nevertheless, these results encouraged further structural manipulation which revealed that the combination of 4- and 5-methoxy substitution in **49** was associated with significant effects on HR and SNRT as was the 4-methoxy and 5-chloro combination exemplified by **50**. However, the combination of a 4-methoxy substituent with either a 6-chloro (**51**) or 7-chloro (**1**) substituent moderated the CV effects, with those of **1** comparable to vehicle in the Langendorff rabbit heart assay. This CV profile was confirmed in a 60-min perfusion protocol at a

Table 6 Antiviral potency and cardiac screening of analogues of **30**

Compound #	R ₁	R ₂	R ₃	R ₄	IC ₅₀ GT-1a enzyme (nM)	EC ₅₀ GT-1b replicon (nM)	% HR change	% SNRT change
30	<i>t</i> -BuOCO	<i>t</i> -Bu		NHSO ₂ cPr	2	12	-25	290
42				OH	247	2,000	-26	37
43		<i>i</i> -Pr		NHSO ₂ cPr	2	17	-32	144
44		<i>t</i> -Bu			4	13	-44	901
45	<i>t</i> -BuOCO	<i>t</i> -Bu		NHSO ₂ cPr	4	52	-19	26
46					2	32	-37	397
47	<i>t</i> -BuOCO	<i>t</i> -Bu		NHSO ₂ cPr	1	25	-9	17

(continued)

Table 6 (continued)

Compound #	R ₁	R ₂	R ₃	R ₄	IC ₅₀ GT-1a enzyme (nM)	EC ₅₀ GT-1b replicon (nM)	% HR change	% SNRT change
33					2	19	-8	18
48					1	7	-13	20
49					1	5	-37	198
50					1	9	-44	104
51					2	10	-11	27
1					1	6	-4	5

drug concentration of 10 μM where the maximal reduction of heart rate associated with **1** was 10% and the maximal increase in SNRT was 14%, values that were similar to the vehicle control in this experiment. This result provides a second demonstration of the significant effects of subtle structural modifications on biological properties in the context of a large molecule in this series of HCV NS3/4A protease inhibitor, with the only difference in the molecular formulae between **30** and **1** being the addition of a chlorine atom [1].

The PK profile of **1** in rats was acceptable, with an oral AUC of 1.0 $\mu\text{M}\cdot\text{h}$ following a 20 mpk dose, 12% oral bioavailability, and high liver levels of 15.2 μM 24-h post-dose, reflective of a more hepatotropic disposition than **30** [1, 42]. An IV PK experiment allowed the determination of the in vivo clearance of **1**, which was 38 mL/min/kg, although the $t_{1/2}$ was reasonable at 4.2 h (Table 7). Although extensive SAR studies were conducted around **1**, with variations at P₁, P₂*, and P₄ examined, none of the analogues synthesized offered an overall profile in vitro and in vivo that surpassed that of the prototype, and **1** was examined in further detail in order to determine its suitability as a candidate for development. The PK profiles of **1** in mouse, dog, and cynomolgus monkey are compiled along with the rat data in Table 7 and reveal moderate clearance in all species with the exception of the cynomolgus monkey, a PK profile that reflects the high turnover of **1** in LMs from this species (50 ± 22 pmol/min mg which compares to 4.9 pmol/min mg in RLM, 4.7 pmol/min mg in dog LM, and 5.8 ± 1.8 in HLM). The measured in vitro clearance values correlated reasonably well with the in vivo results in the dog and monkey but underpredicted in vivo clearance in the rat and the dog, although the data were within twofold in the latter species. This was attributed to direct excretion of **1** into the bile, which amounted to 9% of the dose in the rat and 22% in the dog, and suggested the involvement of liver uptake transporters. Incubation of **1** with individual recombinant CYP enzymes revealed significant metabolic turnover only by CYP 3A4, with metabolism in HLM inhibited by ketoconazole and troleandomycin and selective CYP 3A4 inhibitors, although additional contributions to metabolism by CYP 2D6, CYP 2C9, and CYP1A2 could not be definitively ruled out. Further studies with recombinant CYP enzymes indicated that **1** was not an inhibitor of CYP 2D6, CYP 2C9, CYP 2C19, and CYP 1A2, with IC₅₀ values >40 μM , but **1** was a moderate CYP 3A4 inhibitor with IC₅₀ values of 8, 29, and 27 μM when benzyloxyresorufin (BZR), 7-benzyloxy-trifluoromethylcoumarin (BFC), and midazolam were used as substrate probes, respectively.

The permeability of **1** in a parallel artificial membrane permeability assay (PAMPA) was high (>473 nm/s at pH = 5.5 and >492 nm/s at pH = 7.4) predictive of good absorption [1, 43, 44]. The high membrane permeability associated with **1** has been attributed to its inherent conformational flexibility which allows dynamic modulation of the exposure of its polar surface elements in different environments [44]. However, in a bidirectional Caco-2 cell assay, the measured efflux ratio (ER) was 31-fold at a drug concentration of 5 μM and threefold at the higher concentration of 25 μM , indicative of saturation of efflux [43, 44]. Efflux of **1** (5 μM) was reduced significantly in these assays in the presence of inhibitors

Table 7 Single dose PK profile of **1** in preclinical species

Species	Route	Dose (mpk)	t_{\max} (h)	C_{\max} (μM)	AUC_{0-t} ($\mu\text{M}\cdot\text{h}$)	Clearance ($\text{mL}/\text{min}/\text{kg}$)	$t_{1/2}$ (h)	V_{ss} (L/kg)	%F
Mouse	IV	2			0.77	57.3	4.6	12.6	
	PO	5	6.0	0.13	0.54				28
	IV	5			2.9 ± 0.79	38 ± 10	4.2 ± 0.56	7.9 ± 7.2	
Rat	PO	15	4.0 ± 0	0.18 ± 0.08	1.0 ± 0.27				14 ± 3.7
	IV	1			1.2	18.7	1.0	0.6	
Dog	PO	3	3.0	0.60	2.2				61
	IV	1			1.3 ± 0.35	18.3 ± 5.1	1.3 ± 0.28	0.54 ± 0.18	
	PO	3	1.3 ± 0.58	0.19 ± 0.18	0.41 ± 0.28				11 ± 4.3

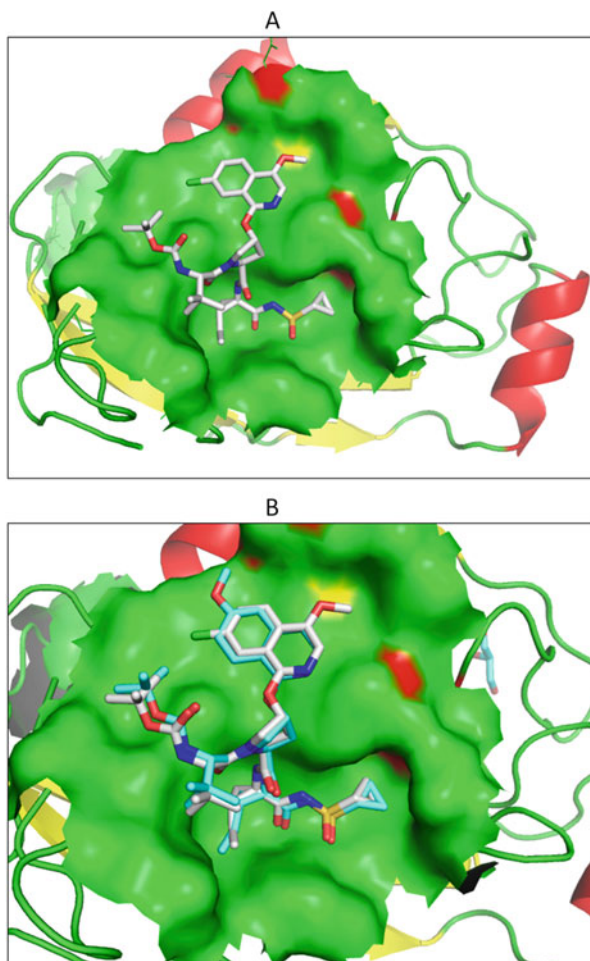
of P-gp and breast cancer resistance protein (BCRP) ($ER = 1.9$) and P-gp and multidrug resistance protein 2 (MRP2) ($ER = 1.4$) but less so in the presence of a BCRP inhibitor alone ($ER = 20$), suggesting that **1** is a substrate for P-gp and, possibly, MRP2. A role for P-gp in the disposition of **1** in vivo was confirmed with studies in P-gp knockout mice where the oral bioavailability increased to $>100\%$ compared to 28% in wild-type animals [43].

The plasma protein binding of **1** was high in rat, dog, and cynomolgus monkey plasma (97.2 – 98.8%) and comparable to human plasma, 98.8% . The V_{ss} in vivo was higher than total body water in mice and rats but similar to the total body water volume in dog and cynomolgus monkey. The liver to plasma ratios of **1** in mouse, rat, dog, and monkey measured at 8-h post-dose were 82, 555, 293 (7 h), and 248, respectively, high levels that persisted out to 24-h post-dose in the rat (300) and dog (410), indicative of a hepatotropic disposition in all of the preclinical species studied. However, **1** did not distribute effectively to CNS, endocrine, reproductive, or fatty tissues.

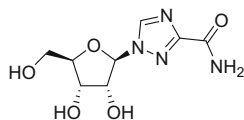
Biochemical profiling indicated that **1** was a potent and competitive inhibitor of recombinant GT-1a and GT-1b HCV NS3/4A proteases with K_i values of 0.4 nM and 0.24 nM, respectively, and an X-ray co-crystal structure highlighted the key drug-target interactions (Fig. 6) [1, 43, 45–47]. In vitro genotypic and phenotypic analysis of the emergence of resistance in GT-1a and GT-1b replicons in response to selective pressure exerted by **1** identified several substitutions that conferred low (5-fold) to moderate (21-fold) resistance to GT-1a virus in transient-transfection susceptibility assays [45]. The primary mutations were either Arg155Lys or Asp168Gly, which interacts in the NS3 protein to form a salt bridge, part of which makes contact with the isoquinoline P_2^* moiety, or at Ile170Thr, a residue interacts with the head group of Arg155 and contributes to the pocket around the Arg155-Asp168 salt bridge. While the Ile170Thr mutation suggests a subtle effect on interactions of the isoquinoline P_2^* heterocycle with the Arg155-Asp168 salt bridge, disruption of the Asp168-Arg155 salt bridge renders the Arg155 side chain mobile, modifying the planarity of the S_2^* region of NS3/4A and thereby affecting binding of the isoquinoline P_2^* heterocycle. In addition, comparison of the single crystal conformation to the bound conformation of **1** (Fig. 7) suggests significant preorganization of the ligand in the P_2^* - P_4 region. Mutations occurring in the S_2^* region would thus be expected to exert an impact on the contact surface with the protein and require disruption of the preorganized conformation of the ligand, with the fold change in resistance reflective of the extent of disruption in the optimal planar S_2^* site. In GT-1b replicons, the same selection pressures resulted in replicons with a higher level of resistance to **1**, with the primary site of mutation mapped to Asp168 and with several substitutions (Asp168Ala/Gly/His/Val/Tyr) observed that conferred high levels (16- to 280-fold) of resistance. The most prevalent GT-1b resistance mutations were Asp168Gly and Asp168Val, and these substitutions had a deleterious impact on replication capacity.

In replicon assays, **1** was a potent inhibitor of GT-1 and GT-4 replication with EC_{50} values of <5 nM but was less potent toward GT-2 and GT-3 replicons where the EC_{50} values ranged from 67 to 1,162 nM, data compiled in Table 8.

Fig. 6 Co-crystal structures of **1** bound to a HCV NS3/4A enzyme construct. (a) Co-crystal structure of **1** bound to a HCV NS3/4A enzyme construct. (b) An overlay of the co-crystal structures of **1** and **30** bound to a HCV NS3/4A enzyme construct



In combination studies, **1** demonstrated additive or synergistic activity when combined with IFN- α , the nucleoside derivative ribavirin (**52**), the HCV NS5A inhibitor **2**, and the allosteric HCV NS5B inhibitor **3**.



52 (ribavirin)

Fig. 7 (a) Single crystal structure of **1**. (b) Overlay of the single crystal structure of **1** with the protease-bound conformation of **1** (green “C” sticks)

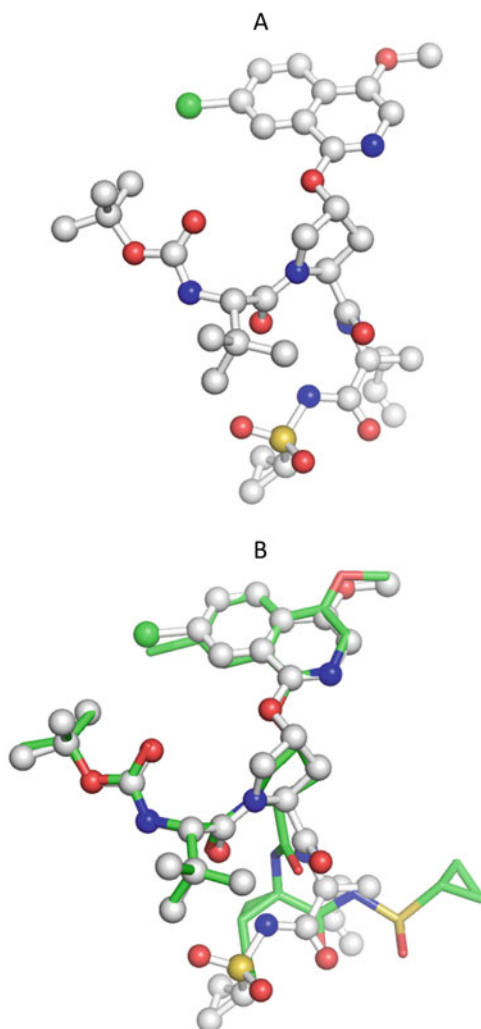


Table 8 Antiviral profile of **1**

HCV NS3 protease inhibition		HCV replicon inhibition	
HCV genotype (strain)	IC ₅₀ (nM)	Genotype (strain)	EC ₅₀ (nM)
1a (H77)	0.70 ± 0.06	1a (H77c, stable cell line)	4.0 ± 0.3
1b (J4L6S)	0.30 ± 0.02	1b (Con1, stable cell line)	1.2 ± 0.3
2a (HC-J6)	15 ± 1	2a (JFH-1, stable cell line)	230 ± 74
2b (HC-J8)	78 ± 2	3a (S52, stable cell line)	1,162 ± 274
3a (S52)	320 ± 13	4a (ED43, transient cell line)	1.8 ± 0.2
4a (ED43)	1.6 ± 0.1		ND
5a (SA13)	1.7 ± 0.2		ND
6a (HK-6A)	0.9 ± 0.1		ND

ND not determined

4 Clinical Studies with Asunaprevir

The clinical development program for **1** began with a double-blind, placebo-controlled sequential SAD study in which doses of 10, 50, 100, 200, 400, 600, and 1,200 mg of **1** were administered as an oral suspension to panels of eight NHVs in order to establish a safety profile and glean insight into plasma pharmacokinetic properties [48–51]. Adverse events (AEs) were generally mild to moderate and comparable to the placebo controls, with headache and diarrhea as the most common events that occurred in both the drug-treated and placebo groups. Most importantly in this short duration study, a detailed analysis of cardiac safety in patients revealed no evidence of an increased risk of adverse cardiac events, and there were no dose- or time-related trends in the QT interval corrected for heart rate [48]. Although **1** was detected in plasma of NHVs at 30 min post-dose, reflective of facile absorption, the PK profile of the drug was complex in nature. The terminal half-life of **1** ranged from 14 to 20 h, but the apparent oral clearance was high, and plasma levels of the compound declined in a biphasic fashion [49–51]. The rapid plasma clearance associated with **1** was consistent with the hepatotropic disposition observed in preclinical species and in subsequent studies evaluating the effect of concomitant administration of a single dose of the OATP inhibitor rifampin; the plasma C_{\max} of **1** was 21-fold higher, although there was considerable variability in the values, while the mean AUC_{inf} increased by 15-fold [52]. The plasma exposure of **1** in the context of dose was nonlinear, with incremental increases in exposure that were greater below 200 mg than above this dose (Table 9) [49–51]. In addition, the plasma exposure was higher following the dosing of **1** as a solution formulation with the mean C_{\max} and AUC_{inf} 4.4- and 1.8-fold higher, respectively, at the 50 mg dose and 10- and 2.8-fold higher, respectively, at the 200 mg dose. Collectively, these data were indicative of solubility- and dissolution-limited absorption, and when a tablet formulation of **1** was dosed concomitantly with a high-fat meal at a dose of 600 mg, the C_{\max} and AUC_{inf} values were 29.6- and 11.5-fold higher, respectively, than administration of the tablet under fasted conditions [49–51].

Based on the PK profile in NHVs, doses of 10, 50, 200, and 600 mg of **1** were selected for a double-blind, placebo-controlled sequential SAD study conducted in HCV GT-1-infected patients to assess the effect of compound on plasma HCV levels [48]. The PK parameters of **1** in this patient population were similar to NHVs although plasma exposure appeared to be slightly higher [48–51]. HCV viral load was followed for 144-h post-drug dosing, and while the virological response to **1** was minimal at the 10 mg dose, mean plasma HCV RNA declined by 0.64 \log_{10} , 2.26 \log_{10} , and 2.87 \log_{10} IU/mL following administration of single 50, 200, and 600 mg doses of **1**, respectively (Fig. 8a). A multiple ascending dose study in which **1** was administered at doses of 200, 400, and 600 mg on a twice daily schedule for 3 days to GT-1 HCV-infected individuals under a double-blind, placebo-controlled protocol confirmed the antiviral effects, with the mean maximal reductions in viral load compiled in Fig. 8b.

Table 9 Mean C_{\max} and AUC_{inf} values following the dosing of **1** as a suspension or solution formulation to NHVs and as a suspension to HCV-infected subjects

NHVs ($n = 6$ per group)			HCV-infected subjects ($n = 5$ per group)		
Dose (mg)	Mean C_{\max} (ng/mL) (SD)	Mean AUC_{inf} (ng•h/mL)	Dose (mg)	Mean C_{\max} (ng/mL) (SD)	Mean AUC_{inf} (ng•h/mL)
10	1.2 ± 0.79	7.6 ± 2.19	10	5.13 ± 5.96	34.5 ± 31.15
50	9.4 ± 2.79	82.3 ± 28.38	50	12.23 ± 4.53	104.7 ± 26.00
50 (solution)	44.02 ± 23.10)	153.9 ± 78.86			
100	38.45 ± 23.25	248.1 ± 100.17			
200	40.12 ± 18.32	423.1 ± 170.56	200	91.00 ± 98.15	763.6 ± 504.59
200 (solution)	446.5 ± 319.99	1,265.1 ± 797.79			
400	110 ± 86.00	638.5 ± 220.71			
600	1,304 ± 2,701.36	3,610.2 ± 6,715.38	600	162.00 ± 55.05	1,288.0 ± 359.65
1,200	1,016 ± 1,327.87	2,805 ± 3,000.24			

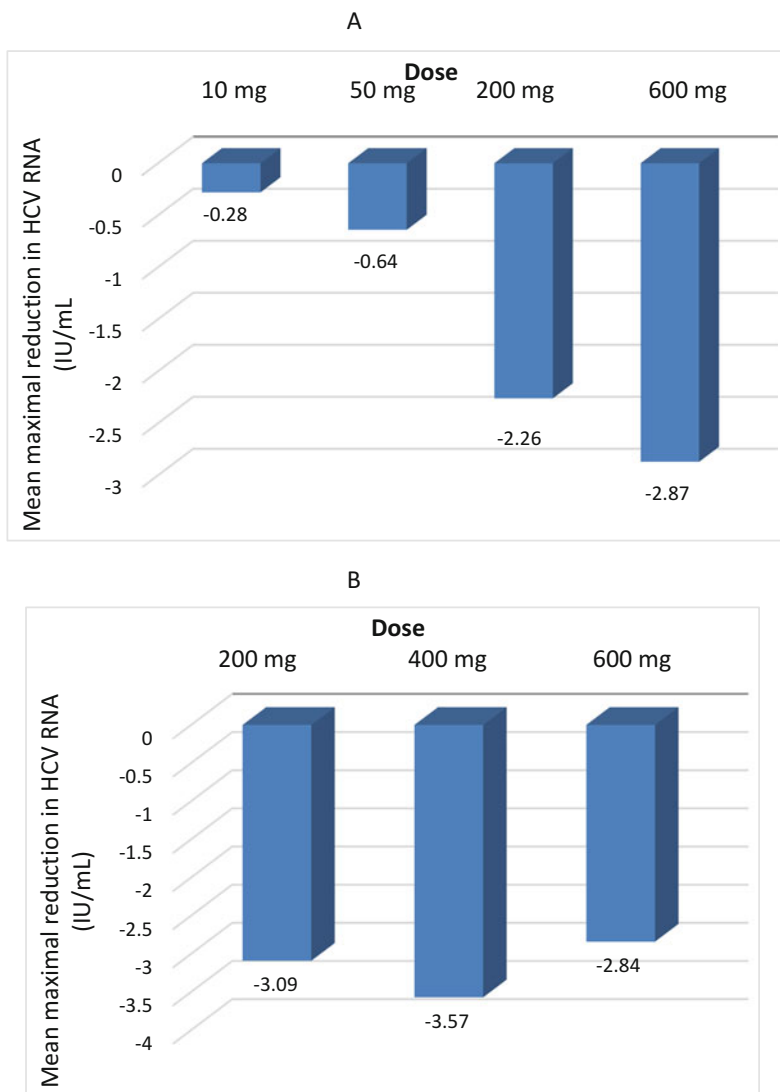


Fig. 8 (a) Mean maximal viral load reduction following oral administration of **1** to GT-1 HIV-infected patients. Maximal viral load reduction was observed at 12-h post-dose following administration of the 10, 50, and 200 mg doses, while the nadir occurred at 24 h following the 600 mg dose of **1**. (b) Mean maximal viral load reduction following oral administration of **1** twice daily to GT-1 HIV-infected patients for 3 days

The development of **1** was part of a broader strategy that sought to advance at least two direct-acting antiviral agents into clinical trials that were designed to be used in combination therapy as a means of addressing concerns surrounding the

rapid development of resistance to mono-therapeutic drug regimens. Viral RNA polymerases are recognized for their poor proofreading ability which leads to the incorporation of mismatched base pairs and the production of viruses with mutations that can resist drug action and lead to virological failure [53–60]. The frequency with which HCV RNA polymerase introduces mutations and the influence of replication rate on virus diversity has been elegantly analyzed by Perelson and explains the rapid emergence of resistance seen with the first-generation HCV NS3 protease inhibitors [61–69]. The HCV NS5A inhibitor **2** progressed into clinical trials contemporaneously with **1**, providing the opportunity to conduct a clinical trial in which the potential of the two compounds to treat a chronic HCV infection was examined [17, 18]. The patient population selected for this trial was comprised of patients who had either failed the existing standard of care therapy at the time, PEG-IFN- α , and the nucleoside analogue **52**, or who had failed to respond to this therapeutic regimen, so-called null responders [70–72]. This patient population was considered to be the most difficult to treat, and a trial against this clinical background was viewed as a stringent evaluation of the potential of DAAs to affect the course of a chronic HCV infection. In this phase IIa clinical trial, a combination of **1** (600 mg BID) and **2** (60 mg QD) was administered to 11 HCV GT-1-infected subjects for 24 weeks. The control arm for this study comprised of 10 GT-1-infected subjects who received the same dosing regimen of **1** and **2** in conjunction with the standard of care therapy of PEG-IFN- α 2a and **52** dosed for 24 weeks. The two patient cohorts were matched for viral load and virus genotype, with the majority infected with GT-1a and with 10/11 patients in the dual combination group and 9/10 in the quadruple arm group expressing the IL28B CT or TT genotypes that predict a poor response to peg-IFN α therapy rather than the responsive CC genotype (Table 10) [73–76]. In the quadruple therapy cohort, all patients had undetectable

Table 10 Results of a clinical trial comparing the combination of **1** and **2** with a quadruple combination of **1**, **2**, PEG-IFN α 2a, and **52**

Therapy	1 + 2	1 + 2 + PEG-IFN α 2a + 52
# of subjects	11	10
# GT1a/GT-1b-	9/2	9/1
HCV RNA (IU/mL)	6.8 \pm 0.6	6.6 \pm 0.8
IL28B genotype	CT or TT: 10/11 (91%) CC: 1/11 (9%)	CT or TT: 9/10 (90%) CC: 1/10 (10%)
<i>Patients with undetectable HCV RNA in plasma</i>		
Week 4	7/11 (64%)	6/10 (60%)
Week 24	5/11 (45%)	10/10 (100%)
Week 12 post-therapy (SVR ₁₂)	4/11 (36%)	10/10 (100%)
Week 24 post-therapy (SVR ₂₄)	4/11 (36%)	9/10 (90%) ^a
Week 48 post-therapy	3/11 (27%)	9/10 (90%)

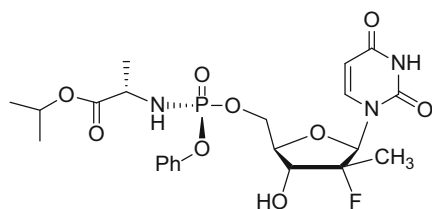
SVR₁₂ and SVR₂₄ = undetectable HCV RNA 12 and 24 weeks, respectively, after completion of 24 weeks of therapy

^aOne patient had detectable but not quantifiable HCV RNA at week 24 but was undetectable on retesting 35 days later

levels of HCV RNA in plasma at the end of therapy, a circumstance that persisted to week 12 post-therapy (SVR₁₂), data compiled in Table 10. However, one patient had detectable HCV RNA in plasma at week 24 after treatment but was undetectable 35 days later; however, this patient was classified as a failure based on the written clinical protocol. In the direct-acting antiviral cohort, 5/11 subjects had undetectable HCV RNA at the end of therapy with 1 GT-1a-infected subject relapsing post-therapy to leave 4/11 subjects who achieved SVR₁₂ (Table 10). In this cohort, both GT-1b-infected subjects achieved SVR₁₂ and SVR₂₄, while viral breakthrough was restricted to the GT-1a-infected subjects. Those subjects experiencing viral breakthrough had peg-IFN α 2a and **52** added to their drug treatment regimen, and while most responded with declines in viral load, the effect was not durable [17].

This study demonstrated for the first time that a chronic HCV infection could be cured with DAA therapy alone in the absence of an exogenous immune stimulant and **52** and was characterized as “a watershed moment” in the development of HCV DAAs [18]. The efficacy of the combination of **1** and **2** in treating GT-1b infections redirected the clinical development program toward Japan where the patient population is comprised predominantly (70%) of subjects infected with this virus genotype. In the phase III clinical trials that formed the basis of marketing approval of the dual combination of **1** and **2** for the treatment of GT-1b infection in Japan, the combination was administered at doses of 100 mg BID and 60 mg QD, respectively, for 24 weeks of therapy [77–85]. This regimen was associated with SVR₁₂ rates of 81% in the non-responder population and 87% in those either ineligible for or intolerant of PEG-IFN α therapy. In a multinational clinical trial conducted in a broad-based patient population infected with GT-1b virus, the SVR₁₂ rates were 90% for those naïve to therapy and 82% for those in the ineligible/intolerant group.

Marketing approval of the dual drug combination of **1** and **2** by the Japanese Pharmaceutical and Medical Devices Agency (PMDA) occurred on July 4, 2014 [8]. The licensing of **1** and **2** represented the first approval of a combination of DAAs for the treatment of HCV infection although the combination of **52** and the nucleoside-based HCV NS5B inhibitor prodrug sofosbuvir (**53**) was approved by the FDA in December of 2013 [86, 87].



53 (sofosbuvir)

Extending the therapeutic utility of **1** and **2** to include the treatment of HCV GT-1a infections required the addition of a third agent, the NS5B inhibitor beclabuvir (**3**), which was ultimately developed as a fixed dose combination comprising of 200 mg of **1**, 30 mg of **2**, and 75 mg of **3** administered on a BID schedule

for 12 weeks [88–93]. In an international phase III clinical study designated the UNITY 1 trial that was conducted in 415 patients infected with HCV GT-1 who were non-cirrhotic, 91% of the patients achieved SVR₁₂. This patient population in this trial comprised of both treatment-naïve and treatment-experienced patients with SVR₁₂ achieved by 92% in the former and 89% in the latter groups with virologic failure occurring in 8% of the patients. In a phase III study conducted in 202 GT-1-infected patients with compensated cirrhosis who resided in the United States, Canada, France, and Australia (UNITY-2), the SVR₁₂ rates were 93% and 87% for patients in the treatment-naïve and treatment-experienced groups, respectively. In this study, the addition of **52** to the therapeutic regimen improved SVR₁₂ rates to 98% for those naïve to treatment and 93% in those who were treatment-experienced. In the UNITY 3 phase III clinical trial that was conducted in Japanese patients infected with GT-1 HCV, SVR₁₂ rates were $\geq 95\%$ in both the larger treatment-naïve ($n = 152$) and the interferon-experienced ($n = 65$) groups following 12 weeks of therapy. In this study, SVR₁₂ rates were similar for this with cirrhosis and those aged ≥ 65 years. These studies contributed to the approval of the fixed dose combination of **1**, **2**, and **3** for marketing as Ximency[®] in Japan on December 20, 2016. Interestingly, a short duration intensification study in which HCV-infected patients were treated with a combination of **1**, **2**, **3**, and **53** for 4 or 6 weeks failed to effect high rates of cure despite 96% of the patients achieving undetectable HCV RNA levels in plasma at the end of therapy [94].

5 Conclusion

The discovery of **1** relied upon an approach rooted in structure-based drug design that identified the beneficial effects of the cyclopropyl-acyl sulfonamide moiety as the optimal P₁-P₁' moiety in a series of tripeptide-based NS3/4A inhibitors. This structural element conferred a significant enhancement in intrinsic enzyme inhibitory activity compared to carboxylic acid-based prototypes that translated effectively to potent antiviral effects in HCV replicons, which had just become available at the time that **11** was first synthesized. The value of the cyclopropyl-acyl sulfonamide in NS3/4A inhibitor drug design is underscored by the widespread adoption of this moiety as a prominent structural element that is present in all of the currently marketed HCV NS3/4A protease inhibitors. The development of the tripeptide-based inhibitors leading to **1** presented several challenges that were associated with exploring drug space beyond the rule-of-5 parameters that were beginning to be widely embraced at the time that **11** was discovered [95–101]. While identifying compounds with targeted PK profiles proved to be less arduous than the rule-of-5 parameters might have predicted, the observations of cardiac side effects in phase I clinical trials with **30** was a major disappointment and a significant hurdle to surmount. However, despite the low throughput associated with the Langendorff isolated rabbit heart assay used to triage compounds for CV effects, by the time that the decision was made to end the clinical development of **30**, the team had been able

to identify **1** by finessing the salient structure-liability relationships after screening approximately 20 compounds. The clinical trial assessing a combination of **1** with the NS5A inhibitor **2**, the discovery of which relied upon the diametrically opposite strategy of phenotypic screening and optimization, in infected HCV patients proved to be of significance to the field [11, 16, 17]. The results of this small clinical study, which demonstrated for the first time that a chronic infection could be cured by DAAs alone, subtended the advent of the well-tolerated small molecule drug combinations that have been widely approved. These DAA combinations are very effective therapeutics for the treatment of chronic HCV infections, effecting high rates of cure after just 8–12 weeks of therapy, a sharp contrast to the 48 weeks of therapy that had to be endured with PEG-IFN- α -based regimens.

Compliance with Ethical Standards

Conflict of Interest: Nicholas A. Meanwell is an employee of Bristol-Myers Squibb and holds stock in the company.

Ethical Approval: This article does not contain any preclinical studies with animals or clinical trials with human participants that were performed by any of the authors.

References

1. Scola PM, Sun L-Q, Wang AX, Chen J, Sin N, Venables BL, Sit S-Y, Chen Y, Cocuzza A, Bilder DM, D'Andrea SV, Zheng B, Hewawasam P, Tu Y, Friborg J, Falk P, Hernandez D, Levine S, Chen C, Yu F, Sheaffer AK, Zhai G, Barry D, Knipe JO, Han Y-H, Schartman R, Donoso M, Mosure K, Sinz MW, Zvyaga T, Good AC, Rajamani R, Kish K, Tredup J, Klei HE, Gao Q, Mueller L, Colonna RJ, Grasela DM, Adams SP, Loy J, Levesque PC, Sun H, Shi H, Sun L, Warner W, Li D, Zhu J, Meanwell NA, McPhee F (2015) The discovery of asunaprevir (BMS-650032), an orally efficacious NS3 protease inhibitor for the treatment of hepatitis C virus infection. *J Med Chem* 57:1730–1752
2. Meanwell NA (2016) 2015 Philip S. Portoghese medicinal chemistry lectureship. Curing hepatitis C virus infection with direct-acting antiviral agents: the arc of a medicinal chemistry triumph. *J Med Chem* 59:7311–7351
3. Reviriego C (2012) Asunaprevir. *Drugs Future* 37:247–254
4. Gentile I, Buonomo AR, Zappulo E, Minei G, Morisco F, Borrelli F, Coppola N, Borgia G (2014) Asunaprevir, a protease inhibitor for the treatment of hepatitis C infection. *Ther Clin Risk Manag* 10:493–504
5. Yang SS, Kao JH (2015) Asunaprevir-containing regimens for the treatment of hepatitis C virus infection. *Expert Rev Gastroenterol Hepatol* 9:9–20
6. Akamatsu N, Sugawara Y, Kokudo N (2015) Asunaprevir (BMS-650032) for the treatment of hepatitis C virus. *Expert Rev Anti-Infect Ther* 13:1307–1317
7. Eley T, Garimella T, Li W, Bertz RJ (2017) Asunaprevir: an HCV protease inhibitor with preferential liver distribution. *Clin Pharmacol Drug Dev* 6:195–200
8. Poole RM (2014) Daclatasvir plus asunaprevir: first global approval. *Drugs* 74:1559–1571
9. Zeuli JD, Adie SK, Rizza SA, Temesgen Z (2015) Asunaprevir plus daclatasvir for the treatment of chronic hepatitis C virus infection. *Drugs Today* 51:629–643
10. Hayes CN, Imamura M, Chayama K (2017) The practical management of chronic hepatitis C infection in Japan – dual therapy of daclatasvir plus asunaprevir. *Expert Rev Gastroenterol Hepatol* 11:103–113

11. Gao M, Nettles RE, Belema M, Snyder LB, Nguyen VN, Fridell RA, Serrano-Wu MH, Langley DR, Sun J-H, O'Boyle II DR, Lemm JA, Wang C, Knipe JO, Chien C, Colonna RJ, Grasela DM, Meanwell NA, Hamann LG (2010) Chemical genetics strategy identifies an HCV NS5A inhibitor with a potent clinical effect. *Nature* 465:96–100
12. Belema M, Nguyen VN, Bachand C, Deon DH, Goodrich JT, James CA, Lavoie R, Lopez OD, Martel A, Romine JL, Ruediger EH, Snyder LB, St. Laurent DR, Yang F, Zhu J, Wong HS, Langley DR, Adams SP, Cantor GH, Chimalakonda A, Fura A, Johnson BM, Knipe JO, Parker DD, Santone KS, Fridell RA, Lemm JA, O'Boyle II DR, Colonna RJ, Gao M, Meanwell NA, Hamann LG (2014) Hepatitis C virus NS5A replication complex inhibitors: the discovery of daclatasvir. *J Med Chem* 57:2013–2032
13. Belema M, Meanwell NA (2014) Discovery of daclatasvir, a pan-genotypic hepatitis C virus NS5A replication complex inhibitor with potent clinical effect. *J Med Chem* 57:5057–5071
14. Gentles RG, Ding M, Bender JA, Bergstrom CP, Grant-Young K, Hewawasam P, Hudyma T, Martin S, Nickel A, Regueiro-Ren A, Tu Y, Yang Z, Yeung K-S, Zheng X, Chao S, Sun J-H, Beno BR, Camac DM, Chang C-H, Gao M, Morin PE, Sheriff S, Tredup J, Wan J, Witmer MR, Xie D, Hanumegowda U, Knipe J, Masure K, Santone KS, Parker DD, Zhuo X, Lemm J, Liu M, Pelosi L, Rigat K, Voss S, Wang Y, Wang Y-K, Colonna RJ, Gao M, Roberts SB, Gao Q, Ng A, Meanwell NA, Kadow JF (2014) Discovery and preclinical characterization of the cyclopropylindolobenzazepine BMS-791325, a potent allosteric inhibitor of the hepatitis C virus NS5B polymerase. *J Med Chem* 57:1855–1879
15. Esposito I, Marciano S, Trinks J (2018) Pharmacokinetic and pharmacodynamic evaluation of daclatasvir, asunaprevir plus beclabuvir as a fixed-dose co-formulation for the treatment of hepatitis C. *Expert Opin Drug Metab Toxicol* 14:649–657
16. Lok AS, Gardiner DF, Lawitz E, Martorell C, Everson GT, Ghalib R, Reindollar R, Rustgi V, McPhee F, Wind-Rotolo M, Persson A, Zhu K, Dimitrova DI, Eley T, Guo T, Grasela DM, Pasquinelli C (2012) Preliminary study of two antiviral agents for hepatitis C genotype 1. *N Engl J Med* 366:216–224
17. Lok AS, Gardiner DF, Hézode C, Lawitz EJ, Bourlière M, Everson GT, Marcellin P, Rodriguez-Torres M, Pol S, Serfaty L, Eley T, Huang S-P, Li J, Wind-Rotolo M, Yu F, McPhee F, Grasela DM, Pasquinelli C (2014) Randomized trial of daclatasvir and asunaprevir with or without PegIFN/RBV for hepatitis C virus genotype 1 null responders. *J Hepatol* 60:490–499
18. Chung RT (2012) A watershed moment in the treatment of hepatitis C. *N Engl J Med* 366:273–275
19. Chayama K, Imamura M, Hayes CN (2016) Hepatitis C virus treatment updated. A new era of all-oral HCV treatment. *Adv Dig Med* 3:153–160
20. Zhang X (2016) Direct anti-HCV agents. *Acta Pharm Sin B* 6:26–31
21. Falade-Nwulia O, Suarez-Cuervo C, Nelson DR, Fried MW, Segal JB, Sulkowski MS (2017) Oral direct-acting agent therapy for hepatitis C virus infection. A systematic review. *Ann Intern Med* 166:637–648
22. Gedda A, Ibrahim YF, Elbahie NM, Ibrahim MA (2017) Direct acting anti-hepatitis C virus drugs: clinical pharmacology and future direction. *J Transl Int Med* 5:8–17
23. Li G, De Clercq E (2017) Current therapy for chronic hepatitis C: the role of direct-acting antivirals. *Antivir Res* 142:83–122
24. Spengler U (2018) Direct antiviral agents (DAAs) – a new age in the treatment of hepatitis C virus infection. *Pharmacol Ther* 183:118–126
25. Campbell JA, Good A (2002) World Patent Application WO-2002/060926 A2, 8 Aug 2002
26. Scola PM, Wang A, Good AC, Sun L, Combrink KD, Campbell JA, Chen J, Tu Y, Sin N, Venables BL, Sit SY, Chen Y, Cocuzza A, Bilder DM, D'Andrea S, Zheng B, Hewawasam P, Ding M, Thuring J, Hernandez D, Yu F, Falk P, Zhai G, Sheaffer AK, Chen C, Lee MS, Barry D, Knipe JO, Han YH, Jenkins S, Gesenberg C, Sinz MW, Santone KS, Zvyaga T, Rajamani R, Klei HE, Colonna RJ, Grasela DM, Hughes E, Chien C, Adams S, Levesque PC, Li D, Zhu J, Meanwell NA, McPhee F (2014) Discovery and early clinical evaluation of BMS-605339, a potent and orally efficacious tripeptidic acylsulfonamide NS3 protease inhibitor for the treatment of hepatitis C virus infection. *J Med Chem* 57:1708–1729

27. Ingallinella P, Altamura S, Bianchi E, Taliani M, Ingenito R, Cortese R, De Francesco R, Steinkühler C, Pessi A (1998) Potent peptide inhibitors of human hepatitis C virus NS3 protease are obtained by optimizing the cleavage products. *Biochemistry* 37:8906–8914
28. Linàs-Brunet M, Bailey M, Fazal G, Goulet S, Halmos T, Laplante S, Maurice R, Poirier M, Poupart M-A, Thibeault D, Wernic D, Lamare D (1998) Peptide-based inhibitors of the hepatitis C virus serine protease. *Bioorg Med Chem Lett* 8:1713–1718
29. Steinkühler C, Biasiol G, Brunetti M, Urbani A, Koch U, Cortese R, Pessi A, De Francesco R (1998) Product inhibition of the hepatitis C virus NS3 protease. *Biochemistry* 37:8899–8905
30. Imperiali B, Abeles RH (1987) Extended binding inhibitors of chymotrypsin that interact with leaving group subsites S1'-S3'. *Biochemistry* 26:4474–4477
31. Meanwell NA (2011) Synopsis of some recent tactical application of bioisosteres in drug design. *J Med Chem* 54:2529–2591
32. Heidler P, Link A (2005) *N*-Acyl-*N*-alkyl-sulfonamide anchors derived from Kenner's safety-catch linker: powerful tools in bioorganic and medicinal chemistry. *Bioorg Med Chem* 13:585–599
33. Ammazalorso A, De Filippis B, Giampietro L, Amoroso R (2017) *N*-acylsulfonamides: synthetic routes and biological potential in medicinal chemistry. *Chem Biol Drug Des* 90:1094–1105
34. Llinas-Brunet M, Bailey MD, Cameron D, Faucher A-M, Ghio E, Goudreau N, Halmos T, Poupart M-A, Rancourt J, Tzantrizos YS, Wernic DM, Simoneau B (2000) Preparation of hepatitis C inhibitory tripeptides. World Patent Application WO 2000/0009543. 24 Feb 2000
35. Llinas-Brunet M, Bailey M, Cameron D, Ghio E, Goudreau N, Poupart M-A, Rancourt J, Tzantrizos YS (2000) Hepatitis C inhibitor peptides. World Patent application WO 2000/0009558, 24 Feb 2000
36. Gunaydin H, Bartberger MD (2016) Stacking with no planarity? *ACS Med Chem Lett* 7:341–344
37. Li J, Smith D, Wong HS, Campbell JA, Meanwell NA, Scola PM (2006) A facile synthesis of 1-substituted cyclopropylsulfonamides. *Synlett* 2006:725–728
38. Venables BL, Sin N, Wang XA, Sun L-Q, Hernandez D, Sheaffer A, Lee M, Franco D, Friberg J, Yu F, Knipe J, Sandquist J, Good AC, Rajamani R, McPhee F, Meanwell NA, Scola PM (2018) P3-P4 Ureas and reverse carbamates as potent HCV NS3 serine protease inhibitors: effective transposition of the P4 hydrogen bond donor. *Bioorg Med Chem Lett* 28:1853–1859
39. Jenkins S, Scola P, McPhee F, Gesenberg C, Sinz M, Arora V, Pilcher G, Santone K (2014) Preclinical pharmacokinetics and in vitro metabolism of BMS-605339: a novel HCV NS3 protease inhibitor. *J Pharm Sci* 103:1891–1902
40. Scola P, Sun L-Q, Gillis, E, Bowsher M, Chen J, Wang X, Sit SY, Chen Y, Zheng Z, D'Andrea S, Sin N, Venables B, Mull E, Chen Q, Kandhasamy S, Pulicharla N, Vishwakrishnan S, Reddy S, Trivedi R, Sinha S, Sivaprasad S, Rao A, Desai S, Ghosh K, Rajamani R, Friberg J, Levine S, Chen C, Falk P, Jenkins S, Kramer M, Haskell R, Johnson K, Loy J, Levesque P, Zhu J, Cockett M, Meanwell N, McPhee F (2015) Discovery of a second generation, pan genotype NS3/4A protease inhibitor (BMS-986144) for the treatment of hepatitis C. In: Proceedings of 250th national ACS meeting and exposition, Boston, MA, 16–20 Aug 2015. MEDI-309
41. Langendorff O (1895) Untersuchungen am überleberden saugerleizen. *Pflugers Arch Gesamte Physiol* 61:291–332
42. Mosure KW, Knipe JO, Browning M, Arora V, Shu Y-Z, Phillip T, McPhee F, Scola P, Balakrishnan A, Soars MG, Santone K, Sinz M (2015) Preclinical pharmacokinetics and in vitro metabolism of asunaprevir (BMS-650032), a potent hepatitis C virus NS3 protease inhibitor. *J Pharm Sci* 104:2813–2823
43. McPhee F, Sheaffer AK, Friberg J, Hernandez D, Falk P, Zhai G, Levine S, Chaniewski S, Yu F, Barry D, Chen C, Lee MS, Mosure K, Sun L-Q, Sinz M, Meanwell NA, Colonna RJ,

- Knipe J, Scola P (2012) Preclinical profile and characterization of the hepatitis C virus NS3 protease inhibitor asunaprevir (BMS-650032). *Antimicrob Agents Chemother* 56:5387–5396
44. Rossi Sebastiano M, Doak BC, Backlund M, Poongavanam V, Over B, Ermondi G, Caron G, Matsson P, Kihlberg J (2018) Impact of dynamically exposed polarity on permeability and solubility of chameleonic drugs beyond the rule of 5. *J Med Chem* 61:4189–4202
 45. McPhee F, Friborg J, Levine S, Chen C, Falk P, Yu F, Hernandez D, Lee MS, Chaniewski S, Sheaffer AK, Pasquinelli C (2012) Resistance analysis of the hepatitis C virus NS3 protease inhibitor asunaprevir. *Antimicrob Agents Chemother* 56:3670–3681
 46. Ali A, Aydin C, Gildemeister R, Romano KP, Cao H, Ozen A, Soumana D, Newton A, Petropoulos CJ, Huang W, Schiffer CA (2013) Evaluating the role of macrocycles in the susceptibility of hepatitis C virus NS3/4A protease inhibitors to drug resistance. *ACS Chem Biol* 8:1469–1478
 47. Soumana DI, Ali A, Schiffer CA (2014) Structural analysis of asunaprevir resistance in HCV NS3/4A protease. *ACS Chem Biol* 9:2485–2490
 48. Pasquinelli C, McPhee F, Eley T, Villegas C, Sandy K, Sheridan P, Persson A, Huang S-P, Hernandez D, Sheaffer AK, Scola P, Marbury T, Lawitz E, Goldwater R, Rodriguez-Torres M, DeMicco M, Wright D, Charlton M, Kraft WK, Lopez-Talavera J-C, Grasela DM (2012) Single- and multiple-ascending-dose studies of the NS3 protease inhibitor asunaprevir in subjects with or without chronic hepatitis C. *Antimicrob Agents Chemother* 56:1838–1844
 49. Eley T, He B, Huang S-P, Li W, Pasquinelli C, Rodrigues AD, Grasela DM, Bertz RJ (2013) Pharmacokinetics of the NS3 protease inhibitor, asunaprevir (ASV, BMS-650032), in phase I studies in subjects with or without chronic hepatitis C. *Clin Pharmacol Drugs Dev* 2:316–327
 50. Eley T, Garimella T, Li W, Bertz RJ (2015) Asunaprevir: a review of preclinical and clinical pharmacokinetics and drug–drug interactions. *Clin Pharmacokinet* 54:1305–1222
 51. Gong J, Eley T, He B, Arora V, Philip T, Jiang H, Easter J, Humphreys WG, Iyer RA, Li W (2016) Characterization of ADME properties of [¹⁴C]asunaprevir (BMS-650032) in humans. *Xenobiotica* 46:52–64
 52. Eley T, Han Y-H, Huang S-P, He B, Li W, Bedford W, Stonier M, Gardiner D, Sims K, Rodrigues AD, Bertz RJ (2015) Organic anion transporting polypeptide-mediated transport of, and inhibition by asunaprevir, an inhibitor of hepatitis C virus NS3 protease. *Clin Pharmacol Ther* 97:159–166
 53. Steinhauer DA, Domingo E, Holland JJ (1992) Lack of evidence for proofreading mechanisms associated with an RNA virus polymerase. *Gene* 122:281–288
 54. Elena SF, Sanjuán R (2005) Adaptive value of high mutation rates of RNA viruses: separating causes from consequences. *J Virol* 79:11555–11558
 55. Barr JN, Fearn R (2010) How RNA viruses maintain their genome integrity. *J Gen Virol* 91:1373–1387
 56. Sanjuán R, Nebot MR, Chirico N, Mansky LM, Belshaw R (2010) Viral mutation rates. *J Virol* 84:9733–9748
 57. Graci JD, Gnädig NF, Galarrage JE, Castro C, Vignuzzi M, Cameron CE (2012) Mutational robustness of an RNA virus influences sensitivity to lethal mutagenesis. *J Virol* 86:2869–2873
 58. Campagnola G, McDonald S, Beaucourt S, Vignuzzi M, Peersen OB (2015) Structure-function relationships underlying the replication fidelity of viral RNA-dependent RNA polymerases. *J Virol* 8:275–286
 59. Shu B, Gong P (2016) Structural basis of viral RNA-dependent RNA polymerase catalysis and translocation. *Proc Natl Acad Sci U S A* 113:4005–4014
 60. Venkataraman S, Prasad BVLS, Selvarajan R (2018) RNA dependent RNA polymerases: insights from structure, function and evolution. *Viruses* 10:76. <https://doi.org/10.3390/v10020076>
 61. Neumann AU, Lam NP, Dahari H, Gretch DR, Wiley TE, Layden TJ, Perelson AS (1998) Hepatitis C viral dynamics in vivo and the antiviral efficacy of interferon- α therapy. *Science* 282:103–107
 62. Perelson AS, Herrmann E, Micol F, Zeuzem S (2005) New kinetic models for the hepatitis C virus. *Hepatology* 42:749–754

63. Shudo E, Ribeiro RM, Perelson AS (2009) Modeling HCV kinetics under therapy using PK and PD information. *Expert Opin Drug Metab Toxicol* 5:321–332
64. Rong L, Perelson AS (2010) Treatment of hepatitis C virus infection with interferon and small molecule direct antivirals: viral kinetics and modeling. *Crit Rev Immunol* 30:131–148
65. Ribeiro RM, Li H, Wang S, Stoddard MB, Learn GH, Korber BT, Bhattacharya T, Guedj J, Parrish EH, Hahn BH, Shaw GM, Perelson AS (2012) Quantifying the diversification of hepatitis C virus (HCV) during primary infection: estimates of the in vivo mutation rate. *PLoS Pathog* 8(8):e1002881. <https://doi.org/10.1371/journal.ppat.1002881>
66. Chatterjee A, Guedj J, Perelson AS (2012) Mathematical modeling of HCV infection: what can it teach us in the era of direct-acting antiviral agents? *Antivir Ther* 17:1171–1182
67. Sarrazin C, Kieffer TL, Bartels D, Hanzelka B, Müh U, Welker M, Wincheringer D, Zhou Y, Chu H-M, Lin C, Weegink C, Reesink H, Zeuzem S, Kwong AD (2007) Dynamic hepatitis C virus genotypic and phenotypic changes in patients treated with the protease inhibitor telaprevir. *Gastroenterology* 132:1767–1777
68. Rong L, Dahari H, Ribeiro RM, Perelson AS (2010) Rapid emergence of protease inhibitor resistance in hepatitis C virus. *Sci Transl Med* 2:1–9
69. Susser S, Welsch C, Wang Y, Zettler M, Domingues FS, Karey U, Hughes E, Ralston R, Tong X, Herrmann E, Zeuzem S, Sarrazin C (2009) Characterization of resistance to the protease inhibitor boceprevir in hepatitis C virus-infected patients. *Hepatology* 50:1709–1718
70. Hilgenfeldt EG, Schlachterman A, Firpi RJ (2015) Hepatitis C: treatment of difficult to treat patients. *World J Hepatol* 7:1953–1963
71. Suzuki H, Kakizaki S, Horiguchi N, Ichikawa T, Sato K, Takagi H, Mori M (2010) Clinical characteristics of null responders to Peg-IFN α 2b/ribavirin therapy for chronic hepatitis C. *World J Hepatol* 2:401–405
72. Palumbo E (2011) Pegylated interferon and ribavirin treatment for hepatitis C virus infection. *Ther Adv Chronic Dis* 2:39–45
73. Ge D, Fellay J, Thompson AJ, Simon JS, Shianna KV, Urban TJ, Heinzen EL, Qiu P, Bertelsen AH, Muir AJ, Sulkowski M, McHutchison JG, Goldstein DB (2009) Genetic variation in IL28B predicts hepatitis C treatment-induced viral clearance. *Nature* 461:399–401
74. Suppiah V, Moldovan M, Ahlenstiel G, Berg T, Weltman M, Lorena Abate M, Bassendine M, Spengler U, Dore GJ, Powell E, Riordan S, Sheridan D, Smedile A, Fragomeli V, Müller T, Bahlo M, Stewart GJ, Booth DR, George J, Hepatitis C Study (2009) IL28B is associated with response to chronic hepatitis C interferon- α and ribavirin therapy. *Nat Genet* 41:1100–1104
75. Tanaka Y, Nishida N, Sugiyama M, Kurosaki M, Matsuura K, Sakamoto N, Nakagawa M, Korenaga M, Hino K, Hige S, Ito Y, Mita E, Tanaka E, Mochida S, Murawaki Y, Honda M, Sakai A, Hiasa Y, Nishiguchi S, Koike A, Sakaida I, Imamura M, Ito K, Yano K, Masaki N, Sugauchi F, Izumi N, Tokunaga K, Mizokami M (2009) Genome-wide association of IL28B with response to pegylated interferon- α and ribavirin therapy for chronic hepatitis C. *Nat Genet* 41:1105–1109
76. Asselah T, Estrabaud E, Bieche I, Lapalus M, De Muynck S, Vidaud M, Saadoun D, Soumelis V, Marcellin P (2010) Hepatitis C: viral and host factors associated with non-response to pegylated interferon plus ribavirin. *Liver Int* 30:1259–1269
77. Chayama K, Takahashi S, Toyota J, Karino Y, Ikeda K, Ishikawa H, Watanabe H, McPhee F, Hughes E, Kumada H (2012) Dual therapy with the nonstructural protein 5A inhibitor, daclatasvir, and the nonstructural protein 3 protease inhibitor, asunaprevir, in hepatitis C virus genotype 1b-infected null responders. *Hepatology* 55:742–748
78. Suzuki Y, Ikeda K, Suzuki F, Toyota J, Karino Y, Chayama K, Kawakami Y, Ishikawa H, Watanabe J, Hu W, Eley T, McPhee F, Hughes E, Kumada H (2013) Dual oral therapy with daclatasvir and asunaprevir for patients with HCV genotype 1b infection and limited treatment options. *J Hepatol* 58:655–662
79. Kumada H, Suzuki Y, Ikeda K, Toyota J, Karino Y, Chayama K, Kawakami Y, Ido A, Yamamoto K, Takaguchi K, Izumi N, Koike K, Takehara T, Kawada N, Sata M, Miyagoshi H, Eley T, McPhee F, Damokosh A, Ishikawa H, Hughes E (2014) Daclatasvir plus asunaprevir for chronic HCV genotype 1b infection. *Hepatology* 59:2083–2091

80. McPhee F, Suzuki Y, Toyota J, Karino Y, Chayama K, Kawakami Y, Yu ML, Ahn SH, Ishikawa H, Bhoire R, Zhou N, Hernandez D, Mendez P, Kumada H (2015) High sustained virologic response to daclatasvir plus asunaprevir in elderly and cirrhotic patients with hepatitis C virus genotype 1b without baseline NS5A polymorphisms. *Adv Ther* 32:637–649
81. Kanda T, Yasui S, Nakamura M, Suzuki E, Arai M, Haga Y, Sasaki R, Wu S, Nakamoto S, Imazeki F, Yokosuka O (2016) Daclatasvir plus asunaprevir treatment for real-world HCV genotype 1-infected patients in Japan. *Int J Med Sci* 13:418–423
82. Kumada H, Suzuki F, Suzuki Y, Toyota J, Karino Y, Chayama K, Kawakami Y, Fujiyama S, Ito T, Itoh Y, Tamura E, Ueki T, Ishikawa H, Hu W, McPhee F, Linaberry M, Hughes E (2016) Randomized comparison of daclatasvir+asunaprevir versus telaprevir+peginterferon/ribavirin in Japanese hepatitis C virus patients. *J Gastroenterol Hepatol* 31:14–22
83. Akuta N, Sezaki H, Suzuki F, Kawamura Y, Hosaka T, Kobayashi M, Kobayashi M, Saitoh S, Suzuki Y, Arase Y, Ikeda K, Kumada H (2017) Favorable efficacy of daclatasvir plus asunaprevir in treatment of elderly Japanese patients infected with HCV genotype 1b aged 70 and older. *J Med Virol* 89:91–98
84. Toyoda H, Kumada T, Tada T, Shimada N, Takaguchi K, Senoh T, Tsuji K, Tachi Y, Hiraoka A, Ishikawa T, Shima T, Okanoue T (2017) Efficacy and tolerability of an IFN-free regimen with DCV/ASV for elderly patients infected with HCV genotype 1B. *J Hepatol* 66:521–527
85. Sezaki H, Suzuki F, Hosaka T, Akuta N, Fujiyama S, Kawamura Y, Kobayashi M, Suzuki Y, Saitoh S, Arase Y, Ikeda K, Kobayashi M, Kumada H (2017) The efficacy and safety of dual oral therapy with daclatasvir and asunaprevir for genotype 1b in Japanese real-life settings. *Liver Int* 37:1325–1333
86. Gane EJ, Stedman CA, Hyland RH, Ding X, Svarovskaia E, Symonds WT, Hindes RG, Berrey MM (2013) Nucleotide polymerase inhibitor sofosbuvir plus ribavirin for hepatitis C. *N Engl J Med* 368:34–44
87. Keating GM (2014) Sofosbuvir: a review of its use in patients with chronic hepatitis C. *Drugs* 74:1127–1146
88. Poordad F, Sievert W, Mollison L, Bennett M, Tse E, Brau N, Levin J, Sepe T, Lee SS, Angus P, Conway B, Pol S, Boyer N, Bronowicki J-P, Jacobson I, Muir AJ, Reddy KR, Tam E, Ortiz-Lasanta G, de Ledinghen V, Sulkowski M, Boparai N, McPhee F, Hughes E, Swenson ES, Yin PD, UNITY-1 Study Group (2013) Fixed-dose combination therapy with daclatasvir, asunaprevir, and beclabuvir for noncirrhotic patients with HCV genotype 1 infection. *J Am Med Assoc* 313:1728–1735
89. Muir AJ, Poordad F, Lalezari J, Everson G, Dore GJ, Herring R, Sheikh A, Kwo P, Hézode C, Pockros PJ, Tran A, Yozviak J, Reau N, Ramji A, Stuart K, Thompson AJ, Vierling J, Freilich B, Cooper J, Ghesquiere W, Yang R, McPhee F, Hughes EA, Swenson ES, Yin PD (2015) Daclatasvir in combination with asunaprevir and beclabuvir for hepatitis C virus genotype 1 infection with compensated cirrhosis. *J Am Med Assoc* 313:1736–1744
90. Hassanein T, Sims KD, Bennett M, Gitlin N, Lawitz E, Nguyen T, Webster L, Younossi Z, Schwartz H, Thuluvath PJ, Zhou H, Rege B, McPhee F, Zhou N, Wind-Rotolo M, Chung E, Griffies A, Grasela DM, Gardiner DF (2015) A randomized trial of daclatasvir in combination with asunaprevir and beclabuvir in patients with chronic hepatitis C virus genotype 4 infection. *J Hepatol* 62:1204–1206
91. Toyota J, Karino Y, Suzuki F, Ikeda F, Ido A, Tanaka K, Takaguchi K, Naganuma A, Tomita E, Chayama K, Fujiyama S, Inada Y, Yoshiji H, Watanabe H, Ishikawa H, Hu W, McPhee F, Linaberry M, Yin PD, Swenson ES, Kumada H (2017) Daclatasvir/asunaprevir/beclabuvir fixed-dose combination in Japanese patients with HCV genotype 1 infection. *J Gastroenterol* 52:385–395
92. Kao JH, Yu ML, Peng CY, Heo J, Chu CJ, Chang TT, Lee YJ, Hu TH, Yoon KT, Paik SW, Lim YS, Ahn SH, Isakov V, McPhee F, Hu W, Swenson ES, Yin PD, Treitel M (2017) Daclatasvir/asunaprevir/beclabuvir, all-oral, fixed-dose combination for patients with chronic hepatitis C virus genotype 1. *J Gastroenterol Hepatol* 32:1998–2005

93. Ahmed AM, Doheim MF, Mattar OM, Sherif NA, Truong DH, Le Hoa PT, Hirayama K, Huy NT (2017) Beclabuvir in combination with asunaprevir and daclatasvir for hepatitis C virus genotype 1 infection: a systematic review and meta-analysis. *J Med Virol* 90:907–918
94. Sulkowski MS, Flamm S, Kayali Z, Lawitz EJ, Kwo P, McPhee F, Torbeyns A, Hughes EA, Swenson ES, Yin PD, Linaberry M (2017) Short-duration treatment for chronic hepatitis C virus with daclatasvir, asunaprevir, beclabuvir and sofosbuvir (FOURward study). *Liver Int* 37:836–842
95. Lipinski CA, Lombardo F, Dominy BW, Feeney PJ (1997) Experimental and computational approaches to estimate solubility and permeability in drug discovery and development settings. *Adv Drug Deliv Rev* 23:3–25
96. Lipinski CA (2000) Drug-like properties and the causes of poor solubility and poor permeability. *J Pharmacol Toxicol Methods* 44:235–249
97. Meanwell NA (2011) Improving drug candidates by design: a focus on physicochemical properties as a means of improving compound disposition and safety. *Chem Res Toxicol* 24:1420–1456
98. Meanwell NA (2016) Improving drug design: an update on recent applications of efficiency metrics, strategies for replacing problematic elements, and compounds in nontraditional drug space. *Chem Res Toxicol* 29:564–616
99. Doak BC, Over B, Giordanetto F, Kihlberg J (2014) Oral druggable space beyond the rule of 5: insights from drugs and clinical candidates. *Chem Biol* 21:1115–1142
100. Doak BC, Zheng J, Dobritzsch D, Kihlberg J (2016) How beyond rule of 5 drugs and clinical candidates bind to their targets. *J Med Chem* 59:2312–2327
101. Zhao H (2011) Lead optimization in the nondrug-like space. *Drug Discov Today* 16:158–163

The Invention of Grazoprevir: An HCV NS3/4a Protease Inhibitor



John A. McCauley and Michael T. Rudd

Contents

1	Introduction	356
2	P2–P4 Macrocyclic Design and Synthesis	358
3	Invention of Vaniprevir	363
4	Bis-Macrocycles	367
5	Invention of Grazoprevir	368
6	Conclusions	381
	References	382

Abstract The development of highly potent and efficacious HCV NS3/4a protease inhibitors has been a key factor in the recent evolution of all-oral HCV infection therapies. While many different NS3/4a inhibitors progressed into clinical development, the P2–P4 macrocycle grazoprevir has proven to be a cornerstone of one of the most effective treatments (ZEPATIER, in combination with NS5a inhibitor elbasvir) leading to sustained virologic response rates of >90%. The path to the invention of grazoprevir was ultimately successful due to a number of key medicinal chemistry decisions and strategies. Molecular modeling inspired the original P2–P4 macrocyclic design, and the flexibility and reliability of the ring-closing metathesis reaction proved instrumental in the rapid synthesis of diverse analogs. The identification of the P2 heterocycle present in grazoprevir was discovered through exploration of novel chemical space enabled by a key synthesis-inspired design strategy. This chapter details the design and synthesis elements of the program in addition to the optimization for broad genotype and mutant enzyme potency, cellular activity, and liver exposure in preclinical species which ultimately led to the invention of grazoprevir.

Keywords Grazoprevir, HCV NS3/4a, Hepatitis C, Protease inhibitor, Ring-closing metathesis, Synthesis-inspired design, ZEPATIER

J. A. McCauley (✉) and M. T. Rudd
Department of Medicinal Chemistry, Merck & Co., Inc., West Point, PA, USA
e-mail: john_mccauley@merck.com

1 Introduction

Hepatitis C virus (HCV) infection [1] continues to represent a major health issue, with estimates of 130 million to 170 million people infected worldwide [2]. While HCV is slow to progress, the disease ultimately leads to liver damage in up to 50% of individuals as well as hepatocellular carcinoma in a significant number of cases [3]. Multiple genotypes of this positive strand RNA *Flaviviridae* virus exist, in addition to virtually unlimited quasispecies [4]. The modest sustained virologic response (SVR) rates for the most common genotype worldwide (gt 1), coupled with significant adverse events (AEs) and extended treatment duration of the previous standard-of-care therapies (pegylated interferon-alpha/ribavirin; PEG-IFN/RBV) [5], sparked a significant effort to identify more effective and better-tolerated treatments. These efforts have focused on direct inhibitors of several key nonstructural proteins essential for viral replication [6].

The treatment of HCV infection has undergone a revolution over the last 10 years. Initially, the PEG-IFN/RBV standard of care has been modified with the addition of NS3/4a protease inhibitors [7]. This treatment change led to increased SVR rates in both naïve and treatment-experienced patients. More recently, all-oral therapies that exhibit SVR rates of better than 90% have eliminated the need for the less-effective interferon-based therapies that showed high rates of intolerable side effects and required difficult dosing regimens. The all-oral therapies currently on the market are based on a several different combinations of inhibitors of NS5b polymerase, NS3/4a protease, and the NS5a replication complex.

This chapter will focus on the discovery of a new class of HCV NS3/4a protease inhibitors by the Merck Sharp & Dohme (MSD) team, located in West Point, PA, USA, and Rome, Italy. These efforts ultimately led to the invention of grazoprevir which, along with NS5a inhibitor elbasvir, is prescribed as ZEPATIER for the treatment of HCV infection.

The HCV NS3 protein consists of two domains: an N-terminal serine protease and a C-terminal RNA helicase [8]. NS4a is a peptide that binds to NS3 and is a critical cofactor for polyprotein maturation. The NS3/4a complex mediates proteolysis of the HCV polyprotein, cleaving four junctions between the nonstructural proteins, and is required for replication [9]. Early work on inhibition of NS3/4a protease focused on the discovery and optimization of peptide-based protease inhibitors. Boehringer Ingelheim showed that the N-terminal hexapeptide product of substrate cleavage (DDIVPC-OH) was an inhibitor of the enzyme (**1**, Fig. 1) [10]. Optimization of this lead led to a sub-micromolar inhibitor, while concurrent

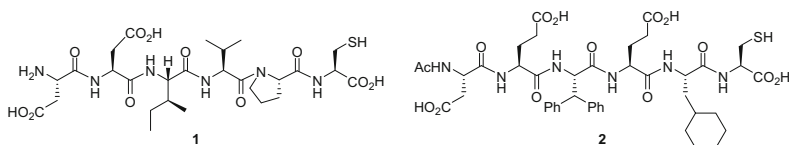


Fig. 1 Peptide-based HCV NS3 inhibitors

work at IRBM also led to the discovery of product inhibition of NS3 [11]. One product of cleavage of the NS4a-NS4b peptide (Ac-DEMEEC-OH) was a competitive inhibitor of NS3 with a K_i of 0.6 μM . Using single mutations and combinatorial techniques, this peptide was optimized to a hexamer (**2**) with an IC_{50} against NS3 protease of 55 nM. In both of these efforts, specific interactions between the peptide inhibitors and NS3 were discovered, and fundamental contributions to SAR were made. These included the recognition that the P1 carboxylic acid was critical for activity. This fundamental and pioneering work formed the basis for the discovery of multiple therapeutic agents in the NS3/4a protease inhibitor class [12].

HCV NS3/4a protease inhibitors that have entered clinical development can be classified by their modes of interaction with the protease, ketoamides that participate in slowly reversible covalent binding events with the active-site serine and typically more rapidly reversible non-covalent inhibitors. Building from the peptide-based inhibitors and incorporation of two different fused proline cores led to the development of the initial NS3/4a protease inhibitors to gain FDA approval, boceprevir (**3**, VICTRELIS) [13] and telaprevir (**4**, INCIVEK/INCIVIO) [14], both of which belong to the ketoamide class of molecules (Fig. 2).

The reversible inhibitor structural class is significantly larger than the covalent binder class and can itself be broken down into three subclasses based on structure: P1–P3 macrocyclic, acyclic, and P2–P4 macrocyclic compounds. The prototypical non-covalent inhibitor is a highly potent P1–P3 macrocycle discovered at Boehringer Ingelheim, ciluprevir (BILN-2061, **5**, Fig. 3) [15] which was the first HCV NS3/4a inhibitor to demonstrate efficacy in the clinic – showing multi-log drops in viral load during a Phase 1b study [16]. Development of ciluprevir was subsequently discontinued due to cardiac findings in rhesus safety studies [17]. Ciluprevir contains several structural features that proved important to the field as a whole, most notably the P1 vinylcyclopropane carboxylic acid and the P1–P3 macrocycle. Following the clinical proof of concept established for the inhibition of the HCV NS3/4a protease mechanism of action with ciluprevir [15, 16], a number of research groups chose this molecule as a starting point for novel compound/series development. Elaboration and modification of the P1–P3 macrocyclic scaffold core, as well as the acyclic scaffold, have provided multiple compounds that have advanced into clinical development. A number of key compounds demonstrate significant breakthroughs with regard to structural features of NS3/4a protease inhibitors. Danoprevir (**6**, Fig. 3) [18–20] is an example of the wide variety of P2 heterocycles that can be employed in this framework. The cyclopropyl sulfonamide replacement for the carboxylic acid in ciluprevir was initially utilized

Fig. 2 Ketoamide HCV NS3 inhibitors

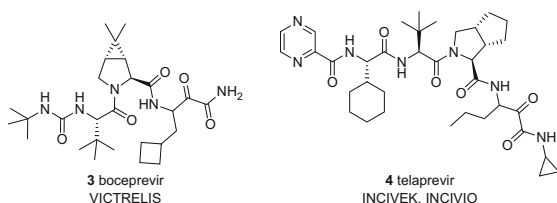


Fig. 3 P1–P3 macrocyclic HCV NS3 inhibitors and acyclic HCV NS3 inhibitors

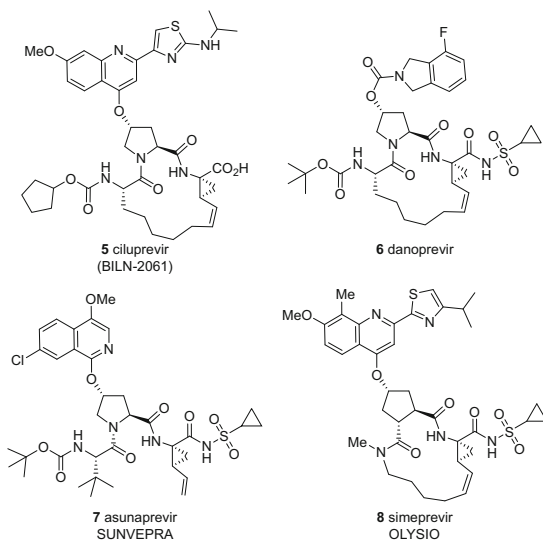
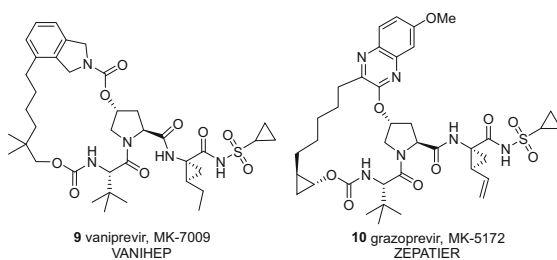


Fig. 4 P2–P4 macrocyclic HCV NS3 inhibitors



by the BMS group in asunaprevir (**7**, SUNVEPRA) [21]. In addition, simeprevir (**8**, OLYSIO) [22] from Medavir/J&J, showed that the central proline could be successfully replaced as well.

The third class of reversible protease inhibitors is the P2–P4 macrocyclic class, which was invented by the MSD team using a modeling-based approach [23]. This effort led to multiple clinical candidates, including the approved protease inhibitors vaniprevir (**9**, VANIHEP) [24, 25] and grazoprevir (**10**, ZEPATIER) [26, 27] (Fig. 4), which are described in detail below.

2 P2–P4 Macrocyclic Design and Synthesis

The starting point for the invention of P2–P4 macrocyclic NS3/4a inhibitors emerged from examining published views of a close analog of BILN-2061 (**5**) bound to the 1–180 protease domain of NS3 protease [28]. This suggested that the P2 thiazolylquinoline portion of the inhibitor lies on a relatively featureless enzyme

surface with binding interactions that provide little apparent basis for the very large contribution to potency derived from that moiety [29]. To rationalize this, the MSD team chose to model **5** bound to the full-length NS3/4a protein, including the significantly larger helicase domain (Fig. 5), to determine the extent of any role the helicase could play in inhibitor binding. The specific role of the helicase in binding has been the subject of debate in the literature [30], though recent X-ray structures have confirmed that the helicase does make contact with NS3 inhibitors [31]. However at the time, no full-length structures with inhibitors bound were available; consequently, a published apoenzyme structure [32] was used as the starting point for docking studies. To permit access of the inhibitor to the active site, the six C-terminal residues (DLEVVT) of the helicase domain that lie in the active site of the apo X-ray structure were truncated. Analysis of **5** docked in the latter structure suggested that the helicase domain could provide a surface over the P2 moiety, including a hydrophobic pocket that appeared to accommodate the thiazolyl substituent.

Specific inhibitor-helicase interactions in this model include His528-carbamate oxygen and Gln526-quinoline. The other key finding from this study was that space between the carbamate cyclopentane and the quinoline ring could potentially accommodate a macrocyclic connection. This concept was supported by reexamination of the helicase C-terminus from the apo structure, overlaid with BILN-2061 (Fig. 6), in which the side chain of Glu628 occupies the same space as the proposed linker. Together, these observations suggested that an alternative P2 quinoline–P4 cyclopentyl macrocyclization to form a structurally distinct series of inhibitors was feasible.

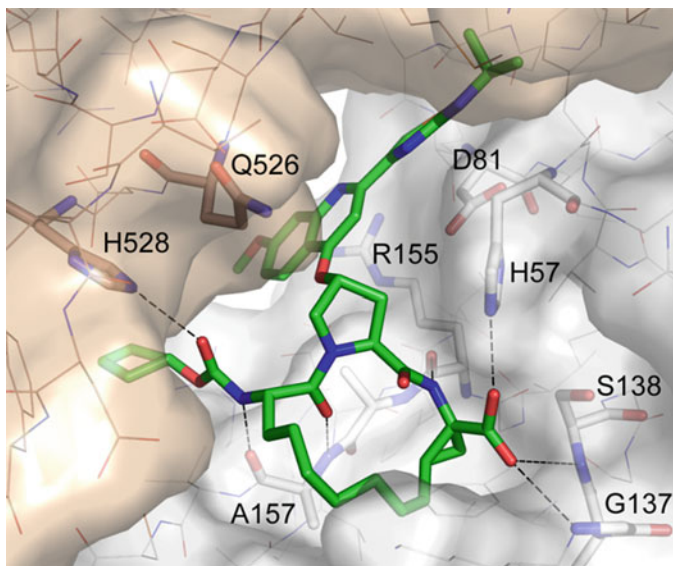


Fig. 5 Model of **5** (green) bound to full-length NS3/4a (protease, white; helicase, light brown) with key protein-inhibitor interactions shown

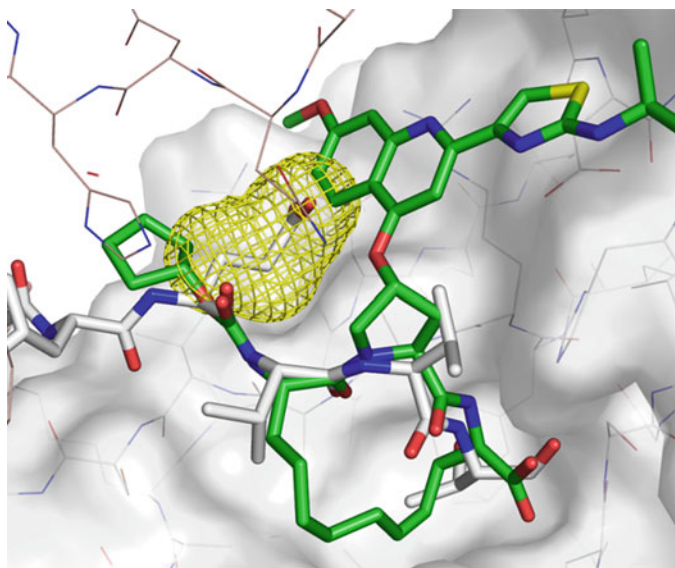
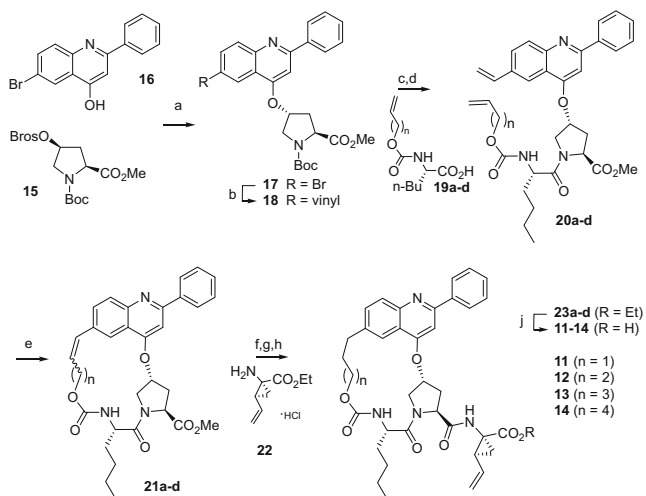


Fig. 6 Model of **5** bound to full-length NS3/4A with helicase C-terminus (white) restored and Glu628 highlighted with mesh surface

To test this hypothesis, the initial molecules targeted were carbamate derivatives **11–14** (Scheme 1, Fig. 7 shows **13** docked and overlaid with BILN-2061), in which the P1–P3 macrocyclic linker was disconnected, the proposed P2–P4 linker was formed, and a simplified 3-phenylquinoline P2 was utilized. Energy scores for the different linker lengths calculated by two methods predicted that the 5- and 6-carbon linkers would show greatest activity (Table 1).

The desired compounds were prepared, as outlined in Scheme 1, via a synthetic sequence featuring a ring-closing metathesis (RCM) reaction [33, 34] as the key macrocycle-forming event. Displacement of the brosylate of proline derivative **15** [35] with bromohydroxyquinoline **16** yielded ether **17**, which was vinylated via a palladium-catalyzed Stille reaction with tributylvinyltin to give **18**. Subsequent removal of the Boc protecting group and coupling with the appropriate norleucine carbamate derivatives **19a–d** afforded key RCM precursors **20a–d**. Ring closure was accomplished in excellent yield (84–93%) with the Zhan 1B catalyst [36] in 1,2-dichloroethane to give macrocyclic olefins **21a–d**. Conversion to the desired products (**11–14**) was carried out via hydrogenation of the styryl olefin, hydrolysis of the proline ester, coupling with cyclopropylaminoester **22** [37] to afford **23a–d** and hydrolysis of the P1 ethyl ester. The RCM reaction was a critical element in this stage of the program, providing a rapid and flexible means of testing the macrocyclization hypothesis. This reaction would continue to have a major impact throughout the program.

Compound **11**, with three carbons between the carbamate oxygen and the P2 quinoline, proved to have very modest activity of 2,000 nM in a genotype 1b



Scheme 1 Conditions: (a) Cs_2CO_3 , NMP, 40°C , 86%; (b) $\text{Bu}_3\text{SnCH}=\text{CH}_2$, $\text{Pd}(\text{PPh}_3)_4$, toluene, 100°C , 79%; (c) 4 N HCl, dioxane; (d) HATU, DIPEA, DMAP, DMF, **19a-d**; (e) Zhan 1B catalyst [36], DCE, ~10 mM, 84–93%; (f) H_2 , 10% Pd/C, EtOAc; (g) LiOH, THF, MeOH, H_2O ; (h) HATU, DIPEA, DMAP, **22**, DMF; (j) LiOH, THF, MeOH, H_2O . Zhan 1B catalyst = 1,3-bis(2,4,6-trimethylphenyl)-4,5-dihydroimidazol-2-ylidene[2-(i-propoxy)-5-(*N,N*-dimethylaminosulfonyl)phenyl] methyleneruthenium (II) dichloride

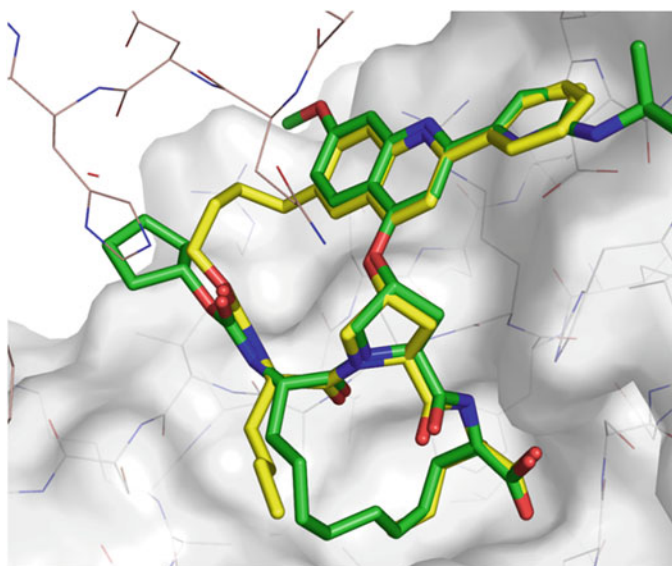
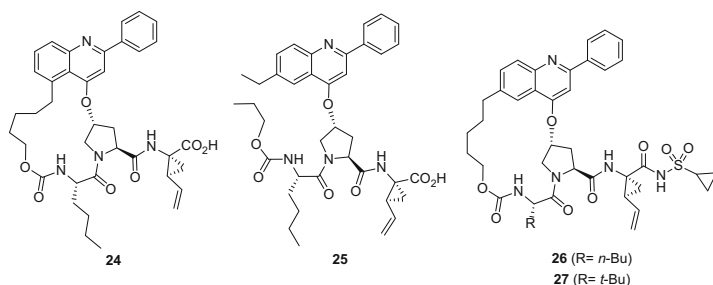


Fig. 7 Target macrocycle **13** (yellow) overlaid with **5** (green)

Table 1 In vitro activity of P2–P4 macrocycles^a

Comp	Modeling		GT 1b K_i (nM) ^b	GT 1b replicon IC_{50} (nM) ^c	
	E_{inter} ^a	Xscore ^a		10% FBS	50% NHS
5			0.3	3	19
11	−69.5	8.09	2,000	–	–
12	−70.5	8.26	145	6,100	>100,000
13	−71.1	8.36	8.5	1,150	5,600
14	−71.4	8.44	25	1,200	9,100
24			4,400	–	–
25			40	4,800	>100,000
26			<0.016	6.7	26
27			<0.016	13	25

^aFor molecular modeling details, see [23]^bNS3/4a protease time-resolved fluorescence assay^cCell-based replicon assay; in the presence of 10% FBS or 50% NHS**Fig. 8** Phenylquinoline analogs

NS3/4A enzyme inhibition assay [38] (Table 1). As predicted however, incremental lengthening of the linker afforded dramatic improvements with optimized activity of 8.5 nM in the case of the C5-linked **13**. The improved enzyme inhibition of **13** also translated to a corresponding improvement in genotype 1b cell-based replicon activity [39]. The point of attachment of the macrocyclic linker on the P2 quinoline was critical to the activity as demonstrated by synthesis of the corresponding 5-substituted derivative **24** (Fig. 8), which proved much less active (K_i 4,400 nM). Synthesis of an acyclic analog, **25**, demonstrated that potency enhancement, particularly in the replicon assay, could be achieved through a P2–P4 macrocyclization strategy. While there are reports of compounds employing a related P2–P4 cyclization strategy [40, 41], the inhibitors had no P2 substituent linked directly to the proline and displayed modest micromolar potencies. Synthesis of the cyclopropylacylsulfonamide analog of one of these P2–P4 compounds had little effect on potency [23].

Replacement of the P1 carboxylic acid functionality in **13** with the cyclopropylacylsulfonamide [42–44] led to a dramatic increase in potency and afforded a

Table 2 Liver exposure of compounds **26** and **27**^a

Compound	C _{max} (nM)	Plasma AUC 0–4 h (μMh)	4 h liver concentration (μM)
26	7	0.006	0.2
27	6	0.01	3.9

^aCompounds dosed at 2 mg/kg PO in PEG400 (*n* = 3)

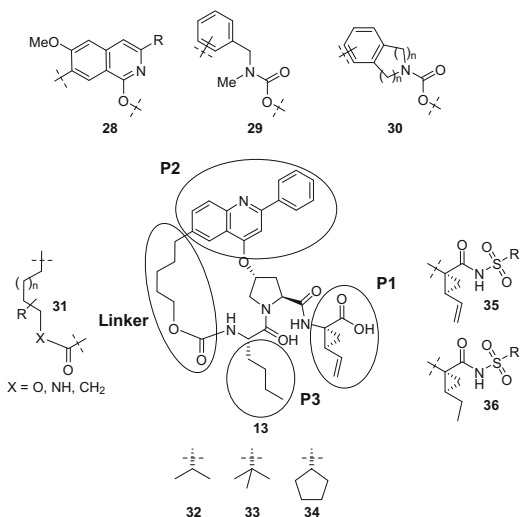
sub-nanomolar inhibitor of NS3/4A protease (**26**, Fig. 8). Disappointingly, given the critical need for liver exposure, oral administration of **26** to rats at 5 mpk P.O. provided low (0.2 μM) compound levels in the liver at 4 h with barely detectable plasma exposure (Table 2). In a surprising result, when the P3 *n*-butyl residue was replaced with the isomeric *t*-butyl group, the resultant inhibitor **27**, which had a very similar in vitro activity profile, was effectively partitioned into the liver with a tissue concentration at 4 h of 3.9 μM, although plasma levels were unimproved. The dramatic impact of this minor structural change on liver levels of **27** strongly suggested that uptake was via an active transporter-mediated process.

3 Invention of Vaniprevir

With the P2–P4 macrocyclization strategy validated by the attractive potency and liver exposure of compound **27** [23], further exploration of the macrocyclic scaffold was initiated. In this investigation, the RCM reaction was again critical. An additional benefit of the P2–P4 macrocyclic class relative to the P1–P3 structural class is the potential to use a range of macrocyclization strategies in advanced process development, including intramolecular Heck or Suzuki reactions, proline amide [45] coupling, or RCM. This contrasts with synthetic approaches to P1–P3 compounds, where an RCM macrocyclization step appears to be the only viable strategy [46]. In the exploration of SAR, however, the RCM provided a flexible way to vary many parts of the molecule while maintaining the reliability of the key ring-forming step [33, 47, 48]. Over the course of the first stage of the NS3 program, this modular synthetic approach was used to explore the P1, P2, and P3 substituents as well as the linker region extensively (Fig. 9). The literature provides examples of significant diversity in substituents in the P2 region, as shown above with compounds **5–8** (Fig. 3). This region tolerated many different substituents in both the direct-linked and carbamate-linked class as shown with **28–30** (Fig. 9) [49, 50]. Substituted linkers of varying length in the carbamate, urea, and amide series were also explored (**31**), along with branched alkyl groups in P3 (**32–34**). In the P1 region, acids and a variety of substituted acylsulfonamides were employed with vinyl, ethyl, and other pendant groups (**35–36**).

Initial optimization of the P2–P4 macrocyclic class led to the highly potent isoindoline compound (**37**, Table 3) with 50 pM activity versus the genotype 1b enzyme and 7 nM activity in the replicon assay (Table 3). Compound **37** also showed liver exposure in rat of 0.91 μM at the 4 h time point following a single

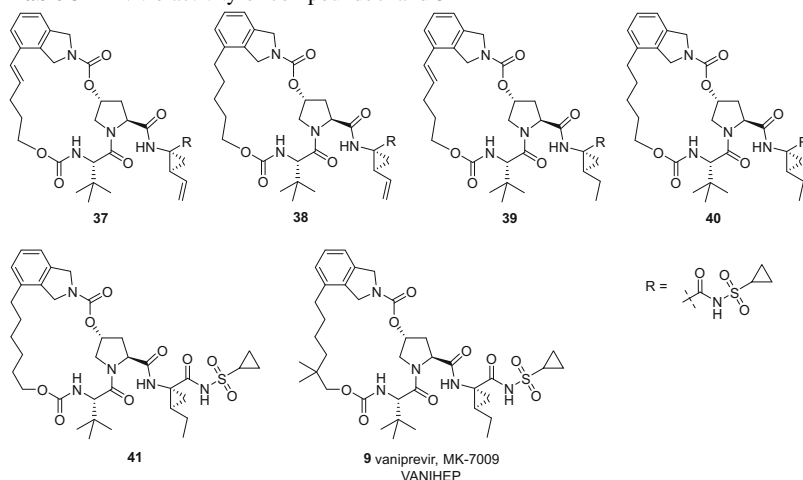
Fig. 9 General description of SAR investigations of the P2–P4 macrocyclic framework of **13**



5 mg/kg oral dose. Based on the need for high liver exposure with any anti-HCV drug [23], rat liver concentrations were used as the primary pharmacokinetic readout for evaluating compounds. On the basis of these data, **37** became an important lead for the program.

A study to examine the effect of saturation of each of the two olefins present in **37** was undertaken as part of extensive SAR studies. Reduction of the macrocyclic olefin provided **38** (Table 3), which had a virtually identical potency and pharmacokinetic profile to that of **37**. Saturation of the P1 vinyl group to the P1 ethyl (**39**) led to a ~fourfold increase in rat liver concentration, but this was accompanied by a ~tenfold loss in potency. The fully saturated compound (**40**), however, maintained much of the potency of **37** but showed improved liver exposure (10.7 μM) at a 5 mg/kg oral dose to rats. These observations underscore the unpredictability of liver exposure of compounds in the program and validated the decision to pursue an empirical strategy. Encouraged by the liver exposure of **40**, the MSD group undertook further profiling of the compound. Interestingly, compound **40** showed significantly reduced genotype 2a replicon activity, as opposed to good activity against genotype 1b. In fact, only **38** in this series was below 100 nM in the genotype 2a replicon assay.

Further work in the linker region of the molecule solved the genotype 2a activity issue. Simple addition of a methylene group (**41**) gave a small boost in genotype 1b replicon activity but also led to a >tenfold increase in genotype 2a replicon activity (Table 3). Somewhat unexpectedly, the liver exposure seen with **41** was about fivefold lower than **40**, even though the structures only differ by one methylene unit in the linker. Installation of a dimethyl group β to the carbamate oxygen gave compound **9**, which showed a concentration of 9.9 μM in rat liver at 4 h following a 5 mg/kg oral dose. Furthermore, replicon activity at both genotypes 1b and 2a was under 10 nM in the presence of 10% FBS, and in the presence of 50% NHS, the

Table 3 In vitro activity of compounds **9** and **37–41**

Compound	GT 1b K_i (nM) ^a	GT 2a K_i (nM) ^a	Replicon IC_{50} (nM) ^b			Rat [liver] at 4 h (μ M) ^c
			1b 10% FBS	1b 50% NHS	2a 10% FBS	
37	0.05	2.6	7	32	150	0.91
38	0.04	0.9	7	27	66	0.52
39	0.45	19	29	110	720	3.8
40	0.18	4.0	10	35	140	10.7
41	0.06	0.9	5.0	27	13	1.9
9 (vaniprevir)	0.05	0.9	3.0	19	9.0	9.0

^aNS3/4a protease time-resolved fluorescence assay

^bCell-based replicon assay; in the presence of 10% FBS or 50% NHS

^c5 mg/kg dosed orally in PEG400 ($n = 2$), liver levels after 4 h

genotype 1b replicon activity showed a very small protein shift to 19 nM. Based on the exploration of the macrocyclic scaffold in the P2 isoindoline series, **9** (MK-7009) was identified as the optimal compound and was subsequently designated vaniprevir [24, 25, 51].

The synthesis of vaniprevir starts with 3-bromo-*o*-xylene (**42**) that was dibrominated with N-bromosuccinimide (NBS) and benzoyl peroxide (Scheme 2) [52]. Displacement of the bromines with benzylamine with concomitant ring closure gave 2-benzyl-4-bromoisindoline (**43**). Installation of the vinyl group and removal of the benzyl protective group with 1-chloroethyl chloroformate [53] and methanol (MeOH) provided **44**. Standard carbamate-forming conditions with **45** and removal of the Boc protecting group gave key intermediate **46**. Compound **46** was deprotected and coupled to linker intermediate **47** to give the bis-olefin **48**. The Zhan 1B metathesis catalyst [36] was used to affect macrocyclization, and the newly formed olefin could be hydrogenated, providing **49**. Ester hydrolysis and coupling to **50** gave vaniprevir (**9**). Subsequent optimization of synthetic routes has led to improved approaches to vaniprevir [45, 54].

and liver pharmacokinetics. Following an oral dose of 10 mg/kg in chimpanzees, **9** shows excellent plasma exposure, and liver biopsy at this dose level shows a liver concentration of 31 μM at 12 h post-dose. This concentration is >1,500-fold greater than the serum-shifted replicon IC_{50} and clearly supported a dosing regimen of, at most, twice per day in chimpanzees.

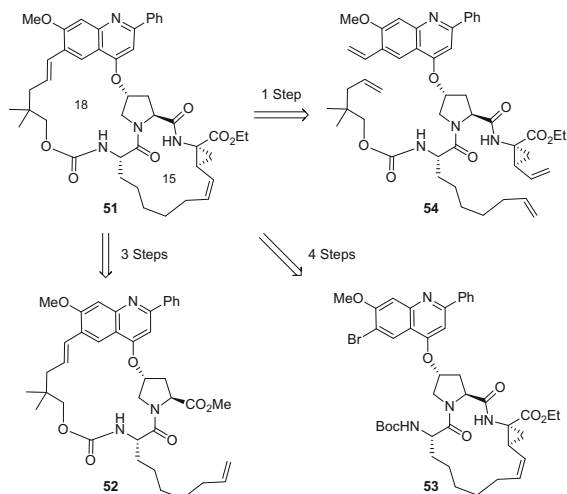
Vaniprevir demonstrates significant liver exposure in multiple preclinical species that persists over a significant timeframe. In particular, the concentrations present represent a significant margin relative to the replicon EC_{50} activity measured in the presence of 50% normal human serum (NHS) at 24 h (Table 4) in the case of rats (31-fold), dogs (46-fold), and rhesus (15-fold) and 12 h in chimpanzees (2,400-fold). The excellent exposure seen with vaniprevir in chimpanzees provided a strong basis for clinical evaluation of an antiviral effect. Further studies of vaniprevir, including clinical investigations of the pharmacokinetic and efficacy profile, led to its approval by the PDMA in Japan as VANIHEP which was used in combination with standard of care interferon treatment and led to increased efficacy in naïve and treatment-experienced patients [56].

4 Bis-Macrocycles

VANIHEP along with other first-generation protease inhibitors provided a good option for many patients with HCV infection, but the focus of HCV drug discovery had quickly shifted to all-oral combination therapies. The MSD team continued investigating NS3/4a inhibitors with the aim of inventing a molecule with improved potency, including activity against multiple genotypes and clinically resistant mutant enzymes, while maintaining the good pharmacokinetic and safety profiles of vaniprevir. These efforts included revisiting the original P2–P4 macrocyclic design and the decision to break the P1–P3 macrocycle. MSD envisioned accessing a compound that contained both the P2–P4 macrocycle and the P1–P3 macrocycle seen in compounds such as **5**, **6**, and **8**. This proposed class of bis-macrocycles were interesting targets from a biological perspective and would be a significant synthetic challenge, with target molecules containing both 18- and 15-membered rings.

Our synthetic planning began with the retrosynthetic analysis of ester **51** (Fig. 10). Initial disconnection of the P1–P3 macrocycle gives **52** which could theoretically yield **51** in three steps. The synthesis of compound **52**, however, would be nontrivial, requiring either a selective RCM of a triolefin, protection of the terminal olefin contained in the P3 side chain, or exploration of non-RCM synthetic routes. Alternatively, initial disconnection of the P2–P4 macrocycle gives a more readily accessible target **53**. This route would most likely deliver target **51** but only after a mostly linear sequence of greater than ten steps. A third possibility would be to form both rings simultaneously via a double-ring-closing metathesis reaction with tetraolefin **54**. The route was attractive because **54** could be synthesized in a convergent manner by formation of the central amide bond from readily available fragments. Furthermore, each macrocycle had been independently

Fig. 10 Bis-macrocycle retrosynthetic analysis



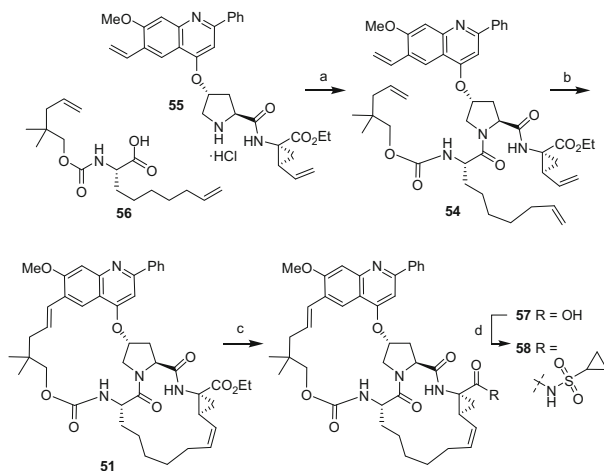
formed via RCM reactions in the literature, and olefin geometry had been controlled in both cases [15, 23]. The double RCM strategy, although convergent, presented significant chemo- and stereoselectivity challenges with the possibility of a variety of undesired ring closures as well as olefin isomers. Encouragement for this high-risk route, however, was provided by a previous report of a remarkably selective intermolecular bis-RCM reaction [57].

In practice, compounds **55** and **56** could be coupled under standard conditions in high yield to give the targeted bis-RCM precursor **54** (Scheme 3). After optimization, exposure of **54** to the Zhan 1B catalyst and *p*-benzoquinone [58] in 1,2-dichloroethane (1 mM) at 70°C for 1 h led to formation of a single major peak by HPLC and isolation of one compound in 66% yield. Proton and carbon NMR analysis along with 2D experiments confirmed that the major reaction product was the desired bis-macrocycle **51** which had been formed with at least 10:1 selectivity over other RCM products. This compound could then be elaborated to targets **57** and **58** in a straightforward manner (Table 5).

The P1 acid and acylsulfonamide bis-macrocycles maintained good enzyme and cellular potency, with compound **58** being one of the most potent compounds made on the program, including against the genotype 3 enzyme. Multiple studies exploring the selectivity of this reaction were undertaken [59], as well as further SAR work that led to a development candidate, MK-6325, that was ultimately discontinued [60].

5 Invention of Grazoprevir

As noted previously, the MSD team set the goal of invention of a second-generation NS3/4a protease inhibitor with significant improvements in activity against the gt 3a enzyme as well as key clinically relevant gt 1 mutant enzymes while maintaining or



Scheme 3 Conditions: (a) HATU, DIPEA, DMF, 79%; (b) Zhan 1B catalyst, DCE, 70°C, 1 mM, 1 h, 66%; (c) LiOH, H₂O, THF, EtOH, 86%; (d) CDI, THF; cyclopropyl sulfonamide, DBU, 40°C, 68%. Zhan 1B catalyst = 1,3-bis(2,4,6-trimethylphenyl)-4,5-dihydroimidazol-2-ylidene [2-(*i*-propoxy)-5-(*N,N*-dimethylaminosulfonyl)phenyl] methylenruthenium (II) dichloride

Table 5 In vitro activity of compounds 57 and 58

Compound	GT 1b K_i (nM) ^a	GT 3a K_i (nM) ^a	Replicon IC ₅₀ (nM) ^b	
			1b 10% FBS	1b 50% NHS
57	0.13	140	10	340
58	0.029	1.2	2	10

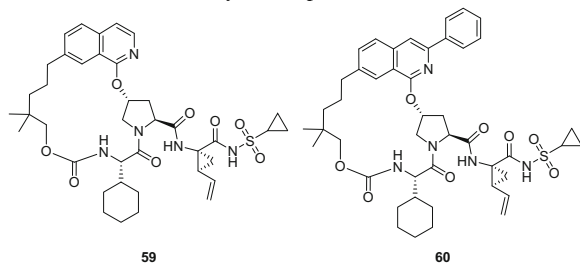
^aNS3/4a protease time-resolved fluorescence assay

^bCell-based replicon assay; in the presence of 10% FBS or 50% NHS

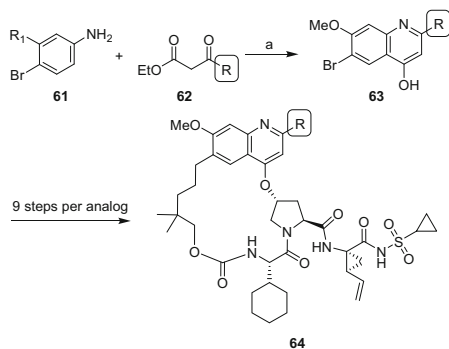
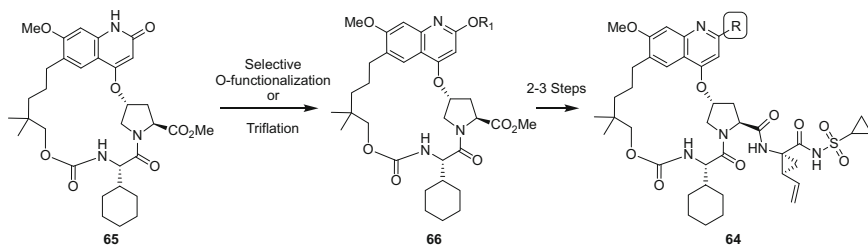
improving the PK profile seen with vaniprevir. In parallel with the above investigations, an additional entry point for enhanced gt 3a activity was provided by a consistent trend for improving gt 3a activity with the addition of a large substituent to the P2 heterocycle in early compounds. The series that was initially focused on toward this goal was the P2 isoquinolines (**59**, Table 6). The addition of a phenyl substituent in the 2-position of the quinoline (**60**) led to a reduced shift between gt 1 and gt 3a activity (Table 6). Given the apparent impact of these substituents, the team decided to more fully explore the SAR at this position with the closely related P2 quinoline.

However, in order to explore this region rapidly, a more efficient synthetic sequence needed to be developed, given that using the standard route utilizing the Conrad-Limpach quinoline synthesis [61] to install the 2-substituent, each analog (e.g., **64**) would require approximately nine steps to complete (Scheme 4).

In order to develop a more versatile route which introduced the 2-substituent near the end of the synthetic route, a P2 quinolone **65** (Scheme 5) was envisioned as a common intermediate for the synthesis of a variety of compounds with diversity in the 2-position.

Table 6 In vitro activity of compounds **59** and **60**

Compound	1b K_i (nM) ^a	3a K_i (nM) ^a	1b replicon IC ₅₀ 50% NHS (nM) ^b	Rat [liver] at 4 h (μM) ^c
59	0.02	200	10	21
60	0.05	45	19	7.8

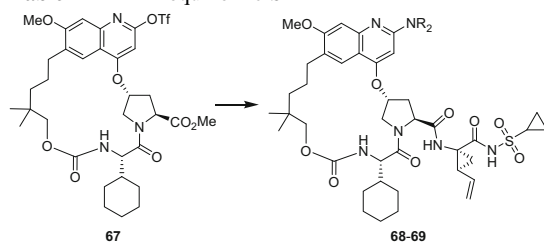
^aNS3/4a protease time-resolved fluorescence assay^bCell-based replicon assay; in the presence of 50% NHS^c5 mg/kg dosed orally in PEG400 ($n = 2$), liver levels after 4 h**Scheme 4** Conditions: (a) polyphosphoric acid, heat**Scheme 5** General synthetic route to substituted quinolines

Macrocyclic quinolone **65** would serve as starting point for O-alkylation or O-arylation as well as the precursor to the equally versatile triflate (**66**) which could participate in Suzuki or various S_NAr reactions to yield a wide variety of 2-substituted quinoline **64** (Scheme 5). In practice, quinolone **65** was prepared in 23% overall yield in seven steps from malonic acid using the standard RCM-enabled strategy. P2 aryl and heteroaryl groups were then accessed via straightforward Suzuki couplings using quinoline-2-triflate **66**, and selective O-alkylation/arylation was carried out directly from the quinolone using a variety of conditions. While the majority of the resulting analogs retained robust HCV NS3 activity, relatively modest gains in potency were realized relative to the parent 2-phenyl [**62**].

With the quinoline-2-triflate in hand, there was also an opportunity to prepare novel analogs that would not have been easily accessible without the newly designed route and versatile intermediate **67**. At MSD, this concept is referred to as synthesis-inspired design and subsequently led to a key breakthrough in the program. One of the subseries of analogs prepared using the triflate intermediate (**67**) was the 2-aminoquinolines shown in Table 7. Both compounds **68** and **69** showed exceptional potency against the genotype 3 enzyme, about tenfold better than similar phenyl quinolones (e.g., **60**). The N-Me analog **68**, however, showed virtually unmeasurable liver concentration in rat following a 5 mg/kg oral dose, and precluded further advancement. In contrast, ethyl carbamate **69** maintained the excellent biochemical and cellular potency while increasing liver concentration ~10,000-fold [**62**].

This positive result prompted additional exploration of less basic N-substituted quinolines and raised the possibility of exploring fused heterocycles as well. Again,

Table 7 2-Aminoquinoline SAR



Compound	NR ₂	GT 1b K _i (nM) ^a	GT 3a K _i (nM) ^a	GT 1b replicon IC ₅₀ (nM) ^b		[Liver] _{4h} (μM) ^c
				10% FBS	50% NHS	
68		0.09	5.4	1.6	90	<0.005
69		0.03	4.3	5.0	27	42

^aNS3/4a protease time-resolved fluorescence assay

^bCell-based replicon assay; in the presence of 10% FBS or 50% NHS

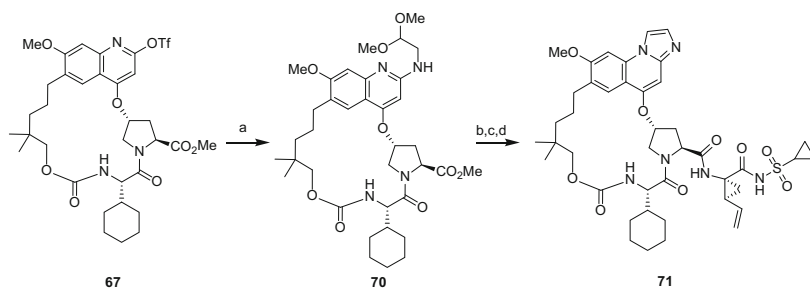
^c5 mg/kg dosed orally in PEG400 (*n* = 2), liver levels after 4 h

the utility of quinoline-2-triflate **67** was exploited to prepare a variety of these analogs including a novel tricyclic imidazoquinoline **71** which was accessed following N-arylation with aminoacetaldehyde dimethyl acetal giving intermediate **70** (Scheme 6). Cyclization under thermal conditions yielded the desired tricycle in moderate yield, and the targeted analog **71** was then prepared using standard conditions.

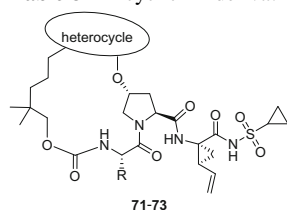
The resultant P2 imidazoquinoline **71** (Table 8) again possessed excellent gt 3a potency (1.8 nM) relative to the corresponding 2-substituted quinolones and represented a novel P2 substituent. Once again, synthesis-inspired design played a key role in this breakthrough. Without the novel synthetic route that generated intermediate **67**, a target like **71** would have been much more of a synthetic challenge, and this area of chemical space may have been evaluated more slowly, if at all. Even though relatively poor gt 1 replicon potency and rat liver exposure plagued this subseries, further investigation of the tricyclic series was clearly warranted, and the related isoquinoline-tricycle **72** was designed to further explore P2-tricycle SAR. Gratifyingly, compound **72** displayed excellent gt 3a potency (1.7 nM) and, in contrast to the corresponding imidazoquinoline **71**, also had good gt 1b replicon activity (3 nM) and rat liver concentration (27 μ M). Substituent effects on the newly introduced fused ring were then explored, with the methoxy analog **73** slightly increasing both potency and rat liver concentration compared to the corresponding unsubstituted analog.

In order to build understanding of the positive effect of the tricycle on potency, the MSD team turned to molecular modeling and docked compounds **74**, **75**, and **76** into both the gt 1 and gt 3a NS3/4a active sites. Figure 11 shows these analogs in the gt 1b active site with the differences between the two genotypes highlighted in red. As expected, the compounds adopt similar conformations, but 2-phenylisoquinoline **75** and phenanthridine **76** extend further into the S2 pocket of the active site than isoquinoline **74**. Given that this region is conserved between gt 1 and gt 3a, the hypothesis was that increasing contacts with conserved regions between the two genotypes should improve potency at gt 3a without compromising the already superior gt 1 potency.

As Fig. 11 illustrates, the P2–P4 linker lies across a region of the active site that is less conserved between genotypes and is also adjacent to two important gt 3a



Scheme 6 Conditions: (a) Aminoacetaldehyde dimethyl acetal, heat. (b) Xylene, acetic acid, heat (c) LiOH·H₂O, THF, methanol (d) 50, HATU, DIPEA, DMAP, DMF

Table 8 Tricyclic P2 derivatives

Compound	Heterocycle	R ^a	GT 1b K_i (nM) ^b	GT 3a K_i (nM) ^b	GT 1b replicon IC ₅₀ (nM) ^c		[Liver] _{4h} (μ M) ^d
					10% FBS	50% NHS	
71		Cyh	0.04	1.8	43	140	0.8
72		Cyp	<0.02	1.7	3	29	27
73		Cyp	<0.02	0.8	4	27	35

^aCyh, cyclohexyl; Cyp, cyclopentyl

^bNS3/4a protease time-resolved fluorescence assay

^cCell-based replicon assay; in the presence of 10% FBS or 50% NHS

^d5 mg/kg dosed orally in PEG400 ($n = 2$), liver levels after 4 h

mutations. The modeling also suggests that the addition of a larger P2 substituent may allow the macrocyclic ring to shift, possibly improving complementarity to the gt 3a site. In addition to the gt 1b to gt 3a changes in this region (D168Q), D168 and R155 mutations are observed in the gt 1 [63] during clinical studies, and these mutations lead to reduced potency for both vaniprevir and the additional MSD clinical candidate, MK-1220 [64]. Given this observation, the strategy was to increase the flexibility in the P2–P4 macrocyclic linker while increasing contacts within the conserved portion of P2 in order to allow for further improvements in the gt 1 mutant profile as well as the gt 3a activity. This strategy led to the proposal of simplifying the P2 heterocycle by “excising” two carbons from tricyclic framework (77), leading to a more flexible linker and a bicyclic P2 (78) as shown in Table 9.

Compound 78 maintained similar gt 1 activity ($K_i = 0.06$ nM) and liver exposure (25 μ M) but did result in a gt 3a potency loss ($K_i = 130$ nM). However, considering the large structural change and only modest loss in gt 3a potency, the related and simpler P2-pyridine isomers (79, 80) were reevaluated. While neither compound displayed high levels of potency, the 3-pyridyl analog 80 had ~twofold improved gt 3a activity even though it is less potent at gt 1b compared to the corresponding 2-pyridyl analog 79. Based upon the level of understanding at the time, this result

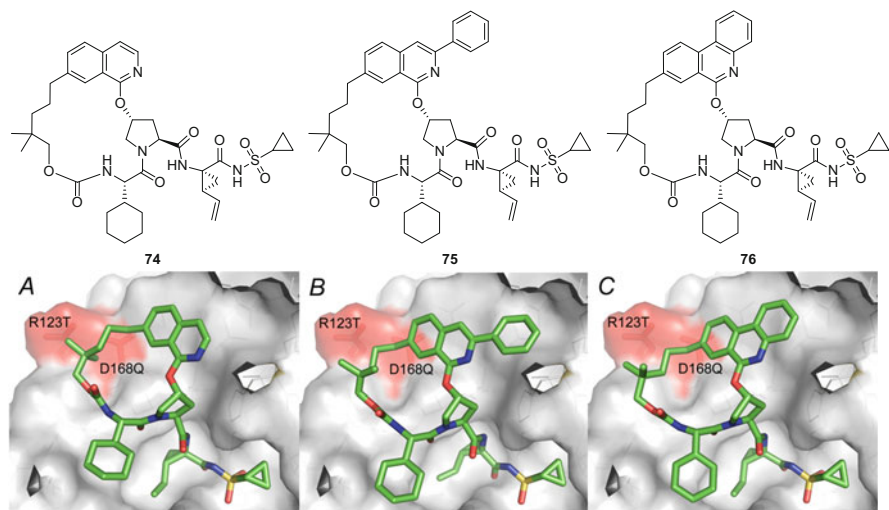
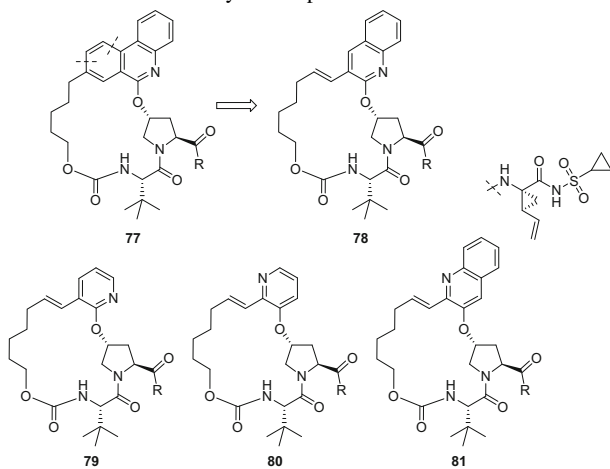


Fig. 11 Compounds **74** (a), **75** (b), and **76** (c) docked in the gt 1b NS3/4a active site. Light red = areas of diversity between the gt 1b and gt 3a enzymes

Table 9 In vitro activity of compounds **78–81**



Compound	GT 1b K_i (nM) ^a	GT 3a K_i (nM) ^a	1b replicon IC ₅₀ 50% NHS (nM) ^b	Rat [liver] at 4 h (μM) ^c
78	0.06	130	21	25
79	1.1	1,200	nd	nd
80	1.9	520	nd	nd
81	0.08	26	44	0.6

^aNS3/4a protease time-resolved fluorescence assay

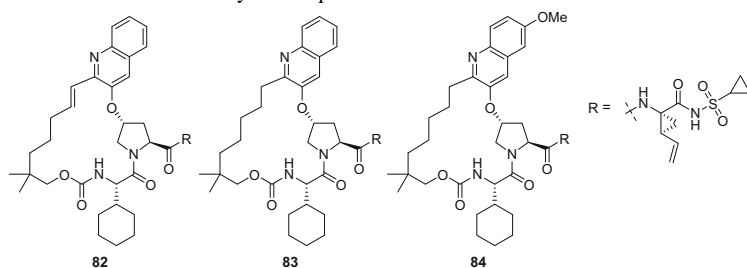
^bCell-based replicon assay; in the presence of 50% NHS

^c5 mg/kg dosed orally in PEG400 ($n = 2$), liver levels after 4 h

was difficult to explain, as there did not appear to be a hydrogen-bonding interaction associated with the pyridyl nitrogen in either position. However, one hypothesis was that a more favorable electrostatic interaction with R155 in the case of compound **80** or a change in hydrogen bonding to active-site water molecules led to the increased potency. Subsequently, crystallographic evidence published in 2012 [65] confirmed aspects of these ideas in the gt 1a R155K active site and indicated the possibility of an ordered water interacting with the 1-nitrogen atom in a quinoxaline ring system equivalent to the 3-pyridyl isomer. Given the improved gt 3a potency of **80** compared to **79**, this equivalent isomeric switch was performed on bicyclic 2-quinoline **78**, giving 3-quinoline **81**. This resulted in a fivefold increase in gt 3a potency ($K_i = 26$ nM), but liver exposure was unfortunately dramatically reduced (4 h liver exposure, **81** = 0.6 μ M vs. **78** = 26 μ M). In light of previous experience in optimizing for high liver concentrations during the development of vaniprevir, a similar strategy was pursued starting with **81** due to its attractive gt 3a profile. Subsequently, this series became the key lead of MSD's second-generation NS3/4a inhibitor program.

As was discovered in the context of first-generation inhibitors, increasing lipophilicity in specific regions of the P2–P4 macrocycles can lead to increases in liver exposure [25, 64]. With this in mind, a dimethyl-containing linker (**82**) was utilized; however only a small increase (0.6–1.5 μ M) in liver exposure was observed (Table 10). Fortunately, this small change in the linker did improve potency and led to nearly a tenfold improvement in gt 3a potency ($K_i = 2.8$ nM) which was almost 20-fold improved over vaniprevir, **9** (gt 3a $K_i = 54$ nM) [25]. Additional profiling of **82** also revealed a dramatic improvement against the key gt 1 mutant R155K [63]

Table 10 In vitro activity of compounds 82–84



Comp	GT 1b K_i (nM) ^a	GT 3a K_i (nM) ^a	GT 1b R155K K_i (nM) ^a	GT 1b A156T K_i (nM) ^a	GT 1b A156V K_i (nM) ^a	GT 1b D168V K_i (nM) ^a	1b replicon IC ₅₀ 50% NHS (nM) ^b	Rat [liver] at 4 h (μ M) ^c
82	0.02	2.8	0.32	18	79	nd	37	1.5
83	0.02	4.0	0.20	27	80	nd	18	63
84	0.02	1.9	0.16	12	64	nd	28	9.8

^aNS3/4a protease time-resolved fluorescence assay

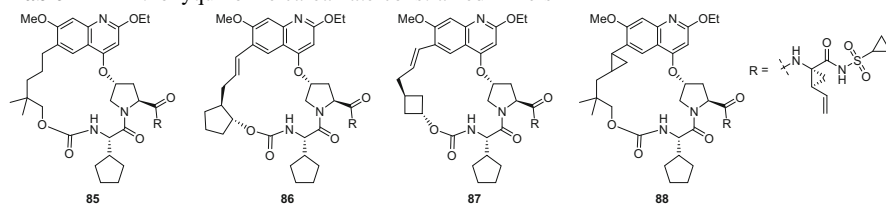
^bCell-based replicon assay; in the presence of 50% NHS

^c5 mg/kg dosed orally in PEG400 ($n = 2$), liver levels after 4 h

($K_i = 0.32$ nM). This sub-nanomolar potency was approximately 50-fold better than vaniprevir (gt 1b R155K $K_i = 19$ nM) and MK-1220 (gt 1b R155K $K_i = 15$ nM). Additionally, the activity of **82** versus A156 mutants was improved 10- to 30-fold compared to MK-1220 but was comparable to that of vaniprevir. As linker SAR was further explored, the olefinic linker in **82** was saturated giving **83**, which resulted in a very similar potency profile but also a dramatic 40-fold increase in the liver exposure (63 μ M at 4 h after a 5 mg/kg oral dose). Large increases in rat liver exposure following small changes in structure such as olefin reduction have been observed throughout the program as discussed above and highlight the need for the rat liver screening strategy [23, 25, 64]. Substituent effects were studied on the quinoline scaffold and found to be similar to the tricyclic phenanthridine with the 7-methoxy substituent (**84**) being optimal due to slight increases in potency against gt 3a and 1b mutants R155K, A156T, and A156V. However, in order to develop a true second-generation compound, additional improvements in gt 1b A156 and D168 mutants were needed.

As part of MSD's overall second-generation HCV NS3/4a protease inhibitor effort, further optimization of a series of P2 ethoxyquinolines was pursued, and a key observation within the context of this series was made, which was critical in the invention of grazoprevir. While exploring additional modifications of the linker starting from analog **85**, it was observed that a variety of cycloalkyl fused rings greatly improved the A156T and A156V potency while generally maintaining gt 3a potency (Table 11) [66]. For example, introduction of a cyclopentyl carbamate (**86**) led to a slight loss in gt 3a potency, but the activity against gt 1b A156T increased >40-fold relative to **85** while still maintaining good rat liver exposure. The reason for this increase in A156 mutant potency is not completely clear, but molecular modeling suggests that **86** can adopt a slightly more open conformation allowing it

Table 11 2-Ethoxyquinoline carbamate-constrained linkers



Compound	GT 3a K_i (nM) ^a	GT 1b replicon IC ₅₀ (nM) ^b	GT 1b mutants K_i (nM) ^a			[Liver] _{4h} (μ M) ^c
			R155K	A156T	A156V	
85	2.2	11	1.3	41	–	35
86	4.6	17	0.5	0.8	15	10.2
87	7.7	16	2.4	4.8	16	–
88^d	1.0	11	0.2	2.8	14	27.0

^aNS3/4a protease time-resolved fluorescence assay

^bCell-based replicon assay; in the presence of 10% FBS

^c5 mg/kg dosed orally in PEG400 ($n = 2$), liver levels after 4 h

^dAbsolute stereochemistry not established

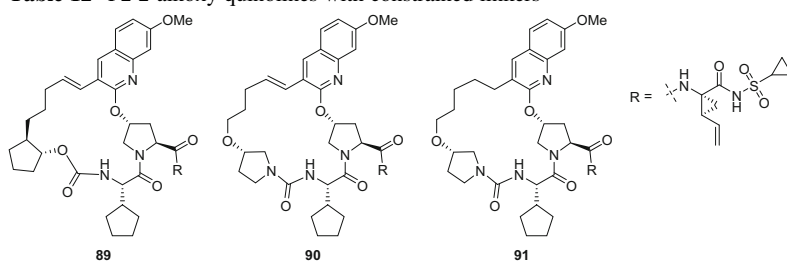
to more readily modulate the position of the macrocyclic ring as it sits atop the increased size of the T156 residue.

Smaller cycloalkyl rings such as 1,3-cyclobutane (**87**) or cyclopropane (**88**) also led to promising profiles across gt 3a and gt 1b mutant enzymes. Cyclobutane **87** lost severalfold gt 3a potency but displays good potency versus A156 mutants, including only a $\sim 3\times$ shift going from A156T to A156V. Introduction of a cyclopropyl fused ring adjacent to the P2 heterocycle led to a compound with the most balanced overall profile within this sub-series as **88** possesses excellent gt 3a ($K_i = 1$ nM) potency, gt 1b replicon activity ($IC_{50} = 11$ nM), and rat liver exposure (27,000 nM at 4 h, 5 mpk). In terms of gt 1b mutant activity, **88** is nearly single-digit nanomolar against both A156T (2.8 nM) and A156V (14 nM), while maintaining sub-nanomolar activity against gt 1b R155K.

While this effect is not fully understood, the impact was seen across a wide variety of P2 groups. In practice, the optimal cyclic constraint varied with different P2 groups and was determined empirically. For example, in the P2 2-quinoline series, the fused cyclopentyl analog **89** only had moderate gt 3a and gt 1b A156T/V potency, but the introduction of an alkoxy pyrrolidine urea (**90**, **91**) gave compounds with promising overall profiles in terms of potency and rat liver exposure (Table 12).

In contrast to the 2-quinolines, a fused cycloalkyl ring was the preferred linker in the 3-quinoline series, and compound **92** possessed excellent potency activity against different genotypes and key mutant enzymes as compared to compound **84** (Table 13). Exploration of different ring sizes led to the identification of a fused cyclopropyl linker which further improved the activity and gave a compound (**93**) with excellent liver exposure as well. As was seen with the 2-ethoxyquinoline class, the ring fusion in **93** allows the macrocycle to shift away from the A156 residue (Fig. 12) thus making it easier to accommodate the increased bulk of the A156T or A156V mutation.

Table 12 P2 2-alkoxy quinolines with constrained linkers

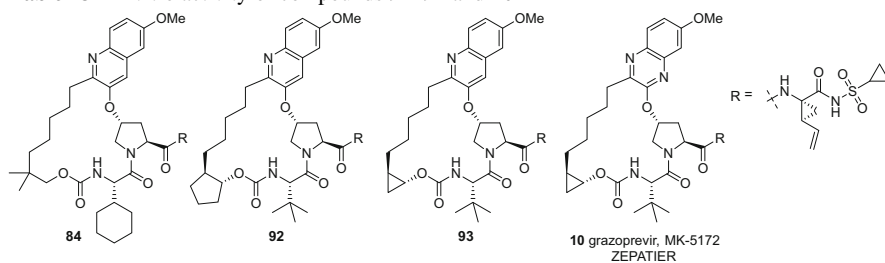


Compound	GT 3a K_i (nM) ^a	GT 1b replicon IC_{50} (nM) ^b	GT 1b mutants K_i (nM) ^a			[Liver] _{4h} (μ M) ^c
			R155K	A156T	A156V	
89	11.6	58	0.2	17	–	30.8
90	3.0	32	0.1	2.9	37	8.6
91	5.9	31	0.1	1.5	22	12.0

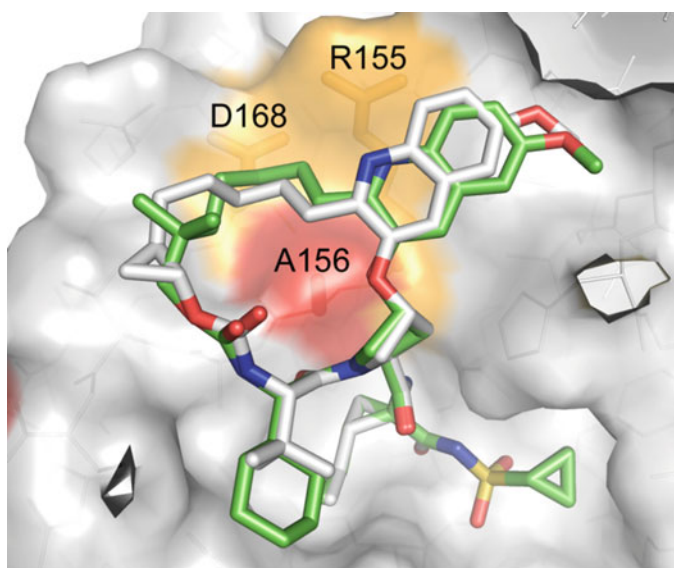
^aNS3/4a protease time-resolved fluorescence assay

^bCell-based replicon assay; in the presence of 10% FBS

^c5 mg/kg dosed orally in PEG400 ($n = 2$), liver levels after 4 h

Table 13 In vitro activity of compounds **92–94** and **10**

Compound	GT 1b K_i (nM) ^a	GT 3a K_i (nM) ^a	GT 1b R155K K_i (nM) ^a	GT 1b A156T K_i (nM) ^a	GT 1b A156V K_i (nM) ^a	GT 1b D168V K_i (nM) ^a	GT 1b replicon IC ₅₀ 50% NHS (nM) ^b	Rat [liver] at 4 h (μM) ^c
84	0.02	1.9	0.16	12	64	nd	28	9.8
92	0.02	0.39	0.07	2.4	11	0.06	16	6.3
93	0.02	0.31	0.02	2.9	5.7	0.05	13	20
10 (grazoprevir)	0.02	0.70	0.07	5.3	12	0.14	7.4	23

^aNS3/4a protease time-resolved fluorescence assay^bCell-based replicon assay; in the presence of 50% NHS^c5 mg/kg dosed orally in PEG400 ($n = 2$), liver levels after 4 h**Fig. 12** Comparison of the energy-minimized conformations of compounds **84** (green) and **93** (white) docked in the gt 1b NS3/4a active site

While compound **93** met high-level criteria for a second-generation HCV protease inhibitor, during more in-depth evaluation, a significant issue emerged which prevented it from advancing further into development. Compound physical properties led to a reduction in the exposure which could be obtained in preclinical species with oral dosing. Specifically, while the crystalline potassium salt of **93** is quite soluble in a variety of aqueous vehicles, it readily disproportionates to a crystalline zwitterionic form that has very low aqueous solubility (<0.009 mg/mL) which significantly limits the amount of compound available to be absorbed. The possibility of a zwitterion is driven by the moderate basicity (calculated $pK_a = 4.47$) [67] of the quinoline P2 group of **93** along with moderate acidity of the acylsulfonamide (calculated $pK_a = 3.67$). Following oral dosing, the formation of zwitterionic species and subsequent crystallization is promoted in the stomach due to the lower native pH [68]. Thus, poor absorption resulted and sufficiently high exposures were not able to be obtained with **93** in preclinical species.

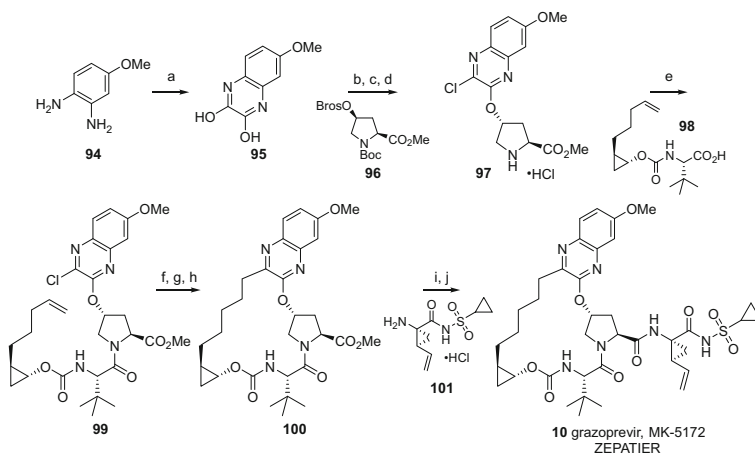
With this knowledge in hand, the attractive overall profile of compound **93** prompted us to examine alternative less basic P2 heterocycles which could maintain the properties of **93** but with reduced risk of zwitterion formation. From this strategy, P2 quinoxalines emerged as a promising subclass, with their lower pK_a reducing the risk of zwitterion formation (calculated $pK_a \sim 1.2$). Incorporating a quinoxaline into the previously optimized linker gave compound **10** (grazoprevir, MK-5172, Table 13) [26, 27]. Overall, **10** maintained the excellent potency against the gt 3a enzyme as well as a broad panel of mutant enzymes and showed excellent rat liver exposure. While the solubility of the potassium salt of **10** was somewhat lower than **93**, no disproportionation was observed, enabling grazoprevir to advance into development. The extended potency profile of grazoprevir is shown in Table 14, and the pan-genotypic potency is evident as well as the very large improvements compared to vaniprevir.

The medicinal chemistry route for grazoprevir (**10**) is shown in Scheme 7 and generally follows the synthetic sequence used for previous compounds. The synthesis starts from 4-methoxy-phenylenediamine hydrochloride (**94**) which was heated

Table 14 Activity of vaniprevir and grazoprevir

Enzyme ^a	Vaniprevir K_i (nM)	Grazoprevir K_i (nM)	Fold improvement
Genotype 1a	0.07	0.01	7×
Genotype 1b	0.06	0.01	6×
Genotype 2a	1.0	0.07	14×
Genotype 2b	1.4	0.14	10×
Genotype 3a	54	0.69	78×
Genotype 4a	nd	0.06	–
Genotype 5a	nd	0.07	–
Genotype 6a	nd	0.03	–
1b R155K	19	0.07	270×
1b D168Y	120	0.23	520×

^aNS3/4a protease time-resolved fluorescence assay



Scheme 7 Conditions: (a) diethyloxalate, TEA, 150°C, 69%; (b) thionyl chloride, DMF, 110°C, 69%; (c) **96** [35], Cs₂CO₃, NMP; (d) HCl, dioxane; (e) **98**, HATU, DIPEA, DMF, 78%; (f) potassium vinyltrifluoroborate, TEA, dichloro[1,1-bis(diphenylphosphino) ferrocene] palladium (II) chloride, EtOH; (g) Zhan 1B catalyst, DCE, 25%; (h) H₂, 10% Pd/C, MeOH, dioxane, 99%; (i) LiOH, THF, water; (j) **101** [69], TBTU, DIPEA, DMAP, DMF, 89%, two steps. Zhan 1B catalyst = 1,3-bis(2,4,6-trimethylphenyl)-4,5-dihydroimidazol-2-ylidene [2-(*i*-propoxy)-5-(*N,N*-dimethylaminosulfonyl)phenyl] methylenruthenium (II) dichloride

Table 15 Pharmacokinetic parameters for the potassium salt of **10** (grazoprevir)^a

Species	Cl (mL/min/kg)	V _d (L/kg)	T _{1/2} (h)	P.O. AUC (μMh)	P.O. [liver] 4 h (μM)	P.O. [liver] 24 h (μM)
Rat	28	3.1	1.4	0.7	23	0.2
Dog	5	0.7	3.0	0.4	nd	1.4

^aRat IV (2 mg/kg, *n* = 3, DMSO), dog IV (0.5 mg/kg, *n* = 3, DMSO), rat P.O. (5 mg/kg, *n* = 3, PEG400), dog P.O. (1 mg/kg, *n* = 3, PEG400)

with diethyloxalate to give **95** in 69% yield. Chemoselective chlorination with thionyl chloride followed by addition to activated *cis*-hydroxyproline derivative **96** [35] and deprotection gives intermediate **97** in 69% yield. Amide coupling with **98**, prepared as a single enantiomer in six steps, yields chloroquinoxaline **99** in 78% yield. Next, vinylation followed by RCM gives the desired macrocycle. While the RCM generally worked well across analog subseries, quinoxalines often performed poorly, and in this case, the targeted macrocycle was isolated in only 25% yield. Reduction of the resulting olefin gave macrocycle **100**, which was readily converted to **10** in 89% yield by hydrolysis and coupling to the known cyclopropylamino acylsulfonamide **101** [69]. Subsequent optimization by the MSD Process Chemistry group has led to improved approaches to grazoprevir [70–72].

The pharmacokinetic properties of grazoprevir were evaluated in multiple species (Table 15). Grazoprevir has moderate plasma clearance of 28 mL/min/kg in rat with a half-life of 1.4 h. When dosed orally at 5 mg/kg, the plasma exposure of

grazoprevir was improved relative to vaniprevir with an AUC of 0.7 μMh . The liver exposure of the compound was also significant (23 μM at 4 h), and at 24 h, the liver concentration of **10** was 0.2 μM , which is >25-fold higher than the IC_{50} in the replicon assay with 50% NHS. In dogs, grazoprevir shows low clearance of 5 mL/min/kg and a 3 h half-life with significant plasma exposure (AUC = 0.4 μMh) after a 1 mg/kg oral dose (Table 15). Dog liver biopsy studies showed that the liver concentration of grazoprevir after the 1 mg/kg oral dose is 1.4 μM at the 24 h time point. As with rats, grazoprevir partitions into liver tissue, and this concentration is well above the IC_{50} in the replicon assay with 50% NHS.

In summary, initial screening for gt 3a activity along with molecular modeling led to the discovery of a series of P2 quinoline macrocycles with excellent broad activity vs. NS3/4a genotypes and clinically observed gt 1 mutant enzymes. This series was optimized for enzyme activity and liver exposure in preclinical species and led to the second-generation NS3/4a protease inhibitor grazoprevir. Clinical and preclinical studies showed that grazoprevir was an effective NS3/4a protease inhibitor and the compound was approved for the treatment of HCV in a single-tablet, fixed-dose combination with the NS5a inhibitor elbasvir under the name ZEPATIER. The invention of elbasvir and the development of ZEPATIER are described elsewhere in this volume.

6 Conclusions

The path to development of HCV NS3/4a protease inhibitors has been a long one but has successfully yielded multiple marketed drugs in multiple subclasses from a number of companies that have been used in conjunction with interferon-based therapies and as part of all-oral direct antiviral treatment regimens.

The program that led to the invention of grazoprevir benefited from a number of chemistry and medicinal chemistry decisions and strategies. Analysis of bound structures, and specifically *in silico* methods to analyze structure when no crystal structure was available, was critical in the formulation of the P2–P4 macrocyclization hypothesis. The ring-closing metathesis reaction was instrumental in testing this hypothesis, and the reaction continued to have impact throughout the program. While structural chemistry provided key guidance in the design of new inhibitor structures, a significant portion of the optimization, particularly improving activity against mutant enzymes and for high liver exposure, was empirical in nature. The flexibility and reliability of the RCM reaction allowed for extensive and rapid evaluation of the macrocyclic framework. Without this reaction, which has only been widely employed in medicinal chemistry for the last 15 years, this investigation would have been much more challenging from a synthetic perspective.

At several points during the invention of grazoprevir, novel designs were also enabled by the discovery and application of new synthetic routes and availability of key advanced intermediates, which made the exploration of chemical space more facile. This aspect of synthesis-inspired design was crucial to the identification of the

optimal P2 heterocycle present in grazoprevir. Furthermore from a medicinal chemistry point of view, the structural properties of the inhibitors described in detail here do not conform well to what has been considered druggable space [73–76]. With high molecular weights in the 750 range and large polar surface areas, identification of compounds that show good plasma pharmacokinetics represents a significant accomplishment. Overall, the strategy the MSD team took from the initial design of P2–P4 macrocycles and optimization for broad genotype and mutant enzyme potency, cellular activity, and liver exposure in preclinical species has proven to be effective with the invention of grazoprevir. Following the invention of grazoprevir, several other P2–P4 macrocyclic HCV NS3/4a protease inhibitors have been more recently approved by the FDA [77, 78]. As part of the single-tablet, fixed-dose combination product ZEPATIER, grazoprevir is positioned to be an important part of the worldwide effort to eliminate HCV infection.

Compliance with Ethical Standards

Conflict of Interest Authors declare that they have no conflict of interest.

Ethical Approval This article does not contain any studies with human participants performed by any of the authors. All applicable international, national, and/or institutional guidelines for the care and use of animals were followed.

References

1. Choo QL, Kuo G, Weiner AJ, Overby LR, Bradley DW, Houghton M (1989) Isolation of a cDNA clone derived from a blood-borne non-A, non-B viral hepatitis genome. *Science* 244:359–362
2. Lavanchy D (2009) The global burden of hepatitis C. *Liver Int* 29 Suppl(1):74–81
3. Marcellin P, Asselah T, Boyer N (2002) Fibrosis and disease progression in hepatitis C. *Hepatology* 36:S47–S56
4. Simmonds P (2004) Genetic diversity and evolution of hepatitis C virus –15 years on. *J Gen Virol* 85:3173–3188
5. Zeuzem S, Berg T, Moeller B, Hinrichsen H, Mauss S, Wedemeyer H, Sarrazin C, Hueppe D, Zehnter E, Manns MP (2009) Expert opinion on the treatment of patients with chronic hepatitis C. *J Viral Hepat* 16:75–90
6. Lindenbach BD, Rice CM (2005) Unravelling hepatitis C virus replication from genome to function. *Nature* 436:933–938
7. Coilly A, Dumortier JRM, Botta-Fridlund D, Latournerie M, Leroy V, Pageaux G-P, Agostini HLN, Giostra E, Moreno C, Roche B, Antonini TM, Guillaud O, Lebray P, Radenne S, Saouli A-C, Calmus Y, Alric L, Debette-Gratien M, De Ledinghen V, Durand FO, Duvoux C, Samuel D, Duclos-Vallée J-C (2015) Multicenter experience with boceprevir or telaprevir to treat hepatitis C recurrence after liver transplantation: when present becomes past, what lessons for future? *Plos One* 10:e0138091
8. Kim JL, Morgenstern KA, Lin C, Fox T, Dwyer MD, Landro JA, Chambers SP, Markland W, Lepre CA et al (1996) Crystal structure of the hepatitis C virus NS3 protease domain complexed with a synthetic NS4A cofactor peptide. *Cell* 87:343–355

9. Grakoui A, McCourt DW, Wychowski C, Feinstone SM, Rice CM (1993) Characterization of the hepatitis C virus-encoded serine proteinase: determination of proteinase-dependent polyprotein cleavage sites. *J Virol* 67:2832–2843
10. Llinas-Brunet M, Bailey M, Fazal G, Goulet S, Halmos T, Laplante S, Maurice R, Poirier M, Poupard M-A, Thibeault D, Wernic D, Lamarre D (1998) Peptide-based inhibitors of the hepatitis C virus serine protease. *Bioorg Med Chem Lett* 8:1713–1718
11. Ingallinella P, Altamura S, Bianchi E, Taliani M, Ingenito R, Cortese R, De Francesco R, Steinkuehler C, Pessi A (1998) Potent peptide inhibitors of human hepatitis C virus NS3 protease are obtained by optimizing the cleavage products. *Biochemistry* 37:8906–8914
12. McCauley JA, Rudd MT (2016) Hepatitis C virus NS3/4a protease inhibitors. *Curr Opin Pharmacol* 30:84–92
13. Venkatraman S, Bogen SL, Arasappan A, Bennett F, Chen K, Jao E, Liu Y-T, Lovey R, Hendrata S, Huang Y, Pan W, Parekh T, Pinto P, Popov V, Pike R, Ruan S, Santhanam B, Vibulbhan B, Wu W, Yang W, Kong J, Liang X, Wong J, Liu R, Butkiewicz N, Chase R, Hart A, Agrawal S, Ingravallo P, Pichardo J, Kong R, Baroudy B, Malcolm B, Guo Z, Prongay A, Madison V, Broske L, Cui X, Cheng K-C, Hsieh TY, Brisson J-M, Prelusky D, Korfmacher W, White R, Bogdanowich-Knipp S, Pavlovsky A, Bradley P, Saksena AK, Ganguly A, Piwinski J, Girijavallabhan V, Njoroge FG (2006) Discovery of (1R,5S)-N-[3-amino-1-(cyclobutylmethyl)-2,3-dioxopropyl]-3-[2(S)-[[[(1,1-dimethylethyl)amino]carbonyl]amino]-3,3-dimethyl-1-oxobutyl]-6,6-dimethyl-3-azabicyclo[3.1.0]hexan-2(S)-carboxamide (SCH 503034), a selective, potent, orally bioavailable hepatitis C virus NS3 protease inhibitor: a potential therapeutic agent for the treatment of hepatitis C infection. *J Med Chem* 49:6074–6086
14. Lin C, Kwong AD, Perni RB (2006) Discovery and development of VX-950, a novel, covalent, and reversible inhibitor of hepatitis C virus NS3/4A serine protease. *Infect Disord Drug Targets* 6:3–16
15. Llinas-Brunet M, Bailey MD, Bolger G, Brochu C, Faucher A-M, Ferland JM, Garneau M, Ghio E, Gorys V, Grand-Maitre C, Halmos T, Lapeyre-Paquette N, Liard F, Poirier M, Rheume M, Tsantrizos YS, Lamarre D (2004) Structure-activity study on a novel series of macrocyclic inhibitors of the hepatitis C virus NS3 protease leading to the discovery of BILN 2061. *J Med Chem* 47:1605–1608
16. Lamarre D, Anderson PC, Bailey M, Beaulieu P, Bolger G, Bonneau P, Bos M, Cameron DR, Cartier M, Cordingley MG, Faucher A-M, Goudreau N, Kawai SH, Kukolj G, Lagace L, LaPlante SR, Narjes H, Poupard M-A, Rancourt J, Sentjens RE, St GR, Simoneau B, Steinmann G, Thibeault D, Tsantrizos YS, Weldon SM, Yong C-L, Llinas-Brunet M (2003) An NS3 protease inhibitor with antiviral effects in humans infected with hepatitis C virus. *Nature* 426:186–189
17. Stoltz JH, Stern JO, Huang Q, Seidler RW, Pack FD, Knight BL (2011) A twenty-eight-day mechanistic time course study in the rhesus monkey with hepatitis C virus protease inhibitor BILN 2061. *Toxicol Pathol* 39:496–501
18. Seiwert SD, Andrews SW, Jiang Y, Serebryany V, Tan H, Kossen K, Rajagopalan PTR, Misialek S, Stevens SK, Stoycheva A, Hong J, Lim SR, Qin X, Rieger R, Condroski KR, Zhang H, Do MG, Lemieux C, Hingorani GP, Hartley DP, Josey JA, Pan L, Beigelman L, Blatt LM (2008) Preclinical characteristics of the hepatitis C virus NS3/4a protease inhibitor ITMN-191 (R7227). *Antimicrob Agents Chemother* 52:4432–4441
19. Forestier N, Larrey D, Marcellin P, Guyader D, Patat A, Rouzier R, Smith PF, Qin X, Lim S, Bradford W, Porter S, Seiwert SD, Zeuzem S (2011) Antiviral activity of danoprevir (ITMN-191/RG7227) in combination with pegylated interferon α -2a and ribavirin in patients with hepatitis C. *J Infect Dis* 204:601–608
20. Forestier N, Larrey D, Guyader D, Marcellin P, Rouzier R, Patat A, Smith P, Bradford W, Porter S, Blatt L, Seiwert SD, Zeuzem S (2011) Treatment of chronic hepatitis C patients with the NS3/4A protease inhibitor danoprevir (ITMN-191/RG7227) leads to robust reductions in viral RNA: a phase 1b multiple ascending dose study. *J Hepatol* 54:1130–1136

21. Scola PM, Sun L-Q, Wang AX, Chen J, Sin N, Venables BL, Sit S-Y, Chen Y, Cocuzza A, Bilder DM, D'Andrea SV, Zheng B, Hewawasam P, Tu Y, Friborg J, Falk P, Hernandez D, Levine S, Chen C, Yu F, Sheaffer AK, Zhai G, Barry D, Knipe JO, Han Y-H, Schartman R, Donoso M, Mosure K, Sinz MW, Zvyaga T, Good AC, Rajamani R, Kish K, Tredup J, Klei HE, Gao Q, Mueller L, Colonna RJ, Grasel DM, Adams SP, Loy J, Levesque PC, Sun H, Shi H, Sun L, Warner W, Li D, Zhu J, Meanwell NA, McPhee F (2014) The discovery of asunaprevir (BMS-650032), an orally efficacious NS3 protease inhibitor for the treatment of hepatitis C virus infection. *J Med Chem* 57:1730–1752
22. Rosenquist Å, Samuelsson B, Johansson P-O, Cummings MD, Lenz O, Raboisson P, Simmen K, Vendeville S, Kock H d, Nilsson M, Horvath A, Kalmeijer R, Rosa G d l, Beumont-Mauviel M (2014) Discovery and development of simeprevir (TMC435), a HCV NS3/4A protease inhibitor. *J Med Chem* 57:1673–1693
23. Liverton NJ, Holloway MK, McCauley JA, Rudd MT, Butcher JW, Carroll SS, DiMuzio J, Fandozzi C, Gilbert KF, Mao S-S, McIntyre CJ, Nguyen KT, Romano JJ, Stahlhut M, Wan B-L, Olsen DB, Vacca JP (2008) Molecular modeling based approach to potent P2-P4 macrocyclic inhibitors of hepatitis C NS3/4A protease. *J Am Chem Soc* 130:4607–4609
24. Liverton NJ, Carroll SS, Di Muzio J, Fandozzi C, Graham DJ, Hazuda D, Holloway MK, Ludmerer SW, McCauley JA, McIntyre CJ, Olsen DB, Rudd MT, Stahlhut M, Vacca JP (2009) MK-7009, a potent and selective inhibitor of hepatitis C virus NS3/4A protease. *Antimicrob Agents Chemother* 54:305–311
25. McCauley JA, McIntyre CJ, Rudd MT, Nguyen KT, Romano JJ, Butcher JW, Gilbert KF, Bush KJ, Holloway MK, Swestock J, Wan B-L, Carroll SS, DiMuzio JM, Graham DJ, Ludmerer SW, Mao S-S, Stahlhut MW, Fandozzi CM, Trainor N, Olsen DB, Vacca JP, Liverton NJ (2010) Discovery of Vaniprevir (MK-7009), a macrocyclic hepatitis C virus NS3/4a protease inhibitor. *J Med Chem* 53:2443–2463
26. Harper S, McCauley JA, Rudd MT, Ferrara M, DiFilippo M, Crescenzi B, Koch U, Petrocchi A, Holloway MK, Butcher JW, Romano JJ, Bush KJ, Gilbert KF, McIntyre CJ, Nguyen KT, Nizi E, Carroll SS, Ludmerer SW, Burlein C, DiMuzio JM, Graham DJ, McHale CM, Stahlhut MW, Olsen DB, Monteagudo E, Cianetti S, Giuliano C, Pucci V, Trainor N, Fandozzi CM, Rowley M, Coleman PJ, Vacca JP, Summa V, Liverton NJ (2012) Discovery of MK-5172, a macrocyclic hepatitis C virus NS3/4a protease inhibitor. *ACS Med Chem Lett* 3:332–336
27. Summa V, Ludmerer SW, McCauley JA, Fandozzi C, Burlein C, Claudio G, Coleman PJ, DiMuzio JM, Ferrara M, Di Filippo M, Gates AT, Graham DJ, Harper S, Hazuda DJ, McHale C, Monteagudo E, Pucci V, Rowley M, Rudd MT, Soriano A, Stahlhut MW, Vacca JP, Olsen DB, Liverton NJ, Carroll SS (2012) MK-5172, a selective inhibitor of hepatitis C virus NS3/4a protease with broad activity across genotypes and resistant variants. *Antimicrob Agents Chemother* 56:4161–4167
28. Tsantrizos YS, Bolger G, Bonneau P, Cameron DR, Goudreau N, Kukulj G, LaPlante SR, Llinas-Brunet M, Nar H, Lamarre D (2003) Macrocyclic inhibitors of the NS3 protease as potential therapeutic agents of hepatitis C virus infection. *Angew Chem Int Ed* 42:1356–1360
29. LaPlante SR, Llinas-Brunet M (2005) Dynamics and structure-based design of drugs targeting the critical serine protease of the hepatitis C virus – from a peptidic substrate to BILN 2061. *Curr Med Chem Anti-Infect Agents* 4:111–132
30. Thibeault D, Massariol M-J, Zhao S, Welchner E, Goudreau N, Gingras R, Llinas-Brunet M, White PW (2009) Use of the fused NS4A peptide-NS3 protease domain to study the importance of the helicase domain for protease inhibitor binding to hepatitis C virus NS3-NS4A. *Biochemistry* 48:744–753
31. Schiering N, D'Arcy A, Villard F, Simic O, Kamke M, Monnet G, Hassiepen U, Svergun DI, Pulfer R, Eder J, Raman P, Bodendorf U (2011) A macrocyclic HCV NS3/4A protease inhibitor interacts with protease and helicase residues in the complex with its full-length target. *Proc Natl Acad Sci U S A* 108:21052–21056
32. Yao N, Reichert P, Taremi SS, Prosis WW, Weber PC (1999) Molecular views of viral polyprotein processing revealed by the crystal structure of the hepatitis C virus bifunctional protease-helicase. *Structure* 7:1353–1363
33. Grubbs RH (2004) Olefin metathesis. *Tetrahedron* 60:7117–7140

34. Grubbs RH (2006) Olefin-metathesis catalysts for the preparation of molecules and materials (Nobel lecture). *Angew Chem Int Ed* 45:3760–3765
35. Arasappan A, Chen KX, Njoroge FG, Parekh TN, Girijavallabhan V (2002) Novel dipeptide macrocycles from 4-Oxo-, -Thio-, and -amino-substituted proline derivatives. *J Org Chem* 67:3923–3926
36. Available from Strem chemicals, catalog #44-0082; CAS# 918870-76-5
37. Beaulieu PL, Gillard J, Bailey MD, Boucher C, Duceppe J-S, Simoneau B, Wang X-J, Zhang L, Grozinger K, Houpis I, Farina V, Heimroth H, Krueger T, Schnaubelt J (2005) Synthesis of (1R,2S)-1-amino-2-vinylcyclopropanecarboxylic acid vinyl-ACCA derivatives: key intermediates for the preparation of inhibitors of the hepatitis C virus NS3 protease. *J Org Chem* 70:5869–5879
38. Mao S-S, DiMuzio J, McHale C, Burlein C, Olsen D, Carroll SS (2008) A time-resolved, internally quenched fluorescence assay to characterize inhibition of hepatitis C virus nonstructural protein 3-4A protease at low enzyme concentrations. *Anal Biochem* 373:1–8
39. Migliaccio G, Tomassini JE, Carroll SS, Tomei L, Altamura S, Bhat B, Bartholomew L, Bosserman MR, Ceccacci A, Colwell LF, Cortese R, De Francesco R, Eldrup AB, Getty KL, Hou XS, LaFemina RL, Ludmerer SW, MacCoss M, McMasters DR, Stahlhut MW, Olsen DB, Hazuda DJ, Flores OA (2003) Characterization of resistance to non-obligate chain-terminating Ribonucleoside analogs that inhibit hepatitis C virus replication in vitro. *J Biol Chem* 278:49164–49170
40. Marchetti A, Ontoria JM, Matassa VG (1999) Synthesis of two novel cyclic diphenyl ether analogs of an inhibitor of HCV NS3 protease. *Synlett* 1999:1000–1002
41. Chen KX, Njoroge FG, Pichardo J, Prongay A, Butkiewicz N, Yao N, Madison V, Girijavallabhan V (2006) Potent 7-hydroxy-1,2,3,4-tetrahydroisoquinoline-3-carboxylic acid-based macrocyclic inhibitors of hepatitis C virus NS3 protease. *J Med Chem* 49:567–574
42. Tu Y, Scola PM, Good AC, Campbell JA (2005) Preparation of prolinamide peptides as hepatitis C virus inhibitors. WO2005054430A2
43. Johansson A, Poliakov A, Kerblom EA, Wiklund K, Lindeberg G, Winiwarer S, Danielson UH, Samuelsson B, Hallberga A (2003) Acyl sulfonamides as potent protease inhibitors of the hepatitis C virus full-length NS3 (protease-helicase/NTPase): a comparative study of different C-terminals. *Biogianic Med Chem* 11:2551–2568
44. Scola PM, Wang AX, Good AC, Sun L-Q, Combrink KD, Campbell JA, Chen J, Tu Y, Sin N, Venables BL, Sit S-Y, Chen Y, Cocuzza A, Bilder DM, D'Andrea S, Zheng B, Hewawasam P, Ding M, Thuring J, Li J, Hernandez D, Yu F, Falk P, Zhai G, Sheaffer AK, Chen C, Lee MS, Barry D, Knipe JO, Li W, Han Y-H, Jenkins S, Gesenberg C, Gao Q, Sinz MW, Santone KS, Zvyaga T, Rajamani R, Klei HE, Colonno RJ, Grasela DM, Hughes E, Chien C, Adams S, Levesque PC, Li D, Zhu J, Meanwell NA, McPhee F (2014) Discovery and early clinical evaluation of BMS-605339, a potent and orally efficacious tripeptidic acylsulfonamide NS3 protease inhibitor for the treatment of hepatitis C virus infection. *J Med Chem* 57:1708–1729
45. Song ZJ, Tellers DM, Jourmet M, Kuethe JT, Lieberman D, Humphrey G, Zhang F, Peng Z, Waters MS, Zewge D, Nolting A, Zhao D, Reamer RA, Dormer PG, Belyk KM, Davies IW, Devine PN, Tschauen DM (2011) Synthesis of vaniprevir (MK-7009): lactamization to prepare a 20-membered macrocycle. *J Org Chem* 76:7804–7815
46. Nicola T, Brenner M, Donsbach K, Kreye P (2005) First scale-up to production scale of a ring closing metathesis reaction forming a 15-membered macrocycle as a precursor of an active pharmaceutical ingredient. *Org Process Res Dev* 9:513–515
47. Van de Weghe P, Eustache J (2005) The application of olefin metathesis to the synthesis of biologically active macrocyclic agents. *Curr Top Med Chem* 5:1495–1519
48. Gradillas A, Perez-Castells J (2006) Macrocyclization by ring-closing metathesis in the total synthesis of natural products: reaction conditions and limitations. *Angew Chem Int Ed* 45:6086–6101

49. McPhee F, Campbell JA, Li W, D'Andrea S, Zheng ZB, Good AC, Carini DJ, Johnson BL, Scola PM (2004) Preparation of macrocyclic isoquinoline peptide inhibitors of hepatitis C virus. WO2004094452A2
50. Ripka A, Campbell JA, Good AC, Scola PM, Sin N, Venables B (2004) Preparation of hydroxyprolinamide peptides as hepatitis C virus inhibitors. US20040048802A1
51. Vacca JP, Rudd MT, Olsen DB, McIntyre CJ, McCauley JA, Ludmerer SW, Liverton NJ, Holloway MK (2008) HCV NS3 protease inhibitors. US7470664
52. Tsue H, Nakashima S, Goto Y, Tatemitsu H, Misumi S, Abraham RJ, Asahi T, Tanaka Y, Okada T et al (1994) Synthesis of rigid porphyrin-quinone compounds for studying mutual orientation effects on electron transfer and their photophysical properties. *Bull Chem Soc Jpn* 67:3067–3075
53. Olofson RA, Martz JT, Senet JP, Piteau M, Malfrout T (1984) A new reagent for the selective, high-yield N-dealkylation of tertiary amines: improved syntheses of naltrexone and nalbuphine. *J Org Chem* 49:2081–2082
54. Kong J, Chen C-y, Balsells-Padros J, Cao Y, Dunn RF, Dolman SJ, Janey J, Li H, Zacuto MJ (2012) Synthesis of the HCV protease inhibitor Vaniprevir (MK-7009) using ring-closing metathesis strategy. *J Org Chem* 77:3820–3828
55. Olsen DB, Davies M-E, Handt L, Koeplinger K, Zhang NR, Ludmerer SW, Graham D, Liverton N, MacCoss M, Hazuda D, Carroll SS (2011) Sustained viral response in a hepatitis C virus-infected chimpanzee via a combination of direct-acting antiviral agents. *Antimicrob Agents Chemother* 55:937–939
56. Hayashi N, Nakamuta M, Takehara T, Kumada H, Takase A, Howe AYM, Ludmerer SW, Mobashery N (2016) Vaniprevir plus peginterferon alfa-2b and ribavirin in treatment-naive Japanese patients with hepatitis C virus genotype 1 infection: a randomized phase III study. *J Gastroenterol* 51:390
57. Smith III AB, Kozmin SA, Adams CM, Paone DV (2000) Assembly of (–)-cylindrocyclophanes A and F via remarkable olefin metathesis dimerizations. *J Am Chem Soc* 122:4984–4985
58. Hong SH, Sanders DP, Lee CW, Grubbs RH (2005) Prevention of undesirable isomerization during olefin metathesis. *J Am Chem Soc* 127:17160–17161
59. McCauley JA, Rudd MT, Nguyen KT, McIntyre CJ, Romano JJ, Bush KJ, Varga SL, Ross III CW, Carroll SS, DiMuzio J, Stahlhut MW, Olsen DB, Lyle TA, Vacca JP, Liverton NJ (2008) Bismacrocyclic inhibitors of hepatitis C NS3/4a protease. *Angew Chem Int Ed* 47:9104–9107
60. Rudd MT, Butcher JW, Nguyen KT, McIntyre CJ, Romano JJ, Gilbert KF, Bush KJ, Liverton NJ, Holloway MK, Harper S, Ferrara M, DiFilippo M, Summa V, Swestock J, Fritzen J, Carroll SS, Burlein C, DiMuzio JM, Gates A, Graham DJ, Huang Q, McClain S, McHale C, Stahlhut MW, Black S, Chase R, Soriano A, Fandozzi CM, Taylor A, Trainor N, Olsen DB, Coleman PJ, Ludmerer SW, McCauley JA (2015) P2-quinazolinones and bis-macrocycles as new templates for next-generation hepatitis C virus NS3/4a protease inhibitors: discovery of MK-2748 and MK-6325. *ChemMedChem* 10:727–735
61. Reitsema RH (1948) The chemistry of 4-hydroxyquinolines. *Chem Rev* 43:47
62. Rudd MT, McCauley JA, Romano JJ, Butcher JW, Bush K, McIntyre CJ, Nguyen KT, Gilbert KF, Lyle TA, Holloway MK, Wan B-L, Vacca JP, Summa V, Harper S, Rowley M, Carroll SS, Burlein C, DiMuzio JM, Gates A, Graham DJ, Huang Q, Ludmerer SW, McClain S, McHale C, Stahlhut M, Fandozzi C, Taylor A, Trainor N, Olsen DB, Liverton NJ (2012) Development of potent macrocyclic inhibitors of genotype 3a HCV NS3/4A protease. *Bioorg Med Chem Lett* 22:7201–7206
63. The R155K mutant arises clinically in gt 1a infected patients, however Merck chose to screen against the gt 1b mutant such that the same background was utilized in relation to the main screening genotype 1 subtype. Where comparison data exist for both gt 1a and 1b R155K, the K_i values are similar, see reference 62
64. Rudd MT, McCauley JA, Butcher JW, Romano JJ, McIntyre CJ, Nguyen KT, Gilbert KF, Bush KJ, Holloway MK, Swestock J, Wan B-L, Carroll SS, DiMuzio JM, Graham DJ, Ludmerer SW,

- Stahlhut MW, Fandozzi CM, Trainor N, Olsen DB, Vacca JP, Liverton NJ (2011) Discovery of MK-1220: a macrocyclic inhibitor of hepatitis C virus NS3/4A protease with improved preclinical plasma exposure. *ACS Med Chem Lett* 2:207–212
65. Romano KP, Ali A, Aydin C, Soumana D, Ozen A, Deveau LM, Silver C, Cao H, Newton A, Petropoulos CJ, Huang W, Schiffer CA (2012) The molecular basis of drug resistance against hepatitis C virus NS3/4A protease inhibitors. *PLoS Pathog* 8:e1002832
 66. Rudd MT, McIntyre CJ, Romano JJ, Butcher JW, Holloway MK, Bush K, Nguyen KT, Gilbert KF, Lyle TA, Liverton NJ, Wan B-L, Summa V, Harper S, Rowley M, Vacca JP, Carroll SS, Burlein C, DiMuzio JM, Gates A, Graham DJ, Huang Q, Ludmerer SW, McClain S, McHale C, Stahlhut M, Fandozzi C, Taylor A, Trainor N, Olsen DB, McCauley JA (2012) Development of macrocyclic inhibitors of HCV NS3/4A protease with cyclic constrained P2-P4 linkers. *Bioorg Med Chem Lett* 22:7207–7213
 67. MarvinSketch, 3.5.2 (2004) ChemAxon Ltd
 68. Monteagudo E, Fonsi M, Chu X, Bleasby K, Evers R, Pucci V, Orsale MV, Cianetti S, Ferrara M, Harper S, Laufer R, Rowley M, Summa V (2010) The metabolism and disposition of a potent inhibitor of hepatitis C virus NS3/4A protease. *Xenobiotica* 40:826–839
 69. Li J, Smith D, Wong HS, Campbell JA, Meanwell NA, Scola PM (2006) A facile synthesis of 1-substituted cyclopropylsulfonamides. *Synlett*:725–728
 70. Xu F, Zhong Y-L, Li H, Qi J, Desmond R, Song ZJ, Park J, Wang T, Truppo M, Humphrey GR, Ruck RT (2017) Asymmetric synthesis of functionalized trans-cyclopropyl building block for grazoprevir. *Org Lett* 19:5880–5883
 71. Williams MJ, Kong J, Chung CK, Brunskill A, Campeau L-C, McLaughlin M (2016) The discovery of quinoxaline-based metathesis catalysts from synthesis of Grazoprevir (MK-5172). *Org Lett* 18:1952–1955
 72. Kuethe J, Zhong Y-L, Yasuda N, Beutner G, Linn K, Kim M, Marcune B, Dreher SD, Humphrey G, Pei T (2013) Development of a practical, asymmetric synthesis of the hepatitis C virus protease inhibitor MK-5172. *Org Lett* 15:4174–4177
 73. Lipinski CA (2004) Lead- and drug-like compounds: the rule-of-five revolution. *Drug Discov Today Technol* 1:337–341
 74. Gleeson MP (2008) Generation of a set of simple, interpretable ADMET rules of thumb. *J Med Chem* 51:817–834
 75. Leeson PD, Springthorpe B (2007) The influence of drug-like concepts on decision-making in medicinal chemistry. *Nat Rev Drug Discov* 6:881–890
 76. Waring MJ (2010) Lipophilicity in drug discovery. *Expert Opin Drug Discovery* 5:235–248
 77. Lawitz EJ, O'Riordan WD, Asatryan A, Freilich BL, Box TD, Overcash JS, Lovell S, Ng TI, Liu W, Campbell A, Lin C-W, Yao B, Kort J (2016) Potent antiviral activities of the direct-acting antivirals ABT-493 and ABT-530 with three-day monotherapy for hepatitis C virus genotype 1 infection. *Antimicrob Agents Chemother* 60:1546–1555
 78. Rodriguez-Torres M, Glass S, Hill J, Freilich B, Hassman D, Di BAM, Taylor JG, Kirby BJ, Dvory-Sobol H, Yang JC, An D, Stamm LM, Brainard DM, Kim S, Krefetz D, Smith W, Marbury T, Lawitz E (2016) GS-9857 in patients with chronic hepatitis C virus genotype 1-4 infection: a randomized, double-blind, dose-ranging phase 1 study. *J Viral Hepat* 23:614

The Discovery and Development of HCV NS3 Protease Inhibitor Paritaprevir



Keith F. McDaniel, Yi-Yin Ku, Ying Sun, Hui-Ju Chen, Jason Shanley, Timothy Middleton, Yat Sun Or, and Dale Kempf

Contents

1	Introduction	390
2	The Abbott-Enanta Collaboration	391
3	Early Chemistry and Virology	392
4	Metabolism and Pharmacokinetics	397
5	Discovery of P3-Heterocyclic Amide Capping Moieties	399
6	Discovery of the P*-Phenanthridine Series	401
7	Designation of ABT-450 as a Preclinical Candidate	405
8	ABT-450 Virology	407
9	Development of ABT-450	409
10	Conclusion	411
	References	412

Abstract Hepatitis C virus (HCV) NS3/4A protease inhibitors play an important role in several of the combination regimens that have revolutionized the treatment of this disease, offering patients an excellent chance for a complete cure. Starting from inhibitors incorporating oxime-based P*-shelf moieties, a collaborative effort between Abbott Laboratories and Enanta Pharmaceuticals generated ABT-450 (paritaprevir, a component of Technivie™ and Viekira Pak™), incorporating novel P*-phenanthridine and P3-amide capping groups and pharmacokinetically boosted by ritonavir. The discovery and development of ABT-450 enabled one of the first IFN-free combination therapies for HCV genotype 1 infection and contributed to the transformation of the treatment of this chronic and deadly disease.

K. F. McDaniel (✉), Y.-Y. Ku, H.-J. Chen, J. Shanley, T. Middleton, and D. Kempf
AbbVie, Inc., North Chicago, IL, USA
e-mail: Keith.f.mcdaniel@abbvie.com; Yiyin.ku@abbvie.com; Hui-ju.chen@abbvie.com;
Jason.shanley@abbvie.com; Timothy.middleton@abbvie.com; Dale.j.kempf@abbvie.com

Y. Sun and Y. S. Or
Enanta Pharmaceuticals, Watertown, MA, USA
e-mail: Yings2006@hotmail.com; Or@enanta.com

Keywords AbbVie, ABT-450, Enanta, Hepatitis C virus (HCV), Macrocyclic, Paritaprevir, Phenanthridine, Protease inhibitor, Ritonavir

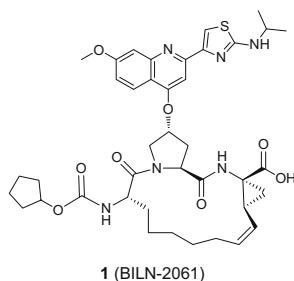
1 Introduction

The discovery of curative therapies for the treatment of hepatitis C virus (HCV) infection represents one of the most striking success stories in modern medicinal chemistry. Early treatments for this disease using pegylated interferon (pegIFN) and the antiviral compound ribavirin were plagued with both poor efficacy and poor tolerability. In contrast, subsequent advances in the discovery and development of HCV direct-acting antivirals (DAAs) now provide patients with an excellent chance for a complete cure. These current treatments utilize various combinations of agents targeting multiple drug targets, including NS3/4A protease inhibitors, NS5B polymerase inhibitors, and NS5A inhibitors, and provide high cure rates (>90–95%) in as short as 8 weeks of treatment and with limited side effects [1]. The intense and concentrated efforts required to advance to this milestone encompass a broad and diverse range of medicinal chemistry approaches, requiring the design and synthesis of extremely complicated chemical matter, as well as key advances which overcame significant biological challenges. The totality of these individual accomplishments demonstrates the power of modern drug discovery to identify increasingly superior treatments for destructive diseases.

Within the field of HCV NS3/4A protease inhibitors, two medicinal chemistry innovations led the field into the modern era. The first came with the development of the ketoamide-based covalent inhibitors telaprevir [2] and boceprevir [3]. These compounds required high doses and three times a day (TID) dosing due to low metabolic stability [4]. Nonetheless they provided substantially improved therapeutic outcomes for genotype (GT) 1 HCV patients and were approved for the treatment of HCV in combination with pegIFN and ribavirin [5, 6]. This combination treatment of HCV-infected patients represented the first breakthrough beyond IFN-based therapies and presaged the remarkable improvements of the past 10 years resulting in curative, IFN-free combination regimens.

A second medicinal chemistry breakthrough was revealed early in the 2000s by scientists at Boehringer Ingelheim, who reported that the strikingly complex non-covalently bound 15-membered ring macrocycle BILN-2061 (**1**, Fig. 1, [7]) demonstrated potent antiviral activity in a 2-day, twice-daily treatment clinical study. This compound demonstrated substantially improved antiviral activity compared to compounds based on ketoamide-based cores and thus offered the promise of an improved dosing regimen. Although further evaluation of BILN-2061 was discontinued due to cardiac toxicity revealed in cynomolgus monkeys [8], this medicinal chemistry tour de force, along with the discoveries of telaprevir and boceprevir, demonstrated that small molecule approaches to the treatment of HCV, while difficult, likely were feasible.

Fig. 1 Structure of BILN-2061



2 The Abbott-Enanta Collaboration

Although the antiviral team at Abbott Laboratories (the pharmaceutical division of Abbott became AbbVie in 2013) made several forays into the discovery of NS3/4A HCV protease inhibitors during the late 1990s and early 2000s, these efforts yielded only limited progress. With the success of other programs targeting HCV polymerase and NS5A inhibitors, however, it became imperative for Abbott to also access protease inhibitors in order to develop a multi-targeted combination regimen that would enable IFN-free HCV therapy. Thus, in December 2006, a collaboration agreement was signed between Abbott and Enanta Pharmaceuticals, a chemistry-driven biotech company based in Watertown, MA, which had developed a substantial portfolio of HCV NS3/4A protease inhibitor patents and patent applications, covering a wide range of cores and structures. Several of the leaders at Enanta had previously worked at Abbott, and therefore the collaboration began on firm and familiar ground. Abbott's experience in the development of HIV protease inhibitors ritonavir and lopinavir (both key ingredients in Abbott's HIV protease inhibitor Kaletra™) also brought substantial value to the collaboration, and a strong research relationship quickly developed between the two organizations.

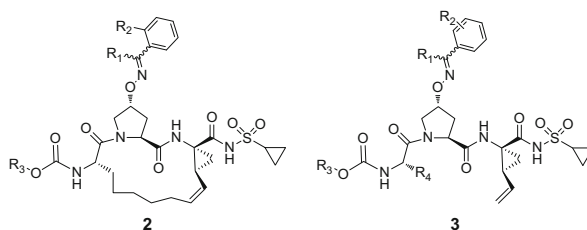
The main goal early in the collaboration was to rapidly evaluate and expand upon the most promising compounds provided by Enanta in search of potential clinical candidates. In order to focus this search, the team made the decision to concentrate its initial efforts on the discovery of agents that demonstrated potency against genotype 1 virus, the most prevalent form of the disease [9], and the genotype most poorly served by the then current pegIFN/ribavirin regimen [10, 11]. The initial target product profile (TPP) also included once-daily (QD) dosing with a favorable therapeutic index, a substantial improvement over the existing therapy. A particularly attractive characteristic of many of the inhibitors discovered at Enanta was the observation of high liver exposures in rat pharmacokinetic (PK) studies, suggesting efficient targeting of liver tissue. Since the primary target organ for HCV antiviral activity is the liver, potent activity might be expected from a HCV protease inhibitor that maintains inhibitory concentrations in the liver but not necessarily in the plasma. At the outset, the combined team faced several challenges. In vitro replication systems for HCV are relatively artificial. They consist of HCV replicons, which encode the nonstructural proteins necessary for replication of subgenomic HCV

RNA but do not encode the structural proteins required for particle formation and new rounds of infection [12]. Furthermore, no validated small animal models for HCV infection existed at that time, and studies in infected chimpanzees, which could provide preclinical proof-of-concept (PoC) and information about liver drug concentrations, were only occasionally available. The above practical difficulties created uncertainty regarding the target preclinical profile of HCV PIs with respect to plasma and liver PK. Nonetheless, compounds that concentrated in the liver and had low exposures in other compartments decreased the likelihood of extra-hepatic toxicity. Therefore, decisions around prioritization of chemical series and advancement of preclinical candidates were based primarily on *in vitro* virology studies along with sophisticated PK studies incorporating both plasma and the liver. Fortunately, plasma HCV RNA is a biomarker for efficacy that can be assessed in early short-term human studies providing PoC and insight into pharmacokinetic/pharmacodynamic (PK/PD) relationships.

3 Early Chemistry and Virology

In addition to the experienced research teams that both parties brought to the collaboration, Enanta also provided the aforementioned robust pipeline of HCV protease inhibitors. Several key features of the known HCV protease inhibitor structural landscape, particularly those utilized in the BILN-2061 framework, were featured in the Enanta portfolio. Thus, P1–P3 macrocycles based on the BILN-2061 core were incorporated into many of the inhibitors (e.g., **2**, Fig. 2), along with more simplified compounds based on a linear core (e.g., **3**, Fig. 2) [13] which eased synthesis demands. A variety of C-terminal carboxylic acid isosteres were also explored, including the acylsulfonamide [14]. While a range of P3-capping groups were examined (R_3), the most potent and promising compounds evaluated in the initial stages of the program utilized carbamate-based P3 moieties. In the linear series most of the P3 side chains (R_4) consisted of relatively simple alkyl groups. The main focus of structural differentiation between early chemical series focused on modifications of the moiety attached to the hydroxy group of the P2 proline (referred to subsequently as the P* group), which boosted potency via hydrophobic interactions with the extensive P*-shelf in the HCV protease active site [15]. From the wide variety of compounds examined by Enanta prior to the partnership and early in the

Fig. 2 P*-oxime series structures



collaboration, the series that came rapidly to the forefront based on biological activity, DMPK properties, and novelty consisted of compounds that contained an oxime-based P^{*}-shelf moiety (Fig. 2). These P^{*}-oximes incorporated a large, flat aromatic group that provided substantial potency via a productive hydrophobic interaction, although at the risk of negatively impacting drug metabolism and pharmacokinetic (DMPK) properties. The P1–P3 macrocyclic P^{*}-oxime inhibitors (**2**) and linear P^{*}-oxime inhibitors (**3**) each provided advantages and disadvantages, as described below, and formed the basis of the first optimized lead compounds to emerge from this effort.

Two cellular assays provided the main biological data collected and examined for compound characterization [16]. The first assay employed cell lines generated to express genotypes 1a (from HCV strain H77) and 1b (from HCV strain Con1) as stably replicating replicons similar in nature to those described previously [12] (referred to herein as the “stable replicon assay”). As compound development progressed, the impact on antiviral activity of protein binding by human serum was measured by comparing the activity of the compounds measured in the stable replicon assay in the presence of 5% fetal bovine serum (FBS) vs. the activity noted in the presence of 5% FBS plus 40% human plasma to measure the impact of plasma protein binding on potency. The second assay (transient replicon assay) used cells transfected with replicons similar to those used to generate the stable cell lines. The extent of replication of the replicons over 3 days was measured. Using this assay, antiviral activity against a panel of resistance-associated substitutions was also gathered through the use of 1a-H77 and 1b-Con1 subgenomic shuttle vector constructs used for introduction of mutations of interest in the NS3 gene. These replicon shuttle vectors allowed insertion of the region encoding the complete NS3 protease domain, and the EC₅₀ values of compounds were evaluated in these transient assays [16].

Although the TPP for the program focused on the generation of compounds with high activity against genotype 1, lead compounds were also profiled for activity against genotypes 2–4 in a tight-binding enzyme assay [17, 18] and against stable replicons containing NS3 from genotype 2a, 3a, 4a, or 6a [16].

As noted above, one series of P^{*}-oxime-based inhibitors investigated in detail incorporated the 15-membered ring P1–P3 macrocycle (**4**, Fig. 3). Early results from

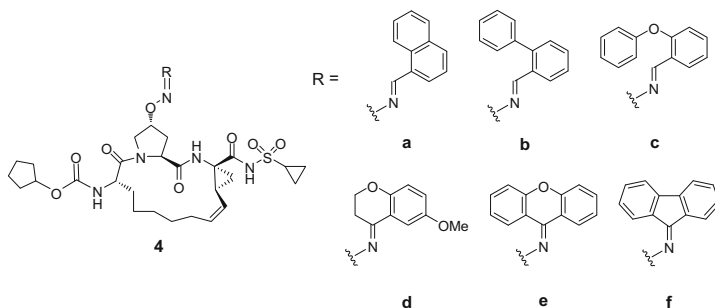


Fig. 3 Representative P1–P3 macrocyclic P^{*}-oxime inhibitors

the Enanta team determined that although oximes generated from both aromatic aldehydes and ketones generally provided potent compounds as measured in biochemical and replicon assays, symmetric compounds proved to be more easily characterized and avoided any potential syn/anti stereochemistry complications potentially present with aldoximes or nonsymmetric ketoximes. Tricyclic systems such as oxime **4f** resulting from condensation of 9*H*-fluoren-9-one bound productively into the P*-shelf (Fig. 4) and provided a potent core from which to evaluate additional SAR.

The second focus of SAR examination in this P1–P3 macrocyclic P*-oxime series centered on the P3-carbamate group located in the southwest quadrant of the molecule (**5**, Fig. 5). A range of carbamates was investigated, with the most potent and practical structures incorporating relatively simple alkyl and cycloalkyl groups such as cyclopentyl (**5a**) and *t*-butyl (**5c**). Examination of the activity of these two

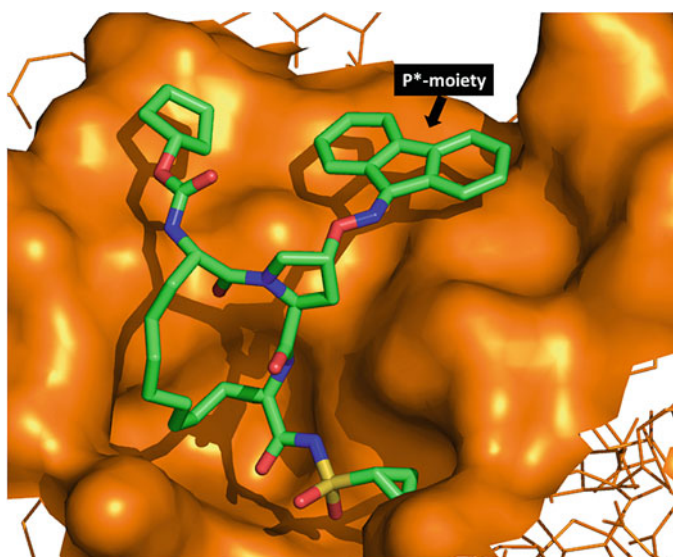


Fig. 4 Model of **4f** in HCV protease

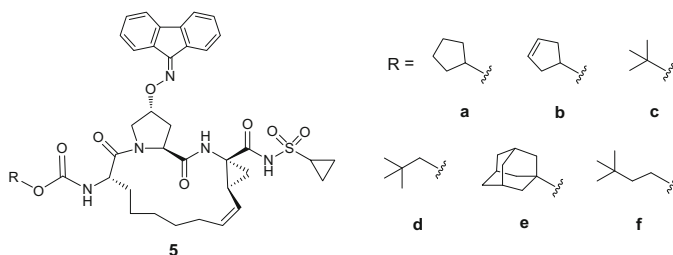


Fig. 5 Representative P3 capping carbamates

compounds against a small panel of resistance-associated substitutions in genotype 1b revealed negligible potency differences, and the impact of human serum binding on activity in a stable replicon assay also failed to differentiate between the two analogs.

The SAR of the less structurally complex linear P*-oxime analogs was also generated and examined (**6**, Fig. 6). Replacement of the macrocycle with a P1-vinyl cyclopropane and simple alkyl groups at P3 interestingly provided linear inhibitors with improved DMPK properties albeit with somewhat reduced potencies. The most promising analogs from this series also incorporated alkyl carbamates (R₁), along with simple alkyl moieties appended in P3 (R₂). The incorporation of polar groups at this R₂ position (e.g., -C(CH₃)₂OH) led to a substantial drop in potency.

From these sets of project compounds, two P*-oxime-based protease inhibitors with structural differences at the carbamate position (cyclopentyl vs. t-butyl) and P1–P3 groups (acyclic vs. macrocyclic) were chosen to advance as optimized leads. The antiviral attributes of these promising analogs (compounds **7** and **8**) were examined in more detail. In the stable replicon assay against genotypes 1a and 1b, macrocyclic inhibitor **8** exhibited superior potency by approximately six- to eight-fold (Table 1). The impact of plasma protein binding on this activity was also determined by measuring the activity of both compounds in the presence of 40%

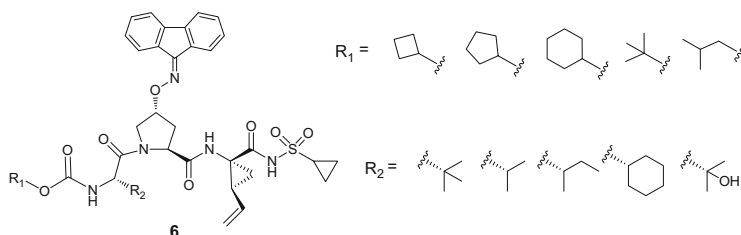
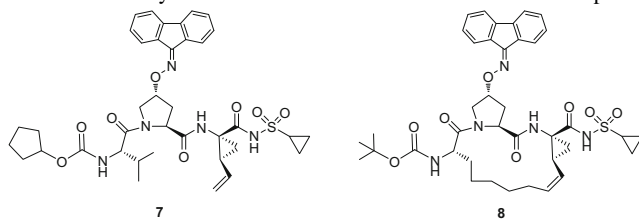


Fig. 6 Linear P*-oxime inhibitors

Table 1 Activity of P*-oxime inhibitors **7** and **8** in the stable replicon assay



Compound	Stable replicon EC ₅₀ (nM)			Fold change in HP
	GT 1a	GT 1b	GT1b, 40% HP	
7	7.0	4.1	169	41
8	0.9	0.7	37	52

human plasma in genotype 1b, which resulted in a similar drop in potency in each case (41–52-fold, Table 1).

Another criterion for evaluation of the two lead compounds was their activity against a panel of resistance-associated substitutions resistant to previously developed NS3/4A inhibitors (Table 2). Compounds **7** and **8** were examined in a transient assay against genotype 1a and 1b wild-type replicons alongside amino acid substitutions that were identified through the use of 1a-H77 and 1b-Con1 subgenomic shuttle vector constructs, as described above. As noted in the stable replicon assay, the macrocyclic inhibitor **8** demonstrated superior activity compared to the linear inhibitor **7** against both genotypes 1a (eightfold) and 1b (threefold) wild-type virus. The difference in potency against the panel of resistance-associated substitutions was even more striking: macrocyclic inhibitor **8** was 7–20-fold more active than the linear inhibitor **7** against substitutions examined in both genotypes 1a and 1b. It should be noted that both compounds registered large decreases in potency vs. the crucial D168V substitution in genotype 1a.

The two lead compounds were also profiled for activity against genotypes 2–4 in a tight-binding enzyme assay [17, 18]. Although both compounds demonstrated similar potency against genotypes 1 and 4 in this assay, the linear inhibitor **7** lost substantially more activity when measured against genotypes 2a and 2b and particularly against genotype 3a (Table 3). While the macrocyclic inhibitor **8** also lost potency vs. genotypes 2 and 3, this drop in activity was much less striking.

Finally, the activity of compounds **7** and **8** in colony selection assays was also evaluated. HCV genotype 1a and 1b subgenomic replicon cell lines were passaged in the presence of **7** and **8** at concentrations of 10-, 100-, and 1,000-fold over their respective EC₅₀. Fewer colonies survived with **8** than with **7** in all of the cell lines, indicating lower prevalence of preexisting substitutions that can confer resistance to

Table 2 Activity of P*-oxime inhibitors **7** and **8** against resistance-associated substitutions

Compound	Transient replicon EC ₅₀ (nM)						
	GT 1a background			GT 1b background			
	WT	D168E (fold loss)	D168V (fold loss)	WT	D168V (fold loss)	A156T (fold loss)	R155K (fold loss)
7	2.1	129 (61×)	>1,000 (>476×)	0.66	184 (279×)	38 (58×)	18 (27×)
8	0.25	6.5 (26×)	127 (508×)	0.23	10 (40×)	2.3 (10×)	2.4 (12×)
7/8	8	20	>7	3	18	17	8

Table 3 Activity of P*-oximes **7** and **8** vs. HCV genotypes 1–4

Compound	Enzyme activity across GT 1–4 in 6 h tight-binding assay (K _i , nM, fold loss for GT 2–4 vs. GT 1)				
	GT 1 (average)	2a (fold loss)	2b (fold loss)	3a (fold loss)	4a (fold loss)
7	0.094	3.8 (40×)	17 (181×)	55 (585×)	0.15 (1.6×)
8	0.075	0.54 (7×)	1.1 (15×)	3.0 (40×)	0.07 (1×)

Table 4 Colony selection assay results for compounds **7** and **8**^a

Compound	1a-H77			1b-con1		1b-N		
	10×	100×	1,000×	10×	100×	10×	100×	1,000×
7	0.97	0.055	0.003	0.50	0.084	>1	0.75	0.053
8	0.06	0.011	0	0.065	0.017	0.91	0.11	0

^aPercent surviving replicon colonies from 10⁵ cells after selection with inhibitor

8 (Table 4). Overall, therefore, by a number of measures, the antiviral activity of the P1–P3 macrocyclic inhibitor **8** was deemed to be superior to the linear inhibitor **7**.

4 Metabolism and Pharmacokinetics

Along with the virology characteristics, the *in vitro* metabolism and *in vivo* PK properties of the P*-oxime-based HCV protease inhibitors were studied. Initial PK results after dosing in rats were highly encouraging. Thus, even though plasma exposures were low after oral dosing, concentrations in rat liver were high and sustained, with continuous concentrations many times above 40% human plasma-adjusted replicon EC₅₀ values for the entire 8-h evaluation period. As mentioned above, this “liver-targeted” profile offered potential advantages in treating HCV infection, in which viral replication is largely confined to hepatocytes. However, further studies on the series revealed two potential liabilities. First, the liver-plasma (L:P) exposure ratio in other preclinical species was substantially lower than in rat. Consequently, the extent to which rat PK experiments could predict liver-targeting in humans was highly uncertain. Second, studies in liver microsome cultures revealed that the analogs were much less stable toward metabolism in human systems compared to rats. Therefore, even if the compounds targeted the liver in humans, sustained concentrations were unlikely given low metabolic stability in liver tissue. To address the first issue, PK studies in larger, non-rodent preclinical species were conducted in which liver biopsies were analyzed for drug concentrations. Ultimately, a study in a HCV-infected non-human primate (chimpanzee) provided insight not only into liver PK but additionally into the PK/PD of this series. To address the second uncertainty, *in vitro* and *in vivo* studies were conducted in the presence of ritonavir, a powerful inhibitor of cytochrome P-450 3A (CYP3A) [19]. Ritonavir, which is used to pharmacokinetically boost HIV protease inhibitors such as lopinavir [20], had also been shown to boost the plasma concentrations of ketoamide-based HCV protease inhibitors [4]. Although the above studies were conducted on multiple analogs in the P*-oxime series, the description below is confined to the lead compounds **7** and **8**.

Total *in vitro* clearance in human, rat, and dog liver microsomes for **7** and **8** is provided in Table 5. As noted with other analogs in the series, stability in human microsomes was markedly lower than in rat microsomes, suggesting that rat PK profiles of these compounds may not be predictive of human. Co-incubation with

Table 5 In vitro metabolism of compounds **7** and **8**

Compound	Liver microsome stability ($Cl_{\text{int vitro}}$, $\mu\text{L}/\text{min}/\mu\text{g}$)			
	Rat liver microsomes	Dog liver microsomes	Human liver microsomes	Human liver microsomes plus ritonavir
7	43	68	118	24
8	71	370	265	<23

Table 6 Preclinical pharmacokinetics of **7** and **8**

Compound	Species	Dose (mg/kg)	C_{max} ($\mu\text{g}/\text{mL}$)	AUC ($\mu\text{g h}/\text{mL}$)
7	Rat	30	0.34	2.2
		50 + RTV (25)	8.2	53
	Dog	10	0.16	1.0
		10 + RTV (10)	13.9	162
	Monkey	2.5	0	0
		15 + RTV (15)	1.3	3.9
8	Rat	5	0	0
		5 + RTV (5)	0.03	0.25
	Dog	5	1.55	0.97
		5 + RTV (5)	16.1	69
	Monkey	2.5	0	0
		10 + RTV (10)	0.59	3.3

ritonavir substantially reduced the in vitro metabolism of both compounds, indicating that the metabolism was primarily mediated by CYP3A. Notably, in vitro clearance in human microsomes in the presence of ritonavir was even lower than in rat liver microsomes, suggesting that suppressive concentrations might be maintained in human liver following co-dosing of these compounds with ritonavir.

The in vitro metabolic interaction of **7** and **8** with ritonavir was confirmed in PK studies of the two compounds (Table 6). In most cases, plasma concentrations following oral dosing without ritonavir were low or undetectable, consistent both with low metabolic stability and with liver-targeting. Indeed, in separate studies, high L:P ratios were observed, particularly in rats (**7**, 785:1 at 3 h, 8,887:1 at 12 h; **8**, 171:1 at 3 h, 454:1 at 6 h). The L:P ratio for **8** was lower in dogs (2:1), although a significant level of liver-targeting was evident in monkeys (L:P 9:1). The effect of ritonavir co-dosing was surprisingly profound: plasma AUC increased by at least 20-fold, to >100-fold in some cases.

The differences in metabolic stability and PK properties of **7** and **8** between preclinical species presented a challenge for the estimation of a projected efficacious human dose. Based on PK/PD studies of HIV protease inhibitors [21] and the fact that HCV replication occurs in the liver, the maintenance of concentrations well in excess of the in vitro 40% human plasma-adjusted EC_{50} was deemed a requirement to achieve the desired initial viral load decline (~4 logs) observed with potent HCV protease inhibitors [7] and required by the TPP. To test this hypothesis and better understand the correlation between antiviral activity and PK, the examination of

Table 7 Liver concentrations of **7** and **8** after co-dosing with ritonavir

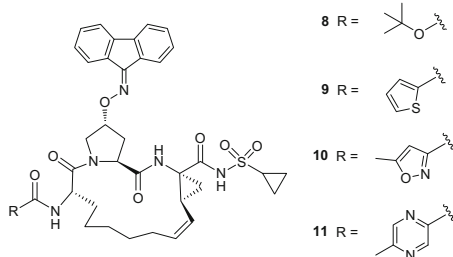
Compound	Species	Dose (mg/kg)	Liver C12 ($\mu\text{g/g}$)
7	Rat	20	50.4
	Dog	15	0.38
	Dog	15 + RTV (15)	53.5
8	Rat	20	15.2
	Dog	15	0.68
	Dog	15 + RTV (15)	56.2

compound **7** in a genotype 1b HCV-infected chimpanzee was initiated. In this study, **7** was dosed orally at 450 mg BID for 7 days and produced a 2.5 log decline in HCV RNA levels, with a liver C_{trough} of 1.1 $\mu\text{g/g}$ (ninefold above the 40% human plasma-adjusted in vitro EC_{50} against the GT1b stable replicon). This in vivo efficacy result not only demonstrated a PoC for this series of HCV protease inhibitors but also helped to define, through additional PK/PD modeling, minimum target 24-h liver concentrations for QD dosing. Since P1–P3 macrocyclic analog **8** was at least fivefold more potent than compound **7**, it appeared likely that liver C_{trough} levels significantly in excess of 0.2 $\mu\text{g/g}$ would be needed to achieve the TPP.

In order to ascertain the effect of differences in metabolic stability observed in microsomes on the persistence of suppressive concentrations in liver, liver biopsies were performed in dogs 12 h after oral dosing of **7** and **8**, either alone or with a ritonavir co-dose. As shown in Table 7, 12-h liver concentrations for both **7** and **8** were lower than target 24-h liver concentrations for humans. Notably, 12-h liver concentrations in rats, in which metabolic stability was substantially higher than in dogs, exceeded those in dogs by ~ 100 -fold and ~ 20 -fold for **7** and **8**, respectively. Likewise, co-dosing either **7** or **8** with ritonavir in dogs resulted in 12-h liver concentrations similar to those observed in rats. Taken together with the low in vitro stability of both compounds in human liver microsomes, these results strongly suggested that achieving high antiviral activity in humans with either **7** or **8** would require ritonavir boosting.

5 Discovery of P3-Heterocyclic Amide Capping Moieties

During the detailed evaluation of P*-oxime HCV protease inhibitors **7** and **8**, a variety of medicinal chemistry efforts continued in an attempt to generate compounds with superior activity and DMPK properties. Multiple modifications of the structure of the macrocycle, the P*-group, the cyclopropyl acyl sulfonamide, and the P3-capping moiety were studied. One simple yet ultimately valuable aspect of this effort involved further examination of the SAR surrounding the P3-carbamate moiety of **8**. As more data became available, one compound that stood out in the P1–P3 macrocyclic P*-oxime series incorporated a 2-thiophene amide moiety for the P3-capping group (**9**) in place of the more standard carbamates. Thiophene amide **9** demonstrated slightly improved activity in the stable replicon assay compared to

Table 8 Potency data for P3-amide analogs

Compound	Stable replicon EC ₅₀ (nM)		GT 1b transient replicon EC ₅₀ (nM)			
	GT 1a	GT 1b	WT	R155K (fold loss)	D168V (fold loss)	A156T (fold loss)
8	1.0	0.9	0.20	2.3 (11×)	10 (50×)	2.3 (12×)
9	0.7	0.2	0.10	0.28 (3×)	0.80 (8×)	0.37 (4×)
10	0.4	0.2	0.10	2.7 (27×)	5.0 (50×)	1.9 (19×)
11	1.9	0.5	1.1	27 (25×)	31 (28×)	10 (10×)

Table 9 Liver microsome stability comparison for P3-capped analogs

Compound	Liver microsome stability (Cl _{int} <i>in vitro</i> , μL/min/μg)		
	Human LM	Rat LM	Dog LM
8	265	71	541
9	330	53	NA
10	213	81	445
11	75	33	28

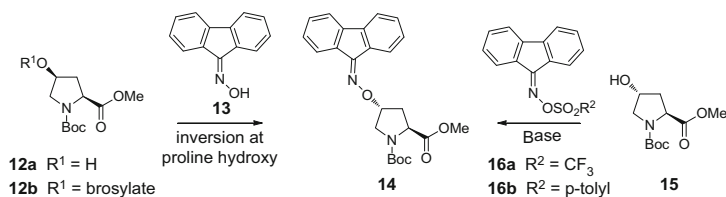
t-butyl carbamate **8** in both genotypes 1a (0.7 nM vs. 0.9 nM for **8**) and 1b (0.2 nM vs. 0.7 nM for **8**) (Table 8). More importantly, thiophene amide **9** demonstrated improved activity compared to **8** against the panel of genotype 1b resistance-associated substitutions, with fold losses in activity of only 3× (R155K), 8× (D168V), and 4× (A156T) compared to 11× (R155K), 50× (D168V), and 12× (A156T), respectively, for carbamate **8**. Although the limited stability of thiophene **9** in human liver microsomes precluded further detailed evaluation of this compound, based upon this observation, a large library of P3-amide capping groups was generated and evaluated. From this library of analogs, several trends stood out. First, methyl-substituted five-membered ring heterocyclic amides, such as isoxazole **10** (Table 8), demonstrated excellent activity against wild-type genotype 1a and 1b replicons and were also potent vs. genotype 1b resistance-associated substitutions R155K, D168V, and A156T in the transient replicon assay. Amides incorporating six-membered ring heterocycles (e.g., **11**) demonstrated moderate activity against both wild-type replicons and resistance-associated substitutions but exhibited substantially improved metabolic stability in human, rat, and dog liver microsomes (Table 9). This improved stability in liver microsomes translated to

improved PK properties. For example, compound **11** exhibited substantially increased exposure ($AUC = 25 \mu\text{g h/mL}$) and bioavailability ($F = 27\%$) in dog PK studies when compared to *t*-butyl carbamate **8**. The incorporation of representative P3-heteroaryl amide capping moieties was therefore included in all subsequent SAR evaluations of new cores.

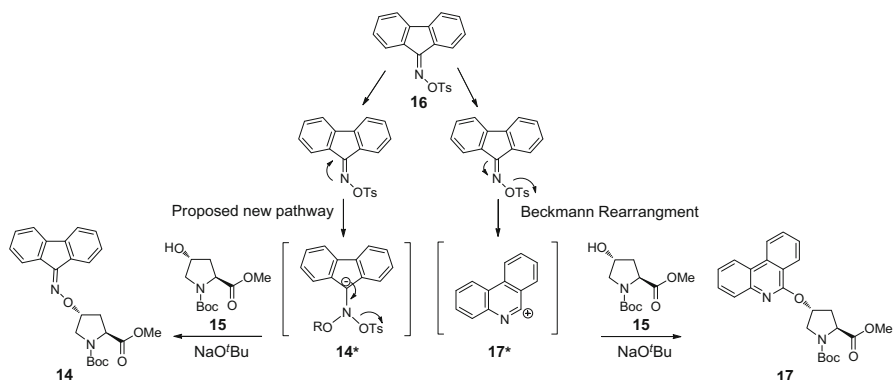
6 Discovery of the P*-Phenanthridine Series

A second discovery with a major impact on the medicinal chemistry program originated from the process chemistry group, an innovation which came in the midst of developing routes suitable for the large-scale preparation of **7** and **8** containing the preferred oxime moiety. The initial synthetic approach to the incorporation of the fluoren-9-one oxime group utilized the Mitsunobu reaction of the fluoren-9-one oxime **13** with *cis*-hydroxy proline **12a** ($R = \text{H}$) to provide intermediate **14** (Scheme 1). A related approach utilized the displacement reaction of the proline brosylate **12b** ($R = \text{brosylate}$). In both cases, inversion of configuration at the proline hydroxyl mandated the use of the *cis*-hydroxy proline intermediate, which was not available in large quantity and required several chemical steps to invert the hydroxyl group from the more readily available *trans*-hydroxy proline **15**.

During the investigation of alternative approaches to intermediate **14**, it was postulated that direct displacement of triflate **16a** ($R^2 = \text{CF}_3$) with *trans*-hydroxy proline **15** could be accomplished by an addition-elimination pathway via formation of a stabilized 6π -electron anionic intermediate (**14***) which could collapse to form **14**, thus avoiding double inversion of the *trans*-hydroxy proline (Scheme 2). Treatment of triflate **16a** with **15** under basic conditions indeed provided **14**, indicating that the reaction did proceed through the reactive intermediate **14***. However, phenanthridine **17** was also formed as a significant product during this reaction (Scheme 2), likely via a Beckmann rearrangement intermediate **17***. The structure determination of **17** was confirmed by 2D NMR analysis. Notably, formation of



Scheme 1 Synthetic approaches to oxime intermediate **14**



Scheme 2 Two observed reaction pathways for the reaction of fluorenone triflate **16a** with *trans*-hydroxy proline **15**

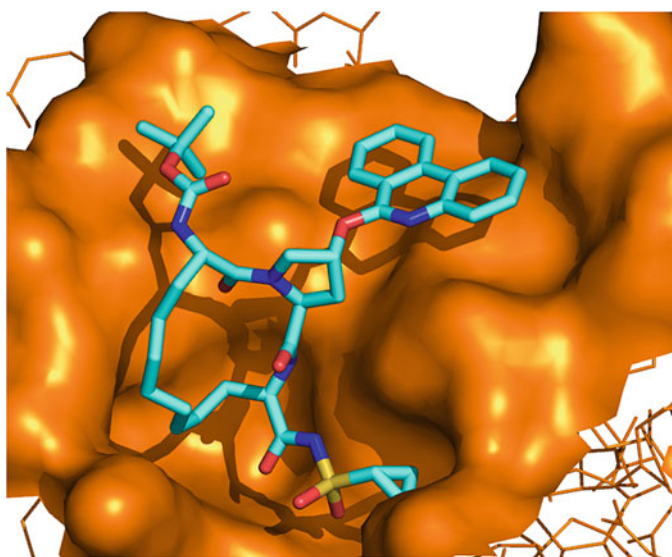
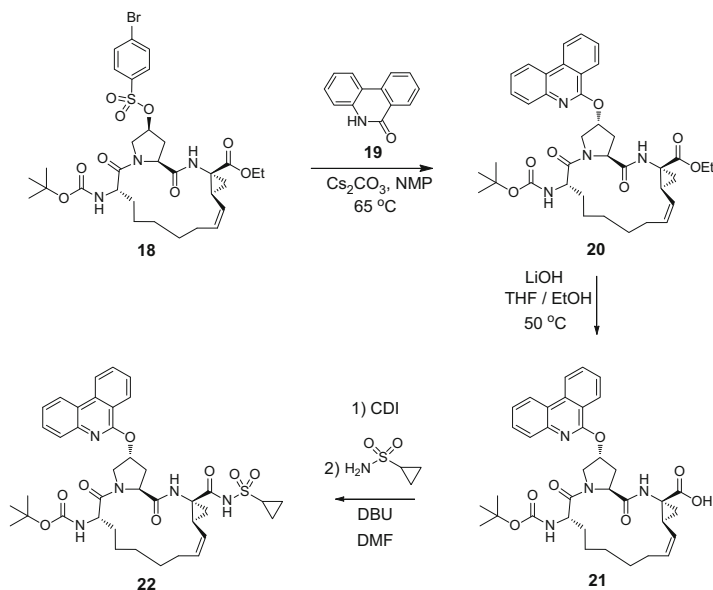


Fig. 7 Model of P*-phenanthridine **22** bound in HCV protease

phenanthridines was not observed when the tosylate **16b** ($R^2 = p\text{-tolyl}$) was reacted with alcohols under similar conditions [22].

The isolation of **17** as a major byproduct provided the opportunity for biological examination of a new class of P*-phenanthridine analogs of oximes **7** and **8**, as it appeared that these new P*-phenanthridine moieties might bind similarly well to the P*-shelf occupied by the P*-fluoren-9-one oxime. Molecular modeling of the P*-phenanthridine supported this hypothesis (Fig. 7).

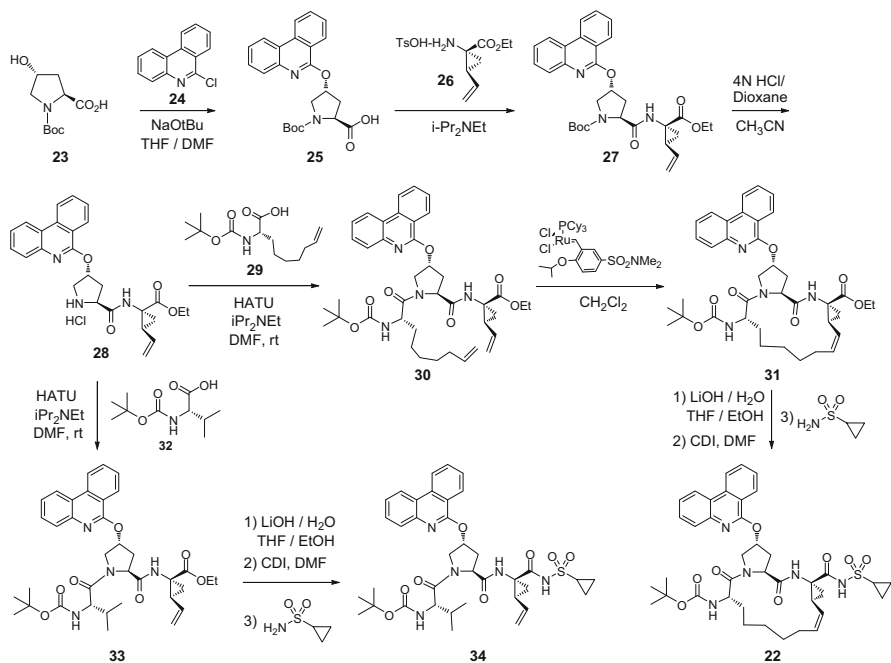
Direct synthesis of the P*-phenanthridine analogs could be accomplished by S_N2 displacement of the advanced intermediate macrocyclic brosylate **18** with



Scheme 3 Initial preparation of P*-phenanthridine **22**

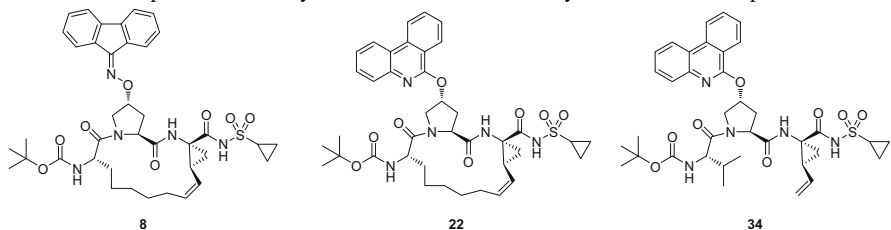
phenanthridinone (**19**) to provide P*-phenanthridine **20** (Scheme 3). Hydrolysis of the ethyl ester followed by incorporation of the preferred acyl sulfonamide generated compound **22**, analogous to oxime **8** but with the phenanthridine P*-shelf moiety in place. However, the preparation of brosylate **18** was inefficient, still requiring inversion of a *cis*-hydroxy proline. Thus, a more practical synthesis was developed based on direct arylation of the preferred *trans*-hydroxy proline with 2-chlorophenanthridine. This synthesis was successfully applied to prepare both the P1–P3 macrocyclic P*-phenanthridine **22** and the linear P*-phenanthridine **34** (Scheme 4).

To our delight, initial analysis of the activity of compound **22** indicated that this phenanthridine moiety might serve as an excellent P*-moiety. In fact, the activity of macrocyclic phenanthridine **22** was found to be comparable or even superior to macrocyclic oxime **8** in the genotype 1a and 1b stable replicon assays and was also of comparable activity against a panel of resistance-associated substitutions (Table 10). The activity of acyclic P*-phenanthridine analogs such as **34** did not match the activity of the macrocyclic analogs, particularly with respect to their activity against the panel of resistance-associated substitutions. Therefore, nearly all additional efforts incorporating P*-phenanthridines were directed toward the macrocyclic series.

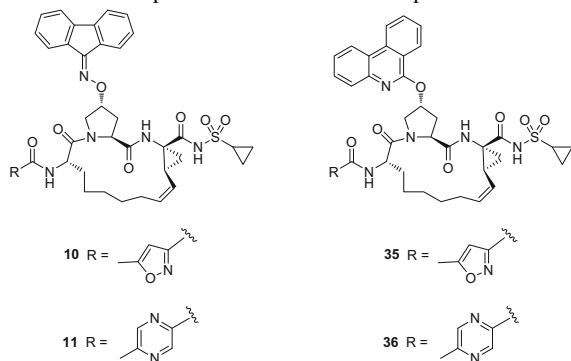


Scheme 4 Improved synthetic route to P*-phenanthridines **22** and **34**

Table 10 Comparison of activity and liver microsome stability of P*-oxime to P*-phenanthridines



Compound	Stable replicon EC ₅₀ (nM)		GT 1b transient replicon EC ₅₀ (nM)				Human LM Cl _{in vitro}
	GT 1a	GT 1b	WT	R155K (fold loss)	D168V (fold loss)	A156T (fold loss)	
8	0.9	0.7	0.3	2.3 (8×)	10 (33×)	2.1 (7×)	265
22	0.7	0.4	0.1	1.2 (12×)	4.8 (48×)	1.5 (15×)	293
34	2.7	0.5	2.6	88 (34×)	252 (97×)	114 (44×)	143

Table 11 Comparison of P*-oxime and P*-phenanthridine P3-heterocyclic amides

Compound	Stable replicon EC ₅₀ (nM)		Fold change in EC ₅₀ relative to wild-type value in GT 1b transient replicon EC ₅₀		
	GT 1a	GT 1b	R155K	D168V	A156T
10	0.4	0.2	27	50	19
35	0.2	0.2	9	9	4
11	1.9	0.5	25	28	9
36	1.0	0.2	21	19	6

Since P3-heteroaryl amide capping groups provided an improvement in both activity and liver microsome stability in the P*-oxime series, a set of analogous amides was generated in the new P*-phenanthridine series. Similar to the two analogous *t*-butyl carbamates **8** and **22**, a comparison of activities of matched pairs revealed that the P*-phenanthridine analogs demonstrated a moderate advantage compared to the P*-oxime analogs in activity against genotypes 1a and 1b in the stable replicon assay as well as the panel of genotype 1b resistance-associated substitutions in the transient replicon assay (Table 11) for both the five-membered ring and the six-membered ring heterocyclic amides. Again, the five-membered ring heterocyclic amides such as 5-methylisoxazole **35** provided the most potent compounds, although 4-methylpyrazine amide **36** also demonstrated an excellent activity profile.

7 Designation of ABT-450 as a Preclinical Candidate

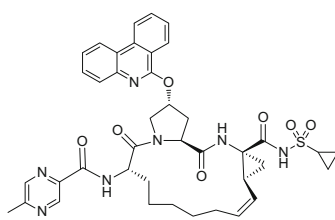
The improved antiviral potency of P*-phenanthridines and the improved spectrum of P3-heteroaryl amides against replicons containing resistance-associated substitutions suggested that the SAR studies had identified optimal compounds qualifying for preclinical candidate status. The antiviral and DMPK properties of optimized compounds **35** and **36** were therefore thoroughly compared. In general, most properties did not greatly discriminate between the two compounds. However, a key distinction was noted in their *in vitro* metabolism profiles: across human, rat,

dog, and monkey liver microsomes, compound **36** demonstrated greater stability (Table 12). The metabolism of both compounds was substantially reduced in the presence of ritonavir. However, the significantly higher stability of compound **36** in HLM without ritonavir offered two potential advantages. First, it was possible that the metabolic stability could be sufficient to support the development of **36** without the need for ritonavir co-dosing, whereas the very low stability of compound **35** did not offer that potential. Second, in the event that ritonavir co-dosing was needed with compound **36**, the dose of ritonavir required to sustain levels sufficiently for QD dosing might be expected to be lower. On the basis of these potential advantages, compound **36** was chosen to progress forward as a preclinical candidate, and designated as ABT-450 (Fig. 8).

The pharmacokinetic profiles of ABT-450 in rat and dog are provided in Table 13. Plasma half-life in rat was short after IV dosing and concentrations were low after oral dosing even with ritonavir (undetectable without ritonavir), consistent with rapid uptake into liver, where the L:P ratio was 385 and 496 at 3 and 8 h after dosing, respectively. Because of higher metabolic stability and lower liver uptake (average L:P ~7), plasma concentrations in dogs were reasonable without ritonavir (41% bioavailability); however, co-dosing with ritonavir increased exposure by >fourfold and sustained plasma levels to 24 h. More importantly, liver levels were increased by three- to fivefold by ritonavir co-dosing (Fig. 9), and average liver concentrations at 12 h after dosing with ritonavir (2.66 $\mu\text{g/g}$) exceed 6-h concentrations with no ritonavir (1.37) by twofold. Taken together with the *in vitro* metabolism data above, these results suggested that ritonavir co-dosing in humans would both elevate and sustain ABT-450 concentrations in both plasma and liver in humans.

Table 12 *In vitro* metabolism of compounds **35** and **36** (ABT-450) in liver microsomes

Species	Liver microsome stability ($Cl_{\text{int vitro}}$, $\mu\text{L}/\text{min}/\mu\text{g}$)	
	Compound 35	Compound 36
Rat	90	50
Dog	95	31
Monkey	301	94
Human	225	88
Human (+RTV)	<23	<23

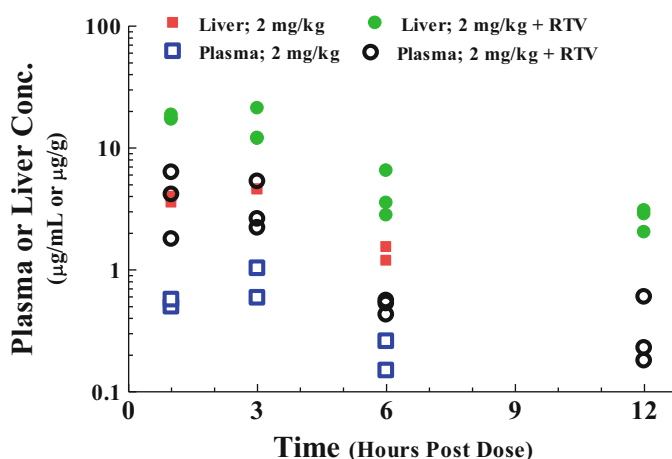


ABT-450

Fig. 8 Structure of ABT-450

Table 13 Preclinical pharmacokinetics of ABT-450

IV dosing:				
Species	Dose (mg/kg)	$t_{1/2}$ (h)	V_{ss} (L/kg)	CLp (L/h kg)
Rat	5	0.4	0.98	3.0
Dog	2.5	1.2	0.15	0.1
Oral dosing:				
Species	Dose (mg/kg)	C_{max} ($\mu\text{g/mL}$)	AUC ($\mu\text{g h/mL}$)	F (%)
Rat	5	0	0	0
	5 + RTV (5)	0.3	0.1	–
Dog	5	6.3	19	41
	5 + RTV (5)	23	85	–

**Fig. 9** Plasma and liver concentrations of ABT-450 in dog, dosed alone (2 mg/kg) or with ritonavir (5 mg/kg)

8 ABT-450 Virology

With the choice of compound ABT-450 as the lead clinical candidate, its antiviral activity was investigated in detail. First, the activity of ABT-450 was evaluated more thoroughly against an expanded panel of genotype 1a and 1b resistance-associated substitutions in the transient replicon assay, with activity and fold changes in EC_{50} relative to wild type shown in Table 14. More substantial reductions in potency against these resistance-associated substitutions were evident in genotype 1a, where D168E and D168V demonstrated the most substantial resistance to ABT-450. Particularly striking was the drop in activity against the clinically relevant 1a D168V substitution, which is known to emerge upon treatment with most first generation HCV protease inhibitors [23–28].

Table 14 Activity of ABT-450 against resistance-associated substitutions

Compound	Fold change in EC ₅₀ relative to wild-type value in transient replicon assay					
	1a			1b		
	R155K	D168E	D168V	R155K	D168V	A-156T
ABT-450	37	14	96	40	159	7

Table 15 Activity of ABT-450 in the presence of human plasma

Compound	Stable replicon EC ₅₀ (nM)					
	Genotype 1a			Genotype 1b		
	No human plasma	40% human plasma	Fold difference	No human plasma	40% human plasma	Fold difference
ABT-450	1.0	17	17	0.21	5.2	25

Table 16 Plasma-corrected replicon activity of ABT-450 against resistance-associated substitutions

Compound	Transient replicon EC ₅₀ (nM) estimate in presence of 40% human plasma					
	1a			1b		
	R155K	D168E	D168V	R155K	D168V	A156T
ABT-450	629	238	1,632	208	827	36

Table 17 Characterization of resistance to ABT-450 by colony selection assay evaluation (colonies per 10⁵ cells)

Compound	1a-H77			1b-Con1		
	10×	100×	500×	10×	100×	500×
ABT-450	117	0	0	127	15	0

The impact of 40% human plasma binding on the activity of ABT-450 was measured in the stable replicon assay, where activity against genotypes 1a and 1b decreased by 17–25-fold in the presence of 40% human plasma (Table 15).

Using these two measures, the impact of plasma protein binding on the activity of ABT-450 against resistance-associated substitutions could also be estimated, by multiplying the EC₅₀ of ABT-450 in the presence of 40% human plasma in the stable replicon assay by the fold difference against each substitution determined in the transient replicon assay (Table 16). According to this analysis, R155K and D168V in genotype 1a and D168V in genotype 1b appeared to represent the most challenging substitutions to overcome.

Colony selection assays using the HCV replicon were utilized to further characterize the activity and resistance profile of ABT-450 and to help guide projected human dose calculations. HCV genotype 1a and 1b subgenomic replicon cell lines were passaged in the presence of ABT-450 at concentrations 10-, 100-, and 500-fold above its EC₅₀. No colonies survived at 100- or 500-fold over the EC₅₀ in genotype 1a or at 500-fold over the EC₅₀ in genotype 1b (Table 17). Among the major

Table 18 Activity of ABT-450 against replicon cell lines with NS3 from different genotypes

Compound	Stable replicon EC ₅₀ (nM) with genotype					
	1a	1b	2a	3a	4a	6a
ABT-450	1.0	0.21	5.3	19	0.09	0.69

substitutions observed in selected colonies in 1a-H77 was R155K, which has been shown to confer resistance to nearly all HCV protease inhibitors, and which exhibited 37-fold reduced susceptibility to ABT-450 in the transient replicon assay. Another major substitution observed in selected colonies was D168V, which confers resistance to P1–P3 macrocyclic acyl sulfonamide HCV protease inhibitors in both genotypes 1a and 1b [23–26]. The presence of this substitution also confirmed results from the transient replicon assay, where a 96- or 159-fold reduced susceptibility to ABT-450 in genotypes 1a or 1b, respectively, had been noted.

In addition to the evaluation of activity vs. genotypes 1a and 1b, ABT-450 was also examined against genotypes 2a, 3a, 4a, and 6a in stable replicon assays [16]. Although ABT-450 demonstrates activity against multiple HCV genotypes, it exhibits reduced potency vs. genotype 3a, (Table 18), as has been noted for HCV protease inhibitors such as simeprevir [29] and asunaprevir [30].

9 Development of ABT-450

As the preclinical development of ABT-450 proceeded, considerable uncertainties were encountered in the prediction of an efficacious human dose for ABT-450. A PK/PD-viral dynamics model was constructed based on the continuous maintenance of liver concentrations sufficient to completely block replication of wild-type (susceptible) virus and produce a ~4-log decline in plasma HCV RNA over short-term (several days) treatment. Key uncertainties in this calculation included the target liver C_{trough} (extrapolated from the chimpanzee study with compound 7), the L:P ratio for humans (conservatively assumed to be similar to dog), and the extent of interaction with ritonavir (dose of ritonavir required, if any). Preclinical toxicology studies were therefore conducted both without and with ritonavir co-dosing to cover a wide exposure range. Overall, ABT-450 exhibited a benign secondary pharmacological profile. Dog CV safety studies suggested low potential for hemodynamic effects or QT prolongation in humans, and in vitro hERG current studies demonstrated a relatively high hERG IC₅₀ (88 µg/mL), representing 33–382-fold the modeled clinical C_{max} range of 0.23–2.7 µg/mL. ABT-450 produced no emesis in ferrets at the targeted plasma concentrations and was negative in genetic toxicity assays. GLP toxicity studies in rats and dogs produced no toxicologically remarkable findings. Based upon these findings, the program advanced ABT-450 into Phase 1 clinical studies.

Phase 1 studies in healthy human volunteers revealed a remarkable pharmacokinetic interaction between ABT-450 and ritonavir. Following a 300 mg single oral dose of ABT-450, co-dosing with a low (100 mg) single dose of ritonavir increased ABT-450 plasma C_{\max} from 0.10 to 2.03 $\mu\text{g}/\text{mL}$ and AUC from 0.35 to 10.5 $\mu\text{g h}/\text{mL}$ (20- and 30-fold, respectively) [31]. The results of dose ranging indicated that the 100 mg dose of ritonavir was optimal for enhancing ABT-450: at higher doses ABT-450 exposure was more sensitive to ABT-450 dose rather than ritonavir dose. The results also indicated that proceeding into efficacy studies without ritonavir co-dosing was unlikely to achieve the desired TPP (~ 4 -log HCV RNA decline in short-term monotherapy studies).

Based on the favorable pharmacokinetic and safety profile in healthy volunteers, the *in vivo* antiviral activity of ABT-450 was examined in a 3-day monotherapy study. In this study, treatment-naïve patients infected with HCV genotype 1 were administered doses of ABT-450/ritonavir (ABT-450/r) of 50/100 mg, 100/100 mg, or 200/100 mg once daily for 3 days. Similar HCV RNA decreases were seen with all ABT-450/ritonavir dosing groups at the end of the 3-day treatment, with the mean maximum HCV RNA decrease from baseline of $4.0 \pm 0.4 \log_{10} \text{IU}/\text{mL}$ [16]. Despite the similarity in viral load of all three arms, analysis of resistance development to ABT-450 over the 3 days of dosing revealed a dose dependence. Phenotypic and genotypic analyses of viral isolates from baseline and at the end of the 3 days of ABT-450/ritonavir monotherapy were performed in order to characterize the selection of resistance-associated substitutions. The most common resistance-associated substitutions were R155K and D168V in genotype 1a and D168V in genotype 1b. Notably, the selection of resistance was significantly lower in isolates from patients in the cohort administered the highest dose, suggesting the creation of a pharmacologic barrier to resistance through higher liver drug concentrations [16]. These results provided the first PoC for this regimen and helped to define the dose of ABT-450/r to explore in subsequent combination studies with other anti-HCV agents.

As the Phase 2 program progressed, ABT-450 (paritaprevir) was examined in longer-term studies, first in combination with the investigational HCV NS5B inhibitor ABT-333 (dasabuvir) and ribavirin, in one of the first examples of IFN-free HCV treatment [32]. In subsequent studies, a third investigational compound, the HCV NS5A inhibitor ABT-267 (ombitasvir), was added to the combination, producing high response rates in genotype 1 HCV-infected patients [33]. These studies supported a large Phase 3 program, in which ABT-450/r (150/100 mg), dasabuvir and ombitasvir in combination, with or without ribavirin, was studied in HCV genotype 1-infected patients for 12 weeks [34, 35]. High ($>95\%$) rates of sustained virologic response (SVR) in these supported the approval of the ritonavir-boosted double and triple combinations, designated as Technivie™ and Viekira Pak™, respectively (Viekirax and Exviera™ outside of the USA), in genotype 1 HCV-infected patients (co-administered with ribavirin for genotype 1a infection). This treatment regimen was approved for use in the USA, Europe, and Japan in 2016 and has since received approval in a wide range of additional countries. It is marketed by AbbVie.

10 Conclusion

The discovery and development of ABT-450 (paritaprevir) described above, incorporating novel P*-phenanthridine and P3-amide capping groups and pharmacokinetically boosted by ritonavir, enabled one of the first IFN-free combination therapies for HCV genotype 1 infection and contributed to the transformation of the treatment of this chronic and deadly disease. However, its activity against other HCV genotypes was more limited, and subsequent to the discovery of ABT-450, the combined Abbott-Enanta discovery team continued their work toward identifying a broad-genotype HCV protease inhibitor with superior activity against resistance-associated substitutions. This effort was eventually fulfilled with the identification of a second agent, glecaprevir, which, in combination with the HCV NS5A inhibitor pibrentasvir, provided $\geq 95\%$ SVR across treatment-naïve patients with HCV genotypes 1–6 with just 8 weeks of treatment [36]. This combination has since been approved in multiple countries and is marketed by AbbVie as Mavyret/Maviret™. The discovery of these and other direct-acting anti-HCV agents has enabled HCV infection to be cured in hundreds of thousands of people and holds promise for millions more who are infected with this virus globally.

Acknowledgments The authors would like to acknowledge the assistance of Tami Pilot-Matias (virology discussions), Charles Hutchins (molecular modeling support), and Lisa Hasvold (proofreading) in the preparation of this manuscript.

Compliance with Ethical Standards

Funding The study was supported by AbbVie.

Conflict of Interest K.F.M., Y.-Y.K, H.-J.C., J.S., T.M., and D.K. are current AbbVie employees and may hold AbbVie stock or options. Y.S. and Y.S.O. are current or former Enanta employees and may hold Enanta stock or options. The design and study conduct for this research were provided by AbbVie and Enanta. AbbVie and Enanta participated in the interpretation of the data and review and approval of the publication.

AbbVie is committed to responsible data sharing regarding the clinical trials we sponsor. This includes access to anonymized, individual and trial-level data (analysis data sets), as well as other information (e.g., protocols and Clinical Study Reports), as long as the trials are not part of an ongoing or planned regulatory submission. This includes requests for clinical trial data for unlicensed products and indications.

This clinical trial data can be requested by any qualified researchers who engage in rigorous, independent scientific research, and will be provided following review and approval of a research proposal and Statistical Analysis Plan (SAP) and execution of a Data Sharing Agreement (DSA). Data requests can be submitted at any time and the data will be accessible for 12 months, with possible extensions considered. For more information on the process, or to submit a request, visit the following link: <https://www.abbvie.com/our-science/clinical-trials/clinical-trials-data-and-information-sharing/data-and-information-sharing-with-qualified-researchers.html>.

Ethical Approval All applicable international, national, and/or institutional guidelines for the care and use of animals were followed. All procedures performed in studies involving human participants were in accordance with the ethical standards of the institutional and/or national research committee and with the 1964 Helsinki declaration and its later amendments or comparable ethical standards.

Informed Consent Informed consent was obtained from all individual participants included in the study.

The authors would like to thank the patients and their families as well as study site staff who participated in the clinical trials of paritaprevir.

References

1. Naggie S, Muir A (2017) Oral combination therapies for hepatitis C virus infection: successes, challenges, and unmet needs. *Annu Rev Med* 68:345–358
2. Grillot A-L, Farmer L, Rao B et al (2011) Discovery and development of telaprevir. *Anti-Cancer Drugs* 209–224
3. Njoroge F, Chen K, Shih N-Y et al (2008) Challenges in modern drug discovery: a case study of boceprevir, an HCV protease inhibitor for the treatment of hepatitis C virus infection. *Acc Chem Res* 41:50–59
4. Kempf D, Klein C, Chen H-J et al (2007) Pharmacokinetic enhancement of the hepatitis C virus protein inhibitors VX-950 and SCH 503034 by co-dosing with ritonavir. *Antivir Chem Chemother* 18:163–167
5. Jacobson I, McHutchison J, Dusheiko G et al (2011) Telaprevir for previously untreated chronic hepatitis C virus infection. *N Engl J Med* 364:2405–2416
6. Poordad F, McCone Jr J, Bacon B et al (2011) Boceprevir for untreated chronic HCV genotype 1 infection. *N Engl J Med* 364:1195–1206
7. Lamarre D, Anderson P, Bailey M et al (2003) An NS3 protease inhibitor with antiviral effects in humans infected with hepatitis C virus. *Nature* 426:186–189
8. Stoltz J, Stern J, Huang Q et al (2011) A twenty-eight-day mechanistic time course study in the rhesus monkey with hepatitis C virus protease inhibitor BILN 2061. *Toxicol Pathol* 39:496–501
9. Gower E, Estes C, Blach S et al (2014) Global epidemiology and genotype distribution of the hepatitis C virus infection. *J Hepatol* 61(Suppl):S45–S57
10. Fried M, Shiffman M, Reddy R et al (2002) Peginterferon alfa-2a plus ribovirin for chronic hepatitis C virus infection. *N Engl J Med* 347:975–982
11. Manns M, McHutchinson J, Gordon S et al (2001) Peginterferon alfa-2b plus ribavirin compared with interferon alfa-2b plus ribavirin for initial treatment of chronic hepatitis C: a randomized trial. *Lancet* 358:958–965
12. Lohmann V, Hoffmann S, Herian U et al (2003) Viral and cellular determinants of hepatitis C virus RNA replication in cell culture. *J Virol* 77:3007–3019
13. Llinas-Brunet M, Bailey M, Ghiro E et al (2004) A systematic approach to the optimization of substrate-based inhibitors of the hepatitis C virus NS3 protease: discovery of potent and specific tripeptide inhibitors. *J Med Chem* 47:6584–6594
14. Scola P, Wang A, Good A et al (2014) Discovery and early clinical evaluation of BMS-605339, a potent and orally efficacious tripeptidic acylsulfonamide NS3 protease inhibitor for the treatment of hepatitis C virus infection. *J Med Chem* 57:1708–1729
15. Llinas-Brunet M, Bailey M, Fazal G (2000) Highly potent and selective peptide-based inhibitors of the hepatitis C virus serine protease: towards smaller inhibitors. *Bioorg Med Chem Lett* 10:2267–2700

16. Pilot-Matias T, Tripathi R, Cohen D et al (2015) *In vitro* and *in vivo* antiviral activity and resistance profile of the hepatitis C virus NS3/4A protease inhibitor ABT-450. *Antimicrob Agents Chemother* 59:988–997
17. Konstantinidis A, Richardson P, Kurtz K et al (2007) Longer wavelength fluorescence energy transfer decapeptide substrates for hepatitis C virus NS3 protease. *Anal Biochem* 368:156–167
18. Morrison J, Stone S (1985) Approaches to the study and analysis of the inhibition of enzymes by slow- and tight-binding inhibitors. *Comments Mol Cell Biophys* 2:347–368
19. Kempf D, Marsh K, Kumar G et al (1997) Pharmacokinetic enhancement of inhibitors of the human immunodeficiency virus protease by coadministration with ritonavir. *Antimicrob Agents Chemother* 41:654–660
20. Sham H, Kempf D, Molla A et al (1998) ABT-378, a highly potent inhibitor of the human immunodeficiency virus protease. *Antimicrob Agents Chemother* 42:3218–3224
21. Shulman N, Zolopa A, Havlir D et al (2002) Virtual inhibitory quotient predicts response to ritonavir boosting of indinavir-based therapy in human immunodeficiency virus-infected patients with ongoing viremia. *Antimicrob Agents Chemother* 46:3907–3916
22. Hassner A, Patchornik G, Pradhan T et al (2007) Intermolecular electrophilic O-amination of alcohols. *J Org Chem* 72:658–661
23. Berger K, Lagace L, Triki I et al (2013) Viral resistance in hepatitis C virus genotype 1-infected patients receiving the NS3 protease inhibitor faldaprevir (BI 201335) in a phase 1b multiple-rising-dose study. *Antimicrob Agents Chemother* 57:4928–4936
24. Lim S, Qin X, Susser S et al (2012) Virologic escape during danoprevir (ITMN-191/RG7227) monotherapy in hepatitis C virus subtype dependent and associated with R155K substitution. *Antimicrob Agents Chemother* 56:271–279
25. McPhee F, Friborg J, Levine S et al (2012) Resistance analysis of the hepatitis C virus NS3 protease inhibitor asunaprevir. *Antimicrob Agents Chemother* 56:3670–3681
26. Reesink H, Fanning G, Farha K et al (2010) Rapid HCV-RNA decline with once daily TMC435: a phase 1 study in healthy volunteers and hepatitis C patients. *Gastroenterology* 138:913–921
27. Sarrazin C, Kieffer T, Bartels D et al (2007) Dynamic hepatitis C virus genotypic and phenotypic changes in patients treated with protease inhibitor telaprevir. *Gastroenterology* 132:1767–1777
28. Susser S, Welsch C, Wang Y et al (2009) Characterization of resistance to the protease inhibitor boceprevir in hepatitis C virus-infected patients. *Hepatology* 50:1709–1718
29. Lenz O, Vijgen L, Berke J et al (2013) Virologic response and characterization of HCV genotype 2-6 in patients receiving TMC435 monotherapy (study TMC435-C202). *J Hepatol* 58:445–451
30. McPhee F, Sheaffer A, Friborg J et al (2012) Preclinical profile and characterization of hepatitis C virus NS3 protease inhibitor asunaprevir (BMS-650032). *Antimicrob Agents Chemother* 56:5387–5396
31. Menon R, Klein C, Podsadecki T et al (2016) Pharmacokinetics and tolerability of paritaprevir, a direct acting antiviral agent for hepatitis C virus treatment, with and without ritonavir in healthy volunteers. *Br J Clin Pharm* 81:929–940
32. Poordad F, Lawitz E, Kowdley K et al (2013) Exploratory study of oral combination antiviral therapy for hepatitis C. *N Engl J Med* 368:45–53
33. Kowdley K, Lawitz E, Poordad F et al (2014) Phase 2b trial of interferon-free therapy for hepatitis C virus genotype 1. *N Engl J Med* 370:222–232
34. Feld J, Kowdley K, Coakley E et al (2014) Treatment of HCV with ABT-450/r-ombitasvir and dasabuvir with ribavirin. *N Engl J Med* 370:1594–1603
35. Ferenci P, Bernstein D, Lalezari J et al (2014) ABT-450/r-ombitasvir and dasabuvir with or without ribavirin for HCV. *N Engl J Med* 370:1983–1982
36. Zeuzem S, Foster G, Wang S et al (2018) Glecaprevir-pibrentasvir for 8 or 12 weeks in HCV genotype 1 or 3 infection. *N Engl J Med* 378:354–369

Discovery and Development of the Next-Generation HCV NS3 Protease Inhibitor Glecaprevir



Guoqiang Wang, Jun Ma, Li-Juan Jiang, Yonghua Gai, Jiang Long,
Bin Wang, Keith F. McDaniel, and Yat Sun Or

Contents

1	Introduction	416
2	Enanta's Early HCV Protease Inhibitor Research	417
3	Identification of PoC Compound in P2-P4 Macrocyclic Series	418
4	Phenyl Alkyl Linker	422
5	Phenyl Alkyl Ether Linker	422
6	Benzyl Alkyl Ether Linker	427
7	Difluoroalkyl Cyclopentyl Ether Linker	428
8	Discovery of ABT-493	431
9	Synthesis of ABT-493	432
10	Preclinical PK Evaluation of ABT-493	433
11	ABT-493 Virology	434
12	Development of ABT-493	434
13	Conclusion	436
	References	437

Abstract The early collaboration between Enanta and Abbott/AbbVie on HCV NS3 protease inhibitor program led to the discovery of ABT-450 (paritaprevir), which is a component of two FDA-approved IFN-free DAA combination therapies (Viekira Pak™ and Technivie™) with approval to treat genotypes 1 and 4, respectively. However, its activity against some key resistant mutants and other HCV genotypes was limited. This chapter reviews our further effort to identify a next-generation HCV protease inhibitor with pan-genotypic activity, excellent

G. Wang (✉), J. Ma, L.-J. Jiang, Y. Gai, J. Long, B. Wang, and Y. S. Or
Enanta Pharmaceuticals, Inc., Watertown, MA, USA
e-mail: guoqiang@enanta.com; junma@enanta.com; ljiang@enanta.com; yonghua.gai@pharmaron.com; jlong@enanta.com; binwang@enanta.com; Or@enanta.com

K. F. McDaniel
AbbVie, Inc., North Chicago, IL, USA
e-mail: Keith.f.mcdaniel@abbvie.com

activity against resistant mutants, and favorable pharmacokinetic (PK) properties, which included the identification of the first proof-of-concept (PoC) compound in P2-P4 macrocyclic series by evaluation of different core structures and the discovery of the candidate compound ABT-493 through extensive SAR studies at P*, P1, and P1' positions and particularly on the linker. In combination with the HCV NS5A inhibitor pibrentasvir, ABT-493 (glecaprevir) was approved by the FDA in August 2017 for treatment of hepatitis C and is marketed by AbbVie as Mavyret™/Maviret™ in multiple countries.

Keywords ABT-493, DAA combination therapy, Glecaprevir, HCV protease inhibitor, P2-P4 macrocyclic, Pan-genotypic

1 Introduction

An unknown virus was first noted in the mid-1970s when posttransfusion patients developed hepatitis not attributable to either the hepatitis A or B viruses and was coined non-A, non-B hepatitis [1]. This previously unidentified virus was unambiguously characterized and identified as the hepatitis C virus (HCV) in 1989. With an estimated 130–170 million people chronically infected worldwide, HCV infection became a major global health epidemic.

HCV is a member of the *Hepacivirus* genus of the family *Flaviviridae* [2, 3] and is a positive-sense, single-stranded RNA virus with a high degree of genetic heterogeneity. It can be classified into six major genotypes that have different geographic distributions. Genotypes 1, 2, and 3 account for more than 90% of the infections in the developed world, with genotype 1 being predominant (~75%) in the USA, Western Europe, and Japan [4]. Prior to the approval of HCV direct-acting antiviral (DAA) therapies, the standard of care (SOC) for treatment of HCV was a combination of pegylated interferon (pegIFN) and the antiviral compound ribavirin (RBV). Unfortunately, this SOC suffered not only from poor efficacy (40–50% sustained viral response achieved for genotype 1-infected patients treated for 48 weeks) but also elicited severe side effects, including rash, nausea, anemia, and depression [5]. It was these limitations which drove anti-HCV drug discovery efforts at Enanta Pharmaceuticals, Inc. (Enanta).

Notably, the serine protease encoded by HCV NS3 and NS4A genes has been an attractive target for the discovery of DAAs. This protease is the viral enzyme responsible for cleaving the HCV polyprotein at four sites yielding mature viral proteins essential for viral RNA replication [6]. In addition to its crucial role in viral replication, the HCV NS3/4A protease also plays a central role in the HCV innate immune evasion strategy by cleaving cellular proteins involved in the host innate antiviral response [7]. The first DAAs approved for the treatment of chronic HCV infection were HCV NS3/4A protease inhibitors (HCV PIs) telaprevir and boceprevir (Fig. 1), each of which was used in combination with pegIFN and RBV. These two inhibitors are linear α -ketoamide derivatives and form a slowly reversible

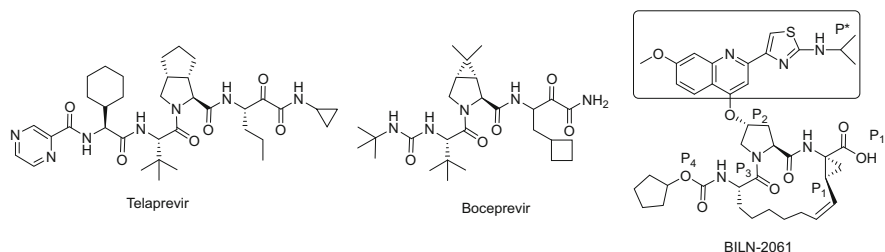


Fig. 1 Structures of telaprevir, boceprevir, and BILN-2061

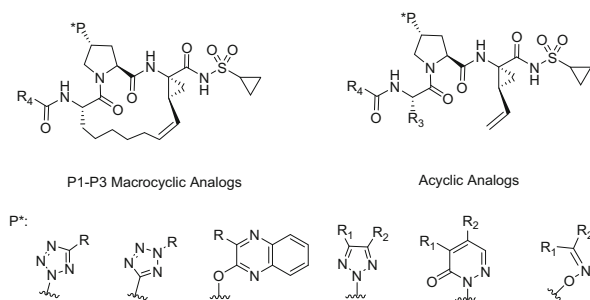


Fig. 2 Two chemotypes and representative P* modifications

covalent bond with the active site of the enzyme. Because of their limited antiviral potency and metabolic instability, these two HCV PIs required high clinical doses and three times a day (TID) administration. The first non-covalently bound fast-reversible HCV NS3/4A protease inhibitor, BILN-2061 (Fig. 1), was discovered by scientists at Boehringer Ingelheim [8]. This compound incorporates a large substituted aryl group, which is attached to the hydroxyl group of P2 proline (referred to subsequently as the P* group). This large P* group is essential for high potency via hydrophobic interactions with the extensive P* shelf in the HCV protease active site.

2 Enanta's Early HCV Protease Inhibitor Research

Early discovery efforts on HCV NS3/4A protease inhibitors at Enanta focused on the development of novel P* shelf groups to improve antiviral potency, targeting single-digit nM EC₅₀ values in stable replicon assay and a pharmacokinetic (PK) profile sufficient to support once daily (QD) administration. Structure-activity-relationship (SAR) studies on two core structures with novel P* shelf groups were performed (Fig. 2). The first structure was a P1-P3 macrocyclic core, which had the same framework as BILN-2061, while the second structure was a more simplified acyclic

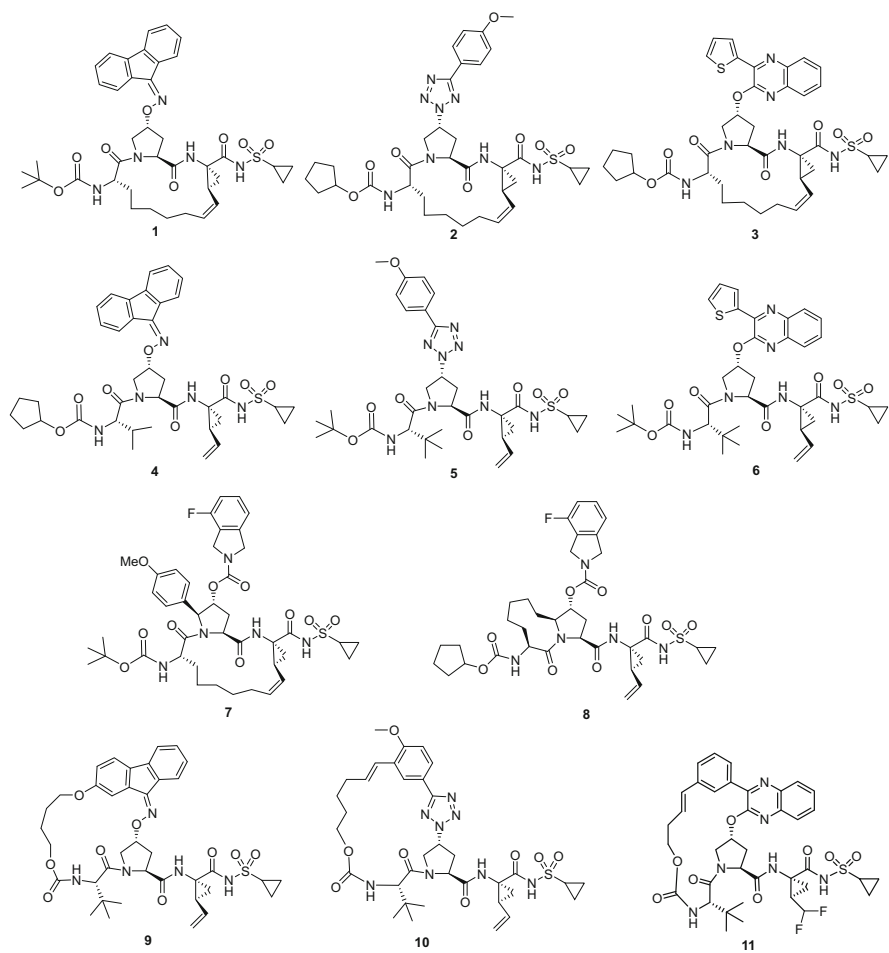
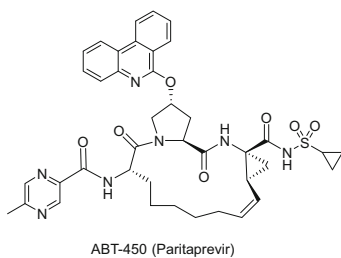
core, first reported by scientists at Boehringer Ingelheim [9]. Many P* shelf groups were examined, and among them, substituted quinoxaliny, 1-tetrazolyl, 3-tetrazolyl, oximyl, and pyridazinonyl P* group analogs showed relatively better HCV potency [10–13]. Furthermore, a variety of C-terminal carboxylic acid isosteres also were explored, including the acylsulfonamides, first described by scientists at Bristol-Myers Squibb [14]. Notably, the acylsulfonamide analogs showed improved potency and metabolic stability. As a result, this group was incorporated into most subsequently prepared compounds. P3 capping groups such as carbamates, ureas, and amides were also examined (R₄ corresponds to alkoxy groups, alkyl/aryl amino groups, and alkyl/aryl groups, respectively), as were P₃ modifications of the acyclic core series via small alkyl substitutions (R₃ corresponds to t-butyl, isopropyl, c-pentyl, c-hexyl, etc.).

Enanta scientists also studied novel P* group substitutions on the P2-P4 macrocyclic core [15–21] (e.g., compounds 9–11 in Fig. 3), which was first reported by scientists at Schering-Plough and Merck [22, 23], and developed novel core structures by substitution on the P2 proline group [24] (e.g., compound 7) and forming a P2-P3 macrocyclic ring (e.g., compound 8) [25]. At this juncture, Enanta had established a substantial portfolio of HCV protease inhibitor patents and patent applications, covering a wide range of cores and structures. Since various structural changes were introduced, the overall structure-activity relationship was unpredictable and needed to be studied further. This early discovery work led to a collaboration with Abbott Laboratories (the pharmaceutical division of Abbott was spun out to AbbVie as a new public company in 2013) in December 2006. Shortly after the collaboration with Abbott began, several lead compounds from the Enanta collection were identified for further evaluation based on antiviral activity, structural differentiation, and early PK evaluation (compounds 1–11, Fig. 3).

Extensive studies by the collaborative team around compound 1 led to the discovery of ABT-450 (paritaprevir) (Fig. 4), which was approved in 2016 with the ritonavir-boosted double and triple combinations (with the NS5B inhibitor dasabuvir and the NS5A inhibitor ombitasvir and co-administered with ribavirin in genotype 1 HCV patients). (See chapter entitled “The Discovery and Development of HCV NS3 Protease Inhibitor Paritaprevir”).

3 Identification of PoC Compound in P2-P4 Macrocyclic Series

Paritaprevir-containing regimens, along with several other early IFN-free, DAA-containing regimens approved for HCV therapy [26, 27], were not equally potent across all HCV genotypes and subpopulations, nor did they consistently retain activity against specific substitutions associated with resistance for other members of the same inhibitor class [28–34]. In addition, several early regimens required different strategies to maximize efficacy, including lengthening of treatment duration

**Fig. 3** Leading compounds 1-11**Fig. 4** Structure of ABT-450 (paritaprevir)

(e.g., from 12 to 16 or 24 weeks) for certain populations or the addition of RBV, which in some patients has been shown to induce undesirable side effects (e.g., nausea, weight loss, or hemolytic anemia) [35–37]. Lower efficacy was also observed in patients with baseline NS3 or NS5A amino acid polymorphisms that confer resistance to components of these regimens [38–43]. Thus, there remained an unmet medical need for a simple, next-generation pegIFN- and RBV-free HCV regimen with potent pan-genotypic activity that could shorten treatment duration and provide high efficacy in treatment-naïve patients or those who had previously failed a DAA-containing regimen. Accordingly, the collaborative discovery teams continued their efforts toward achieving the target product profile (TPP) of a next-generation HCV PI. This TPP included favorable PK properties to support QD dosing without ritonavir boosting, superior activity against all major HCV genotypes and their clinically relevant resistance-associated substitutions, and suitability for potential combination with other DAAs such as an NS5A inhibitor.

Compounds generated in the early stages of SAR examination were tested for (1) anti-HCV activity in the genotype 1a/1b stable replicon assay and (2) metabolic stability with *in vitro* clearance in human liver microsomes as an early indicator of potentially favorable PK properties. As compounds progressed to the second stage of examination, antiviral activity against a panel of resistant mutants was assessed through the use of 1a-H77 and 1b-Con1 subgenomic shuttle vector constructs used for introduction of mutations of interest in the NS3 gene. These replicon shuttle vectors allowed insertion of the region encoding the complete NS3 protease domain without adaptive mutations, and the EC₅₀ values of compounds were measured in transient replicon assays [44]. The impact on antiviral activity of protein binding by human plasma (HP) was also evaluated by comparing the activity of the compounds measured in the presence of 5% fetal bovine serum (FBS) versus activity measured in the presence of 40% HP. Since the next-generation HCV PI compounds required pan-genotypic activity in the TPP, lead compounds also were profiled for their activity against multiple genotypes, especially against genotype 3a, considered the genotype most difficult to treat with DAAs. Further, PK properties were evaluated for potential QD dosing without RTV boosting. Compounds prepared at Enanta were first tested for their activity against genotype 1b in the stable replicon assay and were then delivered to Abbott for detailed evaluations as described in the above screening funnel. All such data described in subsequent discussions herein were generated by the Abbott biology team. Medicinal chemistry teams at Enanta and Abbott worked on complementary next-generation compound series. The progression of analogs of compound **11**, leading ultimately to ABT-493 at Enanta, is detailed below.

The antiviral activity of compounds **1–11** was measured in the stable replicon assay for both genotype 1a and genotype 1b (GT1a/1b), and their metabolic stability was evaluated by their *in vitro* clearance in human liver microsomes (HLM). Most of the compounds displayed activity comparable to ABT-450 against GT1a/1b. Gratifyingly, compound **11** with the P2-P4 macrocyclic core and difluoromethyl P1 substitution showed improved metabolic stability in HLM (HLM Cl_{int vitro}* at 31 μL/min/mg) compared to ABT-450 (HLM Cl_{int vitro}* at 88 μL/min/mg) (Table 1).

Table 1 In vitro metabolism and activity in stable replicon assay for compounds **ABT-450** and **11**

Compound	Stable replicon EC ₅₀ (nM)		HLM Cl _{int vitro} * (μL/min/mg)
	GT 1a	GT 1b	
ABT-450	1.0	0.21	88
11	2.0	2.9	31

Table 2 Rat pharmacokinetics of **11** and **ABT-450**

Compound	Dose (mg/kg)	t _{1/2} (h)	AUC (μg h/mL)	CL _p (L/h kg)
IV dosing:				
11	1	4.5	0.42	2.4
ABT-450	5	0.4	1.88	3.0
Compound	Dose (mg/kg)	C _{max} (μg/mL)	AUC (μg h/mL)	F (%)
Oral dosing:				
11	20	0.067	0.344	4.1
ABT-450	5	0	0	0

Table 3 Activity of compounds **ABT-450** and **11** in the presence of 40% HP and against resistant mutants

Compound	Replicon EC ₅₀ 40% HP (nM)		Fold change in EC ₅₀ relative to wild-type value in transient replicon assay					
			1a			1b		
	1a	1b	R155K	D168E	D168V	R155K	D168V	A-156T
ABT-450	17	5.2	37	14	96	40	159	7
11	84	62	170	127	>1,732	4.9	22	59

Thus, the rat PK profile of compound **11** was studied and compared to ABT-450 (Table 2). Compound **11** demonstrated a longer plasma half-life after IV dosing (4.5 h) than ABT-450 (0.4 h). Both compounds showed low plasma concentration after oral dosing, which was consistent with rapid uptake into the liver, with the liver/plasma ratio at 1,090 for compound **11** and 385 for ABT-450 at 3 h after oral dosing.

To further evaluate compound **11**, an in vivo efficacy study in an HCV-infected chimpanzee model was initiated. In this study, compound **11** was dosed orally at 700 mg twice daily (BID) for 5 days and produced a >4.0 log reduction in viral load. This result provided a positive proof of concept (PoC) for this P2-P4 macrocyclic series of HCV protease inhibitors. Compound **11** was also evaluated for the impact of protein binding by HP on antiviral activity and its activity against resistant mutants (Table 3). Unfortunately, compound **11** showed substantially decreased activity in the replicon assay in the presence of 40% HP (20- to 40-fold loss compared to activity in the presence of 5% FBS) and decreased activity against a panel of genotype 1a resistance-associated substitutions with fold losses in activity of 170× (R155K), 127× (D168E), and >1,732× (D168V).

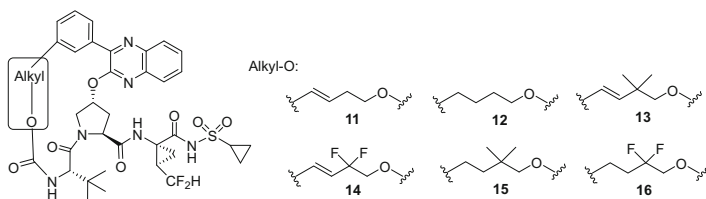


Fig. 5 Phenyl alkyl linker compounds **11–16**

Table 4 In vitro metabolism and activity in stable replicon assay for compounds **11–16**

Compound	Stable replicon EC ₅₀ (nM)		HLM Cl _{int vitro} * (μL/min/mg)
	GT 1a	GT 1b	
11	2.0	2.9	31
12	4.5	2.2	38
13	0.6	0.7	24
14	1.4	2.1	37
15	0.5	1.2	33
16	1.0	0.9	32

4 Phenyl Alkyl Linker

Further SAR studies were performed for the identification of a compound which would satisfy the required TPP. The first modifications examined were saturation of the alkene and various substitutions on the linker. Thus, compounds **12–16** were prepared (Fig. 5), and their in vitro metabolic stability and HCV activity in the stable replicon assay were measured in comparison to compound **11** (Table 4).

One significant finding from the linker modification study was that adding small substitution groups (such as gem-dimethyl and gem-difluoro) on the methylene of the linker improved antiviral HCV activity without negatively impacting metabolic stability. For example, compounds **15** and **16** showed a twofold to fourfold improvement in antiviral HCV activity in the stable replicon assay, while their in vitro clearance in human liver microsomes remained similar to that of compound **12**. The positive effect on antiviral HCV activity by the addition of small substitution groups on the linker also was observed in other linker evaluations.

5 Phenyl Alkyl Ether Linker

Another series of linker modification, a phenyl alkyl ether linker, was constructed by inserting one oxygen atom between the phenyl group and alkyl group of compound **11** [45]. Substitutions on this linker were also examined (Fig. 6). Thus, compounds **17–22** were prepared and compared to compound **11** (Table 5).

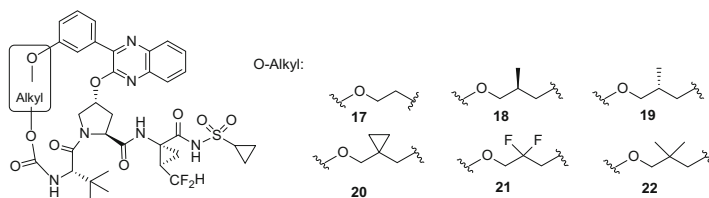


Fig. 6 Phenyl alkyl ether linker compounds **17–22**

Table 5 In vitro metabolism and activity in the stable replicon assay for compounds **11**, **17–22**, and **ABT-450**

Compound	Stable replicon EC ₅₀ (nM)		HLM Cl _{int vitro} * (μL/min/mg)
	GT 1a	GT 1b	
11	2.0	2.9	31
17	1.3	3.3	<23
18	0.42	1.5	32
19	0.7	3.6	27
20	0.45	0.87	33
21	0.45	0.64	24
22	0.24	0.46	<23
ABT-450	1.0	0.21	88

Several compounds incorporating the phenyl alkyl ether linker showed improved metabolic stability. As observed with previous compounds, gem-dimethyl substitution on the alkyl group of the linker improved antiviral HCV activity, while monomethyl substitution was less impactful. For example, compound **22** demonstrated fivefold to eightfold improved antiviral HCV activity as compared to compound **11** and better metabolic stability (Table 5). Cyclopropyl and gem-difluoro substitution on the linker also improved activity, with compounds **20** and **21** displaying an approximate 4-fold increase in antiviral HCV activity. However, compound **17**, one carbon shorter and lacking substitution on the linker, displayed only similar antiviral HCV activity as compared to compound **11** in the stable replicon assay.

Since compound **22** exhibited comparable activity in the stable replicon assay and improved metabolic stability compared to ABT-450, further modifications were performed based on compound **22**. Substitution on the P1' cyclopropyl sulfonamide was examined first (compounds **23a–g**, Fig. 7 and Table 6). The simple methyl-substituted cyclopropyl sulfonamide compound **23a** showed antiviral HCV activity similar to compound **22**. However, compounds **23b** and **23c**, with the introduction of a polar amide group on the cyclopropyl sulfonamide, displayed a substantial loss (>10×) of activity. Compounds **23d–g** with a methyl carboxylic ester, difluoromethyl, hydroxymethyl, and methoxymethyl substitution on the cyclopropyl sulfonamide, respectively, also showed decreased antiviral HCV activity. Thus, cyclopropyl sulfonamide and methylcyclopropylsulfonamide were employed as P1' groups in subsequent SAR examination.

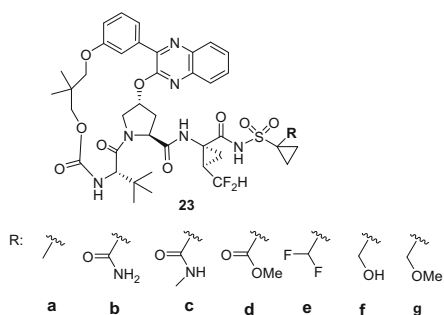


Fig. 7 Optimization on P1' cyclopropyl sulfonamide compounds **22** and **23a–g**

Table 6 Activity in stable replicon assay for compounds **22** and **23a–g**

Compound	Stable replicon EC ₅₀ (nM)	
	GT 1a	GT 1b
22	0.24	0.46
23a	0.25	0.45
23b	4.5	18
23c	6.8	40
23d	1.6	3.9
23e	1.1	2.8
23f	1.0	3.8
23g	1.3	10.4

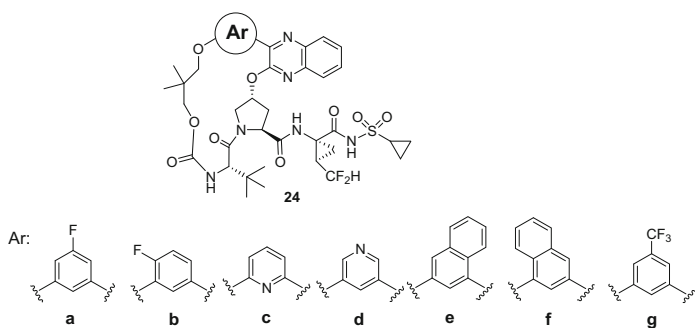
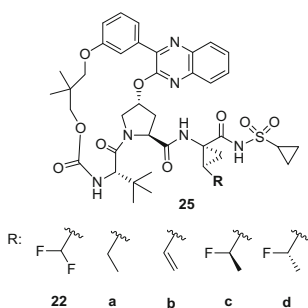


Fig. 8 Optimization on the phenyl alkyl ether linker for compounds **24a–g**

Substitutions on the phenyl group of the phenyl alkyl ether linker concurrent with complete replacement of the phenyl ring with other aromatic groups were also explored. Compounds **24a–g** were prepared (Fig. 8) and evaluated for their antiviral HCV activity (Table 7). Only compound **24b** with *o*-F substitution on the phenyl group demonstrated comparable antiviral HCV activity to compound **22**. Compounds **24a** and **24g**, with *m*-F and *m*-trifluoromethyl substitutions on the phenyl group, respectively, showed reduced antiviral activity compared to compound **22**,

Table 7 Activity in stable replicon assay for compounds **22** and **24a–g**

Compound	Stable replicon EC ₅₀ (nM)	
	GT 1a	GT 1b
22	0.24	0.46
24a	0.81	2.0
24b	0.26	0.39
24c	8.6	24
24d	4.9	15
24e	>100	>100
24f	11	3.8
24g	23	15

**Fig. 9** Optimization of the P1 position for compounds **22**, **25a–d**

with a 4-fold loss for **24a** and >30-fold loss for **24g**. By replacing the phenyl group with pyridyl or naphthyl groups, compounds **24c–f** displayed significant loss of activity. As a result, a phenyl group was used in subsequent SAR studies.

As previously discussed, compounds with a P1 difluoromethyl substitution possessed more favorable metabolic stability than compounds with a P1 vinyl substitution. Therefore, compounds **25a–d** were prepared with a P1 ethyl or 1-fluoroethyl substitution and evaluated for their antiviral HCV activity and metabolic stability in comparison to compound **22** (Fig. 9).

Compounds **22**, **25a**, and **25b** showed comparable activity (<2× difference) in the stable replicon assay and comparable metabolic stability (Table 8). However, compounds **25c** and **25d** incorporating a P1 2-fluoroethyl group demonstrated a significant loss in antiviral activity in biochemical assay, along with somewhat reduced metabolic stability. Therefore, their antiviral activity in stable replicon was not evaluated.

Compounds **22** and **25a** were further evaluated for the impact of protein binding on their activity. Their activity in genotype 1a and genotype 1b stable replicons in the presence of 40% human plasma was measured (Table 9). Compound **22** showed higher protein binding impact with a 91-fold loss for GT1a and a 37-fold loss for GT1b compared to compounds **25a** with an approximate 21-fold and 17-fold loss for GT1a and GT1b, respectively.

Table 8 In vitro metabolism and activity in the stable replicon assay for compounds **22**, **25a–d**

Compound	Stable replicon EC ₅₀ (nM)		HLM Cl _{int} * (μL/min/mg)
	GT 1a	GT 1b	
22	0.24	0.46	33
25a	0.56	0.81	46
25b	0.19	0.35	33
25c	ND	ND	49
25d	ND	ND	59
ABT-450	1.0	0.21	88

ND not determined

Table 9 Activity in the stable replicon assay for compounds **22**, **25a**, and **ABT-450**

Compound	Stable replicon EC ₅₀ (nM)					
	GT 1a	GT1a, 40% HP	Fold change	GT 1b	GT1b, 40% HP	Fold change
22	0.24	22	91	0.46	17	37
25a	0.56	12	21	0.81	14	17
ABT-450	1.0	17	17	0.21	5.2	25

Table 10 Rat pharmacokinetics of compounds **22** and **25a**

Compound	Dose (mg/kg)	C _{max} (μg/mL)	T _{max} (h)	AUC (μg h/mL)
22	30	0.27	2.7	1.43
	100	0.65	4.7	3.7
	300	3.8	4.7	22
25a	30	30	7.3	307
	100	277	10	3,856
	300	259	4.0	2,719

Compounds **22** and **25a** were also evaluated in a single escalating oral dose rat PK study in order to assess their potential for QD dosing without RTV boosting. As shown in Table 10, following a single oral dose of 30 mg/kg, compound **25a** demonstrated a greater than 200-fold higher plasma exposure than compound **22**.

With this favorable PK profile and potent HCV activity in the stable replicon assay, compound **25a** was chosen as a lead compound for further preclinical evaluation. Unfortunately, this compound was found to be a strong PPAR-γ agonist, with a half maximal inhibitory concentration (IC₅₀) of 0.28 μM. Other compounds from the phenyl alkyl ether linker series were also tested for their PPAR-γ activity, and all showed IC₅₀s < 10 μM. Since PPAR-γ agonists have the potential to cause side effects such as edema and congestive heart failure [46–50], reduction of PPAR-γ activity (IC₅₀ > 30 μM; >100-fold decrease compared to compound **25a**) became an important factor in the evaluation of the compounds generated from subsequent SAR studies and was included as a criteria in the TPP.

6 Benzyl Alkyl Ether Linker

Extensive SAR studies were performed on the phenyl alkyl ether linker through modifications on the P* and P3 groups, with the goal of reducing PPAR- γ activity while maintaining or improving antiviral HCV activity. However, most compounds either had no reduction of PPAR- γ activity, significant loss of antiviral HCV activity, or decreased metabolic stability. With this setback, medicinal chemistry efforts were refocused on linker modifications. By transposing the oxygen atom by one carbon away from the phenyl group in the phenyl alkyl ether linker, a benzyl alkyl ether linker was generated. A series of compounds with different P* groups, P1 and P1' substitutions, were prepared (Fig. 10). Gratifyingly, compounds with this linker displayed a significant reduction in PPAR- γ agonistic activity (IC₅₀: 25–56 μ M compared to 0.28 μ M for compound **25a**) while maintaining comparable antiviral HCV activity with compound **25a**.

The PPAR- γ activity and antiviral activity in the stable replicon assay of compounds **26a–g** are displayed in Table 11. All compounds with the benzyl alkyl ether linker demonstrated an approximately 100- to 200-fold reduction in PPAR- γ activity as compared to compound **25a**. Compounds **26b** and **26g**, with differing P* groups (quinoxaliny and quinolinyl, respectively) demonstrated comparable antiviral activity to compound **25a** and were selected for further evaluations, including the impact of protein binding by human plasma on antiviral activity, as well as their activity against resistant mutants.

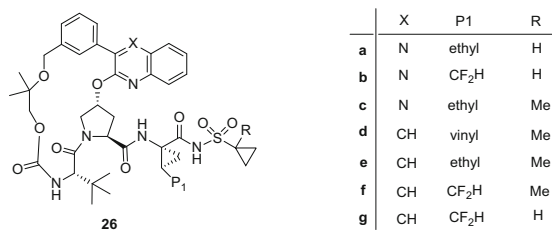


Fig. 10 Compounds with benzyl alkyl ether linker

Table 11 PPAR- γ activity and activity in stable replicon assay for compounds **25a** and **26a–g**

Compound	Stable replicon EC ₅₀ (nM)		PPAR- γ IC ₅₀ (μ M)
	GT 1a	GT 1b	
25a	0.56	0.81	0.28
26a	1.4	1.3	51
26b	0.77	0.76	46
26c	0.80	1.4	48
26d	1.5	0.88	25
26e	2.3	1.6	36
26f	1.3	0.67	50
26g	1.3	0.83	56

Table 12 Activity in stable replicon assay for compounds **26b**, **26g**, and **ABT-450**

Compound	Stable replicon EC ₅₀ (nM)					
	GT 1a	GT1a, 40% HP	Fold change	GT 1b	GT1b, 40% HP	Fold change
26b	0.77	6.3	8	0.76	13	17
26g	1.3	12	9	1.0	8.8	9
ABT-450	1.0	17	17	0.21	5.2	25

Table 13 Activity of compounds **26b**, **26g**, and **ABT-450** against resistant mutants

Compound	Fold change in EC ₅₀ relative to wild-type value in transient replicon assay					
	1a			1b		
	R155K	D168E	D168V	R155K	D168V	A-156T
26b	84	8	1,750	14	30	50
26g	16	13	202	1	6	6
ABT-450	37	14	96	40	159	7

The antiviral HCV activity in the stable replicon assay of compounds **26b** and **26g** in the presence of 40% human plasma was measured (Table 12), and compound **26g** demonstrated less protein binding impact compared to ABT-450. Thus, the presence of 40% human plasma resulted in only 9-fold loss for both GT1a and GT1b in the activity of compound **26g**, compared to 17-fold (GT1a) and 25-fold loss (GT1b) for ABT-450.

Additionally, the activity of compounds **26b** and **26g** was evaluated against a panel of genotype 1a and 1b resistance-associated substitutions in the transient replicon assay, with activity and fold changes in EC₅₀ relative to wild type shown in Table 13. The greatest reductions in potency against these resistance-associated substitutions were evident in genotype 1a, where D168V demonstrated the most substantial resistance to compounds **26b** (1,750-fold change) and **26g** (202-fold change). Compound **26g** displayed much better activity against the panel of genotype 1b resistance-associated substitutions R155K and D168V with fold losses in antiviral activity of only 1× (R155K) and 6× (D168V) compared to 40× (R155K) and 159× (D168V), respectively for ABT-450.

7 Difluoroalkyl Cyclopentyl Ether Linker

Another linker modification, which replaced the benzyl alkyl ether with the difluoroalkyl cyclopentyl ether [51], yielded compound **28** with HCV activity comparable to compound **25a** and without significant PPAR-γ activity (IC₅₀ > 20 μM) (Fig. 11). Initial attempts were made to remove the phenyl group from the linker and replace it with a simple unconjugated alkene. However, during initial studies attempting to form the macrocyclic alkene via ring-closing metathesis (RCM), the allyl group attached to P* quinoxaliny group in the precursor preferentially moved into conjugation with the P* quinoxaliny group. Thus, a difluoro

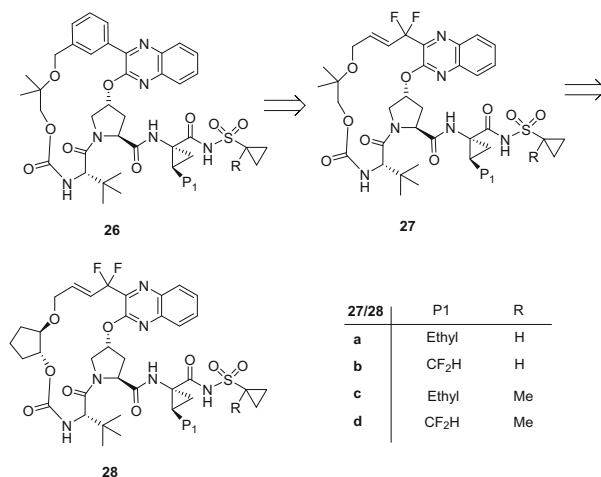


Fig. 11 Design of difluoroalkyl cyclopentyl ether linker compound **28**

Table 14 PPAR- γ activity and activity in the stable replicon assay for compounds **25a** and **27a–d**

Compound	Stable replicon EC ₅₀ (nM)		PPAR- γ IC ₅₀ (μ M)
	GT 1a	GT 1b	
25a	0.56	0.81	0.28
27a	3.8	3.7	37
27b	6.5	3.5	132
27c	1.9	1.8	31
27d	3.5	2.5	166

substitution was introduced at the benzylic position to prevent this migration. Additionally, we hypothesized that this strategy would also improve metabolic stability by the blockade of the potentially labile benzylic position. Accordingly, compounds **27a–d** were prepared (Fig. 11), and their HCV activity in the stable replicon assay and their PPAR- γ activity were evaluated (Table 14). All these compounds were weaker PPAR- γ agonists, particularly the difluoromethyl P1 compounds **27b** and **27d** with IC_{50s} > 100 μ M. However, most compounds displayed decreased HCV activities in the stable replicon assay compared to the compound **25a**. As discussed previously introducing gem-difluoro or gem-dimethyl substitution to the P2–P4 macrocyclic linker showed improved antiviral HCV activity (see Fig. 5 and Table 4). The improved activity is attributed to decreased conformational flexibility imposed by the Thorpe-Ingold effect of the gem-difluoro/gem-dimethyl substitutions. Consequently, to further increase conformational rigidity in the linker region, compound **28** was designed by introducing a cyclopentyl group on the other side of the ether linker.

Compounds **28a–f** were prepared (Fig. 11), and their HCV activity in the stable replicon assay and their PPAR- γ activities were evaluated (Table 15). Gratifyingly, all compounds exhibited HCV activity in the stable replicon assay comparable to

Table 15 PPAR- γ activity and activity in the stable replicon assay for compounds **25a** and **28a–d**

Compound	Stable replicon EC ₅₀ (nM)		PPAR- γ IC ₅₀ (μ M)
	GT 1a	GT 1b	
25a	0.56	0.81	0.28
28a	0.76	1.4	34
28b	1.4	1.6	79
28c	0.88	1.6	20
28d	0.85	0.94	>100

Table 16 Activity in the stable replicon assay for compounds **28b**, **28g**, and **ABT-450**

Compound	Stable replicon EC ₅₀ (nM)					
	GT 1a	GT1a, 40% HP	Fold change	GT 1b	GT1b, 40% HP	Fold change
28b	1.4	8.0	5.7	1.6	21	13
28d	0.85	5.3	6.2	0.94	10	11
ABT-450	1.0	17	17	0.21	5.2	25

Table 17 Activity against resistant mutants of compounds **28b**, **28d**, and **ABT-450**

Compound	Fold change in EC ₅₀ relative to wild-type value in transient replicon assay					
	1a			1b		
	R155K	D168E	D168V	R155K	D168V	A-156T
28b	0.5	2.2	4.0	0.6	1.4	202
28d	0.8	<3.7	3.8	0.7	0.9	181
ABT-450	37	14	96	40	159	7

compound **25a**, and compounds **28b/28d** demonstrated the most significant decrease in PPAR- γ activity with IC₅₀s of 79 μ M for compound **28b** and >100 μ M for compound **28d**. Given their HCV activity in the stable replicon and their PPAR- γ activity, compounds **28b** and **28d** were advanced for evaluation of their human plasma protein binding impact on antiviral activity and for their activity against resistance-associated substitutions.

Compounds **28b** and **28d** underwent testing in the stable replicon assay in the presence of 40% human plasma (Table 16). The impact of plasma protein binding on the activity of both compounds **28b** and **28d** was similar with about 6-fold (GT1a) and 11- to 13-fold (GT1b) potency loss as compared to their activity in the presence of 5% FBS.

The activity of compounds **28b** and **28d** was also evaluated against a panel of genotype 1a and 1b resistance-associated substitutions in the transient replicon assay, with activity and fold changes in EC₅₀ relative to wild type shown in Table 17. These two compounds demonstrated superior activity compared to earlier compounds with a <5-fold change in EC₅₀ relative to wild type for five of six resistance-associated substitutions. The only significant potency loss was observed

for both compounds against the genotype 1b A-156T mutant (>100-fold); however, the viral fitness of the replicon with this particular mutation was low (replication efficiency <19%) [52].

8 Discovery of ABT-493

As mentioned previously, the selected target product profile for the next-generation HCV PIs required that they possess pan-genotypic activity and potential QD dosing without RTV boosting. Based on previously discussed antiviral activity, activity against resistance-associated substitutions and PPAR- γ activity, compounds **26g** and **28d**, chosen from two different linker series for structural diversity, were selected for further evaluation for their pan-genotypic activity and PK properties. Thus the binding constants (K_i) with different genotype HCV proteases of both compounds **26g** and **28d** were measured (Table 18). Compound **28d** demonstrated superior binding affinity to all genotype HCV proteases tested.

Single ascending dose rat PK studies of compounds **26g** and **28d** were performed to evaluate their potential for QD dosing without RTV boosting (Table 19). Compound **28d** demonstrated higher plasma exposure (25 versus 1.7 $\mu\text{g h/mL}$) and a longer half-life (2.8 versus 0.6 h) as compared to compound **26g** following a single 5 mg/kg intravenous (*iv*) dose. Compound **28d** also exhibited better bioavailability (90% vs 46%) compared to compound **26g**, as well as a dose proportional increase in plasma exposure following single oral doses of 5 (22 $\mu\text{g h/mL}$) and 20 mg/kg (101 $\mu\text{g h/mL}$). Notably, no increase in plasma exposure was observed when compound **28d** was co-dosed with RTV.

Table 18 Binding affinity of compounds **26g** and **28d** with HCV proteases of different genotypes

Compound	HCV protease tight-binding biochemical genotype data (K_i , nM)					
	1a	1b	2a	3a	4a	6a
26g	0.22	0.23	0.66	7.5	0.24	NA
28d	0.075	0.063	0.053	0.96	0.092	0.11

Table 19 Rat pharmacokinetics of compounds **26g** and **28d**

Compound	Route	Dose (mg/kg)	$T_{1/2}$ (h)	C_{max} ($\mu\text{g/mL}$)	AUC ($\mu\text{g h/mL}$)	F (%)
26g	<i>iv</i>	5	0.6		1.7	
	Oral	5		0.35	0.78	46
	Oral	30		3.9	13	
	Oral	60		7.8	36	
	Oral	100		11	44	
28d	<i>iv</i>	5	2.8		25	
	Oral	5		6.3	22	90
	Oral	20		28	101	
	Oral	5 + RTV (5)		11	4	

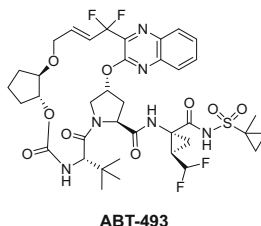
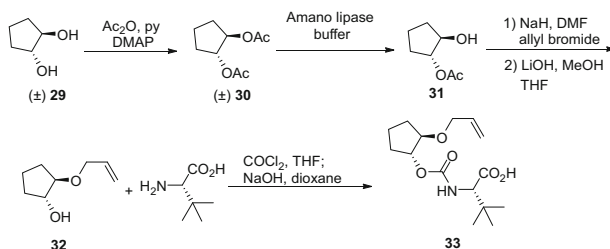


Fig. 12 Structure of ABT-493



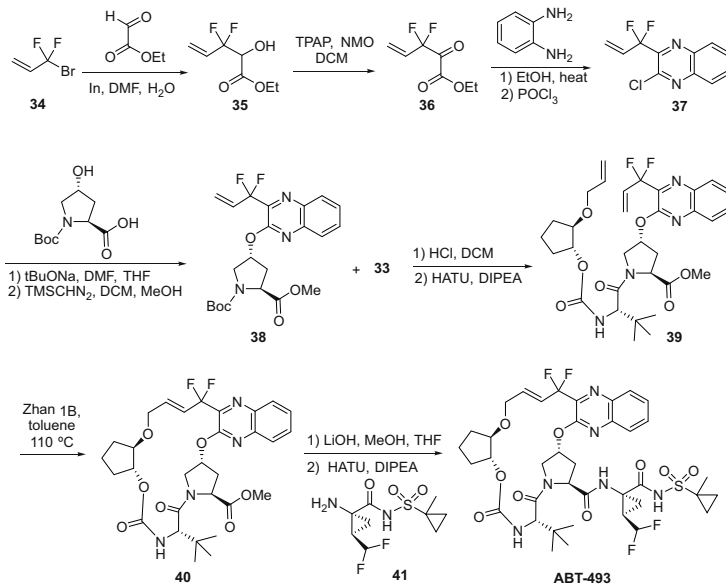
Scheme 1 Synthesis of intermediate compound **33**

Based on virology and preclinical PK data, compound **28d** was chosen to move forward as a preclinical candidate and designated as ABT-493 (Fig. 12).

9 Synthesis of ABT-493

The synthesis of ABT-493 is outlined below, starting with the preparation of the linker region intermediate **33** (Scheme 1). Racemic *trans*-1,2-cyclopentanediol (**29**) was acetylated to give diacetate **30**. Mono-deacetylation was effected in lipase buffer to afford chiral compound **31**. Allyl ether formation in the presence of allyl bromide and sodium hydride in DMF followed by deacetylation delivered allyl ether **32**. Activation of compound **32** with phosgene followed by reacting with (*S*)-2-amino-3,3-dimethylbutanoic acid gave intermediate **33**.

The construction of the quinoxaline fragment of ABT-493 commenced with an indium-mediated Barbier reaction of difluoroallyl bromide **34** with ethyl glyoxalate to afford difluoro alcohol **35**, which was subsequently oxidized by TPAP/NMO to deliver keto ester **36** (Scheme 2). Condensation of **36** with *o*-phenylenediamine in ethanol followed by treatment with POCl₃ gave the chloroquinoxaline intermediate **37**. Coupling of **37** with L-N-Boc-4-hydroxyl-proline under basic conditions proceeded without issue, and the intermediate was esterified to deliver ester **38**. Notably, when the analogous proline methyl ester was utilized to couple with compound **37**, significant epimerization occurred. Boc deprotection followed by amide coupling with intermediate **33** delivered diene **39**. The ring-closing metathesis

**Scheme 2** Synthesis of ABT-493**Table 20** Dog pharmacokinetics of ABT-493

Route	Dose (mg/kg)	$T_{1/2}$ (h)	C_{max} ($\mu\text{g/mL}$)	AUC ($\mu\text{g h/mL}$)	F (%)
<i>iv</i>	1.0	0.6		0.52	
Oral	3		0.79	1.49	95
Oral	10		13	23.7	

of diene **39** proceeded smoothly in toluene to provide the macrocyclic intermediate **40**, when the Zhan 1B was employed as the catalyst. Finally, saponification of intermediate **40**, followed by coupling with amine **41**, provided ABT-493.

10 Preclinical PK Evaluation of ABT-493

As previously described, ABT-493 yielded favorable outcomes from a single 5 mg/kg *iv* dose rat PK study: a plasma half-life of 2.8 h and plasma exposure (AUC) of 25 $\mu\text{g h/mL}$ with oral bioavailability of 90%. In addition to the rat PK evaluation, the ABT-493 PK profile also was evaluated in dog (Table 20). Although ABT-493 displayed a short plasma half-life (0.6 h) and low plasma exposure (AUC 0.52 $\mu\text{g h/mL}$) following a single 1.0 mg/kg *iv* dose, 95% oral bioavailability was achieved after a single 3 mg/kg oral dose, with plasma exposure >20 $\mu\text{g h/mL}$ observed after a single 10 mg/kg oral dose.

Table 21 In vitro antiviral activity of ABT-493

HCV replicon or virus	Mean EC ₅₀ ± SD (nM)
GT1a H77	0.85 ± 0.15
GT1b Con1	0.94 ± 0.35
GT2a JFH-1	2.2 ± 1.1
GT2b	4.6 ± 1.2
GT3a	1.9 ± 0.62
GT4a	2.8 ± 0.41
GT5a	1.4 ± 0.26
GT6a	0.86 ± 0.11
GT6e	0.21 ± 0.05

11 ABT-493 Virology [52]

In transient transfection assays, ABT-493 was shown to retain activity against most of the NS3 amino acid substitutions associated with reduced susceptibility to other currently approved HCV PIs, including those commonly observed at positions 155 and 168 [52]. In colony selection experiments across genotypes 1–6, A156T or A156V substitutions in NS3 were isolated, which demonstrated reduced susceptibility to ABT-493 by 148- to 3,106-fold. However, the replication efficiencies of replicons with these substitutions were low ($\leq 5\%$ in genotype 1a and $\leq 19\%$ in genotype 1b). Furthermore, ABT-493 also maintained activity against replicons containing key resistance-associated substitutions for NS5A and NS5B inhibitors. Selection of ABT-493 was reinforced by colony selection experiments using a combination of ABT-493 and ABT-530, an investigational NS5A inhibitor. Following treatment of either genotype 1a or 1b replicon cells with ABT-493 plus ABT-530, each at tenfold its respective EC₅₀, no replicon cells survived the selection, indicating enhanced suppression of the emergence of drug-resistant colonies by this combination [52]. The antiviral activity of ABT-493 in HCV subgenomic stable replicons containing proteases from HCV genotypes 1a, 1b, 2a, 2b, 3a, 4a, 5a, 6a, and 6e in Huh-7 cells also was investigated. The EC₅₀ values are listed in Table 21. The EC₅₀ values of ABT-493 in this study ranged from 0.21 to 4.6 nM. Importantly, ABT-493 was active against a replicon-containing protease from genotype 3, the most difficult-to-treat HCV genotype, with an EC₅₀ of 1.9 nM. Notably, approved HCV protease inhibitors such as simeprevir, asunaprevir, and ABT-450 had reduced potency against this replicon [44, 53–55].

12 Development of ABT-493

As the preclinical development proceeded, ABT-493 was evaluated in a battery of safety pharmacology assays, including assessment of effects on central nervous system/neurobehavior, cardiovascular, and respiratory function, and no clinical

relevant adverse effects were observed. ABT-493 was not mutagenic or clastogenic as tested in the Ames assay, the *in vitro* chromosomal aberration assay in CHO cells, and *in vivo* rat micronucleus assays. ABT-493 was well tolerated in rodent and dog toxicology studies. No adverse effects were identified at maximal feasible exposures (580 $\mu\text{g h/mL}$ in the rat at the 120 mg/kg/day and 765 $\mu\text{g h/mL}$ in the dog at the 200 mg/kg/day, representing 223- to 294-fold the mean AUC exposure in humans of 2.6 $\mu\text{g h/mL}$ at the 300 mg therapeutic dose) in studies up to 13-week duration. Based upon these benign safety and toxicological profiles in combination with its favorable preclinical virological and pharmacokinetic properties, ABT-493 advanced into Phase 1 clinical studies.

ABT-493 was well tolerated in Phase 1 studies in healthy human volunteers at the doses up to 800 mg once daily for 10 days with steady-state plasma AUC_{0-24} of 64 $\mu\text{g h/mL}$ [56]. Based on PK/PD-viral dynamics modeling and simulations, ABT-493 monotherapy for 3 days in genotype (GT) 3a (which was considered to be the most challenging genotype to treat) subjects was predicted to result in a total viral load reduction of 2.6–4.1 log for AUC values ranging from 1.2 to 4.7 $\mu\text{g h/mL}$ [Chih-Wei Lin, unpublished data]. Thus, the results of Phase 1 dose ranging provided a wide safety window for ABT-493 over the projected efficacious doses. The plasma exposures of ABT-493 were greater than dose proportional with a terminal half-life ranging from 7 to 9 h. Coadministration with ritonavir, a strong inhibitor of cytochrome P450 3A4 which is used to pharmacokinetically boost HIV protease inhibitors such as lopinavir and HCV protease inhibitors such as paritaprevir [57], had minimal boosting effects on both AUC exposure and terminal half-life of ABT-493. Therefore, ABT-493 proceeded into Phase 2 efficacy studies without ritonavir co-dosing.

Based on the favorable pharmacokinetic and safety profile in healthy volunteers, the *in vivo* antiviral activity of ABT-493 was first examined in a PoC 3-day monotherapy study [58]. In this study, treatment-naïve patients infected with HCV genotype 1 were administered doses of ABT-493 ranging from 100 to 700 mg once daily for 3 days. Mean maximal decreases in the HCV plasma viral load from the baseline at the end of the 3-day monotherapy ranged from 3.8 to 4.3 \log_{10} IU/mL. Of note, NS3 amino acid substitutions emerged in only 2 (4%) of the 48 patients in this monotherapy study. This low rate of emergence of amino acid substitutions during monotherapy was consistent with the high barrier to resistance observed for ABT-493 in genotype 1a replicons *in vitro* [52].

As the Phase 2/3 programs progressed, ABT-493 (glecaprevir) was examined in combination with the investigational HCV NS5A inhibitor ABT-530 (pibrentasvir). The combination of glecaprevir and pibrentasvir, two direct-acting antiviral agents (DAA) with distinct anti-HCV mechanisms of action plus non-overlapping resistance profiles, resulted in synergistic inhibition of HCV replication and also suppressed the emergence of drug resistance *in vitro* [52]. In phase 2/3 studies, the fixed-dose combination of 300 mg glecaprevir and 120 mg pibrentasvir, dosed once daily, achieved an overall sustained virologic response (SVR) rate of >99% (modified intent to treat [mITT]) in a total of 2,256 treatment-naïve or treatment-experienced (pegIFN, RBV, and/or sofosbuvir) patients infected with HCV genotypes 1–6 with a treatment duration of 8, 12, or 16 weeks [59, 60]. Twenty-two out

of these 2,256 patients (<1%) experienced virologic failure, and treatment-emergent NS3 substitutions at amino acid positions 56, 80, 156, or 168 were detected in 11 GT-3 patients and 1 GT-1 patient. The combination of glecaprevir and pibrentasvir was also evaluated in HCV GT 1-infected patients who had failed a prior DAA-containing regimen [61]. HCV samples collected from these patients at baseline had diverse resistance profiles and a high prevalence of NS3 or NS5A resistance-associated substitutions due to the patients' failure to their prior DAA treatments. This combination regimen of glecaprevir and pibrentasvir achieved an SVR rate of 96% (mITT), demonstrating its robust efficacy in HCV-infected DAA-experienced patients. High SVR rates in Phase 2/3 studies supported the approval of the glecaprevir/pibrentasvir combination, designated as Mavyret™ (USA) or Maviret™ (ex-USA), for the treatment of patients with chronic HCV genotype 1, 2, 3, 4, 5, or 6 infection without cirrhosis or with compensated cirrhosis and also for patients with HCV GT-1 infection who previously have been treated with a regimen containing an HCV NS5A inhibitor or an NS3/4A protease inhibitor, but not both. This treatment regimen was approved for use in the USA and Europe in August and July 2017, respectively, and has since received approval in a wide range of additional countries (including Japan). It is marketed by AbbVie.

13 Conclusion

As described above, the next-generation HCV protease inhibitor ABT-493 (glecaprevir), which has a favorable PK profile, pan-genotypic activity, and activity against resistance-associated variants, was identified through extensive SAR studies at the P* and P1 positions and through linker modification. In combination with the HCV NS5A inhibitor pibrentasvir, this dual DAA combination regimen achieved $\geq 95\%$ SVR across treatment-naïve patients, without cirrhosis, infected with HCV genotypes 1–6 with just 8 weeks of treatment. This combination has since been approved in multiple countries and is marketed by AbbVie as Mavyret™/Maviret™.

Acknowledgment Authors want to thank Dale J. Kempf and other Abbott medicinal chemistry team members for editing and reviewing this chapter and helpful discussion/idea exchanges during collaboration. Also thanks to Abbott's virology and DMPK teams for the characterizations of all compounds, which were essential for identification of the candidate ABT-493. Authors also want to thank all Joint Steering Committee members from both Enanta and Abbott for their support.

Compliance with Ethical Standards

Funding The study was supported by Enanta Pharmaceuticals, Inc. and AbbVie.

Conflict of Interest G.W., J.M., L.-J.J., J.L., B.W., and Y.S.O. are current Enanta employees who hold Enanta stock options, and all of them and Y.G. may hold Enanta stock. K.F.M. is a current AbbVie employee and may hold AbbVie stock or options. The chemistry research and the preclinical characterization were conducted by Enanta and AbbVie, respectively. The design and conduct of the clinical studies of glecaprevir were provided by AbbVie. AbbVie and Enanta participated in the interpretation of the data and review and approval of the publication.

AbbVie is committed to responsible data sharing regarding the clinical trials it sponsors. This includes access to anonymized, individual and trial-level data (analysis data sets), as well as other information (e.g., protocols and Clinical Study Reports), as long as the trials are not part of an ongoing or planned regulatory submission. This includes requests for clinical trial data for unlicensed products and indications.

This clinical trial data can be requested of AbbVie by any qualified researchers who engage in rigorous, independent scientific research, and will be provided following review and approval of a research proposal and Statistical Analysis Plan (SAP) and execution of a Data Sharing Agreement (DSA). Data requests can be submitted at any time and the data will be accessible for 12 months, with possible extensions considered. For more information on the process, or to submit a request, visit the following link: <https://www.abbvie.com/our-science/clinicaltrials/clinical-trials-data-and-information-sharing/data-and-information-sharing-with-qualifiedresearchers.html>.

Ethical Approval All applicable international, national, and/or institutional guidelines for the care and use of animals were followed in the preclinical research conducted at Enanta and at AbbVie. All procedures performed by AbbVie in studies involving human participants were in accordance with the ethical standards of the institutional and/or national research committee and with the 1964 Helsinki declaration and its later amendments or comparable ethical standards.

Informed Consent Informed consent was obtained from all individual participants included in the study.

The authors would like to thank the patients and their families as well as the study site staff who participated in the clinical trials of glecaprevir.

References

1. Feinstone SM, Kapikian AZ, Purcell RH, Alter HJ, Holland PV (1975) Transfusion associated hepatitis not due to viral hepatitis type A or B. *N Engl J Med* 292:767–770
2. Choo QL, Kuo G, Weiner AJ, Overby LR, Bradley DW, Houghton M (1989) Isolation of a c-DNA clone derived from a blood-borne non-A, non-B viral hepatitis genome. *Science* 244:359–362
3. Takamizawa A, Mori C, Fuke I et al (1991) Structure and organization of the hepatitis C virus genome isolated from human carriers. *J Virol* 65:1105–1113
4. Nakano T, Lau GMG, Lau GML, Sugiyama M, Mizokami M (2012) An updated analysis of hepatitis C virus genotypes and subtypes based on the complete coding region. *Liver Int* 32:339–345
5. Fried MW (2002) Side effects of therapy of hepatitis C and their management. *Hepatology* 36:S237–S244
6. Bartenschlager R, Ahlborn-Laake L, Mous J, Jacobsen H (1994) Kinetic and structural analyses of hepatitis C virus polyprotein processing. *J Virol* 68:5045–5055
7. Horner SM, Gale Jr M (2013) Regulation of hepatic innate immunity by hepatitis C virus. *Nat Med* 19:879–888
8. Llinas-Brunet M, Bailey M, Bolger G et al (2004) Structure activity study on a novel series of macrocyclic inhibitors of the hepatitis C virus NS3 protease leading to the discovery of BILN 2061. *J Med Chem* 47:1605–1608
9. Llinas-Brunet M, Bailey M, Ghire E et al (2004) A systematic approach to the optimization of substrate-based inhibitors of the hepatitis C virus NS3 protease: discovery of potent and specific tripeptide inhibitors. *J Med Chem* 47:6584–6594
10. Miao Z, Sun Y, Wu F, Nakajima S, Xu G, Or YS, Wang Z (2004) Macrocyclic hepatitis C virus (HCV) serine protease NS3 inhibitors, their synthesis and use to prevent HCV infection. WO 2004/072243 A2, ENANTA Pharmaceuticals

11. Nakajima S, Sun Y, Tang D, Xu G, Porter B, Or Y, Wang Z, Miao Z (2004) Preparation of quinoxalinyll macrocyclic hepatitis C serine protease inhibitors. WO 2004/093798 A2, ENANTA Pharmaceuticals
12. Miao Z, Sun Y, Nakajima S, Tang D, Wang Z, Or YS (2004) Preparation of tripeptide hepatitis C serine protease inhibitors. WO2004/113365 A2, ENANTA Pharmaceuticals
13. Wu F, Nakajima S, Or YS, Lu Z, Sun Y, Miao Z, Wang Z (2005) Preparation of aza-peptide macrocyclic hepatitis C serine protease inhibitors. WO 2005/010029 A1, ENANTA Pharmaceuticals
14. Scola P, Wang A, Good A et al (2014) Discovery and early clinical evaluation of BMS-605339, a potent and orally efficacious tripeptidic acylsulfonamide NS3 protease inhibitor for the treatment of hepatitis C virus infection. *J Med Chem* 57:1708–1729
15. Gai Y, Or YS, Wang Z (2009) Macrocyclic quinoxalinyll HCV serine protease inhibitors. WO2009/064975 A1, ENANTA Pharmaceuticals
16. Gai Y, Or YS, Wang Z (2012) Triazole-containing macrocyclic HCV serine protease inhibitors. US 8,273,709 B2, ENANTA Pharmaceuticals
17. Sun Y, Liu D, Or YS, Wang Z (2012) Macrocyclic tetrazolyl hepatitis C serine protease inhibitors. US 8,304,385 B2, ENANTA Pharmaceuticals
18. Sun Y, Gai Y, Or YS, Wang Z (2012) Macrocyclic oximyl hepatitis C serine protease inhibitors. US 8,222,203 B2, ENANTA Pharmaceuticals
19. Liu D, Or YS, Wang Z (2012) Bridged carbocyclic hepatitis C serine protease inhibitors. US 8,283,309 B2, ENANTA Pharmaceuticals
20. Gai Y, Or YS, Wang Z (2013) Fluorinated macrocyclic compounds as hepatitis C virus inhibitors. US 8,372,802 B2, ENANTA Pharmaceuticals
21. Gai Y, Liu D, Moore JD, Or YS, Wang Z (2012) Difluoromethyl-containing macrocyclic compounds as hepatitis C virus inhibitors. US 8,211,891 B2, ENANTA Pharmaceuticals
22. Chen KX, Njoroge FG et al (2006) Potent 7-hydroxy-1,2,3,4-tetrahydroisoquinoline-3-carboxylic acid-based macrocyclic inhibitors of HCV NS3 protease. *J Med Chem* 49:567–574
23. Liverton NJ, Holloway MK et al (2008) Molecular modeling based approach to potent P2-P4 macrocyclic inhibitors of hepatitis C NS3/4A protease. *J Am Chem Soc* 130:4607–4609
24. Moore JD, Or YS, Wang Z (2012) C5-substituted, proline derived, macrocyclic hepatitis C serine protease inhibitors. US 8,263,549 B2, ENANTA Pharmaceuticals
25. Moore JD, Or YS, Wang Z (2011) Bicyclic C5-substituted proline derivatives as inhibitors of the hepatitis C virus NS3 protease. US 8,030,307 B2, ENANTA Pharmaceuticals
26. Kwong AD (2014) The HCV revolution did not happen overnight. *ACS Med Chem Lett* 5:214–220
27. Asselah T, Boyer N, Saadoun D, Martinot-Peignoux M, Marcellin P (2016) Direct-acting antivirals for the treatment of hepatitis C virus infection: optimizing current IFN-free treatment and future perspectives. *Liver Int* 36(Suppl 1):47–57
28. Gottwein JM, Scheel TK, Jensen TB, Ghanem L, Bukh J (2011) Differential efficacy of protease inhibitors against HCV genotypes 2a, 3a, 5a, and 6a NS3/4A protease recombinant viruses. *Gastroenterology* 141:1067–1079
29. Romano KP, Ali A, Aydin C, Soumana D, Ozen A, Deveau LM, Silver C, Cao H, Newton A, Petropoulos CJ, Huang W, Schiffer CA (2012) The molecular basis of drug resistance against hepatitis C virus NS3/4A protease inhibitors. *PLoS Pathog* 8:e1002832
30. Pawlotsky JM (2013) NS5A inhibitors in the treatment of hepatitis C. *J Hepatol* 59:375–382
31. Gao M (2013) Antiviral activity and resistance of HCV NS5A replication complex inhibitors. *Curr Opin Virol* 3:514–520
32. Jensen SB, Serre SB, Humes DG, Ramirez S, Li YP, Bukh J, Gottwein JM (2015) Substitutions at NS3 residue 155, 156, or 168 of hepatitis C virus genotypes 2 to 6 induce complex patterns of protease inhibitor resistance. *Antimicrob Agents Chemother* 59:7426–7436
33. Pawlotsky JM (2016) Hepatitis C virus resistance to direct-acting antiviral drugs in interferon-free regimens. *Gastroenterology* 151:70–86
34. Lahser FC, Bystol K, Curry S, McMonagle P, Xia E, Ingravallo P, Chase R, Liu R, Black T, Hazuda D, Howe AY, Asante-Appiah E (2016) The combination of grazoprevir, a hepatitis C virus (HCV) NS3/4A protease inhibitor, and elbasvir, an HCV NS5A inhibitor, demonstrates a

- high genetic barrier to resistance in HCV genotype 1a replicons. *Antimicrob Agents Chemother* 60:2954–2964
35. Falade-Nwulia O, Suarez-Cuervo C, Nelson DR, Fried MW, Segal JB, Sulkowski MS (2017) Oral direct-acting agent therapy for hepatitis C virus infection: a systematic review. *Ann Intern Med* 166:637–648
 36. Hepatitis C Guidance (2017) AASLD-IDSAs recommendations for testing, managing, and treating adults infected with hepatitis C virus. <http://www.hcvguidelines.org>
 37. European Association for the Study of the Liver (2017) EASL recommendations on treatment of hepatitis C 2016. *J Hepatol* 66:153–194
 38. Merck & Co., Inc. (2016) Zepatier (elbasvir and grazoprevir) tablets, for oral use, package insert. Merck, Whitehouse Station. https://www.merck.com/product/usa/pi_circulars/z/zepatier/zepatier_pi.pdf
 39. Jacobson IM, Asante-Appiah E, Wong P, Black T, Howe A, Wahl J, Robertson MN, Nguyen B-Y, Shaughnessy M, Hwang P, Barr E, Hazuda D (2015) Prevalence and impact of baseline NS5A resistance-associated variants (RAVs) on the efficacy of elbasvir/grazoprevir (EBR/GZR) against GT1a infection. *Hepatology* 62:1393A–1394A
 40. McPhee F, Hernandez D, Yu F, Ueland J, Monikowski A, Carifa A, Falk P, Wang C, Fridell R, Eley T, Zhou N, Gardiner D (2013) Resistance analysis of hepatitis C virus genotype 1 prior treatment null responders receiving daclatasvir and asunaprevir. *Hepatology* 58:902–911
 41. Janssen Products (2013) Olysio (simeprevir). Highlights of prescribing information. Janssen Therapeutics, Titusville
 42. Hernandez D, Zhou N, Ueland J, Monikowski A, McPhee F (2013) Natural prevalence of NS5A polymorphisms in subjects infected with hepatitis C virus genotype 3 and their effects on the antiviral activity of NS5A inhibitors. *J Clin Virol* 57:13–18
 43. Lontok E, Harrington P, Howe A, Kieffer T, Lennerstrand J, Lenz O, McPhee F, Mo H, Parkin N, Pilot-Matias T, Miller V (2015) Hepatitis C virus drug resistance-associated substitutions: state of the art summary. *Hepatology* 62:1623–1632
 44. Pilot-Matias T, Tripathi R, Cohen D et al (2015) In vitro and in vivo antiviral activity and resistance profile of the hepatitis C virus NS3/4A protease inhibitor ABT-450. *Antimicrob Agents Chemother* 59:988–997
 45. Gai Y, Or YS, Wang G (2015) Macrocyclic compounds as HCV virus inhibitors. US 8,936,781 B2, ENANTA Pharmaceuticals
 46. Tang WH, Maroo A (2007) PPAR- γ agonists: safety issues in heart failure. *Diabetes Obes Metab* 9(4):447–454
 47. Nesto RW, Bell D, Bonow RO et al (2003) Thiazolidinedione use, fluid retention, and congestive heart failure: a consensus statement from the American Heart Association and American Diabetes Association. *Circulation* 108:2941–2948
 48. Guan Y, Hao C, Cha DR et al (2005) Thiazolidinediones expand body fluid volume through PPAR- γ stimulation of ENaC-mediated renal salt absorption. *Nat Med* 11:861–866
 49. Rubenstrunk A, Hanf R, Hum DW, Fruchart JC, Staels B (2007) Safety issues and prospects for future generations of PPAR modulators. *Biochim Biophys Acta* 1771:1065–1081
 50. Huang JV, Greyson CR, Schwartz GG (2012) PPAR- γ as a therapeutic target in cardiovascular disease: evidence and uncertainty. *J Lipid Res* 53(9):1738–1754
 51. Or YS, Ma J, Wang G, Long J, Wang B (2012) Macrocyclic proline derived HCV serine protease inhibitors. WO 2012/040167 A1, ENANTA Pharmaceuticals
 52. Ng TI, Tripathi R, Reisch T et al (2018) In vitro antiviral activity and resistance profile of the next-generation hepatitis C virus NS3/4A protease inhibitor glecaprevir. *Antimicrob Agents Chemother* 62(1):e01620–e01617
 53. Lenz O, Vijgen L, Berke J et al (2013) Virologic response and characterization of HCV genotype 2-6 in patients receiving TMC435 monotherapy (study TMC435-C202). *J Hepatol* 58:445–451
 54. McPhee F, Friborg J, Levine S et al (2012) Resistance analysis of the hepatitis C virus NS3 protease inhibitor asunaprevir. *Antimicrob Agents Chemother* 56:3670–3681

55. McPhee F, Sheaffer A, Friborg J et al (2012) Preclinical profile and characterization of hepatitis C virus NS3 protease inhibitor asunaprevir (BMS-650032). *Antimicrob Agents Chemother* 56:5387–5396
56. Lin CW, Dutta S, Asatryan A, Chiu YL, Wang H, Clifton II J, Campbell A, Liu W (2017) Pharmacokinetics, safety and tolerability of single and multiple doses of ABT-493: a first in human study. *J Pharm Sci* 106:645–651
57. Sham H, Kempf D, Molla A et al (1998) ABT-378, a highly potent inhibitor of the human immunodeficiency virus protease. *Antimicrob Agents Chemother* 42:3218–3224
58. Lawitz EJ, O’Riordan WD, Asatryan A, Freilich BL, Box TD, Overcash JS, Lovell S, Ng TI, Liu W, Campbell A, Lin CW, Yao B, Kort J (2016) Potent antiviral activities of the direct-acting antivirals ABT-493 and ABT-530 with three-day monotherapy for hepatitis C virus genotype 1 infection. *Antimicrob Agents Chemother* 60:1546–1555
59. Krishnan P, Schnell G, Tripathi R, Ng T, Reisch T, Beyer J, Dekhtyar T, Irvin M, Xie W, Larsen L, Mensa F, Pilot-Matias T, Collins C (2017) Pooled resistance analysis in HCV genotype 1–6-infected patients treated with glecaprevir/pibrentasvir in phase 2 and 3 clinical trials. *J Hepatol* 66(Suppl 1):S500
60. Puoti M, Foster G, Wang S, Mutimer D, Gane E, Moreno C, Chang TT, Lee SS, Marinho R, Dufour JF, Pol S, Hezode C, Gordon SC, Strasser SI, Thuluvath PJ, Liu R, Pilot-Matias T, Mensa F (2017) High SVR rates with eight and twelve weeks of pangenotypic glecaprevir/pibrentasvir: integrated efficacy and safety analysis of genotype 1-6 patients without cirrhosis. *J Hepatol* 66(Suppl 1):S721
61. Poordad F, Felizarta F, Asatryan A, Sulkowski MS, Reindollar RW, Landis CS, Gordon SC, Flamm SL, Fried MW, Bernstein DE, Lin CW, Liu R, Lovell SS, Ng TI, Kort J, Mensa FJ (2017) Glecaprevir and pibrentasvir for 12 weeks for hepatitis C virus genotype 1 infection and prior direct-acting antiviral treatment. *Hepatology* 66:389–397

Discovery of Voxilaprevir (GS-9857): The Pan-Genotypic Hepatitis C Virus NS3/4A Protease Inhibitor Utilized as a Component of Vosevi[®]



James G. Taylor

Contents

1	Introduction	442
2	HCV NS3/4A Protease Inhibitors: Successes and Challenges	443
3	Exploration of Alternative Core Connectivities	444
4	Discovery of 3-Alkyl Substituted Pyrrolidines as Beneficial in GT3	445
5	Hepatotoxicity Risk Associated With Some HCV NS3/4A Protease Inhibitors	447
6	Improving Pan-Genotypic Potency and Minimizing Protein Adducts: The Discovery of Voxilaprevir	449
7	Voxilaprevir and Vosevi [®] (sofosbuvir/velpatasvir/voxilaprevir) Clinical Antiviral Activity	454
8	Conclusion	455
	References	455

Abstract There has been remarkable progress in the treatment of hepatitis C virus (HCV) infection with the approval of multiple direct acting antiviral (DAA) regimens. Although overall high HCV cure rates are now generally obtained, there are patients who fail the currently approved therapeutics and require a retreatment option. While HCV NS3/4A protease inhibitors (PIs) have proven highly effective for treating genotype (GT) 1 infection, decreased potency against GT2 and/or GT3 along with observed ALT elevation for some PIs has limited the broad utility of this treatment class. Described herein are the discovery efforts resulting in the HCV NS3/4A PI voxilaprevir. Distinct interactions with the conserved NS3 protease catalytic triad were identified that improve GT3 potency and activity against some common resistance variants. Furthermore, multiple parameters were analyzed to determine potential drivers of hepatotoxicity for HCV PIs in the clinic and it was determined that protein adduct formation had a high correlation with clinical ALT elevation. Therefore, structural modifications were made that both improved metabolic stability and reduced protein adduct formation, ultimately resulting in voxilaprevir.

J. G. Taylor (✉)
Gilead Sciences, Foster City, CA, USA
e-mail: james.taylor@gilead.com

Consistent with our optimization strategy, the combination of voxilaprevir with sofosbuvir (NS5B inhibitor) and velpatasvir (NS5A inhibitor) has proven highly effective across genotypes in Phase 3 clinical trials and hepatotoxicity has not been observed. Vosevi[®] (sofosbuvir, velpatasvir, and voxilaprevir) was approved in 2017 as a pan-genotypic treatment option for individuals who have previously failed DAA regimens and, for some DAA-naïve patients, represents a treatment regimen of shortened duration (8 weeks).

Keywords GS-9857, HCV, Hepatitis C virus, Hepatotoxicity, NS3/4A protease, Protein adducts, Single tablet regimen, SOF/VEL/VOX, STR, Vosevi, Voxilaprevir

1 Introduction

The approval of multiple innovative direct-acting antiviral (DAA) agents to treat hepatitis C virus (HCV) infection has resulted in over one million individuals cured. Despite this remarkable progress, HCV infection remains a global health concern with an estimated 71 million people chronically infected worldwide [1]. When left untreated, chronic HCV infection can eventually cause cirrhosis, hepatocellular carcinoma, and liver failure, resulting in approximately 400,000 deaths in 2015 alone [2]. The high viral genetic diversity, wherein there are 8 distinct genotypes (GTs) and at least 86 viral subtypes [3], has historically been a complicating factor in the treatment of HCV infection as the antiviral activity of each DAA is generally distinct across genotypes. The introduction of interferon-sparing oral DAA combination regimens including Harvoni[®] (ledipasvir and sofosbuvir), Viekira Pak[™] (ombitasvir, paritaprevir, ritonavir, and dasabuvir), and Zepatier[®] (elbasvir and grazoprevir) revolutionized the treatment of GT1 HCV infection, resulting in SVR rates ranging from 92 to 100% in GT1 subjects [4]. However, due to the differential antiviral activity of the DAA agents across HCV genotypes, these combination regimens do not represent pan-genotypic treatment options. To address the therapeutic need to treat patients infected with HCV genotypes not susceptible to the initial DAA combinations, next-generation combination regimens containing compounds with potent antiviral activity across all genotypes have been developed. For example, velpatasvir is an NS5A inhibitor with potent picomolar activity across all genotypes tested, and, when combined with sofosbuvir into the oral once-daily single-tablet regimen (STR) Epclusa[®], high SVR rates are obtained across genotypes [5, 6]. Despite the generally high SVR rates obtained for the multiple approved DAA combination regimens, there are patients that still fail these treatment options due to the development of viral mutations (also referred to as variants and substitutions) that are less susceptible to the DAA agents [7]. Voxilaprevir, the discovery described herein, retains significant antiviral activity against some common GT1 NS3/4A resistance-associated substitutions (RAS) and has potent nanomolar cellular activity across all HCV genotypes tested. Voxilaprevir was approved in 2017 as a component of the

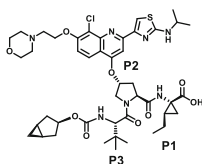
pan-genotypic STR Vosevi[®] (sofosbuvir, velpatasvir, and voxilaprevir). Vosevi[®] provides a treatment option for the most difficult-to-cure patients who have failed prior DAA-based therapies [8, 9], and, for some DAA-naïve patients, Vosevi[®] provides a pan-genotypic option of shortened treatment duration (8 weeks) [8].

2 HCV NS3/4A Protease Inhibitors: Successes and Challenges

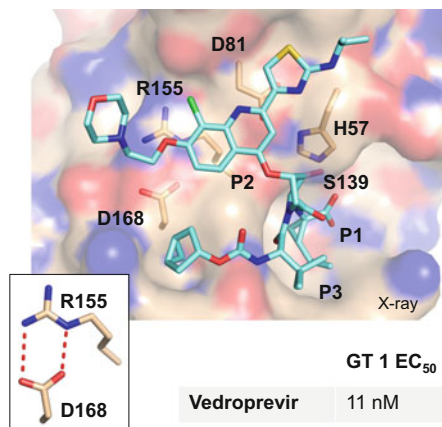
Inhibitors of the NS3/4A protease are an important therapeutic class utilized in the treatment of HCV infection. Indeed the first DAAs approved for the treatment of HCV GT1 infection in 2011 were the covalent reversible NS3/4A PIs telaprevir and boceprevir. Second-generation NS3/4A PIs soon followed that did not rely upon a covalent reversible interaction. Instead, they achieved potency by incorporating large hydrophobic aromatic P2 groups along with highly optimized terminal carboxylic acid or acyl sulfonamide P1 motifs. While these second-generation PIs have substantially improved GT1 potency compared to telaprevir and boceprevir, GT3 (and frequently GT2) potency remains a challenge [10, 11], limiting clinical application in these patient populations. Additionally, alanine transaminase (ALT) elevations, a marker of potential hepatotoxicity, has been observed with some NS3/4A PIs [12], contributing to clinical discontinuation (IDX-320, [13]), clinical dose reductions (asunaprevir [14], grazoprevir [15], and paritaprevir [16]), and/or hepatotoxicity warnings in the prescribing label (asunaprevir [17], grazoprevir [18], and paritaprevir [19]). Therefore, our internal efforts were focused on discovering an NS3/4A PI with a reduced risk of hepatotoxicity while also improving the pan-genotypic profile and activity against common RAS.

The NS3/4A protease is essential for viral replication as it cleaves the nascent HCV polyprotein into the proteins required for viral replication. This is accomplished by a classic Ser-His-Asp catalytic triad (S139, H57, and D81) that is conserved across all genotypes. Due to their necessity, RAS and polymorphisms at these three amino acids have not been observed. In contrast, RAS at other amino acids proximal to the NS3/4A PI binding site have rapidly emerged following PI treatment in GT1 patients (including amino acid positions 155 and 168, [20]). Amino acid variations at position 168 are of particular importance as there is a glutamine in GT3 rather than the aspartate found in all other genotypes, which contributes to a significant loss in GT3 potency for most NS3/4A PIs [11]. The electrostatic interaction formed between D168 and R155 creates an important surface for interaction with aromatic hydrophobic P2 groups. The crystal structure of the HCV NS3/4A PI vedroprevir (**1**) [21] bound to the GT1 NS3/4A protease highlights this interaction (Fig. 1). Accordingly, amino acid variations that disrupt this electrostatic interaction, such as Q168 in GT3, have a significant impact on inhibitor binding affinity. Indeed, vedroprevir GT3 cellular potency (3.6 μ M) is >300-fold lower than for GT1 (11 nM in GT1). The steric clash that would occur

a) Structure of vedroprevir 1 (GS-9451)



b) Vedroprevir bound to GT 1 NS3/4A protease



c) Model highlighting steric clash between GT3 Q168 (filled) and vedroprevir

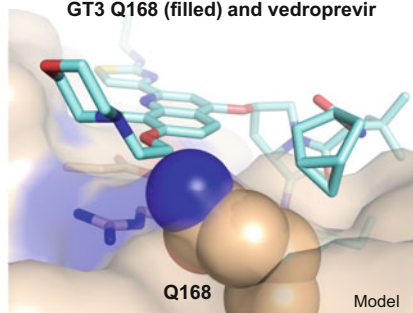


Fig. 1 (a) Chemical structure of vedroprevir and differential vedroprevir interactions with the NS3/4A protease in (b) GT1 and (c) GT3 surrogate (GT1b Q168)

between Q168 and the large P2 group of vedroprevir in the GT3 NS3/4A protease is modeled in Fig. 1c. Decreasing steric bulk of the P2 hydrophobic heterocycle, along with macrocyclization from P2 to P4, were strategies utilized in the discovery of grazoprevir to improve GT3 potency [22]. Even with these structural modifications, grazoprevir loses 2–3 orders of magnitude in both biochemical and cellular potency against GT3 compared to GT1 [11, 23]. Our initial internal discovery efforts were focused on modifications to the central P2 pyrrolidine core with the goal of improving both GT3 potency and activity against common GT1 RAS.

3 Exploration of Alternative Core Connectivities

To improve GT3 potency by minimizing the dependence on the D168/R155 interaction, modifications to the central pyrrolidine core with the goal of shifting the macrocycle away from residues D168 and R155 were initially pursued. Changing connectivity of the P2 heterocycle on the pyrrolidine from the 4-position in compound 2 to the 3-position in analog 3 resulted in a complete loss of GT3 potency (Table 1). Modeling suggested a piperidine with the quinoxaline heterocycle

Table 1 Effect of core replacements on GT3 activity

Compound	GT3 K_i^a (nM)	GT3 EC_{50}^b (nM)
2	0.063	79
3	>100	>4,444
4	>100	4,346
5	30	1,848
6	>100	>4,444
7	>100	>4,444

^a K_i determined by enzymatic assay using an HCV genotype 3a NS3/4A protein

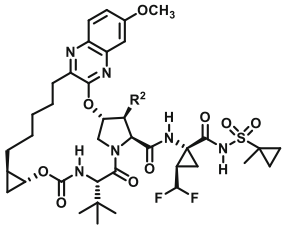

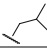
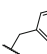
^b EC_{50} determined by cell-based assay using RLuc cells harboring subgenomic genotype 3a replicon

connected at the 4-position (**4**) might be better tolerated, but this change was also detrimental to both GT3 (4,346 nM for compound **4**) and GT1a potency (3.2 vs 543 nM for compounds **2** and **4**, respectively). These effects stand in contrast to IDX-320, wherein the piperidine core proved effective with a P1 to P3 macrocycle for GT 1 potency [13]. Utilizing the [2.2.1] azabicyclic group in compound **5** to enforce a modeling-preferred boat conformation of the piperidine ring improved potency compared to the acyclic piperidine containing analog **4**, but once again this was inferior to the initial 4-substituted pyrrolidine core (**2**). Changing the connection point of the quinoxaline to the 5-position of the piperidine (**6**) or the [2.2.1] azabicyclic variant (**7**) was also not tolerated. As modifications to the macrocycle trajectory were unacceptable, our efforts shifted to direct interactions with the HCV NS3/4A protease catalytic triad.

4 Discovery of 3-Alkyl Substituted Pyrrolidines as Beneficial in GT3

Due to its essential role in enzymatic activity, the catalytic triad (S138, H57, and D81) is conserved across all genotypes and is not a site of viral polymorphisms or resistance. Realizing that H57 is positioned adjacent to the 3-position of the central pyrrolidine core and H57 presents a hydrophobic surface, our efforts shifted toward exploring substituents such as alkyl, substituted alkyl, and cycloalkyl moieties at the pyrrolidine 3-position to exploit potential van der Waals

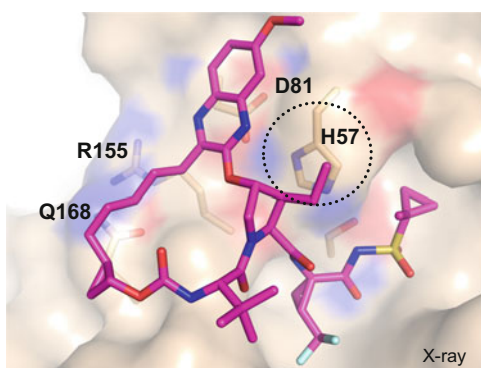
Table 2 Genotype 3 biochemical and cellular potency of 3-substituted pyrrolidine core containing HCV PIs

	Compound	R ²	GT3 Ki ^a (nM)	GT3a EC ₅₀ ^b (nM)	
	2	H	0.165	74	
	8	Me	0.100	20	
	9	Et	0.067	23	
	10	<i>n</i> -Pr	0.120	36	
	11			4.9	1,164
	12			0.630	1,125
	13			0.870	1,107

^aKi determined by enzymatic assay using an HCV genotype 3a NS3/4A protein

^bEC₅₀ determined by cell-based assay using RLuc cells harboring subgenomic genotype 3a replicon

Fig. 2 Crystal structure of 3-ethyl substituted pyrrolidine containing compound **9** bound to GT3 surrogate NS3/4A protease (GT1 D168Q) NS3/4A



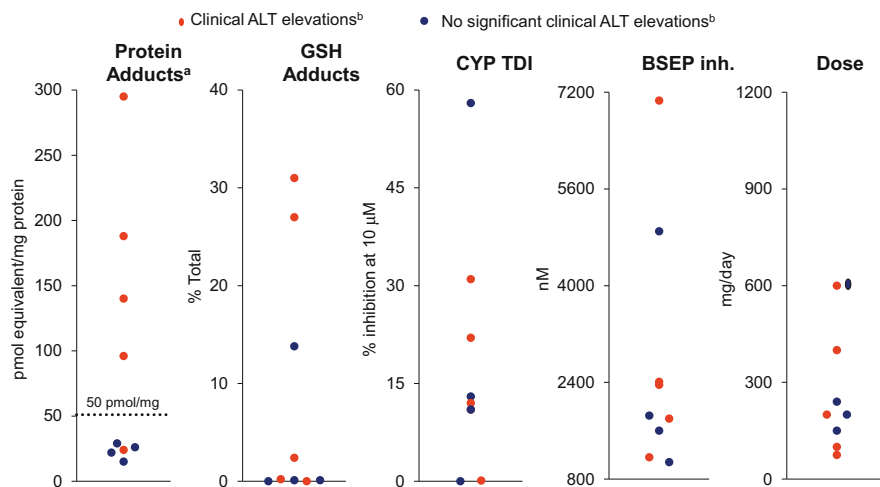
interactions. Consistent with this design strategy, methyl (**8**) and ethyl (**9**) substituted pyrrolidines improved GT3 cellular potency threefold to fourfold (Table 2) versus the unsubstituted pyrrolidine (**2**). The ethyl substituted compound **9** also improved GT3 biochemical potency 2.5-fold versus the unsubstituted pyrrolidine comparator **2** (67 pM vs 165 pM, respectively). The crystal structure of compound **9** bound to a GT3 surrogate NS3/4A protease (GT1 D168Q) demonstrates that the ethyl motif is indeed in van der Waals contact with H57 as we had envisioned (Fig. 2). Further extending to *n*-propyl (**10**) also improved both GT3 cellular and enzymatic potency versus the unsubstituted compound **2**, but this group was inferior to both methyl (**8**) and ethyl (**9**) substituents. More sterically demanding groups including cyclopropyl, isobutyl, and benzyl all resulted in significant potency losses (all >1,000 nM in GT3 cellular assay), which is consistent with space constraints resulting from the P2 quinoxaline and P1 cyclopropyl sulfonamide groups being in close proximity upon inhibitor binding. As the 3-methyl and 3-ethyl pyrrolidine substitutions proved beneficial to GT3 potency, both series were further pursued in parallel as we focused our attention on

drug metabolism and pharmacokinetic properties as well as addressing the hepatotoxicity risk associated with some HCV NS3/4A protease inhibitors.

5 Hepatotoxicity Risk Associated With Some HCV NS3/4A Protease Inhibitors

Potential hepatotoxicity associated with clinical ALT elevations has been observed with some HCV NS3/4A PI containing antiviral therapy regimens, leading to ALT warnings in the prescribing information along with recommendations for ALT monitoring. Identifying drivers of hepatotoxicity, and overcoming this liability, remains a common challenge in drug discovery. Multiple mechanisms can contribute to drug-induced hepatotoxicity, including reactive metabolite formation, immune-response pathways, and inhibition of biliary transporters [24–27]. More generally, hepatotoxicity is also often related to clinical dose. To determine if these factors are associated with HCV NS3/4A protease inhibitor-induced ALT elevations, we evaluated asunaprevir, danoprevir, faldaprevir, glecaprevir, grazoprevir, IDX-320, paritaprevir, vaniprevir, and vedroprevir in radiolabeled protein adduct, glutathione (GSH) adduct, cytochrome P450 (CYP) time-dependent inhibition (TDI), and bile salt export pump (BSEP) inhibition assays. These results, along with clinical dose, were then compared to reports of clinical ALT elevations. Notably, radiolabeled protein adduct formation had a strong correlation with clinical ALT elevation (Fig. 3), wherein all compounds generating >50 pmol equivalent/mg protein radiolabeled protein adducts showed clinical ALT elevations. Consistent with reactive metabolites contributing to ALT elevations, co-administration of ritonavir (to minimize CYP3A-mediated formation of reactive metabolites) with the NS3/4A PI danoprevir resulted in reduced clinical hepatotoxicity [21, 22]. Our internal studies, combined with the danoprevir results above, are consistent with protein adduct formation as an important correlator with clinical ALT elevations for this therapeutic class. Consequently, minimizing radiolabeled protein adduct formation became a priority for our NS3/4A PI discovery efforts.

A PI cyclopropyl-olefin motif is a structural feature common to many HCV NS3/4A PIs, and all five hepatotoxic NS3/4A PIs contain this motif wherein the olefin is either a terminal vinyl group (e.g., compound **14**, in Table 3) or part of a macrocycle. We hypothesized that this olefin could undergo metabolic activation to a reactive epoxide intermediate, which could then react with nucleophiles to form protein adducts (it is probable that the cyclopropyl group would increase the reactivity of the epoxide electrophile). In our discovery efforts, multiple cyclopropyl-olefin-containing analogs were investigated in metabolite identification (Met ID) studies in the presence of glutathione (GSH), and we frequently observed adducts consistent with this proposed metabolic activation pathway. Compound **14** is a specific example where Met ID results suggested GSH addition to an intermediate vinyl-derived epoxide. These metabolic results, along with the clinical hepatotoxicity



- Protein adduct formation generally correlates with clinical ALT for HCV PIs

Fig. 3 Association of clinical ALT elevation with potential risk factors across nine NS3/4A PIs. ^aIn vitro covalent binding determination involved the incubation of 10 µM radiolabeled drug substrate with 1.0 mg/mL human hepatic microsomes (±NADPH regenerating system). The radioactive content in remaining protein pellets was determined by liquid scintillation counter (LSC). ^bALT elevation status derived from package insert for approved compounds (paritaprevir, asunaprevir, grazoprevir, and simeprevir). For compounds not approved in the USA or EMA, positive ALT elevation noted when grade ≥3 ALT elevation occurred in ≥1% of patients or when publications document significant ALT elevation (danoprevir [28, 29]) or serious liver enzyme elevation (IDX-320 [13])

Table 3 Impact of P1 (R¹), P2 (R²), and P1' (R³) modifications on GT3 potency and human microsomal stability

Compound	R ¹	R ²	R ³	GT3 K _i ^a (nM)	GT3 EC ₅₀ ^b (nM)	hCLP ^c (L/h/kg)
14	Vinyl	Me	H	0.094	41	0.64
15	Et	Me	H	0.530	188	0.40
16		Me	H	1.3	419	0.20
17		Me	H	0.92	375	<0.17
18	Vinyl	Et	H	0.081	20	0.84
19	Et	Et	H	0.563	272	0.44
20	Me	Et	Me	0.838	109	0.67
21	CF ₂ H	Et	H	0.043	27	0.20
9	CF ₂ H	Et	Me	0.067	23	0.25
8	CF ₂ H	Me	Me	0.100	20	0.18

^aK_i determined by enzymatic assay using an HCV genotype 3a NS3/4A protein

^bEC₅₀ determined by cell-based assay using RLuc cells harboring subgenomic genotype 3a replicon

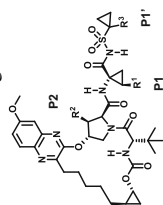
^chMS CLP = human clearance predicted using human microsomal stability assay

association, suggested a significant risk for the cyclopropyl-olefin motif; thus, our efforts focused on identifying alternative, metabolically inert P1 groups that would maintain sufficient antiviral potency and also demonstrate favorable drug metabolism and pharmacokinetic (DMPK) properties.

6 Improving Pan-Genotypic Potency and Minimizing Protein Adducts: The Discovery of Voxilaprevir

The small nature of the HCV NS3/4A protease S1 pocket interacting with the P1 cyclopropyl olefin group is evident by the natural peptide substrates that contain either a cysteine or threonine at this position [30]. Replacing the P1 vinyl (**14**) with an ethyl (**15**) in the 3-methyl pyrrolidine series resulted in an approximate fivefold loss in potency, consistent with the limited space available in this pocket. While the potency loss for **15** was unacceptable, we were encouraged by the improvement in predicted human clearance (hCLp) from 0.64 to 0.40 L/h/kg, which is consistent with removing the metabolically labile vinyl group. Monofluorination (**16**) or difluorination (**17**) of the P1 ethyl group further improved the predicted human clearance (hCLp = 0.20 and <0.17 L/h/kg, respectively), but at further expense to GT3 potency. The 3-ethyl pyrrolidine series was also investigated, yielding a trend toward improved metabolic stability and reduced GT3 potency when the P1 vinyl (**18**) is replaced with ethyl (**19**). Truncation to a P1 methyl group (**20**) significantly improved metabolic stability compared to the vinyl analog (**18**) but came with a significant loss in GT3 biochemical potency (~10-fold). Replacement of the P1 methyl with difluoromethyl afforded compound **21**, which maintained comparable potency to vinyl analog **18**, and also had substantially improved metabolic stability (hCLp = 0.20 L/h/kg). With potency and metabolic stability goals realized for the P1 position, we placed extensive efforts on modifications to the P1' cyclopropyl sulfonamide group, including substitution with multiple alkyl, cycloalkyl, and substituted alkyls (data not shown). Methyl substitution (Table 3, R³ group) was preferred due to pharmacokinetic properties (discussed below), resulting in 3-ethyl pyrrolidine compound **9** and its 3-methyl pyrrolidine variant (**8**). Both compounds were potent in the GT3 cellular potency assay (23 and 20 nM) and had low predicted human clearance (hCLp = 0.25 and 0.18 L/h/kg, respectively). With the discovery that the P1 difluoromethyl substituent afforded favorable potency and stability, we next evaluated the effect of P1 and P1' substitutions on the pharmacokinetic profile.

To enable a once-daily STR containing our NS3/4A PI combined with sofosbuvir and velpatasvir, we needed our NS3/4A PI to have a drug metabolism and pharmacokinetic profile supportive of a low, once-daily dose. Additionally, preferential distribution to the liver was considered a favorable attribute as the liver is the primary site of HCV replication. The combination of 3-substituted pyrrolidines with the different P1 and P1' groups had a dramatic impact on pharmacokinetics (Table 4). Compound **18**, which contained a P1 vinyl and a 3-ethylpyrrolidine, had

Table 4 Drug metabolism and pharmacokinetic profiles of 3-substituted pyrrolidine compounds

Compound	R ¹	R ²	R ³	LogD	hClp ^a (L/h/kg)	Protein adducts (pmol/mg protein)	Rat CL (L/h/kg)	Rat V _{ss} (L/h)	Rat t _{1/2} (h)	Rat F (%)	Rat [liver] @ 6 h (μM)
18	Vinyl	Et	H	4.1	0.84	117	0.88	1.9	2.2		20.9
19	Et	Et	H	4.6	0.44		0.67	3.1	5.0	100	30.2
21	CF ₂ H	Et	H	3.5	0.20		2.0	1.0	0.8	36	1.2
9	CF ₂ H	Et	Me	3.8	0.25	10	1.3	1.7	1.4	31	14.0
8	CF ₂ H	Me	Me	3.5	0.18		2.1	2.2	1.3	100	3.1

^ahClp = Predicted clearance based on incubation with human microsomes

high distribution to the liver in rats (20.9 μM at 6 h) but poor metabolic stability and high level of protein adducts (117 pmol equivalent/mg protein), precluding further advancement of this compound. Replacement of the P1 vinyl with ethyl afforded compound **19**, which had both an improved half-life (5.0 h vs 2.2 h) and liver concentration at 6 h compared to **18** but weaker GT3 potency as already described. While P1 difluoromethyl-containing compound **21** had good potency and metabolic stability, this structural motif had an unexpected negative impact on the apparent volume of distribution at steady state (V_{ss}), half-life, and liver concentration compared to both the vinyl (**18**) and ethyl (**19**) compounds. We hypothesized that the decrease in LogD, which resulted from decreased lipophilicity proximal to the acyl sulfonamide group, contributed to the impaired pharmacokinetics. Consequently, addition of a methyl to the P1' cyclopropyl (**9**) increased the LogD to 3.8 and yielded improved V_{ss} , half-life, and liver concentration at 6 h. The 3-methylpyrrolidine analog **8** was also evaluated, but the liver concentration was inferior to the 3-ethylpyrrolidine comparator **9** (3.1 vs 14.0 μM at 6 h, respectively), consistent with liver loading-LogD relationship observed with compounds **19**, **21**, and **9**. With compound **9** we were able to evaluate the effect of replacing the reactive vinyl group with a metabolically blocked difluoromethyl group on protein adduct formation. As desired, compound **9** had a nearly 12-fold reduction in protein adducts compared to the vinyl containing compound **18** (10 vs 117 pmol equivalent/mg protein, respectively).

Compound **9** was a major advancement for the program because GT3 potency was improved by the 3-ethyl pyrrolidine core, metabolic stability was increased, and protein adduct formation was reduced by replacing the P1 vinyl with a metabolically inert difluoromethyl group. Furthermore, preclinical pharmacokinetics were improved by the introduction of a methyl on the P1' cyclopropyl group. As our ultimate goal was to discover a once-daily compound that could be combined into a STR with sofosbuvir and velpatasvir, we sought to further improve both predicted human metabolic stability and GT3 potency. A human microsomal Met ID study was performed on compound **9**, and three distinct hydroxylated metabolites on the P2 to P4 macrocycle fragment were observed. While the exact location of hydroxylation on the macrocycle could not be determined, we expected that the methylene group attached to the 3-position of the quinoxaline would be the most metabolically labile. If oxidation were to occur at this position, the potential for quinone-methide-type reactive intermediate formation could arise via participation of the quinoxaline methoxy group. Thus, this metabolic pathway could result in protein adducts, potentially explaining the low but measurable level of adducts observed with compound **9** (10 pmol equivalent/mg protein). Therefore, metabolic blocks were explored at this benzylic position to improve metabolic stability and potentially further reduce protein adduct formation. A modest improvement in metabolic stability was realized with the two cyclopropyl diastereomer compounds **22** and **23** (Table 5), but both compounds lost significant GT3 potency. The benzylic monofluoro diastereomeric mixture (**24**) resulted in a small improvement in human microsomal stability, but with a slight loss in GT3 potency. Benzylic difluoro substitution with an adjacent macrocyclic olefin (a structural feature remaining

Table 5 Modifications to macrocycle to improve human microsomal stability and GT3 potency

	9	22	23	24	25	26
GT 3 EC ₅₀ ^a (nM)	23	128	829	35	5.3	6.1
GT 3 K _i ^b (nM)	0.067	1.7	9.4	0.13	0.053	0.063
hCLP ^c (L/h/kg)	0.25	0.21	0.23	0.23	0.25	<0.17

^aK_i determined by enzymatic assay using an HCV genotype 3a NS3/4A protein

^bEC₅₀ determined by cell-based assay using RLuc cells harboring subgenomic genotype 3a replicon

^chCLP = Predicted clearance in human microsomes

after the ring closing metathesis reaction) afforded compound **25**, which was approximately fourfold more potent in GT3 versus the unsubstituted comparator **9** (5.3 vs 23 nM, respectively). However, its human microsomal metabolic stability was unchanged, and we were concerned that the macrocyclic olefin could undergo undesired metabolic activation to a potentially reactive epoxide. Therefore, the olefin was reduced to generate compound **26**, which exhibited similarly improved GT3 biochemical (63 pM) and cellular (6.1 nM) potency versus analog **9** along with improved metabolic stability (hCLP <0.17 L/h/kg). The high metabolic stability of **26** was confirmed in a cryopreserved human hepatocyte stability assay wherein the predicted human clearance was <0.07 L/h/kg. Notably, this compound exhibited superior performance in the protein adduct assay (<1 pmol equivalent/mg protein), supporting our hypothesis that benzylic oxidation of the methylene was giving rise to the low but measurable protein adduct formed with compound **9** and further lowering the risk of clinical hepatotoxicity. Additionally, as the benzylic difluoro in compound **26** is positioned directly above the hydrophobic alkyl portion of the R155 amino acid, van der Waals interactions may contribute to the improved potency for **26** compared to the unsubstituted compound **9** (Fig. 4).

With both pan-genotypic potency and improved antiviral activity against common GT1 RAS being essential attributes of our desired compound profile, compound **26** was evaluated in a range of cellular potency assays. As desired, **26** was highly potent across genotypes (EC₅₀ = 1.5–6.6 nM) with less than a twofold shift between GT1 and GT3 (Table 6). Potency was also maintained against some common RAS including genotype 1a Q80K, 1b R155K, and 1b D168 (<2-fold potency shift), consistent with our design strategy of targeting interactions with the conserved H57 of the catalytic triad. Similar to other NS3/4A PIs, a large shift in potency was observed for the A156T RAS. This was not unexpected as this amino acid is

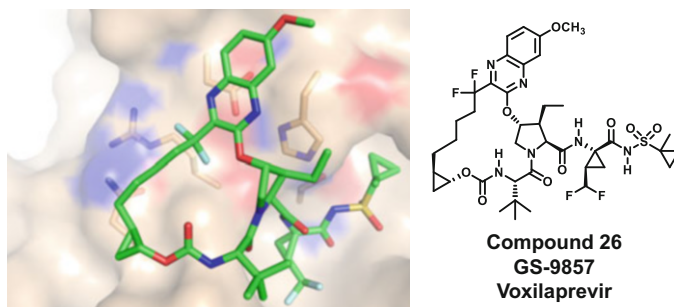


Fig. 4 Crystal structure of voxilaprevir bound to GT1 D168Q (GT3 surrogate) NS3/4A protease

Table 6 Compound **26** pan-genotypic potency and activity against common GT1 RAS

	Genotype (wild-type)								RAS			
	1a	1b	2a	2b	3a	4a	5a	6a	1a Q80K	1a R155K	1b D168E	1a/1b A156T
EC ₅₀ ^a (nM)	3.9	3.3	3.7	6.6	6.1	4.9	1.9	1.5	3.1	2.7	4.0	>500

GT1a (strain H77). GT1b (Con-1). GT2a (JFH-1). GT2b (HM568433) is a NS3 protease chimeric replicon expressed in a 2a subgenomic backbone. GT3a (strain S52) is a subgenomic replicon with adaptive mutations P89L in the protease domain and K583E in the helicase domain. GT4a (ED43). GT5a NS3 protease is expressed in a 1b subgenomic replicon backbone. The 1b protease domain was converted to GT5a protease by changing 34 amino acids to corresponding sequences in the strain SA13. GT6a (consensus) is a NS3 protease chimeric replicon expressed in a 1b subgenomic backbone

^aEC₅₀ determined by cell-based assays using RLuc cells harboring subgenomic genotype replicons of the corresponding genotype

positioned directly below the central P2 pyrrolidine group of NS3/4A PIs, and increasing sterics beyond alanine decreases inhibitor binding.

The drug metabolism and pharmacokinetic properties of compound **26** were profiled in a range of in vitro and in vivo studies. The in vivo half-lives ranged from 0.93 to 4.2 h with the observed clearances being within twofold of the predicted metabolic clearances, suggesting a low in vivo clearance in humans. The V_{ss} was slightly larger than total body water, and preferential liver distribution was high with liver to plasma ratios of >50-fold across species (Table 7). In vitro human and rat hepatocyte uptake studies, in the presence and absence of rifampicin, suggest that preferential liver distribution is mainly driven by transporter-mediated active hepatic uptake. With the projected long half-life in humans supportive of once-daily dosing, decreased risk of hepatotoxicity, potent antiviral activity across genotypes, and improved activity against some common GT1 RAS, compound **26** (voxilaprevir, VOX) was selected for advancement into clinical trials.

Table 7 Drug metabolism and pharmacokinetic profile of compound **26**

	In vitro		In vivo ^{a,b}				
	% Free plasma	CLp ^c (L/h/kg)	CL (L/h/kg)	V _{ss} (L/kg)	t _{1/2} (h)	F/F _a (%)	Liver to plasma ratio, @ 2 h
Rat	0.42	0.39	0.82	0.84	0.93	83/100	>500×
Dog	0.28	0.17	0.19	0.94	4.2	27/30	55×
Monkey	0.91	1.01	0.89	0.80	2.1	10/23	100×
Human	0.46	<0.07					

^aRat iv (1.0 mg/kg), dog iv (0.5 mg/kg), cyno iv (0.5 mg/kg)

^bRat po (3.0 mg/kg), dog po (1.0 mg/kg), cyno po (1.0 mg/kg)

^cCLp = metabolic clearance predicted from microsomal stability for rat, dog, and monkey and from hepatocyte stability for human

F bioavailability, F_a fraction absorbed

7 Voxilaprevir and Vosevi[®] (sofosbuvir/velpatasvir/voxilaprevir) Clinical Antiviral Activity

The safety and pharmacokinetics of voxilaprevir in healthy volunteers were evaluated in a double-blind, placebo-controlled, single- and multiple-dose study at 30, 100, and 300 mg. Voxilaprevir was well tolerated with no clinically significant laboratory abnormalities. Consistent with voxilaprevir having high metabolic stability, the median steady-state half-lives of voxilaprevir ranged from 28 to 41 h, supporting once-daily dosing. Antiviral activity of voxilaprevir as a monotherapy was assessed in a Phase 1b trial evaluating voxilaprevir in subjects infected with HCV GT 1–4 virus. At the 100-mg dose, antiviral activity was observed across all genotypes with median maximal viral load reductions of >3 log₁₀ IU/mL [31]. The 100 mg dose of voxilaprevir was thus selected for advancement into Phase 2 and 3 clinical studies in combination with sofosbuvir and velpatasvir. Four Phase 3 studies (POLARIS-1, POLARIS-2, POLARIS-3, and POLARIS-4) were conducted to assess the antiviral efficacy, safety, and tolerability of SOF/VEL/VOX. In the combined POLARIS-1 and POLARIS-4 studies evaluating SOF/VEL/VOX administered for 12 weeks in DAA-experienced patients with and without compensated cirrhosis, the overall SVR rate was 97%, and high SVR rates were observed irrespective of genotype, prior DAA regimen, or presence of pre-existing RAS [32]. To assess whether the addition of VOX to the SOF/VEL regimen would allow shortening treatment duration for DAA-naïve patients with and without cirrhosis, the POLARIS-2 and POLARIS-3 studies were conducted. A total of 611 DAA-naïve patients were treated with 8 weeks of SOF/VEL/VOX, and the overall SVR12 rate was 95% [33]. In the combined Phase 3 studies, over 1,000 genotype 1–6 HCV-infected patients were treated with SOF/VEL/VOX, and no treatment-related serious adverse events were reported. Consistent with the preclinical optimization efforts, no safety signal of hepatotoxicity was observed.

8 Conclusion

In summary, favorable binding interactions of voxilaprevir with the catalytic triad and R155 of the HCV NS3/4A protease were discovered that contributed to improved potency against GT3 and some common GT1 RAS. In evaluating clinical NS3/4A protease inhibitors, a strong association between protein adduct formation and clinical ALT elevation was identified. To mitigate the risk of clinical hepatotoxicity, multiple structural modifications were introduced that improved metabolic stability and decreased protein adduct formation to <1 pmol equivalent/mg protein. Consistent with this design strategy, hepatotoxicity was not observed with regimens containing voxilaprevir in Phase 3 trials involving over 1,000 patients. The high metabolic stability was further reflected in the human pharmacokinetics wherein the average steady-state half-lives of voxilaprevir ranged from 28 to 41 h in healthy volunteers, supporting once-daily dosing. In a Phase 1b trial evaluating voxilaprevir in subjects infected with HCV GT 1–4 virus, median maximal viral load reductions of >3 log₁₀ IU/mL were observed across genotypes at the 100 mg dose. Voxilaprevir's profile has allowed for its combination with sofosbuvir and velpatasvir into a once-daily STR treatment for HCV infection known as Vosevi[®]. Vosevi[®] represents a treatment option for some of the most difficult-to-cure patients who have failed previous DAA containing regimens. Furthermore, for some DAA-naïve patients, Vosevi[®] provides an option of shortened 8-week treatment duration.

Acknowledgements The author would like to thank the many individuals who contributed to the discovery and development of voxilaprevir. The author would also like to thank the patients and their families as well as study site staff who participated in the clinical trials of Vosevi.

Compliance with Ethical Standards

Conflicts of Interest James G. Taylor is an employee of Gilead Sciences, Inc.

Ethical Approval All procedures performed in the studies involving human participants were in accordance with the ethical standards of the institutional and/or national research committee and with the 1964 Helsinki declaration and its later amendments or comparable ethical standards.

Informed Consent Informed consent was obtained from all individual participants included in the study.

References

1. Polaris Observatory HCV Collaborators (2017) Global prevalence and genotype distribution of hepatitis C virus infection in 2015: a modelling study. *Lancet Gastroenterol Hepatol* 2 (3):161–176
2. WHO (2017) Global hepatitis report, 2017
3. Hedskog C et al (2017) Identification of novel HCV genotype and subtypes in patients treated with Sofosbuvir-based regimens. *J Hepatol* 66

4. Burstow NJ et al (2017) Hepatitis C treatment: where are we now? *Int J Gen Med* 10:39–52
5. Feld JJ et al (2015) Sofosbuvir and velpatasvir for HCV genotype 1, 2, 4, 5, and 6 infection. *N Engl J Med* 373(27):2599–2607
6. Foster GR et al (2015) Sofosbuvir and velpatasvir for HCV genotype 2 and 3 infection. *N Engl J Med* 373(27):2608–2617
7. Pawlotsky JM (2016) Hepatitis C virus resistance to direct-acting antiviral drugs in interferon-free regimens. *Gastroenterology* 151(1):70–86
8. Vosevi (sofosbuvir, velpatasvir, and voxilaprevir) [EMA Summary of Product Characteristics] (2017) Gilead Sciences Ireland UC, Carrigtohill
9. Vosevi (sofosbuvir, velpatasvir, and voxilaprevir) [package insert] (2017) Gilead Sciences, Inc, Foster City
10. Gottwein JM et al (2011) Differential efficacy of protease inhibitors against HCV genotypes 2a, 3a, 5a, and 6a NS3/4A protease recombinant viruses. *Gastroenterology* 141(3):1067–1079
11. Soumana DI et al (2016) Molecular and dynamic mechanism underlying drug resistance in genotype 3 hepatitis C NS3/4A protease. *J Am Chem Soc* 138(36):11850–11859
12. Mishra P, Chen M (2017) Direct-acting antivirals for chronic hepatitis C: can drug properties signal potential for liver injury? *Gastroenterology* 152(6):1270–1274
13. Parsy CC et al (2015) Discovery and structural diversity of the hepatitis C virus NS3/4A serine protease inhibitor series leading to clinical candidate IDX320. *Bioorg Med Chem Lett* 25(22):5427–5436
14. Bronowicki JP et al (2013) Randomized study of asunaprevir plus pegylated interferon-alpha and ribavirin for previously untreated genotype 1 chronic hepatitis C. *Antivir Ther* 18(7):885–893
15. Caro L, Du L, Huang S, Wenning L, Su J, Hwang P, Valesky R, Gilbert C, Gress J, Klaassen F, Gendrano IN, Brunhofer J, Cooreman M, Huisman J, Mobashery N (2013) Relationship between transaminase levels and plasma pharmacokinetics following administration of MK-5172 with pegylated interferon alfa-2b and ribavirin to GT1 treatment-naive HCV patients. In: Proceedings of the 8th international workshop on clinical pharmacology of hepatitis therapy
16. Poordad F et al (2013) Exploratory study of oral combination antiviral therapy for hepatitis C. *N Engl J Med* 368(1):45–53
17. Sunvepra (asunaprevir) (2017) Bristol-Myers Squibb Australia Pty Ltd, Mulgrave
18. Zepatier (elbasvir and grazoprevir) [package insert] (2016) Merck & Co., Inc, Whitehouse Station
19. Viekira Pak (ombitasvir, paritaprevir, and ritonavir tablets; dasabuvir tablets) [package insert] (2014) AbbVie, Inc, Chicago
20. Romano KP et al (2012) The molecular basis of drug resistance against hepatitis C virus NS3/4A protease inhibitors. *PLoS Pathog* 8(7):e1002832
21. Sheng XC et al (2012) Discovery of GS-9451: an acid inhibitor of the hepatitis C virus NS3/4A protease. *Bioorg Med Chem Lett* 22(7):2629–2634
22. Harper S et al (2012) Discovery of MK-5172, a macrocyclic hepatitis C virus NS3/4a protease inhibitor. *ACS Med Chem Lett* 3(4):332–336
23. Yu M et al (2013) In vitro efficacy of approved and experimental antivirals against novel genotype 3 hepatitis C virus subgenomic replicons. *Antivir Res* 100(2):439–445
24. Thompson RA et al (2016) Reactive metabolites: current and emerging risk and Hazard assessments. *Chem Res Toxicol* 29(4):505–533
25. Tujios S, Fontana RJ (2011) Mechanisms of drug-induced liver injury: from bedside to bench. *Nat Rev Gastroenterol Hepatol* 8(4):202–211
26. Stephens C, Andrade RJ, Lucena MI (2014) Mechanisms of drug-induced liver injury. *Curr Opin Allergy Clin Immunol* 14(4):286–292
27. Evans DC et al (2004) Drug-protein adducts: an industry perspective on minimizing the potential for drug bioactivation in drug discovery and development. *Chem Res Toxicol* 17(1):3–16

28. Goelzer P et al (2012) Coadministration of ritonavir with the HCV protease inhibitor danoprevir substantially reduces reactive metabolite formation both in vitro and in vivo (abstract 796). *J Hepatol* 56(2):580A
29. Gane EJ et al (2014) Efficacy and safety of danoprevir-ritonavir plus peginterferon alfa-2a-ribavirin in hepatitis C virus genotype 1 prior null responders. *Antimicrob Agents Chemother* 58(2):1136–1145
30. Lin C (2006) HCV NS3-4A serine protease. In: Tan SL (ed) *Hepatitis C viruses: genomes and molecular biology*. Horizon Scientific Press, Norfolk
31. Rodriguez-Torres M et al (2016) GS-9857 in patients with chronic hepatitis C virus genotype 1-4 infection: a randomized, double-blind, dose-ranging phase 1 study. *J Viral Hepat* 23(8):614–622
32. Bourliere M et al (2017) Sofosbuvir, velpatasvir, and voxilaprevir for previously treated HCV infection. *N Engl J Med* 376(22):2134–2146
33. Jacobson IM et al (2017) Efficacy of 8 weeks of sofosbuvir, velpatasvir, and voxilaprevir in patients with chronic HCV infection: 2 phase 3 randomized trials. *Gastroenterology* 153(1):113–122

Index

A

ABT-072, 182
ABT-450 (paritaprevir), 245, 389, 405, 415, 418
ABT-493 (glecaprevir), 251, 415, 416, 431, 436
ACH-0143422, 134, 135
ACH-1625 (sofavprevir), 242
ACH-2684 (deldeprevir/neceprevir), 245, 246
ACH-3102, 242
Acyl sulfonamide, 317
Adenosine deaminase (ADA), 123
Alanine 1-naphthyl phosphoramidate, 126
Alanine transaminase (ALT), 100, 443
Albinterferon, 99
Albuferon, 107
Alkoxypropylidone urea, 377
ALS-2200, 134
Animal models, 29–55, 71, 152, 157, 269, 277, 392
Antiviral therapy, 35, 43, 69, 88, 100, 149, 447
Asunaprevir (ASV), 193, 223, 231, 242, 317, 333
Australia antigen, 3–9
Awareness, 283, 286
Azidocytidine (R1479), 130

B

Balapiravir, 130
Beclabuvir, 171, 175, 193, 222, 317, 319
Benzimidazoles, 196
Benzodiazepinone, 175
Benzothiadiazines, 182
Benzyl alkyl ether linkers, 427
BI 201335 (faldaprevir), 240

BILB 1941, 171, 174
BILN-2061, 249, 269, 358, 392, 417
Blood tests, 19
Blood transfusion, 6, 8
BMS-605339, 241, 242, 317, 321
BMS-650032 (asunaprevir), 242, 317, 333
BMS-790052 (daclatasvir), 45
BMS-791325, 222
BMS-890068, 242
BMS-929075, 171, 184
BMS-986094, 128
Boceprevir, 102, 107, 231, 238, 262, 293, 308–312, 357, 390, 416, 443
Bovine viral diarrhea virus (BVDV), 184, 219

C

Capecitabine, 130, 131
CD81, 32
Chimpanzees, 3, 9, 48, 130, 154, 366, 392, 409, 421
Chronic active hepatitis (CAH), 10
Chronic infection, 97
Ciluprevir, 231, 236, 243, 357
Cirrhosis, 3, 8, 10, 70, 103, 163, 223, 282, 293, 347, 442, 454
Claudin-1 (CLDN1), 32
Cloning, 4, 11, 19, 71, 88
Con1, 74, 76, 78, 80, 82, 145, 195, 341, 393, 396, 408, 420
Consensus interferon (CIFN), 99, 107
1-Cyclopentyl benzimidazole, 173
Cyclopentyl carbamate, 243, 325, 376
Cyclophilin A (CYPA), 44

- Cyclopropylindolobenzazepines, 221
 Cytidine analogs, 129
 Cytochrome P (CYP), 129, 216, 219, 309, 397, 435, 447
- D**
 Daclatasvir (DCV), 45, 86, 87, 176, 193, 223, 317–319
 Danoprevir, 150, 231, 246, 357, 447
 Dasabuvir, 171, 182, 186, 245, 286, 410, 418, 442
 DDIVPC-OH, 356
 Deaza-2'-C-methyladenosine, 124
 Deldeprevir, 245, 246
 Deleobuvir, 171, 174, 241
 Deoxy-2'-fluorocytidine (2'-FdC), 131
 Deoxy-2'-(*R*)-fluoro-2'-C-methylcytidine (PSI-6130), 131
 Deoxy-2'-(*R*)-fluoro-2'-methyluracil (PSI-6206), 131
 Difluoroalkyl cyclopentyl ether linkers, 428
 Diphosphates, 118, 141, 158
 Direct-acting antivirals (DAA), 20, 71, 98, 142, 262, 345, 390, 416, 441
 combination therapy, 415
 Drug development, 69, 85, 183, 277, 286, 294
 Drug resistance, 81, 86, 98, 107, 281, 309, 339, 434
- E**
 Electrophilic trap, 293, 312
 Encephalomyocarditis virus (EMCV), 73, 75
 Eplclusa, 142, 165, 278, 442
- F**
 Faldaprevir, 174, 231, 240, 241, 447
 Filibuvir, 171, 177
 Flaviviridae, 19, 53, 194, 294, 356, 416
 Fluoro-*C*-methyl cytidine, 141
 Fluoro-*C*-methyl nucleoside, 141
 Fluoro-*C*-methyl uridine, 117, 141
 Fumaryl acetoacetate hydrolase, 51
- G**
 GB virus B (GBV-B), 49, 53, 55, 331
 Genome organization, 31, 54, 72, 88
 Glecaprevir, 108, 231, 251–253, 415, 436, 447
 Glycoproteins, 31, 38, 99, 160, 295
 Grazoprevir, 231, 250, 252, 253, 355, 368, 411
 GS-9256, 247
 GS-9451 (vedoprevir), 243, 247
 GS-9587 (voxilaprevir), 251
 GS-9857, 441
 GSK625433, 171, 179
 GSK2485852, 171, 184
 GT-1b virus, 318
 Guanosine analogs, 126
- H**
 Harvoni, 141
 HCV-371, 171, 177
 HCV-BK, 76, 80
 HCV cell culture (HCVcc) system, 82
 HCV-N, 80
 Hepaciviruses, 29, 48–55, 416
 Hepatitis A virus (HAV), 3, 9
 Hepatitis B surface antigen (HBsAg), 8
 Hepatitis B virus (HBV), 3, 9, 75, 118, 172
 Hepatitis, chronic active hepatitis (CAH), 10
 non-A/non-B hepatitis (NANBH), 3, 9–13, 19–24, 47
 posttransfusion, 3, 7, 8, 19, 24, 416
 Hepatitis C virus (HCV), 3–457
 cell culture system, 69
 polymerases, 26, 121, 171, 263, 391
 polyprotein, 31, 36, 39–42, 74, 264, 356, 416, 443
 protease, inhibitors, 43, 47, 231, 262–277, 285, 293, 296, 310, 379, 391–411, 416, 431–436
 proteins, 29, 36, 43
 replication, 29, 41–53, 70–87, 117, 141, 144, 194, 232, 398
 RNA, 13, 30–51, 150, 172, 179, 195, 268, 274, 342–347, 392, 409
 Hepatitis D virus (HDV), 22, 73, 106
 Hepatocellular carcinoma (HCC), 8, 293
 Hepatoma cell lines, 22, 51, 75, 76, 121
 transplantation, 51
 Hepatotoxicity, 52, 106, 441, 443, 447, 454
 Huh7 hepatoma, 51, 75, 76, 121
 Human immunodeficiency virus (HIV), 13, 15, 20, 42, 128, 159, 163, 164, 172, 187, 194, 219, 263, 281, 286, 294, 331
 protease inhibitors, 42, 177, 264, 295, 391, 397, 398, 435
 reverse transcriptase, 122
 Human liver chimeric mice, 29, 51
 Human vesicle-associated membrane protein-associated protein A (hVAP-A), 78

I

IDX-184, 128
 IDX-320, 245, 443
 IDX-375, 171, 181
 INCIVEK, 231, 238, 252, 262–267, 277, 357
 Indolobenzazepines, 193, 200–222
 Indolobenzodiazepine, 201
 Inflammation, 13, 97, 101, 281
 Interferon (IFN), 10, 20, 42, 79, 97–108,
 186, 231
 albinterferon, 99
 consensus (CIFN), 99, 107
 IFN- α , 51, 97, 100, 103, 194, 317
 IFN- β , 99, 106
 IFN- λ , 99, 106
 peginterferons (PegIFNs), 97, 102–107,
 262, 317, 416, 420, 435
 Interferon-free therapies, 47, 50, 141, 231
 Interferon-stimulated genes (ISGs), 49
 Internal ribosomal entry site (IRES), 31, 71
 INX-189 (BMS-986094), 128
 ITMN-191, 246

J

JFH-1, 22, 44, 79–85, 128, 161, 341, 434, 453
 JNJ-54257099, 135
 JTK-109, 171, 173, 174

K

Ketoamides, 231, 237, 293–311, 357, 390,
 397, 416

L

L-570310, 238
 Life cycle, viral, 19, 32, 40, 47, 52, 71, 82, 107,
 171, 293
 Lipo-viro-particle (LVP), 33
 Liver, 3–14, 141–164
 microsomes, 211, 217, 325, 397–405,
 420, 422
 targeting, 121, 129, 141–165, 398
 Lomibuvir, 171, 178, 179
 Lopinavir, 391, 397, 435

M

Macrocycles, 176, 231, 235–251, 355,
 367–382, 390, 444
 MAVS, 42
 Mericitabine, 132, 142, 150, 151, 246

Methyladenosine (2'-C-MeA), 121, 124, 127
 Methylcytidine (2'-O-MeC), 119, 121, 122,
 129–131, 143
 Methylguanosine, 124, 126, 127, 129
 Mice, genetic humanization, 52
 human liver chimeric, 29, 51
 MicroRNA-122 (miR-122), 34
 Miravirsen/SPC3649, 34
 MK-608, 125
 MK-1220, 250, 373, 376
 MK-2748, 249, 250
 MK-3281, 171, 175
 MK-4519, 249
 MK-5172 (grazoprevir), 250, 358, 378, 380
 MK-6325, 251, 368
 MK-7009 (vaniprevir), 249, 250, 365, 366
 MK-8876, 171, 184
 Monophosphates, 102, 117, 141–153, 163
 Morpholine carboxamides, 201, 208
 Mouse models, 48–55, 177, 183, 270
 MS-1/MS-2, 5

N

NANBV, 3
 Narlaprevir, 231, 240, 252
 Neceprevir, 245, 246
 Nesbuvir, 171, 183
 NM283 (valopicitabine), 129
 Nonalcoholic fatty liver disease (NAFLD), 13
 Non-A/non-B hepatitis (NANBH), 3, 9–13,
 19–24, 47
 blood-borne, 19
 Non-nucleoside inhibitors (NNIs),
 47, 171–187
 Non-primate hepaciviruses (NPHV),
 29, 53, 54
 Nonstructural proteins (NS), 71
 Norway rat hepacivirus (NrHV), 55
 NS2 protease, 32, 40, 72, 75, 82, 84, 295
 NS3 protease, 12, 40, 317, 355
 helicase, 42
 protease, 293, 415
 NS4 protease, 12
 NS4A protease, 12, 41, 317, 355
 NS4B protease, 43
 NS5A, 12, 43, 69, 442
 NS5B protease, 12, 45, 117, 141, 171, 442
 NTPase/helicase, 31, 42
 Nucleoside diphosphate (NDP), 118, 120
 kinase (NDPK), 118, 120, 148, 158
 Nucleoside monophosphate (NMP), 118
 kinase (NMPK), 118

- Nucleosides, 117, 141
 analogues, 101, 117–135, 141–146, 345
 inhibitors, 47, 119, 121, 143, 194, 246
- Nucleotides, 117, 141
 inhibitors, 47, 117, 239, 263
- O**
- Occludin (OCLN), 32
- Odalasvir, 244
- OLYSIO, 176, 231, 243, 246, 253, 286, 358, 409, 434
- Ombitasvir, 182, 245, 246, 286, 410, 418, 442
- P**
- P2-P4 macrocyclic, 415
- P7, 39, 71, 75, 83, 295
- Palm domain/site, 45, 161, 171, 179, 184, 186, 221
- Pan-genotypic, 415
- Paritaprevir, 182, 231, 245, 253, 286, 389–411, 418, 435, 447, 448
- Peginterferons (PegIFNs), 97, 102–107, 262, 317, 416, 420, 435
- Pegylation, 97, 102, 262, 317
- Phenanthridine, 245, 372, 389, 401–405, 411
- Phenyl alkyl linkers, 422
- Phosphatidylinositol-4-phosphate (PI4P), 78
- Phosphoramidate, 117, 141, 152–160
- PHX-1766, 247
- PI4KIII α , 44
- Piperazine, 175, 213, 217
 carboxamides, 193, 211–216
- Piperidine, 444, 445
 carboxamide, 196
- Polymerase, 171
 inhibitors, 193, 390
- Polymerase chain reaction (PCR), 9, 11, 24, 75, 100
- Posttransfusion hepatitis, 3, 7, 8, 19, 24, 416
- P*-oxime inhibitors, 393
- P*-phenanthridine, 401
- PPAR- γ , 426, 427, 431
- Primary care providers, 283
- Prodrugs, 126, 141, 150–156
- Proteases, 26, 30, 40, 43, 71–86, 158
 inhibitors (PI), 102, 107, 150, 262, 355, 389, 399, 415, 441–453
- Protein adducts, 441
- PSI-6130, 131, 141–144, 149
- PSI-6206, 131, 141, 146–163
- PSI-6419 (*N*¹-pentylloxycarbonyl PSI-6130), 130, 131
- PSI-7672, 157
- PSI-7851, 141, 157–162
- PSI-7977 (GS-7977, sofosbuvir), 117, 134, 141, 158
- PSI-8118, 157
- PSI-352707, 157, 158, 160
- PSI-352938, 129, 162, 163
- PSI-353661, 129
- Purine nucleoside phosphorylase (PNP), 123
- Pyrazoles, 179, 195, 197
- Pyrrolidines, 3-alkyl substituted, 445–450
- R**
- R1626 (balapiravir), 130
- R7128 (mericitabine), 130, 132, 133
- R7227, 245, 246
- Radalbuvir, 171, 179
- Replication-enhancing mutations (REMs), 76
- Replication systems, 72
- Resistance, 141, 441
- Resistance-associated substitutions (RAS), 393–411, 421, 431, 434, 442
- RG7109, 171, 182
- RG7128, 141
- Ribavirin (RBV), 97–107, 128, 132, 142, 174, 178, 181, 183, 194, 223, 238, 262, 280, 311, 317, 340, 356, 390, 410, 416
- Ribavirin-free, 231
- Ribonucleoside kinase (rNK), 118
- Ribonucleosides, 148
- Ribozyme, 73, 74
- Ring-closing metathesis, 355
- Ritonavir, 176, 182, 245, 286, 389–406, 411, 420, 435, 442, 447
- RNA polymerase, 118, 135, 157, 199, 275, 345
 RNA-dependent (RdRp), 31, 45, 71, 141, 142
- Rodent hepaciviruses (RHV), 29, 49, 54
- S**
- SB-750330, 171, 181
- Scavenger receptor B1 (SR-B1), 32
- SCH-503034 (boceprevir), 102, 107, 231, 238, 262, 293, 308–312, 357, 390, 416, 443
- SCH-900518 (narlaprevir), 240
- Serine protease, 26, 41, 232, 293, 295, 356, 416
- Setrobuvir, 171, 181
- Simeprevir, 176, 231, 243, 246, 253, 286, 358, 409, 434, 448
- Single tablet regimen (STR), 187, 441, 442
- Sofosbuvir, 47, 55, 107, 117, 136, 141–165, 186, 239, 244, 251, 277, 286, 346, 435, 442, 450, 455

SOF/VEL/VOX, 441
SOVALDI, 141, 142, 165, 277, 286
Sovaprevir, 231, 242
S282T, 141, 149, 159–165
Steatohepatitis (NASH), 13
Stigma, 283
Sustained virologic response (SVR), 3, 10, 14, 97, 100, 163, 435
Synthesis-inspired design, 355

T

Tegobuvir, 171, 184
Telaprevir, 231, 238, 252, 262–267, 277, 357
Thiophene-2-carboxylic acids, 178
Thumb domain/site, 45, 161, 171–180, 199, 206, 221
TMC647055, 171, 176
Togaviridae, 21
Transfusion-associated hepatitis (TAH), 3, 8, 12
Triphosphates, 117, 141, 163, 184
Tubercidin (7-deaza-adenosine), 124
Tupaia belangeri, 48

U

Undecapeptide lead, 238, 293–298
Untranslated regions (UTRs), 31, 34
Uprifosbuvir, 135

Uridine analogs, 133, 146, 148, 153
Urokinase plasminogen activator, 51

V

Vaniprevir (VANIHEP), 232, 250, 252, 358, 363–381, 447
VCH-759, 171
Vedroprevir, 231, 243, 443, 444, 447
Velpatasvir, 251, 253, 449, 451, 455
VICTRELIS (boceprevir), 102, 107, 231, 238, 262, 277, 293, 308–312, 357, 390, 416, 443
Viral adaptation, 53
Viroporin, 31, 40
Virus identification, 19
Vosevi, 141, 165, 253, 441, 443, 454
Voxilaprevir (GS-9857), 232, 251–253, 441, 449
VX-135, 134
VX-950, 238, 262–287

X

Xenotransplantation, 51
Ximency, 176, 223, 318, 347

Z

ZEPATIER (grazoprevir), 231, 250, 252, 253, 355, 358, 368, 411